



## ARTICLE

# Synthesis and characterization of novel 2-(1-benzyl-3-[4-fluorophenyl]-1*H*-pyrazol-4-yl)-7-fluoro-4*H*-chromen-4-one derivatives

Kiran S. Hon | Hemantkumar N. Akolkar | Bhausahab K. Karale

P.G. and Research, Department of Chemistry, Radhabai Kale Mahila Mahavidyalaya, Ahmednagar, Maharashtra, India

**Correspondence**

Bhausahab K. Karale, P.G. and Research, Department of Chemistry, Radhabai Kale Mahila Mahavidyalaya, Ahmednagar, Maharashtra 414 001, India.  
Email: bkkarale@yahoo.com

**Abstract**

Novel 1-benzyl-3-(4-fluorophenyl)-1*H*-pyrazole-4-carbaldehydes **3a** to **3e** were synthesized via Vilsmeier-Haack reaction of the appropriate 1-benzyl-2-(1-(4-fluorophenyl)ethylidene)hydrazines, derived from 4-fluoroacetophenone **1** with substituted 2-benzylhydrazines **2a** to **2e**. The base catalyzed condensation of 1-benzyl-3-(4-fluorophenyl)-1*H*-pyrazole-4-carbaldehydes **3a** to **3e** with 1-(4-fluoro-2-hydroxyphenyl)ethanone **4** gave (*E*)-3-(1-benzyl-3-(4-fluorophenyl)-1*H*-pyrazol-4-yl)-1-(4-fluoro-2-hydroxyphenyl)prop-2-en-1-ones **5a** to **5e**. On cyclization with dimethyl sulfoxide (DMSO)/I<sub>2</sub>, compounds **5a** to **5e** gave 2-(1-benzyl-3-(4-fluorophenyl)-1*H*-pyrazol-4-yl)-7-fluoro-4*H*-chromen-4-ones **6a** to **6e**. Structures of all novel compounds were confirmed by infrared (IR), proton nuclear magnetic resonance (<sup>1</sup>H NMR), carbon nuclear magnetic resonance (<sup>13</sup>C NMR), and mass spectral data. All the synthesized compounds were screened for their antibacterial activities.

## 1 | INTRODUCTION

Chromones (4*H*-1-benzopyran-4-one, 4*H*-chromen-4-one) are the heterocyclic compound widely distributed in nature.<sup>[1]</sup> Chromone-containing compounds display various pharmacological properties such as antifungal,<sup>[2]</sup> antimalarial,<sup>[3]</sup> anticancer,<sup>[4]</sup> antibacterial,<sup>[5]</sup> and are also well known as an antidiabetic and cardiovascular agents.<sup>[6,7]</sup> Pyrazole-containing compounds show antiangiogenic,<sup>[8]</sup> antimalarial,<sup>[9]</sup> antifungal,<sup>[10]</sup> antitubercular,<sup>[11]</sup> antimicrobial,<sup>[11]</sup> and anticancer<sup>[12]</sup> activities.

Currently, there are more than 200 pharmaceutical drugs available in market containing fluorine atom. Fluorine and fluorine-containing substituent can impart many effects on properties of organic compounds.<sup>[13,14]</sup> Fluorine-containing compounds exhibit fungicidal,<sup>[15]</sup> herbicidal,<sup>[16]</sup> antiviral,<sup>[17]</sup> antipyretic,<sup>[18]</sup> and analgesic<sup>[19]</sup> activities.

Considering the biological importance of chromone, pyrazole, and fluorine nucleus, we have reported the synthesis, characterization, and antibacterial screening of

novel 1-benzyl-3-(4-fluorophenyl)-1*H*-pyrazole-4-carbaldehydes **3a** to **3e**, (*E*)-3-(1-benzyl-3-(4-fluorophenyl)-1*H*-pyrazol-4-yl)-1-(4-fluoro-2-hydroxyphenyl)prop-2-en-1-ones **5a** to **5e** and 2-(1-benzyl-3-(4-fluorophenyl)-1*H*-pyrazol-4-yl)-7-fluoro-4*H*-chromen-4-one derivatives **6a** to **6e**.

## 2 | RESULT AND DISCUSSION

1-Benzyl-3-(4-fluorophenyl)-1*H*-pyrazole-4-carbaldehydes **3a** to **3e** were synthesized via the Vilsmeier-Haack reaction of the appropriate 1-benzyl-2-(1-(4-fluorophenyl)ethylidene)hydrazines, derived from 4-fluoroacetophenone **1** with substituted 2-benzylhydrazines **2a** to **2e**.<sup>[20]</sup> (*E*)-3-(1-Benzyl-3-(4-fluorophenyl)-1*H*-pyrazol-4-yl)-1-(4-fluoro-2-hydroxyphenyl)prop-2-en-1-ones **5a** to **5e** were synthesized from the reaction of 1-benzyl-3-(4-fluorophenyl)-1*H*-pyrazole-4-carbaldehydes **3a** to **3e** with 1-(4-fluoro-2-hydroxyphenyl)ethanone **4** in 10% aq. KOH. The synthesis of 2-(1-benzyl-3-(4-fluorophenyl)-1*H*-pyrazol-4-yl)-

7-fluoro-4*H*-chromen-4-ones **6a** to **6e** was achieved by reaction of (*E*)-3-(1-benzyl-3-(4-fluorophenyl)-1*H*-pyrazol-4-yl)-1-(4-fluoro-2-hydroxyphenyl)prop-2-en-1-ones **5a** to **5e** with dimethyl sulfoxide (DMSO)/I<sub>2</sub> (Scheme 1 and Section 3).

Structures of all the synthesized compounds were confirmed by using infrared (IR), proton nuclear magnetic resonance (<sup>1</sup>H NMR), carbon nuclear magnetic resonance (<sup>13</sup>C NMR), and liquid chromatography-mass spectrometry (LC-MS) spectroscopic techniques.

## 2.1 | Antibacterial activities

All the synthesized compounds were screened for their antibacterial activities. The bacterial strains *Staphylococcus aureus*, *Bacillus subtilis*, *Escherichia coli*, and *Pseudomonas aeruginosa* were used. The zone of inhibition in millimeter was determined by the well diffusion method at 1 mg/mL of concentration, and Ampicillin was used as reference drugs. The results of antibacterial activity are shown in Table 1.

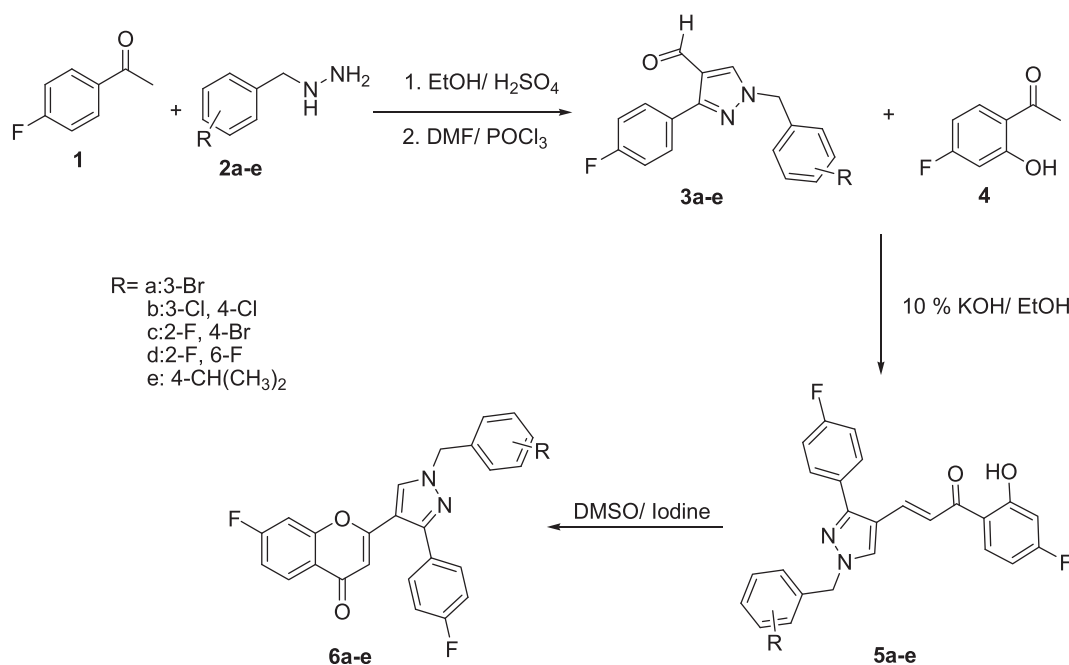
The results given in Table 1 indicated that compounds **3c**, **3d**, **3d**, **6a**, **6b**, **6c**, and **6d** exhibited good antibacterial activity against *E. coli* bacterial strain. Compounds **3c** to **3e**, **5e**, and **6a** to **6e** exhibited good antibacterial activity against *P. aeruginosa*. While compounds **3e** and **6a** to **6d** exhibited good antibacterial activity against *B. subtilis* and *S. aureus* compared with the standard Ampicillin. While other compounds were found to be less to moderately active against all bacterial strains.

## 3 | EXPERIMENTAL

The melting points were measured on a DBK melting point apparatus and are uncorrected. IR spectra were recorded on Shimadzu IR Affinity 1S (attenuated total reflection [ATR]) Fourier transform infrared (FTIR) spectrophotometer. <sup>1</sup>H NMR (400 MHz) and <sup>13</sup>C NMR (100 MHz) spectra were recorded on Varian 400 spectrophotometer using tetramethylsilane (TMS) as an internal standard and DMSO-*d*<sub>6</sub> as solvent, and chemical shifts were expressed as δ parts per million units. Mass spectra were obtained on Shimadzu (LC-MS) mass spectrometer.

### 3.1 | General procedure for synthesis of 1-benzyl-3-(4-fluorophenyl)-1*H*-pyrazole-4-carbaldehydes (**3a-e**)

A mixture of substituted 1-benzylhydrazine (0.01 mol) and catalytic amount of concentrated H<sub>2</sub>SO<sub>4</sub> was added to a solution of 1-(4-fluorophenyl)ethanone (0.01 mol) in 20 mL of ethanol. The mixture was refluxed for 1 hour, and the 1-benzyl-2-(1-(4-fluorophenyl)ethylidene)hydrazine formed was filtered and dried. A mixture of dimethylformamide (DMF) and phosphoryl chloride (POCl<sub>3</sub>) was cooled with constant stirring at 0°C. A solution of 1-benzyl-2-(1-(4-fluorophenyl)ethylidene)hydrazine in DMF was added dropwise to the reaction mixture and then heated at 70 to 80°C for 5 hours. After completion of reaction, contents were cooled to room temperature and poured onto ice-cold water, and then it was made alkaline with saturated K<sub>2</sub>CO<sub>3</sub> solution. The



**SCHEME 1** Synthetic approach to the title compounds

**TABLE 1** Antibacterial activities of the synthesized compounds (zone of inhibition in millimeter)

Compound	<i>Escherichia coli</i>	<i>Pseudomonas aeruginosa</i>	<i>Bacillus subtilis</i>	<i>Staphylococcus aureus</i>
3a	8	10	10	12
3b	9	10	10	11
3c	14	13	12	12
3d	15	14	12	13
3e	16	15	14	17
5a	9	11	12	11
5b	9	10	10	12
5c	8	10	10	9
5d	10	11	10	9
5e	12	14	13	12
6a	16	15	14	16
6b	14	15	14	16
6c	16	14	16	17
6d	14	15	15	16
6e	12	14	9	10
Ampicillin	16	15	17	18

precipitate formed was crystallized from ethanol to get pure 1-benzyl-3-(4-fluorophenyl)-1H-pyrazole-4-carbaldehydes **3a-e**.

### 3.2 | 1-(3-Bromobenzyl)-3-(4-fluorophenyl)-1H-pyrazole-4-carbaldehyde (3a)

Yield: 71%, White solid, mp 58–60°C. IR ( $\nu_{\max}/\text{cm}^{-1}$ ): 3112 (=C–H), 2820 (aldehyde C–H), 1674 (C=O), 1655 (C=N);  $^1\text{H}$  NMR spectrum (400 MHz, DMSO- $d_6$ ):  $\delta$  = 5.45 (s, 2H, –CH<sub>2</sub>), 7.25–7.35 (m, 4H, Ar–H), 7.52–7.60 (m, 2H, Ar–H), 7.86–7.90 (m, 2H, Ar–H), 8.72 (s, 1H, pyrazolyl-H), 9.86 (s, 1H, –CHO);  $^{13}\text{C}$  NMR (100 MHz, DMSO- $d_6$ ):  $\delta$  = 53.92, 115.17, 115.38, 120.48, 127.96, 128.36, 130.10, 130.52, 130.61, 130.85, 131.24, 137.09, 138.35, 150.91, 161.21, 163.66, 184.33; MS (LC-MS):  $m/z$  358.95 (M + H)<sup>+</sup>.

### 3.3 | 1-(3,4-Dichlorobenzyl)-3-(4-fluorophenyl)-1H-pyrazole-4-carbaldehyde (3b)

Yield: 65%, White solid. mp 190–192°C; IR ( $\nu_{\max}/\text{cm}^{-1}$ ): 3112 (=C–H), 2820 (aldehyde C–H), 1674 (C=O), 1655 (C=N);  $^1\text{H}$  NMR spectrum (400 MHz, DMSO- $d_6$ ):  $\delta$  = 5.46 (s, 2H, –CH<sub>2</sub>), 7.26–7.36 (m, 3H, Ar–H), 7.64–7.68 (m, 2H, Ar–H), 7.86–7.89 (m, 2H, Ar–H), 8.72 (s, 1H, pyrazolyl-H), 9.86 (s, 1H, –CHO); MS (LC-MS):  $m/z$  349 (M + H)<sup>+</sup>.

### 3.4 | 1-(4-Bromo-2-fluorobenzyl)-3-(4-fluorophenyl)-1H-pyrazole-4-carbaldehyde (3c)

Yield: 69%; White solid; mp 64–66°C; IR ( $\nu_{\max}/\text{cm}^{-1}$ ): 3113 (=C–H), 2822 (aldehyde C–H), 1673 (C=O), 1656 (C=N);  $^1\text{H}$  NMR (400 MHz, DMSO- $d_6$ ):  $\delta$  = 5.49 (s, 2H, –CH<sub>2</sub>), 7.29 (t, 2H,  $J$  = 8.8 Hz, Ar–H), 7.35 (t, 1H,  $J$  = 8 Hz, Ar–H), 7.45 (d, 1H,  $J$  = 8.4 Hz, Ar–H), 7.61 (d, 1H,  $J$  = 8.4 Hz, Ar–H), 7.86 (dd, 2H,  $J$  = 8 and 6 Hz, Ar–H), 8.67 (s, 1H, pyrazolyl-H), 9.86 (s, 1H, –CHO);  $^{13}\text{C}$  NMR (100 MHz, DMSO- $d_6$ ):  $\delta$  = 49.66, 115.40, 115.62, 116.20, 116.42, 119.34, 119.58, 121.08, 121.23, 123.26, 123.35, 127.44, 127.85, 128.02, 128.05, 130.53, 130.61, 131.57, 131.60, 131.77, 131.86, 134.57, 152.82, 159.01, 161.53, 161.97, 164.45, 184.20; MS (LC-MS):  $m/z$  376.95 (M + H)<sup>+</sup>.

### 3.5 | 1-(2,6-Difluorobenzyl)-3-(4-fluorophenyl)-1H-pyrazole-4-carbaldehyde (3d)

Yield: 61%; White solid; mp 68–70°C; IR ( $\nu_{\max}/\text{cm}^{-1}$ ): 3112 (=C–H), 2824 (aldehyde C–H), 1677 (C=O), 1654 (C=N);  $^1\text{H}$  NMR (400 MHz, DMSO- $d_6$ ):  $\delta$  = 5.52 (s, 2H, –CH<sub>2</sub>), 7.18 (t, 2H,  $J$  = 8 Hz, Ar–H), 7.26 (t, 2H,  $J$  = 8.8 Hz, Ar–H), 7.50 (t, 1H,  $J$  = 8 Hz, Ar–H), 7.83 (m, 2H, Ar–H), 8.66 (s, 1H, pyrazolyl-H), 9.85 (s, 1H, –CHO);  $^{13}\text{C}$  NMR (100 MHz, DMSO- $d_6$ ):  $\delta$  = 43.32, 111.38, 111.57, 111.75, 112.00, 115.17, 115.38, 120.24,

127.96, 130.49, 130.57, 131.43, 131.53, 131.64, 138.50, 150.59, 159.75, 161.20, 162.15, 163.64, 184.38; MS (LC-MS):  $m/z$  317.05 (M + H)<sup>+</sup>.

### 3.6 | 1-(4-Isopropylbenzyl)-3-(4-fluorophenyl)-1H-pyrazole-4-carbaldehyde (3e)

Yield: 64%; White solid; mp 52–54°C; IR ( $\nu_{\max}/\text{cm}^{-1}$ ): 3111 (C–H), 2821 (aldehyde C–H), 1672 (C=O), 1656 (C=N); <sup>1</sup>H NMR (400 MHz, DMSO-*d*<sub>6</sub>):  $\delta$  = 1.1 (d, 6H, –CH<sub>3</sub>), 2.8 (m, 1H, –CH), 5.4 (s, 2H, –CH<sub>2</sub>), 7.23–7.30 (m, 6H, Ar–H), 7.86–7.90 (m, 2H, Ar–H), 7.45 (d, 1H,  $J$  = 8.4 Hz, Ar–H), 7.61 (d, 1H,  $J$  = 8.4 Hz, Ar–H), 7.86 (dd, 2H,  $J$  = 8 and 6 Hz, Ar–H), 8.67 (s, 1H, pyrazolyl-H), 9.85 (s, 1H, –CHO); MS (LC-MS):  $m/z$  323.05 (M + H)<sup>+</sup>.

### 3.7 | General procedure for synthesis of (E)-3-(1-Benzyl-3-(4-fluorophenyl)-1H-pyrazol-4-yl)-1-(4-fluoro-2-hydroxyphenyl)prop-2-en-1-ones (5a-e)

A mixture of 1-benzyl-3-(4-fluorophenyl)-1H-pyrazole-4-carbaldehydes **3a** to **3e** (0.005 mol) with 1-(4-fluoro-2-hydroxyphenyl)ethanone **4** (0.005 mol) was stirred in ethanolic KOH (10%) for 16 hours at room temperature. After completion of reaction, contents were poured onto ice-cold water and then acidified with concentrated hydrochloric acid (HCl). The precipitate formed was filtered off, washed with water, and crystallized from ethanol to get the pure product **5a-e**.

### 3.8 | (E)-3-(1-(3-Bromobenzyl)-3-(4-fluorophenyl)-1H-pyrazol-4-yl)-1-(4-fluoro-2-hydroxyphenyl)prop-2-en-1-one (5a)

Yield: 74%; Yellow solid; mp 80–82°C; IR ( $\nu_{\max}/\text{cm}^{-1}$ ): 1637 (C=O), 1590 (C=N), 1569 (C=C); <sup>1</sup>H NMR (400 MHz, DMSO-*d*<sub>6</sub>):  $\delta$  = 5.46 (s, 2H, –CH<sub>2</sub>), 6.82–6.89 (m, 2H, Ar–H), 7.33–7.39 (m, 4H, Ar–H), 7.53–7.61 (m, 4H, Ar–H), 7.70–7.81 (AB quartet, 2H,  $J$  = 15.6 Hz, =C–H), 8.21 (dd, 1H,  $J$  = 8 and 6.8 Hz, Ar–H), 8.75 (s, 1H, pyrazolyl-H), 13.09 (s, 1H, –OH); <sup>13</sup>C NMR (100 MHz, DMSO-*d*<sub>6</sub>):  $\delta$  = 54.73, 104.12, 104.36, 106.79, 107.02, 115.65, 115.86, 117.58, 119.62, 121.84, 126.97, 128.52, 130.36, 130.44, 130.63, 130.90, 132.31, 133.04, 133.16, 135.87, 139.10, 151.29, 161.01, 163.46, 164.46, 164.60, 165.14, 167.67, 192.09; MS (LC-MS):  $m/z$  495.10 (M + H)<sup>+</sup>.

### 3.9 | (E)-3-(1-(3,4-Dichlorobenzyl)-3-(4-fluorophenyl)-1H-pyrazol-4-yl)-1-(4-fluoro-2-hydroxyphenyl)prop-2-en-1-one (5b)

Yield: 72%; Yellow solid; mp 158–160°C; IR ( $\nu_{\max}/\text{cm}^{-1}$ ): 1641 (C=O), 1594 (C=N), 1524 (C=C); <sup>1</sup>H NMR (400 MHz, DMSO-*d*<sub>6</sub>):  $\delta$  = 5.47 (s, 2H, –CH<sub>2</sub>), 6.81–6.87 (m, 2H, Ar–H), 7.33–7.44 (m, 3H, Ar–H), 7.59 (dd, 2H,  $J$  = 8 and 6 Hz, Ar–H), 7.66–7.68 (m, 2H, Ar–H), 7.69–7.81 (AB quartet, 2H,  $J$  = 15.6 Hz, =CH), 8.19 (t, 1H,  $J$  = 8 Hz, Ar–H), 8.73 (s, 1H, pyrazolyl-H), 13.07 (s, 1H, –OH); <sup>13</sup>C NMR (100 MHz, DMSO-*d*<sub>6</sub>):  $\delta$  = 55.34, 104.98, 105.22, 106.86, 107.08, 115.76, 115.97, 116.83, 118.83, 127.23, 128.22, 129.90, 129.97, 130.48, 130.56, 131.06, 131.49, 131.60, 132.92, 133.22, 135.43, 136.10, 152.44, 166.03, 166.18, 192.06; MS (LC-MS):  $m/z$  485.05 (M + H)<sup>+</sup>.

### 3.10 | (E)-3-(1-(4-Bromo-2-fluorobenzyl)-3-(4-fluorophenyl)-1H-pyrazol-4-yl)-1-(4-fluoro-2-hydroxyphenyl)prop-2-en-1-one (5c)

Yield: 71%; Yellow solid; mp 118–120°C; IR ( $\nu_{\max}/\text{cm}^{-1}$ ): 1638 (C=O), 1587 (C=N), 1574 (C=C); <sup>1</sup>H NMR (400 MHz, DMSO-*d*<sub>6</sub>):  $\delta$  = 5.48 (s, 2H, –CH<sub>2</sub>), 6.81–6.89 (m, 2H, Ar–H), 7.32–7.40 (m, 3H, Ar–H), 7.48 (dd, 1H,  $J$  = 8 and 2 Hz, Ar–H), 7.57 (dd, 2H,  $J$  = 8 and 6 Hz, Ar–H), 7.63 (dd, 1H,  $J$  = 8 and 2 Hz, Ar–H), 7.69–7.82 (AB quartet, 2H,  $J$  = 15.6 Hz, =CH), 8.23 (dd, 1H,  $J$  = 8 and 6.8 Hz, Ar–H), 8.72 (s, 1H, pyrazolyl-H), 13.10 (s, 1H, –OH); <sup>13</sup>C NMR (100 MHz, DMSO-*d*<sub>6</sub>):  $\delta$  = 49.07, 104.13, 104.37, 106.82, 107.03, 115.66, 115.74, 115.87, 117.60, 118.92, 119.16, 119.67, 121.97, 122.07, 122.64, 122.79, 128.00, 128.46, 130.39, 130.47, 132.29, 132.38, 132.43, 133.12, 133.23, 135.80, 151.35, 158.82, 161.02, 161.32, 163.47, 164.47, 164.60, 165.16, 167.68, 192.13; MS (LC-MS):  $m/z$  515 (M + H)<sup>+</sup>.

### 3.11 | (E)-3-(1-(2,6-Difluorobenzyl)-3-(4-fluorophenyl)-1H-pyrazol-4-yl)-1-(4-fluoro-2-hydroxyphenyl)prop-2-en-1-one (5d)

Yield: 74%; Yellow solid; mp 184–186°C; IR ( $\nu_{\max}/\text{cm}^{-1}$ ): 1640 (C=O), 1596 (C=N), 1568 (C=C); <sup>1</sup>H NMR (400 MHz, DMSO-*d*<sub>6</sub>):  $\delta$  = 5.49 (s, 2H, –CH<sub>2</sub>), 6.81–6.89 (m, 2H, Ar–H), 7.17 (t, 2H,  $J$  = 8 Hz, Ar–H), 7.33 (t, 2H,  $J$  = 8 Hz, Ar–H), 7.48–7.56 (m, 3H, Ar–H), 7.7 (d, 1H,  $J$  = 15.8 Hz, =C–H), 7.83 (d, 1H,  $J$  = 15.6 Hz, =C–H), 8.26 (dd, 1H,  $J$  = 8 and 6.8 Hz, Ar–H), 8.74 (s, 1H, pyrazolyl-H), 13.14 (s, 1H, –OH); <sup>13</sup>C NMR (100 MHz, DMSO-*d*<sub>6</sub>):  $\delta$  = 43.47, 104.09, 104.32, 106.73, 106.95, 111.37, 111.56,



111.75, 111.93, 111.99, 115.59, 115.65, 115.81, 117.45, 119.49, 128.45, 128.48, 130.37, 130.45, 131.37, 131.47, 131.57, 132.10, 133.17, 133.28, 135.82, 151.32, 159.71, 159.79, 161.02, 162.20, 162.27, 163.47, 164.63, 164.77, 165.19, 167.71, 193.20; MS (LC-MS):  $m/z$  453.15 (M + H)<sup>+</sup>.

### 3.12 | (E)-3-(1-(4-Isopropylbenzyl)-3-(4-fluorophenyl)-1H-pyrazol-4-yl)-1-(4-fluoro-2-hydroxyphenyl)prop-2-en-1-one (5e)

Yield: 77%; Yellow solid; mp 130-132°C; IR ( $\nu_{\max}/\text{cm}^{-1}$ ): 1635 (C=O), 1595 (C=N), 1567 (C=C); <sup>1</sup>H NMR (400 MHz, DMSO-*d*<sub>6</sub>):  $\delta$  = 1.17 (d, 6H, CH<sub>3</sub>), 2.87 (m, 1H, —C—H), 5.39 (s, 2H, —CH<sub>2</sub>), 6.82-6.89 (m, 2H, Ar—H), 7.25-7.37 (m, 6H, Ar—H), 7.57-7.61 (m, 2H, Ar—H), 7.70-7.81 (AB quartet, 2H,  $J$  = 15.8 Hz, =C—H), 8.23 (dd, 1H,  $J$  = 8 and 6.8 Hz, Ar—H), 8.74 (s, 1H, pyrazolyl-H), 13.13 (s, 1H, —OH); <sup>13</sup>C NMR (100 MHz, DMSO-*d*<sub>6</sub>):  $\delta$  = 23.75, 33.12, 55.41, 104.13, 104.36, 106.79, 107.01, 115.63, 115.75, 115.84, 117.56, 119.36, 126.06, 127.92, 128.63, 130.35, 130.43, 132.01, 133.06, 133.17, 133.90, 136.05, 148.22, 151.04, 160.98, 163.42, 164.49, 164.63, 165.14, 167.67, 192.13; MS (LC-MS):  $m/z$  459.15 (M + H)<sup>+</sup>.

### 3.13 | General procedure for synthesis of 2-(1-benzyl-3-(4-fluorophenyl)-1H-pyrazol-4-yl)-7-fluoro-4H-chromen-4-ones (6a-e)

Compound **5a** to **5e** (0.002 mol) was dissolved in 15-mL DMSO. To this solution, catalytic amount of iodine was added. The reaction mixture was heated to 140°C for 2 hours. After completion of reaction (checked by thin-layer chromatography [TLC]), content were cooled and poured over crushed ice. The product obtained was filtered, washed with cold water and 10% sodium thiosulphate solution followed by cold water, and crystallized from ethanol to get the pure product **6a** to **6e**.

### 3.14 | 2-(1-(3-Bromobenzyl)-3-(4-fluorophenyl)-1H-pyrazol-4-yl)-7-fluoro-4H-chromen-4-one (6a)

Yield: 77%; White solid; mp 200-202°C; IR ( $\nu_{\max}/\text{cm}^{-1}$ ): 3112 (=C—H), 1641 (C=O), 1622 (C=N), 1597 (C=C); <sup>1</sup>H NMR (400 MHz, DMSO-*d*<sub>6</sub>):  $\delta$  = 5.46 (s, 2H, —CH<sub>2</sub>), 6.32 (s, 1H), 7.19 (dd, 1H,  $J$  = 8 and 2 Hz, Ar—H), 7.30-7.62 (m, 9H, Ar—H), 8.19 (dd, 1H,  $J$  = 8 and 6.8 Hz, Ar—H), 8.71 (s, 1H, pyrazolyl-H); <sup>13</sup>C NMR (100 MHz, DMSO-*d*<sub>6</sub>):  $\delta$  = 54.87, 104.56, 104.82, 107.24, 110.95, 112.30, 113.82, 115.32, 115.54, 116.69, 119.55, 120.72, 122.07, 127.24, 127.74, 127.84, 129.20, 130.97, 131.12, 133.66,

139.25, 149.39, 158.12, 158.50, 158.89, 159.28, 159.63, 163.82, 175.80; MS (LC-MS):  $m/z$  495.10 (M + H)<sup>+</sup>.

### 3.15 | 2-(1-(3,4-Dichlorobenzyl)-3-(4-fluorophenyl)-1H-pyrazol-4-yl)-7-fluoro-4H-chromen-4-one (6b)

Yield: 65%; White solid; mp 148-150°C; IR ( $\nu_{\max}/\text{cm}^{-1}$ ): 3059 (=C—H), 1645 (C=O), 1620 (C=N), 1598 (C=C); <sup>1</sup>H NMR (400 MHz, DMSO-*d*<sub>6</sub>):  $\delta$  = 5.47 (s, 2H, —CH<sub>2</sub>), 6.32 (s, 1H), 7.19 (d, 1H,  $J$  = 8 Hz, Ar—H), 7.27-7.70 (m, 8H, Ar—H), 8.19 (t, 1H,  $J$  = 8 Hz, Ar—H), 8.70 (s, 1H, pyrazolyl-H); <sup>13</sup>C NMR (100 MHz, DMSO-*d*<sub>6</sub>):  $\delta$  = 54.13, 104.83, 107.23, 110.87, 113.74, 115.32, 115.54, 116.61, 120.59, 127.80, 128.53, 129.00, 130.25, 131.06, 131.39, 133.71, 137.48, 157.96, 158.34, 158.73, 159.10, 175.70; MS (LC-MS):  $m/z$  483.10 (M + H)<sup>+</sup>.

### 3.16 | 2-(1-(4-Bromo-2-fluorobenzyl)-3-(4-fluorophenyl)-1H-pyrazol-4-yl)-7-fluoro-4H-chromen-4-one (6c)

Yield: 69%; White solid; mp 220-222°C; IR ( $\nu_{\max}/\text{cm}^{-1}$ ): 3065 (=C—H), 1643 (C=O), 1620 (C=N), 1594 (C=C); <sup>1</sup>H NMR (400 MHz, DMSO-*d*<sub>6</sub>):  $\delta$  = 5.49 (s, 2H, —CH<sub>2</sub>), 6.31 (s, 1H), 7.19 (dd, 1H,  $J$  = 8 and 6.8 Hz, Ar—H), 7.25-7.78 (m, 8H, Ar—H), 8.05 (dd, 1H,  $J$  = 8 and 6.8 Hz, Ar—H), 8.67 (s, 1H, pyrazolyl-H); <sup>13</sup>C NMR (100 MHz, DMSO-*d*<sub>6</sub>):  $\delta$  = 48.46, 104.43, 104.69, 107.01, 111.87, 113.66, 113.89, 115.14, 115.35, 118.85, 119.09, 120.41, 121.87, 121.96, 122.62, 122.77, 127.48, 127.59, 127.96, 128.77, 130.43, 130.83, 130.91, 132.24, 133.50, 149.04, 156.26, 156.40, 158.73, 159.23, 161.01, 161.24, 163.46, 165.97, 175.44; MS (LC-MS):  $m/z$  513.10 (M + H)<sup>+</sup>.

### 3.17 | 2-(1-(2,6-Difluorobenzyl)-3-(4-fluorophenyl)-1H-pyrazol-4-yl)-7-fluoro-4H-chromen-4-one (6d)

Yield: 72%; White solid; mp 140-142°C; IR ( $\nu_{\max}/\text{cm}^{-1}$ ): 3110 (=C—H), 1648 (C=O), 1622 (C=N), 1594 (C=C); <sup>1</sup>H NMR (400 MHz, DMSO-*d*<sub>6</sub>):  $\delta$  = 5.51 s (2H, —CH<sub>2</sub>), 6.31 (s, 1H), 7.16-7.57 (m, 9H, Ar—H), 8.04 (dd, 1H,  $J$  = 8 and 6.8 Hz, Ar—H), 8.66 (s, 1H, pyrazolyl-H); <sup>13</sup>C NMR (100 MHz, DMSO-*d*<sub>6</sub>):  $\delta$  = 43.31, 104.41, 104.66, 106.95, 111.43, 111.70, 111.75, 111.93, 113.58, 113.80, 115.09, 115.30, 120.38, 127.43, 127.54, 128.80, 130.81, 130.89, 131.44, 131.54, 133.25, 148.96, 156.23, 156.37, 159.17, 159.74, 161.00, 162.16, 163.44, 165.94, 175.41; MS (LC-MS):  $m/z$  451.05 (M + H)<sup>+</sup>.

### 3.18 | 2-(1-(4-Isopropylbenzyl)-3-(4-fluorophenyl)-1H-pyrazol-4-yl)-7-fluoro-4H-chromen-4-one (6e)

Yield: 67%; White solid; mp 280-282°C; IR ( $\nu_{\max}/\text{cm}^{-1}$ ): 3066 (=C-H), 1644 (C=O), 1620 (C=N), 1592(C=C);  $^1\text{H}$  NMR (400 MHz, DMSO- $d_6$ ):  $\delta$  = 1.18 (d, 6H, -CH<sub>3</sub>), 2.87 (m, 1H, -C-H), 5.39 (s, 2H, -CH<sub>2</sub>), 6.30 (s, 1H), 7.18-7.36 (m, 8H, Ar-H), 7.58-7.62 (m, 2H, Ar-H), 8.05 (dd, 1H,  $J$  = 8 and 6.8 Hz, Ar-H), 8.68 (s, 1H, pyrazolyl-H);  $^{13}\text{C}$  NMR (100 MHz, DMSO- $d_6$ ):  $\delta$  = 23.76, 33.12, 55.20, 104.44, 104.70, 106.90, 111.81, 113.67, 113.90, 115.16, 115.37, 120.44, 126.57, 127.52, 127.98, 128.98, 130.85, 130.93, 133.17, 133.83, 148.22, 148.76, 156.30, 156.43, 159.46, 161.00, 163.44, 165.99, 175.46; MS (LC-MS):  $m/z$  457.15 (M + H)<sup>+</sup>.

## 4 | CONCLUSION

In conclusion, we have synthesized a series of novel 2-(1-benzyl-3-(4-fluorophenyl)-1H-pyrazol-4-yl)-7-fluoro-4H-chromen-4-ones **6a** to **6e** from 1-benzyl-3-(4-fluorophenyl)-1H-pyrazole-4-carbaldehydes **3a** to **3e**. All synthesized compounds are characterized by using spectral methods and screened for their antibacterial activities.

## ORCID

Hemantkumar N. Akolkar  <https://orcid.org/0000-0003-0882-1324>

## REFERENCES

- [1] J. Reis, A. Gaspar, N. Milhazes, F. M. Borges, *J. Med. Chem.* **2017**, 60(19), 7941.
- [2] O. Prakash, R. Kumar, V. Parkash, *Eur. J. Med. Chem.* **2008**, 43, 435.
- [3] P. Lerdsiriruk, C. Maicheen, J. Ungwitayatorn, *Bioorg. Chem.* **2014**, 57, 142.
- [4] K. N. Gopalan, A. Joseph, S. Moorkoth, *Int. J. Pharm. Biosci. Technol.* **2013**, 1, 130.
- [5] M. Momin, D. Ramjugernath, H. Chenia, N. A. Koorbanally, *J. Chem.* **2013**, 13, 50.

- [6] O. Bozdog-Dundar, M. Ceylan-Unlusoy, E. J. Verspohl, R. Ertan, *Arzneim. Forsch.* **2007**, 57, 532.
- [7] M. Ceylan-Ünlüsoy, E. J. Verspohl, R. Ertan, *J. Enzyme. Inhib. Med. Chem.* **2010**, 25, 784.
- [8] M. S. Christodoulou, S. Liekens, K. M. Kasiotis, S. A. Haroutounian, *Bioorg. Med. Chem.* **2010**, 18, 4338.
- [9] A. A. Bekhit, A. Hymete, H. Asfaw, A. A. Bekhit, *Arch. Pharm. Chem. Life Sci.* **2012**, 345, 147.
- [10] C. B. Vicentini, C. Romagnoli, E. Andreotti, D. Mares, *J. Agric. Food Chem.* **2007**, 55, 10331.
- [11] R. B. Pathak, P. T. Chovatia, H. H. Parekh, *Bioorg. Med. Chem. Lett.* **2012**, 22, 5129.
- [12] I. Bouabdallah, L. A. M'Barek, A. Zyad, A. Ramdani, I. Zidane, A. Melhaoui, *Nat. Pro. Res.* **2006**, 20(11), 1024.
- [13] Y. Zhou, J. Wang, Z. Gu, S. Wang, W. Zhu, J. L. Acen, V. A. Soloshonok, K. Izawa, H. Liu, *Chem. Rev.* **2016**, 116(2), 422.
- [14] J. Wang, M. Sánchez-Roselló, J. L. Aceña, C. Pozo, A. E. Sorochinsky, S. Fustero, V. A. Soloshonok, H. Liu, *Chem. Rev.* **2014**, 114(4), 2432.
- [15] A. Guan, C. Liu, G. Huang, H. Li, S. Hao, Y. Xu, Y. Xie, Z. Li, *J. Fluorine Chem.* **2014**, 160, 82.
- [16] G. Li, X. Qian, J. Cui, Q. Huang, D. Cui, R. Zhang, F. Liu, *J. Fluorine Chem.* **2006**, 127, 182.
- [17] H. Chen, S. Q. Huang, J. Y. Xie, *J. Fluorine Chem.* **2006**, 127, 1130.
- [18] S. G. Kucukguzel, S. Rollas, H. Erdeniz, A. C. Kiraz, M. Ekinci, A. Vidin, *Eur. J. Med. Chem.* **2000**, 35, 761.
- [19] T. P. Gregory, C. D. Darlene, M. S. David, *Pestic. Biochem. Phys.* **1998**, 60, 177.
- [20] M. A. Kira, M. O. Abdel-Rahman, K. Z. Gadalla, *Tetrahedron Lett.* **1969**, 10, 109.

## SUPPORTING INFORMATION

Additional supporting information may be found online in the Supporting Information section at the end of this article.

**How to cite this article:** Hon KS, Akolkar HN, Karale BK. Synthesis and characterization of novel 2-(1-benzyl-3-[4-fluorophenyl]-1H-pyrazol-4-yl)-7-fluoro-4H-chromen-4-one derivatives. *J Heterocyclic Chem.* 2020;1-6. <https://doi.org/10.1002/jhet.3894>

# Microwave Assisted Synthesis and Antibacterial Activity of New 1,3,4-Thiadiazoles and 1,2,4-Triazoles Derived from 2-{2-[2-(4-Fluorophenyl)-4-methylthiazol-5-yl]-1*H*-benzo[*d*]imidazol-1-yl}acetohydrazide

N. R. Darekar<sup>a,b</sup>, B. K. Karale<sup>a</sup>, H. N. Akolkar<sup>a</sup>, and A. S. Burungale<sup>b,\*</sup>

<sup>a</sup> P.G. and Research, Department of Chemistry, Rayat Shikshan Sanstha's Radhabai Kale Mahila Mahavidyalaya, Maharashtra, Ahmednagar, 414001 India

<sup>b</sup> P.G. and Research, Department of Chemistry, Rayat Shikshan Sanstha's S. M. Joshi College, Hadapsar, Maharashtra, Pune, 411028 India

\*e-mail: hemantakolkar@gmail.com

Received July 7, 2020; revised August 18, 2020; accepted August 31, 2020

**Abstract**—A series of novel derivatives of 1-(2-{2-[2-(4-fluorophenyl)-4-methylthiazol-5-yl]-1*H*-benzo[*d*]imidazol-1-yl}acetyl)-4-phenylthiosemicarbazide, 5-({2-[2-(4-fluorophenyl)-4-methylthiazol-5-yl]-1*H*-benzo[*d*]imidazol-1-yl}methyl)-4-phenyl-4*H*-1,2,4-triazole-3-thiol and 5-({2-[2-(4-fluorophenyl)-4-methylthiazol-5-yl]-1*H*-benzo[*d*]imidazol-1-yl}methyl)-*N*-phenyl-1,3,4-thiadiazol-2-amine have been synthesized by the conventional method as well as using MW irradiation. All newly synthesized compounds have been tested for antibacterial activity. Several products have demonstrated moderate activity against gram positive and gram negative bacterial strains.

**Keywords:** 1,3,4-thiadiazole, 1,2,4-triazole, microwave irradiation, antibacterial activity

**DOI:** 10.1134/S1070363220090200

Antimycobacterial and antimicrobial activities have been well established and studied in depth for benzimidazole [1, 2], thiazole [3, 4], 1,3,4-thiadiazole [5–7], and 1,2,4-triazole [8, 9] derivatives.

Pharmacological importance associated with those compounds inspired us to synthesize novel benzimidazole and thiazole containing 1,3,4-thiadiazoles and 1,2,4-triazoles under conventional and MW irradiation. All newly synthesized compounds were evaluated for their antibacterial activity.

## RESULTS AND DISCUSSION

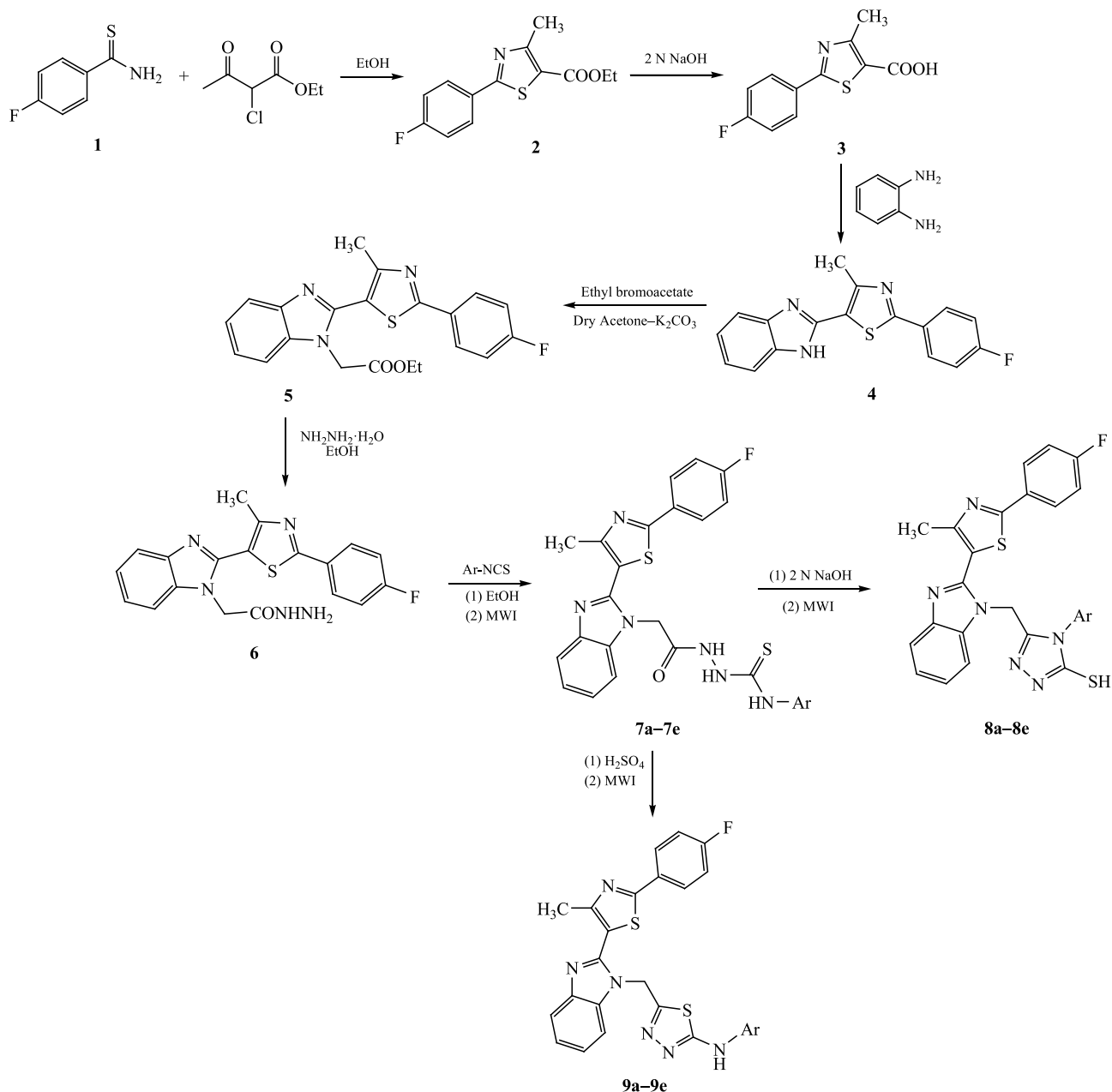
Synthesis of 2-{2-[2-(4-fluorophenyl)-4-methylthiazol-5-yl]-1*H*-benzo[*d*]imidazol-1-yl}acetohydrazide **6** was carried out by the known method (Scheme 1) [10–12].

A novel series of 1-(2-{2-[2-(4-fluorophenyl)-4-methylthiazol-5-yl]-1*H*-benzo[*d*]imidazol-1-yl}acetyl)-4-phenylthiosemicarbazide **7a–7e** was synthesized from the intermediate **6** and substituted aryl isothiocyanates by conventional method and under MW irradiation [10, 13]. Their molecular structures were supported by

IR, <sup>1</sup>H and <sup>13</sup>C NMR spectra. Reaction of compounds **7a–7e** in presence of NaOH under conventional conditions or MW irradiation gave 1,2,4-triazole derivatives **8a–8e** [10, 13]. In IR spectra of the products **8a–8e** no bands at ca. 3100 cm<sup>-1</sup> characteristic for –NH group were recorded. In <sup>1</sup>H NMR spectra of those compounds characteristic singlets of S–H were recorded at ca. 14.00 ppm. Similar reaction of compounds **7a–7e** in acidic media under conventional conditions or MW irradiation gave 1,3,4-thiadiazoles **9a–9e** [10, 13]. The NH group of compound **9a** was recorded in IR spectrum by the band at 3201 cm<sup>-1</sup> and in <sup>1</sup>H NMR spectrum by a singlet at 9.50 ppm.

The MW irradiation method proved to be more efficient in the synthesis of thiosemicarbazides **7a–7e**, 1,2,4-triazoles **8a–8e** and 1,3,4-thiadiazoles **9a–9e** derivatives than the conventional heating. It reduced the reaction time from hours to 5–10 min and increased the products yield up to 77–88% over the conventional method (60–74%) (Table 1).

**In vitro antibacterial activity.** All the synthesized compounds were tested against gram positive bacterial

**Scheme 1.** Synthesis of derivatives of thiosemicarbazide (**7a–7e**), 1,2,4-triazole (**8a–8e**), and 1,3,4-thiadiazole (**9a–9e**).

strains *Staphylococcus aureus* (NCIM 2079), *Bacillus subtilis* (NCIM 2063), and gram negative bacterial strains *Escherichia coli* (NCIM 2810), *Salmonella abony* (NCIM 2257). The zone of inhibition in mm was determined by the well diffusion method at concentration of 1 mg/mL, and Ciprofloxacin was used as the reference drug (Table 2). Compounds **7a**, **7d**, **7e**, **8d**, and **9e** demonstrated moderate activity against both gram positive and

gram negative bacteria while other compounds were characterized by low activity or none.

## EXPERIMENTAL

All organic solvents and reagents were acquired from commercial sources and used as received. The melting points were measured on a DBK melting point apparatus and are uncorrected. Microwave irradiation was carried out in a Raga's synthetic microwave oven.

**Table 1.** Synthesis data for the products

Comp. no.	Ar	Conventional method		Microwave method	
		time, min	yield, %	time, min	yield, %
7a	3-Chlorophenyl	90	74	7.0	88
7b	2-Chlorophenyl	90	70	6.5	85
7c	2,4-Dichlorophenyl	90	75	7.5	84
7d	4-Chlorophenyl	90	68	8.0	82
7e	3,4-Dichlorophenyl	90	72	9.5	87
8a	3-Chlorophenyl	150	65	8.5	80
8b	2-Chlorophenyl	150	68	9.0	78
8c	2,4-Dichlorophenyl	150	62	8.0	81
8d	4-Chlorophenyl	150	66	7.5	83
8e	3,4-Dichlorophenyl	150	70	8.5	79
9a	3-Chlorophenyl	240	68	9.0	77
9b	2-Chlorophenyl	240	62	9.5	85
9c	2,4-Dichlorophenyl	240	67	8.5	83
9d	4-Chlorophenyl	240	60	8.5	78
9e	3,4-Dichlorophenyl	240	66	8.0	81

**Table 2.** Antibacterial tests data for the synthesized compounds

Compound	Zone of inhibition, mm			
	<i>S. aureus</i>	<i>B. subtilis</i>	<i>E. coli</i>	<i>S. abony</i>
7a	16	15	14	17
7b	15	11	–	15
7c	15	14	–	13
7d	15	13	14	15
7e	16	16	17	16
8a	–	–	–	12
8b	–	–	11	10
8c	–	–	13	–
8d	15	17	13	18
8e	–	–	10	10
9a	11	12	12	16
9b	13	12	14	13
9c	12	12	14	–
9d	11	12	12	13
9e	13	15	14	16
Ciprofloxacin	23	28	26	40

FTIR spectra were recorded on a Shimadzu IR Affinity 1S (ATR) spectrophotometer.  $^1\text{H}$  and  $^{13}\text{C}$  NMR spectra were measured on a Bruker Advance 400 spectrometer using TMS as an internal standard and  $\text{DMSO-}d_6$  as a solvent. Mass spectra were measured on a Waters, Q-TOF micromass (ESI-MS) mass spectrometer.

**Synthesis of 1-(2-{2-[2-(4-fluorophenyl)-4-methylthiazol-5-yl]-1H-benzo[d]imidazol-1-yl}acetyl)-4-phenylthiosemicarbazide (7a–7e).** *Conventional method.* Equimolar amounts (0.01 mmol) of acid hydrazide **6** and aryl isothiocyanate **5** were dissolved

in 15 mL of ethanol and refluxed for 90 min. Reaction progress was monitored by TLC. Upon completion of the reaction the solid product was filtered off and crystallized from ethanol to give the corresponding pure compounds **7a–7e** (Table 1).

*Microwave method.* The mixture of equimolar amounts (0.01 mmol) of acid hydrazide **6** and aryl isothiocyanates **5** was dissolved in 15 mL of ethanol and subjected to MW irradiation for 5 to 10 min at 350 W. Reaction progress was monitored by TLC. Upon completion of the reaction the precipitated product was filtered off and crystallized



from ethanol to give the corresponding pure compounds **7a–7e** (Table 2).

**4-(3-Chlorophenyl)-1-(2-{2-[2-(4-fluorophenyl)-4-methylthiazol-5-yl]-1H-benzo[d]imidazol-1-yl}acetyl)thiosemicarbazide (7a).** White solid, mp 194–196°C. IR spectrum,  $\nu$ ,  $\text{cm}^{-1}$ : 3367 (N–H), 3277 (N–H), 3248 (N–H), 1672 (C=O), 1232 (C–F).  $^1\text{H}$  NMR spectrum,  $\delta$ , ppm: 10.51 s (1H, NH), 9.99 s (1H, NH), 9.80 s (1H, NH), 8.05 d. d (2H,  $J = 5.6$  and  $8.8$  Hz, ArH), 7.75 d (1H,  $J = 8$  Hz, ArH), 7.58 d (2H,  $J = 8$  Hz, ArH), 7.19–7.40 m (7H, ArH), 5.07 s (2H,  $\text{CH}_2$ ), 2.51 s (3H,  $\text{CH}_3$ ).  $^{13}\text{C}$  NMR spectrum,  $\delta_{\text{C}}$ , ppm: 166.22, 162.25, 155.01, 145.38, 142.48, 140.42, 135.87, 132.21, 129.76, 129.14, 128.64, 128.55, 123.14, 122.52, 119.29, 118.91, 116.50, 116.27, 110.98, 45.56, 16.47. LC-MS:  $m/z$ : 551.06  $[M + H]^+$ .

**4-(2-Chlorophenyl)-1-(2-{2-[2-(4-fluorophenyl)-4-methylthiazol-5-yl]-1H-benzo[d]imidazol-1-yl}acetyl)thiosemicarbazide (7b).** White solid, mp 226–228°C. IR spectrum,  $\nu$ ,  $\text{cm}^{-1}$ : 3365 (N–H), 3277 (N–H), 3245 (N–H), 1674 (C=O), 1231 (C–F).  $^1\text{H}$  NMR spectrum,  $\delta$ , ppm: 10.55 s (1H, NH), 9.98 s (1H, NH), 9.60 s (1H, NH), 8.05 d. d (2H,  $J = 5.2$  and  $8.8$  Hz, ArH), 7.75 d (1H,  $J = 8$  Hz, ArH), 7.29–7.57 m (9H, ArH), 5.06 s (2H,  $\text{CH}_2$ ), 2.52 s (3H,  $\text{CH}_3$ ).  $^{13}\text{C}$  NMR spectrum,  $\delta_{\text{C}}$ , ppm: 166.22, 155.01, 145.37, 142.48, 135.87, 129.39, 129.14, 128.66, 128.57, 127.21, 123.09, 122.51, 119.27, 118.94, 116.48, 116.26, 111.01, 45.50, 16.48. LC-MS:  $m/z$ : 551.06  $[M + H]^+$ .

**4-(2,4-Dichlorophenyl)-1-(2-{2-[2-(4-fluorophenyl)-4-methylthiazol-5-yl]-1H-benzo[d]imidazol-1-yl}acetyl)thiosemicarbazide (7c),** White solid, mp 220–222°C. IR spectrum,  $\nu$ ,  $\text{cm}^{-1}$ : 3366 (N–H), 3275 (N–H), 3246 (N–H), 1671 (C=O), 1232 (C–F).  $^1\text{H}$  NMR spectrum,  $\delta$ , ppm: 10.52 s (1H, NH), 10.03 s (1H, NH), 9.58 s (1H, NH), 8.01 d. d (2H,  $J = 5.6$  and  $8.4$  Hz, ArH), 7.71 d (1H,  $J = 8$  Hz, ArH), 7.66 s (1H, ArH), 7.25–7.52 m (7H, ArH), 5.02 s (2H,  $\text{CH}_2$ ), 2.48 s (3H,  $\text{CH}_3$ ). LC-MS:  $m/z$ : 585  $[M + H]^+$ .

**4-(4-Chlorophenyl)-1-(2-{2-[2-(4-fluorophenyl)-4-methylthiazol-5-yl]-1H-benzo[d]imidazol-1-yl}acetyl)thiosemicarbazide (7d).** White solid, mp 160–162°C. IR spectrum,  $\nu$ ,  $\text{cm}^{-1}$ : 3367 (N–H), 3278 (N–H), 3247 (N–H), 1672 (C=O), 1232 (C–F).  $^1\text{H}$  NMR spectrum,  $\delta$ , ppm: 10.46 s (1H, NH), 9.89 s (1H, NH), 9.74 s (1H, NH), 8.01 d. d (2H,  $J = 5.6$  and  $8.8$  Hz, ArH), 7.71 d (1H,  $J = 7.6$  Hz, ArH), 7.54 d (1H,  $J = 8$  Hz, ArH), 7.41 d (2H,  $J = 7.6$  Hz, ArH), 7.25–7.36 m (6H, ArH), 5.04 s (2H,  $\text{CH}_2$ ), 2.48 s (3H,  $\text{CH}_3$ ).  $^{13}\text{C}$  NMR spectrum,  $\delta_{\text{C}}$ , ppm:

166.25, 162.28, 155.02, 145.42, 142.49, 137.91, 135.88, 129.16, 128.67, 128.58, 128.09, 123.18, 122.54, 119.31, 118.94, 116.51, 116.29, 110.98, 45.57, 16.48. LC-MS:  $m/z$ : 551  $[M + H]^+$ .

**4-(3,4-Dichlorophenyl)-1-(2-{2-[2-(4-fluorophenyl)-4-methylthiazol-5-yl]-1H-benzo[d]imidazol-1-yl}acetyl)thiosemicarbazide (7e).** White solid, mp 188–190°C. IR spectrum,  $\nu$ ,  $\text{cm}^{-1}$ : 3367 (N–H), 3276 (N–H), 3244 (N–H), 1671 (C=O), 1231 (C–F).  $^1\text{H}$  NMR spectrum,  $\delta$ , ppm: 10.51 s (1H, NH), 10.07 s (1H, NH), 9.88 s (1H, NH), 7.29–8.05 m (11H, ArH), 5.07 s (2H,  $\text{CH}_2$ ), 2.50 s (3H,  $\text{CH}_3$ ).  $^{13}\text{C}$  NMR spectrum,  $\delta_{\text{C}}$ , ppm: 166.21, 164.73, 162.25, 154.99, 145.38, 142.48, 139.09, 135.84, 129.95, 129.10, 128.62, 128.53, 123.14, 122.52, 119.29, 118.90, 116.47, 116.25, 110.95, 45.55, 16.45. LC-MS:  $m/z$ : 585  $[M + H]^+$ .

**Synthesis of 5-({2-[2-(4-fluorophenyl)-4-methylthiazol-5-yl]-1H-benzo[d]imidazol-1-yl}methyl)-4-phenyl-4H-1,2,4-triazole-3-thiol (8a–8e).** *Conventional method.* The mixture of an appropriate thiosemicarbazide **7a–7e** (0.001 mol) with 10 mL of 2 N NaOH solution was refluxed for 2.5 h. Progress of the reaction was monitored by TLC. After completion of the reaction, the mixture was poured onto crushed ice and acidified with acetic acid. The product was filtered off and crystallized from ethanol to give the corresponding pure compound **8a–8e** (Table 1).

*Microwave method.* The mixture of an appropriate thiosemicarbazide **7a–7e** (0.01 mol) with 2 N NaOH solution was subjected to MW irradiation at 350W for 5–10 min. Progress of the reaction was monitored by TLC. After completion of the process, the mixture was poured onto crushed ice and acidified with dilute acetic acid. The product was filtered off and crystallized from DMF/water to afford the corresponding pure compound **8a–8e** (Table 1).

**4-(3-Chlorophenyl)-5-({2-[2-(4-fluorophenyl)-4-methylthiazol-5-yl]-1H-benzo[d]imidazol-1-yl}methyl)-4H-1,2,4-triazole-3-thiol (8a).** White solid, mp 230–232°C. IR spectrum,  $\nu$ ,  $\text{cm}^{-1}$ : 2939 (=C–H), 1640 (C=N), 1218 (C–F).  $^1\text{H}$  NMR spectrum,  $\delta$ , ppm: 6.99–8.01 m (12H, ArH), 5.50 s (2H,  $\text{CH}_2$ ), 2.41 s (3H,  $\text{CH}_3$ ).  $^{13}\text{C}$  NMR spectrum,  $\delta_{\text{C}}$ , ppm: 168.42, 165.99, 162.27, 154.71, 146.50, 144.53, 142.42, 135.27, 135.13, 133.19, 130.51, 128.94, 128.63, 128.54, 127.65, 126.28, 123.15, 122.51, 119.22, 118.71, 116.55, 116.32, 111.21, 40.50, 16.62. LC-MS:  $m/z$ : 533.11  $[M + H]^+$ .

**4-(2-Chlorophenyl)-5-({2-[2-(4-fluorophenyl)-4-methylthiazol-5-yl]-1H-benzo[d]imidazol-1-yl}-**

**methyl)-4H-1,2,4-triazole-3-thiol (8b).** White solid, mp 226–228°C. IR spectrum,  $\nu$ ,  $\text{cm}^{-1}$ : 2936 (=C–H), 1638 (C=N), 1219 (C–F).  $^1\text{H}$  NMR spectrum,  $\delta$ , ppm: 7.13–7.99 m (12H, ArH), 5.31 s (2H,  $\text{CH}_2$ ), 2.40 s (3H,  $\text{CH}_3$ ).  $^{13}\text{C}$  NMR spectrum,  $\delta_{\text{C}}$ , ppm: 165.87, 154.76, 142.49, 130.81, 129.92, 128.51, 127.92, 122.43, 119.16, 116.57, 116.35, 111.35, 40.12, 16.63. LC-MS:  $m/z$ : 532.98  $[M + \text{H}]^+$ .

**4-(2,4-Dichlorophenyl)-5-({2-[2-(4-fluorophenyl)-4-methylthiazol-5-yl]-1H-benzo[d]imidazol-1-yl}-methyl)-4H-1,2,4-triazole-3-thiol (8c).** White solid, mp 230–232°C. IR spectrum,  $\nu$ ,  $\text{cm}^{-1}$ : 2938 (=C–H), 1635 (C=N), 1221 (C–F).  $^1\text{H}$  NMR spectrum,  $\delta$ , ppm: 7.23–7.97 m (11H, ArH), 5.38 s (2H,  $\text{CH}_2$ ), 2.40 s (3H,  $\text{CH}_3$ ). LC-MS:  $m/z$ : 567.00  $[M + \text{H}]^+$ .

**4-(4-Chlorophenyl)-5-({2-[2-(4-fluorophenyl)-4-methylthiazol-5-yl]-1H-benzo[d]imidazol-1-yl}methyl)-4H-1,2,4-triazole-3-thiol (8d).** White solid, mp 210–212°C. IR spectrum,  $\nu$ ,  $\text{cm}^{-1}$ : 2935 (=C–H), 1639 (C=N), 1219 (C–F).  $^1\text{H}$  NMR spectrum,  $\delta$ , ppm: 14.00 s (1H, SH), 7.17–8.01 m (12H, ArH), 5.51 s (2H,  $\text{CH}_2$ ), 2.41 s (3H,  $\text{CH}_3$ ).  $^{13}\text{C}$  NMR spectrum,  $\delta_{\text{C}}$ , ppm: 168.51, 166.04, 154.75, 147.24, 144.53, 142.39, 135.16, 134.44, 131.49, 129.41, 129.31, 129.03, 128.65, 128.56, 123.29, 122.65, 119.33, 118.58, 116.59, 116.37, 111.09, 38.88, 16.57. LC-MS:  $m/z$ : 533.05  $[M + \text{H}]^+$ .

**4-(3,4-Dichlorophenyl)-5-({2-[2-(4-fluorophenyl)-4-methylthiazol-5-yl]-1H-benzo[d]imidazol-1-yl}-methyl)-4H-1,2,4-triazole-3-thiol (8e).** White solid, mp 220–222°C. IR spectrum,  $\nu$ ,  $\text{cm}^{-1}$ : 2938 (=C–H), 1637 (C=N), 1222 (C–F).  $^1\text{H}$  NMR spectrum,  $\delta$ , ppm: 14.00 s (1H, SH), 7.17–8.01 m (12H, ArH), 5.51 s (2H,  $\text{CH}_2$ ), 2.41 s (3H,  $\text{CH}_3$ ).  $^{13}\text{C}$  NMR spectrum,  $\delta_{\text{C}}$ , ppm: 168.53, 166.09, 162.30, 154.68, 146.94, 144.47, 142.35, 135.08, 132.63, 131.74, 131.15, 129.54, 129.03, 128.67, 128.59, 127.86, 123.25, 122.67, 119.32, 118.57, 116.55, 116.33, 111.09, 16.64. LC-MS:  $m/z$ : 567.05  $[M + \text{H}]^+$ .

**Synthesis of 5-({2-[2-(4-fluorophenyl)-4-methylthiazol-5-yl]-1H-benzo[d]imidazol-1-yl}-methyl)-N-phenyl-1,3,4-thiadiazol-2-amine (9a–9e).** *Conventional method.* The mixture of an appropriate thiosemicarbazide **7a–7e** (0.001 mol) with 5 mL of conc.  $\text{H}_2\text{SO}_4$  was stirred for 4 h at RT. After completion of process, the mixture was poured onto crushed ice and neutralized with liquid  $\text{NH}_3$ , a solid product was formed. It was filtered off and washed with methanol to afford the corresponding pure compound **9a–9e** (Table 1).

*Microwave method.* The mixture of an appropriate thiosemicarbazide **7a–7e** (0.01 mol) with 5 mL of conc.  $\text{H}_2\text{SO}_4$  was subjected to MW irradiation for 5 to 10 min at 350 W. After completion of the process the mixture was poured onto crushed ice and neutralized with liquid  $\text{NH}_3$ . The precipitated solid was filtered off and crystallized from water–DMF to afford the corresponding pure thiadiazole **9a–9e** (Table 1).

**N-(3-Chlorophenyl)-5-({2-[2-(4-fluorophenyl)-4-methylthiazol-5-yl]-1H-benzo[d]imidazol-1-yl}-methyl)-1,3,4-thiadiazol-2-amine (9a).** White solid, mp 130–132°C. IR spectrum,  $\nu$ ,  $\text{cm}^{-1}$ : 3201 (N–H), 3039 (=C–H), 1606 (C=N), 1232 (C–F).  $^1\text{H}$  NMR spectrum,  $\delta$ , ppm: 9.5 s (1H, NH), 7.05–8.18 m (12H, ArH), 5.85 s (2H,  $\text{CH}_2$ ), 2.40 s (3H,  $\text{CH}_3$ ).  $^{13}\text{C}$  NMR spectrum,  $\delta_{\text{C}}$ , ppm: 165.80, 165.01, 154.67, 144.15, 142.18, 134.57, 129.11, 128.54, 128.19, 127.31, 123.71, 123.02, 122.35, 121.10, 118.99, 118.11, 116.07, 115.85, 110.74, 42.31, 15.98. LC-MS:  $m/z$ : 533.15  $[M + \text{H}]^+$ .

**N-(2-Chlorophenyl)-5-({2-[2-(4-fluorophenyl)-4-methylthiazol-5-yl]-1H-benzo[d]imidazol-1-yl}methyl)-1,3,4-thiadiazol-2-amine (9b).** White solid, mp 140–142°C. IR spectrum,  $\nu$ ,  $\text{cm}^{-1}$ : 3203 (N–H), 3038 (=C–H), 1607 (C=N), 1232 (C–F).  $^1\text{H}$  NMR spectrum,  $\delta$ , ppm: 9.2 s (1H, NH), 8.17 d (1H,  $J = 8.8$  Hz, ArH), 8.01–8.02 m (2H, ArH), 7.72 d. d (2H,  $J = 13.2$  and 8 Hz, ArH), 7.26–7.44 m (6H, ArH), 7.03 t (1H,  $J = 7.2$  Hz, ArH), 5.84 s (2H,  $\text{CH}_2$ ), 2.47 s (3H,  $\text{CH}_3$ ).  $^{13}\text{C}$  NMR spectrum,  $\delta_{\text{C}}$ , ppm: 166.30, 165.51, 162.30, 155.75, 155.17, 144.65, 142.69, 136.91, 135.08, 129.61, 129.05, 128.69, 128.61, 127.81, 124.22, 123.52, 122.86, 122.70, 121.61, 119.50, 118.61, 116.57, 116.35, 111.25, 42.81, 16.48. LC-MS:  $m/z$ : 533.10  $[M + \text{H}]^+$ .

**N-(2,4-Dichlorophenyl)-5-({2-[2-(4-fluorophenyl)-4-methylthiazol-5-yl]-1H-benzo[d]imidazol-1-yl}-methyl)-1,3,4-thiadiazol-2-amine (9c).** White solid, mp 230–232°C. IR spectrum,  $\nu$ ,  $\text{cm}^{-1}$ : 3201 (N–H), 3037 (=C–H), 1608 (C=N), 1231 (C–F).  $^1\text{H}$  NMR spectrum,  $\delta$ , ppm: 9.2 s (1H, NH), 8.29 d (1H,  $J = 8.4$  Hz, ArH), 8.04 m (2H, ArH), 7.74 d. d (2H,  $J = 14.8$  and 7.2 Hz, ArH), 7.60 s (1H, ArH), 7.32–7.38 m (5H, ArH), 5.86 s (2H,  $\text{CH}_2$ ), 2.49 s (3H,  $\text{CH}_3$ ).  $^{13}\text{C}$  NMR spectrum,  $\delta_{\text{C}}$ , ppm: 166.30, 165.04, 156.19, 155.16, 144.64, 142.68, 136.09, 135.06, 128.89, 128.69, 128.61, 127.80, 126.60, 123.52, 123.02, 122.86, 122.12, 119.50, 118.59, 116.57, 116.35, 111.25, 42.78, 16.49. LC-MS:  $m/z$ : 567.05  $[M + \text{H}]^+$ .

**N-(4-Chlorophenyl)-5-({2-[2-(4-fluorophenyl)-4-methylthiazol-5-yl]-1H-benzo[d]imidazol-1-yl}-**

**methyl)-1,3,4-thiadiazol-2-amine (9d).** White solid, mp 210–212°C. IR spectrum,  $\nu$ ,  $\text{cm}^{-1}$ : 3202 (N–H), 3039 (=C–H), 1605 (C=N), 1232 (C–F).  $^1\text{H}$  NMR spectrum,  $\delta$ , ppm: 10.2 s (1H, NH), 8.04 m (1H, ArH), 7.73 d. d (2H,  $J = 17$  and 7.6 Hz, ArH), 7.56 d (1H,  $J = 8$  Hz, ArH), 7.33–7.50 m (4H, ArH), 5.86 s (2H,  $\text{CH}_2$ ), 2.49 s (3H,  $\text{CH}_3$ ).  $^{13}\text{C}$  NMR spectrum,  $\delta_{\text{C}}$ , ppm: 166.30, 164.66, 162.29, 155.16, 154.64, 144.63, 142.68, 139.13, 135.06, 129.01, 128.84, 128.68, 128.59, 125.41, 123.50, 122.84, 119.49, 118.89, 118.60, 116.55, 116.33, 111.23, 42.80, 16.48. LC-MS:  $m/z$ : 533.05 [ $M + \text{H}$ ] $^+$ .

***N*-(3,4-Dichlorophenyl)-5-({2-[2-(4-fluorophenyl)-4-methylthiazol-5-yl]-1*H*-benzo[*d*]imidazol-1-yl}-methyl)-1,3,4-thiadiazol-2-amine (9e).** White solid, mp 180–182°C. IR spectrum,  $\nu$ ,  $\text{cm}^{-1}$ : 3202 (N–H), 3035 (=C–H), 1604 (C=N), 1231 (C–F).  $^1\text{H}$  NMR spectrum,  $\delta$ , ppm: 10.5 s (1H, NH), 6.5–8.4 m (11H, ArH), 5.86 s (2H,  $\text{CH}_2$ ), 2.4 s (3H,  $\text{CH}_3$ ).  $^{13}\text{C}$  NMR spectrum,  $\delta_{\text{C}}$ , ppm: 166.29, 164.39, 162.35, 155.23, 144.65, 142.69, 140.07, 135.08, 131.25, 130.71, 128.65, 123.50, 123.13, 119.50, 118.56, 117.52, 116.51, 111.20, 42.77, 16.49. LC-MS:  $m/z$ : 567.05 [ $M + \text{H}$ ] $^+$ .

### CONCLUSIONS

The new series of derivatives of 1,2,4-triazole **8a–8e** and 1,3,4-thiadiazole **9a–9e** have been synthesized by conventional as well as MW irradiation methods from 2-{{2-[2-(4-fluorophenyl)-4-methylthiazol-5-yl]-1*H*-benzo[*d*]imidazol-1-yl}acetohydrazide. MW irradiation at 350 W reduces the reaction time from hours to 5–10 min and increases the yield of products from 60–74 to 77–88%. All the newly synthesized compounds have been tested for their antibacterial activity. Compounds **7a**, **7d**, **7e**, **8d**, and **9e** are characterized by moderate activity against both gram positive and gram negative bacterial strains.

### ACKNOWLEDGMENTS

Authors are thankful to Department of Science and Technology, New Delhi for providing financial assistance for research facilities under FIST programme.

### CONFLICT OF INTEREST

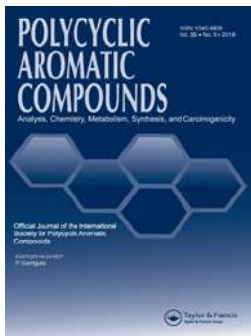
No conflict of interest was declared by the authors.

### SUPPLEMENTARY MATERIAL

Supplementary material are available for this article at <https://doi.org/10.1134/S1070363220090200> and are accessible for authorized users.

### REFERENCES

- Sirim, M.M., Krishna, V.S., Sriram, D., and Tan, O.U., *Eur. J. Med. Chem.*, 2020, vol. 188, p. 112010. <https://doi.org/10.1016/j.ejmech.2019.112010>
- Dokla, E.M.E., Abutaleb, N.S., Milik, S.N., Li, D., El-baz, K., Shalaby, M.A.W., Al-Karaki, R., Nasr, M., Klein, C.D., Abouzid, K.A.M., and Seleem, M.N., *Eur. J. Med. Chem.*, 2020, vol. 18615, p. 111850. <https://doi.org/10.1016/j.ejmech.2019.111850>
- Abdel-Galil, E., Moawad, E.B., El-Mekabaty, A., and Said, G.E., *Synth. Commun.*, 2018, vol. 48, no. 16, p. 2083. <https://doi.org/10.1080/00397911.2018.1482349>
- Shaikh, M.S., Palkar, M.B., Patel, H.M., Rane, R.A., Alwan, W.S., Shaikh, M.M., Shaikh, I.M., Hampannavar, G.A., and Karpoornath, R., *RSC Adv.*, 2014, vol. 4, p. 62308. <https://doi.org/10.1039/C4RA11752B>
- Chandra Sekhar, D., Venkata Rao, D.V., Tejeswara Rao, A., Luv kumar, U., and Jha, A., *Russ. J. Gen. Chem.*, 2019, vol. 89, p. 770. <https://doi.org/10.1134/S1070363219040224>
- Yusuf, M., Khan, R.A., Khan, M., and Ahmed, B., *Chemistry Select*, 2017, vol. 2, no. 4, p. 1323. <https://doi.org/10.1002/slct.201601137>
- Onkol, T., Dogruer, D.S., Uzun, L., Adak, S., Ozkan, S., and Şahin, M.F., *J. Enzyme Inhib. Med. Chem.*, 2008, vol. 23, no. 2, p. 277. <https://doi.org/10.1080/14756360701408697>
- Stec, A.P., Biernasiuk, A., Malm, A., and Pitucha, M., *J. Heterocycl. Chem.*, 2017, vol. 54, no. 5, p. 2867. <https://doi.org/10.1002/jhet.2893>
- Gao, F., Wang, T., Xiao, J., and Huang, G., *Eur. J. Med. Chem.*, 2019, vol. 173, p. 274. <https://doi.org/10.1016/j.ejmech.2019.04.043>
- Akolkar, H.N., Karale, B.K., Randhavane, P.V., and Dalavi, N.R., *Indian J. Chem. B*, 2017, vol. 56, p. 348. <http://nopr.niscair.res.in/handle/123456789/40728>
- Karale, B.K., Takate, S.J., Salve, S.P., Zaware, B.H., and Jadhav, S.S., *Indian J. Chem. B*, 2014, vol. 53, p. 339. <http://nopr.niscair.res.in/handle/123456789/27403>
- Phillip, M., *J. Chem. Soc. C.*, 1971, p. 1143.
- Dengale, S.G., Karale, B.K., Akolkar, H.N., Darekar, N.R., and Deshmukh, K.K., *Russ. J. Gen. Chem.*, 2019, vol. 89, p. 1535. <https://doi.org/10.1134/S1070363219070259>




## Design, Synthesis and Biological Evaluation of Novel Furan & Thiophene Containing Pyrazolyl Pyrazolines as Antimalarial Agents

Hemantkumar N. Akolkar , Sujata G. Dengale , Keshav K. Deshmukh ,  
**Bhausahab K. Karale** , Nirmala R. Darekar , Vijay M. Khedkar & Mubarak H. Shaikh

To cite this article: Hemantkumar N. Akolkar , Sujata G. Dengale , Keshav K. Deshmukh , Bhausahab K. Karale , Nirmala R. Darekar , Vijay M. Khedkar & Mubarak H. Shaikh (2020): Design, Synthesis and Biological Evaluation of Novel Furan & Thiophene Containing Pyrazolyl Pyrazolines as Antimalarial Agents, Polycyclic Aromatic Compounds, DOI: [10.1080/10406638.2020.1821231](https://doi.org/10.1080/10406638.2020.1821231)


To link to this article: <https://doi.org/10.1080/10406638.2020.1821231>

 View supplementary material 

 Published online: 14 Sep 2020.

 Submit your article to this journal 

 Article views: 9

 View related articles 

 View Crossmark data 





# Design, Synthesis and Biological Evaluation of Novel Furan & Thiophene Containing Pyrazolyl Pyrazolines as Antimalarial Agents

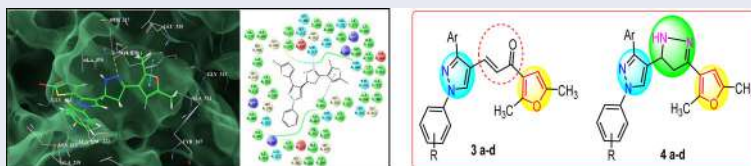
Hemantkumar N. Akolkar<sup>a</sup>, Sujata G. Dengale<sup>b</sup>, Keshav K. Deshmukh<sup>b</sup>, Bhausaheb K. Karale<sup>a</sup>, Nirmala R. Darekar<sup>a</sup>, Vijay M. Khedkar<sup>c</sup>, and Mubarak H. Shaikh<sup>a</sup>

<sup>a</sup>P.G. and Research, Department of Chemistry, Radhabai Kale Mahila Mahavidyalaya, Ahmednagar, India;

<sup>b</sup>P.G. and Research, Department of Chemistry, Sangamner Nagarpalika Arts, D. J. Malpani Commerce, B.N. Sarada Science College, Sangamner, India; <sup>c</sup>Department of Pharmaceutical Chemistry, School of Pharmacy, Vishwakarma University, Pune, India

## ABSTRACT

In search for novel compounds targeting Malaria, based on the *in silico* molecular docking binding affinity data, the novel furans containing pyrazolyl chalcones (**3a-d**) and pyrazoline derivatives (**4a-d**) were synthesized. The formation of the synthesized compound were confirmed by spectral analysis like IR, <sup>1</sup>H NMR, <sup>13</sup>C NMR and mass spectrometry. Compounds with thiophene and pyrazoline ring **4b** (0.47  $\mu$ M), **4c** (0.47  $\mu$ M) and **4d** (0.21  $\mu$ M) exhibited excellent anti-malarial activity against *Plasmodium falciparum* compared with standard antimalarial drug Quinine (0.83  $\mu$ M). To check the selectivity furthermore, compounds were tested for antimicrobial activity and none of the synthesized compound exhibited significant potency compared with the standard antibacterial drug Chloramphenicol and antifungal drug Nystatin respectively. So, it can be resolved that the produced compounds show selectively toward antimalarial activity and have the potential to be explored further.



## ARTICLE HISTORY

Received 7 August 2020

Accepted 5 September 2020


## KEYWORDS

Antimalarial; antimicrobial; chalcones; pfENR inhibitor; pyrazole-pyrazolines; thiophene

## Introduction

Life-threatening disease Malaria is caused by *Plasmodium* parasites that are spread to people through the bites of infected female Anopheles mosquitoes. Out of five *Plasmodium* Parasites *Plasmodium falciparum* produces high levels of blood-stage parasites that sequester in critical organs in all age groups.<sup>1</sup> As per the World Health Organization report in 2018, in sub Saharan Africa 11 million pregnant women were infected with malaria and 872 000 children were born with a low birth weight. Around 24 million children estimated to be infected with the *P. falciparum* parasite in the region; out of these, 1.8 million had severe anemia and 12 million had

**CONTACT** Hemantkumar N. Akolkar  [hemantakolkar@gmail.com](mailto:hemantakolkar@gmail.com)  P.G. and Research, Department of Chemistry, Radhabai Kale Mahila Mahavidyalaya, Ahmednagar, Maharashtra 414001, India.

 Supplemental data for this article is available online at <https://doi.org/10.1080/10406638.2020.1821231>.



moderate anemia.<sup>2</sup> Mortality and morbidity caused by malaria are continually increasing. This subject is the consequence of the ever-increasing development of parasite resistance to drugs and also increased mosquito resistance to insecticides which is one of the most critical complications in controlling malaria over recent years.<sup>3</sup>

*P. falciparum* enoyl-acyl carrier protein (ACP) reductase (ENR) is an enzyme in type II fatty acid synthesis (FAS II) pathway which catalyzes the NADH-dependent reduction of trans-2-enoyl-ACP to acyl-ACP and plays important role in completion of the fatty acid elongation cycles. Due to its role in the parasite's fatty acid pathway, PfENR has been known as one of the most promising antimalarial targets for structure-based drug design.<sup>4-6</sup> Triclosan, a broadly used antibiotic, is effective inhibitor of PfENR enzyme activity. Several efforts have been taken in the recent past in the direction of the identification of new antimalarials using pharmacophore modeling, molecular docking and MD simulations.<sup>7-12</sup>

Pyrazole is a well-known class of nitrogen containing heterocyclic compounds and play important role in agricultural and medicinal field. Pyrazole and its derivatives are known to possess antibacterial,<sup>13</sup> antipyretic,<sup>14</sup> fungistatic,<sup>15</sup> anticonvulsant,<sup>16</sup> antitubercular,<sup>17</sup> antipyretic,<sup>18</sup> insecticides,<sup>19</sup> and anti-inflammatory<sup>20</sup> activities. Pyrazoline containing compounds are recognized to possess various pharmacological activities like antimalarial,<sup>21,22</sup> anticancer,<sup>23</sup> anti-inflammatory,<sup>24</sup> analgesic,<sup>24</sup> antitumor,<sup>25</sup> antimicrobial<sup>26</sup> and antidepressant activities.<sup>27</sup> Furan containing compounds possess lipoxygenase inhibitor,<sup>28</sup> urotensin-II receptor antagonists,<sup>29</sup> fungicidal,<sup>30</sup> epidermal growth factor receptor inhibitors and anticancer<sup>31</sup> etc. activities. Chalcone is a natural pigment found in plant and is an important intermediate for the synthesis of flavonoids. Varieties of biological activities are associated with chalcones and their derivatives such as antiplasmodial,<sup>32</sup> nematicide,<sup>33</sup> antiallergenic,<sup>34</sup> antimalarial,<sup>35</sup> anti-HIV,<sup>36</sup> anti-cancer,<sup>37</sup> anti-inflammatory<sup>38</sup> and anti-tuberculosis.<sup>39</sup>

So, considering the biological importance of pyrazoles, furan and chalcone, herein we report the design of a small library of furan containing pyrazolyl pyrazoline derivatives by molecular hybridization approach targeting PfENR using the *in silico* molecular docking technique. The promising results obtained from this *in silico* study served the basis for the synthesis of these molecules followed by evaluation of their antimalarial potential.

Molecular docking technique plays significant role in lead identification/optimization and in the mechanistic study by predicting the binding affinity and the thermodynamic interactions leading the binding of a ligand to its biological receptor. Thus, with the objective to identify novel leads targeting the crucial antimalarial target *Plasmodium falciparum* enoyl-ACP reductase (PfENR or FabI) (pdb code: 1NHG), molecular docking was carried out using the GLIDE (Grid-based LIgand Docking with Energetics) program of the Schrodinger Molecular modeling package.<sup>40-42</sup> A small library of 8 molecules comprising furan containing pyrazolyl pyrazoline derivatives (**3a-3d**, **4a-4d**) was docked against PfENR. The ensuing docking conformation revealed that these molecules changed a binding mode which is corresponding with the active site of pfENR and were found to be involved in a series of bonded and non-bonded interactions with the residues lining the active site. Their docking scores varied from -6.979 to -8.222 with an average docking score of -7.563 signifying a potent binding affinity to PfENR. In order to get a quantitative insight into the most significantly interacting residues and their associated thermodynamic interactions, a detailed per-residue interaction analysis was carried out (Table S1, Supporting Information). This analysis showed that the furan containing pyrazolyl chalcones (**3a-d**) (Figure 1) were deeply embedded into the active site of PfENR engaging in a sequence of favorable *van der Waals* interactions observed with Ile:C369, Phe:C368, IleA323, Ala:A320, Ala:A319, Arg:A318, Ser:A317, Leu:A315, Pro:A314, Gly:A313, Ala:A312, Lys:A285, Met:A281, Tyr:A277, Tyr:A267, Thr:A266, Leu:A265, Gly:A112, Tyr:A111, Gly:A110 and Asp:A107 residues through the 1,3-substituted-1*H*-pyrazol-4-yl scaffold while the 1-(2,5-Dimethylfuran-3-yl) prop-2-en-1-one

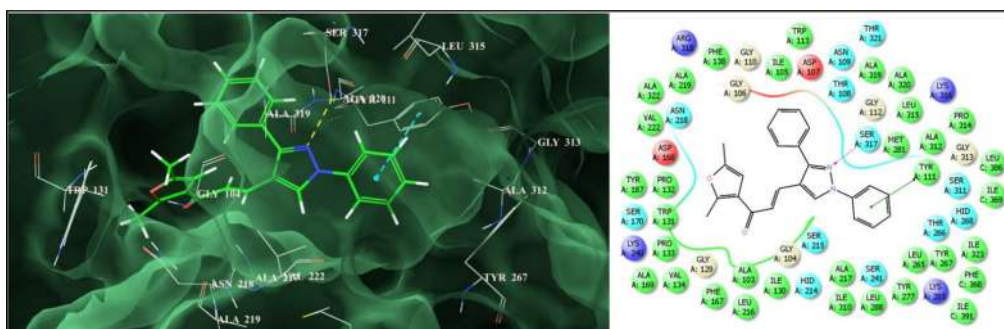


**Figure 1.** Binding mode of **3a** into the active site of *Plasmodium falciparum* enoyl-ACP reductase (on right side: pink lines represent the hydrogen bond while green lines signify  $\pi$ - $\pi$  stacking interactions).

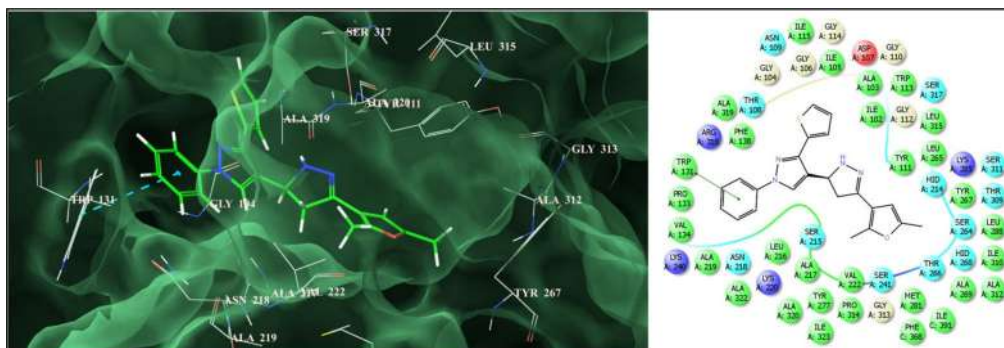
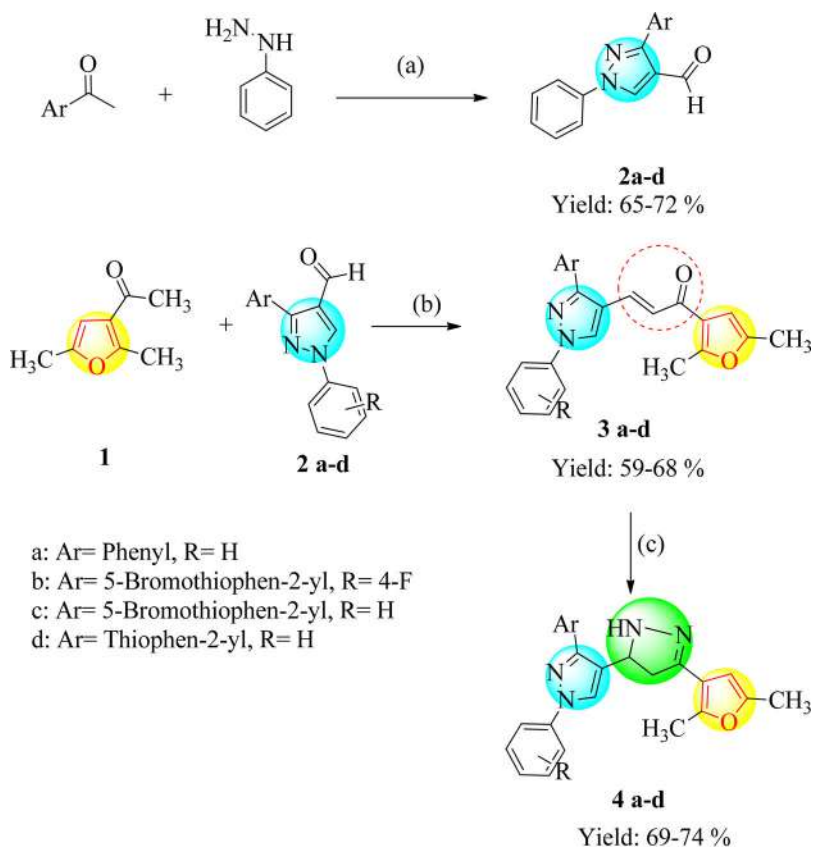


**Figure 2.** Binding mode of **4d** into the active site of *Plasmodium falciparum* enoyl-ACP reductase (on right side: pink lines represent the hydrogen bond while green lines signify  $\pi$ - $\pi$  stacking interactions).

component of the molecules was seen to be involved in similar interactions with Asn:A218, Ala:A217, Leu:A216, Ser:A215, Trp:A131, Gly:A106, Ile:A105, Gly:A104 residues of the active site.

Furthermore the enhanced binding affinity of these molecule is also attributed to significant electrostatic interactions observed with Arg:A318, Ser:A317, Lys:A285, Asp:A236, Asn:A218, Ala:A217, Ser:A215, Tyr:A111, Gly:A110, Asp:A107, Gly:A104 residues lining the active site. On the other hand, the furan containing pyrazoline derivatives (**4a-d**) (Figure 2) were also seen to be stabilized into the active of *Pf*ENR through a network of significant *van der Waals* interactions observed with (2,5-dimethylfuran-3-yl)-1*H*-pyrazolyl scaffold *via* Ile:C369, Phe:C368, Ala:A320, Ser:A317, Leu:A315, Pro:A314, Gly:A313, Ala:A312, Lys:A285, Tyr:A267, Thr:A266, Leu:A265, Gly:A112, Tyr:A111, Gly:A110, Gly:A106 and Ile:A105 while other half of the molecule i.e., 2-thiophenyl-1-phenyl-1*H*-pyrazole showed similar type of interactions with Ile:A323, Ala:A319, Arg:A318, Met:A281, Tyr:A277, Val:A222, Ala:A219, Asn:A218, Ala:A217, Leu:A216, Ser:A215, Trp:A131, Ile:A130, Trp:A113, Asp:A107, Gly:A104 residues.

Further the enhanced binding affinity of the molecules is also attributed to favorable electrostatic interactions observed with Arg:A318, Ser:A317, Glu:A289, Lys:A285, Asp:A236, Asn:A218, Ala:A217, Ser:A215, Tyr:A111, Gly:A110, Asp:A107 and Gly:A104. While these non-bonded interactions (*van der Waals* and electrostatic) were observed to be the major driving force for the mechanical interlocking of these novel furan containing pyrazolyl pyrazoline derivatives into the active site *Pf*ENR, the enhanced binding affinity of these molecules is also contributed by very prominent hydrogen bonding interaction observed for **3a** (Ser:A317(2.708 Å)), **4a** (Ser:A317(2.783 Å)), **4b** (Ser:A317(2.462 Å)) and **4c** (Ser:A317(2.462 Å)). Furthermore these



**Reagents and conditions:** (a): i) EtOH, reflux, 2 hr ii) DMF/POCl<sub>3</sub>, 0-10° C;  
 (b) 10 % aq. KOH, EtOH, RT, 14hr; (c) NH<sub>2</sub>NH<sub>2</sub>·H<sub>2</sub>O, EtOH, AcOH, 6hr

**Scheme 1.** Synthesis of pyrazolyl chalcones (3a-d) and pyrazolyl pyrazolines (4a-d).

molecules were also engaged in a very close  $\pi$ - $\pi$  stacking interactions: **3a**: Tyr: A111(2.669 Å), **3b**: Tyr:A267(2.529 Å), **3c**: Tyr:A267(2.541 Å), **3d**: Tyr:A267(2.335 Å), **4a**: Tyr:A111(2.602 Å), **4b**: Trp:A131(2.073 Å), **4c**: TyrA:111(2.073 Å) and **4d**: TrpA131(2.538 Å) (Figures S1-S6, Supporting Information).

This type of bonded interactions i.e., hydrogen bonding and  $\pi$ - $\pi$  stacking are known to serve as an “anchor” to guide the alignment of a molecule into the 3D space of enzyme’s active site and facilitate the non-bonded interactions (*Van der Waals* and electrostatic) as well. Overall, the in-silico binding affinity data suggested that these furans containing pyrazolyl pyrazoline derivatives (**3a-d**, **4a-d**) could be developed as novel scaffold to arrive at compounds with high selectivity and potency *Plasmodium falciparum*.

## Results and discussion

### Chemistry

The novel series of furan containing pyrazolyl chalcones (**3a-d**) and pyrazoline derivatives (**4a-d**) were synthesized from commercially available starting materials (Scheme 1). Initially, pyrazole aldehyde **2a-d** was formed by the condensation between substituted acetophenone and phenyl

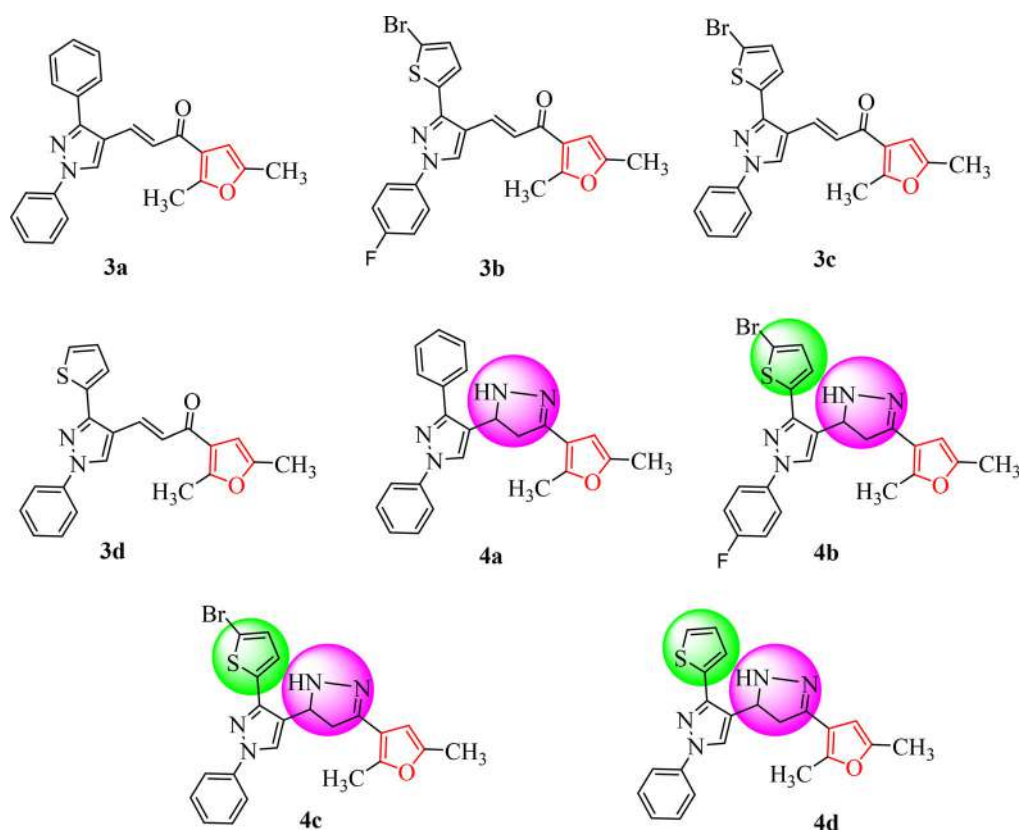


**Figure 3.** The newly synthesized compounds structure **3a-d** & **4a-d**.

hydrazine followed by Vilsmeier-Haack formylation reaction (Scheme 1). Then furan containing pyrazolyl chalcones **3a-d** were synthesized by base-catalyzed Claisen-Schmidt condensation of 1-(2,5-dimethylfuran-3-yl)ethanone **1** and substituted pyrazole aldehyde **2a-d**.<sup>43</sup> Finally, the furan containing pyrazolyl chalcones **3a-d** and hydrazine hydrate in ethanol solvent using catalytic amount of acetic acid at reflux condition for 6 hr afforded the corresponding pyrazolyl pyrazolines (**4a-d**) in quantitative isolated yield (69–74%) (Scheme 1).

The newly synthesized compounds structures were shown in Figure 3. The newly synthesized compound's structures were confirmed by IR, <sup>1</sup>H NMR, <sup>13</sup>C NMR, mass spectral data. For compound **3a**, in IR spectrum the stretching band for C=O was detected at 1657 cm<sup>-1</sup>. In the <sup>1</sup>H NMR spectrum of compound **3a**, the proton of pyrazole and furan ring resonate as a singlet at δ 9.31 and δ 6.60 ppm respectively. Also, singlet for two -CH<sub>3</sub> were observed at δ 2.27 and δ 2.50 ppm. The <sup>13</sup>C NMR spectrum of compound **3a** showed signal at δ 184.41 ppm due to C=O and δ 12.89 and δ 13.93 ppm is due to two -CH<sub>3</sub>. Mass spectrum confirms the formation of compound **3a** showed m/z = 369 (M + H)<sup>+</sup>.

Secondly, in the IR spectrum of compound **4a**, -N-H stretching band observed at 3252 cm<sup>-1</sup>. The <sup>1</sup>H NMR spectrum of compound **4a**, the CH<sub>2</sub> protons of the pyrazoline ring resonated as a pair of doublets of doublets at δ 2.88 ppm and 3.35 ppm. The CH proton appeared as triplet at δ 4.87 ppm due to vicinal coupling with two protons of the methylene group. In the <sup>13</sup>C NMR spectra of the compound **4a** carbons of the pyrazoline ring were observed at δ 41.97 ppm and 54.67 ppm. All the other aromatic and aliphatic protons and carbons were observed at expected regions. Mass spectrum confirms the formation of compound **4a** showed m/z = 383 (M + H)<sup>+</sup>.

**Table 1.** Antimalarial ( $\mu\text{M}$ ), Antibacterial (MIC in  $\mu\text{g/mL}$ ) & Antifungal (MIC in  $\mu\text{g/mL}$ ) activity.

Cpd	Antimalarial activity Plasmodium falciparum	Antibacterial activity				Antifungal activity			Molecular Docking Score
		EC	PA	SA	SP	CA	AN	AC	
<b>3a</b>	1.46	200	200	250	250	500	500	500	-7.814
<b>3b</b>	3.93	100	250	250	200	1000	500	500	-7.032
<b>3c</b>	2.16	62.5	200	125	250	500	>1000	>1000	-7.192
<b>3d</b>	3.07	100	100	200	200	1000	500	500	-7.118
<b>4a</b>	6.31	125	100	100	100	500	500	500	-6.979
<b>4b</b>	0.47	100	200	100	100	250	500	500	-8.157
<b>4c</b>	0.47	125	125	200	200	1000	>1000	>1000	-8.222
<b>4d</b>	0.21	200	100	125	100	500	500	500	-7.988
Chloroquine	0.06	-	-	-	-	-	-	-	-
Quinine	0.83	-	-	-	-	-	-	-	-
CP	-	50	50	50	50	-	-	-	-
NS	-	-	-	-	-	100	100	100	-

Cpd: Compound; EC: *Escherichia coli*; PA: *Pseudomonas aeruginosa*; SA: *Staphylococcus aureus*; SP: *Streptococcus pyogenes*; CA: *Candida albicans*; AN: *Aspergillus niger*; AC: *Aspergillus clavatus*; CP: Chloramphenicol; NS: Nystatin.

## Biological evaluation

### *In vitro* antimalarial screening

All the synthesized novel compounds were tested for antimalarial activities. The *in vitro* antimalarial assay was carried out according to the micro assay protocol of Rieckmann and coworkers with minor modifications.<sup>44–47</sup> The results were recorded as the minimum inhibitory concentrations ( $\mu\text{M}$  MIC) chloroquine and quinine were used as the reference drug (Table 1).

Herein, we have synthesized four chalcone and pyrazoline derivatives respectively. Structure activity relationship (SAR) plays very important role while displaying the antimalarial activity. All the synthesized chalcone derivatives (**3a–d**) exhibited less potency compared to the standard drug. But pyrazoline derivatives exhibited excellent antimalarial activity compared to the standard drug. In compound **4a**, thiophene ring was absent and pyrazoline ring is present, so, the compound **4a** exhibited less potency compared to the standard drug. Now, in compound **4b**, bromo substituted thiophene and pyrazoline rings are present along with the fluorine at the para position on benzene ring. Interestingly, this compound **4b** (0.47  $\mu\text{M}$ ), exhibited excellent activity compared to the standard drug quinine (0.83  $\mu\text{M}$ ). Again, in compound **4c**, bromo substituted thiophene and pyrazoline rings are present but no fluorine at the para position of benzene ring. Though fluorine is absent on benzene ring in compound **4c** (0.47  $\mu\text{M}$ ), it exhibited same potency as that of compound **4b** compared to the standard drug quinine (0.83  $\mu\text{M}$ ). Finally, in compound **4d**, there were no substitution on the thiophene and benzene ring. In compound **4d** plane thiophene, plane benzene ring and pyrazoline ring constructed in a single molecular framework. Compound **4d** (0.21  $\mu\text{M}$ ), exhibited four-fold more antimalarial activity compared to the standard drug quinine (0.83  $\mu\text{M}$ ). From SAR, we can conclude that for the antimalarial activity thiophene, pyrazoline and benzene ring were very important in a single molecular framework.

### Antimicrobial activities

Further, all the novel synthesized compounds were also screened for antimicrobial activities against the bacterial strains *Escherichia coli* (MTCC 443), *Staphylococcus aureus* (MTCC 96), *Pseudomonas aeruginosa* (MTCC 1688), *Streptococcus pyogenes* (MTCC 442) and fungal strains *Aspergillus clavatus* (MTCC 1323), *Candida albicans* (MTCC 227) and *Aspergillus niger* (MTCC 282). The minimum inhibitory concentration (MIC) was determined by the broth dilution method. Chloramphenicol and Nystatin were used as reference drugs for antibacterial and antifungal activity, respectively. The results of antibacterial and antifungal activity were given in Table 1.



The results given in Table 1 indicated that none of the synthesized compound exhibited significant potency toward the standard antibacterial drug Chloramphenicol and antifungal drug Nystatin. Hence, from above result we can conclude that the synthesized compounds show selectively antimalarial activity and negligible antimicrobial activity.

## Conclusion

In conclusion, Considering the importance of enoyl-ACP reductase (*Pf*ENR) in *Plasmodium*, a small library of 8 molecules comprising furan containing pyrazolyl pyrazoline derivatives (**3a-d**, **4a-d**) was designed and docked against *Pf*ENR. Based on the *in silico* binding affinity data, synthesis was carried out for these novel furans containing pyrazolyl pyrazoline derivatives (**3a-d**, **4a-d**) and was evaluated for activity against *Plasmodium falciparum*. The synthesized compounds shown selectively antimalarial activity with minimal antimicrobial activity. Compounds (**3a-d**) exhibited less antimalarial activity compared to the standard drug. From the series of compounds (**4a-d**), compound **4b** (0.47  $\mu$ M), **4c** (0.47  $\mu$ M) and **4d** (0.21  $\mu$ M) exhibited more antimalarial activity compared to the standard drug quinine (0.83  $\mu$ M). Compound **4d** shows four-fold more activity compared to the standard drug quinine. From the SAR, we have distinguished areas of the pyrazolyl chalcones and pyrazolyl pyrazolines framework where variations can be made to expand the pharmacokinetic profile as well as features required to improve inhibitor effectiveness. This innovative molecular scaffold presents breakthrough for optimization to develop effective *Pf*ENR inhibitors.

## Experimental

### General

All the reagents, solvents and chemicals were taken from commercial sources found to be and used as such without purification. The physical constant like melting points were measured on a DBK melting point apparatus and are uncorrected. IR spectra were recorded on Shimadzu IR Affinity 1S (ATR) FTIR spectrophotometer.  $^1\text{H}$  NMR (400 MHz) and  $^{13}\text{C}$  NMR (100 MHz) spectra were recorded on Bruker Advance II 400 spectrophotometer using TMS as an internal standard and DMSO- $d_6$  as solvent and chemical shifts were expressed as  $\delta$  ppm units. Mass spectra were obtained on Waters, Q-TOF micro mass (ESI-MS) mass spectrometer.

### General procedure for the synthesis of pyrazolyl chalcones (**3a-d**)

A mixture of 1-(2,5-dimethylfuran-3-yl)ethanone **1** (0.05 mol), substituted pyrazole aldehyde **2** (0.05 mol) and 10% aqueous potassium hydroxide (10 mL) in ethanol (50 mL) was stirred at room temperature for 14 h. The progress of the reaction was monitored by TLC. After completion of the reaction, the reaction mixture was transferred into crushed ice and neutralized by dil. HCl. The precipitation observed, filtered it, washed with water and dried. The crystallization of product carried out in ethanol.

### (*E*)-1-(2,5-Dimethylfuran-3-yl)-3-(1,3-diphenyl-1H-pyrazol-4-yl)prop-2-en-1-one (**3a**)

Yield: 61%, yellow solid; mp: 80–82  $^{\circ}\text{C}$ ; IR ( $\nu_{\text{max}}$ ,  $\text{cm}^{-1}$ ): 2921 (=C-H), 2855 (C-H), 1657 (C=O), 1454 (C=N);  $^1\text{H}$ -NMR (400 MHz, DMSO- $d_6$ ,  $\delta$ , ppm): 9.31 (s, 1H, Pyrazole-H), 7.93 (d, 2H,  $J=7.9$  Hz), 7.38–7.68 (m, 10H, Ar-H), 6.60 (s, 1H, Furan-H), 2.53 (s, 3H,  $-\text{CH}_3$ ), 2.27 (s, 3H,  $-\text{CH}_3$ );  $^{13}\text{C}$  NMR (100 MHz, DMSO- $d_6$ ,  $\delta$ , ppm): 184.4 (C=O), 159.9, 152.8, 149.7, 138.9, 132.2, 132.0, 129.6, 128.8, 128.5, 128.6, 128.4, 127.1, 123.8, 122.1, 118.6, 117.6, 105.9, 13.9 ( $\text{CH}_3$ ), 12.9 ( $\text{CH}_3$ ); MS(ESI-MS):  $m/z$  369.11 (M + H).<sup>+</sup>

***(E)-3-(3-(5-Bromothiophen-2-yl)-1-(4-fluorophenyl)-1H-pyrazol-4-yl)-1-(2,5-dimethylfuran-3-yl)prop-2-en-1-one (3b)***

Yield: 59%, yellow solid, mp: 112–114 °C; IR ( $\nu_{\max}$ ,  $\text{cm}^{-1}$ ): 2923 (=C–H), 2856 (C–H), 1656 (C=O), 1455 (C=N);  $^1\text{H-NMR}$  (400 MHz, DMSO- $d_6$ ,  $\delta$ , ppm): 9.25 (s, 1H, Pyrazole-H), 7.90 (dd, 2H,  $J=4.7$  & 9.0 Hz, Ar–H), 7.64 (d, 1H,  $J=15.4$  Hz, olefinic-H), 7.39–7.45 (m, 3H, Ar–H), 7.34 (d, 1H,  $J=3.8$  Hz, Ar–H), 7.25 (d, 1H,  $J=3.8$  Hz, Ar–H), 6.61 (s, 1H, Furan-H), 2.55 (s, 3H,  $-\text{CH}_3$ ), 2.28 (s, 3H,  $-\text{CH}_3$ );  $^{13}\text{C NMR}$  (100 MHz, DMSO- $d_6$ ,  $\delta$ , ppm): 184.2, 162.0, 159.6, 157.1, 149.7, 145.7, 135.4, 135.1, 131.4, 130.8, 128.9, 127.3, 124.6, 122.0, 120.7, 120.6, 117.3, 116.6, 116.3, 112.5, 105.9, 13.9, 12.9; MS (ESI-MS):  $m/z$  472.89 (M + H).<sup>+</sup>

***(E)-3-(3-(5-Bromothiophen-2-yl)-1-phenyl-1H-pyrazol-4-yl)-1-(2,5-dimethylfuran-3-yl)prop-2-en-1-one (3c)***

Yield: 68%, yellow solid, mp 120–114 °C; IR ( $\nu_{\max}$ ,  $\text{cm}^{-1}$ ): 2921 (=C–H), 2855 (C–H), 1699 (C=O), 1454 (C=N);  $^1\text{H-NMR}$  (400 MHz, DMSO- $d_6$ ,  $\delta$ , ppm): 9.14 (s, 1H, Pyrazole-H), 7.87 (d, 2H,  $J=7.8$  Hz, Ar–H), 7.70 (d, 1H,  $J=15$  Hz, olefinic-H), 7.52 (t, 2H,  $J=8$  Hz, Ar–H), 7.36–7.40 (m, 2H, Ar–H), 7.20 (s, 2H, Ar–H), 6.55 (s, 1H, Furan-H), 2.57 (s, 3H,  $-\text{CH}_3$ ), 2.29 (s, 3H,  $-\text{CH}_3$ );  $^{13}\text{C NMR}$  (100 MHz, DMSO- $d_6$ ,  $\delta$ , ppm): 184.3, 157.1, 149.7, 145.7, 138.6, 135.5, 131.4, 130.9, 129.7, 128.8, 127.3, 127.3, 124.6, 122.0, 118.6, 117.4, 112.5, 105.9, 13.9, 12.9; MS(ESI-MS):  $m/z$  454.57 (M + H).<sup>+</sup>

***(E)-1-(2,5-Dimethylfuran-3-yl)-3-(1-phenyl-3-(thiophen-2-yl)-1H-pyrazol-4-yl)prop-2-en-1-one (3d)***

Yield: 62%, yellow solid, mp 124–126 °C; IR ( $\nu_{\max}$ ,  $\text{cm}^{-1}$ ): 2921 (=C–H), 2715 (C–H), 1652 (C=O), 1456 (C=N);  $^1\text{H-NMR}$  (400 MHz, DMSO- $d_6$ ,  $\delta$ , ppm): 8.56 (s, 1H, Pyrazole-H), 7.91 (d, 2H,  $J=7.8$  Hz, Ar–H), 7.76 (d, 1H,  $J=15.4$  Hz, olefinic-H), 7.60 (d, 1H,  $J=5.1$  Hz, Ar–H), 7.54 (t, 2H,  $J=8.2$  Hz, Ar–H), 7.35–7.44 (m, 3H, Ar–H), 7.21 (dd, 1H,  $J=5.0$  & 3.7 Hz, Ar–H), 6.59 (s, 1H, Furan-H), 2.57 (s, 3H,  $-\text{CH}_3$ ), 2.29 (s, 3H,  $-\text{CH}_3$ );  $^{13}\text{C NMR}$  (100 MHz, DMSO- $d_6$ ,  $\delta$ , ppm): 184.4, 157.0, 149.7, 146.8, 138.7, 133.5, 131.5, 129.7, 128.7, 128.1, 127.3, 127.2, 126.8, 124.3, 122.1, 118.6, 117.4, 105.9, 13.9, 12.9; MS(ESI-MS):  $m/z$  375.10 (M + H).<sup>+</sup>

***General procedure for synthesis of pyrazolyl-pyrazoline (4a-d)***

A mixture of chalcone **3a-d** (0.001 mol) and hydrazine hydrate (0.004 mol) in solvent ethanol (10 ml) was refluxed in presence of catalytic amount of glacial acetic acid for 6 h. The progress of the reaction was monitored by TLC. After completion of the reaction, the reaction mixture was transferred into crushed ice. The precipitation observed, filtered it, washed with water and dried. The crystallization of product carried out in ethanol to get pure pyrazolines.

***4-(4,5-Dihydro-3-(2,5-dimethylfuran-3-yl)-1H-pyrazol-5-yl)-1,3-diphenyl-1H-pyrazole (4a)***

Yield: 74%, white solid, mp 102–104 °C; IR ( $\nu_{\max}$ ,  $\text{cm}^{-1}$ ): 3306 (N–H), 3049 (Ar–H), 1592 (C=N);  $^1\text{H-NMR}$  (400 MHz, DMSO- $d_6$ ,  $\delta$ , ppm): 8.56 (s, 1H, pyrazole-H), 7.90 (d, 2H,  $J=7.8$  Hz, Ar–H), 7.76 (d, 2H,  $J=8.3$  Hz, Ar–H), 7.47–7.52 (m, 4H, Ar–H), 7.41 (t, 1H,  $J=7.3$  Hz, Ar–H), 7.31 (t, 1H,  $J=7.4$  Hz, Ar–H), 7.20 (s, 1H, N–H), 6.19 (s, 1H, furan-H), 4.87 (t, 1H,  $J=10.7$  Hz, pyrazoline-H), 3.34 (dd, 1H,  $J=10.5$  & 15.6 Hz, pyrazoline-H), 2.88 (dd, 1H,  $J=11.1$  & 16.1 Hz, pyrazoline-H), 2.38 (s, 3H,  $\text{CH}_3$ ), 2.20 (s, 3H,  $\text{CH}_3$ );  $^{13}\text{C NMR}$  (100 MHz, DMSO- $d_6$ ,  $\delta$ , ppm): 150.4, 149.3, 147.6, 145.1, 139.5, 132.9, 129.5, 128.6, 127.9, 127.2, 126.2, 123.2, 118.1, 115.2, 105.9, 54.7, 41.9, 13.3, 12.9; MS (ESI-MS):  $m/z$  383.04 (M + H).<sup>+</sup>

**3-(5-Bromothiophen-2-yl)-1-(4-fluorophenyl)-4-(4,5-dihydro-3-(2,5-dimethylfuran-3-yl)-1H-pyrazol-5-yl)-1H-pyrazole (4b)**

Yield: 69%, white solid, mp 98–100 °C; IR ( $\nu_{\max}$ ,  $\text{cm}^{-1}$ ): 3310 (N–H), 3046 (Ar–H), 1594 (C=N);  $^1\text{H}$  NMR (400 MHz, DMSO- $d_6$ ,  $\delta$ , ppm): 8.54 (s, 1H, pyrazole-H), 7.88 (m, 2H, Ar–H), 7.35 (t, 2H,  $J=8.7$  Hz, Ar–H), 7.28 (dd, 2H,  $J=3.8$  Hz, Ar–H), 7.21 (s, 1H, N–H), 6.20 (s, 1H, furan-H), 4.93 (t, 1H,  $J=10.68$  Hz, pyrazoline-H), 3.37 (dd, 1H,  $J=10.7$  & 16.5 Hz, pyrazoline-H), 2.86 (dd, 1H,  $J=10.9$  & 16.1 Hz, pyrazoline-H), 2.38 (s, 3H,  $\text{CH}_3$ ), 2.20 (s, 3H,  $\text{CH}_3$ );  $^{13}\text{C}$  NMR (100 MHz, DMSO- $d_6$ ,  $\delta$ , ppm): 161.6, 159.1, 149.3, 147.7, 145.3, 144.1, 136.9, 135.6, 131.2, 128.0, 126.6, 122.6, 120.2, 120.2, 116.4, 116.2, 115.1, 111.5, 105.9, 54.3, 41.1, 13.3, 12.9; MS (ESI-MS):  $m/z$  486.93 (M + H).<sup>+</sup>

**3-(5-Bromothiophen-2-yl)-4-(4,5-dihydro-3-(2,5-dimethylfuran-3-yl)-1H-pyrazol-5-yl)-1-phenyl-1H-pyrazole (4c)**

Yield: 72%, white solid, mp 122–124 °C; IR ( $\nu_{\max}$ ,  $\text{cm}^{-1}$ ): 3303 (N–H), 3096 (Ar–H), 1593 (C=N),  $^1\text{H}$  NMR (400 MHz, DMSO- $d_6$ ,  $\delta$ , ppm): 8.55 (s, 1H, pyrazole-H), 7.84 (d, 2H,  $J=7.9$  Hz, Ar–H), 7.51 (t, 2H,  $J=7.6$  Hz, Ar–H), 7.22–7.34 (m, 4H, Ar–H), 6.20 (s, 1H, furan-H), 4.94 (t, 1H,  $J=10.6$  Hz, pyrazoline-H), 3.38 (m, 1H, pyrazoline-H), 2.88 (dd, 1H,  $J=12.1$  & 16.1 Hz, pyrazoline-H), 2.39 (s, 3H,  $\text{CH}_3$ ), 2.20 (s, 3H,  $\text{CH}_3$ );  $^{13}\text{C}$  NMR (100 MHz, DMSO- $d_6$ ,  $\delta$ , ppm): 149.3, 147.7, 145.2, 144.0, 139.0, 137.0, 131.2, 129.6, 127.8, 126.6, 126.5, 122.5, 118.0, 115.1, 111.4, 105.9, 54.4, 41.1, 13.3, 12.9; MS (ESI-MS):  $m/z$  468.95 (M + H).<sup>+</sup>

**4-(4,5-Dihydro-3-(2,5-dimethylfuran-3-yl)-1H-pyrazol-5-yl)-1-phenyl-3-(thiophen-2-yl)-1H-pyrazole (4d)**

Yield: 70%, white solid, mp 96–98 °C; IR ( $\nu_{\max}$ ,  $\text{cm}^{-1}$ ): 3336 (N–H), 3067 (Ar–H), 1501 (C=N);  $^1\text{H}$  NMR (400 MHz, DMSO- $d_6$ ,  $\delta$ , ppm): 8.53 (s, 1H, pyrazole-H), 7.86 (d, 1H,  $J=8$  Hz, Ar–H), 7.58 (d, 1H,  $J=4.9$  Hz, Ar–H), 7.47–7.52 (m, 3H, Ar–H), 7.31 (t, 1H,  $J=7.3$  Hz, Ar–H), 7.15–7.20 (m, 2H, Ar–H), 6.21 (s, 1H, furan-H), 4.98 (t, 1H,  $J=10.5$  Hz, pyrazoline-H), 3.42 (m, 1H, pyrazoline-H), 2.89 (dd, 1H,  $J=10.7$  & 16.1 Hz, pyrazoline-H), 2.39 (s, 3H,  $\text{CH}_3$ ), 2.20 (s, 3H,  $\text{CH}_3$ );  $^{13}\text{C}$  NMR (100 MHz, DMSO- $d_6$ ,  $\delta$ , ppm): 149.3, 147.7, 145.1, 144.9, 139.2, 135.0, 129.6, 127.9, 127.4, 126.3, 126.0, 125.8, 122.6, 118.1, 115.1, 105.9, 54.5, 41.3, 13.3, 12.9; MS (ESI-MS):  $m/z$  389.03 (M + H).<sup>+</sup>

**Experimental protocol for biological activity****Antimalarial assay**

The antimalarial activity of the synthesized compounds was carried out in the Microcare laboratory & TRC, Surat, Gujarat. According to the micro assay protocol of Rieckmann and coworkers the *in vitro* antimalarial assay was carried out in 96 well microtiter plates. To maintain *P. falciparum* strain culture in medium Roswell Park Memorial Institute (RPMI) 1640 supplemented with 25 mM (4-(2-hydroxyethyl)-1-piperazineethanesulfonic acid) (HEPES), 1% D-glucose, 0.23% sodium bicarbonate and 10% heat inactivated human serum. To obtain only the ring stage parasitized cells, 5% D-sorbitol treatment required to synchronized the asynchronous parasites of *P. falciparum*. To determine the percent parasitaemia (rings) and uniformly maintained with 50% RBCs ( $\text{O}^+$ ) an initial ring stage parasitaemia of 0.8 to 1.5% at 3% hematocrit in a total volume of 200  $\mu\text{l}$  of medium RPMI-1640 was carried out for the assay. A stock solution of 5 mg/ml of each of the test samples was prepared in DMSO and subsequent dilutions were prepared with culture medium. To the test wells to obtain final concentrations (at five-fold dilutions) ranging between 0.4  $\mu\text{g/ml}$  to 100  $\mu\text{g/ml}$  in duplicate well containing parasitized cell preparation the diluted samples in 20  $\mu\text{l}$  volume were added. In a candle jar, the culture plates were incubated at 37 °C. Thin

blood smears from each well were prepared and stained with Jaswant Singh-Bhattacharji (JSB) stain after 36 to 40 h incubation. To record maturation of ring stage parasites into trophozoites and schizonts in presence of different concentrations of the test agents the slides were microscopically observed. The minimum inhibitory concentrations (MIC) was recorded as the test concentration which inhibited the complete maturation into schizonts. Chloroquine was used as the reference drug.

After incubation for 38 hours, and percent maturation inhibition with respect to control group, the mean number of rings, trophozoites and schizonts recorded per 100 parasites from duplicate wells.

### **Molecular docking**

The crystal structure of *Plasmodium Falciparum* Enoyl-Acyl-Carrier-Protein Reductase (*Pf*ENR or FabI) in complex with its inhibitor Triclosan was retrieved from the protein data bank (PDB) (pdb code: 1NHG) and refined using the protein preparation wizard. It involves eliminating all crystallographically observed water (as no conserved interaction is reported with co-crystallized water molecules), addition of missing side chain/hydrogen atoms. Considering the appropriate ionization states for the acidic as well as basic amino acid residues, the appropriate charge and protonation state were assigned to the protein structure corresponding to pH 7.0 followed by thorough minimization, using OPLS-2005 force-field, of the obtained structure to relieve the steric clashes due to addition of hydrogen atoms. The 3D structures of the furan containing pyrazolyl chalcones (**3a-d**) were sketched using the build panel in Maestro and were optimized using the Ligand Preparation module followed by energy minimization using OPLS-2005 force-field until their average root mean square deviation (RMSD) reached 0.001 Å. The active site of *Pf*ENR was defined using receptor grid generation panel to include residues within a 10 Å radius around the co-crystallized ligand. Using this setup, flexible docking was carried using the extra precision (XP) Glide scoring function to gauge the binding affinities of these molecules and to identify binding mode within the target. The obtained results as docking poses were visualized and analyzed quantitatively for the thermodynamic elements of interactions with the residues lining the active site of the enzyme using the Maestro's Pose Viewer utility.

### **Acknowledgements**

Authors are thankful to Microcare laboratory and TRC, Surat, Gujarat for providing antimicrobial and antimalarial activities and Director, SAIF, Panjab University, Chandigarh for providing spectral data; Schrodinger Inc. for providing the software to perform the *in silico* study.

### **Disclosure statement**

No potential conflict of interest was reported by the author(s).

### **Funding**

Authors are thankful to Department of Science and Technology, New Delhi for providing financial assistance for research facilities under DST-FIST programme.

### **References**

1. E. A. Ashley, A. Pyae Phyo, and C. J. Woodrow, "Malaria," *The Lancet* 391, no. 10130 (2018): 1608–21.
2. World Health Organization. "World Malaria Report 2019" (World Health Organization, Geneva, 2019). Licence: CC BY-NC-SA 3.0 IGO.

3. J. Talapko, I. Skrlec, T. Alebic, M. Jukic, and A. Vcev, "Malaria: The Past and the Present," *Microorganisms* 7 (2019): 179.
4. R. J. Heath, and C. O. Rock, "Enoyl-Acyl Carrier Protein Reductase (fabI) Plays a Determinant Role in Completing Cycles of Fatty Acid Elongation in Escherichia coli," *The Journal of Biological Chemistry* 270, no. 44 (1995): 26538–42.
5. R. F. Waller, S. A. Ralph, M. B. Reed, V. Su, J. D. Douglas, D. E. Minnikin, A. F. Cowman, G. S. Besra, and G. I. McFadden, "A Type II Pathway for Fatty Acid Biosynthesis Presents Drug Targets in Plasmodium falciparum," *Antimicrobial Agents and Chemotherapy* 47, no. 1 (2003): 297–301.
6. G. Nicola, C. A. Smith, E. Lucumi, M. R. Kuo, L. Karagyzov, D. A. Fidock, J. C. Sacchetti, and R. Abagyan, "Discovery of Novel Inhibitors Targeting Enoyl-Acyl Carrier Protein Reductase in Plasmodium falciparum by Structure-Based Virtual Screening," *Biochemical and Biophysical Research Communications* 358, no. 3 (2007): 686–91.
7. N. Surolia, and A. Surolia, "Triclosan Offers Protection against Blood Stages of Malaria by Inhibiting enoyl-ACP Reductase of Plasmodium falciparum," *Nature Medicine* 7, no. 2 (2001): 167–73.
8. S. Sharma, T. N. C. Ramya, A. Surolia, and N. Surolia, "Triclosan as a Systemic Antibacterial Agent in a Mouse Model of Acute Bacterial Challenge," *Antimicrobial Agents and Chemotherapy* 47, no. 12 (2003): 3859–66.
9. R. P. Samal, V. M. Khedkar, R. R. S. Pissurlenkar, A. G. Bwalya, D. Tasdemir, R. A. Joshi, P. R. Rajamohan, V. G. Puranik, and E. C. Coutinho, "Design, Synthesis, Structural Characterization by IR, (1) H, (13) C, (15) N, 2D-NMR, X-Ray Diffraction and Evaluation of a New Class of Phenylaminoacetic Acid Benzylidene Hydrazines as pFENR Inhibitors," *Chemical Biology & Drug Design* 81, no. 6 (2013): 715–29.
10. M. Chhibber, G. Kumar, P. Parasuraman, T. N. C. Ramya, N. Surolia, and A. Surolia, "Novel Diphenyl Ethers: Design, Docking Studies, Synthesis and Inhibition of Enoyl ACP Reductase of Plasmodium falciparum and Escherichia coli," *Bioorganic & Medicinal Chemistry* 14, no. 23 (2006): 8086–98.
11. V. A. Morde, M. S. Shaikh, R. R. S. Pissurlenkar, and E. C. Coutinho, "Molecular Modeling Studies, Synthesis, and Biological Evaluation of Plasmodium falciparum Enoyl-Acyl Carrier Protein Reductase (PfENR) Inhibitors," *Molecular Diversity* 13, no. 4 (2009): 501–17.
12. A. Manhas, A. Patel, M. Y. Lone, P. K. Jha, and P. C. Jha, "Identification of PfENR Inhibitors: A Hybrid Structure-Based Approach in Conjunction with Molecular Dynamics Simulations," *Journal of Cellular Biochemistry* 119, no. 10 (2018): 8490–500.
13. M. A. Berghot, and E. B. Moawad, "Convergent Synthesis and Antibacterial Activity of Pyrazole and Pyrazoline Derivatives of Diazepam," *European Journal of Pharmaceutical Sciences: Official Journal of the European Federation for Pharmaceutical Sciences* 20, no. 2 (2003): 173–9.
14. J. N. Dominguez, J. E. Charris, M. Caparelli, and F. Riggione, "Synthesis and Antimalarial Activity of Substituted Pyrazole Derivatives," *Arzneimittel-Forschung* 52, no. 6 (2002): 482–8.
15. R. Sridhar, P. T. Perumal, S. Etti, G. Shanmugam, M. N. Ponnuswamy, V. R. Prabavathy, and N. Mathivanan, "Design, Synthesis and anti-Microbial Activity of 1H-Pyrazole Carboxylates," *Bioorganic & Medicinal Chemistry Letters* 14, no. 24 (2004): 6035–40.
16. Shivapura Viveka, Dinesha Dinesha, Prasanna Shama, Shivalingegowda Naveen, Neratur Krishnappagowda Lokanath, and Gundibasappa Karikannar Nagaraja, "Design, Synthesis, Anticonvulsant and Analgesic Studies of New Pyrazole Analogues: A Knoevenagel Reaction Approach," *RSC Advances* 5, no. 115 (2015): 94786–95.
17. Z. Xu, C. Gao, Q. C. Ren, X. F. Song, L. S. Feng, and Z. S. Lv, "Recent Advances of Pyrazole-Containing Derivatives as Anti-Tubercular Agents," *European Journal of Medicinal Chemistry* 139, (2017): 429–40.
18. R. S. Fabiane, T. S. Vanessa, R. Viviane, P. B. Lysandro, R. O. Marli, G. B. Helio, Z. Nilo, A. P. M. Marcos, and F. M. Carlos, "Hypothermic and Antipyretic Effects of 3-Methyl- and 3-Phenyl-5-Hydroxy-5-Trichloromethyl-4,5-Dihydro-1H-Pyrazole-1-Carboxyamides in Mice," *European Journal of Pharmacology* 451 (2002): 141–7.
19. A. Ana, R. C. Jose, P. C. Fernando, D. O. Agel, J. G. Maria, H. Antonio, L. Fernando, and M. Andres, "Efficient Tautomerization Hydrazone-Azomethine Imine under Microwave Irradiation. Synthesis of [4,3] and [5,3]Bipyrazoles," *Tetrahedron* 54 (1998): 13167–80.
20. K. O. Mohammed, and Y. M. Nissan, "Synthesis, Molecular Docking, and Biological Evaluation of Some Novel Hydrazones and Pyrazole Derivatives as Anti-Inflammatory Agents," *Chemical Biology & Drug Design* 84, no. 4 (2014): 473–88.
21. B. Insuasty, A. Montoya, D. Becerra, J. Quiroga, R. Abonia, S. Robledo, I. D. Velez, Y. Upegui, M. Noguera, and J. Cobo, "Synthesis of Novel Analogs of 2-pyrazoline Obtained from [(7-Chloroquinolin-4-yl)Amino]Chalcones and Hydrazine as Potential Antitumor and Antimalarial Agents," *European Journal of Medicinal Chemistry* 67 (2013): 252–62.
22. G. Kumar, O. Tanwar, J. Kumar, M. Akhter, S. Sharma, C. R. Pillai, M. M. Alam, and M. S. Zama, "Pyrazole-Pyrazoline as Promising Novel Antimalarial Agents: A Mechanistic Study," *European Journal of Medicinal Chemistry* 149 (2018): 139–47.



23. R. Alam, A. Alam, and A. K. Panda Rahisuddin, "Design, Synthesis and Cytotoxicity Evaluation of Pyrazolyl Pyrazoline and Pyrazolyl Aminopyrimidine Derivatives as Potential Anticancer Agents," *Medicinal Chemistry Research* 27 (2018): 560–70.
24. S. Viveka, D. P. Shama, G. K. Nagaraja, S. Ballav, and S. Kerkar, "Design and Synthesis of Some New Pyrazolyl-Pyrazolines as Potential Anti-Inflammatory, Analgesic and Antibacterial Agents," *European Journal of Medicinal Chemistry* 101 (2015): 442–51.
25. H. Khanam, A. Mashrai, A. Sherwani, M. Owais, and N. Siddiqui, "Synthesis and Anti-Tumor Evaluation of B-Ring Substituted Steroidal Pyrazoline Derivatives," *Steroids* 78, (2013): 1263–72.
26. S. K. Sahu, M. Banerjee, A. Samantray, C. Behera, and M. A. Azam, "Synthesis, Analgesic, anti-Inflammatory and Antimicrobial Activities of Some Novel Pyrazoline Derivatives," *Tropical Journal of Pharmaceutical Research* 7, no. 2 (2008): 961–8.
27. M. Johnson, B. Younglove, L. Lee, R. LeBlanc, H. Holt, Jr, P. Hills, H. Mackay, T. Brown, S. L. Mooberry, and M. Lee, "Design, Synthesis, and Biological Testing of Pyrazoline Derivatives of combretastatin-A4," *Bioorganic & Medicinal Chemistry Letters* 17, no. 21 (2007): 5897–901.
28. J. Vinayagam, R. L. Gajbhiye, L. Mandal, M. Arumugam, A. Achari, and P. Jaisankar, "Substituted Furans as Potent Lipoxigenase Inhibitors: Synthesis, in Vitro and Molecular Docking Studies," *Bioorganic Chemistry* 71 (2017): 97–101.
29. C. J. Lim, N. H. Kim, H. J. Park, B. H. Lee, K. S. Oh, and K. Y. Yi, "Synthesis and SAR of 5-Aryl-Furan-2-Carboxamide Derivatives as Potent urotensin-II Receptor Antagonists," *Bioorganic & Medicinal Chemistry Letters* 29, no. 4 (2019): 577–80.
30. B. Wang, Y. Shi, Y. Zhan, L. Zhang, Y. Zhang, L. Wang, X. Zhang, Y. Li, Z. Li, and B. Li, "Synthesis and Biological Activity of Novel Furan/Thiophene and Piperazine-Containing (Bis)1,2,4-Triazole Mannich Bases," *Chinese Journal of Chemistry* 33, no. 10 (2015): 1124–34.
31. Z. Lan, D. Xinshan, W. Jiaofeng, M. Guangpeng, L. Congchong, C. Guzhou, Z. Qingchun, and H. Chun, "Design, Synthesis and Biological Activities of N-(Furan-2-Ylmethyl)-1H-Indole-3-Carboxamide Derivatives as Epidermal Growth Factor Receptor Inhibitors and Anticancer Agents," *Chemical Research in Chinese Universities* 33, no. 3 (2017): 365–72.
32. M. L. Go, M. Liu, P. Wilairat, P. J. Rosenthal, K. J. Saliba, and K. Kirk, "Anti-plasmodial Chalcones Inhibit Sorbitol-Induced Hemolysis of Plasmodium falciparum-Infected Erythrocytes," *Antimicrobial Agents and Chemotherapy* 48, no. 9 (2004): 3241–5.
33. J. A. Gonzalez, and A. Estevez-Braun, "Effect of (E)-Chalcone on Potato-Cyst Nematodes *Globodera pallida* and *G. rostochiensis*," *Journal of Agricultural and Food Chemistry* 46 (1998): 1163–5.
34. M. Yoshimura, A. Sano, J. L. Kamei, and A. Obata, "Identification and Quantification of Metabolites of Orally Administered Naringenin Chalcone in Rats," *Journal of Agricultural and Food Chemistry* 57, no. 14 (2009): 6432–7.
35. M. Chen, T. G. Theander, S. B. Christensen, L. Hviid, L. Zhai, and A. Kharazmi, "Licochalcone A, a New Antimalarial Agent, Inhibits in Vitro Growth of the Human Malaria Parasite *Plasmodium falciparum* and Protects Mice from *P. yoelii* Infection," *Antimicrobial Agents and Chemotherapy* 38, no. 7 (1994): 1470–5.
36. L. Mishra, R. Sinha, H. Itokawa, K. F. Bastow, Y. Tachibana, Y. Nakanishi, N. Kilgore, and K. H. Lee, "Anti-HIV and Cytotoxic Activities of Ru(II)/Ru(III) Polypyridyl Complexes Containing 2,6-(2'-Benzimidazolyl)-Pyridine/Chalcone as Co-Ligand," *Bioorganic & Medicinal Chemistry* 9, no. 7 (2001): 1667–71.
37. C. Jin, Y. J. Liang, H. He, and L. Fu, "Synthesis and Antitumor Activity of Novel Chalcone Derivatives," *Biomedicine & Pharmacotherapy = Biomedecine & Pharmacotherapie* 67, no. 3 (2013): 215–7.
38. F. Herencia, M. L. Ferrándiz, A. Ubeda, J. N. Domínguez, J. E. Charris, G. M. Lobo, and M. J. Alcaraz, "Synthesis and anti-Inflammatory Activity of Chalcone Derivatives," *Bioorganic & Medicinal Chemistry Letters* 8, no. 10 (1998): 1169–74.
39. Y. Qian, G. Y. Ma, Y. Yang, K. Cheng, Q. Z. Zheng, W. J. Mao, L. Shi, J. Zhao, and H. L. Zhu, "Synthesis, Molecular Modeling and Biological Evaluation of Dithiocarbamates as Novel Antitubulin Agents," *Bioorganic & Medicinal Chemistry* 18, no. 12 (2010): 4310–6.
40. R. A. Friesner, J. L. Banks, R. B. Murphy, T. A. Halgren, J. J. Klicic, D. T. Mainz, M. P. Repasky, E. H. Knoll, M. Shelley, J. K. Perry, et al. "Glide: A New Approach for Rapid, Accurate Docking and Scoring. 1. Method and Assessment of Docking accuracy," *Journal of Medicinal Chemistry* 47, no. 7 (2004): 1739–49.
41. R. A. Friesner, R. B. Murphy, M. P. Repasky, L. L. Frye, J. R. Greenwood, T. A. Halgren, P. C. Sanschagrin, and D. T. Mainz, "Extra Precision Glide: Docking and Scoring Incorporating a Model of Hydrophobic Enclosure for Protein-Ligand Complexes," *Journal of Medicinal Chemistry* 49, no. 21 (2006): 6177–96.
42. T. A. Halgren, R. B. Murphy, R. A. Friesner, H. S. Beard, L. L. Frye, W. T. Pollard, and J. L. Banks, "Glide: A New Approach for Rapid, Accurate Docking and Scoring. 2. Enrichment Factors in Database Screening," *Journal of Medicinal Chemistry* 47, no. 7 (2004): 1750–9.

43. S. J. Takate, A. D. Shinde, B. K. Karale, H. Akolkar, L. Nawale, D. Sarkar, and P. C. Mhaske, "Thiazolyl-Pyrazole Derivatives as Potential Antimycobacterial Agents," *Bioorganic & Medicinal Chemistry Letters* 29, no. 10 (2019): 1199–202.
44. K. H. Rieckmann, G. H. Campbell, L. J. Sax, and J. E. Ema, "Drug Sensitivity of plasmodium falciparum. An In-Vitro Micro Technique," *The Lancet* 311, no. 8054 (1978): 22–3.
45. R. Panjarathinam, *Text Book of Medical Parasitology*, 2nd ed. (Chennai: Orient Longman Pvt. Ltd., 2007), 329–331.
46. C. Lambros, and J. P. Vanderberg, "Synchronization of Plasmodium falciparum Erythrocytic Stages in Culture," *The Journal of Parasitology* 65, no. 3 (1979): 418–20.
47. J. S. B. Singh, "Stain; a Review," *Indian Journal of Malariology* 10 (1956): 117–29.


 Cite this: *RSC Adv.*, 2020, 10, 26997

# Nanostructured N doped TiO<sub>2</sub> efficient stable catalyst for Kabachnik–Fields reaction under microwave irradiation†

 Sachin P. Kunde,<sup>ab</sup> Kaluram G. Kanade,<sup>ac</sup> Bhausaheb K. Karale,<sup>a</sup> Hemant N. Akolkar,<sup>a</sup> Sudhir S. Arbuj,<sup>d</sup> Pratibha V. Randhavane,<sup>a</sup> Santosh T. Shinde,<sup>a</sup> Mubarak H. Shaikh<sup>a</sup> and Aniruddha K. Kulkarni<sup>e</sup>

Herein, we report nitrogen-doped TiO<sub>2</sub> (N-TiO<sub>2</sub>) solid-acid nanocatalysts with heterogeneous structure employed for the solvent-free synthesis of  $\alpha$ -aminophosphonates through Kabachnik–Fields reaction. N-TiO<sub>2</sub> were synthesized by direct amination using triethylamine as a source of nitrogen at low temperature and optimized by varying the volume ratios of TiCl<sub>4</sub>, methanol, water, and triethylamine, under identical conditions. An X-ray diffraction (XRD) study showed the formation of a rutile phase and the crystalline size is 10 nm. The nanostructural features of N-TiO<sub>2</sub> were examined by HR-TEM analysis, which showed they had rod-like morphology with a diameter of  $\sim$ 7 to 10 nm. Diffuse reflectance spectra show the extended absorbance in the visible region with a narrowing in the band gap of 2.85 eV, and the high resolution XPS spectrum of the N 1s region confirmed successful doping of N in the TiO<sub>2</sub> lattice. More significantly, we found that as-synthesized N-TiO<sub>2</sub> showed significantly higher catalytic activity than commercially available TiO<sub>2</sub> for the synthesis of a novel series of  $\alpha$ -amino phosphonates via Kabachnik–Fields reaction under microwave irradiation conditions. The improved catalytic activity is due to the presence of strong and Bronsted acid sites on a porous nanorod surface. This work signifies N-TiO<sub>2</sub> is an efficient stable catalyst for the synthesis of  $\alpha$ -aminophosphonate derivatives.

Received 21st May 2020

Accepted 7th July 2020

DOI: 10.1039/d0ra04533k

[rsc.li/rsc-advances](http://rsc.li/rsc-advances)

## 1 Introduction

In recent years, organophosphorus compounds have received much attention due to their widespread applications in medicinal and agriculture industries.<sup>1,2</sup>  $\alpha$ -Aminophosphonates are one such biological important framework that are structural mimics of amino acids. For example, glyphosate (*N*-(phosphonomethyl)glycine) is extensively utilized in agriculture as a systemic herbicide and Alafosfalin is used as an antibacterial agent<sup>3</sup> (Fig. 1). The bioactivity of these molecules such as antimicrobial,<sup>4</sup> antioxidant,<sup>5</sup> anti-inflammatory,<sup>6</sup> enzyme inhibitors<sup>7</sup> and antibacterial<sup>8</sup> is one of the reasons for them to be of

immense interest in synthetic organic chemistry. It has been demonstrated that on incorporation of heterocycles such as thiophene,<sup>9</sup> benzothiazoles,<sup>10</sup> thiadiazoles,<sup>11</sup> and pyrazole<sup>12</sup> into the  $\alpha$ -aminophosphonates scaffold, the resulting compounds exhibited interesting biological activities. Pyrazole derivatives of  $\alpha$ -aminophosphonates have been rarely reported in the literature,<sup>13,14</sup> thus synthesis of novel pyrazole derivatives of  $\alpha$ -aminophosphonates is important to research.

Although several protocols for the synthesis of  $\alpha$ -aminophosphonates are reported, one of the most important is the Kabachnik–Fields reaction.<sup>15,16</sup> This involves a one-pot three-component coupling of a carbonyl compound, an amine and alkylphosphite. These protocols has been accomplished in presence of a variety of catalyst such as TiCl<sub>4</sub>,<sup>17</sup> CuI,<sup>18</sup> hexanesulphonic sodium salt,<sup>19</sup> trifluoroacetic acid (TFA),<sup>20</sup> In(OTf)<sub>3</sub>,<sup>21</sup> BiCl<sub>3</sub>,<sup>22</sup> Cu(OTf)<sub>2</sub>,<sup>23</sup> SbCl<sub>3</sub>/Al<sub>2</sub>O<sub>3</sub>,<sup>24</sup> InCl<sub>3</sub>,<sup>25</sup> LiClO<sub>4</sub>,<sup>26</sup> ZrOCl<sub>2</sub>,<sup>27</sup> TsCl,<sup>28</sup> Mg(ClO<sub>4</sub>)<sub>2</sub>,<sup>29</sup> and Na<sub>2</sub>CaP<sub>2</sub>O<sub>3</sub><sup>30</sup> in presence or

<sup>a</sup>PG and Research Centre, Radhabai Kale Mahila Mahavidyalaya, Ahmednagar, 414 001 India. E-mail: kgkanade@yahoo.co.in

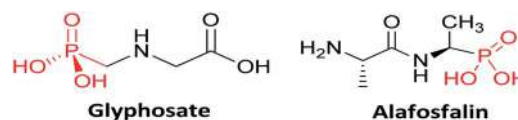
<sup>b</sup>PG and Research Centre, Mahatma Phule Arts, Science and Commerce College, Panvel, 410 206, India

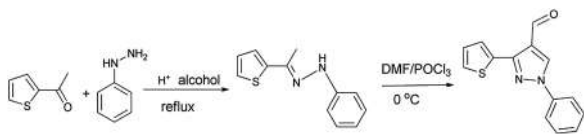
<sup>c</sup>PG and Research Centre, Yashwantrao Chavan Institute of Science, Satara, 415 001 India

<sup>d</sup>Centre for Materials for Electronics Technology (C-MET), Department of Electronics and Information Technology (DeitY), Government of India, Panchavati, Off Pashan Road, Pune-411 008, India

<sup>e</sup>Dr. John Barnabas School for Biological Studies, Department of Chemistry, Ahmednagar College, Ahmednagar-414 001, India

† Electronic supplementary information (ESI) available. See DOI: 10.1039/d0ra04533k


 Fig. 1 Some biological active  $\alpha$ -aminophosphonate.

Scheme 1 Synthesis of 1-phenyl-5-(thiophen-2-yl)-1H-pyrrole-3-carbaldehyde.

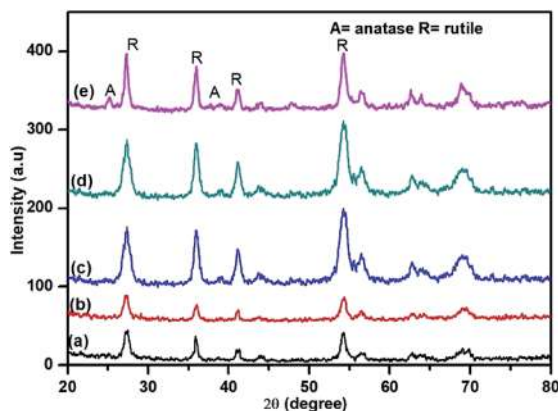


Fig. 2 X-ray diffraction patterns of (a) TN0 (TiO<sub>2</sub>), (b) TN1, (c) TN2 (d) TN3 (e) TN4.

even in the absence of a solvent. However, most of these existing procedures are sluggish, require long reaction times, use of strong acidic conditions, give unsatisfactory yields and also suffer from the formation of many side products. Moreover, in all alternatives microwave reaction proved to be a kind of promising medium for such reaction.<sup>31</sup>

In the last few years, the application of transition metal oxides gained particular interest as a heterogeneous catalyst for various organic synthesis.<sup>32</sup> Among all transition metal oxides the use of nanocrystalline titania (TiO<sub>2</sub>) has been grown extensively owing to their outstanding physiochemical properties, which furnished their wide applications in sensors,<sup>33</sup> pigments,<sup>34</sup> photovoltaic cells,<sup>35</sup> and catalysis.<sup>36</sup> Also, the use of potential titania catalyst attracted in organic synthesis due to its environmental compatibility, inexpensive, safe, stable, reusable and earth-abundant. It has been proven the desired property of TiO<sub>2</sub> was attained by fulfilling requirements in terms of unique morphology, high crystallinity and mixed-phase composition,

Table 1 Phase composition and crystallite size of as-prepared samples from analysis of XRD

Sample	Rutile	Anatase	Crystallite size (nm)
TN0	100	0	25
TN1	98	2	19
TN2	94	6	16
TN3	95	5	12
TN4	91	9	9

the ability of oxidizing and reducing ability under suitable irradiation makes promising greener alternative approach towards important organic transformations compared to other expensive, toxic, transition metal oxides. Moreover, the phase composition and the degree of crystallinity of the titania sample plays an important role in catalytic activity.<sup>8</sup> In the past several organic transformations such as oxidation of primary alcohols,<sup>37</sup> synthesis of xanthenes,<sup>38</sup> Friedel-Crafts alkylation,<sup>39</sup> Beckmann rearrangement<sup>40</sup> efficiently utilizes TiO<sub>2</sub> as a heterogeneous reusable catalyst. In the literature several reports have been debated to influence nitrogen doping on photocatalytic activity of nanocrystalline TiO<sub>2</sub>. However, the effect is unrevealed for catalytic applications in organic synthesis. Recently, Hosseini-Sarvari explored the use of commercial TiO<sub>2</sub> in the synthesis of  $\alpha$ -aminophosphonates *via* Kabachnik-Fields reactions.<sup>41</sup>

In present investigation, we have prepared nanostructured N doped TiO<sub>2</sub> and also investigation emphasis was given on the synthesis of a series of a novel diethyl(1-phenyl-3-(thiophen-2-yl)-1H-pyrazol-4-yl)(phenylamino) methylphosphonates under microwave irradiation.

## 2 Experimental sections

### 2.1 Synthesis of N doped TiO<sub>2</sub> nanorods

The nanostructured N-TiO<sub>2</sub> were synthesized by previously reported method with some modification.<sup>42,43</sup> In a typical procedure, 0.5 mL of titanium tetrachloride (TiCl<sub>4</sub>) was added in absolute methanol (25 mL) with constant stirring at room temperature. To this solution requisite quantity a 0.1–2 M aqueous triethylamine solution is injected rapidly. The resulting solution was refluxed for 24 h with constant stirring. The white precipitate formed was collected and washed with ethanol several times followed by centrifugation (10 000 rpm for 20 min). The precipitate was dried at 473 K for 24 h. To control the final morphologies of samples, the sample were synthesized as function of volume ratio of TiCl<sub>4</sub>, methanol, water, and triethylamine. The sample prepared in volume ratio 1 : 10 : 50 : 0, 1 : 10 : 50 : 1, 1 : 10 : 50 : 2, 2 : 10 : 50 : 2, and 2 : 10 : 50 : 4 were denoted as TN0 (pure TiO<sub>2</sub>), TN1, TN2, TN3 and TN4 respectively.

### 2.2 Synthesis of 1-phenyl-5-(thiophen-2-yl)-1H-pyrrole-3-carbaldehyde

1-Phenyl-5-(thiophene-2-yl)-1H-pyrrole-3-carbaldehyde were obtained *via* the Vilsmeier-Haack reaction of the appropriate phenylhydrazones, derived from the reaction of 2-acetyl thiophene with phenylhydrazine<sup>44</sup> (Scheme 1).

### 2.3 Synthesis of diethyl(1-phenyl-3-(thiophene-2-yl)-1H-pyrazole-4-yl)(phenylamino)methylphosphonates

In a typical procedure, the pyrazolealdehyde **1** (1 mmol), aniline **2** (1 mmol), triethyl phosphite **3** (1.1 mmol) and N-TiO<sub>2</sub> (12 mol%) were taken in a round bottom flask equipped with a condenser and subjected to microwave irradiation for (10–15 min) using 420 W (RAGA's Microwave system) (Scheme 3). The





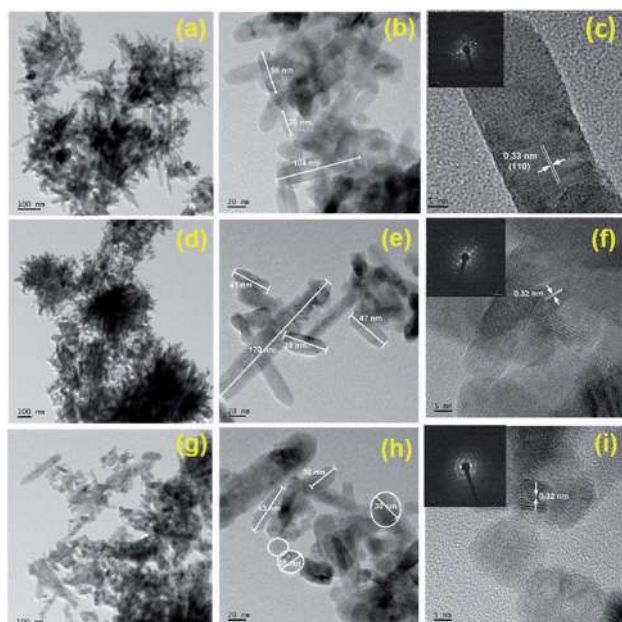


Fig. 3 HR-TEM images of (a–c) TN0, (d–f) TN1, and (g–i) TN2; inset c, f and h SAED pattern of TN0, TN2 and TN3 respectively.

progress of the reaction was monitored by TLC. After the reaction was completed, the reaction mixture extracted using ethyl acetate and insoluble catalyst separated by filtration. The crude product was purified by silica gel column chromatography using *n*-hexane/ethyl acetate as eluent. The product structure was determined by FTIR,  $^1\text{H}$  NMR, and LS-MS.

## 2.4 Samples characterization

The phase purity and crystallinity were examined by X-ray diffraction (XRD) technique (Advance, Bruker AXS D8) using  $\text{Cu K}\alpha 1$  (1.5406 Å) radiation with scanning  $2\theta$  range from 20 to 80°. For FE-TEM analysis samples were prepared by evaporating dilute solution on carbon-coated grids. FE-TEM measurements were carried using the JEOL SS2200 instrument operated at an

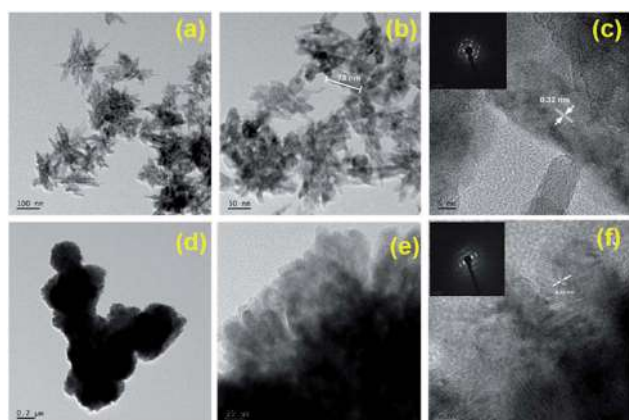


Fig. 4 HR-TEM images of (a–c) TN3 and (d–f) TN4; inset c, and f SAED pattern of TN3, and TN4 respectively.

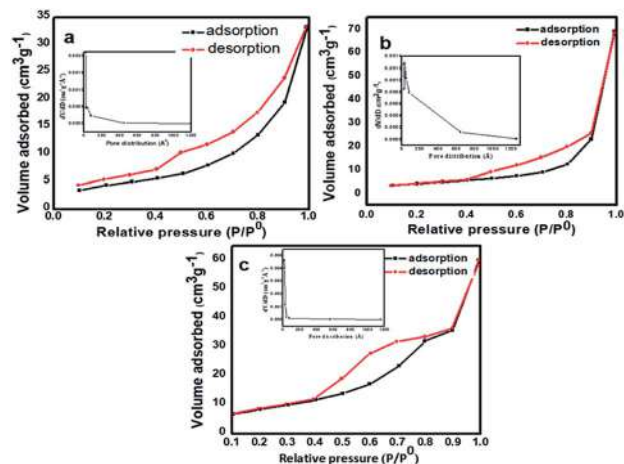


Fig. 5 Nitrogen ( $\text{N}_2$ ) adsorption–desorption isotherms of (a) TN0 ( $\text{TiO}_2$ ), (b) TN2 ( $\text{N-TiO}_2$ ), (c) TN4 ( $\text{N-TiO}_2$ ). Insets show their corresponding pore size distributions.

accelerating voltage of 300 kV. The Brunauer–Emmett–Teller (BET) surface area of nanocatalysts was examined using the Quantachrome v 11.02 nitrogen instrument. The optical properties of the powder samples were studied using UV-vis diffuse reflectance absorption spectra (UV-DRS) were recorded on the Perkin-Elmer Lambda-950 spectrophotometer in the wavelength range of 200–800 nm. Powder samples were used for XPS measurements. The XPS measurements of powdered samples were carried out on a VG Microtech ESCA3000 instrument. Fourier transform infrared (FTIR) spectra of prepared samples were recorded on a Shimadzu Affinity 1-S spectrophotometer in over a range of 400–4000  $\text{cm}^{-1}$ .  $^1\text{H}$  NMR was recorded in DMSO- $d_6$  solvent on a Bruker Advance-400 spectrometer with tetramethylsilane (TMS) as an internal reference.

## 3 Results and discussions

### 3.1 Structural study

Nanostructured  $\text{TiO}_2$  and N doped  $\text{TiO}_2$  were synthesized by a simple refluxing method. The phase purity and phase formation of as-synthesized material were analysed by powder X-ray diffraction pattern. Fig. 2 compares powder XRD patterns of  $\text{TiO}_2$  and N doped  $\text{TiO}_2$  samples. The peak position and peak intensity of the pure  $\text{TiO}_2$  powder can be indexed into rutile phases (Fig. 2). Further, it is observed that an increase in the amount N-dopant (triethylamine) the intensity of the diffraction

Table 2 BET specific surface area and pore size distribution of  $\text{TiO}_2$  and N- $\text{TiO}_2$

Sample	Surface area ( $\text{m}^2 \text{g}^{-1}$ )	Pore volume ( $\text{cm}^3 \text{g}^{-1}$ )	Pore radius (Å)
TN0	21.956	0.051	18.108
TN2	40.359	0.215	30.811
TN4	53.589	0.101	18.041





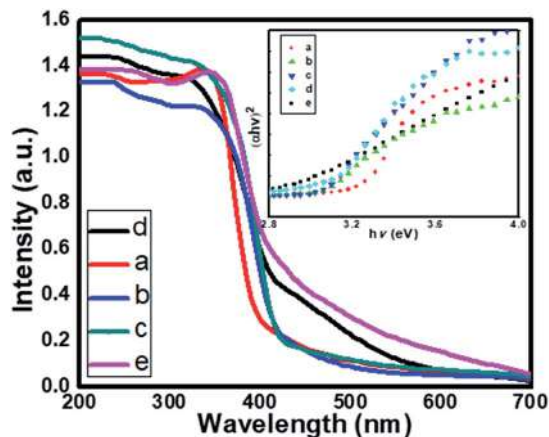


Fig. 6 UV-DRS spectra of (a) TN0 (TiO<sub>2</sub>), (b) TN1 (c) TN2 (d) TN3 (N-TiO<sub>2</sub>), (e) TN4. Inset shows Tauc plot of TiO<sub>2</sub> and N-TiO<sub>2</sub> samples.

peaks of the rutile phase decreases, while that of anatase phase increases, indicating that the fraction of the anatase phase gradually increases at the expense of the rutile phase during this condition (sample TN2–TN4). The phase composition of rutile and anatase phase of TiO<sub>2</sub> evaluated from the peak intensity using the following equation,

$$f_A = \frac{1}{1 + \frac{I_R}{K I_A}} \quad K = 0 : 79; f_A > 0.2; K_{1/4} = 0 : 68; f_A \leq 0.2$$

where  $f_A$  is the fraction of the anatase phase, and  $I_A$  and  $I_R$  are the intensities of the anatase (1 0 1) and rutile (1 1 0) diffraction peaks, respectively. The higher molar concentration of triethylamine is favourable for the transformation from rutile to anatase.<sup>45,46</sup> Therefore, the phase composition of TiO<sub>2</sub> samples, *i.e.* the fraction of anatase and rutile, can be facilely controlled through adjusting the concentration of triethylamine. The slight shift of rutile (1 1 0) diffraction peaks towards a higher angle with an increase in the amount of N dopant suggesting

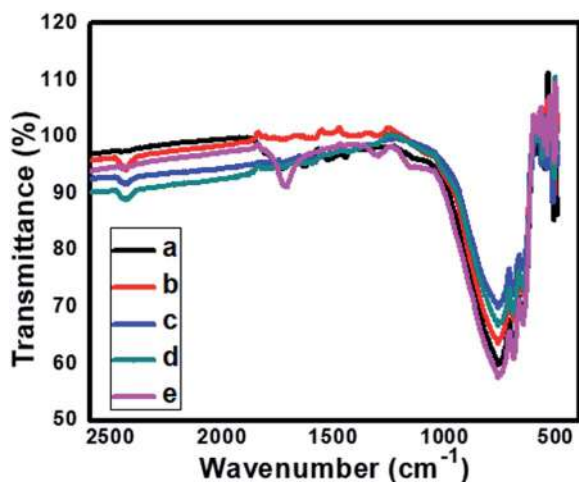


Fig. 7 FTIR spectra of (a) TN0 pure (TiO<sub>2</sub>), (b) TN1 (N-TiO<sub>2</sub>), (c) TN2, (d) TN3 and (e) TN4.

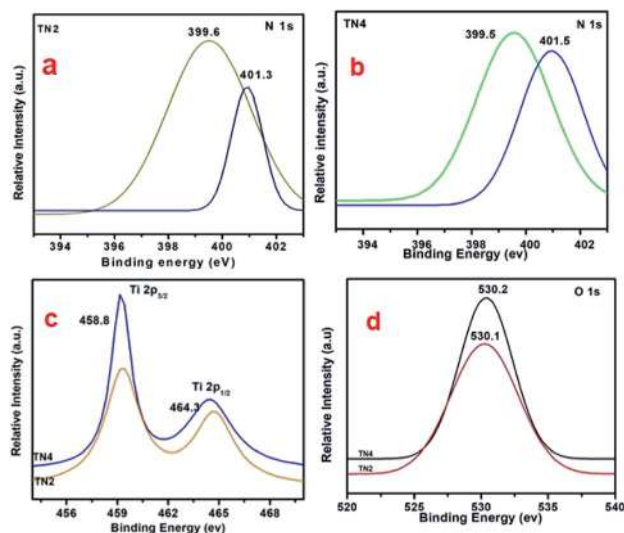
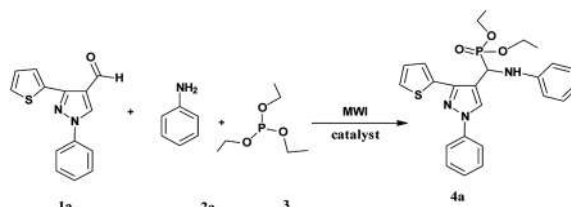


Fig. 8 (a and b) High resolution spectrum of N 1s region (c) high resolution spectrum of Ti 2p region (d) high resolution spectrum of O 1s region.

the incorporation of nitrogen in the TiO<sub>2</sub> crystal structure. The crystallite size is calculated from each (1 1 0) peak in the XRD pattern using the Sherrer formula.<sup>39</sup> The average crystalline size are 25, 19, 16, 12 and 9 nm for TN0, TN1, TN2, TN3, and TN4 respectively (Table 1). From, XRD analysis it is clear that with an increase in the concentration of nitrogen in TiO<sub>2</sub>, fraction of anatase increases phase and crystalline size decreases.

### 3.2 Surface and morphological study

Transmission electron microscopy (TEM) and high-resolution transmission electron microscopy (HRTEM) analysis were performed to study morphology and crystallinity of as-synthesized pure and N doped TiO<sub>2</sub> materials (Fig. 3). The pure TiO<sub>2</sub> (TN0) sample seems flowerlike nanostructures (Fig. 3a). At high-resolution it reveals that each flower microstructure consisting several nanorods. The length of nanorods are in the range of 50–70 nm and diameter is about 10–15 nm (Fig. 3b). Fig. 3c shows the lattice fringes of the material with interplanar spacing  $d$  spacing 0.33 nm matches well (1 0 0) plane of rutile TiO<sub>2</sub>. Fig. 3c inset shows a selected area diffraction pattern in which bright spots observed that confirm the TiO<sub>2</sub> nanorods are in nanocrystalline nature. It was observed that addition of N dopant, resulting sample TN1 and TN2 grows into new superstructure consisting nanorods of length 30–50 nm and spheres



Scheme 2 Standard model reaction.



**Table 3** Comparative study of catalysts used for the synthesis of  $\alpha$ -aminophosphonate<sup>a</sup>

Entry	Catalyst	Time (minutes)	Yield <sup>b</sup> (%)
1	—	20	Trace
2	Acetic acid	20	30
3	Commercial ZnO	15	20
4	Commercial TiO <sub>2</sub>	15	30
5	TN0	10	72
6	TN1	10	73
7	TN2	10	76
8	TN3	10	85
9	TN4	10	95

<sup>a</sup> Reaction condition: aldehyde(1a) (1 mmol), aniline (1 mmol), triethylphosphite (1.1 mmol), catalyst, MW power 420 watt. <sup>b</sup> Isolated yield.

of diameter 20–30 nm, particles size is obviously smaller than TN0 (Fig. 3d and h). HRTEM results are consistent with XRD results. The *d*-spacing is about 0.325 Å between adjacent lattice planes of the N doped TiO<sub>2</sub>.

It was revealed that with doubling concentration of TiCl<sub>4</sub>, sample TN3 and TN4 were grown into very fine agglomerated nanorods (Fig. 4). Further, it is observed that these nanorods having size in length 30–40 nm and diameter is around 7–10 nm which is lower than pure TiO<sub>2</sub>. Fig. 4f inset shows selected area diffraction pattern shows, surprisingly, ring-like pattern unlike TiO<sub>2</sub>, indicates N-TiO<sub>2</sub> nanorods are in polycrystalline nature. From HR-TEM results it is concluded that increase in concentration of TiCl<sub>4</sub> and triethylamine reduces the size of the nanorods.

The specific surface area of as-prepared samples was studied by (N<sub>2</sub>) nitrogen gas adsorption–desorption measurement at 77 K using the Brunauer–Emmett–Teller (BET) method. The N<sub>2</sub> adsorption–desorption isotherm of N-TiO<sub>2</sub> nanoparticles is shown in Fig. 5. The pure TiO<sub>2</sub> shows type IV isotherm according to IUPAC classification,<sup>47</sup> which are typical characteristics of a material with pore size in the range of 1.5–100 nm Fig. 5a. The shape of the hysteresis loop is H<sub>3</sub> type may associates due to the agglomeration of nanoparticles forming slit-like pores, reflected in TEM images. At higher relative pressure (*p/p*<sup>0</sup>) the slope shows increased uptake of adsorbate as pores become filled; inflection point typically occurs near

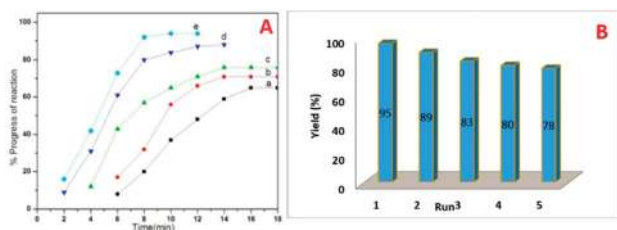


**Fig. 9** (A) Progress of reaction (a) TN0 (b) TN1 (c) TN2 (d) TN3 and (e) TN4. (B) Reusability of catalyst TN4; reaction condition: aldehyde (1a) (1 mmol), aniline (2a) (1 mmol), triethylphosphite 3 (1.1 mmol), N-TiO<sub>2</sub> (12 mol%), MW power 420 watt.

**Table 4** Optimization of the concentration of catalyst<sup>a</sup>

Sr. no.	Concentration of catalyst (mol%)	Yield <sup>b</sup> (%)
1	3	69
2	6	76
3	9	86
4	12	95
5	15	95

<sup>a</sup> Reaction condition: aldehyde (1a) (1 mmol), aniline (1 mmol), triethylphosphite (1.1 mmol), N-TiO<sub>2</sub> catalyst, MW power 420 watt. <sup>b</sup> Isolated yield.

completion of the first monolayer. The BET surface area of pure TiO<sub>2</sub> is found to be 21.956 m<sup>2</sup> g<sup>-1</sup>. The pore size distribution of prepared samples was investigated by Barrett–Joyner–Halenda (BJH) method Fig. 5(a)–(c) insets. The average pore diameter of pure TiO<sub>2</sub> nanoparticles is 18 nm which demonstrates the material is mesoporous nature. Further, it is observed that the incorporation of nitrogen in TiO<sub>2</sub> nanoparticles the surface area shifts towards higher values. The adsorption–desorption isotherms of nitrogen-doped TiO<sub>2</sub> samples display the type II isotherm according to IUPAC classification.<sup>46</sup> The specific BET surface area of samples TN<sub>2</sub> and TN<sub>4</sub> are 40.359 m<sup>2</sup> g<sup>-1</sup> and 53.589 m<sup>2</sup> g<sup>-1</sup> respectively (Fig. 5b and 4c). This observation specifies a decrease in the particle size of TiO<sub>2</sub> nanoparticles specific surface area increases which are in consisting of XRD and TEM results. The Brunauer–Emmett–Teller (BET) specific surface areas, pore volumes and mean pore and mean pore diameters of samples TN0, TN2, and TN4 are summarized in Table 2.

### 3.3 Optical and electronic property studies

The optical property of the as-synthesized material was analyzed by UV-Vis diffuse absorbance spectra as shown in Fig. 6. Fig. 6 displays the comparative UV-DRS spectra of pristine TiO<sub>2</sub> and a series of N doped TiO<sub>2</sub> samples. The absorption edge for the pure TiO<sub>2</sub> (TN0) is observed at around 410 nm (Fig. 6a), which is consistent with the band gap of the rutile phase.<sup>45</sup> The N doped TiO<sub>2</sub> nanostructures show strong absorption in the visible region (410–600 nm). The redshift clearly indicates the

**Table 5** Screening of solvents<sup>a</sup>

Entry	Solvent	Yield (%) <sup>b</sup>
1	Ethanol	85
2	Methanol	87
3	Dichloromethane	55
4	THF	58
6	Toluene	60
7	Neat	95

<sup>a</sup> Reaction condition: aldehyde (1a) (1 mmol), aniline (1 mmol), triethylphosphite (1.1 mmol), N-TiO<sub>2</sub> catalyst, solvent, MW power 420 watt. <sup>b</sup> Isolated yield.



successful doping of N in the lattice of TiO<sub>2</sub>. Moreover, as the concentration of triethylamine increases redshift of N-TiO<sub>2</sub> also increases which confirms higher nitrogen doping and a higher fraction of absorption of photons from the visible region. The band gap of as-synthesized material calculated by using the Tauc plot shown in Fig. 6 (insets). The band gap ( $E_g$ ) for the sample TN0, TN1, TN2, TN3, and TN4, were observed to 3.15, 3.09, 3.07, 3.03 and 2.85 eV respectively. The decrease in the band gap is attributed to higher mixing of the (O/N) 2p level is developed in the Ti-3d level falls at the top of the VB, therefore, band gap reduced compared to the pristine TiO<sub>2</sub> nanostructure.

### 3.4 FT-IR spectroscopy

Fig. 7 shows comparative FTIR spectra for pure and N doped TiO<sub>2</sub>. The absorption peak signal in the range of 400–1100 cm<sup>-1</sup> is characteristic of the formation of O-Ti-O lattice. The absorption at 668 cm<sup>-1</sup>, 601 cm<sup>-1</sup>, 546 cm<sup>-1</sup> and 419 cm<sup>-1</sup> corresponds to Ti-O vibrations.<sup>48,49</sup> Further, for the sample TN1–TN3 the IR bands centred at 1400–1435 cm<sup>-1</sup> indicates nitrogen doping in the TiO<sub>2</sub> sample. The band located at 1070 cm<sup>-1</sup> is attributed to Ti-N bond vibrations. Also, it is observed that the band at 1335 cm<sup>-1</sup> for pure TiO<sub>2</sub> is shifted towards longer wavenumber 1430 cm<sup>-1</sup> supports for the claim of N doping in TiO<sub>2</sub> lattice. Further it is also observed that some of the minor the peaks of pure TiO<sub>2</sub> are rather different than the N-doped TiO<sub>2</sub>, this indicates the incorporation of nitrogen in TiO<sub>2</sub> lattices. The peak centered at 1600–2180 cm<sup>-1</sup> is ascribed due to -OH stretching frequency. From, IR spectra it is clear that N<sub>2</sub> is successfully incorporated in the lattice of TiO<sub>2</sub>.

### 3.5 X-ray photoelectron spectroscopy

The XPS were used for chemical identification and electronic state of dopant nitrogen in sample TN2 and TN4. The high resolution XPS spectra of N 1s on deconvolution shows two different peaks at 399.6 and 401.5 eV indicates nitrogen present in two different electronic state (Fig. 8a and b). The peak at 399.6 is attributed to presence of interstitial N or N-Ti-O linkage. The result is consistent with previous reports.<sup>43</sup> The peak at 401.5 is attributed to presence of N in oxidized state as NO or NO<sub>2</sub>. The concentration of nitrogen on surface of TN2 and TN4 are 2.8% and 3.4% respectively. Fig. 8c shows the peak at 458.8 and 458.3 is attributed to Ti 2p<sub>3/2</sub> and Ti 2p<sub>1/2</sub>, in good agreement the presence of Ti(IV) in TiO<sub>2</sub>. The peak at binding energy 530.1 and 530.2 eV of sample are attributed to O 1s (Fig. 8d).

### 3.6 Catalytic study in synthesis of $\alpha$ -aminophosphonates

In order to find out the best experimental condition, the reaction of pyrazolaldehyde **1a**, aniline **2a** and triethylphosphite **3** under microwave irradiation is considered as standard model reaction (Scheme 2).

In the absence of a catalyst, the standard model reaction gave a small amount of product (Table 3 entry 1). These results specify catalyst is required to occur reaction. In order to check the catalytic utility, the model reaction carried out in the presence of a variety of catalysts (Table 3 entry 2–9). The N-TiO<sub>2</sub> NRs

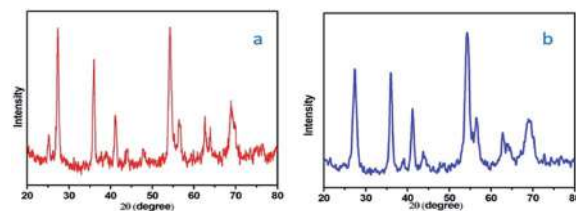


Fig. 10 XRD of sample TN4 (a) before reaction (b) after reaction.

gave better results than acetic acid, commercial ZnO and commercial TiO<sub>2</sub>.

Inspiring these results, we further studied the progress of reaction at different time intervals, we observed the sample N-doped TiO<sub>2</sub> catalyzes efficiently than undoped TiO<sub>2</sub>, and this may be attributed to the higher surface area (Fig. 9A).

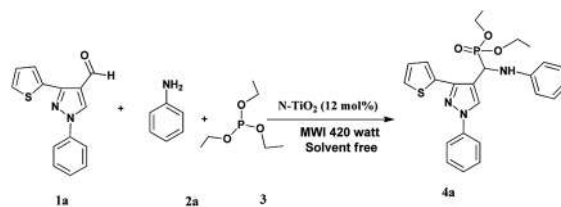
The optimum concentration of the catalyst was investigated by performing the model reaction at different concentrations such as 3, 6, 9, 12 and 15 mol%. The reaction yielded in 69, 76, 86, 95 and 95% yields respectively (Table 4). This shows that 12 mol% of TN<sub>4</sub> is adequate for the reaction by considering the yield of the product.

To evaluate the effect of solvents, different solvents such as ethanol, methanol, dichloromethane, THF, 1,4-dioxane and toluene were used for the model reaction in presence of N-TiO<sub>2</sub> catalyst. The reaction proceed with better yield in polar protic solvent (Table 5, entries 1, 2). However it was observed that the usage of solvents slows down the rate of reaction and gives the desired product in lower yields than that for neat condition (Table 5, entries 1–6).

The recyclability of the catalyst was then examined and the outcomes are shown in Fig. 9B. After the completion of reaction, the reaction mixture was extracted with ethyl acetate. The residual catalyst was washed with acetone, dried under vacuum at 100 °C and reused for consequent reactions. The recovered catalyst could be used for 5 times without obvious loss of catalytic activity.

The difference between the XRD of fresh catalyst and reused catalyst shown in Fig. 10.

The usefulness of optimized reaction condition for model reaction (12 mmol % of catalyst, solvent-free, MWI) was extended for the synthesis of a series of novel  $\alpha$ -amino-phosphonates (**4a–I**) by reacting pyrazolaldehyde (**1a–c**), anilines (**2a–d**) and triethylphosphite (**3**) in excellent yields (Scheme 3).



Scheme 3 Optimized reaction condition for synthesis of diethyl(1-phenyl-3-(thiophen-2-yl)-1H-pyrazol-4-yl)(phenylamino) methylphosphonates



Table 6 Microwave assisted synthesis of novel diethyl(1-phenyl-3-(thiophen-2-yl)-1H-pyrazol-4-yl)(phenylamino)methylphosphonates<sup>a</sup>

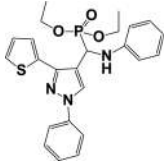
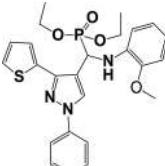
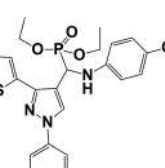
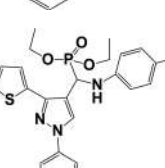
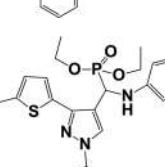
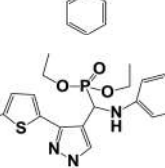
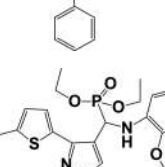
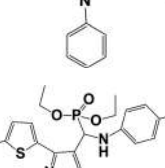
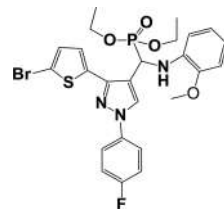
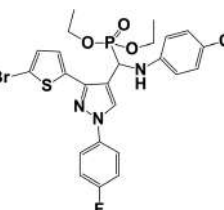
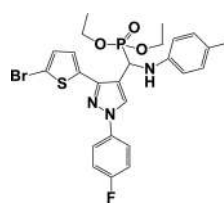
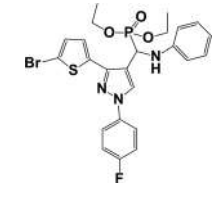
Entry	Product	M.P. (°C)	Yield <sup>b</sup> (%)
4a		218	95
4b		220	79
4c		208	92
4d		216	79
4e		180	86
4f		200	82
4g		162	85
4h		190	71

Table 6 (Contd.)

Entry	Product	M.P. (°C)	Yield <sup>b</sup> (%)
4i		195	81
4j		120	76
4k		210	89
4l		190	75

<sup>a</sup> Reaction condition: aldehyde (1 mmol), aniline (1 mmol), triethylphosphite (1.1 mmol), N-TiO<sub>2</sub> (12 mol%), MW power 420 watt.  
<sup>b</sup> Isolated yield.

The obtained product **4a–l** was characterized by spectroscopic techniques (Table 6).

The spectroscopic data of synthesized compounds are given in ESI (S-2 to S-26).†

## 4 Conclusions

In summary, we have prepared N doped TiO<sub>2</sub> nanorods by thermal hydrolysis method using triethylamine as the source of nitrogen at relatively low temperatures. The XRD analysis showed that with varying composition molar ratios of TiCl<sub>4</sub>, CH<sub>3</sub>OH, H<sub>2</sub>O, and (C<sub>2</sub>H<sub>5</sub>)<sub>3</sub>N, phase composition of rutile to anatase also tunes. FTIR spectra show the chemical environment of doping by the formation of the N-Ti-O and Ti-O-Ti bond. The morphological study performed by the FE-TEM technique shows the formation of well-developed nanorods of size in length 30–40 nm and diameter is around 7–10 nm, which is lower than pure TiO<sub>2</sub>. Further, BET analysis N-TiO<sub>2</sub> shows the maximum specific surface area 53.4 m<sup>2</sup> g<sup>-1</sup> which is 2.5 times





higher than pure TiO<sub>2</sub>. The as-synthesized materials were employed for the synthesis of  $\alpha$ -aminophosphonates via Kabachnik–Fields reaction under microwave irradiation. The N-TiO<sub>2</sub> shows remarkable catalytic activity for aminophosphonate derivatives compared with TiO<sub>2</sub> and other similar nanocatalysts.

## Conflicts of interest

There are no conflicts to declare.

## Acknowledgements

SPK is gratefully acknowledged UGC New Delhi for the award of Senior Research Fellowship (F.11-16/2013(SA-I)). The authors are thankful to parent institute Rayat Shikshan Sanstha, Satara.

## Notes and references

- L. G. Costa, *Toxicol. Sci.*, 2018, **162**(1), 24–35.
- M. Eto, *Organophosphorus pesticides*, CRC press, 2018.
- A. Mucha, P. Kafarski and L. Berlicki, *J. Med. Chem.*, 2011, **54**(17), 5955–5980.
- M. K. Awad, M. F. Abdel-Aal, F. M. Atlam and H. A. Hekal, *Spectrochim. Acta, Part A*, 2018, **206**, 78–88.
- M. M. Azaam, E. R. Kenawy, A. S. El-din, A. A. Khamis and M. A. El-Magd, *J. Saudi Chem. Soc.*, 2018, **22**(1), 34–41.
- R. Damiche and S. Chafaa, *J. Mol. Struct.*, 2017, **1130**, 1009–1017.
- Z. Chen, P. Marce, R. Resende, P. M. Alzari, A. C. Frasch, J. M. Van den Elsen, S. J. Crennell and A. G. Watts, *Eur. J. Med.*, 2018, **158**, 25–33.
- A. Hellal, S. Chafaa, N. Chafai and L. Touafri, *J. Mol. Struct.*, 2017, **1134**, 217–225.
- D. Rogacz, J. Lewkowski, M. Siedlarek, R. Karpowicz, A. Kowalczyk and P. Rychter, *Materials*, 2019, **12**(12), 2018.
- L. Jin, B. Song, G. Zhang, R. Xu, S. Zhang, X. Gao and S. Yang, *Bioorg. Med. Chem. Lett.*, 2006, **16**(6), 537–1543.
- S. M. Lu and R. Y. Chen, *Org. Prep. Proced. Int.*, 2000, **32**(3), 302–306.
- A. G. Nikalje, P. A. Gawhane, S. V. Tiwari, J. N. Sangshetti and M. G. Damale, *Anti-Cancer Agents Med. Chem.*, 2018, **18**(9), 1267–1280.
- C. W. Guo, S. H. Wu, F. L. Chen, Z. Y. Han, X. H. Fu and R. Wan, *Phosphorus, Sulfur Silicon Relat. Elem.*, 2016, **191**(9), 1250–1255.
- L. Wu, B. Song, P. S. Bhadury, S. Yang, D. Hu and L. Jin, *J. Heterocycl. Chem.*, 2011, **48**, 389–396.
- W. Fan, Y. Queneau and F. Popowycz, *RSC Adv.*, 2018, **8**, 31496–31501.
- B. Rajendra Prasad Reddy, P. Vasu Govardhana Reddy and B. N. Reddy, *New J. Chem.*, 2015, **39**, 9605–9610.
- Y. T. Reddy, P. N. Reddy, B. S. Kumar, P. Rajput, N. Sreenivasulu and B. Rajitha, *Phosphorus, Sulfur Silicon Relat. Elem.*, 2007, **182**(1), 161–165.
- H. Fang, X. Xie, B. Hong, Y. Zhao and M. Fang, *Phosphorus, Sulfur Silicon Relat. Elem.*, 2011, **186**(11), 2145–2155.
- K. S. Niralwad, B. B. Shingate and M. S. Shingare, *Ultrason. Sonochem.*, 2010, **17**(5), 760–763.
- T. Akiyama, M. Sanada and K. Fuchibe, *Synlett*, 2003, **10**, 1463–1464.
- R. Ghosh, S. Maiti, A. Chakraborty and D. K. Maiti, *J. Mol. Catal. A: Chem.*, 2004, **210**(1–2), 53–57.
- Z. P. Zhan and J. P. Li, *Synth. Commun.*, 2005, **35**(19), 2501–2508.
- A. S. Paraskar and A. Sudalai, *ARKIVOC*, 2006, 183–189.
- K. S. Ambica, S. C. Taneja, M. S. Hundal and K. K. Kapoor, *Tetrahedron Lett.*, 2008, **49**, 2208–2212.
- B. C. Ranu, A. Hajraa and U. Jana, *Org. Lett.*, 1999, **1**, 1141–1143.
- N. Azizi, F. Rajabi and M. R. Saidi, *Tetrahedron Lett.*, 2004, **45**, 9233–9236.
- S. Bhagat and A. K. Chakraborti, *J. Org. Chem.*, 2008, **73**, 6029–6032.
- B. Kaboudin and E. Jafari, *Synlett*, 2008, **12**, 1837–1839.
- S. Bhagat and A. K. Chakraborti, *J. Org. Chem.*, 2007, **72**, 1263–1266.
- A. Elmakssoudi, M. Zahouily, A. Mezdar, A. Rayadh and S. Sebti, *C. R. Chim.*, 2005, **8**, 1954–1959.
- A. Tajti, E. Szatmári, F. Perdih, G. Keglevich and E. Balint, *Molecules*, 2019, **24**(8), 1640.
- S. P. Kunde, K. G. Kanade, B. K. Karale, H. N. Akolkar, P. V. Randhavane and S. T. Shinde, *Arabian J. Chem.*, 2019, **12**, 5212–5222.
- S. Ardizzone, C. L. Bianchi, G. Cappelletti, S. Gialanella, C. Pirola and V. Ragaini, *J. Phys. Chem. C*, 2007, **111**(35), 13222–13231.
- J. P. Jalava, *Part. Part. Syst. Charact.*, 2006, **23**(2), 159–164.
- M. Pelaez, N. T. Nolan, S. C. Pillai, M. K. Seery, P. Falaras, A. G. Kontos, P. S. Dunlop, J. W. Hamilton, J. A. Byrne, K. O'shea and M. H. Entezari, *Appl. Catal. B*, 2012, **125**, 331–349.
- G. C. Nakhate, V. S. Nikam, K. G. Kanade, S. S. Arbut, B. B. Kale and J. O. Baeg, *Mater. Chem. Phys.*, 2010, **124**(2–3), 976–981.
- D. I. Enache, J. K. Edwards, P. Landon, B. Solsona-Espriu, A. F. Carley, A. A. Herzing, M. Watanabe, C. J. Kiely, D. W. Knight and G. J. Hutchings, *Science*, 2006, **311**, 362–365.
- B. F. Mirjalilia, A. Bamoniri, A. Akbari and N. Taghavinia, *J. Iran. Chem. Soc.*, 2011, **8**, S129–S134.
- L. Kantam, S. Laha, J. Yadav and B. Sreedhar, *Tetrahedron Lett.*, 2006, **47**, 6213–6216.
- H. S. Sarvar and M. H. Sarvari, *J. Chem. Res.*, 2003, **2**, 176–178.
- M. Hosseini-Sarvari, *Tetrahedron*, 2008, **64**(23), 5459–5466.
- Y. Wang, L. Zhang, K. Deng, X. Chen and Z. Zou, *J. Phys. Chem. C*, 2007, **111**, 2709–2714.
- L. Hu, J. Wang, J. Zhang, Q. Zhang and Z. Liu, *RSC Adv.*, 2014, **4**, 420–427.
- B. F. Abdel-wahab, R. E. Khidre and A. A. Farahat, *ARKIVOC*, 2011, (i), 196–245.
- J. Senthilnathan and L. Philip, *Chem. Eng. J.*, 2010, **16**(1–2), 83–92.





## Paper

- 46 T. C. Jagadale, S. P. Takale, R. S. Sonawane, H. M. Joshi, S. I. Patil, B. B. Kale and S. B. Ogale, *J. Phys. Chem. C*, 2008, **11293**, 14595–14602.
- 47 S. Y. Choi, M. Mamak, N. Coombs, N. Chopra and G. A. Ozin, *Adv. Funct. Mater.*, 2004, **14**(4), 335–344.
- 48 X. Chen, X. Wang, Y. Hou, J. Huang, L. Wu and X. Fu, *J. Catal.*, 2008, **255**(1), 59–67.
- 49 M. Hema, A. Y. Arasi, P. Tamilselvi and R. Anbarasan, *Chem. Sci. Trans.*, 2012, **2**, 239–245.





## ARTICLE

# Synthesis of 3-(trifluoromethyl)-1-(perfluorophenyl)-1*H*-pyrazol-5(4*H*)-one derivatives via Knoevenagel condensation and their biological evaluation

Sujata G. Dengale<sup>1</sup> | Hemantkumar N. Akolkar<sup>2</sup> | Bhausahab K. Karale<sup>2</sup> |  
Nirmala R. Darekar<sup>2</sup> | Sadhana D. Mhaske<sup>3</sup> | Mubarak H. Shaikh<sup>2</sup> |  
Dipak N. Raut<sup>4</sup> | Keshav K. Deshmukh<sup>1</sup>

<sup>1</sup>P.G. and Research, Department of Chemistry, Sangamner Nagarpalika Arts, D. J. Malpani Commerce and B. N. Sarada Science College, Sangamner, India

<sup>2</sup>P.G. and Research, Department of Chemistry, Radhabai Kale Mahila Mahavidyalaya, Ahmednagar, India

<sup>3</sup>Department of Chemistry, Dadapatil Rajale College, Pathardi, India

<sup>4</sup>Amrutvahini College of Pharmacy, Sangamner, India

## Correspondence

Hemantkumar N. Akolkar, P.G. and Research, Department of Chemistry, Radhabai Kale Mahila Mahavidyalaya, Ahmednagar, Maharashtra, India, 414001. Email: hemantakolkar@gmail.com

## Abstract

In search of new active molecules, a small focused library of the synthesis of 3-(trifluoromethyl)-1-(perfluorophenyl)-1*H*-pyrazol-5(4*H*)-one derivatives (**4a-d**, **5a-f**, and **6a-e**) has been efficiently prepared via the Knoevenagel condensation approach. All the derivatives were synthesized by conventional and non-conventional methods like ultrasonication and microwave irradiation, respectively. Several derivatives exhibited excellent anti-inflammatory activity compared to the standard drug. Furthermore, the synthesized compounds were found to have potential antioxidant activity. In addition, to rationalize the observed biological activity data, an *in silico* absorption, distribution, metabolism, and excretion (ADME) prediction study also been carried out. The results of the *in vitro* and *in silico* studies suggest that the 3-(trifluoromethyl)-1-(perfluorophenyl)-1*H*-pyrazol-5(4*H*)-one derivatives (**4a-d**, **5a-f**, and **6a-e**) may possess the ideal structural requirements for the further development of novel therapeutic agents.

## KEYWORDS

ADME prediction, anti-inflammatory, antioxidant, Knoevenagel, microwave, pyrazole, ultrasonication

## 1 | INTRODUCTION

The pyrazole ring is a prominent heterocyclic structural compound found in several pharmaceutically active compounds. This is because of its use in pharmacological activity and ease of synthesis. Furthermore, the selective functionalization of pyrazole with diverse substituents was also found to improve their range of action in various fields. Pyrazole containing heterocycles shows various biological activity, such as antibacterial,<sup>[1]</sup> antifungal,<sup>[2]</sup> antimicrobial,<sup>[3]</sup> anti-inflammatory,<sup>[4a]</sup> antioxidant,<sup>[4b]</sup> insecticidal,<sup>[5]</sup> antiviral,<sup>[6]</sup> anti-nitric oxide

synthase,<sup>[7]</sup> glycogen receptor antagonist,<sup>[8]</sup> anticancer,<sup>[9]</sup> antienzyme,<sup>[10]</sup> immunosuppressant,<sup>[11]</sup> anti-fatty acid amide hydrolase (FAAH),<sup>[12]</sup> and liver-x-receptor [LXR] partial agonist activities.<sup>[13]</sup>

Fluorine or fluorine-based compounds are of great interest in synthetic and medicinal chemistry. The position of the fluorine atom in an organic molecule plays a vital role in agrochemicals, pharmaceuticals, and materials<sup>[14]</sup> as it changes the pharmacokinetic and pharmacodynamic properties of the molecule owing to its high membrane permeability, metabolic stability, lipophilicity, and binding affinity.<sup>[15]</sup>

Perfluoro-alkylated and trifluoro-methylated pyrazoles represent pharmacologically related core structures that are present in many important drugs and agrochemicals, such as fluazolate (herbicide), penthiopyrad (fungicide), razaxaban (anticoagulant), deracoxib, celecoxib (anti-inflammatory), and penflufen (fungicidal) (Figure 1).<sup>[16]</sup> So, the modern trend is moving more in the direction of the synthesis of a collection of fluorine-containing molecules in order to find excellent biological activity.

Ultrasonic irradiation is a new technology that has been widely used in chemical reactions. When ultrasonic waves pass through a liquid medium, a large number of microbubbles form, grow, and collapse in very short times, about a few microseconds. The formation and violent collapse of small vacuum bubbles takes place due to the ultrasonication waves generated in alternating high pressure and low pressure in liquids, and the phenomenon is known as cavitation. It causes high-speed imposing liquid jets and strong hydrodynamic shear forces. The deagglomeration of nanometer-

sized materials was carried out using these effects. In this aspect, for high-speed mixers and agitator bead mills, ultrasonication is an alternative.<sup>[17]</sup>

In the preparative chemist's toolkit, microwave heating is a valuable technique. Due to a modern scientific microwave apparatus, it is possible to access elevated temperatures in an easy, safe, and reproducible way.<sup>[18]</sup> In recent years, microwave-assisted organic synthesis (MAOs)<sup>[19]</sup> has been emerged as a new "lead" in organic synthesis. Important advantages of this technology include a highly accelerated rate of the reaction and a decrease in reaction time, with an increase in the yield and quality of the product. The current technique is considered an important method toward green chemistry as this technique is more environmentally friendly. The conventional method of organic synthesis usually needs a longer heating time; tedious apparatus setup, which results in the higher cost of the process; and the excessive use of solvents/reagents, which leads to environmental pollution. This growth of green chemistry

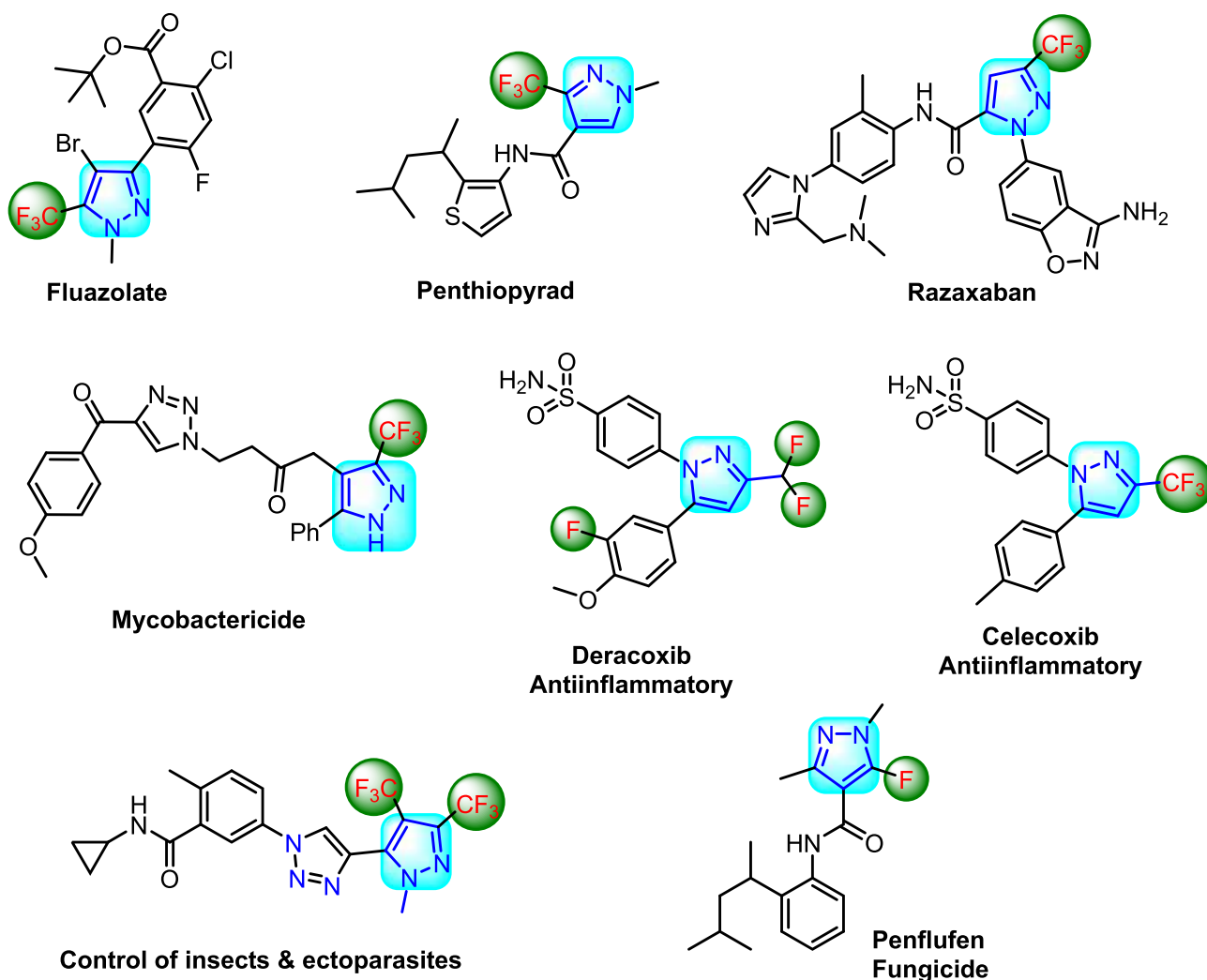


FIGURE 1 Structure of pyrazole- and fluorine-containing commercially available drugs

holds significant potential for a reduction of the byproduct, a reduction in waste production, and lowering of the energy costs. Due to its ability to couple directly with the reaction molecule and bypass thermal conductivity, leading to a rapid rise in the temperature, microwave irradiation has been used to improve many organic syntheses.<sup>[20]</sup> Knoevenagel condensation reactions are carried out by the condensation of aldehyde and the active methylene group using different catalysts such as piperidine,  $\text{InCl}_3$ ,  $\text{TiCl}_4$ ,  $\text{LiOH}$ ,  $\text{ZnCl}_2$ , and  $\text{NbCl}_5$ .<sup>[20,21]</sup> They are also carried out using  $\text{NaAlO}_2$ -promoted mesoporous catalysts,<sup>[22]</sup> ionic liquid,<sup>[23]</sup> monodisperse carbon nanotube-based NiCu nanohybrids,<sup>[24]</sup> and MAOs.<sup>[25]</sup> This is one of the most important methodologies used in synthetic organic chemistry for the formation of a C—C double bond.

From our study, the results demonstrated that green methodologies are less hazardous than classical synthesis methods, as well more efficient and economical and environmentally friendly; short reaction times and excellent yields are observed for those reactions in which conventional heating is replaced by microwave irradiation. Keeping in mind the 12 principles of green chemistry, in continuation of our research work,<sup>[26]</sup> and the advantages of microwave irradiation and activities associated with pyrazole and fluorine, we construct pyrazole and fluorine in one molecular framework as new 3-(trifluoromethyl)-1-(perfluorophenyl)-1*H*-pyrazol-5(4*H*)-one derivatives under conventional, as well as microwave, irradiation and ultrasonication and evaluated their anti-inflammatory and antioxidant activity. In addition to this, we have also performed *in silico* absorption, distribution, metabolism, and excretion (ADME) predictions for the synthesized compounds.

## 2 | RESULTS AND DISCUSSION

### 2.1 | Chemistry

A facile, economic, and green protocol for the cyclocondensation of 2-(perfluorophenyl)-5-(trifluoromethyl)-

2,4-dihydro-3*H*-pyrazol-3-one (**3**) with different aldehydes has been achieved.

The key starting material 3-(trifluoromethyl)-1-(perfluorophenyl)-1*H*-pyrazol-5(4*H*)-one (**3**) was synthesized by the condensation of 1-(perfluorophenyl)hydrazine (**1**) and ethyl 4,4,4-trifluoro-3-oxobutanoate (**2**) in ethanol<sup>[27]</sup> (Scheme 1).

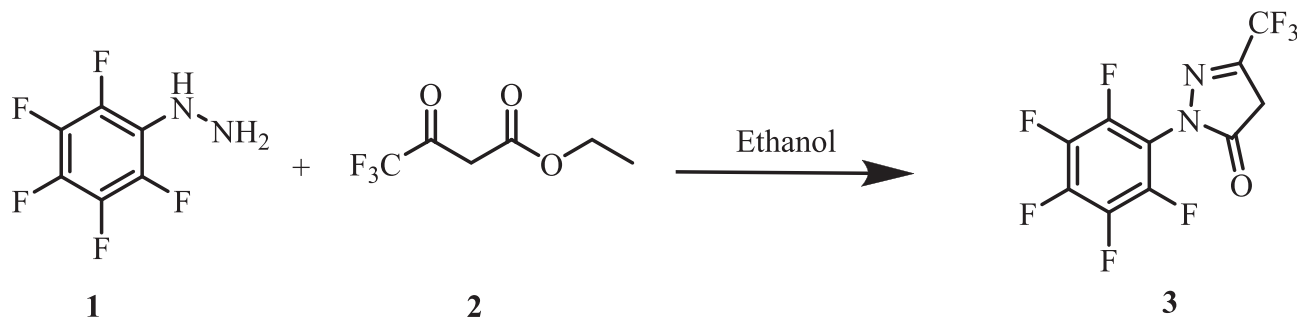
Initially, we carried out the reaction between 2-(perfluorophenyl)-5-(trifluoromethyl)-2,4-dihydro-3*H*-pyrazol-3-one (2 mmol) (**3**) and 1-phenyl-3-(thiophen-2-yl)-1*H*-pyrazole-4-carbaldehyde (2 mmol) refluxed in acetic acid as a model reaction (Scheme 2). Initially, the model reaction was carried out in ethanol without using acetic acid, and it was observed that a very low yield of product (20%) was obtained even after 2 hr. Therefore, improving the yield intervention of the catalyst was thought to be necessary. So, we decided to use acetic acid as a catalyst to promote this transformation at room temperature. At room temperature, the yield of product (45%) was found to be increased in 3 hr, so we decided to provide heating to the reaction mixture to achieve maximum product yield.

When the reaction mixture refluxed in acetic acid, product formation took place after 2 hr, and the yield of the product was 72% (Table 1).

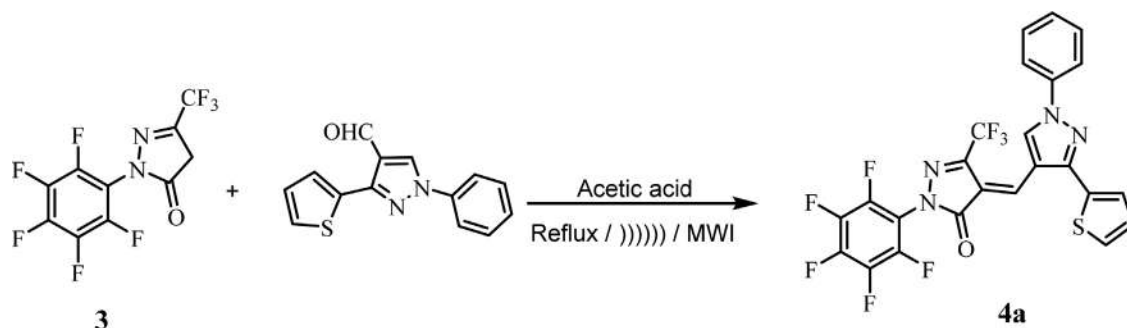
To check the ultrasonication's specific effect on this reaction, under ultrasound irradiation at 35–40°C, we carried out the model reaction using the optimized reaction conditions in hand to check whether the reaction could be accelerated with further improved product yield within a short reaction time (Scheme 2).

It was observed that, under ultrasonic conditions, the conversion rate of a reactant to product increased with less time (Table 1). Thus, when considering the basic green chemistry concept, ultrasonic irradiation was found to have a beneficial effect on the synthesis of Knoevenagel derivatives (**4a-d**, **5a-f**, and **6a-e**), which was superior to the traditional method with respect to yield and reaction time (Table 1).

To accomplish the goal and significance of green chemistry, the model reaction was carried out under



**SCHEME 1** Synthesis of 3-(trifluoromethyl)-1-(perfluorophenyl)-1*H*-pyrazol-5(4*H*)-one **3**



**SCHEME 2** Model reaction for conventional, ultrasonication, and microwave irradiation methods

**TABLE 1** Synthesis of 3-(trifluoromethyl)-1-(perfluorophenyl)-1H-pyrazol-5(4H)-one derivatives (**4a-d**, **5a-f**, and **6a-e**)

Cpd	R <sub>1</sub>	R <sub>2</sub>	R <sub>3</sub>	R <sub>4</sub>	m. p. (°C)	Conventional method <sup>a</sup>		Ultrasound method <sup>b</sup>		Microwave method <sup>c</sup>	
						Time (min)	Yield <sup>d</sup> (%)	Time (min)	Yield <sup>d</sup> (%)	Time (min)	Yield <sup>d</sup> (%)
<b>4a</b>	H	H	-	-	224–226	120	72	20	81	6.5	84
<b>4b</b>	Br	F	-	-	232–234	120	75	18	78	6.5	81
<b>4c</b>	Cl	H	-	-	216–218	120	70	20	76	6.0	80
<b>4d</b>	Br	H	-	-	230–232	120	64	16	70	6.5	76
<b>5a</b>	H	H	OMe	-	202–204	120	70	21	76	5.5	84
<b>5b</b>	H	H	H	-	186–188	120	66	17	72	6.0	80
<b>5c</b>	F	H	OMe	-	180–182	120	68	16	75	7.0	82
<b>5d</b>	H	H	Me	-	206–208	120	65	16	71	6.5	79
<b>5e</b>	H	H	OCF <sub>3</sub>	-	142–144	120	62	18	70	6.5	76
<b>5f</b>	H	Cl	Cl	-	212–214	120	70	19	80	5.5	84
<b>6a</b>	Me	Cl	Me	H	188–190	120	66	18	76	6.0	78
<b>6b</b>	H	Cl	Me	H	180–182	120	62	17	72	7.5	75
<b>6c</b>	H	Cl	H	H	176–178	120	59	18	79	7.0	80
<b>6d</b>	H	Cl	H	Cl	212–214	120	64	20	72	7.0	78
<b>6e</b>	H	H	Me	H	180–182	120	60	18	80	7.5	82

Abbreviation: Cpd, compound.

<sup>a</sup>Reaction conditions: Compound (**3**) (2 mmol) and 1-phenyl-3-(thiophen-2-yl)-1H-pyrazole-4-carbaldehyde (2 mmol) refluxed in acetic acid.

<sup>b</sup>Compound (**3**) (2 mmol) and 1-phenyl-3-(thiophen-2-yl)-1H-pyrazole-4-carbaldehyde (2 mmol) in acetic acid under ultrasound irradiation.

<sup>c</sup>Compound (**3**) (2 mmol) and 1-phenyl-3-(thiophen-2-yl)-1H-pyrazole-4-carbaldehyde (2 mmol) in acetic acid under microwave irradiation.

<sup>d</sup>Isolated yield. m.p.: melting point.

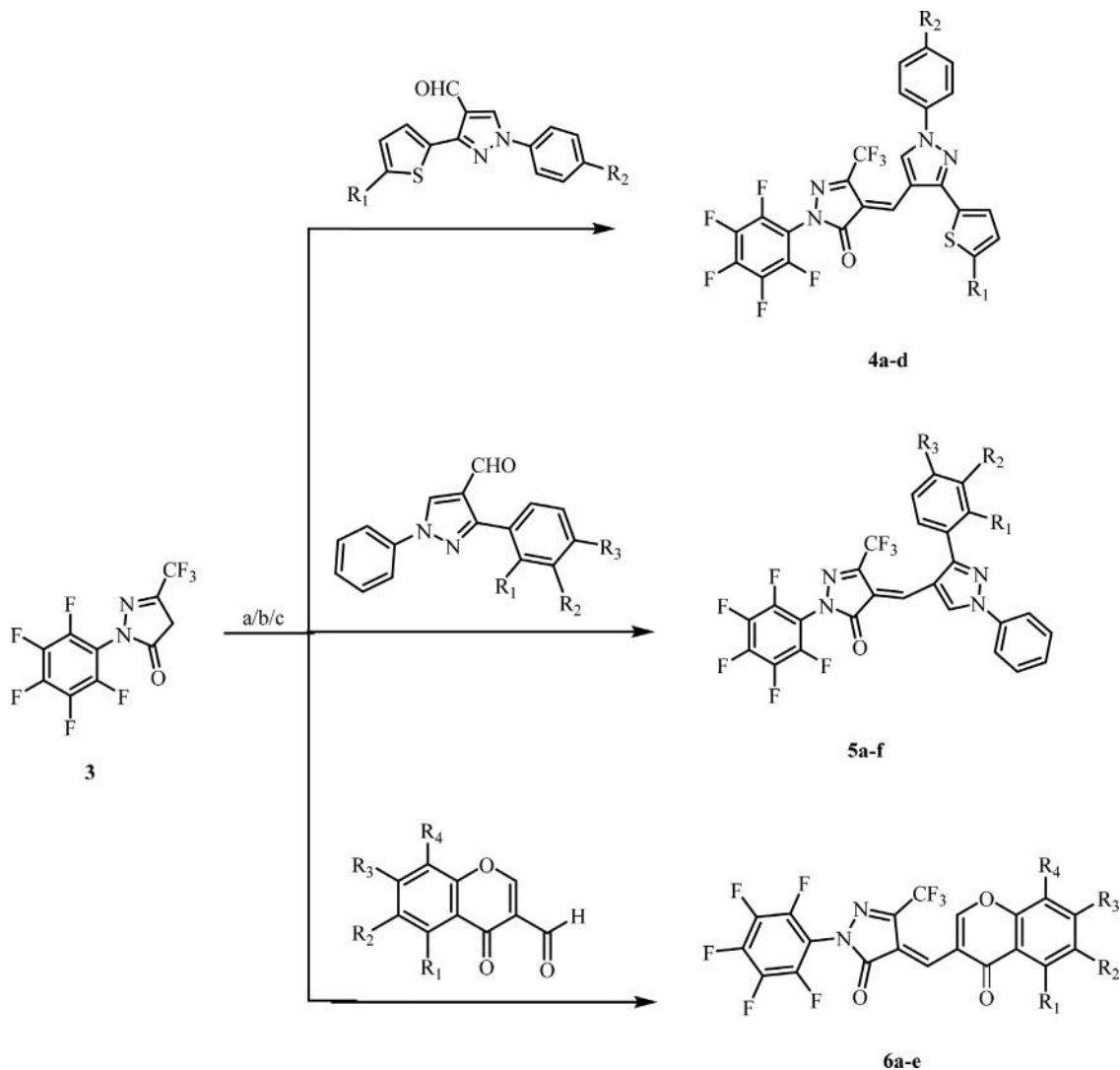
microwave irradiation for a period of time indicated in Table 1 at 350 W (Scheme 2). Fortunately, the product formation occurred in 6.5 min, with an 84% increase in yield.

So, from the above experiments, it can be concluded that, when the reaction was carried out under the conventional method, it gave comparatively low yields of products with longer reaction times, while the same reaction carried out under the influence of ultrasonic irradiation and microwave irradiation gave excellent yields of the products in short reaction times.

Finally, we assessed the scope and generality of this method for the Knoevenagel condensation between 2-(perfluorophenyl)-5-(trifluoromethyl)-2,4-dihydro-3H-pyrazol-3-one (**3**) and different aldehydes (Scheme 3), achieved under conventional and nonconventional methods like the ultrasound and microwave methods, respectively. With respect to the substituent present on the aromatic ring of aldehyde, under the optimized conditions, the corresponding products were obtained in high to excellent yields (Table 1).

More importantly, hetero aryl aldehydes were observed to be well tolerated under optimized conditions,





**SCHEME 3** Synthesis of 3-(trifluoromethyl)-1-(perfluorophenyl)-1H-pyrazol-5(4H)-one derivatives (**4a-d**, **5a-f**, and **6a-e**). Reaction conditions: **a** = Refluxed in acetic acid. **b** = Under ultrasound irradiation in acetic acid. **c** = Under microwave irradiation using acetic acid as a solvent

furnishing the product in good yields. All the synthesized compounds (**4a-d**, **5a-f**, and **6a-e**) were confirmed by IR,  $^1\text{H}$  NMR,  $^{13}\text{C}$  NMR, and mass spectra.

The formation of (4E)-3-(trifluoromethyl)-1-(perfluorophenyl)-4-((1-phenyl-3-(thiophen-2-yl)-1H-pyrazol-4-yl)methylene)-1H-pyrazol-5(4H)-one **4a-d** was confirmed by IR,  $^1\text{H}$  NMR,  $^{13}\text{C}$  NMR, and mass spectra. In the IR spectrum of compound **4a**, the peaks observed at  $1,681\text{ cm}^{-1}$  indicate the presence of C=O group. In the  $^1\text{H}$  NMR spectrum of compound **4a**, two singlets were observed at  $\delta$  8.11 and 10.10 ppm for pyrazolyl and olefinic proton, respectively. The  $^{13}\text{C}$  NMR spectrum of compound **4a** revealed that the peak appearing at  $\delta$  161.4 ppm is due to the presence of carbonyl carbon. The structure of compound **4a** was also confirmed by a molecular ion peak at  $m/z$  555.01 ( $M + \text{H}$ ) $^+$ . Similarly, the

synthesis of (4E)-3-(trifluoromethyl)-1-(perfluorophenyl)-4-((1,3-diphenyl-1H-pyrazol-4-yl)methylene)-1H-pyrazol-5(4H)-ones **5a-f** was also confirmed by spectral techniques. In the IR spectrum of compound **5a**, the peak observed at  $1,701\text{ cm}^{-1}$  corresponded to the C=O group. In the  $^1\text{H}$  NMR spectrum of compound **5a**, the three singlets observed at  $\delta$  3.92, 8.11, and 10.10 ppm confirm the presence of  $-\text{OCH}_3$ , pyrazolyl proton, and olefinic proton, respectively. The  $^{13}\text{C}$  NMR spectrum of compound **5a** showed peaks at  $\delta$  162.5 and 55.5 ppm, confirming the presence of carbonyl carbon and methoxy carbon, respectively. Furthermore, the structure of compound **5a** was also confirmed by a molecular ion peak at  $m/z$  573.21 ( $M + \text{H}$ ) $^+$ .

Furthermore, the formation of (Z)-4-([4-oxo-4H-chromen-3-yl]methylene)-2-(perfluorophenyl)-5-(trifluoromethyl)-2,4-dihydro-3H-pyrazol-3-one **6a-e** was

confirmed by various spectral techniques. The IR spectrum of compound **6a** showed absorption peaks at 1,707 and 1,666  $\text{cm}^{-1}$  corresponding to two carbonyl groups present in the molecules. The  $^1\text{H}$  NMR spectrum of compound **6a** showed four singlets at  $\delta$  2.54 and  $\delta$  3.01 ppm for two  $-\text{CH}_3$ ,  $\delta$  8.50 ppm for chromone ring proton, and  $\delta$  10.54 ppm for olefinic proton. The  $^{13}\text{C}$  NMR spectrum of compound **6a** showed that two signals appear at  $\delta$  175.4 and 164.2 ppm for the carbonyl carbon of chromone and pyrazolone ring, respectively. In addition, two signals for methyl carbon appear at  $\delta$  22.2 and 18.6 ppm. The structure of compound **6a** was also confirmed by mass spectra and by a molecular ion peak observed at  $m/z$  537.11 ( $\text{M} + \text{H}$ ) $^+$ . Similarly, all the synthesized compounds were characterized by the spectral analysis. Structures of all the synthesized derivatives are shown in Figure S1 (Supporting Information).

## 2.2 | Biological activity

### 2.2.1 | Anti-inflammatory activity

The newly synthesized 3-(trifluoromethyl)-1-(perfluorophenyl)-1*H*-pyrazol-5(4*H*)-one derivatives (**4a-d**, **5a-f**, and **6a-e**) ( $\text{EC}_{50}$  range =  $0.6483 \pm 0.221$ – $0.8519 \pm 0.281$   $\mu\text{g}/\text{ml}$ ) exhibited moderate anti-inflammatory activity compared to the standard drug diclofenac sodium. Among all the synthesized compounds, except compounds **4c**, **5c**, **5e**, **6d**, and **6e**, all other compounds exhibited a minimum inhibitory concentration (MIC) of 200  $\mu\text{g}/\text{ml}$  compared to the standard drug diclofenac sodium (Table 2).

The percent inhibition of compounds in the in vitro anti-inflammatory model is shown in Figure 2. Furthermore, the comparative percent inhibition of compounds in the in vitro anti-inflammatory model is shown in Figure 3.

### 2.2.2 | Antioxidant activity

In the present study, antioxidant activity of the synthesized compounds has been assessed in vitro by the DPPH radical scavenging assay.<sup>[28]</sup> Ascorbic acid (AA) has been used as a standard drug for the comparison of antioxidant activity, and the observed results are summarized in Table 2.

According to the DPPH assay, compounds **5a**, **5d**, **5e**, **5f**, **6a**, **6b**, and **6e** ( $\text{IC}_{50}$  = <100  $\mu\text{g}/\text{ml}$ ) exhibited excellent antioxidant activity compared to the standard antioxidant drug AA ( $\text{IC}_{50}$  = <50  $\mu\text{g}/\text{ml}$ ). The remaining synthesized compounds display comparable antioxidant activity than

**TABLE 2** Anti-inflammatory and antioxidant activity of 3-(trifluoromethyl)-1-(perfluorophenyl)-1*H*-pyrazol-5(4*H*)-one derivatives (MIC in  $\mu\text{g}/\text{ml}$ )

Compound	Anti-inflammatory	Antioxidant
<b>4a</b>	200	>100
<b>4b</b>	200	>400
<b>4c</b>	400	>200
<b>4d</b>	200	>200
<b>5a</b>	200	<100
<b>5b</b>	200	>200
<b>5c</b>	NT	NT
<b>5d</b>	200	<100
<b>5e</b>	800	<100
<b>5f</b>	200	<100
<b>6a</b>	200	<100
<b>6b</b>	200	<100
<b>6c</b>	200	>200
<b>6d</b>	800	>100
<b>6e</b>	400	<100
Diclofenac sodium	50	-
Ascorbic acid	-	<50

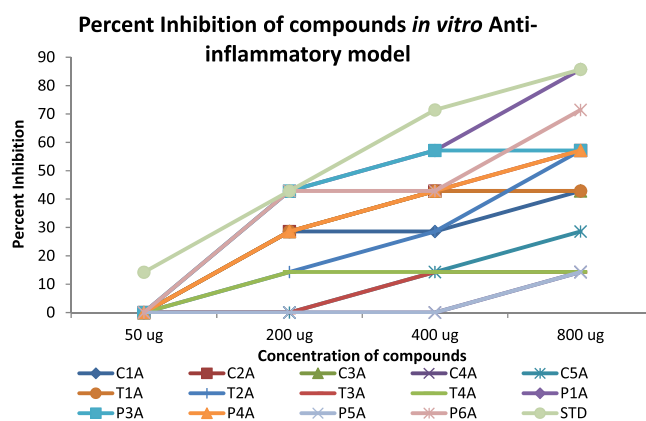


**FIGURE 2** The percent inhibition of compounds in an in vitro anti-inflammatory model

the standard drug butylated hydroxytoluene (Table 2). The percent inhibition of compounds in the in vitro antioxidant model is shown in Figure 4.

## 2.3 | Computational study

### 2.3.1 | In silico ADME

An important task for the lead compounds is early prediction of drug likeness properties as it resolves the cost

**FIGURE 3** The comparative percent inhibition of compounds in an in vitro anti-inflammatory model

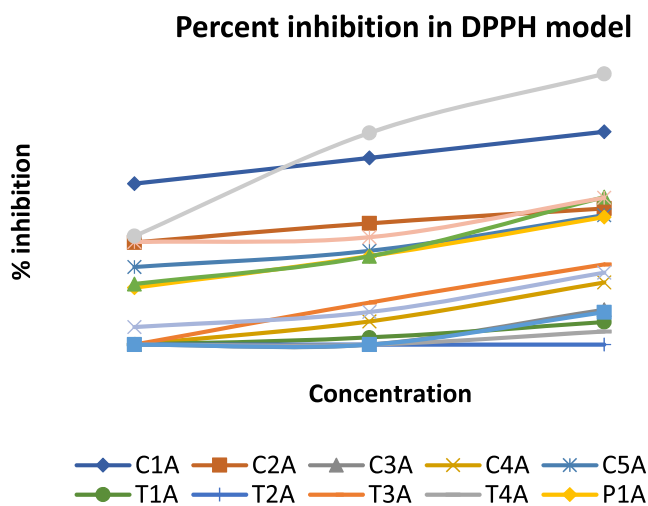
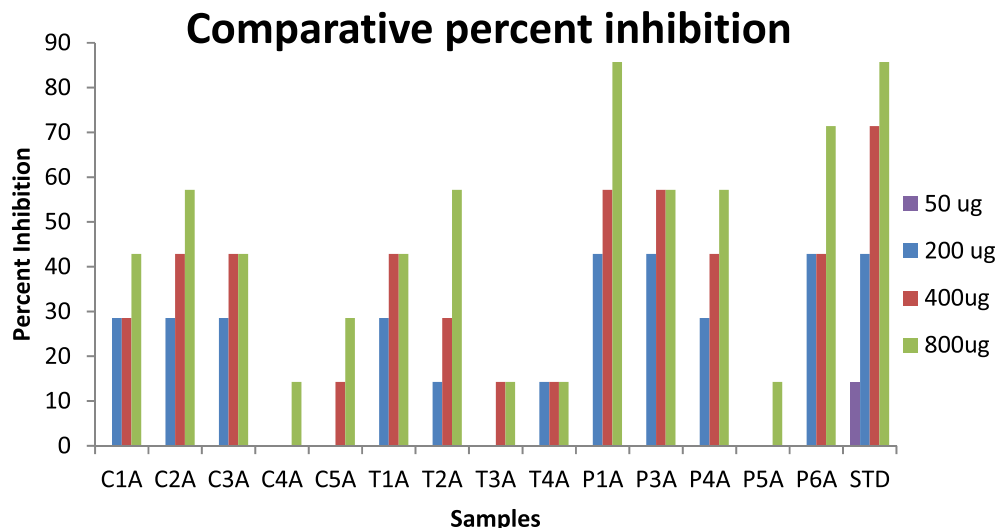


**FIGURE 4** The percent inhibition of compounds in an in vitro antioxidant model

and time issues of drug development and discovery. Due to the inadequate drug likeness properties of many active agents with a significant biological activity, these compounds have failed in clinical trials.<sup>[29]</sup> On the basis of Lipinski's rule of five, the drug likeness properties were analyzed by ADME parameters using the Molinspiration online property calculation toolkit,<sup>[30]</sup> and data are summarized in Table 3.

All the compounds exhibited noteworthy values for the various parameters analyzed and showed good drug-like characteristics based on Lipinski's rule of five and its variants, which characterized these agents to be likely orally active. For the synthesized compound **6e**, the data obtained were within the range of accepted values. Parameters such as the number of rotatable bonds and total polar surface area are linked with the intestinal absorption; results showed that all

synthesized compounds had good absorption. The in silico assessment of all the synthetic compounds has shown that they have very good pharmacokinetic properties, which are reflected in their physicochemical values, thus ultimately enhancing the pharmacological properties of these molecules.

### 3 | EXPERIMENTAL SECTION

All organic solvents were acquired from Poona Chemical Laboratory, Pune and Research-Lab Fine Chem Industries, Mumbai and were used as such without further purification. The melting points were measured on a DBK melting point apparatus and are uncorrected. Microwave irradiation was carried out in Raga's synthetic microwave oven. IR spectra were recorded on Shimadzu IR Affinity 1S (ATR) fourier transform infrared spectrophotometer. <sup>1</sup>H NMR (500 MHz) and <sup>13</sup>C NMR (125 MHz) spectra were recorded on Bruker Advance neo 500 spectrophotometers using tetramethylsilane as an internal standard, and CDCl<sub>3</sub> and dimethyl sulphoxide-*d*<sub>6</sub> as solvent and chemical shifts, respectively, were expressed as  $\delta$  ppm units. Mass spectra were obtained on Waters quadrupole time-of-flight micromass (ESI-MS) mass spectrometer.

#### 3.1 | General procedure for the synthesis of synthesize new 3-(trifluoromethyl)-1-(perfluorophenyl)-1H-pyrazol-5(4H)-one derivatives (4a-d, 5a-f and 6a-e)

**Conventional method:** An equimolar amount of 2-(perfluorophenyl)-5-(trifluoromethyl)-2,4-dihydro-3H-pyrazol-3-

TABLE 3 Pharmacokinetic parameters of (4a-d, 5a-f, and 6a-e) compounds

Entry	% ABS	TPSA (Å <sup>2</sup> )	n- ROTB	MV	MW	miLog P	n- ON	n- OHNH	Lipinski violation	Drug likeness model score
Rule	-	-	-	-	<500	≤5	<10	<5	≤1	-
4a	90.81	52.72	5	397.75	554.42	5.83	5	0	2	-0.68
4b	90.81	52.72	5	420.56	651.31	6.92	5	0	2	-0.84
4c	90.81	52.72	5	411.28	588.87	6.63	5	0	2	-0.25
4d	90.81	52.72	5	415.63	633.32	6.76	5	0	2	-0.56
5a	87.62	61.96	6	432.58	578.42	6.10	6	0	2	-0.46
5b	90.81	52.72	5	407.04	548.39	6.04	5	0	2	-0.80
5c	87.62	61.96	6	437.51	596.41	6.19	6	0	2	-0.22
5d	90.81	52.72	5	423.60	562.42	6.49	5	0	2	-0.51
5e	87.62	61.96	7	447.32	632.39	7.01	6	0	2	-0.45
5f	90.81	52.72	5	434.11	617.28	7.33	5	0	2	-0.36
6a	86.53	65.11	3	374.21	536.76	6.25	5	0	2	-0.53
6b	86.53	65.11	3	357.65	522.74	5.87	5	0	2	-0.36
6c	86.53	65.11	3	341.09	508.71	5.49	5	0	2	-0.32
6d	86.53	65.11	3	354.62	543.15	6.10	5	0	2	-0.93
6e	86.53	65.11	3	344.11	488.29	5.26	5	0	1	-0.81

Abbreviations: % ABS, percentage absorption; TPSA, topological polar surface area; n-ROTB, number of rotatable bonds; MV, molecular volume; MW, molecular weight; miLogP, logarithm of partition coefficient of compound between n-octanol and water; n-ON acceptors, number of hydrogen bond acceptors; n-OHNH donors, number of hydrogen bonds donors.

one (3) (0.002 mol) and substituted aldehydes (0.002 mol) was taken in a round-bottom flask using glacial acetic acid (5 ml) as a solvent and were refluxed for the period of time indicated in Table 1. The progress of the reaction was monitored by thin layer chromatography (TLC). After completion of reaction, the mixture was cooled and poured into ice-cold water. The obtained solid was filtered and washed with water and dried and purified by crystallization from ethyl acetate to obtain pure compounds (4a-d, 5a-f, and 6a-e).

**Ultrasound method:** A mixture of 2-(perfluorophenyl)-5-(trifluoromethyl)-2,4-dihydro-3H-pyrazol-3-one (3) (0.002 mol) and substituted aldehydes (0.002 mol) in acetic acid (5 ml) was taken in a 50-ml round-bottom flask. The mixture was irradiated in the water bath of an ultrasonic cleaner at 35–40°C for a period of time indicated in Table 1. After completion of the reaction (monitored by TLC), the mixture was poured into ice-cold water, and the obtained solid was collected by simple filtration and washed successively with water. The crude product was purified by crystallization from ethyl acetate to obtain pure compounds (4a-d, 5a-f, and 6a-e).

**Microwave irradiation method:** An equimolar amount of 2-(perfluorophenyl)-5-(trifluoromethyl)-

2,4-dihydro-3H-pyrazol-3-one (3) (0.002 mol) and substituted aldehydes (0.002 mol) was taken in a round-bottom flask (RBF) using glacial acetic acid (5 ml) as a solvent, and the contents of RBF were subjected to MW irradiation for the period of time indicated in Table 1 at 350 W. The progress of the reaction was monitored by TLC. After completion of reaction, the mixture was cooled and poured into ice-cold water. The obtained solid was filtered and washed with water and dried and purified by crystallization from ethyl acetate to obtain pure compounds (4a-d, 5a-f, and 6a-e).

### 3.1.1 | (4E)-3-(Trifluoromethyl)-1-(perfluorophenyl)-4-((1-phenyl-3-(thiophen-2-yl)-1H-pyrazol-4-yl)methylene)-1H-pyrazol-5(4H)-one (4a)

Orange solid; Wt. 930 mg, Yield 84%; IR( $\nu_{\max}$ /cm<sup>-1</sup>): 2,926 (=C–H), 1,681 (C=O), 1,598 (C=N), 1,519 (C=C), 1,234 (C–F); <sup>1</sup>H NMR spectrum,  $\delta$ , ppm: 7.35–7.91 (m, 8H, Ar–H), 8.11 (s, 1H, pyrazolyl-H), 10.10 (s, 1H, =C–H); <sup>13</sup>C NMR spectrum,  $\delta_C$ , ppm: 161.4 (C=O), 151.7, 140.1, 137.8, 134.9, 131.1, 130.0, 129.6, 129.1,

128.70, 128.6, 119.7, 115.7, 113.5; MS (ESI-MS):  $m/z$  555.01 (M + H)<sup>+</sup>.

### 3.1.2 | (4E)-4-((3-(5-Bromothiophen-2-yl)-1-(4-fluorophenyl)-1H-pyrazol-4-yl)methylene)-3-(trifluoromethyl)-1-(perfluorophenyl)-1H-pyrazol-5(4H)-one (4b)

Orange solid; Wt. 1.05 g; Yield 81%; IR ( $\nu_{\max}/\text{cm}^{-1}$ ): 2,927 (C–H), 1,680 (C=O), 1,598 (C=N), 1,516 (C=C), 1,231 (C–F); <sup>1</sup>H NMR spectrum,  $\delta$ , ppm: 7.16 (d, 1H,  $J$  = 3.50 Hz, Ar–H), 7.26–7.19 (m, 3H, Ar–H), 7.84 (dd, 2H,  $J$  = 5.00 Hz and 9.00 Hz, Ar–H), 8.10 (s, 1H, pyrazole-H), 10.11 (s, 1H, =C–H); MS:  $m/z$  651.03 (M + H)<sup>+</sup>.

### 3.1.3 | (4E)-4-((3-[5-Chlorothiophen-2-yl]-1-phenyl-1H-pyrazol-4-yl)methylene)-3-(trifluoromethyl)-1-(perfluorophenyl)-1H-pyrazol-5(4H)-one (4c)

Orange solid; Wt. 873 mg; Yield 80%; IR ( $\nu_{\max}/\text{cm}^{-1}$ ): 2,926 (C–H), 1,682 (C=O), 1,597 (C=N), 1,518 (C=C), 1,232 (C–F); <sup>1</sup>H NMR spectrum,  $\delta$ , ppm: 7.07 (s, 1H, Ar–H), 7.26–7.18 (s, 1H, Ar–H), 7.44 (d, 1H,  $J$  = 6.00 Hz, Ar–H), 7.52 (m, 2H, Ar–H), 7.86 (d, 2H,  $J$  = 7.00 Hz, Ar–H), 8.11 (s, 1H, pyrazole-H), 10.16 (s, 1H, =C–H); <sup>13</sup>C NMR spectrum,  $\delta_{\text{C}}$ , ppm: 162.4 (C=O), 151.3, 139.5, 138.3, 135.0, 133.5, 130.8, 130.0, 128.8, 127.6, 127.4, 120.0, 116.3, 114.6; MS:  $m/z$  547.11 (M + H)<sup>+</sup>.

### 3.1.4 | (4E)-4-((3-(5-Bromothiophen-2-yl)-1-phenyl-1H-pyrazol-4-yl)methylene)-3-(trifluoromethyl)-1-(perfluorophenyl)-1H-pyrazol-5(4H)-one (4d)

Orange solid; Wt. 960 mg; Yield 76%; IR ( $\nu_{\max}/\text{cm}^{-1}$ ): 2,926 (C–H), 1,681 (C=O), 1,597 (C=N), 1,520 (C=C), 1,235 (C–F); <sup>1</sup>H NMR spectrum,  $\delta$ , ppm: 7.16 (d, 1H,  $J$  = 4.00 Hz, Ar–H), 7.21 (d, 1H,  $J$  = 3.50 Hz, Ar–H), 7.44 (t, 1H,  $J$  = 7.50 Hz, Ar–H), 7.52 (t, 2H,  $J$  = 7.50 Hz, Ar–H), 7.75–7.86 (d, 2H,  $J$  = 7.50 Hz, Ar–H), 8.47 (s, 1H, pyrazole-H), 10.16 (s, 1H, =C–H); <sup>13</sup>C NMR spectrum,  $\delta_{\text{C}}$ , ppm: 183.2 (C=O), 162.3, 151.2, 143.2, 142.9, 139.4, 138.3, 134.9, 133.7, 133.4, 131.2, 130.6, 129.8, 129.1, 128.8, 128.5, 128.2, 120.6, 119.9, 119.6, 116.2, 115.9, 114.6; MS:  $m/z$  633.05 (M + H).

### 3.1.5 | (4Z)-3-(Trifluoromethyl)-4-((3-[4-methoxyphenyl]-1-phenyl-1H-pyrazol-4-yl)methylene)-1-(perfluorophenyl)-1H-pyrazol-5(4H)-one (5a)

Orange solid; Wt. 971 mg; Yield 84%; IR ( $\nu_{\max}/\text{cm}^{-1}$ ): 3,141 (C–H), 1,703 (C=O), 1,595 (C=N), 1,514 (C=C), 1,224 (C–F); <sup>1</sup>H NMR spectrum,  $\delta$ , ppm: 3.92 (s, 3H, –OCH<sub>3</sub>), 7.10 (d, 2H,  $J$  = 8.50 Hz, Ar–H), 7.51 (t, 2H,  $J$  = 8.50 Hz, Ar–H), 7.62 (d, 2H,  $J$  = 8.50 Hz, Ar–H), 7.90 (d, 2H,  $J$  = 9.00 Hz, Ar–H), 7.99 (s, 1H, pyrazole-H), 10.19 (s, 1H, =C–H); <sup>13</sup>C NMR spectrum,  $\delta_{\text{C}}$ , ppm: 162.5 (C=O), 161.1, 158.7, 143.3, 141.4, 138.6, 134.9, 130.7, 129.7, 128.5, 122.6, 120.1, 116.8, 114.7, 113.7, 55.5 (OCH<sub>3</sub>); MS:  $m/z$  579.21 (M + H)<sup>+</sup>.

### 3.1.6 | (4Z)-3-(Trifluoromethyl)-1-(perfluorophenyl)-4-([1,3-diphenyl-1H-pyrazol-4-yl)methylene)-1H-pyrazol-5(4H)-one (5b)

Orange solid; Wt. 876 mg; Yield 80%; IR ( $\nu_{\max}/\text{cm}^{-1}$ ): 3,142 (C–H), 1,701 (C=O), 1,595 (C=N), 1,510 (C=C), 1,223 (C–F); <sup>1</sup>H NMR spectrum,  $\delta$ , ppm: 7.42 (m, 1H, Ar–H), 7.52 (t, 2H,  $J$  = 7.50 Hz, Ar–H), 7.57–7.58 (m, 3H, Ar–H), 7.68 (dd, 2H,  $J$  = 7.50 and 2.00 Hz, Ar–H), 7.90 (d, 2H,  $J$  = 8.00 Hz, Ar–H), 8.00 (s, 1H, pyrazole-H), 10.22 (s, 1H, =C–H); <sup>13</sup>C NMR spectrum,  $\delta_{\text{C}}$ , ppm: 162.5 (C=O), 158.8, 143.0, 141.2, 138.6, 134.9, 130.3, 129.9, 129.7, 129.4, 129.2, 128.6, 120.0, 116.8, 114.0; MS:  $m/z$  549.19 (M + H)<sup>+</sup>.

### 3.1.7 | (4Z)-4-((3-[2-Fluoro-4-methoxyphenyl]-1-phenyl-1H-pyrazol-4-yl)methylene)-3-(trifluoromethyl)-1-(perfluorophenyl)-1H-pyrazol-5(4H)-one (5c)

Orange solid; Wt. 1.06 g; Yield 82%; IR ( $\nu_{\max}/\text{cm}^{-1}$ ): 3,145 (C–H), 1,702 (C=O), 1,596 (C=N), 1,512 (C=C), 1,221 (C–F); <sup>1</sup>H NMR spectrum,  $\delta$ , ppm: 3.91 (s, 3H, –OCH<sub>3</sub>), 6.82 (dd, 1H,  $J$  = 2.50 and 12.00 Hz, Ar–H), 6.91 (dd, 1H,  $J$  = 2.00 and 8.50 Hz, Ar–H), 7.42 (t, 1H,  $J$  = 7.50 Hz, Ar–H), 7.58–7.49 (m, 2H, Ar–H), 7.79 (d, 1H,  $J$  = 2.50 Hz, Ar–H), 7.88 (d, 2H,  $J$  = 7.50 Hz, Ar–H), 8.52 (s, 1H, pyrazole-H), 10.20 (s, 1H, =C–H); <sup>13</sup>C NMR spectrum,  $\delta_{\text{C}}$ , ppm: 162.7 (C=O), 162.6, 162.5, 154.1, 141.2, 138.6, 134.7, 132.5, 129.7, 128.5, 120.0, 117.6, 113.9, 111.2, 110.3, 102.2, 102.0, 55.8 (OCH<sub>3</sub>); MS:  $m/z$  653.26 (M + H)<sup>+</sup>.



### 3.1.8 | (4Z)-3-(Trifluoromethyl)-1-(perfluorophenyl)-4-([1-phenyl-3-p-tolyl-1H-pyrazol-4-yl]methylene)-1H-pyrazol-5(4H)-one (5d)

Orange solid; Wt. 887 mg; Yield 79%; IR ( $\nu_{\max}/\text{cm}^{-1}$ ): 3,143 (=C–H), 1,701 (C=O), 1,594 (C=N), 1,511 (C=C), 1,220 (C–F);  $^1\text{H}$  NMR spectrum,  $\delta$ , ppm: 2.44 (s, 3H, –CH<sub>3</sub>), 7.45 (d, 1H,  $J = 7.50$  Hz, Ar–H), 7.51 (t, 1H,  $J = 7.50$  Hz, Ar–H), 7.62 (d, 1H,  $J = 8.00$  Hz, Ar–H), 7.65 (d, 1H,  $J = 8.00$  Hz, Ar–H), 9.90 (s, 1H, pyrazole-H), 11.96 (s, 1H, =C–H); MS:  $m/z$  563.08 (M + H)<sup>+</sup>.

### 3.1.9 | (4Z)-3-(Trifluoromethyl)-1-(perfluorophenyl)-4-((1-phenyl-3-(4-[trifluoro methoxy]phenyl)-1H-pyrazol-4-yl)methylene)-1H-pyrazol-5(4H)-one (5e)

Orange solid; Wt. 960 mg; Yield 76%; IR ( $\nu_{\max}/\text{cm}^{-1}$ ): 3,145 (=C–H), 1,700 (C=O), 1,595 (C=N), 1,517 (C=C), 1,225 (C–F);  $^1\text{H}$  NMR spectrum,  $\delta$ , ppm: 7.42–7.44 (m, 3H, Ar–H), 7.51–7.54 (m, 2H, Ar–H), 7.71 (d, 1H,  $J = 2.00$  Hz, Ar–H), 7.73 (d, 1H,  $J = 2.00$  Hz, Ar–H), 7.88 (d, 1H,  $J = 2.00$  Hz, Ar–H), 7.90 (d, 1H,  $J = 3.50$  Hz, Ar–H), 7.92 (s, 1H, pyrazole-H), 10.21 (s, 1H, =C–H);  $^{13}\text{C}$  NMR spectrum,  $\delta_{\text{C}}$ , ppm: 162.4 (C=O), 157.3, 150.5, 143.2, 142.9, 140.3, 138.5, 134.9, 130.9, 129.8, 129.0, 128.7, 121.5, 120.6, 120.0, 118.4, 116.6, 114.4; MS:  $m/z$  633.23 (M + H)<sup>+</sup>.

### 3.1.10 | (4Z)-4-((3-[3,4-Dichlorophenyl]-1-phenyl-1H-pyrazol-4-yl)methylene)-3-(trifluoromethyl)-1-(perfluorophenyl)-1H-pyrazol-5(4H)-one (5f)

Orange solid; Wt. 1.03 g; Yield 84%; IR ( $\nu_{\max}/\text{cm}^{-1}$ ): 3,144 (=C–H), 1,701 (C=O), 1,596 (C=N), 1,517 (C=C), 1,227 (C–F);  $^1\text{H}$  NMR spectrum,  $\delta$ , ppm: 7.44 (m, 1H, Ar–H), 7.48 (d, 1H,  $J = 2.00$  Hz, Ar–H), 7.50 (d, 1H,  $J = 2.00$  Hz, Ar–H), 7.53 (d, 1H,  $J = 7.50$  Hz, Ar–H), 7.67 (d, 1H,  $J = 8.50$  Hz, Ar–H), 7.83 (d, 1H,  $J = 2.00$  Hz, Ar–H), 7.87–7.89 (m, 2H, Ar–H), 7.89 (s, 1H, pyrazole-H), 10.18 (s, 1H, =C–H);  $^{13}\text{C}$  NMR spectrum,  $\delta_{\text{C}}$ , ppm: 162.3 (C=O), 156.1, 143.2, 142.9, 139.7, 138.4, 135.0, 134.5, 133.7, 131.2, 131.1, 130.3, 129.8, 128.8, 128.3, 120.0, 116.4, 114.7; MS:  $m/z$  617.15 (M + H)<sup>+</sup>.

### 3.1.11 | (Z)-4-([6-Chloro-5,7-dimethyl-4-oxo-4H-chromen-3-yl]methylene)-2-(perfluorophenyl)-5-(trifluoromethyl)-2,4-dihydro-3H-pyrazol-3-one (6a)

Orange solid; Wt. 900 mg; Yield 84%; IR ( $\nu_{\max}/\text{cm}^{-1}$ ): 3,074 (=C–H), 1,707 (C=O), 1,666 (C=O), 1,624 (C=N), 1,508 (C=C), 1,192 (C–F);  $^1\text{H}$  NMR spectrum,  $\delta$ , ppm: 2.54 (s, 3H, –CH<sub>3</sub>), 3.01 (s, 3H, –CH<sub>3</sub>), 7.26 (s, 1H, Ar–H), 8.50 (s, 1H, chromone-H), 10.54 (s, 1H, =C–H);  $^{13}\text{C}$  NMR spectrum,  $\delta_{\text{C}}$ , ppm: 175.4 (C=O), 164.2 (C=O), 162.3, 155.1, 144.5, 143.4, 143.3, 139.7, 134.7, 120.9, 120.2, 119.4, 118.3, 118.2, 118.1, 22.2 (–CH<sub>3</sub>), 18.6 (–CH<sub>3</sub>); MS:  $m/z$  537.11 (M + H)<sup>+</sup>.

### 3.1.12 | (Z)-4-([6-Chloro-7-methyl-4-oxo-4H-chromen-3-yl]methylene)-2-(perfluorophenyl)-5-(trifluoromethyl)-2,4-dihydro-3H-pyrazol-3-one (6b)

Orange solid; Wt. 783 mg; Yield 75%; IR ( $\nu_{\max}/\text{cm}^{-1}$ ): 3,076 (=C–H), 1,705 (C=O), 1,664 (C=O), 1,627 (C=N), 1,508 (C=C), 1,192 (C–F);  $^1\text{H}$  NMR spectrum,  $\delta$ , ppm: 2.54 (s, 3H, –CH<sub>3</sub>), 7.47 (s, 1H, Ar–H), 8.24 (s, 1H, Ar–H), 8.48 (s, 1H, chromone-H), 10.62 (s, 1H, =C–H); MS:  $m/z$  523.08 (M + H)<sup>+</sup>.

### 3.1.13 | (Z)-4-([6-Chloro-4-oxo-4H-chromen-3-yl]methylene)-2-(perfluorophenyl)-5-(trifluoromethyl)-2,4-dihydro-3H-pyrazol-3-one (6c)

Orange solid; Wt. 812 mg; Yield 80%; IR ( $\nu_{\max}/\text{cm}^{-1}$ ): 3,074 (=C–H), 1,707 (C=O), 1,662 (C=O), 1,621 (C=N), 1,509 (C=C), 1,193 (C–F);  $^1\text{H}$  NMR spectrum,  $\delta$ , ppm: 7.55 (d, 1H,  $J = 9.00$  Hz, Ar–H), 7.73 (d, 1H,  $J = 2.50$  and 9.00 Hz, Ar–H), 8.26 (d, 1H,  $J = 2.50$  Hz, Ar–H), 8.47 (s, 1H, chromone-H), 10.63 (s, 1H, =C–H); MS:  $m/z$  509.08 (M + H)<sup>+</sup>.

### 3.1.14 | (Z)-4-([6,8-Dichloro-4-oxo-4H-chromen-3-yl]methylene)-2-(perfluorophenyl)-5-(trifluoromethyl)-2,4-dihydro-3H-pyrazol-3-one (6d)

Orange solid; Wt. 845 mg; Yield 78%; IR ( $\nu_{\max}/\text{cm}^{-1}$ ): 3,078 (=C–H), 1,707 (C=O), 1,665 (C=O), 1,626 (C=N), 1,506 (C=C), 1,194 (C–F);  $^1\text{H}$  NMR spectrum,  $\delta$ , ppm: 7.83 (d, 1H,  $J = 2.50$  Hz, Ar–H), 8.17 (d, 1H,  $J = 2.50$  Hz, Ar–H), 8.40 (s, 1H, chromone-H), 10.66 (s, 1H, =C–H); MS:  $m/z$  543.07 (M + H)<sup>+</sup>.

### 3.1.15 | (Z)-4-([7-Methyl-4-oxo-4H-chromen-3-yl]methylene)-2-(perfluorophenyl)-5-(trifluoromethyl)-2,4-dihydro-3H-pyrazol-3-one (6e)

Orange solid; Wt. 800 mg; Yield 82%; IR ( $\nu_{\max}/\text{cm}^{-1}$ ): 3,076 (=C–H), 1,703 (C=O), 1,666 (C=O), 1,627 (C=N), 1,510 (C=C), 1,193 (C–F);  $^1\text{H}$  NMR spectrum,  $\delta$ , ppm: 2.51 (s, 3H, –CH<sub>3</sub>), 7.48 (d, 1H,  $J = 8.00$  Hz, Ar–H), 7.60 (dd, 1H,  $J = 8.00$  and 2.00 Hz, Ar–H), 8.08 (d, 1H,  $J = 1.50$  Hz), 8.54 (s, 1H, chromone-H), 10.64 (s, 1H, =C–H);  $^{13}\text{C}$  NMR spectrum,  $\delta_{\text{C}}$ , ppm: 174.5 (C=O), 165.5 (C=O), 162.4, 154.2, 143.4, 142.4, 137.5, 136.3, 126.2, 120.9, 123.3, 120.2, 118.6, 118.5, 118.2, 118.1, 21.1 (–CH<sub>3</sub>); MS:  $m/z$  489.14 (M + H)<sup>+</sup>.

## 3.2 | Anti-inflammatory activity

All the synthesized compounds were screened for their in vitro anti-inflammatory activities against the standard drug diclofenac sodium. The minimum inhibitory concentration was determined by the well diffusion method at 1 mg/ml of concentration. (Table 2). A volume of 1 ml of diclofenac sodium at different concentrations (50, 100, 200, 400, 800, and 1,000  $\mu\text{g}/\text{ml}$ ) was homogenized with 1 ml of aqueous solution of bovine serum albumin (5%) and incubated at 27°C for 15 minutes. The mixture of distilled water and bismuth sulphite agar constituted the control tube. Denaturation of the proteins was caused by placing the mixture in a water bath for 10 minutes at 70°C. The mixture was cooled within the ambient room temperature, and the activity of each mixture was measured at 255 nm. Each test was conducted thrice. The following formula was used to calculate inhibition percentage:

$$\% \text{inhibition} = \frac{\text{absorbance of control} - \text{absorbance of sample}}{\text{absorbance of control}} \times 100.$$

## 3.3 | In silico ADME

In the present study, we have calculated molecular volume (MV), molecular weight (MW), logarithm of partition coefficient (miLog  $P$ ), number of hydrogen bond acceptors (n-ON), number of hydrogen bonds donors (n-OHNH), topological polar surface area (TPSA), number of rotatable bonds (n-ROTB), and Lipinski's rule of five<sup>[31]</sup> using the Molinspiration online property calculation toolkit.<sup>[30]</sup> Absorption (% ABS) was calculated by: %

ABS =  $109 - (0.345 \times \text{TPSA})$ .<sup>[32]</sup> Drug likeness model score (a collective property of physicochemical properties, pharmacokinetics, and pharmacodynamics of a compound that is represented by a numerical value) was computed by MolSoft software.<sup>[33]</sup>

## 4 | CONCLUSIONS

In conclusion, we have constructed pyrazole and fluorine in one molecular framework as new 3-(trifluoromethyl)-1-(perfluorophenyl)-1H-pyrazol-5(4H)-one derivatives under conventional and nonconventional methods like microwave irradiation and ultrasonication, respectively, via Knoevenagel condensation and evaluated their biological activity. Ultrasonication and microwave irradiation can shorten the reaction time from a few hours to a few minutes and increases the product yield (74–84%) compared to the conventional method (59–75%). The synthesized compounds exhibited promising anti-inflammatory activity compared to the standard drug diclofenac sodium. Similarly, the synthesized compound displayed promising antioxidant activity compared to the standard drug. Furthermore, an analysis of the ADME parameters for synthesized compounds showed good drug-like properties and can be developed as an oral drug candidate, thus suggesting that compounds from the present series can be further optimized and developed as a lead molecule.

## ACKNOWLEDGMENT

The authors are thankful to the Department of Science and Technology, New Delhi for providing research facilities under FIST scheme and to CIF, Savitribai Phule Pune University, Pune and SAIF, Panjab University, Chandigarh for providing spectral facilities.

## CONFLICT OF INTEREST

The authors declare no conflict of interest, financial or otherwise.

## REFERENCES

- [1] M. Bhat, G. K. Nagaraja, R. Kayarmar, S. K. Peethamber, M. Shefeeulla, *RSC Adv.* **2016**, 6, 59375.
- [2] A. L. Luz, C. D. Kassotis, H. M. Stapleton, J. N. Meyer, *Toxicology* **2018**, 393, 150.
- [3] P. Khloya, S. Kumar, P. Kaushik, P. Surain, D. Kaushik, P. K. Sharma, *Bioorg. Med. Chem. Lett.* **2015**, 25, 1177.
- [4] (a) Y. R. Li, C. Li, J. C. Liu, M. Guo, T. Y. Zhang, L. P. Sun, C. J. Zheng, H. R. Piao, *Bioorg. Med. Chem. Lett.* **2015**, 25, 5052. (b) S. A. Ali, S. M. Awad, A. M. Said, S. Mahgouba, H. Tahaa, N. M. Ahmed, *J. Enzyme Inhib. Med. Chem.* **2020**, 35, 847.
- [5] X. L. Deng, J. Xie, Y. Q. Li, D. K. Yuan, X. P. Hu, L. Zhang, Q. M. Wang, M. Chi, X. L. Yang, *Chin. Chem. Lett.* **2016**, 27, 566.

- [6] H. Jia, F. Bai, N. Liu, X. Liang, P. Zhan, C. Ma, X. Jiang, X. Liu, *Eur. J. Med. Chem.* **2016**, *123*, 202.
- [7] C. I. Nieto, M. P. Cabildo, M. P. Cornago, D. Sanz, R. M. Claramunt, I. Alkorta, J. Elguero, J. A. Garcia, A. Lopez, D. A. Castroviejo, *J. Mol. Struct.* **2015**, *1100*, 518.
- [8] S. Shu, X. Cai, J. Li, Y. Feng, A. Dai, J. Wang, D. Yang, M. W. Wang, H. Liu, *Bioorg. Med. Chem.* **2016**, *24*, 2852.
- [9] R. Dummer, P. A. Ascierto, H. J. Gogas, A. Arance, M. Mandala, G. Liskay, C. Garbe, D. Schadendorf, L. Krajsova, R. Gutzmer, V. C. Sileni, C. Dutriaux, J. W. Groot, N. Yamazaki, C. Loquai, L. A. M. D. Parseval, M. D. Pickard, V. Sandor, C. Robert, K. T. Flaherty, *Lancet Oncol.* **2018**, *19*, 6035.
- [10] E. Therrien, G. Larouche, N. Nguyen, J. Rahil, A. M. Lemieux, Z. Li, M. Fournel, T. P. Yan, A. J. Landry, S. Lefebvre, J. J. Wang, K. Macbeth, C. Heise, A. Nguyen, J. M. Besterman, R. Deziel, A. Wahhab, *Bioorg. Med. Chem. Lett.* **2015**, *25*, 2514.
- [11] X. H. Lv, Q. S. Li, Z. L. Ren, M. J. Chu, J. Sun, X. Zhang, M. Xing, H. L. Zhu, H. Q. Cao, *Eur. J. Med. Chem.* **2016**, *108*, 586.
- [12] M. A. Tabrizi, P. G. Baraldi, E. Ruggiero, G. Saponaro, S. Baraldi, R. Romagnoli, A. Martinelli, T. Tuccinardi, *Eur. J. Med. Chem.* **2015**, *97*, 289.
- [13] E. Kick, R. Martin, Y. Xie, B. Flatt, E. Schweiger, T. L. Wang, B. Busch, M. Nyman, X. H. Gu, G. Yan, B. Wagner, M. Nanao, L. Nguyen, T. Stout, A. Plonowski, I. Schulman, J. Ostrowski, T. Kirchgessner, R. Wexler, R. Mohan, *Bioorg. Med. Chem. Lett.* **2015**, *25*, 372.
- [14] a) K. Muller, C. Faeh, F. Diederich, *Science* **2007**, *317*, 1881. b) W. K. Hagmann, *J. Med. Chem.* **2008**, *51*, 4359. c) R. E. Banks, B. E. Smart, J. C. Tatlow, *Organo Fluorine Chemistry. Principles and Commercial Applications*, Plenum, New York **1994**. d) S. Purser, P. R. Moore, S. Swallow, V. Gouverneur, *Chem. Soc. Rev.* **2008**, *37*, 320. e) P. Jeschke, *ChemBioChem* **2004**, *5*, 570.
- [15] a) D. O'Hagan, *Chem. Soc. Rev.* **2008**, *37*, 308. b) H. J. Bohm, D. Banner, S. Bendels, M. Kansy, B. Kuhn, K. Muller, U. ObstSander, M. Stahl, *ChemBioChem* **2004**, *5*, 637. (c) P. Nagender, D. Pulakesh, G. Gouverneur, N. Shibata, *Org. Lett.* **2018**, *20*, 1526. (d) D. Pulakesh, G. Satoshi, P. Nagender, U. Hiroto, T. Etsuko, N. Shibata, *Chem. Sci.* **2018**, *9*, 3276. (e) P. Nagender, S. Takuya, K. Mikhail, T. Etsuko, S. Yuji, N. Shibata, *Chem. Commun.* **2018**, *54*, 4294. (f) D. K. Swaroop, N. Ravi Kumar, P. Nagender, G. Jitender Dev, N. Jagadeesh Babu, B. Narsaiah, *Eur. J. Org. Chem.* **2019**, *2019*, 3654. <https://doi.org/10.1002/ejoc.201900482>. (g) P. Nagender, H. Kyosuke, N. Shibata, *Chem. Commun.* **2018**, *54*, 7171.
- [16] (a) I. I. Gerus, R. X. Mironetz, I. S. Kondratov, A. V. Bezdudny, Y. V. Dmytriv, O. V. Shishkin, V. S. Starova, O. A. Zaporozhets, A. A. Tolmachev, P. K. Mykhailiuk, *J. Org. Chem.* **2012**, *77*, 47. (b) B. D. Maxwell, *J. Labell. Compd. Radiopharm.* **2000**, *43*, 645.
- [17] T. G. Leighton, *The acoustic bubble*, Academic Press, London **1994**, p. 531.
- [18] C. O. Kappe, A. Stadler, D. Dallinger, *Microwaves in Organic and Medicinal Chemistry*, 2nd ed., Wiley-VCH, Weinheim **2012**.
- [19] (a) A. S. William, F. B. Aleksel, C. Ron, Organic synthesis: The science behind art. in *Royal Society of Chemistry (Great Britain)*, RSC publications, Cambridge, **1998**. (b) *Organic Synthesis Co. II vol*; **1935**. (c) *Comprehensive Organic Synthesis Book Volumes*, John Wiley & Sons, Hoboken, NJ, **1991**.
- [20] (a) T. Syed, A. Yahya, J. A. Alsheri, *Lett. Org. Chem.* **2020**, *17*, 157. (b) S. Mallouk, K. Bougrin, A. Laghzizil, R. Benhida, *Molecules* **2010**, *15*, 813. (c) J. S. Biradar, B. S. Sasidhar, *Eur. J. Med. Chem.* **2011**, *46*, 6112. (d) M. B. Ansari, H. Jin, M. N. Parvin, S. E. Park, *Catal. Today* **2012**, *185*, 211.
- [21] (a) M. A. Pasha, K. Manjula, J. Saudi, *Chem. Soc.* **2011**, *15*, 283. (b) Y. Ogiwara, K. Takahashi, T. Kitazawa, N. Sakai, *J. Org. Chem.* **2015**, *80*, 3101. (c) P. Leelavathi, S. R. Kumar, *J. Mol. Catal. A Chem.* **2005**, *240*, 99. (d) J. V. Schijndel, A. C. Luiz, D. Molendijk, J. Meuldijk, *Green Chem. Lett. Rev.* **2017**, *10*, 404.
- [22] S. Ramesh, F. Devred, D. P. Debecker, *ChemistrySelect* **2020**, *5*, 300.
- [23] R. B. Ardakani, N. Safaeian, M. Oftadeh, M. F. Mehrjardi, *Theor. Chem. Acc.* **2020**, *139*, 45.
- [24] N. Zengin, H. Burhan, A. Savk, H. Goksu, F. Sen, *Scie. Rep.* **2020**, *10*, 12758.
- [25] A. R. Bhat, M. H. Najjar, R. S. Dongre, M. S. Akhter, *Res. Green Sust. Chem.*, **2020**, *3*, 100008. <https://doi.org/10.1016/j.jrgsc.2020.06.001>.
- [26] (a) K. S. Hon, H. N. Akolkar, B. K. Karale, *J. Het. Chem.* **2020**, *57*, 1692. (b) S. P. Kunde, K. G. Kanade, B. K. Karale, H. N. Akolkar, S. S. Arbuj, P. V. Randhavane, S. T. Shinde, M. H. Shaikh, A. K. Kulkarni, *RSC Adv.* **2020**, *10*, 26997. (c) S. J. Takate, A. D. Shinde, B. K. Karale, H. Akolkar, L. Nawale, D. Sarkar, P. C. Mhaske, *Bioorg. Med. Chem. Lett.* **2019**, *29*, 1999. (d) S. P. Kunde, K. G. Kanade, B. K. Karale, H. N. Akolkar, P. V. Randhavane, S. T. Shinde, *Res. Chem. Intermed.* **2017**, *43*, 7277. (e) R. S. Endait, B. K. Karale, H. N. Akolkar, P. V. Randhavane, *Indian J. Het. Chem.* **2016**, *26*, 141.
- [27] B. S. Furniss, A. J. Hannaford, P. W. G. Smith, A. R. Tatchell, *Vogel's Text Book of Practical Organic Chemistry*, 5th ed., Addison Wesley Longman Limited, England **1998**.
- [28] S. Kandia, A. L. Charles, *Food Chem.* **2019**, *287*, 338.
- [29] S. Zhang, Y. Luo, L. Q. He, Z. J. Liu, A. Q. Jiang, Y. H. Yang, H. L. Zhu, *Bioorg. Med. Chem.* **2013**, *21*, 3723.
- [30] Molinspiration Chemoinformatics Brastislava, Slovak Republic. <http://www.molinspiration.com/cgi-bin/properties>; **2014**.
- [31] C. A. Lipinski, L. Lombardo, B. W. Dominy, P. J. Feeney, *Adv. Drug Del. Rev.* **2001**, *46*, 3.
- [32] Y. Zhao, M. H. Abraham, J. Lee, A. Hersey, N. C. Luscombe, G. Beck, B. Sherborne, I. Cooper, *Pharm. Res.* **2002**, *19*, 1446.
- [33] Drug-Likeness and Molecular Property Prediction. <http://www.molsoft.com/mprop/>.

## SUPPORTING INFORMATION

Additional supporting information may be found online in the Supporting Information section at the end of this article.

**How to cite this article:** Dengale SG, Akolkar HN, Karale BK, et al. Synthesis of 3-(trifluoromethyl)-1-(perfluorophenyl)-1H-pyrazol-5 (4H)-one derivatives via Knoevenagel condensation and their biological evaluation. *J Chin Chem Soc.* 2020;1–12. <https://doi.org/10.1002/jccs.202000357>



## Microwave-assisted Synthesis, Characterization, and Antibacterial Screening of Some Pyrazolone Derivatives

Bhauasaheb Kisan. Karale<sup>1\*</sup>, Sarita G. Kundlikar<sup>1</sup>, Hemantkumar N. Akolkar<sup>1</sup>, Pratibha V. Randhavane<sup>1</sup>,  
Sushama J. Takate<sup>2</sup>

<sup>1</sup>Department of Chemistry, Radhabai Kale Mahila Mahavidyalaya, Ahmednagar, Maharashtra, India

<sup>2</sup>Department of Chemistry, New Arts, Science and Commerce College, Ahmednagar, Maharashtra, India

**ABSTRACT** 1-(4-(4-Chlorophenyl)thiazol-2-yl)-3-propyl-1H-pyrazol-5(4H)-one **5** was prepared by the reaction of 1-(4-(4-chlorophenyl)thiazol-2-yl)hydrazine and ethyl 3-oxohexanoate. Compound **5** was condensed with different 4-formylpyrazoles **8a-f** to give product **9a-f** through Knoevenagel condensation. The reaction was carried out by both conventional and non-conventional methods. The structures of all the newly synthesized compounds were confirmed with the help of spectral techniques. All the compounds were screened for antibacterial activity. Compounds **9a**, **9d**, and **9e** exhibited good antibacterial activity against *Bacillus subtilis*.

**KEYWORDS** Knoevenagel condensation, Pyrazolone, Thiazoles, Thiophene.

How to cite this article: Karale, B.K., Kundlikar, S.G., Akolkar, H.N., Randhavane, P.V., Takate, S.J. Microwave-assisted Synthesis, Characterization, and Antibacterial Screening of Some Pyrazolone Derivatives, *Indian J. Heterocycl. Chem.*, 2020, 30, 355-360. (DocID: <https://connectjournals.com/01951.2020.30.355>)

### INTRODUCTION

The Knoevenagel condensation reaction has been widely employed for C-C bond formation in organic synthesis<sup>[1]</sup> and their products are the key intermediates for the synthesis of various natural and therapeutic drugs, polymer, and perfumes.<sup>[2,3]</sup> Lewis bases and acids have been reported as catalysts in the Knoevenagel condensation, including Ni-SiO<sub>2</sub>,<sup>[4]</sup> synthetic phosphate Na<sub>2</sub>CaP<sub>2</sub>O<sub>7</sub>,<sup>[5]</sup> Ca<sub>2</sub>P<sub>2</sub>O<sub>7</sub>,<sup>[5]</sup> and natural phosphate ([NP]/KF or NP/NaNO<sub>3</sub>).<sup>[6]</sup> Ionic liquids<sup>[7]</sup> have been also used as catalysts in Knoevenagel condensation.

Thiazoles and their derivatives have attracted continuing interest over the years because of their varied biological activities such as anti-inflammatory,<sup>[8]</sup> antitubercular,<sup>[9]</sup> antimicrobial,<sup>[10]</sup> angiogenesis,<sup>[11]</sup> and neuroprotective.<sup>[12]</sup> Various pyrazole derivatives exhibit anti-inflammatory,<sup>[13]</sup> analgesic,<sup>[13]</sup> antiproliferative,<sup>[14]</sup> and antihepatotoxic<sup>[15]</sup> activities.

Thiophene is sulfur-containing a five-membered heterocyclic compound. Various biological activities

associated with thiophene derivatives are BACE1 inhibitors,<sup>[16]</sup> HIV protease inhibitor,<sup>[17]</sup> antibreast cancer,<sup>[18]</sup> acetylcholinesterase inhibitors,<sup>[19]</sup> and antidepressant.<sup>[20]</sup>

The pyrazolone skeleton exists in the core structure of several biologically active compounds and natural products.<sup>[21]</sup> Antipyrine<sup>[22]</sup> was the first synthetic drug containing pyrazolone ring as the main framework which has been used as an analgesic and antipyretic. Pyrazolone derivatives show a broad spectrum of biological activities such as severe acute respiratory syndrome-coronavirus 3C-like protease inhibitors,<sup>[23]</sup> cytotoxic,<sup>[24]</sup> antitubulin,<sup>[25]</sup> anaplastic lymphoma kinase inhibitors,<sup>[25]</sup> anti-inflammatory,<sup>[26]</sup> and analgesic.<sup>[26]</sup> Some of the chlorine-containing compounds exhibit anti-inflammatory,<sup>[27]</sup> analgesic,<sup>[28]</sup> antibacterial,<sup>[29]</sup> and antifungal<sup>[30]</sup> activities.

The application of microwave (MW) and ultrasound irradiation as a non-conventional energy source for the activation of reactions has now become a very popular and useful technology in organic chemistry.<sup>[31-33]</sup> These methods lead to enhanced conversion rates, higher yields, and easier work-up.

\*Corresponding author: E-mail: [bkkarale@yahoo.com](mailto:bkkarale@yahoo.com)

Journal Homepage

[www.connectjournals.com/ijhc](http://www.connectjournals.com/ijhc)

Published & Hosted by

CONNECT  
Journals

[www.connectjournals.com](http://www.connectjournals.com)



## Synthesis and Antibacterial Screening of Some New Pyrazolylchromones and Pyrazolylcoumaran-3-ones

Sushama J. Takate<sup>1</sup>, Supriya P. Salve<sup>1</sup>, Sushama B. Dare<sup>1</sup>, Bhausaheb K. Karale<sup>2</sup>, Hemantkumar N. Akolkar<sup>2</sup>, Dnyaneshwar B. Falke<sup>1</sup>, Rahul B. Ghungurde<sup>1</sup>, Sadhana D. Mhaske<sup>3\*</sup>

<sup>1</sup>Department of Chemistry, New Arts, Commerce and Science College, Ahmednagar; Affiliated to SPPU, Pune, Maharashtra, India

<sup>2</sup>Department of Chemistry, Radhabai Kale Mahila Mahavidyalaya, Ahmednagar; Affiliated to SPPU, Pune, Maharashtra, India

<sup>3</sup>Department of Chemistry, Dadapatil Rajale Arts, Science and Commerce College, Adinathnagar; Affiliated to SPPU, Pune, Maharashtra, India

**ABSTRACT** Some new pyrazolylchromones **4a-e** (flavone analogs) and pyrazolylcoumaran-3-ones **5a-e** (aurone analogs) were synthesized by refluxing chalcones **3a-e** in dimethyl sulfoxide/ $I_2$  and Pyridine/ $Hg(OAc)_2$ , respectively. Spectral techniques such as infrared, proton nuclear magnetic resonance, and mass spectrometry were used to confirm the structures of newly synthesized compounds. These compounds were studied for their antibacterial activities toward *Bacillus subtilis*, *Staphylococcus aureus*, *Escherichia coli*, and *Salmonella typhi*. Some of these compounds showed promising activity against test organisms.

**KEYWORDS:** Pyrazoles, Flavones, Aurones, Antibacterial activity.

**How to cite this article:** Takate, S.J., Salve, S.P., Dare, S.B., Karale, B.K., Akolkar, H.N., Falke, D.B., Ghungurde, R.B., Mhaske, S.D. Synthesis and Antibacterial Screening of Some New Pyrazolylchromones and Pyrazolylcoumaran-3-ones. *Indian J. Heterocycl. Chem.*, 2020, 30, 525-530. (DocID: <https://connectjournals.com/01951.2020.30.525>)

### INTRODUCTION

Treatment of various diseases is a worldwide serious issue. The emergence of newer infectious diseases, multidrug resistance developing in microbial strains, diseases due to homeostatic disturbances, toxicity associated with existing drugs have created a need of selective, potential therapeutic agents. In search of potential therapeutic agents, many natural and synthetic compounds have been investigated. Many of the natural products are heterocycles which possess medicinal properties and serve as lead molecules for drug discovery.<sup>[1]</sup> Lead modification is an important step in drug design and development.

Pyrazole containing compounds are medicinally useful because of their various therapeutic properties, including antimicrobial,<sup>[2,3]</sup> anti-inflammatory,<sup>[4]</sup> antitubercular,<sup>[5]</sup>

antitumor,<sup>[6]</sup> antidiabetic,<sup>[7]</sup> and antiviral and antioxidant<sup>[8]</sup> properties.

Flavonoids are extensively studied plant products for their biological potential. Chalcones are important intermediates in the flavonoid synthetic pathway and also have medicinal properties.<sup>[9]</sup> These are known to exhibit antibacterial,<sup>[10]</sup> antitubercular,<sup>[11]</sup> anti-inflammatory,<sup>[12,13]</sup> antimalarial,<sup>[14]</sup> antifungal,<sup>[15]</sup> and antiviral<sup>[16]</sup> activities. Synthetic chalcones with heterocyclic rings have been investigated for medicinal properties and are also used in the synthesis of various heterocycles. Pyrazole containing chalcones exhibits potential antimicrobial,<sup>[17]</sup> antioxidant,<sup>[18]</sup> and anticancer<sup>[19]</sup> activities.

Flavones and aurones are medicinally useful members of the flavonoid family. Flavones are widely known for their interesting bioactivities. As a consequence of the

\*Corresponding author: E-mail: [mhaskesadhana@gmail.com](mailto:mhaskesadhana@gmail.com)

Published & Hosted by:

Journal Homepage:  
[www.connectjournals.com/ijhc](http://www.connectjournals.com/ijhc)

**CONNECT** Journals™  
[www.connectjournals.com](http://www.connectjournals.com)

©2020 Connect Journals





ARTICLE

# Synthesis of 3-(trifluoromethyl)-1-(perfluorophenyl)-1*H*-pyrazol-5(4*H*)-one derivatives via Knoevenagel condensation and their biological evaluation

Sujata G. Dengale<sup>1</sup> | Hemantkumar N. Akolkar<sup>2</sup> | Bhausahab K. Karale<sup>2</sup> |  
Nirmala R. Darekar<sup>2</sup> | Sadhana D. Mhaske<sup>3</sup> | Mubarak H. Shaikh<sup>2</sup> |  
Dipak N. Raut<sup>4</sup> | Keshav K. Deshmukh<sup>1</sup>

<sup>1</sup>P.G. and Research, Department of Chemistry, Sangamner Nagarpalika Arts, D. J. Malpani Commerce and B. N. Sarada Science College, Sangamner, India

<sup>2</sup>P.G. and Research, Department of Chemistry, Radhabai Kale Mahila Mahavidyalaya, Ahmednagar, India

<sup>3</sup>Department of Chemistry, Dadapatil Rajale College, Pathardi, India

<sup>4</sup>Amrutvahini College of Pharmacy, Sangamner, India

## Correspondence

Hemantkumar N. Akolkar, P.G. and Research, Department of Chemistry, Radhabai Kale Mahila Mahavidyalaya, Ahmednagar, Maharashtra, India, 414001.  
Email: hemantakolkar@gmail.com

## Abstract

In search of new active molecules, a small focused library of the synthesis of 3-(trifluoromethyl)-1-(perfluorophenyl)-1*H*-pyrazol-5(4*H*)-one derivatives (**4a-d**, **5a-f**, and **6a-e**) has been efficiently prepared via the Knoevenagel condensation approach. All the derivatives were synthesized by conventional and non-conventional methods like ultrasonication and microwave irradiation, respectively. Several derivatives exhibited excellent anti-inflammatory activity compared to the standard drug. Furthermore, the synthesized compounds were found to have potential antioxidant activity. In addition, to rationalize the observed biological activity data, an *in silico* absorption, distribution, metabolism, and excretion (ADME) prediction study also been carried out. The results of the *in vitro* and *in silico* studies suggest that the 3-(trifluoromethyl)-1-(perfluorophenyl)-1*H*-pyrazol-5(4*H*)-one derivatives (**4a-d**, **5a-f**, and **6a-e**) may possess the ideal structural requirements for the further development of novel therapeutic agents.

## KEYWORDS

ADME prediction, anti-inflammatory, antioxidant, Knoevenagel, microwave, pyrazole, ultrasonication

## 1 | INTRODUCTION

The pyrazole ring is a prominent heterocyclic structural compound found in several pharmaceutically active compounds. This is because of its use in pharmacological activity and ease of synthesis. Furthermore, the selective functionalization of pyrazole with diverse substituents was also found to improve their range of action in various fields. Pyrazole containing heterocycles shows various biological activity, such as antibacterial,<sup>[1]</sup> antifungal,<sup>[2]</sup> antimicrobial,<sup>[3]</sup> anti-inflammatory,<sup>[4a]</sup> antioxidant,<sup>[4b]</sup> insecticidal,<sup>[5]</sup> antiviral,<sup>[6]</sup> anti-nitric oxide

synthase,<sup>[7]</sup> glycogen receptor antagonist,<sup>[8]</sup> anticancer,<sup>[9]</sup> anti-enzyme,<sup>[10]</sup> immunosuppressant,<sup>[11]</sup> anti-fatty acid amide hydrolase (FAAH),<sup>[12]</sup> and liver-x-receptor [LXR] partial agonist activities.<sup>[13]</sup>

Fluorine or fluorine-based compounds are of great interest in synthetic and medicinal chemistry. The position of the fluorine atom in an organic molecule plays a vital role in agrochemicals, pharmaceuticals, and materials<sup>[14]</sup> as it changes the pharmacokinetic and pharmacodynamic properties of the molecule owing to its high membrane permeability, metabolic stability, lipophilicity, and binding affinity.<sup>[15]</sup>



## ARTICLE

# Synthesis and characterization of novel 2-(1-benzyl-3-[4-fluorophenyl]-1*H*-pyrazol-4-yl)-7-fluoro-4*H*-chromen-4-one derivatives

Kiran S. Hon | Hemantkumar N. Akolkar | Bhausahab K. Karale

P.G. and Research, Department of Chemistry, Radhabai Kale Mahila Mahavidyalaya, Ahmednagar, Maharashtra, India

**Correspondence**

Bhausahab K. Karale, P.G. and Research, Department of Chemistry, Radhabai Kale Mahila Mahavidyalaya, Ahmednagar, Maharashtra 414 001, India.  
Email: bkkarale@yahoo.com

**Abstract**

Novel 1-benzyl-3-(4-fluorophenyl)-1*H*-pyrazole-4-carbaldehydes **3a** to **3e** were synthesized via Vilsmeier-Haack reaction of the appropriate 1-benzyl-2-(1-(4-fluorophenyl)ethylidene)hydrazines, derived from 4-fluoroacetophenone **1** with substituted 2-benzylhydrazines **2a** to **2e**. The base catalyzed condensation of 1-benzyl-3-(4-fluorophenyl)-1*H*-pyrazole-4-carbaldehydes **3a** to **3e** with 1-(4-fluoro-2-hydroxyphenyl)ethanone **4** gave (*E*)-3-(1-benzyl-3-(4-fluorophenyl)-1*H*-pyrazol-4-yl)-1-(4-fluoro-2-hydroxyphenyl)prop-2-en-1-ones **5a** to **5e**. On cyclization with dimethyl sulfoxide (DMSO)/I<sub>2</sub>, compounds **5a** to **5e** gave 2-(1-benzyl-3-(4-fluorophenyl)-1*H*-pyrazol-4-yl)-7-fluoro-4*H*-chromen-4-ones **6a** to **6e**. Structures of all novel compounds were confirmed by infrared (IR), proton nuclear magnetic resonance (<sup>1</sup>H NMR), carbon nuclear magnetic resonance (<sup>13</sup>C NMR), and mass spectral data. All the synthesized compounds were screened for their antibacterial activities.

## 1 | INTRODUCTION

Chromones (4*H*-1-benzopyran-4-one, 4*H*-chromen-4-one) are the heterocyclic compound widely distributed in nature.<sup>[1]</sup> Chromone-containing compounds display various pharmacological properties such as antifungal,<sup>[2]</sup> antimalarial,<sup>[3]</sup> anticancer,<sup>[4]</sup> antibacterial,<sup>[5]</sup> and are also well known as an antidiabetic and cardiovascular agents.<sup>[6,7]</sup> Pyrazole-containing compounds show antiangiogenic,<sup>[8]</sup> antimalarial,<sup>[9]</sup> antifungal,<sup>[10]</sup> antitubercular,<sup>[11]</sup> antimicrobial,<sup>[11]</sup> and anticancer<sup>[12]</sup> activities.

Currently, there are more than 200 pharmaceutical drugs available in market containing fluorine atom. Fluorine and fluorine-containing substituent can impart many effects on properties of organic compounds.<sup>[13,14]</sup> Fluorine-containing compounds exhibit fungicidal,<sup>[15]</sup> herbicidal,<sup>[16]</sup> antiviral,<sup>[17]</sup> antipyretic,<sup>[18]</sup> and analgesic<sup>[19]</sup> activities.

Considering the biological importance of chromone, pyrazole, and fluorine nucleus, we have reported the synthesis, characterization, and antibacterial screening of

novel 1-benzyl-3-(4-fluorophenyl)-1*H*-pyrazole-4-carbaldehydes **3a** to **3e**, (*E*)-3-(1-benzyl-3-(4-fluorophenyl)-1*H*-pyrazol-4-yl)-1-(4-fluoro-2-hydroxyphenyl)prop-2-en-1-ones **5a** to **5e** and 2-(1-benzyl-3-(4-fluorophenyl)-1*H*-pyrazol-4-yl)-7-fluoro-4*H*-chromen-4-one derivatives **6a** to **6e**.

## 2 | RESULT AND DISCUSSION

1-Benzyl-3-(4-fluorophenyl)-1*H*-pyrazole-4-carbaldehydes **3a** to **3e** were synthesized via the Vilsmeier-Haack reaction of the appropriate 1-benzyl-2-(1-(4-fluorophenyl)ethylidene)hydrazines, derived from 4-fluoroacetophenone **1** with substituted 2-benzylhydrazines **2a** to **2e**.<sup>[20]</sup> (*E*)-3-(1-Benzyl-3-(4-fluorophenyl)-1*H*-pyrazol-4-yl)-1-(4-fluoro-2-hydroxyphenyl)prop-2-en-1-ones **5a** to **5e** were synthesized from the reaction of 1-benzyl-3-(4-fluorophenyl)-1*H*-pyrazole-4-carbaldehydes **3a** to **3e** with 1-(4-fluoro-2-hydroxyphenyl)ethanone **4** in 10% aq. KOH. The synthesis of 2-(1-benzyl-3-(4-fluorophenyl)-1*H*-pyrazol-4-yl)-

7-fluoro-4*H*-chromen-4-ones **6a** to **6e** was achieved by reaction of (*E*)-3-(1-benzyl-3-(4-fluorophenyl)-1*H*-pyrazol-4-yl)-1-(4-fluoro-2-hydroxyphenyl)prop-2-en-1-ones **5a** to **5e** with dimethyl sulfoxide (DMSO)/I<sub>2</sub> (Scheme 1 and Section 3).

Structures of all the synthesized compounds were confirmed by using infrared (IR), proton nuclear magnetic resonance (<sup>1</sup>H NMR), carbon nuclear magnetic resonance (<sup>13</sup>C NMR), and liquid chromatography-mass spectrometry (LC-MS) spectroscopic techniques.

## 2.1 | Antibacterial activities

All the synthesized compounds were screened for their antibacterial activities. The bacterial strains *Staphylococcus aureus*, *Bacillus subtilis*, *Escherichia coli*, and *Pseudomonas aeruginosa* were used. The zone of inhibition in millimeter was determined by the well diffusion method at 1 mg/mL of concentration, and Ampicillin was used as reference drugs. The results of antibacterial activity are shown in Table 1.

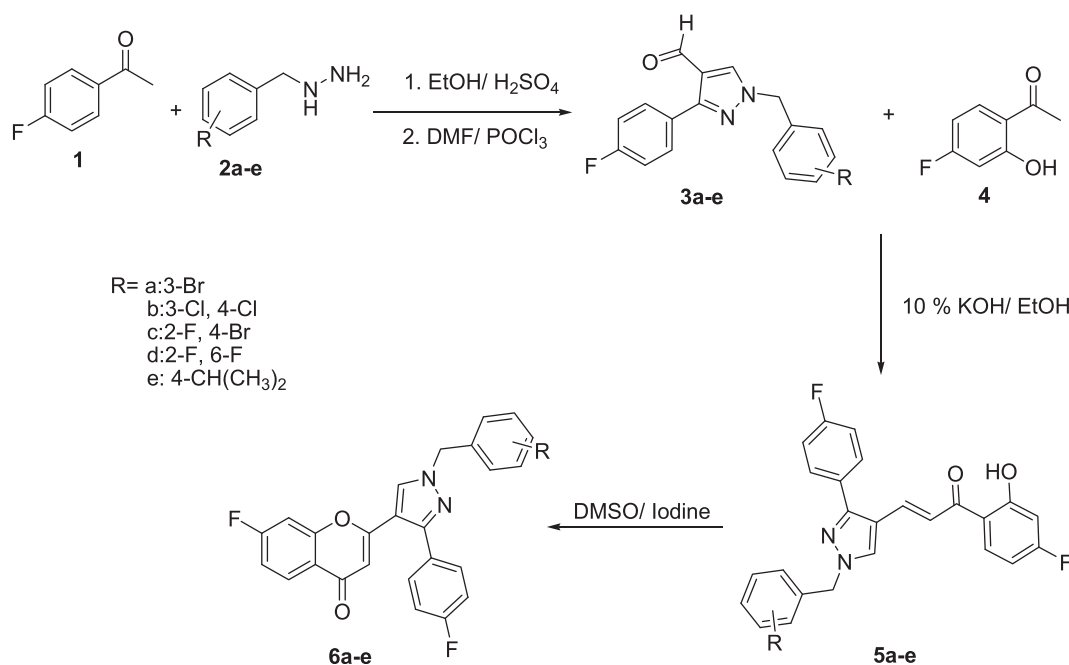
The results given in Table 1 indicated that compounds **3c**, **3d**, **3d**, **6a**, **6b**, **6c**, and **6d** exhibited good antibacterial activity against *E. coli* bacterial strain. Compounds **3c** to **3e**, **5e**, and **6a** to **6e** exhibited good antibacterial activity against *P. aeruginosa*. While compounds **3e** and **6a** to **6d** exhibited good antibacterial activity against *B. subtilis* and *S. aureus* compared with the standard Ampicillin. While other compounds were found to be less to moderately active against all bacterial strains.

## 3 | EXPERIMENTAL

The melting points were measured on a DBK melting point apparatus and are uncorrected. IR spectra were recorded on Shimadzu IR Affinity 1S (attenuated total reflection [ATR]) Fourier transform infrared (FTIR) spectrophotometer. <sup>1</sup>H NMR (400 MHz) and <sup>13</sup>C NMR (100 MHz) spectra were recorded on Varian 400 spectrophotometer using tetramethylsilane (TMS) as an internal standard and DMSO-*d*<sub>6</sub> as solvent, and chemical shifts were expressed as δ parts per million units. Mass spectra were obtained on Shimadzu (LC-MS) mass spectrometer.

### 3.1 | General procedure for synthesis of 1-benzyl-3-(4-fluorophenyl)-1*H*-pyrazole-4-carbaldehydes (**3a-e**)

A mixture of substituted 1-benzylhydrazine (0.01 mol) and catalytic amount of concentrated H<sub>2</sub>SO<sub>4</sub> was added to a solution of 1-(4-fluorophenyl)ethanone (0.01 mol) in 20 mL of ethanol. The mixture was refluxed for 1 hour, and the 1-benzyl-2-(1-(4-fluorophenyl)ethylidene)hydrazine formed was filtered and dried. A mixture of dimethylformamide (DMF) and phosphoryl chloride (POCl<sub>3</sub>) was cooled with constant stirring at 0°C. A solution of 1-benzyl-2-(1-(4-fluorophenyl)ethylidene)hydrazine in DMF was added dropwise to the reaction mixture and then heated at 70 to 80°C for 5 hours. After completion of reaction, contents were cooled to room temperature and poured onto ice-cold water, and then it was made alkaline with saturated K<sub>2</sub>CO<sub>3</sub> solution. The



**SCHEME 1** Synthetic approach to the title compounds

**TABLE 1** Antibacterial activities of the synthesized compounds (zone of inhibition in millimeter)

Compound	<i>Escherichia coli</i>	<i>Pseudomonas aeruginosa</i>	<i>Bacillus subtilis</i>	<i>Staphylococcus aureus</i>
3a	8	10	10	12
3b	9	10	10	11
3c	14	13	12	12
3d	15	14	12	13
3e	16	15	14	17
5a	9	11	12	11
5b	9	10	10	12
5c	8	10	10	9
5d	10	11	10	9
5e	12	14	13	12
6a	16	15	14	16
6b	14	15	14	16
6c	16	14	16	17
6d	14	15	15	16
6e	12	14	9	10
Ampicillin	16	15	17	18

precipitate formed was crystallized from ethanol to get pure 1-benzyl-3-(4-fluorophenyl)-1H-pyrazole-4-carbaldehydes **3a-e**.

### 3.2 | 1-(3-Bromobenzyl)-3-(4-fluorophenyl)-1H-pyrazole-4-carbaldehyde (3a)

Yield: 71%, White solid, mp 58–60°C. IR ( $\nu_{\max}/\text{cm}^{-1}$ ): 3112 (=C–H), 2820 (aldehyde C–H), 1674 (C=O), 1655 (C=N);  $^1\text{H}$  NMR spectrum (400 MHz, DMSO- $d_6$ ):  $\delta$  = 5.45 (s, 2H, –CH<sub>2</sub>), 7.25–7.35 (m, 4H, Ar–H), 7.52–7.60 (m, 2H, Ar–H), 7.86–7.90 (m, 2H, Ar–H), 8.72 (s, 1H, pyrazolyl-H), 9.86 (s, 1H, –CHO);  $^{13}\text{C}$  NMR (100 MHz, DMSO- $d_6$ ):  $\delta$  = 53.92, 115.17, 115.38, 120.48, 127.96, 128.36, 130.10, 130.52, 130.61, 130.85, 131.24, 137.09, 138.35, 150.91, 161.21, 163.66, 184.33; MS (LC-MS):  $m/z$  358.95 (M + H)<sup>+</sup>.

### 3.3 | 1-(3,4-Dichlorobenzyl)-3-(4-fluorophenyl)-1H-pyrazole-4-carbaldehyde (3b)

Yield: 65%, White solid. mp 190–192°C; IR ( $\nu_{\max}/\text{cm}^{-1}$ ): 3112 (=C–H), 2820 (aldehyde C–H), 1674 (C=O), 1655 (C=N);  $^1\text{H}$  NMR spectrum (400 MHz, DMSO- $d_6$ ):  $\delta$  = 5.46 (s, 2H, –CH<sub>2</sub>), 7.26–7.36 (m, 3H, Ar–H), 7.64–7.68 (m, 2H, Ar–H), 7.86–7.89 (m, 2H, Ar–H), 8.72 (s, 1H, pyrazolyl-H), 9.86 (s, 1H, –CHO); MS (LC-MS):  $m/z$  349 (M + H)<sup>+</sup>.

### 3.4 | 1-(4-Bromo-2-fluorobenzyl)-3-(4-fluorophenyl)-1H-pyrazole-4-carbaldehyde (3c)

Yield: 69%; White solid; mp 64–66°C; IR ( $\nu_{\max}/\text{cm}^{-1}$ ): 3113 (=C–H), 2822 (aldehyde C–H), 1673 (C=O), 1656 (C=N);  $^1\text{H}$  NMR (400 MHz, DMSO- $d_6$ ):  $\delta$  = 5.49 (s, 2H, –CH<sub>2</sub>), 7.29 (t, 2H,  $J$  = 8.8 Hz, Ar–H), 7.35 (t, 1H,  $J$  = 8 Hz, Ar–H), 7.45 (d, 1H,  $J$  = 8.4 Hz, Ar–H), 7.61 (d, 1H,  $J$  = 8.4 Hz, Ar–H), 7.86 (dd, 2H,  $J$  = 8 and 6 Hz, Ar–H), 8.67 (s, 1H, pyrazolyl-H), 9.86 (s, 1H, –CHO);  $^{13}\text{C}$  NMR (100 MHz, DMSO- $d_6$ ):  $\delta$  = 49.66, 115.40, 115.62, 116.20, 116.42, 119.34, 119.58, 121.08, 121.23, 123.26, 123.35, 127.44, 127.85, 128.02, 128.05, 130.53, 130.61, 131.57, 131.60, 131.77, 131.86, 134.57, 152.82, 159.01, 161.53, 161.97, 164.45, 184.20; MS (LC-MS):  $m/z$  376.95 (M + H)<sup>+</sup>.

### 3.5 | 1-(2,6-Difluorobenzyl)-3-(4-fluorophenyl)-1H-pyrazole-4-carbaldehyde (3d)

Yield: 61%; White solid; mp 68–70°C; IR ( $\nu_{\max}/\text{cm}^{-1}$ ): 3112 (=C–H), 2824 (aldehyde C–H), 1677 (C=O), 1654 (C=N);  $^1\text{H}$  NMR (400 MHz, DMSO- $d_6$ ):  $\delta$  = 5.52 (s, 2H, –CH<sub>2</sub>), 7.18 (t, 2H,  $J$  = 8 Hz, Ar–H), 7.26 (t, 2H,  $J$  = 8.8 Hz, Ar–H), 7.50 (t, 1H,  $J$  = 8 Hz, Ar–H), 7.83 (m, 2H, Ar–H), 8.66 (s, 1H, pyrazolyl-H), 9.85 (s, 1H, –CHO);  $^{13}\text{C}$  NMR (100 MHz, DMSO- $d_6$ ):  $\delta$  = 43.32, 111.38, 111.57, 111.75, 112.00, 115.17, 115.38, 120.24,



127.96, 130.49, 130.57, 131.43, 131.53, 131.64, 138.50, 150.59, 159.75, 161.20, 162.15, 163.64, 184.38; MS (LC-MS):  $m/z$  317.05 (M + H)<sup>+</sup>.

### 3.6 | 1-(4-Isopropylbenzyl)-3-(4-fluorophenyl)-1H-pyrazole-4-carbaldehyde (3e)

Yield: 64%; White solid; mp 52–54°C; IR ( $\nu_{\max}/\text{cm}^{-1}$ ): 3111 (C–H), 2821 (aldehyde C–H), 1672 (C=O), 1656 (C=N); <sup>1</sup>H NMR (400 MHz, DMSO-*d*<sub>6</sub>):  $\delta$  = 1.1 (d, 6H, –CH<sub>3</sub>), 2.8 (m, 1H, –CH), 5.4 (s, 2H, –CH<sub>2</sub>), 7.23–7.30 (m, 6H, Ar–H), 7.86–7.90 (m, 2H, Ar–H), 7.45 (d, 1H,  $J$  = 8.4 Hz, Ar–H), 7.61 (d, 1H,  $J$  = 8.4 Hz, Ar–H), 7.86 (dd, 2H,  $J$  = 8 and 6 Hz, Ar–H), 8.67 (s, 1H, pyrazolyl-H), 9.85 (s, 1H, –CHO); MS (LC-MS):  $m/z$  323.05 (M + H)<sup>+</sup>.

### 3.7 | General procedure for synthesis of (E)-3-(1-Benzyl-3-(4-fluorophenyl)-1H-pyrazol-4-yl)-1-(4-fluoro-2-hydroxyphenyl)prop-2-en-1-ones (5a-e)

A mixture of 1-benzyl-3-(4-fluorophenyl)-1H-pyrazole-4-carbaldehydes **3a** to **3e** (0.005 mol) with 1-(4-fluoro-2-hydroxyphenyl)ethanone **4** (0.005 mol) was stirred in ethanolic KOH (10%) for 16 hours at room temperature. After completion of reaction, contents were poured onto ice-cold water and then acidified with concentrated hydrochloric acid (HCl). The precipitate formed was filtered off, washed with water, and crystallized from ethanol to get the pure product **5a-e**.

### 3.8 | (E)-3-(1-(3-Bromobenzyl)-3-(4-fluorophenyl)-1H-pyrazol-4-yl)-1-(4-fluoro-2-hydroxyphenyl)prop-2-en-1-one (5a)

Yield: 74%; Yellow solid; mp 80–82°C; IR ( $\nu_{\max}/\text{cm}^{-1}$ ): 1637 (C=O), 1590 (C=N), 1569 (C=C); <sup>1</sup>H NMR (400 MHz, DMSO-*d*<sub>6</sub>):  $\delta$  = 5.46 (s, 2H, –CH<sub>2</sub>), 6.82–6.89 (m, 2H, Ar–H), 7.33–7.39 (m, 4H, Ar–H), 7.53–7.61 (m, 4H, Ar–H), 7.70–7.81 (AB quartet, 2H,  $J$  = 15.6 Hz, =C–H), 8.21 (dd, 1H,  $J$  = 8 and 6.8 Hz, Ar–H), 8.75 (s, 1H, pyrazolyl-H), 13.09 (s, 1H, –OH); <sup>13</sup>C NMR (100 MHz, DMSO-*d*<sub>6</sub>):  $\delta$  = 54.73, 104.12, 104.36, 106.79, 107.02, 115.65, 115.86, 117.58, 119.62, 121.84, 126.97, 128.52, 130.36, 130.44, 130.63, 130.90, 132.31, 133.04, 133.16, 135.87, 139.10, 151.29, 161.01, 163.46, 164.46, 164.60, 165.14, 167.67, 192.09; MS (LC-MS):  $m/z$  495.10 (M + H)<sup>+</sup>.

### 3.9 | (E)-3-(1-(3,4-Dichlorobenzyl)-3-(4-fluorophenyl)-1H-pyrazol-4-yl)-1-(4-fluoro-2-hydroxyphenyl)prop-2-en-1-one (5b)

Yield: 72%; Yellow solid; mp 158–160°C; IR ( $\nu_{\max}/\text{cm}^{-1}$ ): 1641 (C=O), 1594 (C=N), 1524 (C=C); <sup>1</sup>H NMR (400 MHz, DMSO-*d*<sub>6</sub>):  $\delta$  = 5.47 (s, 2H, –CH<sub>2</sub>), 6.81–6.87 (m, 2H, Ar–H), 7.33–7.44 (m, 3H, Ar–H), 7.59 (dd, 2H,  $J$  = 8 and 6 Hz, Ar–H), 7.66–7.68 (m, 2H, Ar–H), 7.69–7.81 (AB quartet, 2H,  $J$  = 15.6 Hz, =CH), 8.19 (t, 1H,  $J$  = 8 Hz, Ar–H), 8.73 (s, 1H, pyrazolyl-H), 13.07 (s, 1H, –OH); <sup>13</sup>C NMR (100 MHz, DMSO-*d*<sub>6</sub>):  $\delta$  = 55.34, 104.98, 105.22, 106.86, 107.08, 115.76, 115.97, 116.83, 118.83, 127.23, 128.22, 129.90, 129.97, 130.48, 130.56, 131.06, 131.49, 131.60, 132.92, 133.22, 135.43, 136.10, 152.44, 166.03, 166.18, 192.06; MS (LC-MS):  $m/z$  485.05 (M + H)<sup>+</sup>.

### 3.10 | (E)-3-(1-(4-Bromo-2-fluorobenzyl)-3-(4-fluorophenyl)-1H-pyrazol-4-yl)-1-(4-fluoro-2-hydroxyphenyl)prop-2-en-1-one (5c)

Yield: 71%; Yellow solid; mp 118–120°C; IR ( $\nu_{\max}/\text{cm}^{-1}$ ): 1638 (C=O), 1587 (C=N), 1574 (C=C); <sup>1</sup>H NMR (400 MHz, DMSO-*d*<sub>6</sub>):  $\delta$  = 5.48 (s, 2H, –CH<sub>2</sub>), 6.81–6.89 (m, 2H, Ar–H), 7.32–7.40 (m, 3H, Ar–H), 7.48 (dd, 1H,  $J$  = 8 and 2 Hz, Ar–H), 7.57 (dd, 2H,  $J$  = 8 and 6 Hz, Ar–H), 7.63 (dd, 1H,  $J$  = 8 and 2 Hz, Ar–H), 7.69–7.82 (AB quartet, 2H,  $J$  = 15.6 Hz, =CH), 8.23 (dd, 1H,  $J$  = 8 and 6.8 Hz, Ar–H), 8.72 (s, 1H, pyrazolyl-H), 13.10 (s, 1H, –OH); <sup>13</sup>C NMR (100 MHz, DMSO-*d*<sub>6</sub>):  $\delta$  = 49.07, 104.13, 104.37, 106.82, 107.03, 115.66, 115.74, 115.87, 117.60, 118.92, 119.16, 119.67, 121.97, 122.07, 122.64, 122.79, 128.00, 128.46, 130.39, 130.47, 132.29, 132.38, 132.43, 133.12, 133.23, 135.80, 151.35, 158.82, 161.02, 161.32, 163.47, 164.47, 164.60, 165.16, 167.68, 192.13; MS (LC-MS):  $m/z$  515 (M + H)<sup>+</sup>.

### 3.11 | (E)-3-(1-(2,6-Difluorobenzyl)-3-(4-fluorophenyl)-1H-pyrazol-4-yl)-1-(4-fluoro-2-hydroxyphenyl)prop-2-en-1-one (5d)

Yield: 74%; Yellow solid; mp 184–186°C; IR ( $\nu_{\max}/\text{cm}^{-1}$ ): 1640 (C=O), 1596 (C=N), 1568 (C=C); <sup>1</sup>H NMR (400 MHz, DMSO-*d*<sub>6</sub>):  $\delta$  = 5.49 (s, 2H, –CH<sub>2</sub>), 6.81–6.89 (m, 2H, Ar–H), 7.17 (t, 2H,  $J$  = 8 Hz, Ar–H), 7.33 (t, 2H,  $J$  = 8 Hz, Ar–H), 7.48–7.56 (m, 3H, Ar–H), 7.7 (d, 1H,  $J$  = 15.8 Hz, =C–H), 7.83 (d, 1H,  $J$  = 15.6 Hz, =C–H), 8.26 (dd, 1H,  $J$  = 8 and 6.8 Hz, Ar–H), 8.74 (s, 1H, pyrazolyl-H), 13.14 (s, 1H, –OH); <sup>13</sup>C NMR (100 MHz, DMSO-*d*<sub>6</sub>):  $\delta$  = 43.47, 104.09, 104.32, 106.73, 106.95, 111.37, 111.56,



111.75, 111.93, 111.99, 115.59, 115.65, 115.81, 117.45, 119.49, 128.45, 128.48, 130.37, 130.45, 131.37, 131.47, 131.57, 132.10, 133.17, 133.28, 135.82, 151.32, 159.71, 159.79, 161.02, 162.20, 162.27, 163.47, 164.63, 164.77, 165.19, 167.71, 193.20; MS (LC-MS):  $m/z$  453.15 (M + H)<sup>+</sup>.

### 3.12 | (E)-3-(1-(4-Isopropylbenzyl)-3-(4-fluorophenyl)-1H-pyrazol-4-yl)-1-(4-fluoro-2-hydroxyphenyl)prop-2-en-1-one (5e)

Yield: 77%; Yellow solid; mp 130-132°C; IR ( $\nu_{\max}/\text{cm}^{-1}$ ): 1635 (C=O), 1595 (C=N), 1567 (C=C); <sup>1</sup>H NMR (400 MHz, DMSO-*d*<sub>6</sub>):  $\delta$  = 1.17 (d, 6H, CH<sub>3</sub>), 2.87 (m, 1H, —C—H), 5.39 (s, 2H, —CH<sub>2</sub>), 6.82-6.89 (m, 2H, Ar—H), 7.25-7.37 (m, 6H, Ar—H), 7.57-7.61 (m, 2H, Ar—H), 7.70-7.81 (AB quartet, 2H,  $J$  = 15.8 Hz, =C—H), 8.23 (dd, 1H,  $J$  = 8 and 6.8 Hz, Ar—H), 8.74 (s, 1H, pyrazolyl-H), 13.13 (s, 1H, —OH); <sup>13</sup>C NMR (100 MHz, DMSO-*d*<sub>6</sub>):  $\delta$  = 23.75, 33.12, 55.41, 104.13, 104.36, 106.79, 107.01, 115.63, 115.75, 115.84, 117.56, 119.36, 126.06, 127.92, 128.63, 130.35, 130.43, 132.01, 133.06, 133.17, 133.90, 136.05, 148.22, 151.04, 160.98, 163.42, 164.49, 164.63, 165.14, 167.67, 192.13; MS (LC-MS):  $m/z$  459.15 (M + H)<sup>+</sup>.

### 3.13 | General procedure for synthesis of 2-(1-benzyl-3-(4-fluorophenyl)-1H-pyrazol-4-yl)-7-fluoro-4H-chromen-4-ones (6a-e)

Compound **5a** to **5e** (0.002 mol) was dissolved in 15-mL DMSO. To this solution, catalytic amount of iodine was added. The reaction mixture was heated to 140°C for 2 hours. After completion of reaction (checked by thin-layer chromatography [TLC]), content were cooled and poured over crushed ice. The product obtained was filtered, washed with cold water and 10% sodium thiosulphate solution followed by cold water, and crystallized from ethanol to get the pure product **6a** to **6e**.

### 3.14 | 2-(1-(3-Bromobenzyl)-3-(4-fluorophenyl)-1H-pyrazol-4-yl)-7-fluoro-4H-chromen-4-one (6a)

Yield: 77%; White solid; mp 200-202°C; IR ( $\nu_{\max}/\text{cm}^{-1}$ ): 3112 (=C—H), 1641 (C=O), 1622 (C=N), 1597 (C=C); <sup>1</sup>H NMR (400 MHz, DMSO-*d*<sub>6</sub>):  $\delta$  = 5.46 (s, 2H, —CH<sub>2</sub>), 6.32 (s, 1H), 7.19 (dd, 1H,  $J$  = 8 and 2 Hz, Ar—H), 7.30-7.62 (m, 9H, Ar—H), 8.19 (dd, 1H,  $J$  = 8 and 6.8 Hz, Ar—H), 8.71 (s, 1H, pyrazolyl-H); <sup>13</sup>C NMR (100 MHz, DMSO-*d*<sub>6</sub>):  $\delta$  = 54.87, 104.56, 104.82, 107.24, 110.95, 112.30, 113.82, 115.32, 115.54, 116.69, 119.55, 120.72, 122.07, 127.24, 127.74, 127.84, 129.20, 130.97, 131.12, 133.66,

139.25, 149.39, 158.12, 158.50, 158.89, 159.28, 159.63, 163.82, 175.80; MS (LC-MS):  $m/z$  495.10 (M + H)<sup>+</sup>.

### 3.15 | 2-(1-(3,4-Dichlorobenzyl)-3-(4-fluorophenyl)-1H-pyrazol-4-yl)-7-fluoro-4H-chromen-4-one (6b)

Yield: 65%; White solid; mp 148-150°C; IR ( $\nu_{\max}/\text{cm}^{-1}$ ): 3059 (=C—H), 1645 (C=O), 1620 (C=N), 1598 (C=C); <sup>1</sup>H NMR (400 MHz, DMSO-*d*<sub>6</sub>):  $\delta$  = 5.47 (s, 2H, —CH<sub>2</sub>), 6.32 (s, 1H), 7.19 (d, 1H,  $J$  = 8 Hz, Ar—H), 7.27-7.70 (m, 8H, Ar—H), 8.19 (t, 1H,  $J$  = 8 Hz, Ar—H), 8.70 (s, 1H, pyrazolyl-H); <sup>13</sup>C NMR (100 MHz, DMSO-*d*<sub>6</sub>):  $\delta$  = 54.13, 104.83, 107.23, 110.87, 113.74, 115.32, 115.54, 116.61, 120.59, 127.80, 128.53, 129.00, 130.25, 131.06, 131.39, 133.71, 137.48, 157.96, 158.34, 158.73, 159.10, 175.70; MS (LC-MS):  $m/z$  483.10 (M + H)<sup>+</sup>.

### 3.16 | 2-(1-(4-Bromo-2-fluorobenzyl)-3-(4-fluorophenyl)-1H-pyrazol-4-yl)-7-fluoro-4H-chromen-4-one (6c)

Yield: 69%; White solid; mp 220-222°C; IR ( $\nu_{\max}/\text{cm}^{-1}$ ): 3065 (=C—H), 1643 (C=O), 1620 (C=N), 1594 (C=C); <sup>1</sup>H NMR (400 MHz, DMSO-*d*<sub>6</sub>):  $\delta$  = 5.49 (s, 2H, —CH<sub>2</sub>), 6.31 (s, 1H), 7.19 (dd, 1H,  $J$  = 8 and 6.8 Hz, Ar—H), 7.25-7.78 (m, 8H, Ar—H), 8.05 (dd, 1H,  $J$  = 8 and 6.8 Hz, Ar—H), 8.67 (s, 1H, pyrazolyl-H); <sup>13</sup>C NMR (100 MHz, DMSO-*d*<sub>6</sub>):  $\delta$  = 48.46, 104.43, 104.69, 107.01, 111.87, 113.66, 113.89, 115.14, 115.35, 118.85, 119.09, 120.41, 121.87, 121.96, 122.62, 122.77, 127.48, 127.59, 127.96, 128.77, 130.43, 130.83, 130.91, 132.24, 133.50, 149.04, 156.26, 156.40, 158.73, 159.23, 161.01, 161.24, 163.46, 165.97, 175.44; MS (LC-MS):  $m/z$  513.10 (M + H)<sup>+</sup>.

### 3.17 | 2-(1-(2,6-Difluorobenzyl)-3-(4-fluorophenyl)-1H-pyrazol-4-yl)-7-fluoro-4H-chromen-4-one (6d)

Yield: 72%; White solid; mp 140-142°C; IR ( $\nu_{\max}/\text{cm}^{-1}$ ): 3110 (=C—H), 1648 (C=O), 1622 (C=N), 1594 (C=C); <sup>1</sup>H NMR (400 MHz, DMSO-*d*<sub>6</sub>):  $\delta$  = 5.51 s (2H, —CH<sub>2</sub>), 6.31 (s, 1H), 7.16-7.57 (m, 9H, Ar—H), 8.04 (dd, 1H,  $J$  = 8 and 6.8 Hz, Ar—H), 8.66 (s, 1H, pyrazolyl-H); <sup>13</sup>C NMR (100 MHz, DMSO-*d*<sub>6</sub>):  $\delta$  = 43.31, 104.41, 104.66, 106.95, 111.43, 111.70, 111.75, 111.93, 113.58, 113.80, 115.09, 115.30, 120.38, 127.43, 127.54, 128.80, 130.81, 130.89, 131.44, 131.54, 133.25, 148.96, 156.23, 156.37, 159.17, 159.74, 161.00, 162.16, 163.44, 165.94, 175.41; MS (LC-MS):  $m/z$  451.05 (M + H)<sup>+</sup>.

### 3.18 | 2-(1-(4-Isopropylbenzyl)-3-(4-fluorophenyl)-1H-pyrazol-4-yl)-7-fluoro-4H-chromen-4-one (6e)

Yield: 67%; White solid; mp 280-282°C; IR ( $\nu_{\max}/\text{cm}^{-1}$ ): 3066 (=C-H), 1644 (C=O), 1620 (C=N), 1592(C=C);  $^1\text{H}$  NMR (400 MHz, DMSO- $d_6$ ):  $\delta$  = 1.18 (d, 6H, -CH<sub>3</sub>), 2.87 (m, 1H, -C-H), 5.39 (s, 2H, -CH<sub>2</sub>), 6.30 (s, 1H), 7.18-7.36 (m, 8H, Ar-H), 7.58-7.62 (m, 2H, Ar-H), 8.05 (dd, 1H,  $J$  = 8 and 6.8 Hz, Ar-H), 8.68 (s, 1H, pyrazolyl-H);  $^{13}\text{C}$  NMR (100 MHz, DMSO- $d_6$ ):  $\delta$  = 23.76, 33.12, 55.20, 104.44, 104.70, 106.90, 111.81, 113.67, 113.90, 115.16, 115.37, 120.44, 126.57, 127.52, 127.98, 128.98, 130.85, 130.93, 133.17, 133.83, 148.22, 148.76, 156.30, 156.43, 159.46, 161.00, 163.44, 165.99, 175.46; MS (LC-MS):  $m/z$  457.15 (M + H)<sup>+</sup>.

## 4 | CONCLUSION

In conclusion, we have synthesized a series of novel 2-(1-benzyl-3-(4-fluorophenyl)-1H-pyrazol-4-yl)-7-fluoro-4H-chromen-4-ones **6a** to **6e** from 1-benzyl-3-(4-fluorophenyl)-1H-pyrazole-4-carbaldehydes **3a** to **3e**. All synthesized compounds are characterized by using spectral methods and screened for their antibacterial activities.

## ORCID

Hemantkumar N. Akolkar  <https://orcid.org/0000-0003-0882-1324>

## REFERENCES

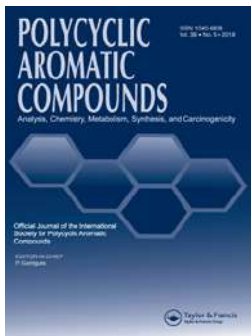
- [1] J. Reis, A. Gaspar, N. Milhazes, F. M. Borges, *J. Med. Chem.* **2017**, *60*(19), 7941.
- [2] O. Prakash, R. Kumar, V. Parkash, *Eur. J. Med. Chem.* **2008**, *43*, 435.
- [3] P. Lerdisirisuk, C. Maicheen, J. Ungwitayatorn, *Bioorg. Chem.* **2014**, *57*, 142.
- [4] K. N. Gopalan, A. Joseph, S. Moorkoth, *Int. J. Pharm. Biosci. Technol.* **2013**, *1*, 130.
- [5] M. Momin, D. Ramjugernath, H. Chenia, N. A. Koorbanally, *J. Chem.* **2013**, *13*, 50.

- [6] O. Bozdog-Dundar, M. Ceylan-Unlusoy, E. J. Verspohl, R. Ertan, *Arzneim. Forsch.* **2007**, *57*, 532.
- [7] M. Ceylan-Ünlüsoy, E. J. Verspohl, R. Ertan, *J. Enzyme. Inhib. Med. Chem.* **2010**, *25*, 784.
- [8] M. S. Christodoulou, S. Liekens, K. M. Kasiotis, S. A. Haroutounian, *Bioorg. Med. Chem.* **2010**, *18*, 4338.
- [9] A. A. Bekhit, A. Hymete, H. Asfaw, A. A. Bekhit, *Arch. Pharm. Chem. Life Sci.* **2012**, *345*, 147.
- [10] C. B. Vicentini, C. Romagnoli, E. Andreotti, D. Mares, *J. Agric. Food Chem.* **2007**, *55*, 10331.
- [11] R. B. Pathak, P. T. Chovatia, H. H. Parekh, *Bioorg. Med. Chem. Lett.* **2012**, *22*, 5129.
- [12] I. Bouabdallah, L. A. M'Barek, A. Zyad, A. Ramdani, I. Zidane, A. Melhaoui, *Nat. Pro. Res.* **2006**, *20*(11), 1024.
- [13] Y. Zhou, J. Wang, Z. Gu, S. Wang, W. Zhu, J. L. Acen, V. A. Soloshonok, K. Izawa, H. Liu, *Chem. Rev.* **2016**, *116*(2), 422.
- [14] J. Wang, M. Sánchez-Roselló, J. L. Aceña, C. Pozo, A. E. Sorochinsky, S. Fustero, V. A. Soloshonok, H. Liu, *Chem. Rev.* **2014**, *114*(4), 2432.
- [15] A. Guan, C. Liu, G. Huang, H. Li, S. Hao, Y. Xu, Y. Xie, Z. Li, *J. Fluorine Chem.* **2014**, *160*, 82.
- [16] G. Li, X. Qian, J. Cui, Q. Huang, D. Cui, R. Zhang, F. Liu, *J. Fluorine Chem.* **2006**, *127*, 182.
- [17] H. Chen, S. Q. Huang, J. Y. Xie, *J. Fluorine Chem.* **2006**, *127*, 1130.
- [18] S. G. Kucukguzel, S. Rollas, H. Erdeniz, A. C. Kiraz, M. Ekinci, A. Vidin, *Eur. J. Med. Chem.* **2000**, *35*, 761.
- [19] T. P. Gregory, C. D. Darlene, M. S. David, *Pestic. Biochem. Phys.* **1998**, *60*, 177.
- [20] M. A. Kira, M. O. Abdel-Rahman, K. Z. Gadalla, *Tetrahedron Lett.* **1969**, *10*, 109.

## SUPPORTING INFORMATION

Additional supporting information may be found online in the Supporting Information section at the end of this article.

**How to cite this article:** Hon KS, Akolkar HN, Karale BK. Synthesis and characterization of novel 2-(1-benzyl-3-[4-fluorophenyl]-1H-pyrazol-4-yl)-7-fluoro-4H-chromen-4-one derivatives. *J Heterocyclic Chem.* 2020;1-6. <https://doi.org/10.1002/jhet.3894>




## Design, Synthesis and Biological Evaluation of Novel Furan & Thiophene Containing Pyrazolyl Pyrazolines as Antimalarial Agents

**Hemantkumar N. Akolkar**, Sujata G. Dengale, Keshav K. Deshmukh, Bhausahab K. Karale, Nirmala R. Darekar, Vijay M. Khedkar & Mubarak H. Shaikh

To cite this article: Hemantkumar N. Akolkar, Sujata G. Dengale, Keshav K. Deshmukh, Bhausahab K. Karale, Nirmala R. Darekar, Vijay M. Khedkar & Mubarak H. Shaikh (2020): Design, Synthesis and Biological Evaluation of Novel Furan & Thiophene Containing Pyrazolyl Pyrazolines as Antimalarial Agents, Polycyclic Aromatic Compounds, DOI: [10.1080/10406638.2020.1821231](https://doi.org/10.1080/10406638.2020.1821231)

To link to this article: <https://doi.org/10.1080/10406638.2020.1821231>

 View supplementary material 

 Published online: 14 Sep 2020.

 Submit your article to this journal 

 Article views: 9

 View related articles 

 View Crossmark data 



# Design, Synthesis and Biological Evaluation of Novel Furan & Thiophene Containing Pyrazolyl Pyrazolines as Antimalarial Agents

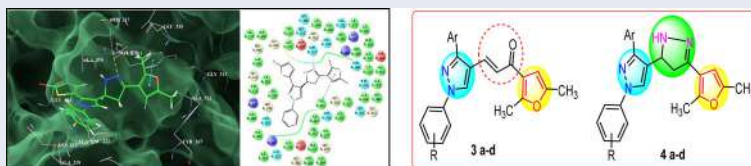
Hemantkumar N. Akolkar<sup>a</sup>, Sujata G. Dengale<sup>b</sup>, Keshav K. Deshmukh<sup>b</sup>, Bhausaheb K. Karale<sup>a</sup>, Nirmala R. Darekar<sup>a</sup>, Vijay M. Khedkar<sup>c</sup>, and Mubarak H. Shaikh<sup>a</sup>

<sup>a</sup>P.G. and Research, Department of Chemistry, Radhabai Kale Mahila Mahavidyalaya, Ahmednagar, India;

<sup>b</sup>P.G. and Research, Department of Chemistry, Sangamner Nagarpalika Arts, D. J. Malpani Commerce, B.N. Sarada Science College, Sangamner, India; <sup>c</sup>Department of Pharmaceutical Chemistry, School of Pharmacy, Vishwakarma University, Pune, India

## ABSTRACT

In search for novel compounds targeting Malaria, based on the *in silico* molecular docking binding affinity data, the novel furans containing pyrazolyl chalcones (**3a-d**) and pyrazoline derivatives (**4a-d**) were synthesized. The formation of the synthesized compound were confirmed by spectral analysis like IR, <sup>1</sup>H NMR, <sup>13</sup>C NMR and mass spectrometry. Compounds with thiophene and pyrazoline ring **4b** (0.47  $\mu$ M), **4c** (0.47  $\mu$ M) and **4d** (0.21  $\mu$ M) exhibited excellent anti-malarial activity against *Plasmodium falciparum* compared with standard antimalarial drug Quinine (0.83  $\mu$ M). To check the selectivity furthermore, compounds were tested for antimicrobial activity and none of the synthesized compound exhibited significant potency compared with the standard antibacterial drug Chloramphenicol and antifungal drug Nystatin respectively. So, it can be resolved that the produced compounds show selectively toward antimalarial activity and have the potential to be explored further.



## ARTICLE HISTORY

Received 7 August 2020

Accepted 5 September 2020


## KEYWORDS

Antimalarial; antimicrobial; chalcones; pfENR inhibitor; pyrazole-pyrazolines; thiophene

## Introduction

Life-threatening disease Malaria is caused by *Plasmodium* parasites that are spread to people through the bites of infected female Anopheles mosquitoes. Out of five *Plasmodium* Parasites *Plasmodium falciparum* produces high levels of blood-stage parasites that sequester in critical organs in all age groups.<sup>1</sup> As per the World Health Organization report in 2018, in sub Saharan Africa 11 million pregnant women were infected with malaria and 872 000 children were born with a low birth weight. Around 24 million children estimated to be infected with the *P. falciparum* parasite in the region; out of these, 1.8 million had severe anemia and 12 million had

**CONTACT** Hemantkumar N. Akolkar  [hemantakolkar@gmail.com](mailto:hemantakolkar@gmail.com)  P.G. and Research, Department of Chemistry, Radhabai Kale Mahila Mahavidyalaya, Ahmednagar, Maharashtra 414001, India.

 Supplemental data for this article is available online at <https://doi.org/10.1080/10406638.2020.1821231>.

moderate anemia.<sup>2</sup> Mortality and morbidity caused by malaria are continually increasing. This subject is the consequence of the ever-increasing development of parasite resistance to drugs and also increased mosquito resistance to insecticides which is one of the most critical complications in controlling malaria over recent years.<sup>3</sup>

*P. falciparum* enoyl-acyl carrier protein (ACP) reductase (ENR) is an enzyme in type II fatty acid synthesis (FAS II) pathway which catalyzes the NADH-dependent reduction of trans-2-enoyl-ACP to acyl-ACP and plays important role in completion of the fatty acid elongation cycles. Due to its role in the parasite's fatty acid pathway, PfENR has been known as one of the most promising antimalarial targets for structure-based drug design.<sup>4-6</sup> Triclosan, a broadly used antibiotic, is effective inhibitor of PfENR enzyme activity. Several efforts have been taken in the recent past in the direction of the identification of new antimalarials using pharmacophore modeling, molecular docking and MD simulations.<sup>7-12</sup>

Pyrazole is a well-known class of nitrogen containing heterocyclic compounds and play important role in agricultural and medicinal field. Pyrazole and its derivatives are known to possess antibacterial,<sup>13</sup> antipyretic,<sup>14</sup> fungistatic,<sup>15</sup> anticonvulsant,<sup>16</sup> antitubercular,<sup>17</sup> antipyretic,<sup>18</sup> insecticides,<sup>19</sup> and anti-inflammatory<sup>20</sup> activities. Pyrazoline containing compounds are recognized to possess various pharmacological activities like antimalarial,<sup>21,22</sup> anticancer,<sup>23</sup> anti-inflammatory,<sup>24</sup> analgesic,<sup>24</sup> antitumor,<sup>25</sup> antimicrobial<sup>26</sup> and antidepressant activities.<sup>27</sup> Furan containing compounds possess lipoxygenase inhibitor,<sup>28</sup> urotensin-II receptor antagonists,<sup>29</sup> fungicidal,<sup>30</sup> epidermal growth factor receptor inhibitors and anticancer<sup>31</sup> etc. activities. Chalcone is a natural pigment found in plant and is an important intermediate for the synthesis of flavonoids. Varieties of biological activities are associated with chalcones and their derivatives such as antiplasmodial,<sup>32</sup> nematicide,<sup>33</sup> antiallergenic,<sup>34</sup> antimalarial,<sup>35</sup> anti-HIV,<sup>36</sup> anti-cancer,<sup>37</sup> anti-inflammatory<sup>38</sup> and anti-tuberculosis.<sup>39</sup>

So, considering the biological importance of pyrazoles, furan and chalcone, herein we report the design of a small library of furan containing pyrazolyl pyrazoline derivatives by molecular hybridization approach targeting PfENR using the *in silico* molecular docking technique. The promising results obtained from this *in silico* study served the basis for the synthesis of these molecules followed by evaluation of their antimalarial potential.

Molecular docking technique plays significant role in lead identification/optimization and in the mechanistic study by predicting the binding affinity and the thermodynamic interactions leading the binding of a ligand to its biological receptor. Thus, with the objective to identify novel leads targeting the crucial antimalarial target *Plasmodium falciparum* enoyl-ACP reductase (PfENR or FabI) (pdb code: 1NHG), molecular docking was carried out using the GLIDE (Grid-based LIgand Docking with Energetics) program of the Schrodinger Molecular modeling package.<sup>40-42</sup> A small library of 8 molecules comprising furan containing pyrazolyl pyrazoline derivatives (**3a-3d**, **4a-4d**) was docked against PfENR. The ensuing docking conformation revealed that these molecules changed a binding mode which is corresponding with the active site of pfENR and were found to be involved in a series of bonded and non-bonded interactions with the residues lining the active site. Their docking scores varied from -6.979 to -8.222 with an average docking score of -7.563 signifying a potent binding affinity to PfENR. In order to get a quantitative insight into the most significantly interacting residues and their associated thermodynamic interactions, a detailed per-residue interaction analysis was carried out (Table S1, Supporting Information). This analysis showed that the furan containing pyrazolyl chalcones (**3a-d**) (Figure 1) were deeply embedded into the active site of PfENR engaging in a sequence of favorable *van der Waals* interactions observed with Ile:C369, Phe:C368, IleA323, Ala:A320, Ala:A319, Arg:A318, Ser:A317, Leu:A315, Pro:A314, Gly:A313, Ala:A312, Lys:A285, Met:A281, Tyr:A277, Tyr:A267, Thr:A266, Leu:A265, Gly:A112, Tyr:A111, Gly:A110 and Asp:A107 residues through the 1,3-substituted-1*H*-pyrazol-4-yl scaffold while the 1-(2,5-Dimethylfuran-3-yl) prop-2-en-1-one



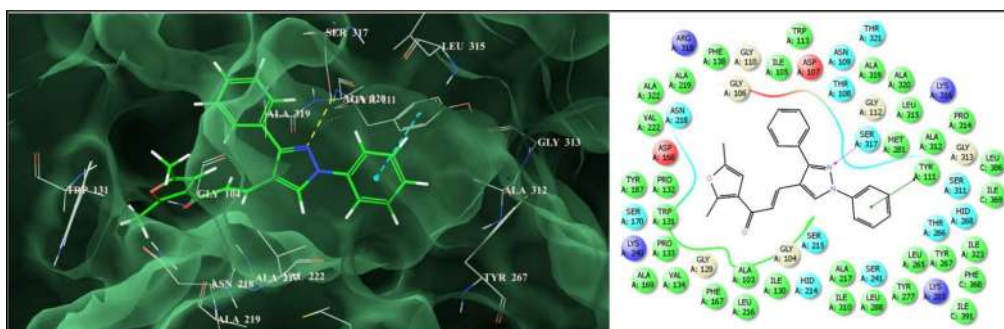


**Figure 1.** Binding mode of **3a** into the active site of *Plasmodium falciparum* enoyl-ACP reductase (on right side: pink lines represent the hydrogen bond while green lines signify  $\pi$ - $\pi$  stacking interactions).

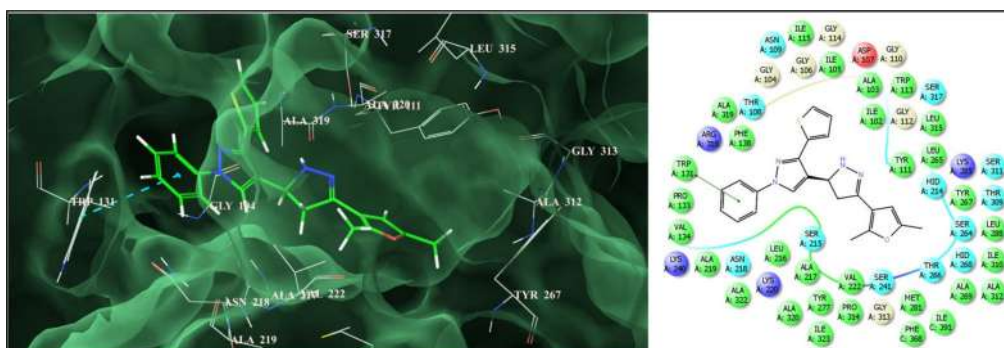
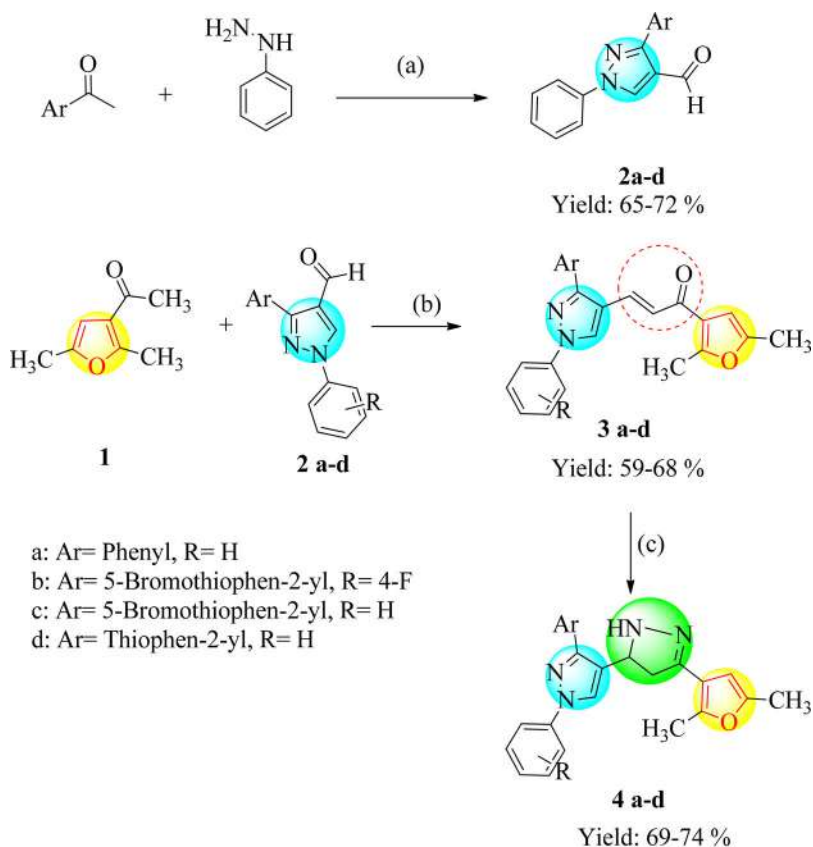


**Figure 2.** Binding mode of **4d** into the active site of *Plasmodium falciparum* enoyl-ACP reductase (on right side: pink lines represent the hydrogen bond while green lines signify  $\pi$ - $\pi$  stacking interactions).

component of the molecules was seen to be involved in similar interactions with Asn:A218, Ala:A217, Leu:A216, Ser:A215, Trp:A131, Gly:A106, Ile:A105, Gly:A104 residues of the active site.

Furthermore the enhanced binding affinity of these molecule is also attributed to significant electrostatic interactions observed with Arg:A318, Ser:A317, Lys:A285, Asp:A236, Asn:A218, Ala:A217, Ser:A215, Tyr:A111, Gly:A110, Asp:A107, Gly:A104 residues lining the active site. On the other hand, the furan containing pyrazoline derivatives (**4a-d**) (Figure 2) were also seen to be stabilized into the active of *Pf*ENR through a network of significant *van der Waals* interactions observed with (2,5-dimethylfuran-3-yl)-1*H*-pyrazolyl scaffold *via* Ile:C369, Phe:C368, Ala:A320, Ser:A317, Leu:A315, Pro:A314, Gly:A313, Ala:A312, Lys:A285, Tyr:A267, Thr:A266, Leu:A265, Gly:A112, Tyr:A111, Gly:A110, Gly:A106 and Ile:A105 while other half of the molecule i.e., 2-thiophenyl-1-phenyl-1*H*-pyrazole showed similar type of interactions with Ile:A323, Ala:A319, Arg:A318, Met:A281, Tyr:A277, Val:A222, Ala:A219, Asn:A218, Ala:A217, Leu:A216, Ser:A215, Trp:A131, Ile:A130, Trp:A113, Asp:A107, Gly:A104 residues.

Further the enhanced binding affinity of the molecules is also attributed to favorable electrostatic interactions observed with Arg:A318, Ser:A317, Glu:A289, Lys:A285, Asp:A236, Asn:A218, Ala:A217, Ser:A215, Tyr:A111, Gly:A110, Asp:A107 and Gly:A104. While these non-bonded interactions (*van der Waals* and electrostatic) were observed to be the major driving force for the mechanical interlocking of these novel furan containing pyrazolyl pyrazoline derivatives into the active site *Pf*ENR, the enhanced binding affinity of these molecules is also contributed by very prominent hydrogen bonding interaction observed for **3a** (Ser:A317(2.708 Å)), **4a** (Ser:A317(2.783 Å)), **4b** (Ser:A317(2.462 Å)) and **4c** (Ser:A317(2.462 Å)). Furthermore these



**Reagents and conditions:** (a): i) EtOH, reflux, 2 hr ii) DMF/POCl<sub>3</sub>, 0-10° C;  
 (b) 10 % aq. KOH, EtOH, RT, 14hr; (c) NH<sub>2</sub>NH<sub>2</sub>·H<sub>2</sub>O, EtOH, AcOH, 6hr

**Scheme 1.** Synthesis of pyrazolyl chalcones (**3a-d**) and pyrazolyl pyrazolines (**4a-d**).

molecules were also engaged in a very close  $\pi$ - $\pi$  stacking interactions: **3a**: Tyr: A111(2.669 Å), **3b**: Tyr:A267(2.529 Å), **3c**: Tyr:A267(2.541 Å), **3d**: Tyr:A267(2.335 Å), **4a**: Tyr:A111(2.602 Å), **4b**: Trp:A131(2.073 Å), **4c**: TyrA:111(2.073 Å) and **4d**: TrpA131(2.538 Å) (Figures S1-S6, Supporting Information).

This type of bonded interactions i.e., hydrogen bonding and  $\pi$ - $\pi$  stacking are known to serve as an “anchor” to guide the alignment of a molecule into the 3D space of enzyme’s active site and facilitate the non-bonded interactions (*Van der Waals* and electrostatic) as well. Overall, the in-silico binding affinity data suggested that these furans containing pyrazolyl pyrazoline derivatives (**3a-d**, **4a-d**) could be developed as novel scaffold to arrive at compounds with high selectivity and potency *Plasmodium falciparum*.

## Results and discussion

### Chemistry

The novel series of furan containing pyrazolyl chalcones (**3a-d**) and pyrazoline derivatives (**4a-d**) were synthesized from commercially available starting materials (Scheme 1). Initially, pyrazole aldehyde **2a-d** was formed by the condensation between substituted acetophenone and phenyl

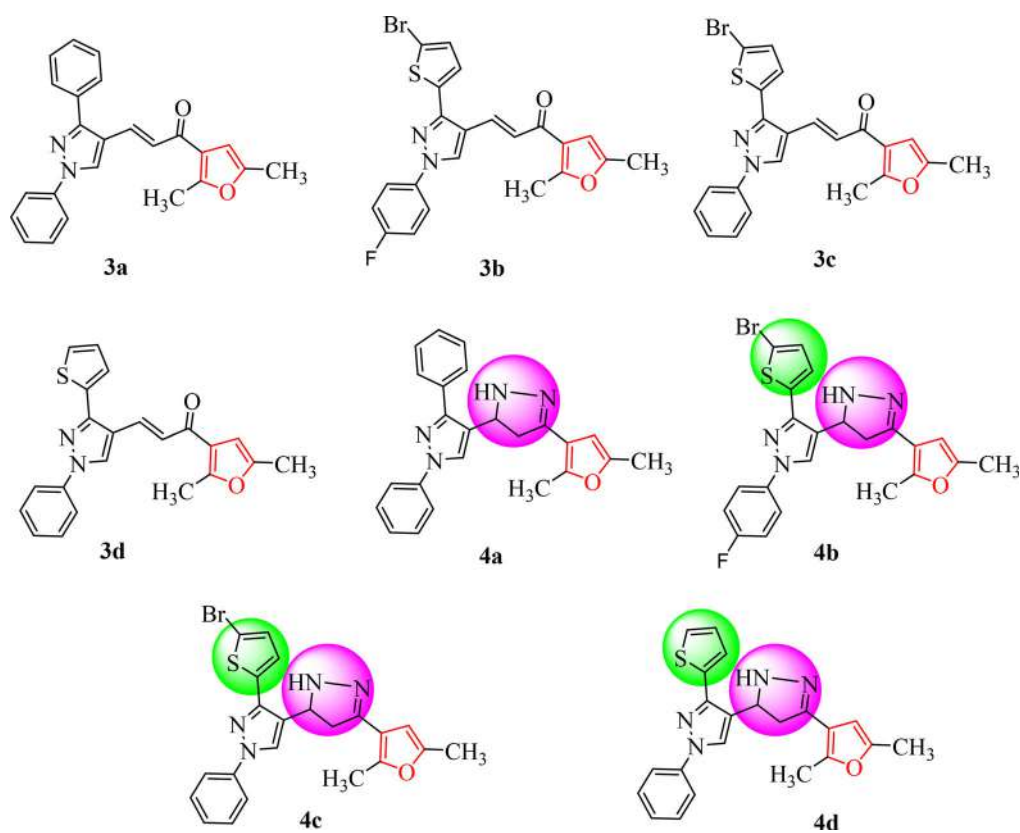


**Figure 3.** The newly synthesized compounds structure **3a-d** & **4a-d**.

hydrazine followed by Vilsmeier-Haack formylation reaction (Scheme 1). Then furan containing pyrazolyl chalcones **3a-d** were synthesized by base-catalyzed Claisen-Schmidt condensation of 1-(2,5-dimethylfuran-3-yl)ethanone **1** and substituted pyrazole aldehyde **2a-d**.<sup>43</sup> Finally, the furan containing pyrazolyl chalcones **3a-d** and hydrazine hydrate in ethanol solvent using catalytic amount of acetic acid at reflux condition for 6 hr afforded the corresponding pyrazolyl pyrazolines (**4a-d**) in quantitative isolated yield (69–74%) (Scheme 1).

The newly synthesized compounds structures were shown in Figure 3. The newly synthesized compound's structures were confirmed by IR, <sup>1</sup>H NMR, <sup>13</sup>C NMR, mass spectral data. For compound **3a**, in IR spectrum the stretching band for C=O was detected at 1657 cm<sup>-1</sup>. In the <sup>1</sup>H NMR spectrum of compound **3a**, the proton of pyrazole and furan ring resonate as a singlet at δ 9.31 and δ 6.60 ppm respectively. Also, singlet for two -CH<sub>3</sub> were observed at δ 2.27 and δ 2.50 ppm. The <sup>13</sup>C NMR spectrum of compound **3a** showed signal at δ 184.41 ppm due to C=O and δ 12.89 and δ 13.93 ppm is due to two -CH<sub>3</sub>. Mass spectrum confirms the formation of compound **3a** showed m/z = 369 (M + H)<sup>+</sup>.

Secondly, in the IR spectrum of compound **4a**, -N-H stretching band observed at 3252 cm<sup>-1</sup>. The <sup>1</sup>H NMR spectrum of compound **4a**, the CH<sub>2</sub> protons of the pyrazoline ring resonated as a pair of doublets of doublets at δ 2.88 ppm and 3.35 ppm. The CH proton appeared as triplet at δ 4.87 ppm due to vicinal coupling with two protons of the methylene group. In the <sup>13</sup>C NMR spectra of the compound **4a** carbons of the pyrazoline ring were observed at δ 41.97 ppm and 54.67 ppm. All the other aromatic and aliphatic protons and carbons were observed at expected regions. Mass spectrum confirms the formation of compound **4a** showed m/z = 383 (M + H)<sup>+</sup>.

**Table 1.** Antimalarial ( $\mu\text{M}$ ), Antibacterial (MIC in  $\mu\text{g/mL}$ ) & Antifungal (MIC in  $\mu\text{g/mL}$ ) activity.

Cpd	Antimalarial activity Plasmodium falciparum	Antibacterial activity				Antifungal activity			Molecular Docking Score
		EC	PA	SA	SP	CA	AN	AC	
<b>3a</b>	1.46	200	200	250	250	500	500	500	-7.814
<b>3b</b>	3.93	100	250	250	200	1000	500	500	-7.032
<b>3c</b>	2.16	62.5	200	125	250	500	>1000	>1000	-7.192
<b>3d</b>	3.07	100	100	200	200	1000	500	500	-7.118
<b>4a</b>	6.31	125	100	100	100	500	500	500	-6.979
<b>4b</b>	0.47	100	200	100	100	250	500	500	-8.157
<b>4c</b>	0.47	125	125	200	200	1000	>1000	>1000	-8.222
<b>4d</b>	0.21	200	100	125	100	500	500	500	-7.988
Chloroquine	0.06	-	-	-	-	-	-	-	-
Quinine	0.83	-	-	-	-	-	-	-	-
CP	-	50	50	50	50	-	-	-	-
NS	-	-	-	-	-	100	100	100	-

Cpd: Compound; EC: *Escherichia coli*; PA: *Pseudomonas aeruginosa*; SA: *Staphylococcus aureus*; SP: *Streptococcus pyogenes*; CA: *Candida albicans*; AN: *Aspergillus niger*; AC: *Aspergillus clavatus*; CP: Chloramphenicol; NS: Nystatin.

## Biological evaluation

### *In vitro* antimalarial screening

All the synthesized novel compounds were tested for antimalarial activities. The *in vitro* antimalarial assay was carried out according to the micro assay protocol of Rieckmann and coworkers with minor modifications.<sup>44–47</sup> The results were recorded as the minimum inhibitory concentrations ( $\mu\text{M}$  MIC) chloroquine and quinine were used as the reference drug (Table 1).

Herein, we have synthesized four chalcone and pyrazoline derivatives respectively. Structure activity relationship (SAR) plays very important role while displaying the antimalarial activity. All the synthesized chalcone derivatives (**3a–d**) exhibited less potency compared to the standard drug. But pyrazoline derivatives exhibited excellent antimalarial activity compared to the standard drug. In compound **4a**, thiophene ring was absent and pyrazoline ring is present, so, the compound **4a** exhibited less potency compared to the standard drug. Now, in compound **4b**, bromo substituted thiophene and pyrazoline rings are present along with the fluorine at the para position on benzene ring. Interestingly, this compound **4b** (0.47  $\mu\text{M}$ ), exhibited excellent activity compared to the standard drug quinine (0.83  $\mu\text{M}$ ). Again, in compound **4c**, bromo substituted thiophene and pyrazoline rings are present but no fluorine at the para position of benzene ring. Though fluorine is absent on benzene ring in compound **4c** (0.47  $\mu\text{M}$ ), it exhibited same potency as that of compound **4b** compared to the standard drug quinine (0.83  $\mu\text{M}$ ). Finally, in compound **4d**, there were no substitution on the thiophene and benzene ring. In compound **4d** plane thiophene, plane benzene ring and pyrazoline ring constructed in a single molecular framework. Compound **4d** (0.21  $\mu\text{M}$ ), exhibited four-fold more antimalarial activity compared to the standard drug quinine (0.83  $\mu\text{M}$ ). From SAR, we can conclude that for the antimalarial activity thiophene, pyrazoline and benzene ring were very important in a single molecular framework.

### Antimicrobial activities

Further, all the novel synthesized compounds were also screened for antimicrobial activities against the bacterial strains *Escherichia coli* (MTCC 443), *Staphylococcus aureus* (MTCC 96), *Pseudomonas aeruginosa* (MTCC 1688), *Streptococcus pyogenes* (MTCC 442) and fungal strains *Aspergillus clavatus* (MTCC 1323), *Candida albicans* (MTCC 227) and *Aspergillus niger* (MTCC 282). The minimum inhibitory concentration (MIC) was determined by the broth dilution method. Chloramphenicol and Nystatin were used as reference drugs for antibacterial and antifungal activity, respectively. The results of antibacterial and antifungal activity were given in Table 1.

The results given in Table 1 indicated that none of the synthesized compound exhibited significant potency toward the standard antibacterial drug Chloramphenicol and antifungal drug Nystatin. Hence, from above result we can conclude that the synthesized compounds show selectively antimalarial activity and negligible antimicrobial activity.

## Conclusion

In conclusion, Considering the importance of enoyl-ACP reductase (*Pf*ENR) in *Plasmodium*, a small library of 8 molecules comprising furan containing pyrazolyl pyrazoline derivatives (**3a-d**, **4a-d**) was designed and docked against *Pf*ENR. Based on the *in silico* binding affinity data, synthesis was carried out for these novel furans containing pyrazolyl pyrazoline derivatives (**3a-d**, **4a-d**) and was evaluated for activity against *Plasmodium falciparum*. The synthesized compounds shown selectively antimalarial activity with minimal antimicrobial activity. Compounds (**3a-d**) exhibited less antimalarial activity compared to the standard drug. From the series of compounds (**4a-d**), compound **4b** (0.47  $\mu$ M), **4c** (0.47  $\mu$ M) and **4d** (0.21  $\mu$ M) exhibited more antimalarial activity compared to the standard drug quinine (0.83  $\mu$ M). Compound **4d** shows four-fold more activity compared to the standard drug quinine. From the SAR, we have distinguished areas of the pyrazolyl chalcones and pyrazolyl pyrazolines framework where variations can be made to expand the pharmacokinetic profile as well as features required to improve inhibitor effectiveness. This innovative molecular scaffold presents breakthrough for optimization to develop effective *Pf*ENR inhibitors.

## Experimental

### General

All the reagents, solvents and chemicals were taken from commercial sources found to be and used as such without purification. The physical constant like melting points were measured on a DBK melting point apparatus and are uncorrected. IR spectra were recorded on Shimadzu IR Affinity 1S (ATR) FTIR spectrophotometer.  $^1\text{H}$  NMR (400 MHz) and  $^{13}\text{C}$  NMR (100 MHz) spectra were recorded on Bruker Advance II 400 spectrophotometer using TMS as an internal standard and DMSO- $d_6$  as solvent and chemical shifts were expressed as  $\delta$  ppm units. Mass spectra were obtained on Waters, Q-TOF micro mass (ESI-MS) mass spectrometer.

### General procedure for the synthesis of pyrazolyl chalcones (**3a-d**)

A mixture of 1-(2,5-dimethylfuran-3-yl)ethanone **1** (0.05 mol), substituted pyrazole aldehyde **2** (0.05 mol) and 10% aqueous potassium hydroxide (10 mL) in ethanol (50 mL) was stirred at room temperature for 14 h. The progress of the reaction was monitored by TLC. After completion of the reaction, the reaction mixture was transferred into crushed ice and neutralized by dil. HCl. The precipitation observed, filtered it, washed with water and dried. The crystallization of product carried out in ethanol.

### (*E*)-1-(2,5-Dimethylfuran-3-yl)-3-(1,3-diphenyl-1H-pyrazol-4-yl)prop-2-en-1-one (**3a**)

Yield: 61%, yellow solid; mp: 80–82  $^{\circ}\text{C}$ ; IR ( $\nu_{\text{max}}$ ,  $\text{cm}^{-1}$ ): 2921 (=C-H), 2855 (C-H), 1657 (C=O), 1454 (C=N);  $^1\text{H}$ -NMR (400 MHz, DMSO- $d_6$ ,  $\delta$ , ppm): 9.31 (s, 1H, Pyrazole-H), 7.93 (d, 2H,  $J=7.9$  Hz), 7.38–7.68 (m, 10H, Ar-H), 6.60 (s, 1H, Furan-H), 2.53 (s, 3H,  $-\text{CH}_3$ ), 2.27 (s, 3H,  $-\text{CH}_3$ );  $^{13}\text{C}$  NMR (100 MHz, DMSO- $d_6$ ,  $\delta$ , ppm): 184.4 (C=O), 159.9, 152.8, 149.7, 138.9, 132.2, 132.0, 129.6, 128.8, 128.5, 128.6, 128.4, 127.1, 123.8, 122.1, 118.6, 117.6, 105.9, 13.9 ( $\text{CH}_3$ ), 12.9 ( $\text{CH}_3$ ); MS(ESI-MS):  $m/z$  369.11 (M + H).<sup>+</sup>



***(E)-3-(3-(5-Bromothiophen-2-yl)-1-(4-fluorophenyl)-1H-pyrazol-4-yl)-1-(2,5-dimethylfuran-3-yl)prop-2-en-1-one (3b)***

Yield: 59%, yellow solid, mp: 112–114 °C; IR ( $\nu_{\max}$ ,  $\text{cm}^{-1}$ ): 2923 (=C–H), 2856 (C–H), 1656 (C=O), 1455 (C=N);  $^1\text{H-NMR}$  (400 MHz, DMSO- $d_6$ ,  $\delta$ , ppm): 9.25 (s, 1H, Pyrazole-H), 7.90 (dd, 2H,  $J=4.7$  & 9.0 Hz, Ar–H), 7.64 (d, 1H,  $J=15.4$  Hz, olefinic-H), 7.39–7.45 (m, 3H, Ar–H), 7.34 (d, 1H,  $J=3.8$  Hz, Ar–H), 7.25 (d, 1H,  $J=3.8$  Hz, Ar–H), 6.61 (s, 1H, Furan-H), 2.55 (s, 3H,  $-\text{CH}_3$ ), 2.28 (s, 3H,  $-\text{CH}_3$ );  $^{13}\text{C NMR}$  (100 MHz, DMSO- $d_6$ ,  $\delta$ , ppm): 184.2, 162.0, 159.6, 157.1, 149.7, 145.7, 135.4, 135.1, 131.4, 130.8, 128.9, 127.3, 124.6, 122.0, 120.7, 120.6, 117.3, 116.6, 116.3, 112.5, 105.9, 13.9, 12.9; MS (ESI-MS):  $m/z$  472.89 (M + H).<sup>+</sup>

***(E)-3-(3-(5-Bromothiophen-2-yl)-1-phenyl-1H-pyrazol-4-yl)-1-(2,5-dimethylfuran-3-yl)prop-2-en-1-one (3c)***

Yield: 68%, yellow solid, mp 120–114 °C; IR ( $\nu_{\max}$ ,  $\text{cm}^{-1}$ ): 2921 (=C–H), 2855 (C–H), 1699 (C=O), 1454 (C=N);  $^1\text{H-NMR}$  (400 MHz, DMSO- $d_6$ ,  $\delta$ , ppm): 9.14 (s, 1H, Pyrazole-H), 7.87 (d, 2H,  $J=7.8$  Hz, Ar–H), 7.70 (d, 1H,  $J=15$  Hz, olefinic-H), 7.52 (t, 2H,  $J=8$  Hz, Ar–H), 7.36–7.40 (m, 2H, Ar–H), 7.20 (s, 2H, Ar–H), 6.55 (s, 1H, Furan-H), 2.57 (s, 3H,  $-\text{CH}_3$ ), 2.29 (s, 3H,  $-\text{CH}_3$ );  $^{13}\text{C NMR}$  (100 MHz, DMSO- $d_6$ ,  $\delta$ , ppm): 184.3, 157.1, 149.7, 145.7, 138.6, 135.5, 131.4, 130.9, 129.7, 128.8, 127.3, 127.3, 124.6, 122.0, 118.6, 117.4, 112.5, 105.9, 13.9, 12.9; MS(ESI-MS):  $m/z$  454.57 (M + H).<sup>+</sup>

***(E)-1-(2,5-Dimethylfuran-3-yl)-3-(1-phenyl-3-(thiophen-2-yl)-1H-pyrazol-4-yl)prop-2-en-1-one (3d)***

Yield: 62%, yellow solid, mp 124–126 °C; IR ( $\nu_{\max}$ ,  $\text{cm}^{-1}$ ): 2921 (=C–H), 2715 (C–H), 1652 (C=O), 1456 (C=N);  $^1\text{H-NMR}$  (400 MHz, DMSO- $d_6$ ,  $\delta$ , ppm): 8.56 (s, 1H, Pyrazole-H), 7.91 (d, 2H,  $J=7.8$  Hz, Ar–H), 7.76 (d, 1H,  $J=15.4$  Hz, olefinic-H), 7.60 (d, 1H,  $J=5.1$  Hz, Ar–H), 7.54 (t, 2H,  $J=8.2$  Hz, Ar–H), 7.35–7.44 (m, 3H, Ar–H), 7.21 (dd, 1H,  $J=5.0$  & 3.7 Hz, Ar–H), 6.59 (s, 1H, Furan-H), 2.57 (s, 3H,  $-\text{CH}_3$ ), 2.29 (s, 3H,  $-\text{CH}_3$ );  $^{13}\text{C NMR}$  (100 MHz, DMSO- $d_6$ ,  $\delta$ , ppm): 184.4, 157.0, 149.7, 146.8, 138.7, 133.5, 131.5, 129.7, 128.7, 128.1, 127.3, 127.2, 126.8, 124.3, 122.1, 118.6, 117.4, 105.9, 13.9, 12.9; MS(ESI-MS):  $m/z$  375.10 (M + H).<sup>+</sup>

***General procedure for synthesis of pyrazolyl-pyrazoline (4a-d)***

A mixture of chalcone **3a-d** (0.001 mol) and hydrazine hydrate (0.004 mol) in solvent ethanol (10 ml) was refluxed in presence of catalytic amount of glacial acetic acid for 6 h. The progress of the reaction was monitored by TLC. After completion of the reaction, the reaction mixture was transferred into crushed ice. The precipitation observed, filtered it, washed with water and dried. The crystallization of product carried out in ethanol to get pure pyrazolines.

***4-(4,5-Dihydro-3-(2,5-dimethylfuran-3-yl)-1H-pyrazol-5-yl)-1,3-diphenyl-1H-pyrazole (4a)***

Yield: 74%, white solid, mp 102–104 °C; IR ( $\nu_{\max}$ ,  $\text{cm}^{-1}$ ): 3306 (N–H), 3049 (Ar–H), 1592 (C=N);  $^1\text{H-NMR}$  (400 MHz, DMSO- $d_6$ ,  $\delta$ , ppm): 8.56 (s, 1H, pyrazole-H), 7.90 (d, 2H,  $J=7.8$  Hz, Ar–H), 7.76 (d, 2H,  $J=8.3$  Hz, Ar–H), 7.47–7.52 (m, 4H, Ar–H), 7.41 (t, 1H,  $J=7.3$  Hz, Ar–H), 7.31 (t, 1H,  $J=7.4$  Hz, Ar–H), 7.20 (s, 1H, N–H), 6.19 (s, 1H, furan-H), 4.87 (t, 1H,  $J=10.7$  Hz, pyrazoline-H), 3.34 (dd, 1H,  $J=10.5$  & 15.6 Hz, pyrazoline-H), 2.88 (dd, 1H,  $J=11.1$  & 16.1 Hz, pyrazoline-H), 2.38 (s, 3H,  $\text{CH}_3$ ), 2.20 (s, 3H,  $\text{CH}_3$ );  $^{13}\text{C NMR}$  (100 MHz, DMSO- $d_6$ ,  $\delta$ , ppm): 150.4, 149.3, 147.6, 145.1, 139.5, 132.9, 129.5, 128.6, 127.9, 127.2, 126.2, 123.2, 118.1, 115.2, 105.9, 54.7, 41.9, 13.3, 12.9; MS (ESI-MS):  $m/z$  383.04 (M + H).<sup>+</sup>

**3-(5-Bromothiophen-2-yl)-1-(4-fluorophenyl)-4-(4,5-dihydro-3-(2,5-dimethylfuran-3-yl)-1H-pyrazol-5-yl)-1H-pyrazole (4b)**

Yield: 69%, white solid, mp 98–100 °C; IR ( $\nu_{\max}$ ,  $\text{cm}^{-1}$ ): 3310 (N–H), 3046 (Ar–H), 1594 (C=N);  $^1\text{H}$  NMR (400 MHz, DMSO- $d_6$ ,  $\delta$ , ppm): 8.54 (s, 1H, pyrazole-H), 7.88 (m, 2H, Ar–H), 7.35 (t, 2H,  $J=8.7$  Hz, Ar–H), 7.28 (dd, 2H,  $J=3.8$  Hz, Ar–H), 7.21 (s, 1H, N–H), 6.20 (s, 1H, furan-H), 4.93 (t, 1H,  $J=10.68$  Hz, pyrazoline-H), 3.37 (dd, 1H,  $J=10.7$  & 16.5 Hz, pyrazoline-H), 2.86 (dd, 1H,  $J=10.9$  & 16.1 Hz, pyrazoline-H), 2.38 (s, 3H,  $\text{CH}_3$ ), 2.20 (s, 3H,  $\text{CH}_3$ );  $^{13}\text{C}$  NMR (100 MHz, DMSO- $d_6$ ,  $\delta$ , ppm): 161.6, 159.1, 149.3, 147.7, 145.3, 144.1, 136.9, 135.6, 131.2, 128.0, 126.6, 122.6, 120.2, 120.2, 116.4, 116.2, 115.1, 111.5, 105.9, 54.3, 41.1, 13.3, 12.9; MS (ESI-MS):  $m/z$  486.93 (M + H).<sup>+</sup>

**3-(5-Bromothiophen-2-yl)-4-(4,5-dihydro-3-(2,5-dimethylfuran-3-yl)-1H-pyrazol-5-yl)-1-phenyl-1H-pyrazole (4c)**

Yield: 72%, white solid, mp 122–124 °C; IR ( $\nu_{\max}$ ,  $\text{cm}^{-1}$ ): 3303 (N–H), 3096 (Ar–H), 1593 (C=N),  $^1\text{H}$  NMR (400 MHz, DMSO- $d_6$ ,  $\delta$ , ppm): 8.55 (s, 1H, pyrazole-H), 7.84 (d, 2H,  $J=7.9$  Hz, Ar–H), 7.51 (t, 2H,  $J=7.6$  Hz, Ar–H), 7.22–7.34 (m, 4H, Ar–H), 6.20 (s, 1H, furan-H), 4.94 (t, 1H,  $J=10.6$  Hz, pyrazoline-H), 3.38 (m, 1H, pyrazoline-H), 2.88 (dd, 1H,  $J=12.1$  & 16.1 Hz, pyrazoline-H), 2.39 (s, 3H,  $\text{CH}_3$ ), 2.20 (s, 3H,  $\text{CH}_3$ );  $^{13}\text{C}$  NMR (100 MHz, DMSO- $d_6$ ,  $\delta$ , ppm): 149.3, 147.7, 145.2, 144.0, 139.0, 137.0, 131.2, 129.6, 127.8, 126.6, 126.5, 122.5, 118.0, 115.1, 111.4, 105.9, 54.4, 41.1, 13.3, 12.9; MS (ESI-MS):  $m/z$  468.95 (M + H).<sup>+</sup>

**4-(4,5-Dihydro-3-(2,5-dimethylfuran-3-yl)-1H-pyrazol-5-yl)-1-phenyl-3-(thiophen-2-yl)-1H-pyrazole (4d)**

Yield: 70%, white solid, mp 96–98 °C; IR ( $\nu_{\max}$ ,  $\text{cm}^{-1}$ ): 3336 (N–H), 3067 (Ar–H), 1501 (C=N);  $^1\text{H}$  NMR (400 MHz, DMSO- $d_6$ ,  $\delta$ , ppm): 8.53 (s, 1H, pyrazole-H), 7.86 (d, 1H,  $J=8$  Hz, Ar–H), 7.58 (d, 1H,  $J=4.9$  Hz, Ar–H), 7.47–7.52 (m, 3H, Ar–H), 7.31 (t, 1H,  $J=7.3$  Hz, Ar–H), 7.15–7.20 (m, 2H, Ar–H), 6.21 (s, 1H, furan-H), 4.98 (t, 1H,  $J=10.5$  Hz, pyrazoline-H), 3.42 (m, 1H, pyrazoline-H), 2.89 (dd, 1H,  $J=10.7$  & 16.1 Hz, pyrazoline-H), 2.39 (s, 3H,  $\text{CH}_3$ ), 2.20 (s, 3H,  $\text{CH}_3$ );  $^{13}\text{C}$  NMR (100 MHz, DMSO- $d_6$ ,  $\delta$ , ppm): 149.3, 147.7, 145.1, 144.9, 139.2, 135.0, 129.6, 127.9, 127.4, 126.3, 126.0, 125.8, 122.6, 118.1, 115.1, 105.9, 54.5, 41.3, 13.3, 12.9; MS (ESI-MS):  $m/z$  389.03 (M + H).<sup>+</sup>

**Experimental protocol for biological activity****Antimalarial assay**

The antimalarial activity of the synthesized compounds was carried out in the Microcare laboratory & TRC, Surat, Gujarat. According to the micro assay protocol of Rieckmann and coworkers the *in vitro* antimalarial assay was carried out in 96 well microtiter plates. To maintain *P. falciparum* strain culture in medium Roswell Park Memorial Institute (RPMI) 1640 supplemented with 25 mM (4-(2-hydroxyethyl)-1-piperazineethanesulfonic acid) (HEPES), 1% D-glucose, 0.23% sodium bicarbonate and 10% heat inactivated human serum. To obtain only the ring stage parasitized cells, 5% D-sorbitol treatment required to synchronized the asynchronous parasites of *P. falciparum*. To determine the percent parasitaemia (rings) and uniformly maintained with 50% RBCs ( $\text{O}^+$ ) an initial ring stage parasitaemia of 0.8 to 1.5% at 3% hematocrit in a total volume of 200  $\mu\text{l}$  of medium RPMI-1640 was carried out for the assay. A stock solution of 5 mg/ml of each of the test samples was prepared in DMSO and subsequent dilutions were prepared with culture medium. To the test wells to obtain final concentrations (at five-fold dilutions) ranging between 0.4  $\mu\text{g/ml}$  to 100  $\mu\text{g/ml}$  in duplicate well containing parasitized cell preparation the diluted samples in 20  $\mu\text{l}$  volume were added. In a candle jar, the culture plates were incubated at 37 °C. Thin

blood smears from each well were prepared and stained with Jaswant Singh-Bhattacharji (JSB) stain after 36 to 40 h incubation. To record maturation of ring stage parasites into trophozoites and schizonts in presence of different concentrations of the test agents the slides were microscopically observed. The minimum inhibitory concentrations (MIC) was recorded as the test concentration which inhibited the complete maturation into schizonts. Chloroquine was used as the reference drug.

After incubation for 38 hours, and percent maturation inhibition with respect to control group, the mean number of rings, trophozoites and schizonts recorded per 100 parasites from duplicate wells.

### **Molecular docking**

The crystal structure of *Plasmodium Falciparum* Enoyl-Acyl-Carrier-Protein Reductase (*Pf*ENR or FabI) in complex with its inhibitor Triclosan was retrieved from the protein data bank (PDB) (pdb code: 1NHG) and refined using the protein preparation wizard. It involves eliminating all crystallographically observed water (as no conserved interaction is reported with co-crystallized water molecules), addition of missing side chain/hydrogen atoms. Considering the appropriate ionization states for the acidic as well as basic amino acid residues, the appropriate charge and protonation state were assigned to the protein structure corresponding to pH 7.0 followed by thorough minimization, using OPLS-2005 force-field, of the obtained structure to relieve the steric clashes due to addition of hydrogen atoms. The 3D structures of the furan containing pyrazolyl chalcones (**3a-d**) were sketched using the build panel in Maestro and were optimized using the Ligand Preparation module followed by energy minimization using OPLS-2005 force-field until their average root mean square deviation (RMSD) reached 0.001 Å. The active site of *Pf*ENR was defined using receptor grid generation panel to include residues within a 10 Å radius around the co-crystallized ligand. Using this setup, flexible docking was carried using the extra precision (XP) Glide scoring function to gauge the binding affinities of these molecules and to identify binding mode within the target. The obtained results as docking poses were visualized and analyzed quantitatively for the thermodynamic elements of interactions with the residues lining the active site of the enzyme using the Maestro's Pose Viewer utility.

### **Acknowledgements**

Authors are thankful to Microcare laboratory and TRC, Surat, Gujarat for providing antimicrobial and antimalarial activities and Director, SAIF, Panjab University, Chandigarh for providing spectral data; Schrodinger Inc. for providing the software to perform the *in silico* study.

### **Disclosure statement**

No potential conflict of interest was reported by the author(s).

### **Funding**

Authors are thankful to Department of Science and Technology, New Delhi for providing financial assistance for research facilities under DST-FIST programme.

### **References**

1. E. A. Ashley, A. Pyae Phyo, and C. J. Woodrow, "Malaria," *The Lancet* 391, no. 10130 (2018): 1608–21.
2. World Health Organization. "World Malaria Report 2019" (World Health Organization, Geneva, 2019). Licence: CC BY-NC-SA 3.0 IGO.

3. J. Talapko, I. Skrlec, T. Alebic, M. Jukic, and A. Vcev, "Malaria: The Past and the Present," *Microorganisms* 7 (2019): 179.
4. R. J. Heath, and C. O. Rock, "Enoyl-Acyl Carrier Protein Reductase (fabI) Plays a Determinant Role in Completing Cycles of Fatty Acid Elongation in Escherichia coli," *The Journal of Biological Chemistry* 270, no. 44 (1995): 26538–42.
5. R. F. Waller, S. A. Ralph, M. B. Reed, V. Su, J. D. Douglas, D. E. Minnikin, A. F. Cowman, G. S. Besra, and G. I. McFadden, "A Type II Pathway for Fatty Acid Biosynthesis Presents Drug Targets in Plasmodium falciparum," *Antimicrobial Agents and Chemotherapy* 47, no. 1 (2003): 297–301.
6. G. Nicola, C. A. Smith, E. Lucumi, M. R. Kuo, L. Karagyzov, D. A. Fidock, J. C. Sacchetti, and R. Abagyan, "Discovery of Novel Inhibitors Targeting Enoyl-Acyl Carrier Protein Reductase in Plasmodium falciparum by Structure-Based Virtual Screening," *Biochemical and Biophysical Research Communications* 358, no. 3 (2007): 686–91.
7. N. Surolia, and A. Surolia, "Triclosan Offers Protection against Blood Stages of Malaria by Inhibiting enoyl-ACP Reductase of Plasmodium falciparum," *Nature Medicine* 7, no. 2 (2001): 167–73.
8. S. Sharma, T. N. C. Ramya, A. Surolia, and N. Surolia, "Triclosan as a Systemic Antibacterial Agent in a Mouse Model of Acute Bacterial Challenge," *Antimicrobial Agents and Chemotherapy* 47, no. 12 (2003): 3859–66.
9. R. P. Samal, V. M. Khedkar, R. R. S. Pissurlenkar, A. G. Bwalya, D. Tasdemir, R. A. Joshi, P. R. Rajamohan, V. G. Puranik, and E. C. Coutinho, "Design, Synthesis, Structural Characterization by IR, (1) H, (13) C, (15) N, 2D-NMR, X-Ray Diffraction and Evaluation of a New Class of Phenylaminoacetic Acid Benzylidene Hydrazines as pFENR Inhibitors," *Chemical Biology & Drug Design* 81, no. 6 (2013): 715–29.
10. M. Chhibber, G. Kumar, P. Parasuraman, T. N. C. Ramya, N. Surolia, and A. Surolia, "Novel Diphenyl Ethers: Design, Docking Studies, Synthesis and Inhibition of Enoyl ACP Reductase of Plasmodium falciparum and Escherichia coli," *Bioorganic & Medicinal Chemistry* 14, no. 23 (2006): 8086–98.
11. V. A. Morde, M. S. Shaikh, R. R. S. Pissurlenkar, and E. C. Coutinho, "Molecular Modeling Studies, Synthesis, and Biological Evaluation of Plasmodium falciparum Enoyl-Acyl Carrier Protein Reductase (PfENR) Inhibitors," *Molecular Diversity* 13, no. 4 (2009): 501–17.
12. A. Manhas, A. Patel, M. Y. Lone, P. K. Jha, and P. C. Jha, "Identification of PfENR Inhibitors: A Hybrid Structure-Based Approach in Conjunction with Molecular Dynamics Simulations," *Journal of Cellular Biochemistry* 119, no. 10 (2018): 8490–500.
13. M. A. Berghot, and E. B. Moawad, "Convergent Synthesis and Antibacterial Activity of Pyrazole and Pyrazoline Derivatives of Diazepam," *European Journal of Pharmaceutical Sciences: Official Journal of the European Federation for Pharmaceutical Sciences* 20, no. 2 (2003): 173–9.
14. J. N. Dominguez, J. E. Charris, M. Caparelli, and F. Riggione, "Synthesis and Antimalarial Activity of Substituted Pyrazole Derivatives," *Arzneimittel-Forschung* 52, no. 6 (2002): 482–8.
15. R. Sridhar, P. T. Perumal, S. Etti, G. Shanmugam, M. N. Ponnuswamy, V. R. Prabavathy, and N. Mathivanan, "Design, Synthesis and anti-Microbial Activity of 1H-Pyrazole Carboxylates," *Bioorganic & Medicinal Chemistry Letters* 14, no. 24 (2004): 6035–40.
16. Shivapura Viveka, Dinesha Dinesha, Prasanna Shama, Shivalingegowda Naveen, Neratur Krishnappagowda Lokanath, and Gundibasappa Karikannar Nagaraja, "Design, Synthesis, Anticonvulsant and Analgesic Studies of New Pyrazole Analogues: A Knoevenagel Reaction Approach," *RSC Advances* 5no. 115 (2015): 94786–95.
17. Z. Xu, C. Gao, Q. C. Ren, X. F. Song, L. S. Feng, and Z. S. Lv, "Recent Advances of Pyrazole-Containing Derivatives as Anti-Tubercular Agents," *European Journal of Medicinal Chemistry* 139, (2017): 429–40.
18. R. S. Fabiane, T. S. Vanessa, R. Viviane, P. B. Lysandro, R. O. Marli, G. B. Helio, Z. Nilo, A. P. M. Marcos, and F. M. Carlos, "Hypothermic and Antipyretic Effects of 3-Methyl- and 3-Phenyl-5-Hydroxy-5-Trichloromethyl-4,5-Dihydro-1H-Pyrazole-1-Carboxyamides in Mice," *European Journal of Pharmacology* 451 (2002): 141–7.
19. A. Ana, R. C. Jose, P. C. Fernando, D. O. Agel, J. G. Maria, H. Antonio, L. Fernando, and M. Andres, "Efficient Tautomerization Hydrazone-Azomethine Imine under Microwave Irradiation. Synthesis of [4,3] and [5,3]Bipyrazoles," *Tetrahedron* 54 (1998): 13167–80.
20. K. O. Mohammed, and Y. M. Nissan, "Synthesis, Molecular Docking, and Biological Evaluation of Some Novel Hydrazones and Pyrazole Derivatives as Anti-Inflammatory Agents," *Chemical Biology & Drug Design* 84, no. 4 (2014): 473–88.
21. B. Insuasty, A. Montoya, D. Becerra, J. Quiroga, R. Abonia, S. Robledo, I. D. Velez, Y. Upegui, M. Noguera, and J. Cobo, "Synthesis of Novel Analogs of 2-pyrazoline Obtained from [(7-Chloroquinolin-4-yl)Amino]Chalcones and Hydrazine as Potential Antitumor and Antimalarial Agents," *European Journal of Medicinal Chemistry* 67 (2013): 252–62.
22. G. Kumar, O. Tanwar, J. Kumar, M. Akhter, S. Sharma, C. R. Pillai, M. M. Alam, and M. S. Zama, "Pyrazole-Pyrazoline as Promising Novel Antimalarial Agents: A Mechanistic Study," *European Journal of Medicinal Chemistry* 149 (2018): 139–47.

23. R. Alam, A. Alam, and A. K. Panda Rahisuddin, "Design, Synthesis and Cytotoxicity Evaluation of Pyrazolyl Pyrazoline and Pyrazolyl Aminopyrimidine Derivatives as Potential Anticancer Agents," *Medicinal Chemistry Research* 27 (2018): 560–70.
24. S. Viveka, D. P. Shama, G. K. Nagaraja, S. Ballav, and S. Kerkar, "Design and Synthesis of Some New Pyrazolyl-Pyrazolines as Potential Anti-Inflammatory, Analgesic and Antibacterial Agents," *European Journal of Medicinal Chemistry* 101 (2015): 442–51.
25. H. Khanam, A. Mashrai, A. Sherwani, M. Owais, and N. Siddiqui, "Synthesis and Anti-Tumor Evaluation of B-Ring Substituted Steroidal Pyrazoline Derivatives," *Steroids* 78, (2013): 1263–72.
26. S. K. Sahu, M. Banerjee, A. Samantray, C. Behera, and M. A. Azam, "Synthesis, Analgesic, anti-Inflammatory and Antimicrobial Activities of Some Novel Pyrazoline Derivatives," *Tropical Journal of Pharmaceutical Research* 7, no. 2 (2008): 961–8.
27. M. Johnson, B. Younglove, L. Lee, R. LeBlanc, H. Holt, Jr, P. Hills, H. Mackay, T. Brown, S. L. Mooberry, and M. Lee, "Design, Synthesis, and Biological Testing of Pyrazoline Derivatives of combretastatin-A4," *Bioorganic & Medicinal Chemistry Letters* 17, no. 21 (2007): 5897–901.
28. J. Vinayagam, R. L. Gajbhiye, L. Mandal, M. Arumugam, A. Achari, and P. Jaisankar, "Substituted Furans as Potent Lipoxigenase Inhibitors: Synthesis, in Vitro and Molecular Docking Studies," *Bioorganic Chemistry* 71 (2017): 97–101.
29. C. J. Lim, N. H. Kim, H. J. Park, B. H. Lee, K. S. Oh, and K. Y. Yi, "Synthesis and SAR of 5-Aryl-Furan-2-Carboxamide Derivatives as Potent urotensin-II Receptor Antagonists," *Bioorganic & Medicinal Chemistry Letters* 29, no. 4 (2019): 577–80.
30. B. Wang, Y. Shi, Y. Zhan, L. Zhang, Y. Zhang, L. Wang, X. Zhang, Y. Li, Z. Li, and B. Li, "Synthesis and Biological Activity of Novel Furan/Thiophene and Piperazine-Containing (Bis)1,2,4-Triazole Mannich Bases," *Chinese Journal of Chemistry* 33, no. 10 (2015): 1124–34.
31. Z. Lan, D. Xinshan, W. Jiaofeng, M. Guangpeng, L. Congchong, C. Guzhou, Z. Qingchun, and H. Chun, "Design, Synthesis and Biological Activities of N-(Furan-2-Ylmethyl)-1H-Indole-3-Carboxamide Derivatives as Epidermal Growth Factor Receptor Inhibitors and Anticancer Agents," *Chemical Research in Chinese Universities* 33, no. 3 (2017): 365–72.
32. M. L. Go, M. Liu, P. Wilairat, P. J. Rosenthal, K. J. Saliba, and K. Kirk, "Anti-plasmodial Chalcones Inhibit Sorbitol-Induced Hemolysis of Plasmodium falciparum-Infected Erythrocytes," *Antimicrobial Agents and Chemotherapy* 48, no. 9 (2004): 3241–5.
33. J. A. Gonzalez, and A. Estevez-Braun, "Effect of (E)-Chalcone on Potato-Cyst Nematodes *Globodera pallida* and *G. rostochiensis*," *Journal of Agricultural and Food Chemistry* 46 (1998): 1163–5.
34. M. Yoshimura, A. Sano, J. L. Kamei, and A. Obata, "Identification and Quantification of Metabolites of Orally Administered Naringenin Chalcone in Rats," *Journal of Agricultural and Food Chemistry* 57, no. 14 (2009): 6432–7.
35. M. Chen, T. G. Theander, S. B. Christensen, L. Hviid, L. Zhai, and A. Kharazmi, "Licochalcone A, a New Antimalarial Agent, Inhibits in Vitro Growth of the Human Malaria Parasite *Plasmodium falciparum* and Protects Mice from *P. yoelii* Infection," *Antimicrobial Agents and Chemotherapy* 38, no. 7 (1994): 1470–5.
36. L. Mishra, R. Sinha, H. Itokawa, K. F. Bastow, Y. Tachibana, Y. Nakanishi, N. Kilgore, and K. H. Lee, "Anti-HIV and Cytotoxic Activities of Ru(II)/Ru(III) Polypyridyl Complexes Containing 2,6-(2'-Benzimidazolyl)-Pyridine/Chalcone as Co-Ligand," *Bioorganic & Medicinal Chemistry* 9, no. 7 (2001): 1667–71.
37. C. Jin, Y. J. Liang, H. He, and L. Fu, "Synthesis and Antitumor Activity of Novel Chalcone Derivatives," *Biomedicine & Pharmacotherapy = Biomedecine & Pharmacotherapie* 67, no. 3 (2013): 215–7.
38. F. Herencia, M. L. Ferrándiz, A. Ubeda, J. N. Domínguez, J. E. Charris, G. M. Lobo, and M. J. Alcaraz, "Synthesis and anti-Inflammatory Activity of Chalcone Derivatives," *Bioorganic & Medicinal Chemistry Letters* 8, no. 10 (1998): 1169–74.
39. Y. Qian, G. Y. Ma, Y. Yang, K. Cheng, Q. Z. Zheng, W. J. Mao, L. Shi, J. Zhao, and H. L. Zhu, "Synthesis, Molecular Modeling and Biological Evaluation of Dithiocarbamates as Novel Antitubulin Agents," *Bioorganic & Medicinal Chemistry* 18, no. 12 (2010): 4310–6.
40. R. A. Friesner, J. L. Banks, R. B. Murphy, T. A. Halgren, J. J. Klicic, D. T. Mainz, M. P. Repasky, E. H. Knoll, M. Shelley, J. K. Perry, et al. "Glide: A New Approach for Rapid, Accurate Docking and Scoring. 1. Method and Assessment of Docking accuracy," *Journal of Medicinal Chemistry* 47, no. 7 (2004): 1739–49.
41. R. A. Friesner, R. B. Murphy, M. P. Repasky, L. L. Frye, J. R. Greenwood, T. A. Halgren, P. C. Sanschagrin, and D. T. Mainz, "Extra Precision Glide: Docking and Scoring Incorporating a Model of Hydrophobic Enclosure for Protein-Ligand Complexes," *Journal of Medicinal Chemistry* 49, no. 21 (2006): 6177–96.
42. T. A. Halgren, R. B. Murphy, R. A. Friesner, H. S. Beard, L. L. Frye, W. T. Pollard, and J. L. Banks, "Glide: A New Approach for Rapid, Accurate Docking and Scoring. 2. Enrichment Factors in Database Screening," *Journal of Medicinal Chemistry* 47, no. 7 (2004): 1750–9.



43. S. J. Takate, A. D. Shinde, B. K. Karale, H. Akolkar, L. Nawale, D. Sarkar, and P. C. Mhaske, "Thiazolyl-Pyrazole Derivatives as Potential Antimycobacterial Agents," *Bioorganic & Medicinal Chemistry Letters* 29, no. 10 (2019): 1199–202.
44. K. H. Rieckmann, G. H. Campbell, L. J. Sax, and J. E. Ema, "Drug Sensitivity of plasmodium falciparum. An In-Vitro Micro Technique," *The Lancet* 311, no. 8054 (1978): 22–3.
45. R. Panjarathinam, *Text Book of Medical Parasitology*, 2nd ed. (Chennai: Orient Longman Pvt. Ltd., 2007), 329–331.
46. C. Lambros, and J. P. Vanderberg, "Synchronization of Plasmodium falciparum Erythrocytic Stages in Culture," *The Journal of Parasitology* 65, no. 3 (1979): 418–20.
47. J. S. B. Singh, "Stain; a Review," *Indian Journal of Malariology* 10 (1956): 117–29.


 Cite this: *RSC Adv.*, 2020, 10, 26997

# Nanostructured N doped TiO<sub>2</sub> efficient stable catalyst for Kabachnik–Fields reaction under microwave irradiation†

 Sachin P. Kunde,<sup>ab</sup> Kaluram G. Kanade,<sup>ac</sup> Bhausheb K. Karale,<sup>a</sup> Hemant N. Akolkar,<sup>a</sup> Sudhir S. Arbuj,<sup>d</sup> Pratibha V. Randhavane,<sup>a</sup> Santosh T. Shinde,<sup>a</sup> Mubarak H. Shaikh<sup>a</sup> and Aniruddha K. Kulkarni<sup>e</sup>

Herein, we report nitrogen-doped TiO<sub>2</sub> (N-TiO<sub>2</sub>) solid-acid nanocatalysts with heterogeneous structure employed for the solvent-free synthesis of  $\alpha$ -aminophosphonates through Kabachnik–Fields reaction. N-TiO<sub>2</sub> were synthesized by direct amination using triethylamine as a source of nitrogen at low temperature and optimized by varying the volume ratios of TiCl<sub>4</sub>, methanol, water, and triethylamine, under identical conditions. An X-ray diffraction (XRD) study showed the formation of a rutile phase and the crystalline size is 10 nm. The nanostructural features of N-TiO<sub>2</sub> were examined by HR-TEM analysis, which showed they had rod-like morphology with a diameter of  $\sim$ 7 to 10 nm. Diffuse reflectance spectra show the extended absorbance in the visible region with a narrowing in the band gap of 2.85 eV, and the high resolution XPS spectrum of the N 1s region confirmed successful doping of N in the TiO<sub>2</sub> lattice. More significantly, we found that as-synthesized N-TiO<sub>2</sub> showed significantly higher catalytic activity than commercially available TiO<sub>2</sub> for the synthesis of a novel series of  $\alpha$ -amino phosphonates via Kabachnik–Fields reaction under microwave irradiation conditions. The improved catalytic activity is due to the presence of strong and Bronsted acid sites on a porous nanorod surface. This work signifies N-TiO<sub>2</sub> is an efficient stable catalyst for the synthesis of  $\alpha$ -aminophosphonate derivatives.

Received 21st May 2020

Accepted 7th July 2020

DOI: 10.1039/d0ra04533k

[rsc.li/rsc-advances](http://rsc.li/rsc-advances)

## 1 Introduction

In recent years, organophosphorus compounds have received much attention due to their widespread applications in medicinal and agriculture industries.<sup>1,2</sup>  $\alpha$ -Aminophosphonates are one such biological important framework that are structural mimics of amino acids. For example, glyphosate (*N*-(phosphonomethyl)glycine) is extensively utilized in agriculture as a systemic herbicide and Alafosfalin is used as an antibacterial agent<sup>3</sup> (Fig. 1). The bioactivity of these molecules such as antimicrobial,<sup>4</sup> antioxidant,<sup>5</sup> anti-inflammatory,<sup>6</sup> enzyme inhibitors<sup>7</sup> and antibacterial<sup>8</sup> is one of the reasons for them to be of

immense interest in synthetic organic chemistry. It has been demonstrated that on incorporation of heterocycles such as thiophene,<sup>9</sup> benzothiazoles,<sup>10</sup> thiadiazoles,<sup>11</sup> and pyrazole<sup>12</sup> into the  $\alpha$ -aminophosphonates scaffold, the resulting compounds exhibited interesting biological activities. Pyrazole derivatives of  $\alpha$ -aminophosphonates have been rarely reported in the literature,<sup>13,14</sup> thus synthesis of novel pyrazole derivatives of  $\alpha$ -aminophosphonates is important to research.

Although several protocols for the synthesis of  $\alpha$ -aminophosphonates are reported, one of the most important is the Kabachnik–Fields reaction.<sup>15,16</sup> This involves a one-pot three-component coupling of a carbonyl compound, an amine and alkylphosphite. These protocols has been accomplished in presence of a variety of catalyst such as TiCl<sub>4</sub>,<sup>17</sup> CuI,<sup>18</sup> hexanesulphonic sodium salt,<sup>19</sup> trifluoroacetic acid (TFA),<sup>20</sup> In(OTf)<sub>3</sub>,<sup>21</sup> BiCl<sub>3</sub>,<sup>22</sup> Cu(OTf)<sub>2</sub>,<sup>23</sup> SbCl<sub>3</sub>/Al<sub>2</sub>O<sub>3</sub>,<sup>24</sup> InCl<sub>3</sub>,<sup>25</sup> LiClO<sub>4</sub>,<sup>26</sup> ZrOCl<sub>2</sub>,<sup>27</sup> TsCl,<sup>28</sup> Mg(ClO<sub>4</sub>)<sub>2</sub>,<sup>29</sup> and Na<sub>2</sub>CaP<sub>2</sub>O<sub>3</sub><sup>30</sup> in presence or

<sup>a</sup>PG and Research Centre, Radhabai Kale Mahila Mahavidyalaya, Ahmednagar, 414 001 India. E-mail: kgkanade@yahoo.co.in

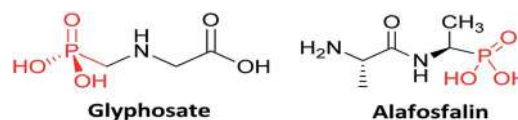
<sup>b</sup>PG and Research Centre, Mahatma Phule Arts, Science and Commerce College, Panvel, 410 206, India

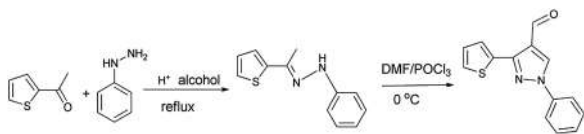
<sup>c</sup>PG and Research Centre, Yashwantrao Chavan Institute of Science, Satara, 415 001 India

<sup>d</sup>Centre for Materials for Electronics Technology (C-MET), Department of Electronics and Information Technology (DeitY), Government of India, Panchavati, Off Pashan Road, Pune-411 008, India

<sup>e</sup>Dr. John Barnabas School for Biological Studies, Department of Chemistry, Ahmednagar College, Ahmednagar-414 001, India

† Electronic supplementary information (ESI) available. See DOI: 10.1039/d0ra04533k


 Fig. 1 Some biological active  $\alpha$ -aminophosphonate.

Scheme 1 Synthesis of 1-phenyl-5-(thiophen-2-yl)-1H-pyrrole-3-carbaldehyde.

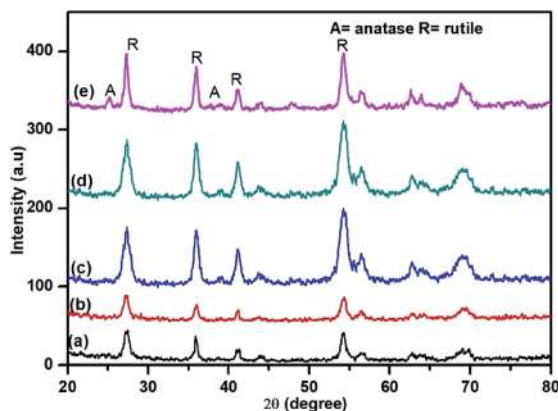


Fig. 2 X-ray diffraction patterns of (a) TN0 (TiO<sub>2</sub>), (b) TN1, (c) TN2 (d) TN3 (e) TN4.

even in the absence of a solvent. However, most of these existing procedures are sluggish, require long reaction times, use of strong acidic conditions, give unsatisfactory yields and also suffer from the formation of many side products. Moreover, in all alternatives microwave reaction proved to be a kind of promising medium for such reaction.<sup>31</sup>

In the last few years, the application of transition metal oxides gained particular interest as a heterogeneous catalyst for various organic synthesis.<sup>32</sup> Among all transition metal oxides the use of nanocrystalline titania (TiO<sub>2</sub>) has been grown extensively owing to their outstanding physicochemical properties, which furnished their wide applications in sensors,<sup>33</sup> pigments,<sup>34</sup> photovoltaic cells,<sup>35</sup> and catalysis.<sup>36</sup> Also, the use of potential titania catalyst attracted in organic synthesis due to its environmental compatibility, inexpensive, safe, stable, reusable and earth-abundant. It has been proven the desired property of TiO<sub>2</sub> was attained by fulfilling requirements in terms of unique morphology, high crystallinity and mixed-phase composition,

Table 1 Phase composition and crystallite size of as-prepared samples from analysis of XRD

Sample	Rutile	Anatase	Crystallite size (nm)
TN0	100	0	25
TN1	98	2	19
TN2	94	6	16
TN3	95	5	12
TN4	91	9	9

the ability of oxidizing and reducing ability under suitable irradiation makes promising greener alternative approach towards important organic transformations compared to other expensive, toxic, transition metal oxides. Moreover, the phase composition and the degree of crystallinity of the titania sample plays an important role in catalytic activity.<sup>8</sup> In the past several organic transformations such as oxidation of primary alcohols,<sup>37</sup> synthesis of xanthenes,<sup>38</sup> Friedel-Crafts alkylation,<sup>39</sup> Beckmann rearrangement<sup>40</sup> efficiently utilizes TiO<sub>2</sub> as a heterogeneous reusable catalyst. In the literature several reports have been debated to influence nitrogen doping on photocatalytic activity of nanocrystalline TiO<sub>2</sub>. However, the effect is unrevealed for catalytic applications in organic synthesis. Recently, Hosseini-Sarvari explored the use of commercial TiO<sub>2</sub> in the synthesis of  $\alpha$ -aminophosphonates *via* Kabachnik-Fields reactions.<sup>41</sup>

In present investigation, we have prepared nanostructured N doped TiO<sub>2</sub> and also investigation emphasis was given on the synthesis of a series of a novel diethyl(1-phenyl-3-(thiophen-2-yl)-1H-pyrazol-4-yl)(phenylamino) methylphosphonates under microwave irradiation.

## 2 Experimental sections

### 2.1 Synthesis of N doped TiO<sub>2</sub> nanorods

The nanostructured N-TiO<sub>2</sub> were synthesized by previously reported method with some modification.<sup>42,43</sup> In a typical procedure, 0.5 mL of titanium tetrachloride (TiCl<sub>4</sub>) was added in absolute methanol (25 mL) with constant stirring at room temperature. To this solution requisite quantity a 0.1–2 M aqueous triethylamine solution is injected rapidly. The resulting solution was refluxed for 24 h with constant stirring. The white precipitate formed was collected and washed with ethanol several times followed by centrifugation (10 000 rpm for 20 min). The precipitate was dried at 473 K for 24 h. To control the final morphologies of samples, the sample were synthesized as function of volume ratio of TiCl<sub>4</sub>, methanol, water, and triethylamine. The sample prepared in volume ratio 1 : 10 : 50 : 0, 1 : 10 : 50 : 1, 1 : 10 : 50 : 2, 2 : 10 : 50 : 2, and 2 : 10 : 50 : 4 were denoted as TN0 (pure TiO<sub>2</sub>), TN1, TN2, TN3 and TN4 respectively.

### 2.2 Synthesis of 1-phenyl-5-(thiophen-2-yl)-1H-pyrrole-3-carbaldehyde

1-Phenyl-5-(thiophene-2-yl)-1H-pyrrole-3-carbaldehyde were obtained *via* the Vilsmeier-Haack reaction of the appropriate phenylhydrazones, derived from the reaction of 2-acetyl thiophene with phenylhydrazine<sup>44</sup> (Scheme 1).

### 2.3 Synthesis of diethyl(1-phenyl-3-(thiophene-2-yl)-1H-pyrazole-4-yl)(phenylamino)methylphosphonates

In a typical procedure, the pyrazolealdehyde **1** (1 mmol), aniline **2** (1 mmol), triethyl phosphite **3** (1.1 mmol) and N-TiO<sub>2</sub> (12 mol%) were taken in a round bottom flask equipped with a condenser and subjected to microwave irradiation for (10–15 min) using 420 W (RAGA's Microwave system) (Scheme 3). The



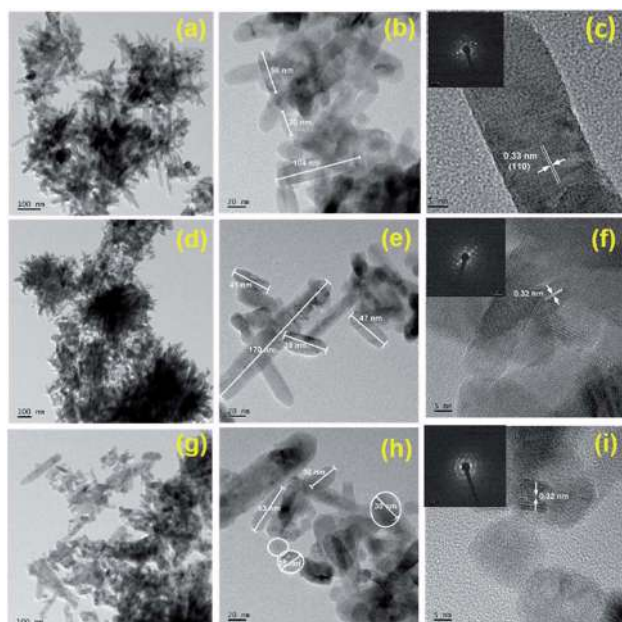


Fig. 3 HR-TEM images of (a–c) TN0, (d–f) TN1, and (g–i) TN2; inset c, f and h SAED pattern of TN0, TN2 and TN3 respectively.

progress of the reaction was monitored by TLC. After the reaction was completed, the reaction mixture extracted using ethyl acetate and insoluble catalyst separated by filtration. The crude product was purified by silica gel column chromatography using *n*-hexane/ethyl acetate as eluent. The product structure was determined by FTIR,  $^1\text{H}$  NMR, and LS-MS.

## 2.4 Samples characterization

The phase purity and crystallinity were examined by X-ray diffraction (XRD) technique (Advance, Bruker AXS D8) using  $\text{Cu K}\alpha 1$  (1.5406 Å) radiation with scanning  $2\theta$  range from 20 to 80°. For FE-TEM analysis samples were prepared by evaporating dilute solution on carbon-coated grids. FE-TEM measurements were carried using the JEOL SS2200 instrument operated at an

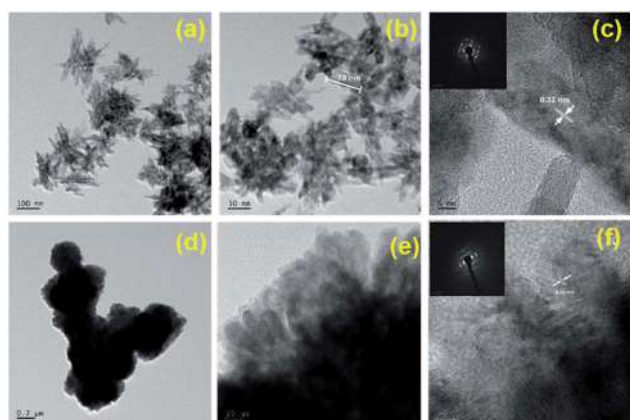


Fig. 4 HR-TEM images of (a–c) TN3 and (d–f) TN4; inset c, and f SAED pattern of TN3, and TN4 respectively.

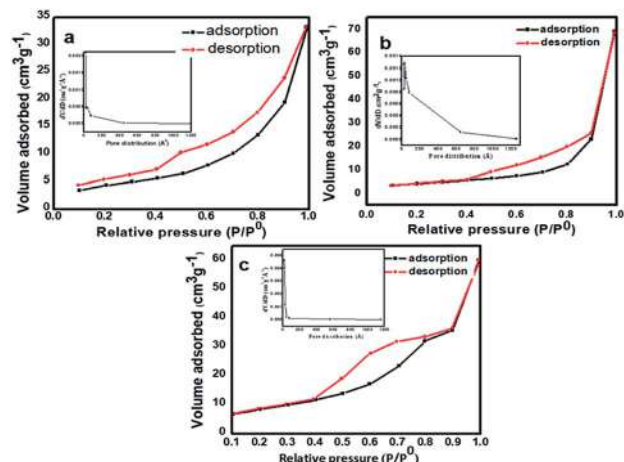


Fig. 5 Nitrogen ( $\text{N}_2$ ) adsorption–desorption isotherms of (a) TN0 ( $\text{TiO}_2$ ), (b) TN2 ( $\text{N-TiO}_2$ ), (c) TN4 ( $\text{N-TiO}_2$ ). Insets show their corresponding pore size distributions.

accelerating voltage of 300 kV. The Brunauer–Emmett–Teller (BET) surface area of nanocatalysts was examined using the Quantachrome v 11.02 nitrogen instrument. The optical properties of the powder samples were studied using UV-vis diffuse reflectance absorption spectra (UV-DRS) were recorded on the Perkin-Elmer Lambda-950 spectrophotometer in the wavelength range of 200–800 nm. Powder samples were used for XPS measurements. The XPS measurements of powdered samples were carried out on a VG Microtech ESCA3000 instrument. Fourier transform infrared (FTIR) spectra of prepared samples were recorded on a Shimadzu Affinity 1-S spectrophotometer in over a range of 400–4000  $\text{cm}^{-1}$ .  $^1\text{H}$  NMR was recorded in DMSO- $d_6$  solvent on a Bruker Advance-400 spectrometer with tetramethylsilane (TMS) as an internal reference.

## 3 Results and discussions

### 3.1 Structural study

Nanostructured  $\text{TiO}_2$  and N doped  $\text{TiO}_2$  were synthesized by a simple refluxing method. The phase purity and phase formation of as-synthesized material were analysed by powder X-ray diffraction pattern. Fig. 2 compares powder XRD patterns of  $\text{TiO}_2$  and N doped  $\text{TiO}_2$  samples. The peak position and peak intensity of the pure  $\text{TiO}_2$  powder can be indexed into rutile phases (Fig. 2). Further, it is observed that an increase in the amount N-dopant (triethylamine) the intensity of the diffraction

Table 2 BET specific surface area and pore size distribution of  $\text{TiO}_2$  and N- $\text{TiO}_2$

Sample	Surface area ( $\text{m}^2 \text{g}^{-1}$ )	Pore volume ( $\text{cm}^3 \text{g}^{-1}$ )	Pore radius (Å)
TN0	21.956	0.051	18.108
TN2	40.359	0.215	30.811
TN4	53.589	0.101	18.041





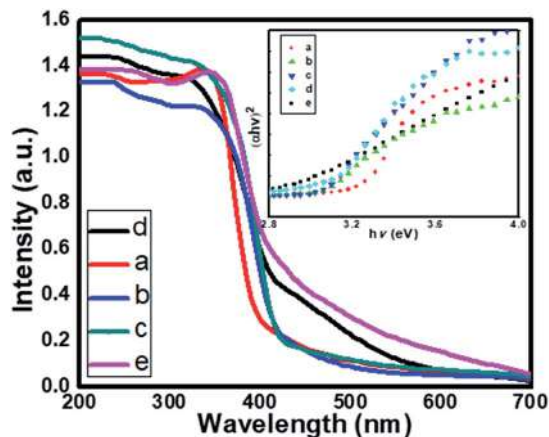


Fig. 6 UV-DRS spectra of (a) TN0 (TiO<sub>2</sub>), (b) TN1 (c) TN2 (d) TN3 (N-TiO<sub>2</sub>), (e) TN4. Inset shows Tauc plot of TiO<sub>2</sub> and N-TiO<sub>2</sub> samples.

peaks of the rutile phase decreases, while that of anatase phase increases, indicating that the fraction of the anatase phase gradually increases at the expense of the rutile phase during this condition (sample TN2–TN4). The phase composition of rutile and anatase phase of TiO<sub>2</sub> evaluated from the peak intensity using the following equation,

$$f_A = \frac{1}{1 + \frac{I_R}{K I_A}} \quad K = 0 : 79; f_A > 0.2; K_{1/4} = 0 : 68; f_A \leq 0.2$$

where  $f_A$  is the fraction of the anatase phase, and  $I_A$  and  $I_R$  are the intensities of the anatase (1 0 1) and rutile (1 1 0) diffraction peaks, respectively. The higher molar concentration of triethylamine is favourable for the transformation from rutile to anatase.<sup>45,46</sup> Therefore, the phase composition of TiO<sub>2</sub> samples, *i.e.* the fraction of anatase and rutile, can be facilely controlled through adjusting the concentration of triethylamine. The slight shift of rutile (1 1 0) diffraction peaks towards a higher angle with an increase in the amount of N dopant suggesting

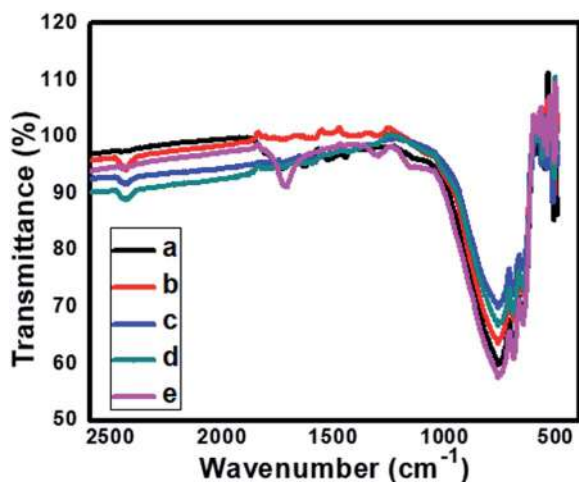


Fig. 7 FTIR spectra of (a) TN0 pure (TiO<sub>2</sub>), (b) TN1 (N-TiO<sub>2</sub>), (c) TN2, (d) TN3 and (e) TN4.

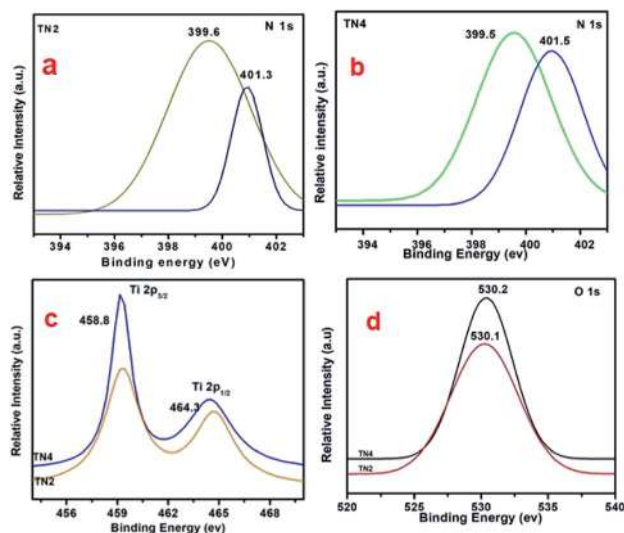
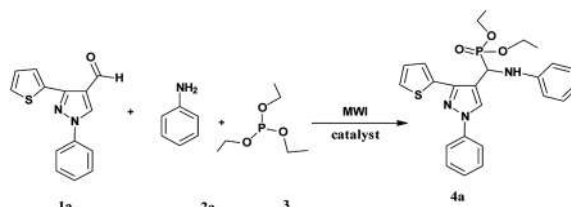


Fig. 8 (a and b) High resolution spectrum of N 1s region (c) high resolution spectrum of Ti 2p region (d) high resolution spectrum of O 1s region.

the incorporation of nitrogen in the TiO<sub>2</sub> crystal structure. The crystallite size is calculated from each (1 1 0) peak in the XRD pattern using the Sherrer formula.<sup>39</sup> The average crystalline size are 25, 19, 16, 12 and 9 nm for TN0, TN1, TN2, TN3, and TN4 respectively (Table 1). From, XRD analysis it is clear that with an increase in the concentration of nitrogen in TiO<sub>2</sub>, fraction of anatase increases phase and crystalline size decreases.

### 3.2 Surface and morphological study

Transmission electron microscopy (TEM) and high-resolution transmission electron microscopy (HRTEM) analysis were performed to study morphology and crystallinity of as-synthesized pure and N doped TiO<sub>2</sub> materials (Fig. 3). The pure TiO<sub>2</sub> (TN0) sample seems flowerlike nanostructures (Fig. 3a). At high-resolution it reveals that each flower microstructure consisting several nanorods. The length of nanorods are in the range of 50–70 nm and diameter is about 10–15 nm (Fig. 3b). Fig. 3c shows the lattice fringes of the material with interplanar spacing  $d$  spacing 0.33 nm matches well (1 0 0) plane of rutile TiO<sub>2</sub>. Fig. 3c inset shows a selected area diffraction pattern in which bright spots observed that confirm the TiO<sub>2</sub> nanorods are in nanocrystalline nature. It was observed that addition of N dopant, resulting sample TN1 and TN2 grows into new superstructure consisting nanorods of length 30–50 nm and spheres



Scheme 2 Standard model reaction.





**Table 3** Comparative study of catalysts used for the synthesis of  $\alpha$ -aminophosphonate<sup>a</sup>

Entry	Catalyst	Time (minutes)	Yield <sup>b</sup> (%)
1	—	20	Trace
2	Acetic acid	20	30
3	Commercial ZnO	15	20
4	Commercial TiO <sub>2</sub>	15	30
5	TN0	10	72
6	TN1	10	73
7	TN2	10	76
8	TN3	10	85
9	TN4	10	95

<sup>a</sup> Reaction condition: aldehyde(1a) (1 mmol), aniline (1 mmol), triethylphosphite (1.1 mmol), catalyst, MW power 420 watt. <sup>b</sup> Isolated yield.

of diameter 20–30 nm, particles size is obviously smaller than TN0 (Fig. 3d and h). HRTEM results are consistent with XRD results. The *d*-spacing is about 0.325 Å between adjacent lattice planes of the N doped TiO<sub>2</sub>.

It was revealed that with doubling concentration of TiCl<sub>4</sub>, sample TN3 and TN4 were grown into very fine agglomerated nanorods (Fig. 4). Further, it is observed that these nanorods having size in length 30–40 nm and diameter is around 7–10 nm which is lower than pure TiO<sub>2</sub>. Fig. 4f inset shows selected area diffraction pattern shows, surprisingly, ring-like pattern unlike TiO<sub>2</sub>, indicates N-TiO<sub>2</sub> nanorods are in polycrystalline nature. From HR-TEM results it is concluded that increase in concentration of TiCl<sub>4</sub> and triethylamine reduces the size of the nanorods.

The specific surface area of as-prepared samples was studied by (N<sub>2</sub>) nitrogen gas adsorption–desorption measurement at 77 K using the Brunauer–Emmett–Teller (BET) method. The N<sub>2</sub> adsorption–desorption isotherm of N-TiO<sub>2</sub> nanoparticles is shown in Fig. 5. The pure TiO<sub>2</sub> shows type IV isotherm according to IUPAC classification,<sup>47</sup> which are typical characteristics of a material with pore size in the range of 1.5–100 nm Fig. 5a. The shape of the hysteresis loop is H<sub>3</sub> type may associates due to the agglomeration of nanoparticles forming slit-like pores, reflected in TEM images. At higher relative pressure (*p/p*<sup>0</sup>) the slope shows increased uptake of adsorbate as pores become filled; inflection point typically occurs near

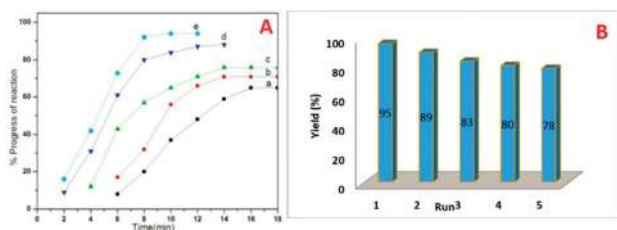


**Fig. 9** (A) Progress of reaction (a) TN0 (b) TN1 (c) TN2 (d) TN3 and (e) TN4. (B) Reusability of catalyst TN4; reaction condition: aldehyde (1a) (1 mmol), aniline (2a) (1 mmol), triethylphosphite 3 (1.1 mmol), N-TiO<sub>2</sub> (12 mol%), MW power 420 watt.

**Table 4** Optimization of the concentration of catalyst<sup>a</sup>

Sr. no.	Concentration of catalyst (mol%)	Yield <sup>b</sup> (%)
1	3	69
2	6	76
3	9	86
4	12	95
5	15	95

<sup>a</sup> Reaction condition: aldehyde (1a) (1 mmol), aniline (1 mmol), triethylphosphite (1.1 mmol), N-TiO<sub>2</sub> catalyst, MW power 420 watt. <sup>b</sup> Isolated yield.

completion of the first monolayer. The BET surface area of pure TiO<sub>2</sub> is found to be 21.956 m<sup>2</sup> g<sup>-1</sup>. The pore size distribution of prepared samples was investigated by Barrett–Joyner–Halenda (BJH) method Fig. 5(a)–(c) insets. The average pore diameter of pure TiO<sub>2</sub> nanoparticles is 18 nm which demonstrates the material is mesoporous nature. Further, it is observed that the incorporation of nitrogen in TiO<sub>2</sub> nanoparticles the surface area shifts towards higher values. The adsorption–desorption isotherms of nitrogen-doped TiO<sub>2</sub> samples display the type II isotherm according to IUPAC classification.<sup>46</sup> The specific BET surface area of samples TN<sub>2</sub> and TN<sub>4</sub> are 40.359 m<sup>2</sup> g<sup>-1</sup> and 53.589 m<sup>2</sup> g<sup>-1</sup> respectively (Fig. 5b and 4c). This observation specifies a decrease in the particle size of TiO<sub>2</sub> nanoparticles specific surface area increases which are in consisting of XRD and TEM results. The Brunauer–Emmett–Teller (BET) specific surface areas, pore volumes and mean pore and mean pore diameters of samples TN0, TN2, and TN4 are summarized in Table 2.

### 3.3 Optical and electronic property studies

The optical property of the as-synthesized material was analyzed by UV-Vis diffuse absorbance spectra as shown in Fig. 6. Fig. 6 displays the comparative UV-DRS spectra of pristine TiO<sub>2</sub> and a series of N doped TiO<sub>2</sub> samples. The absorption edge for the pure TiO<sub>2</sub> (TN0) is observed at around 410 nm (Fig. 6a), which is consistent with the band gap of the rutile phase.<sup>45</sup> The N doped TiO<sub>2</sub> nanostructures show strong absorption in the visible region (410–600 nm). The redshift clearly indicates the

**Table 5** Screening of solvents<sup>a</sup>

Entry	Solvent	Yield (%) <sup>b</sup>
1	Ethanol	85
2	Methanol	87
3	Dichloromethane	55
4	THF	58
6	Toluene	60
7	Neat	95

<sup>a</sup> Reaction condition: aldehyde (1a) (1 mmol), aniline (1 mmol), triethylphosphite (1.1 mmol), N-TiO<sub>2</sub> catalyst, solvent, MW power 420 watt. <sup>b</sup> Isolated yield.



successful doping of N in the lattice of TiO<sub>2</sub>. Moreover, as the concentration of triethylamine increases redshift of N-TiO<sub>2</sub> also increases which confirms higher nitrogen doping and a higher fraction of absorption of photons from the visible region. The band gap of as-synthesized material calculated by using the Tauc plot shown in Fig. 6 (insets). The band gap ( $E_g$ ) for the sample TN0, TN1, TN2, TN3, and TN4, were observed to 3.15, 3.09, 3.07, 3.03 and 2.85 eV respectively. The decrease in the band gap is attributed to higher mixing of the (O/N) 2p level is developed in the Ti-3d level falls at the top of the VB, therefore, band gap reduced compared to the pristine TiO<sub>2</sub> nanostructure.

### 3.4 FT-IR spectroscopy

Fig. 7 shows comparative FTIR spectra for pure and N doped TiO<sub>2</sub>. The absorption peak signal in the range of 400–1100 cm<sup>-1</sup> is characteristic of the formation of O-Ti-O lattice. The absorption at 668 cm<sup>-1</sup>, 601 cm<sup>-1</sup>, 546 cm<sup>-1</sup> and 419 cm<sup>-1</sup> corresponds to Ti-O vibrations.<sup>48,49</sup> Further, for the sample TN1–TN3 the IR bands centred at 1400–1435 cm<sup>-1</sup> indicates nitrogen doping in the TiO<sub>2</sub> sample. The band located at 1070 cm<sup>-1</sup> is attributed to Ti-N bond vibrations. Also, it is observed that the band at 1335 cm<sup>-1</sup> for pure TiO<sub>2</sub> is shifted towards longer wavenumber 1430 cm<sup>-1</sup> supports for the claim of N doping in TiO<sub>2</sub> lattice. Further it is also observed that some of the minor the peaks of pure TiO<sub>2</sub> are rather different than the N-doped TiO<sub>2</sub>, this indicates the incorporation of nitrogen in TiO<sub>2</sub> lattices. The peak centered at 1600–2180 cm<sup>-1</sup> is ascribed due to -OH stretching frequency. From, IR spectra it is clear that N<sub>2</sub> is successfully incorporated in the lattice of TiO<sub>2</sub>.

### 3.5 X-ray photoelectron spectroscopy

The XPS were used for chemical identification and electronic state of dopant nitrogen in sample TN2 and TN4. The high resolution XPS spectra of N 1s on deconvolution shows two different peaks at 399.6 and 401.5 eV indicates nitrogen present in two different electronic state (Fig. 8a and b). The peak at 399.6 is attributed to presence of interstitial N or N-Ti-O linkage. The result is consistent with previous reports.<sup>43</sup> The peak at 401.5 is attributed to presence of N in oxidized state as NO or NO<sub>2</sub>. The concentration of nitrogen on surface of TN2 and TN4 are 2.8% and 3.4% respectively. Fig. 8c shows the peak at 458.8 and 458.3 is attributed to Ti 2p<sub>3/2</sub> and Ti 2p<sub>1/2</sub>, in good agreement the presence of Ti(IV) in TiO<sub>2</sub>. The peak at binding energy 530.1 and 530.2 eV of sample are attributed to O 1s (Fig. 8d).

### 3.6 Catalytic study in synthesis of $\alpha$ -aminophosphonates

In order to find out the best experimental condition, the reaction of pyrazolaldehyde **1a**, aniline **2a** and triethylphosphite **3** under microwave irradiation is considered as standard model reaction (Scheme 2).

In the absence of a catalyst, the standard model reaction gave a small amount of product (Table 3 entry 1). These results specify catalyst is required to occur reaction. In order to check the catalytic utility, the model reaction carried out in the presence of a variety of catalysts (Table 3 entry 2–9). The N-TiO<sub>2</sub> NRs

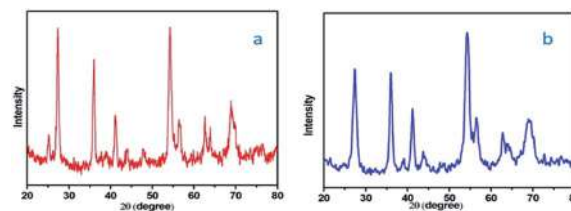


Fig. 10 XRD of sample TN4 (a) before reaction (b) after reaction.

gave better results than acetic acid, commercial ZnO and commercial TiO<sub>2</sub>.

Inspiring these results, we further studied the progress of reaction at different time intervals, we observed the sample N-doped TiO<sub>2</sub> catalyzes efficiently than undoped TiO<sub>2</sub>, and this may be attributed to the higher surface area (Fig. 9A).

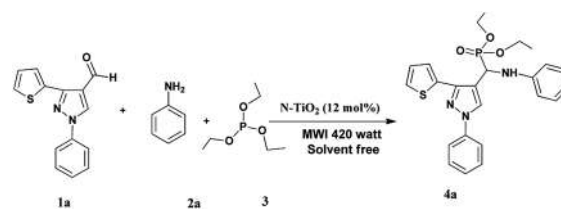
The optimum concentration of the catalyst was investigated by performing the model reaction at different concentrations such as 3, 6, 9, 12 and 15 mol%. The reaction yielded in 69, 76, 86, 95 and 95% yields respectively (Table 4). This shows that 12 mol% of TN<sub>4</sub> is adequate for the reaction by considering the yield of the product.

To evaluate the effect of solvents, different solvents such as ethanol, methanol, dichloromethane, THF, 1,4-dioxane and toluene were used for the model reaction in presence of N-TiO<sub>2</sub> catalyst. The reaction proceed with better yield in polar protic solvent (Table 5, entries 1, 2). However it was observed that the usage of solvents slows down the rate of reaction and gives the desired product in lower yields than that for neat condition (Table 5, entries 1–6).

The recyclability of the catalyst was then examined and the outcomes are shown in Fig. 9B. After the completion of reaction, the reaction mixture was extracted with ethyl acetate. The residual catalyst was washed with acetone, dried under vacuum at 100 °C and reused for consequent reactions. The recovered catalyst could be used for 5 times without obvious loss of catalytic activity.

The difference between the XRD of fresh catalyst and reused catalyst shown in Fig. 10.

The usefulness of optimized reaction condition for model reaction (12 mmol % of catalyst, solvent-free, MWI) was extended for the synthesis of a series of novel  $\alpha$ -amino-phosphonates (**4a–I**) by reacting pyrazolaldehyde (**1a–c**), anilines (**2a–d**) and triethylphosphite (**3**) in excellent yields (Scheme 3).



Scheme 3 Optimized reaction condition for synthesis of diethyl(1-phenyl-3-(thiophen-2-yl)-1H-pyrazol-4-yl)(phenylamino) methylphosphonates



Table 6 Microwave assisted synthesis of novel diethyl(1-phenyl-3-(thiophen-2-yl)-1H-pyrazol-4-yl)(phenylamino)methylphosphonates<sup>a</sup>

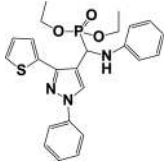
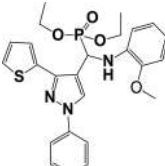
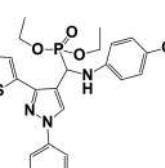
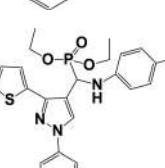
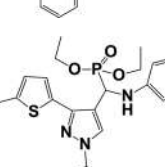
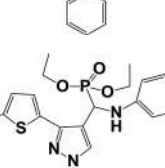
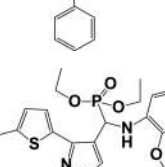
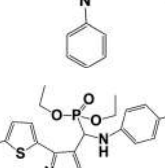
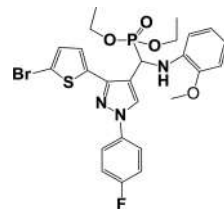
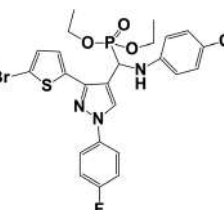
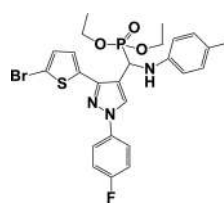
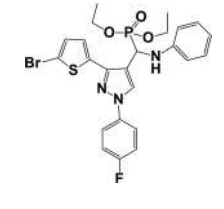
Entry	Product	M.P. (°C)	Yield <sup>b</sup> (%)
4a		218	95
4b		220	79
4c		208	92
4d		216	79
4e		180	86
4f		200	82
4g		162	85
4h		190	71

Table 6 (Contd.)

Entry	Product	M.P. (°C)	Yield <sup>b</sup> (%)
4i		195	81
4j		120	76
4k		210	89
4l		190	75

<sup>a</sup> Reaction condition: aldehyde (1 mmol), aniline (1 mmol), triethylphosphite (1.1 mmol), N-TiO<sub>2</sub> (12 mol%), MW power 420 watt.  
<sup>b</sup> Isolated yield.

The obtained product **4a–l** was characterized by spectroscopic techniques (Table 6).

The spectroscopic data of synthesized compounds are given in ESI (S-2 to S-26).†

## 4 Conclusions

In summary, we have prepared N doped TiO<sub>2</sub> nanorods by thermal hydrolysis method using triethylamine as the source of nitrogen at relatively low temperatures. The XRD analysis showed that with varying composition molar ratios of TiCl<sub>4</sub>, CH<sub>3</sub>OH, H<sub>2</sub>O, and (C<sub>2</sub>H<sub>5</sub>)<sub>3</sub>N, phase composition of rutile to anatase also tunes. FTIR spectra show the chemical environment of doping by the formation of the N-Ti-O and Ti-O-Ti bond. The morphological study performed by the FE-TEM technique shows the formation of well-developed nanorods of size in length 30–40 nm and diameter is around 7–10 nm, which is lower than pure TiO<sub>2</sub>. Further, BET analysis N-TiO<sub>2</sub> shows the maximum specific surface area 53.4 m<sup>2</sup> g<sup>-1</sup> which is 2.5 times



higher than pure TiO<sub>2</sub>. The as-synthesized materials were employed for the synthesis of  $\alpha$ -aminophosphonates via Kabachnik–Fields reaction under microwave irradiation. The N-TiO<sub>2</sub> shows remarkable catalytic activity for aminophosphonate derivatives compared with TiO<sub>2</sub> and other similar nanocatalysts.

## Conflicts of interest

There are no conflicts to declare.

## Acknowledgements

SPK is gratefully acknowledged UGC New Delhi for the award of Senior Research Fellowship (F.11-16/2013(SA-I)). The authors are thankful to parent institute Rayat Shikshan Sanstha, Satara.

## Notes and references

- L. G. Costa, *Toxicol. Sci.*, 2018, **162**(1), 24–35.
- M. Eto, *Organophosphorus pesticides*, CRC press, 2018.
- A. Mucha, P. Kafarski and L. Berlicki, *J. Med. Chem.*, 2011, **54**(17), 5955–5980.
- M. K. Awad, M. F. Abdel-Aal, F. M. Atlam and H. A. Hekal, *Spectrochim. Acta, Part A*, 2018, **206**, 78–88.
- M. M. Azaam, E. R. Kenawy, A. S. El-din, A. A. Khamis and M. A. El-Magd, *J. Saudi Chem. Soc.*, 2018, **22**(1), 34–41.
- R. Damiche and S. Chafaa, *J. Mol. Struct.*, 2017, **1130**, 1009–1017.
- Z. Chen, P. Marce, R. Resende, P. M. Alzari, A. C. Frasch, J. M. Van den Elsen, S. J. Crennell and A. G. Watts, *Eur. J. Med.*, 2018, **158**, 25–33.
- A. Hellal, S. Chafaa, N. Chafai and L. Touafri, *J. Mol. Struct.*, 2017, **1134**, 217–225.
- D. Rogacz, J. Lewkowski, M. Siedlarek, R. Karpowicz, A. Kowalczyk and P. Rychter, *Materials*, 2019, **12**(12), 2018.
- L. Jin, B. Song, G. Zhang, R. Xu, S. Zhang, X. Gao and S. Yang, *Bioorg. Med. Chem. Lett.*, 2006, **16**(6), 537–1543.
- S. M. Lu and R. Y. Chen, *Org. Prep. Proced. Int.*, 2000, **32**(3), 302–306.
- A. G. Nikalje, P. A. Gawhane, S. V. Tiwari, J. N. Sangshetti and M. G. Damale, *Anti-Cancer Agents Med. Chem.*, 2018, **18**(9), 1267–1280.
- C. W. Guo, S. H. Wu, F. L. Chen, Z. Y. Han, X. H. Fu and R. Wan, *Phosphorus, Sulfur Silicon Relat. Elem.*, 2016, **191**(9), 1250–1255.
- L. Wu, B. Song, P. S. Bhadury, S. Yang, D. Hu and L. Jin, *J. Heterocycl. Chem.*, 2011, **48**, 389–396.
- W. Fan, Y. Queneau and F. Popowycz, *RSC Adv.*, 2018, **8**, 31496–31501.
- B. Rajendra Prasad Reddy, P. Vasu Govardhana Reddy and B. N. Reddy, *New J. Chem.*, 2015, **39**, 9605–9610.
- Y. T. Reddy, P. N. Reddy, B. S. Kumar, P. Rajput, N. Sreenivasulu and B. Rajitha, *Phosphorus, Sulfur Silicon Relat. Elem.*, 2007, **182**(1), 161–165.
- H. Fang, X. Xie, B. Hong, Y. Zhao and M. Fang, *Phosphorus, Sulfur Silicon Relat. Elem.*, 2011, **186**(11), 2145–2155.
- K. S. Niralwad, B. B. Shingate and M. S. Shingare, *Ultrason. Sonochem.*, 2010, **17**(5), 760–763.
- T. Akiyama, M. Sanada and K. Fuchibe, *Synlett*, 2003, **10**, 1463–1464.
- R. Ghosh, S. Maiti, A. Chakraborty and D. K. Maiti, *J. Mol. Catal. A: Chem.*, 2004, **210**(1–2), 53–57.
- Z. P. Zhan and J. P. Li, *Synth. Commun.*, 2005, **35**(19), 2501–2508.
- A. S. Paraskar and A. Sudalai, *ARKIVOC*, 2006, 183–189.
- K. S. Ambica, S. C. Taneja, M. S. Hundal and K. K. Kapoor, *Tetrahedron Lett.*, 2008, **49**, 2208–2212.
- B. C. Ranu, A. Hajraa and U. Jana, *Org. Lett.*, 1999, **1**, 1141–1143.
- N. Azizi, F. Rajabi and M. R. Saidi, *Tetrahedron Lett.*, 2004, **45**, 9233–9236.
- S. Bhagat and A. K. Chakraborti, *J. Org. Chem.*, 2008, **73**, 6029–6032.
- B. Kaboudin and E. Jafari, *Synlett*, 2008, **12**, 1837–1839.
- S. Bhagat and A. K. Chakraborti, *J. Org. Chem.*, 2007, **72**, 1263–1266.
- A. Elmakssoudi, M. Zahouily, A. Mezdar, A. Rayadh and S. Sebti, *C. R. Chim.*, 2005, **8**, 1954–1959.
- A. Tajti, E. Szatmári, F. Perdih, G. Keglevich and E. Balint, *Molecules*, 2019, **24**(8), 1640.
- S. P. Kunde, K. G. Kanade, B. K. Karale, H. N. Akolkar, P. V. Randhavane and S. T. Shinde, *Arabian J. Chem.*, 2019, **12**, 5212–5222.
- S. Ardizzone, C. L. Bianchi, G. Cappelletti, S. Gialanella, C. Pirola and V. Ragaini, *J. Phys. Chem. C*, 2007, **111**(35), 13222–13231.
- J. P. Jalava, *Part. Part. Syst. Charact.*, 2006, **23**(2), 159–164.
- M. Pelaez, N. T. Nolan, S. C. Pillai, M. K. Seery, P. Falaras, A. G. Kontos, P. S. Dunlop, J. W. Hamilton, J. A. Byrne, K. O'shea and M. H. Entezari, *Appl. Catal. B*, 2012, **125**, 331–349.
- G. C. Nakhate, V. S. Nikam, K. G. Kanade, S. S. Arbut, B. B. Kale and J. O. Baeg, *Mater. Chem. Phys.*, 2010, **124**(2–3), 976–981.
- D. I. Enache, J. K. Edwards, P. Landon, B. Solsona-Espriu, A. F. Carley, A. A. Herzing, M. Watanabe, C. J. Kiely, D. W. Knight and G. J. Hutchings, *Science*, 2006, **311**, 362–365.
- B. F. Mirjalilia, A. Bamoniri, A. Akbari and N. Taghavinia, *J. Iran. Chem. Soc.*, 2011, **8**, S129–S134.
- L. Kantam, S. Laha, J. Yadav and B. Sreedhar, *Tetrahedron Lett.*, 2006, **47**, 6213–6216.
- H. S. Sarvar and M. H. Sarvari, *J. Chem. Res.*, 2003, **2**, 176–178.
- M. Hosseini-Sarvari, *Tetrahedron*, 2008, **64**(23), 5459–5466.
- Y. Wang, L. Zhang, K. Deng, X. Chen and Z. Zou, *J. Phys. Chem. C*, 2007, **111**, 2709–2714.
- L. Hu, J. Wang, J. Zhang, Q. Zhang and Z. Liu, *RSC Adv.*, 2014, **4**, 420–427.
- B. F. Abdel-wahab, R. E. Khidre and A. A. Farahat, *ARKIVOC*, 2011, (i), 196–245.
- J. Senthilnathan and L. Philip, *Chem. Eng. J.*, 2010, **16**(1–2), 83–92.



## Paper

- 46 T. C. Jagadale, S. P. Takale, R. S. Sonawane, H. M. Joshi, S. I. Patil, B. B. Kale and S. B. Ogale, *J. Phys. Chem. C*, 2008, **11293**, 14595–14602.
- 47 S. Y. Choi, M. Mamak, N. Coombs, N. Chopra and G. A. Ozin, *Adv. Funct. Mater.*, 2004, **14**(4), 335–344.
- 48 X. Chen, X. Wang, Y. Hou, J. Huang, L. Wu and X. Fu, *J. Catal.*, 2008, **255**(1), 59–67.
- 49 M. Hema, A. Y. Arasi, P. Tamilselvi and R. Anbarasan, *Chem. Sci. Trans.*, 2012, **2**, 239–245.







## ARTICLE

# Synthesis of 3-(trifluoromethyl)-1-(perfluorophenyl)-1*H*-pyrazol-5(4*H*)-one derivatives via Knoevenagel condensation and their biological evaluation

Sujata G. Dengale<sup>1</sup> | Hemantkumar N. Akolkar<sup>2</sup> | Bhausahab K. Karale<sup>2</sup> |  
Nirmala R. Darekar<sup>2</sup> | Sadhana D. Mhaske<sup>3</sup> | Mubarak H. Shaikh<sup>2</sup> |  
Dipak N. Raut<sup>4</sup> | Keshav K. Deshmukh<sup>1</sup>

<sup>1</sup>P.G. and Research, Department of Chemistry, Sangamner Nagarpalika Arts, D. J. Malpani Commerce and B. N. Sarada Science College, Sangamner, India

<sup>2</sup>P.G. and Research, Department of Chemistry, Radhabai Kale Mahila Mahavidyalaya, Ahmednagar, India

<sup>3</sup>Department of Chemistry, Dadapatil Rajale College, Pathardi, India

<sup>4</sup>Amrutvahini College of Pharmacy, Sangamner, India

## Correspondence

Hemantkumar N. Akolkar, P.G. and Research, Department of Chemistry, Radhabai Kale Mahila Mahavidyalaya, Ahmednagar, Maharashtra, India, 414001. Email: hemantakolkar@gmail.com

## Abstract

In search of new active molecules, a small focused library of the synthesis of 3-(trifluoromethyl)-1-(perfluorophenyl)-1*H*-pyrazol-5(4*H*)-one derivatives (**4a-d**, **5a-f**, and **6a-e**) has been efficiently prepared via the Knoevenagel condensation approach. All the derivatives were synthesized by conventional and non-conventional methods like ultrasonication and microwave irradiation, respectively. Several derivatives exhibited excellent anti-inflammatory activity compared to the standard drug. Furthermore, the synthesized compounds were found to have potential antioxidant activity. In addition, to rationalize the observed biological activity data, an *in silico* absorption, distribution, metabolism, and excretion (ADME) prediction study also been carried out. The results of the *in vitro* and *in silico* studies suggest that the 3-(trifluoromethyl)-1-(perfluorophenyl)-1*H*-pyrazol-5(4*H*)-one derivatives (**4a-d**, **5a-f**, and **6a-e**) may possess the ideal structural requirements for the further development of novel therapeutic agents.

## KEYWORDS

ADME prediction, anti-inflammatory, antioxidant, Knoevenagel, microwave, pyrazole, ultrasonication

## 1 | INTRODUCTION

The pyrazole ring is a prominent heterocyclic structural compound found in several pharmaceutically active compounds. This is because of its use in pharmacological activity and ease of synthesis. Furthermore, the selective functionalization of pyrazole with diverse substituents was also found to improve their range of action in various fields. Pyrazole containing heterocycles shows various biological activity, such as antibacterial,<sup>[1]</sup> antifungal,<sup>[2]</sup> antimicrobial,<sup>[3]</sup> anti-inflammatory,<sup>[4a]</sup> antioxidant,<sup>[4b]</sup> insecticidal,<sup>[5]</sup> antiviral,<sup>[6]</sup> anti-nitric oxide

synthase,<sup>[7]</sup> glycogen receptor antagonist,<sup>[8]</sup> anticancer,<sup>[9]</sup> antienzyme,<sup>[10]</sup> immunosuppressant,<sup>[11]</sup> anti-fatty acid amide hydrolase (FAAH),<sup>[12]</sup> and liver-x-receptor [LXR] partial agonist activities.<sup>[13]</sup>

Fluorine or fluorine-based compounds are of great interest in synthetic and medicinal chemistry. The position of the fluorine atom in an organic molecule plays a vital role in agrochemicals, pharmaceuticals, and materials<sup>[14]</sup> as it changes the pharmacokinetic and pharmacodynamic properties of the molecule owing to its high membrane permeability, metabolic stability, lipophilicity, and binding affinity.<sup>[15]</sup>

Perfluoro-alkylated and trifluoro-methylated pyrazoles represent pharmacologically related core structures that are present in many important drugs and agrochemicals, such as fluazolate (herbicide), penthiopyrad (fungicide), razaxaban (anticoagulant), deracoxib, celecoxib (anti-inflammatory), and penflufen (fungicidal) (Figure 1).<sup>[16]</sup> So, the modern trend is moving more in the direction of the synthesis of a collection of fluorine-containing molecules in order to find excellent biological activity.

Ultrasonic irradiation is a new technology that has been widely used in chemical reactions. When ultrasonic waves pass through a liquid medium, a large number of microbubbles form, grow, and collapse in very short times, about a few microseconds. The formation and violent collapse of small vacuum bubbles takes place due to the ultrasonication waves generated in alternating high pressure and low pressure in liquids, and the phenomenon is known as cavitation. It causes high-speed imposing liquid jets and strong hydrodynamic shear forces. The deagglomeration of nanometer-

sized materials was carried out using these effects. In this aspect, for high-speed mixers and agitator bead mills, ultrasonication is an alternative.<sup>[17]</sup>

In the preparative chemist's toolkit, microwave heating is a valuable technique. Due to a modern scientific microwave apparatus, it is possible to access elevated temperatures in an easy, safe, and reproducible way.<sup>[18]</sup> In recent years, microwave-assisted organic synthesis (MAOs)<sup>[19]</sup> has been emerged as a new "lead" in organic synthesis. Important advantages of this technology include a highly accelerated rate of the reaction and a decrease in reaction time, with an increase in the yield and quality of the product. The current technique is considered an important method toward green chemistry as this technique is more environmentally friendly. The conventional method of organic synthesis usually needs a longer heating time; tedious apparatus setup, which results in the higher cost of the process; and the excessive use of solvents/reagents, which leads to environmental pollution. This growth of green chemistry

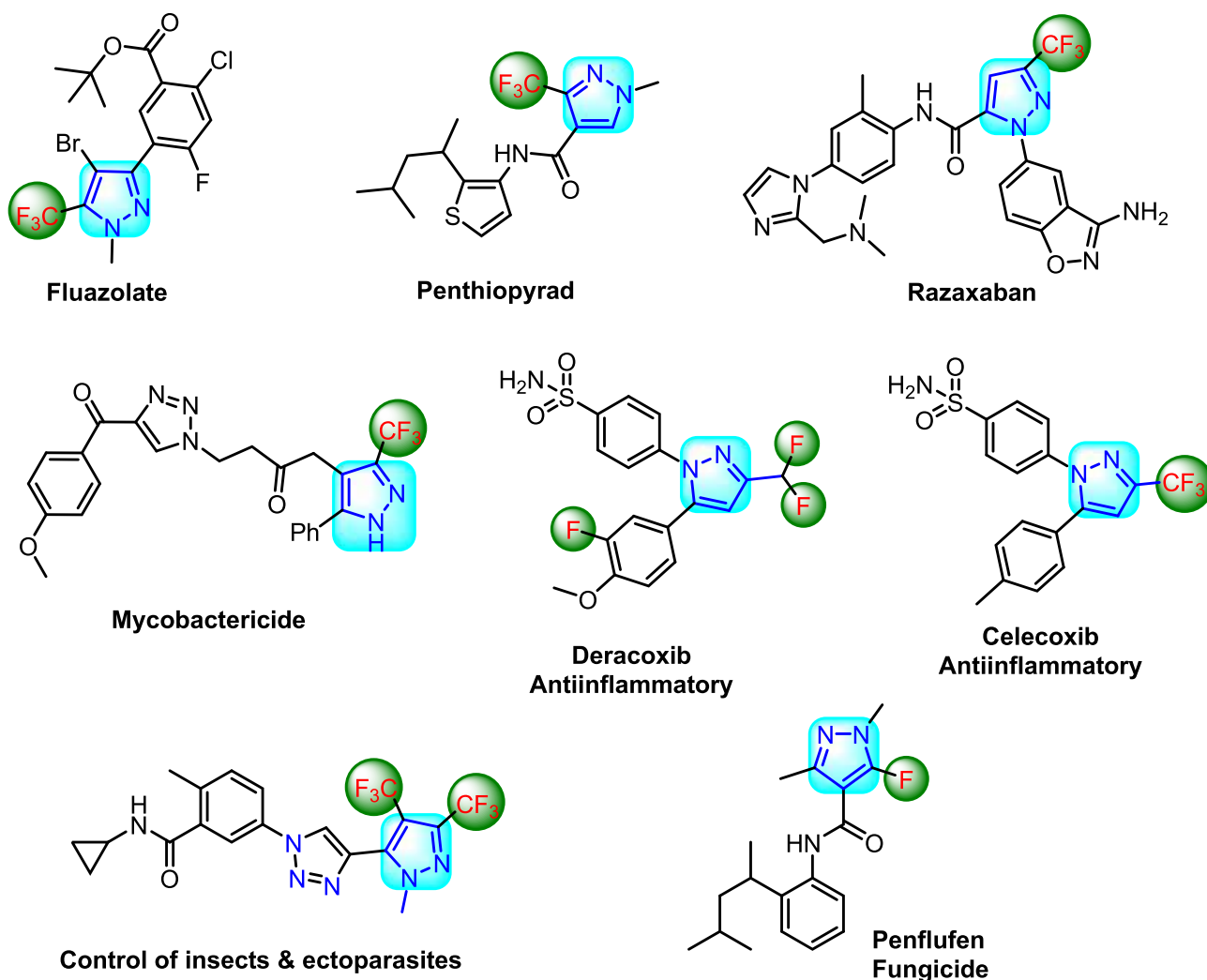


FIGURE 1 Structure of pyrazole- and fluorine-containing commercially available drugs

holds significant potential for a reduction of the byproduct, a reduction in waste production, and lowering of the energy costs. Due to its ability to couple directly with the reaction molecule and bypass thermal conductivity, leading to a rapid rise in the temperature, microwave irradiation has been used to improve many organic syntheses.<sup>[20]</sup> Knoevenagel condensation reactions are carried out by the condensation of aldehyde and the active methylene group using different catalysts such as piperidine,  $\text{InCl}_3$ ,  $\text{TiCl}_4$ ,  $\text{LiOH}$ ,  $\text{ZnCl}_2$ , and  $\text{NbCl}_5$ .<sup>[20,21]</sup> They are also carried out using  $\text{NaAlO}_2$ -promoted mesoporous catalysts,<sup>[22]</sup> ionic liquid,<sup>[23]</sup> monodisperse carbon nanotube-based NiCu nanohybrids,<sup>[24]</sup> and MAOs.<sup>[25]</sup> This is one of the most important methodologies used in synthetic organic chemistry for the formation of a C—C double bond.

From our study, the results demonstrated that green methodologies are less hazardous than classical synthesis methods, as well more efficient and economical and environmentally friendly; short reaction times and excellent yields are observed for those reactions in which conventional heating is replaced by microwave irradiation. Keeping in mind the 12 principles of green chemistry, in continuation of our research work,<sup>[26]</sup> and the advantages of microwave irradiation and activities associated with pyrazole and fluorine, we construct pyrazole and fluorine in one molecular framework as new 3-(trifluoromethyl)-1-(perfluorophenyl)-1*H*-pyrazol-5(4*H*)-one derivatives under conventional, as well as microwave, irradiation and ultrasonication and evaluated their anti-inflammatory and antioxidant activity. In addition to this, we have also performed *in silico* absorption, distribution, metabolism, and excretion (ADME) predictions for the synthesized compounds.

## 2 | RESULTS AND DISCUSSION

### 2.1 | Chemistry

A facile, economic, and green protocol for the cyclocondensation of 2-(perfluorophenyl)-5-(trifluoromethyl)-

2,4-dihydro-3*H*-pyrazol-3-one (**3**) with different aldehydes has been achieved.

The key starting material 3-(trifluoromethyl)-1-(perfluorophenyl)-1*H*-pyrazol-5(4*H*)-one (**3**) was synthesized by the condensation of 1-(perfluorophenyl)hydrazine (**1**) and ethyl 4,4,4-trifluoro-3-oxobutanoate (**2**) in ethanol<sup>[27]</sup> (Scheme 1).

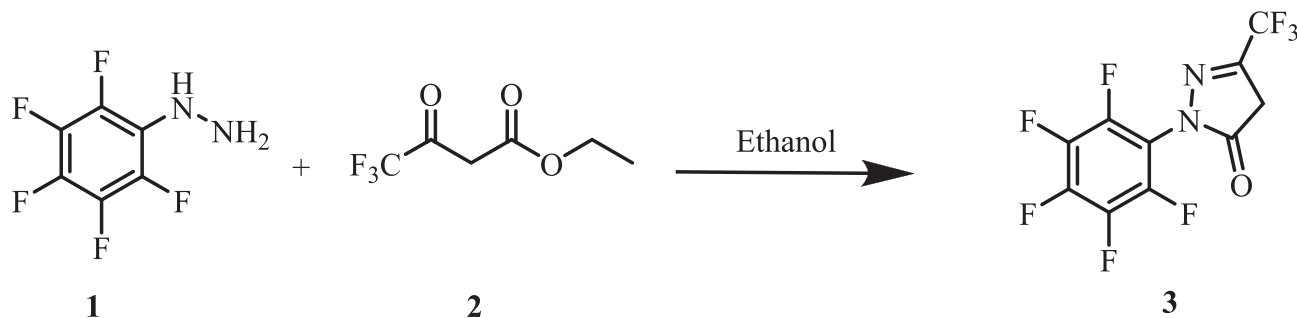
Initially, we carried out the reaction between 2-(perfluorophenyl)-5-(trifluoromethyl)-2,4-dihydro-3*H*-pyrazol-3-one (2 mmol) (**3**) and 1-phenyl-3-(thiophen-2-yl)-1*H*-pyrazole-4-carbaldehyde (2 mmol) refluxed in acetic acid as a model reaction (Scheme 2). Initially, the model reaction was carried out in ethanol without using acetic acid, and it was observed that a very low yield of product (20%) was obtained even after 2 hr. Therefore, improving the yield intervention of the catalyst was thought to be necessary. So, we decided to use acetic acid as a catalyst to promote this transformation at room temperature. At room temperature, the yield of product (45%) was found to be increased in 3 hr, so we decided to provide heating to the reaction mixture to achieve maximum product yield.

When the reaction mixture refluxed in acetic acid, product formation took place after 2 hr, and the yield of the product was 72% (Table 1).

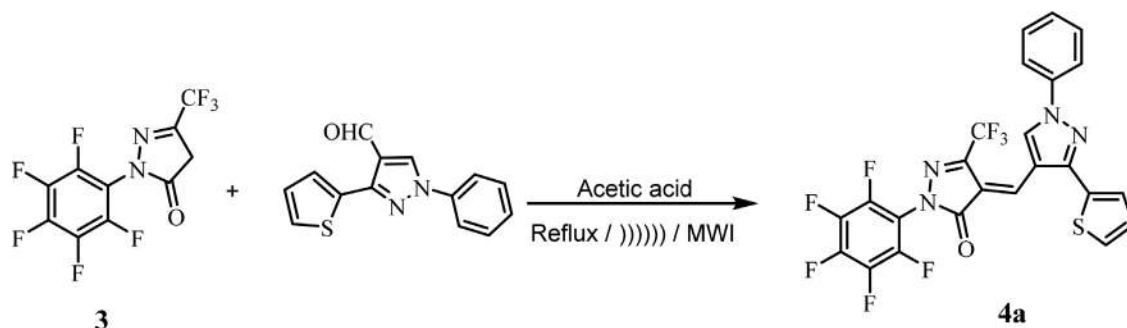
To check the ultrasonication's specific effect on this reaction, under ultrasound irradiation at 35–40°C, we carried out the model reaction using the optimized reaction conditions in hand to check whether the reaction could be accelerated with further improved product yield within a short reaction time (Scheme 2).

It was observed that, under ultrasonic conditions, the conversion rate of a reactant to product increased with less time (Table 1). Thus, when considering the basic green chemistry concept, ultrasonic irradiation was found to have a beneficial effect on the synthesis of Knoevenagel derivatives (**4a-d**, **5a-f**, and **6a-e**), which was superior to the traditional method with respect to yield and reaction time (Table 1).

To accomplish the goal and significance of green chemistry, the model reaction was carried out under



**SCHEME 1** Synthesis of 3-(trifluoromethyl)-1-(perfluorophenyl)-1*H*-pyrazol-5(4*H*)-one **3**



**SCHEME 2** Model reaction for conventional, ultrasonication, and microwave irradiation methods

**TABLE 1** Synthesis of 3-(trifluoromethyl)-1-(perfluorophenyl)-1H-pyrazol-5(4H)-one derivatives (**4a-d**, **5a-f**, and **6a-e**)

Cpd	R <sub>1</sub>	R <sub>2</sub>	R <sub>3</sub>	R <sub>4</sub>	m. p. (°C)	Conventional method <sup>a</sup>		Ultrasound method <sup>b</sup>		Microwave method <sup>c</sup>	
						Time (min)	Yield <sup>d</sup> (%)	Time (min)	Yield <sup>d</sup> (%)	Time (min)	Yield <sup>d</sup> (%)
<b>4a</b>	H	H	-	-	224–226	120	72	20	81	6.5	84
<b>4b</b>	Br	F	-	-	232–234	120	75	18	78	6.5	81
<b>4c</b>	Cl	H	-	-	216–218	120	70	20	76	6.0	80
<b>4d</b>	Br	H	-	-	230–232	120	64	16	70	6.5	76
<b>5a</b>	H	H	OMe	-	202–204	120	70	21	76	5.5	84
<b>5b</b>	H	H	H	-	186–188	120	66	17	72	6.0	80
<b>5c</b>	F	H	OMe	-	180–182	120	68	16	75	7.0	82
<b>5d</b>	H	H	Me	-	206–208	120	65	16	71	6.5	79
<b>5e</b>	H	H	OCF <sub>3</sub>	-	142–144	120	62	18	70	6.5	76
<b>5f</b>	H	Cl	Cl	-	212–214	120	70	19	80	5.5	84
<b>6a</b>	Me	Cl	Me	H	188–190	120	66	18	76	6.0	78
<b>6b</b>	H	Cl	Me	H	180–182	120	62	17	72	7.5	75
<b>6c</b>	H	Cl	H	H	176–178	120	59	18	79	7.0	80
<b>6d</b>	H	Cl	H	Cl	212–214	120	64	20	72	7.0	78
<b>6e</b>	H	H	Me	H	180–182	120	60	18	80	7.5	82

Abbreviation: Cpd, compound.

<sup>a</sup>Reaction conditions: Compound (**3**) (2 mmol) and 1-phenyl-3-(thiophen-2-yl)-1H-pyrazole-4-carbaldehyde (2 mmol) refluxed in acetic acid.

<sup>b</sup>Compound (**3**) (2 mmol) and 1-phenyl-3-(thiophen-2-yl)-1H-pyrazole-4-carbaldehyde (2 mmol) in acetic acid under ultrasound irradiation.

<sup>c</sup>Compound (**3**) (2 mmol) and 1-phenyl-3-(thiophen-2-yl)-1H-pyrazole-4-carbaldehyde (2 mmol) in acetic acid under microwave irradiation.

<sup>d</sup>Isolated yield. m.p.: melting point.

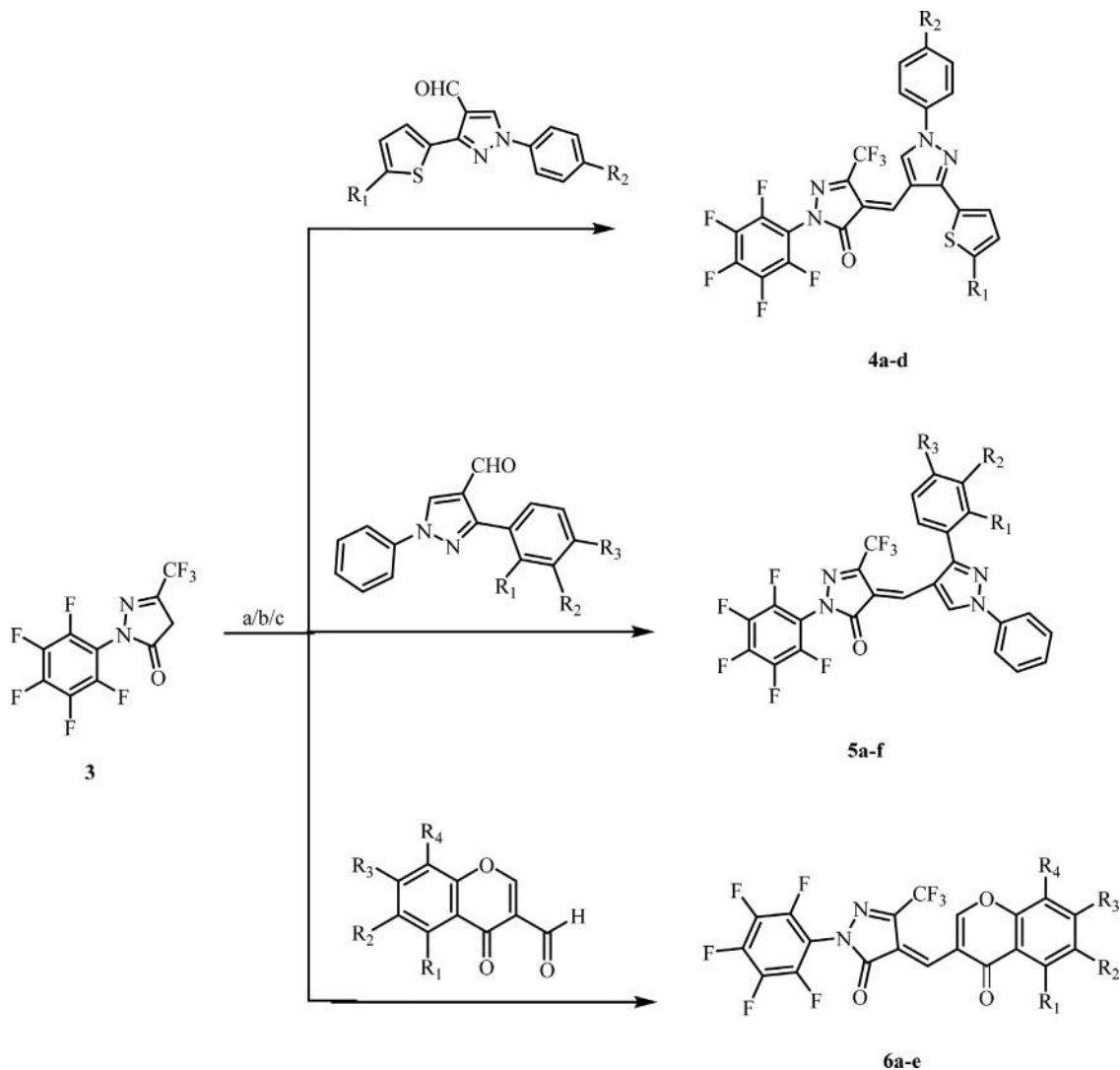
microwave irradiation for a period of time indicated in Table 1 at 350 W (Scheme 2). Fortunately, the product formation occurred in 6.5 min, with an 84% increase in yield.

So, from the above experiments, it can be concluded that, when the reaction was carried out under the conventional method, it gave comparatively low yields of products with longer reaction times, while the same reaction carried out under the influence of ultrasonic irradiation and microwave irradiation gave excellent yields of the products in short reaction times.

Finally, we assessed the scope and generality of this method for the Knoevenagel condensation between 2-(perfluorophenyl)-5-(trifluoromethyl)-2,4-dihydro-3H-pyrazol-3-one (**3**) and different aldehydes (Scheme 3), achieved under conventional and nonconventional methods like the ultrasound and microwave methods, respectively. With respect to the substituent present on the aromatic ring of aldehyde, under the optimized conditions, the corresponding products were obtained in high to excellent yields (Table 1).

More importantly, hetero aryl aldehydes were observed to be well tolerated under optimized conditions,





**SCHEME 3** Synthesis of 3-(trifluoromethyl)-1-(perfluorophenyl)-1H-pyrazol-5(4H)-one derivatives (**4a-d**, **5a-f**, and **6a-e**). Reaction conditions: **a** = Refluxed in acetic acid. **b** = Under ultrasound irradiation in acetic acid. **c** = Under microwave irradiation using acetic acid as a solvent

furnishing the product in good yields. All the synthesized compounds (**4a-d**, **5a-f**, and **6a-e**) were confirmed by IR,  $^1\text{H}$  NMR,  $^{13}\text{C}$  NMR, and mass spectra.

The formation of (4E)-3-(trifluoromethyl)-1-(perfluorophenyl)-4-((1-phenyl-3-(thiophen-2-yl)-1H-pyrazol-4-yl)methylene)-1H-pyrazol-5(4H)-one **4a-d** was confirmed by IR,  $^1\text{H}$  NMR,  $^{13}\text{C}$  NMR, and mass spectra. In the IR spectrum of compound **4a**, the peaks observed at  $1,681\text{ cm}^{-1}$  indicate the presence of C=O group. In the  $^1\text{H}$  NMR spectrum of compound **4a**, two singlets were observed at  $\delta$  8.11 and 10.10 ppm for pyrazolyl and olefinic proton, respectively. The  $^{13}\text{C}$  NMR spectrum of compound **4a** revealed that the peak appearing at  $\delta$  161.4 ppm is due to the presence of carbonyl carbon. The structure of compound **4a** was also confirmed by a molecular ion peak at  $m/z$  555.01 ( $M + \text{H}$ ) $^+$ . Similarly, the

synthesis of (4E)-3-(trifluoromethyl)-1-(perfluorophenyl)-4-((1,3-diphenyl-1H-pyrazol-4-yl)methylene)-1H-pyrazol-5(4H)-ones **5a-f** was also confirmed by spectral techniques. In the IR spectrum of compound **5a**, the peak observed at  $1,701\text{ cm}^{-1}$  corresponded to the C=O group. In the  $^1\text{H}$  NMR spectrum of compound **5a**, the three singlets observed at  $\delta$  3.92, 8.11, and 10.10 ppm confirm the presence of  $-\text{OCH}_3$ , pyrazolyl proton, and olefinic proton, respectively. The  $^{13}\text{C}$  NMR spectrum of compound **5a** showed peaks at  $\delta$  162.5 and 55.5 ppm, confirming the presence of carbonyl carbon and methoxy carbon, respectively. Furthermore, the structure of compound **5a** was also confirmed by a molecular ion peak at  $m/z$  573.21 ( $M + \text{H}$ ) $^+$ .

Furthermore, the formation of (Z)-4-([4-oxo-4H-chromen-3-yl]methylene)-2-(perfluorophenyl)-5-(trifluoromethyl)-2,4-dihydro-3H-pyrazol-3-one **6a-e** was

confirmed by various spectral techniques. The IR spectrum of compound **6a** showed absorption peaks at 1,707 and 1,666  $\text{cm}^{-1}$  corresponding to two carbonyl groups present in the molecules. The  $^1\text{H}$  NMR spectrum of compound **6a** showed four singlets at  $\delta$  2.54 and  $\delta$  3.01 ppm for two  $-\text{CH}_3$ ,  $\delta$  8.50 ppm for chromone ring proton, and  $\delta$  10.54 ppm for olefinic proton. The  $^{13}\text{C}$  NMR spectrum of compound **6a** showed that two signals appear at  $\delta$  175.4 and 164.2 ppm for the carbonyl carbon of chromone and pyrazolone ring, respectively. In addition, two signals for methyl carbon appear at  $\delta$  22.2 and 18.6 ppm. The structure of compound **6a** was also confirmed by mass spectra and by a molecular ion peak observed at  $m/z$  537.11 ( $\text{M} + \text{H}$ ) $^+$ . Similarly, all the synthesized compounds were characterized by the spectral analysis. Structures of all the synthesized derivatives are shown in Figure S1 (Supporting Information).

## 2.2 | Biological activity

### 2.2.1 | Anti-inflammatory activity

The newly synthesized 3-(trifluoromethyl)-1-(perfluorophenyl)-1*H*-pyrazol-5(4*H*)-one derivatives (**4a-d**, **5a-f**, and **6a-e**) ( $\text{EC}_{50}$  range =  $0.6483 \pm 0.221$ – $0.8519 \pm 0.281$   $\mu\text{g}/\text{ml}$ ) exhibited moderate anti-inflammatory activity compared to the standard drug diclofenac sodium. Among all the synthesized compounds, except compounds **4c**, **5c**, **5e**, **6d**, and **6e**, all other compounds exhibited a minimum inhibitory concentration (MIC) of 200  $\mu\text{g}/\text{ml}$  compared to the standard drug diclofenac sodium (Table 2).

The percent inhibition of compounds in the in vitro anti-inflammatory model is shown in Figure 2. Furthermore, the comparative percent inhibition of compounds in the in vitro anti-inflammatory model is shown in Figure 3.

### 2.2.2 | Antioxidant activity

In the present study, antioxidant activity of the synthesized compounds has been assessed in vitro by the DPPH radical scavenging assay.<sup>[28]</sup> Ascorbic acid (AA) has been used as a standard drug for the comparison of antioxidant activity, and the observed results are summarized in Table 2.

According to the DPPH assay, compounds **5a**, **5d**, **5e**, **5f**, **6a**, **6b**, and **6e** ( $\text{IC}_{50}$  = <100  $\mu\text{g}/\text{ml}$ ) exhibited excellent antioxidant activity compared to the standard antioxidant drug AA ( $\text{IC}_{50}$  = <50  $\mu\text{g}/\text{ml}$ ). The remaining synthesized compounds display comparable antioxidant activity than

**TABLE 2** Anti-inflammatory and antioxidant activity of 3-(trifluoromethyl)-1-(perfluorophenyl)-1*H*-pyrazol-5(4*H*)-one derivatives (MIC in  $\mu\text{g}/\text{ml}$ )

Compound	Anti-inflammatory	Antioxidant
<b>4a</b>	200	>100
<b>4b</b>	200	>400
<b>4c</b>	400	>200
<b>4d</b>	200	>200
<b>5a</b>	200	<100
<b>5b</b>	200	>200
<b>5c</b>	NT	NT
<b>5d</b>	200	<100
<b>5e</b>	800	<100
<b>5f</b>	200	<100
<b>6a</b>	200	<100
<b>6b</b>	200	<100
<b>6c</b>	200	>200
<b>6d</b>	800	>100
<b>6e</b>	400	<100
Diclofenac sodium	50	-
Ascorbic acid	-	<50

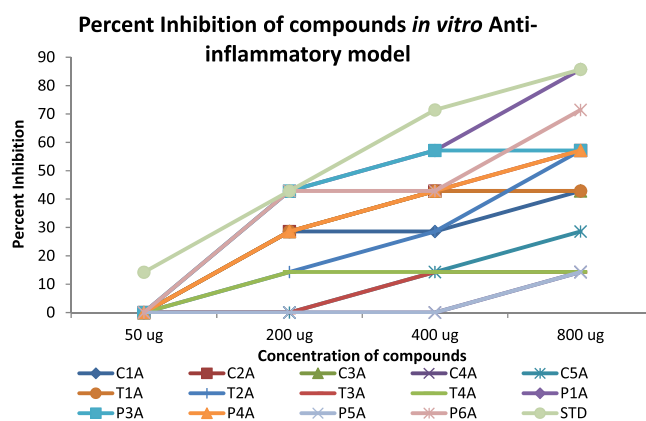


**FIGURE 2** The percent inhibition of compounds in an in vitro anti-inflammatory model

the standard drug butylated hydroxytoluene (Table 2). The percent inhibition of compounds in the in vitro antioxidant model is shown in Figure 4.

## 2.3 | Computational study

### 2.3.1 | In silico ADME

An important task for the lead compounds is early prediction of drug likeness properties as it resolves the cost

**FIGURE 3** The comparative percent inhibition of compounds in an in vitro anti-inflammatory model

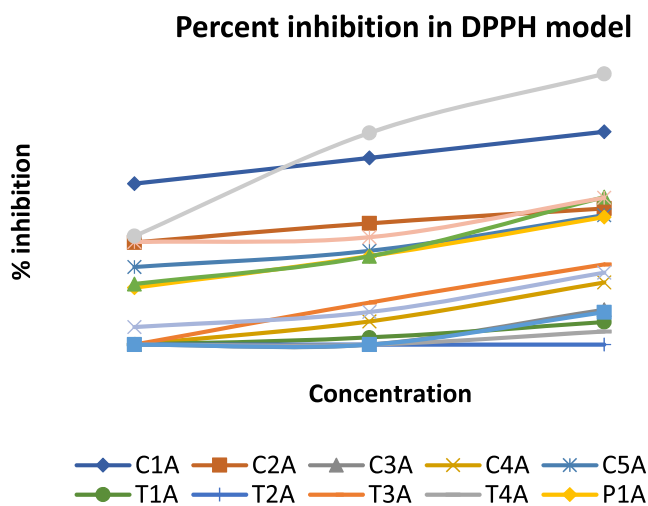
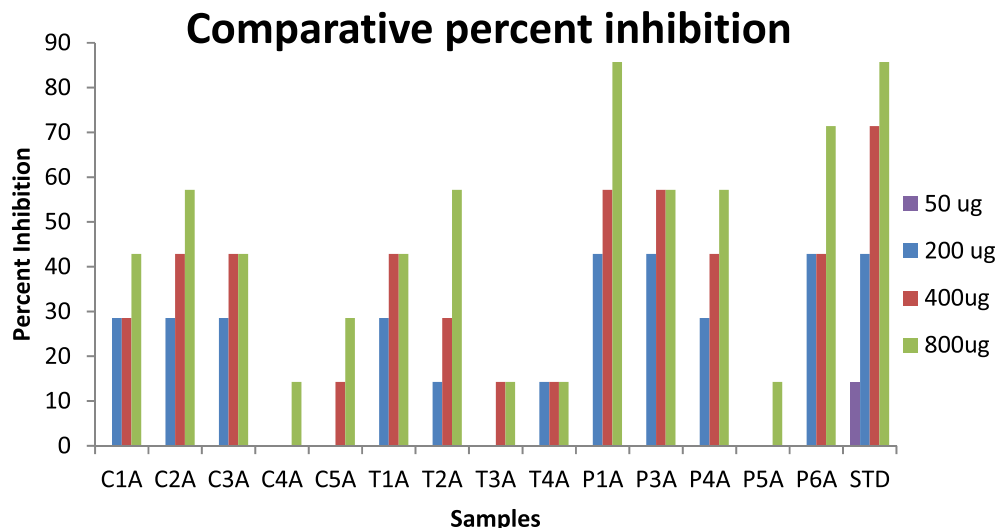


**FIGURE 4** The percent inhibition of compounds in an in vitro antioxidant model

and time issues of drug development and discovery. Due to the inadequate drug likeness properties of many active agents with a significant biological activity, these compounds have failed in clinical trials.<sup>[29]</sup> On the basis of Lipinski's rule of five, the drug likeness properties were analyzed by ADME parameters using the Molinspiration online property calculation toolkit,<sup>[30]</sup> and data are summarized in Table 3.

All the compounds exhibited noteworthy values for the various parameters analyzed and showed good drug-like characteristics based on Lipinski's rule of five and its variants, which characterized these agents to be likely orally active. For the synthesized compound **6e**, the data obtained were within the range of accepted values. Parameters such as the number of rotatable bonds and total polar surface area are linked with the intestinal absorption; results showed that all

synthesized compounds had good absorption. The in silico assessment of all the synthetic compounds has shown that they have very good pharmacokinetic properties, which are reflected in their physicochemical values, thus ultimately enhancing the pharmacological properties of these molecules.

### 3 | EXPERIMENTAL SECTION

All organic solvents were acquired from Poona Chemical Laboratory, Pune and Research-Lab Fine Chem Industries, Mumbai and were used as such without further purification. The melting points were measured on a DBK melting point apparatus and are uncorrected. Microwave irradiation was carried out in Raga's synthetic microwave oven. IR spectra were recorded on Shimadzu IR Affinity 1S (ATR) fourier transform infrared spectrophotometer. <sup>1</sup>H NMR (500 MHz) and <sup>13</sup>C NMR (125 MHz) spectra were recorded on Bruker Advance neo 500 spectrophotometers using tetramethylsilane as an internal standard, and CDCl<sub>3</sub> and dimethyl sulphoxide-*d*<sub>6</sub> as solvent and chemical shifts, respectively, were expressed as  $\delta$  ppm units. Mass spectra were obtained on Waters quadrupole time-of-flight micromass (ESI-MS) mass spectrometer.

#### 3.1 | General procedure for the synthesis of synthesize new 3-(trifluoromethyl)-1-(perfluorophenyl)-1H-pyrazol-5(4H)-one derivatives (4a-d, 5a-f and 6a-e)

**Conventional method:** An equimolar amount of 2-(perfluorophenyl)-5-(trifluoromethyl)-2,4-dihydro-3H-pyrazol-3-

TABLE 3 Pharmacokinetic parameters of (4a-d, 5a-f, and 6a-e) compounds

Entry	% ABS	TPSA (Å <sup>2</sup> )	n- ROTB	MV	MW	miLog P	n- ON	n- OHNH	Lipinski violation	Drug likeness model score
Rule	-	-	-	-	<500	≤5	<10	<5	≤1	-
4a	90.81	52.72	5	397.75	554.42	5.83	5	0	2	-0.68
4b	90.81	52.72	5	420.56	651.31	6.92	5	0	2	-0.84
4c	90.81	52.72	5	411.28	588.87	6.63	5	0	2	-0.25
4d	90.81	52.72	5	415.63	633.32	6.76	5	0	2	-0.56
5a	87.62	61.96	6	432.58	578.42	6.10	6	0	2	-0.46
5b	90.81	52.72	5	407.04	548.39	6.04	5	0	2	-0.80
5c	87.62	61.96	6	437.51	596.41	6.19	6	0	2	-0.22
5d	90.81	52.72	5	423.60	562.42	6.49	5	0	2	-0.51
5e	87.62	61.96	7	447.32	632.39	7.01	6	0	2	-0.45
5f	90.81	52.72	5	434.11	617.28	7.33	5	0	2	-0.36
6a	86.53	65.11	3	374.21	536.76	6.25	5	0	2	-0.53
6b	86.53	65.11	3	357.65	522.74	5.87	5	0	2	-0.36
6c	86.53	65.11	3	341.09	508.71	5.49	5	0	2	-0.32
6d	86.53	65.11	3	354.62	543.15	6.10	5	0	2	-0.93
6e	86.53	65.11	3	344.11	488.29	5.26	5	0	1	-0.81

Abbreviations: % ABS, percentage absorption; TPSA, topological polar surface area; n-ROTB, number of rotatable bonds; MV, molecular volume; MW, molecular weight; miLogP, logarithm of partition coefficient of compound between n-octanol and water; n-ON acceptors, number of hydrogen bond acceptors; n-OHNH donors, number of hydrogen bonds donors.

one (3) (0.002 mol) and substituted aldehydes (0.002 mol) was taken in a round-bottom flask using glacial acetic acid (5 ml) as a solvent and were refluxed for the period of time indicated in Table 1. The progress of the reaction was monitored by thin layer chromatography (TLC). After completion of reaction, the mixture was cooled and poured into ice-cold water. The obtained solid was filtered and washed with water and dried and purified by crystallization from ethyl acetate to obtain pure compounds (4a-d, 5a-f, and 6a-e).

**Ultrasound method:** A mixture of 2-(perfluorophenyl)-5-(trifluoromethyl)-2,4-dihydro-3H-pyrazol-3-one (3) (0.002 mol) and substituted aldehydes (0.002 mol) in acetic acid (5 ml) was taken in a 50-ml round-bottom flask. The mixture was irradiated in the water bath of an ultrasonic cleaner at 35–40°C for a period of time indicated in Table 1. After completion of the reaction (monitored by TLC), the mixture was poured into ice-cold water, and the obtained solid was collected by simple filtration and washed successively with water. The crude product was purified by crystallization from ethyl acetate to obtain pure compounds (4a-d, 5a-f, and 6a-e).

**Microwave irradiation method:** An equimolar amount of 2-(perfluorophenyl)-5-(trifluoromethyl)-

2,4-dihydro-3H-pyrazol-3-one (3) (0.002 mol) and substituted aldehydes (0.002 mol) was taken in a round-bottom flask (RBF) using glacial acetic acid (5 ml) as a solvent, and the contents of RBF were subjected to MW irradiation for the period of time indicated in Table 1 at 350 W. The progress of the reaction was monitored by TLC. After completion of reaction, the mixture was cooled and poured into ice-cold water. The obtained solid was filtered and washed with water and dried and purified by crystallization from ethyl acetate to obtain pure compounds (4a-d, 5a-f, and 6a-e).

### 3.1.1 | (4E)-3-(Trifluoromethyl)-1-(perfluorophenyl)-4-((1-phenyl-3-(thiophen-2-yl)-1H-pyrazol-4-yl)methylene)-1H-pyrazol-5(4H)-one (4a)

Orange solid; Wt. 930 mg, Yield 84%; IR( $\nu_{\max}$ /cm<sup>-1</sup>): 2,926 (=C-H), 1,681 (C=O), 1,598 (C=N), 1,519 (C=C), 1,234 (C-F); <sup>1</sup>H NMR spectrum,  $\delta$ , ppm: 7.35–7.91 (m, 8H, Ar-H), 8.11 (s, 1H, pyrazolyl-H), 10.10 (s, 1H, =C-H); <sup>13</sup>C NMR spectrum,  $\delta_C$ , ppm: 161.4 (C=O), 151.7, 140.1, 137.8, 134.9, 131.1, 130.0, 129.6, 129.1,

128.70, 128.6, 119.7, 115.7, 113.5; MS (ESI-MS):  $m/z$  555.01 (M + H)<sup>+</sup>.

### 3.1.2 | (4E)-4-((3-(5-Bromothiophen-2-yl)-1-(4-fluorophenyl)-1H-pyrazol-4-yl)methylene)-3-(trifluoromethyl)-1-(perfluorophenyl)-1H-pyrazol-5(4H)-one (4b)

Orange solid; Wt. 1.05 g; Yield 81%; IR ( $\nu_{\max}/\text{cm}^{-1}$ ): 2,927 (C–H), 1,680 (C=O), 1,598 (C=N), 1,516 (C=C), 1,231 (C–F); <sup>1</sup>H NMR spectrum,  $\delta$ , ppm: 7.16 (d, 1H,  $J$  = 3.50 Hz, Ar–H), 7.26–7.19 (m, 3H, Ar–H), 7.84 (dd, 2H,  $J$  = 5.00 Hz and 9.00 Hz, Ar–H), 8.10 (s, 1H, pyrazole-H), 10.11 (s, 1H, =C–H); MS:  $m/z$  651.03 (M + H)<sup>+</sup>.

### 3.1.3 | (4E)-4-((3-[5-Chlorothiophen-2-yl]-1-phenyl-1H-pyrazol-4-yl)methylene)-3-(trifluoromethyl)-1-(perfluorophenyl)-1H-pyrazol-5(4H)-one (4c)

Orange solid; Wt. 873 mg; Yield 80%; IR ( $\nu_{\max}/\text{cm}^{-1}$ ): 2,926 (C–H), 1,682 (C=O), 1,597 (C=N), 1,518 (C=C), 1,232 (C–F); <sup>1</sup>H NMR spectrum,  $\delta$ , ppm: 7.07 (s, 1H, Ar–H), 7.26–7.18 (s, 1H, Ar–H), 7.44 (d, 1H,  $J$  = 6.00 Hz, Ar–H), 7.52 (m, 2H, Ar–H), 7.86 (d, 2H,  $J$  = 7.00 Hz, Ar–H), 8.11 (s, 1H, pyrazole-H), 10.16 (s, 1H, =C–H); <sup>13</sup>C NMR spectrum,  $\delta_{\text{C}}$ , ppm: 162.4 (C=O), 151.3, 139.5, 138.3, 135.0, 133.5, 130.8, 130.0, 128.8, 127.6, 127.4, 120.0, 116.3, 114.6; MS:  $m/z$  547.11 (M + H)<sup>+</sup>.

### 3.1.4 | (4E)-4-((3-(5-Bromothiophen-2-yl)-1-phenyl-1H-pyrazol-4-yl)methylene)-3-(trifluoromethyl)-1-(perfluorophenyl)-1H-pyrazol-5(4H)-one (4d)

Orange solid; Wt. 960 mg; Yield 76%; IR ( $\nu_{\max}/\text{cm}^{-1}$ ): 2,926 (C–H), 1,681 (C=O), 1,597 (C=N), 1,520 (C=C), 1,235 (C–F); <sup>1</sup>H NMR spectrum,  $\delta$ , ppm: 7.16 (d, 1H,  $J$  = 4.00 Hz, Ar–H), 7.21 (d, 1H,  $J$  = 3.50 Hz, Ar–H), 7.44 (t, 1H,  $J$  = 7.50 Hz, Ar–H), 7.52 (t, 2H,  $J$  = 7.50 Hz, Ar–H), 7.75–7.86 (d, 2H,  $J$  = 7.50 Hz, Ar–H), 8.47 (s, 1H, pyrazole-H), 10.16 (s, 1H, =C–H); <sup>13</sup>C NMR spectrum,  $\delta_{\text{C}}$ , ppm: 183.2 (C=O), 162.3, 151.2, 143.2, 142.9, 139.4, 138.3, 134.9, 133.7, 133.4, 131.2, 130.6, 129.8, 129.1, 128.8, 128.5, 128.2, 120.6, 119.9, 119.6, 116.2, 115.9, 114.6; MS:  $m/z$  633.05 (M + H).

### 3.1.5 | (4Z)-3-(Trifluoromethyl)-4-((3-[4-methoxyphenyl]-1-phenyl-1H-pyrazol-4-yl)methylene)-1-(perfluorophenyl)-1H-pyrazol-5(4H)-one (5a)

Orange solid; Wt. 971 mg; Yield 84%; IR ( $\nu_{\max}/\text{cm}^{-1}$ ): 3,141 (C–H), 1,703 (C=O), 1,595 (C=N), 1,514 (C=C), 1,224 (C–F); <sup>1</sup>H NMR spectrum,  $\delta$ , ppm: 3.92 (s, 3H, –OCH<sub>3</sub>), 7.10 (d, 2H,  $J$  = 8.50 Hz, Ar–H), 7.51 (t, 2H,  $J$  = 8.50 Hz, Ar–H), 7.62 (d, 2H,  $J$  = 8.50 Hz, Ar–H), 7.90 (d, 2H,  $J$  = 9.00 Hz, Ar–H), 7.99 (s, 1H, pyrazole-H), 10.19 (s, 1H, =C–H); <sup>13</sup>C NMR spectrum,  $\delta_{\text{C}}$ , ppm: 162.5 (C=O), 161.1, 158.7, 143.3, 141.4, 138.6, 134.9, 130.7, 129.7, 128.5, 122.6, 120.1, 116.8, 114.7, 113.7, 55.5 (OCH<sub>3</sub>); MS:  $m/z$  579.21 (M + H)<sup>+</sup>.

### 3.1.6 | (4Z)-3-(Trifluoromethyl)-1-(perfluorophenyl)-4-([1,3-diphenyl-1H-pyrazol-4-yl)methylene)-1H-pyrazol-5(4H)-one (5b)

Orange solid; Wt. 876 mg; Yield 80%; IR ( $\nu_{\max}/\text{cm}^{-1}$ ): 3,142 (C–H), 1,701 (C=O), 1,595 (C=N), 1,510 (C=C), 1,223 (C–F); <sup>1</sup>H NMR spectrum,  $\delta$ , ppm: 7.42 (m, 1H, Ar–H), 7.52 (t, 2H,  $J$  = 7.50 Hz, Ar–H), 7.57–7.58 (m, 3H, Ar–H), 7.68 (dd, 2H,  $J$  = 7.50 and 2.00 Hz, Ar–H), 7.90 (d, 2H,  $J$  = 8.00 Hz, Ar–H), 8.00 (s, 1H, pyrazole-H), 10.22 (s, 1H, =C–H); <sup>13</sup>C NMR spectrum,  $\delta_{\text{C}}$ , ppm: 162.5 (C=O), 158.8, 143.0, 141.2, 138.6, 134.9, 130.3, 129.9, 129.7, 129.4, 129.2, 128.6, 120.0, 116.8, 114.0; MS:  $m/z$  549.19 (M + H)<sup>+</sup>.

### 3.1.7 | (4Z)-4-((3-[2-Fluoro-4-methoxyphenyl]-1-phenyl-1H-pyrazol-4-yl)methylene)-3-(trifluoromethyl)-1-(perfluorophenyl)-1H-pyrazol-5(4H)-one (5c)

Orange solid; Wt. 1.06 g; Yield 82%; IR ( $\nu_{\max}/\text{cm}^{-1}$ ): 3,145 (C–H), 1,702 (C=O), 1,596 (C=N), 1,512 (C=C), 1,221 (C–F); <sup>1</sup>H NMR spectrum,  $\delta$ , ppm: 3.91 (s, 3H, –OCH<sub>3</sub>), 6.82 (dd, 1H,  $J$  = 2.50 and 12.00 Hz, Ar–H), 6.91 (dd, 1H,  $J$  = 2.00 and 8.50 Hz, Ar–H), 7.42 (t, 1H,  $J$  = 7.50 Hz, Ar–H), 7.58–7.49 (m, 2H, Ar–H), 7.79 (d, 1H,  $J$  = 2.50 Hz, Ar–H), 7.88 (d, 2H,  $J$  = 7.50 Hz, Ar–H), 8.52 (s, 1H, pyrazole-H), 10.20 (s, 1H, =C–H); <sup>13</sup>C NMR spectrum,  $\delta_{\text{C}}$ , ppm: 162.7 (C=O), 162.6, 162.5, 154.1, 141.2, 138.6, 134.7, 132.5, 129.7, 128.5, 120.0, 117.6, 113.9, 111.2, 110.3, 102.2, 102.0, 55.8 (OCH<sub>3</sub>); MS:  $m/z$  653.26 (M + H)<sup>+</sup>.



### 3.1.8 | (4Z)-3-(Trifluoromethyl)-1-(perfluorophenyl)-4-([1-phenyl-3-p-tolyl-1H-pyrazol-4-yl]methylene)-1H-pyrazol-5(4H)-one (5d)

Orange solid; Wt. 887 mg; Yield 79%; IR ( $\nu_{\max}/\text{cm}^{-1}$ ): 3,143 (=C–H), 1,701 (C=O), 1,594 (C=N), 1,511 (C=C), 1,220 (C–F);  $^1\text{H}$  NMR spectrum,  $\delta$ , ppm: 2.44 (s, 3H, –CH<sub>3</sub>), 7.45 (d, 1H,  $J = 7.50$  Hz, Ar–H), 7.51 (t, 1H,  $J = 7.50$  Hz, Ar–H), 7.62 (d, 1H,  $J = 8.00$  Hz, Ar–H), 7.65 (d, 1H,  $J = 8.00$  Hz, Ar–H), 9.90 (s, 1H, pyrazole-H), 11.96 (s, 1H, =C–H); MS:  $m/z$  563.08 (M + H)<sup>+</sup>.

### 3.1.9 | (4Z)-3-(Trifluoromethyl)-1-(perfluorophenyl)-4-((1-phenyl-3-(4-[trifluoro methoxy]phenyl)-1H-pyrazol-4-yl)methylene)-1H-pyrazol-5(4H)-one (5e)

Orange solid; Wt. 960 mg; Yield 76%; IR ( $\nu_{\max}/\text{cm}^{-1}$ ): 3,145 (=C–H), 1,700 (C=O), 1,595 (C=N), 1,517 (C=C), 1,225 (C–F);  $^1\text{H}$  NMR spectrum,  $\delta$ , ppm: 7.42–7.44 (m, 3H, Ar–H), 7.51–7.54 (m, 2H, Ar–H), 7.71 (d, 1H,  $J = 2.00$  Hz, Ar–H), 7.73 (d, 1H,  $J = 2.00$  Hz, Ar–H), 7.88 (d, 1H,  $J = 2.00$  Hz, Ar–H), 7.90 (d, 1H,  $J = 3.50$  Hz, Ar–H), 7.92 (s, 1H, pyrazole-H), 10.21 (s, 1H, =C–H);  $^{13}\text{C}$  NMR spectrum,  $\delta_{\text{C}}$ , ppm: 162.4 (C=O), 157.3, 150.5, 143.2, 142.9, 140.3, 138.5, 134.9, 130.9, 129.8, 129.0, 128.7, 121.5, 120.6, 120.0, 118.4, 116.6, 114.4; MS:  $m/z$  633.23 (M + H)<sup>+</sup>.

### 3.1.10 | (4Z)-4-((3-[3,4-Dichlorophenyl]-1-phenyl-1H-pyrazol-4-yl)methylene)-3-(trifluoromethyl)-1-(perfluorophenyl)-1H-pyrazol-5(4H)-one (5f)

Orange solid; Wt. 1.03 g; Yield 84%; IR ( $\nu_{\max}/\text{cm}^{-1}$ ): 3,144 (=C–H), 1,701 (C=O), 1,596 (C=N), 1,517 (C=C), 1,227 (C–F);  $^1\text{H}$  NMR spectrum,  $\delta$ , ppm: 7.44 (m, 1H, Ar–H), 7.48 (d, 1H,  $J = 2.00$  Hz, Ar–H), 7.50 (d, 1H,  $J = 2.00$  Hz, Ar–H), 7.53 (d, 1H,  $J = 7.50$  Hz, Ar–H), 7.67 (d, 1H,  $J = 8.50$  Hz, Ar–H), 7.83 (d, 1H,  $J = 2.00$  Hz, Ar–H), 7.87–7.89 (m, 2H, Ar–H), 7.89 (s, 1H, pyrazole-H), 10.18 (s, 1H, =C–H);  $^{13}\text{C}$  NMR spectrum,  $\delta_{\text{C}}$ , ppm: 162.3 (C=O), 156.1, 143.2, 142.9, 139.7, 138.4, 135.0, 134.5, 133.7, 131.2, 131.1, 130.3, 129.8, 128.8, 128.3, 120.0, 116.4, 114.7; MS:  $m/z$  617.15 (M + H)<sup>+</sup>.

### 3.1.11 | (Z)-4-([6-Chloro-5,7-dimethyl-4-oxo-4H-chromen-3-yl]methylene)-2-(perfluorophenyl)-5-(trifluoromethyl)-2,4-dihydro-3H-pyrazol-3-one (6a)

Orange solid; Wt. 900 mg; Yield 84%; IR ( $\nu_{\max}/\text{cm}^{-1}$ ): 3,074 (=C–H), 1,707 (C=O), 1,666 (C=O), 1,624 (C=N), 1,508 (C=C), 1,192 (C–F);  $^1\text{H}$  NMR spectrum,  $\delta$ , ppm: 2.54 (s, 3H, –CH<sub>3</sub>), 3.01 (s, 3H, –CH<sub>3</sub>), 7.26 (s, 1H, Ar–H), 8.50 (s, 1H, chromone-H), 10.54 (s, 1H, =C–H);  $^{13}\text{C}$  NMR spectrum,  $\delta_{\text{C}}$ , ppm: 175.4 (C=O), 164.2 (C=O), 162.3, 155.1, 144.5, 143.4, 143.3, 139.7, 134.7, 120.9, 120.2, 119.4, 118.3, 118.2, 118.1, 22.2 (–CH<sub>3</sub>), 18.6 (–CH<sub>3</sub>); MS:  $m/z$  537.11 (M + H)<sup>+</sup>.

### 3.1.12 | (Z)-4-([6-Chloro-7-methyl-4-oxo-4H-chromen-3-yl]methylene)-2-(perfluorophenyl)-5-(trifluoromethyl)-2,4-dihydro-3H-pyrazol-3-one (6b)

Orange solid; Wt. 783 mg; Yield 75%; IR ( $\nu_{\max}/\text{cm}^{-1}$ ): 3,076 (=C–H), 1,705 (C=O), 1,664 (C=O), 1,627 (C=N), 1,508 (C=C), 1,192 (C–F);  $^1\text{H}$  NMR spectrum,  $\delta$ , ppm: 2.54 (s, 3H, –CH<sub>3</sub>), 7.47 (s, 1H, Ar–H), 8.24 (s, 1H, Ar–H), 8.48 (s, 1H, chromone-H), 10.62 (s, 1H, =C–H); MS:  $m/z$  523.08 (M + H)<sup>+</sup>.

### 3.1.13 | (Z)-4-([6-Chloro-4-oxo-4H-chromen-3-yl]methylene)-2-(perfluorophenyl)-5-(trifluoromethyl)-2,4-dihydro-3H-pyrazol-3-one (6c)

Orange solid; Wt. 812 mg; Yield 80%; IR ( $\nu_{\max}/\text{cm}^{-1}$ ): 3,074 (=C–H), 1,707 (C=O), 1,662 (C=O), 1,621 (C=N), 1,509 (C=C), 1,193 (C–F);  $^1\text{H}$  NMR spectrum,  $\delta$ , ppm: 7.55 (d, 1H,  $J = 9.00$  Hz, Ar–H), 7.73 (d, 1H,  $J = 2.50$  and 9.00 Hz, Ar–H), 8.26 (d, 1H,  $J = 2.50$  Hz, Ar–H), 8.47 (s, 1H, chromone-H), 10.63 (s, 1H, =C–H); MS:  $m/z$  509.08 (M + H)<sup>+</sup>.

### 3.1.14 | (Z)-4-([6,8-Dichloro-4-oxo-4H-chromen-3-yl]methylene)-2-(perfluorophenyl)-5-(trifluoromethyl)-2,4-dihydro-3H-pyrazol-3-one (6d)

Orange solid; Wt. 845 mg; Yield 78%; IR ( $\nu_{\max}/\text{cm}^{-1}$ ): 3,078 (=C–H), 1,707 (C=O), 1,665 (C=O), 1,626 (C=N), 1,506 (C=C), 1,194 (C–F);  $^1\text{H}$  NMR spectrum,  $\delta$ , ppm: 7.83 (d, 1H,  $J = 2.50$  Hz, Ar–H), 8.17 (d, 1H,  $J = 2.50$  Hz, Ar–H), 8.40 (s, 1H, chromone-H), 10.66 (s, 1H, =C–H); MS:  $m/z$  543.07 (M + H)<sup>+</sup>.

### 3.1.15 | (Z)-4-([7-Methyl-4-oxo-4H-chromen-3-yl]methylene)-2-(perfluorophenyl)-5-(trifluoromethyl)-2,4-dihydro-3H-pyrazol-3-one (6e)

Orange solid; Wt. 800 mg; Yield 82%; IR ( $\nu_{\max}/\text{cm}^{-1}$ ): 3,076 (=C–H), 1,703 (C=O), 1,666 (C=O), 1,627 (C=N), 1,510 (C=C), 1,193 (C–F);  $^1\text{H}$  NMR spectrum,  $\delta$ , ppm: 2.51 (s, 3H, –CH<sub>3</sub>), 7.48 (d, 1H,  $J = 8.00$  Hz, Ar–H), 7.60 (dd, 1H,  $J = 8.00$  and 2.00 Hz, Ar–H), 8.08 (d, 1H,  $J = 1.50$  Hz), 8.54 (s, 1H, chromone-H), 10.64 (s, 1H, =C–H);  $^{13}\text{C}$  NMR spectrum,  $\delta_{\text{C}}$ , ppm: 174.5 (C=O), 165.5 (C=O), 162.4, 154.2, 143.4, 142.4, 137.5, 136.3, 126.2, 120.9, 123.3, 120.2, 118.6, 118.5, 118.2, 118.1, 21.1 (–CH<sub>3</sub>); MS:  $m/z$  489.14 (M + H)<sup>+</sup>.

## 3.2 | Anti-inflammatory activity

All the synthesized compounds were screened for their in vitro anti-inflammatory activities against the standard drug diclofenac sodium. The minimum inhibitory concentration was determined by the well diffusion method at 1 mg/ml of concentration. (Table 2). A volume of 1 ml of diclofenac sodium at different concentrations (50, 100, 200, 400, 800, and 1,000  $\mu\text{g}/\text{ml}$ ) was homogenized with 1 ml of aqueous solution of bovine serum albumin (5%) and incubated at 27°C for 15 minutes. The mixture of distilled water and bismuth sulphite agar constituted the control tube. Denaturation of the proteins was caused by placing the mixture in a water bath for 10 minutes at 70°C. The mixture was cooled within the ambient room temperature, and the activity of each mixture was measured at 255 nm. Each test was conducted thrice. The following formula was used to calculate inhibition percentage:

$$\% \text{inhibition} = \frac{\text{absorbance of control} - \text{absorbance of sample}}{\text{absorbance of control}} \times 100.$$

## 3.3 | In silico ADME

In the present study, we have calculated molecular volume (MV), molecular weight (MW), logarithm of partition coefficient (miLog  $P$ ), number of hydrogen bond acceptors (n-ON), number of hydrogen bonds donors (n-OHNH), topological polar surface area (TPSA), number of rotatable bonds (n-ROTB), and Lipinski's rule of five<sup>[31]</sup> using the Molinspiration online property calculation toolkit.<sup>[30]</sup> Absorption (% ABS) was calculated by: %

ABS = 109 – (0.345 × TPSA).<sup>[32]</sup> Drug likeness model score (a collective property of physicochemical properties, pharmacokinetics, and pharmacodynamics of a compound that is represented by a numerical value) was computed by MolSoft software.<sup>[33]</sup>

## 4 | CONCLUSIONS

In conclusion, we have constructed pyrazole and fluorine in one molecular framework as new 3-(trifluoromethyl)-1-(perfluorophenyl)-1H-pyrazol-5(4H)-one derivatives under conventional and nonconventional methods like microwave irradiation and ultrasonication, respectively, via Knoevenagel condensation and evaluated their biological activity. Ultrasonication and microwave irradiation can shorten the reaction time from a few hours to a few minutes and increases the product yield (74–84%) compared to the conventional method (59–75%). The synthesized compounds exhibited promising anti-inflammatory activity compared to the standard drug diclofenac sodium. Similarly, the synthesized compound displayed promising antioxidant activity compared to the standard drug. Furthermore, an analysis of the ADME parameters for synthesized compounds showed good drug-like properties and can be developed as an oral drug candidate, thus suggesting that compounds from the present series can be further optimized and developed as a lead molecule.

## ACKNOWLEDGMENT

The authors are thankful to the Department of Science and Technology, New Delhi for providing research facilities under FIST scheme and to CIF, Savitribai Phule Pune University, Pune and SAIF, Panjab University, Chandigarh for providing spectral facilities.

## CONFLICT OF INTEREST

The authors declare no conflict of interest, financial or otherwise.

## REFERENCES

- [1] M. Bhat, G. K. Nagaraja, R. Kayarmar, S. K. Peethamber, M. Shefeeulla, *RSC Adv.* **2016**, 6, 59375.
- [2] A. L. Luz, C. D. Kassotis, H. M. Stapleton, J. N. Meyer, *Toxicology* **2018**, 393, 150.
- [3] P. Khloya, S. Kumar, P. Kaushik, P. Surain, D. Kaushik, P. K. Sharma, *Bioorg. Med. Chem. Lett.* **2015**, 25, 1177.
- [4] (a) Y. R. Li, C. Li, J. C. Liu, M. Guo, T. Y. Zhang, L. P. Sun, C. J. Zheng, H. R. Piao, *Bioorg. Med. Chem. Lett.* **2015**, 25, 5052. (b) S. A. Ali, S. M. Awad, A. M. Said, S. Mahgouba, H. Tahaa, N. M. Ahmed, *J. Enzyme Inhib. Med. Chem.* **2020**, 35, 847.
- [5] X. L. Deng, J. Xie, Y. Q. Li, D. K. Yuan, X. P. Hu, L. Zhang, Q. M. Wang, M. Chi, X. L. Yang, *Chin. Chem. Lett.* **2016**, 27, 566.

- [6] H. Jia, F. Bai, N. Liu, X. Liang, P. Zhan, C. Ma, X. Jiang, X. Liu, *Eur. J. Med. Chem.* **2016**, *123*, 202.
- [7] C. I. Nieto, M. P. Cabildo, M. P. Cornago, D. Sanz, R. M. Claramunt, I. Alkorta, J. Elguero, J. A. Garcia, A. Lopez, D. A. Castroviejo, *J. Mol. Struct.* **2015**, *1100*, 518.
- [8] S. Shu, X. Cai, J. Li, Y. Feng, A. Dai, J. Wang, D. Yang, M. W. Wang, H. Liu, *Bioorg. Med. Chem.* **2016**, *24*, 2852.
- [9] R. Dummer, P. A. Ascierto, H. J. Gogas, A. Arance, M. Mandala, G. Liskay, C. Garbe, D. Schandendorf, L. Krajsova, R. Gutzmer, V. C. Sileni, C. Dutriaux, J. W. Groot, N. Yamazaki, C. Loquai, L. A. M. D. Parseval, M. D. Pickard, V. Sandor, C. Robert, K. T. Flaherty, *Lancet Oncol.* **2018**, *19*, 6035.
- [10] E. Therrien, G. Larouche, N. Nguyen, J. Rahil, A. M. Lemieux, Z. Li, M. Fournel, T. P. Yan, A. J. Landry, S. Lefebvre, J. J. Wang, K. Macbeth, C. Heise, A. Nguyen, J. M. Besterman, R. Deziel, A. Wahhab, *Bioorg. Med. Chem. Lett.* **2015**, *25*, 2514.
- [11] X. H. Lv, Q. S. Li, Z. L. Ren, M. J. Chu, J. Sun, X. Zhang, M. Xing, H. L. Zhu, H. Q. Cao, *Eur. J. Med. Chem.* **2016**, *108*, 586.
- [12] M. A. Tabrizi, P. G. Baraldi, E. Ruggiero, G. Saponaro, S. Baraldi, R. Romagnoli, A. Martinelli, T. Tuccinardi, *Eur. J. Med. Chem.* **2015**, *97*, 289.
- [13] E. Kick, R. Martin, Y. Xie, B. Flatt, E. Schweiger, T. L. Wang, B. Busch, M. Nyman, X. H. Gu, G. Yan, B. Wagner, M. Nanao, L. Nguyen, T. Stout, A. Plonowski, I. Schulman, J. Ostrowski, T. Kirchgessner, R. Wexler, R. Mohan, *Bioorg. Med. Chem. Lett.* **2015**, *25*, 372.
- [14] a) K. Muller, C. Faeh, F. Diederich, *Science* **2007**, *317*, 1881. b) W. K. Hagmann, *J. Med. Chem.* **2008**, *51*, 4359. c) R. E. Banks, B. E. Smart, J. C. Tatlow, *Organo Fluorine Chemistry. Principles and Commercial Applications*, Plenum, New York **1994**. d) S. Purser, P. R. Moore, S. Swallow, V. Gouverneur, *Chem. Soc. Rev.* **2008**, *37*, 320. e) P. Jeschke, *ChemBioChem* **2004**, *5*, 570.
- [15] a) D. O'Hagan, *Chem. Soc. Rev.* **2008**, *37*, 308. b) H. J. Bohm, D. Banner, S. Bendels, M. Kansy, B. Kuhn, K. Muller, U. ObstSander, M. Stahl, *ChemBioChem* **2004**, *5*, 637. (c) P. Nagender, D. Pulakesh, G. Gouverneur, N. Shibata, *Org. Lett.* **2018**, *20*, 1526. (d) D. Pulakesh, G. Satoshi, P. Nagender, U. Hiroto, T. Etsuko, N. Shibata, *Chem. Sci.* **2018**, *9*, 3276. (e) P. Nagender, S. Takuya, K. Mikhail, T. Etsuko, S. Yuji, N. Shibata, *Chem. Commun.* **2018**, *54*, 4294. (f) D. K. Swaroop, N. Ravi Kumar, P. Nagender, G. Jitender Dev, N. Jagadeesh Babu, B. Narsaiah, *Eur. J. Org. Chem.* **2019**, *2019*, 3654. <https://doi.org/10.1002/ejoc.201900482>. (g) P. Nagender, H. Kyosuke, N. Shibata, *Chem. Commun.* **2018**, *54*, 7171.
- [16] (a) I. I. Gerus, R. X. Mironetz, I. S. Kondratov, A. V. Bezdudny, Y. V. Dmytriv, O. V. Shishkin, V. S. Starova, O. A. Zaporozhets, A. A. Tolmachev, P. K. Mykhailiuk, *J. Org. Chem.* **2012**, *77*, 47. (b) B. D. Maxwell, *J. Labell. Compd. Radiopharm.* **2000**, *43*, 645.
- [17] T. G. Leighton, *The acoustic bubble*, Academic Press, London **1994**, p. 531.
- [18] C. O. Kappe, A. Stadler, D. Dallinger, *Microwaves in Organic and Medicinal Chemistry*, 2nd ed., Wiley-VCH, Weinheim **2012**.
- [19] (a) A. S. William, F. B. Aleksel, C. Ron, Organic synthesis: The science behind art. in *Royal Society of Chemistry (Great Britain)*, RSC publications, Cambridge, **1998**. (b) *Organic Synthesis Co. II vol*; **1935**. (c) *Comprehensive Organic Synthesis Book Volumes*, John Wiley & Sons, Hoboken, NJ, **1991**.
- [20] (a) T. Syed, A. Yahya, J. A. Alsheri, *Lett. Org. Chem.* **2020**, *17*, 157. (b) S. Mallouk, K. Bougrin, A. Laghzizil, R. Benhida, *Molecules* **2010**, *15*, 813. (c) J. S. Biradar, B. S. Sasidhar, *Eur. J. Med. Chem.* **2011**, *46*, 6112. (d) M. B. Ansari, H. Jin, M. N. Parvin, S. E. Park, *Catal. Today* **2012**, *185*, 211.
- [21] (a) M. A. Pasha, K. Manjula, J. Saudi, *Chem. Soc.* **2011**, *15*, 283. (b) Y. Ogiwara, K. Takahashi, T. Kitazawa, N. Sakai, *J. Org. Chem.* **2015**, *80*, 3101. (c) P. Leelavathi, S. R. Kumar, *J. Mol. Catal. A Chem.* **2005**, *240*, 99. (d) J. V. Schijndel, A. C. Luiz, D. Molendijk, J. Meuldijk, *Green Chem. Lett. Rev.* **2017**, *10*, 404.
- [22] S. Ramesh, F. Devred, D. P. Debecker, *ChemistrySelect* **2020**, *5*, 300.
- [23] R. B. Ardakani, N. Safaeian, M. Oftadeh, M. F. Mehrjardi, *Theor. Chem. Acc.* **2020**, *139*, 45.
- [24] N. Zengin, H. Burhan, A. Savk, H. Goksu, F. Sen, *Scie. Rep.* **2020**, *10*, 12758.
- [25] A. R. Bhat, M. H. Najjar, R. S. Dongre, M. S. Akhter, *Res. Green Sust. Chem.*, **2020**, *3*, 100008. <https://doi.org/10.1016/j.jrgsc.2020.06.001>.
- [26] (a) K. S. Hon, H. N. Akolkar, B. K. Karale, *J. Het. Chem.* **2020**, *57*, 1692. (b) S. P. Kunde, K. G. Kanade, B. K. Karale, H. N. Akolkar, S. S. Arbuj, P. V. Randhavane, S. T. Shinde, M. H. Shaikh, A. K. Kulkarni, *RSC Adv.* **2020**, *10*, 26997. (c) S. J. Takate, A. D. Shinde, B. K. Karale, H. Akolkar, L. Nawale, D. Sarkar, P. C. Mhaske, *Bioorg. Med. Chem. Lett.* **2019**, *29*, 1999. (d) S. P. Kunde, K. G. Kanade, B. K. Karale, H. N. Akolkar, P. V. Randhavane, S. T. Shinde, *Res. Chem. Intermed.* **2017**, *43*, 7277. (e) R. S. Endait, B. K. Karale, H. N. Akolkar, P. V. Randhavane, *Indian J. Het. Chem.* **2016**, *26*, 141.
- [27] B. S. Furniss, A. J. Hannaford, P. W. G. Smith, A. R. Tatchell, *Vogel's Text Book of Practical Organic Chemistry*, 5th ed., Addison Wesley Longman Limited, England **1998**.
- [28] S. Kandia, A. L. Charles, *Food Chem.* **2019**, *287*, 338.
- [29] S. Zhang, Y. Luo, L. Q. He, Z. J. Liu, A. Q. Jiang, Y. H. Yang, H. L. Zhu, *Bioorg. Med. Chem.* **2013**, *21*, 3723.
- [30] Molinspiration Chemoinformatics Brastislava, Slovak Republic. <http://www.molinspiration.com/cgi-bin/properties>; **2014**.
- [31] C. A. Lipinski, L. Lombardo, B. W. Dominy, P. J. Feeney, *Adv. Drug Del. Rev.* **2001**, *46*, 3.
- [32] Y. Zhao, M. H. Abraham, J. Lee, A. Hersey, N. C. Luscombe, G. Beck, B. Sherborne, I. Cooper, *Pharm. Res.* **2002**, *19*, 1446.
- [33] Drug-Likeness and Molecular Property Prediction. <http://www.molsoft.com/mprop/>.

## SUPPORTING INFORMATION

Additional supporting information may be found online in the Supporting Information section at the end of this article.

**How to cite this article:** Dengale SG, Akolkar HN, Karale BK, et al. Synthesis of 3-(trifluoromethyl)-1-(perfluorophenyl)-1H-pyrazol-5 (4H)-one derivatives via Knoevenagel condensation and their biological evaluation. *J Chin Chem Soc.* 2020;1–12. <https://doi.org/10.1002/jccs.202000357>

# Microwave Assisted Synthesis and Antibacterial Activity of New 1,3,4-Thiadiazoles and 1,2,4-Triazoles Derived from 2-{2-[2-(4-Fluorophenyl)-4-methylthiazol-5-yl]-1*H*-benzo[*d*]imidazol-1-yl}acetohydrazide

N. R. Darekar<sup>a,b</sup>, B. K. Karale<sup>a</sup>, H. N. Akolkar<sup>a</sup>, and A. S. Burungale<sup>b,\*</sup>

<sup>a</sup> P.G. and Research, Department of Chemistry, Rayat Shikshan Sanstha's Radhabai Kale Mahila Mahavidyalaya, Maharashtra, Ahmednagar, 414001 India

<sup>b</sup> P.G. and Research, Department of Chemistry, Rayat Shikshan Sanstha's S. M. Joshi College, Hadapsar, Maharashtra, Pune, 411028 India

\*e-mail: hemantakolkar@gmail.com

Received July 7, 2020; revised August 18, 2020; accepted August 31, 2020

**Abstract**—A series of novel derivatives of 1-(2-{2-[2-(4-fluorophenyl)-4-methylthiazol-5-yl]-1*H*-benzo[*d*]imidazol-1-yl}acetyl)-4-phenylthiosemicarbazide, 5-({2-[2-(4-fluorophenyl)-4-methylthiazol-5-yl]-1*H*-benzo[*d*]imidazol-1-yl}methyl)-4-phenyl-4*H*-1,2,4-triazole-3-thiol and 5-({2-[2-(4-fluorophenyl)-4-methylthiazol-5-yl]-1*H*-benzo[*d*]imidazol-1-yl}methyl)-*N*-phenyl-1,3,4-thiadiazol-2-amine have been synthesized by the conventional method as well as using MW irradiation. All newly synthesized compounds have been tested for antibacterial activity. Several products have demonstrated moderate activity against gram positive and gram negative bacterial strains.

**Keywords:** 1,3,4-thiadiazole, 1,2,4-triazole, microwave irradiation, antibacterial activity

**DOI:** 10.1134/S1070363220090200

Antimycobacterial and antimicrobial activities have been well established and studied in depth for benzimidazole [1, 2], thiazole [3, 4], 1,3,4-thiadiazole [5–7], and 1,2,4-triazole [8, 9] derivatives.

Pharmacological importance associated with those compounds inspired us to synthesize novel benzimidazole and thiazole containing 1,3,4-thiadiazoles and 1,2,4-triazoles under conventional and MW irradiation. All newly synthesized compounds were evaluated for their antibacterial activity.

## RESULTS AND DISCUSSION

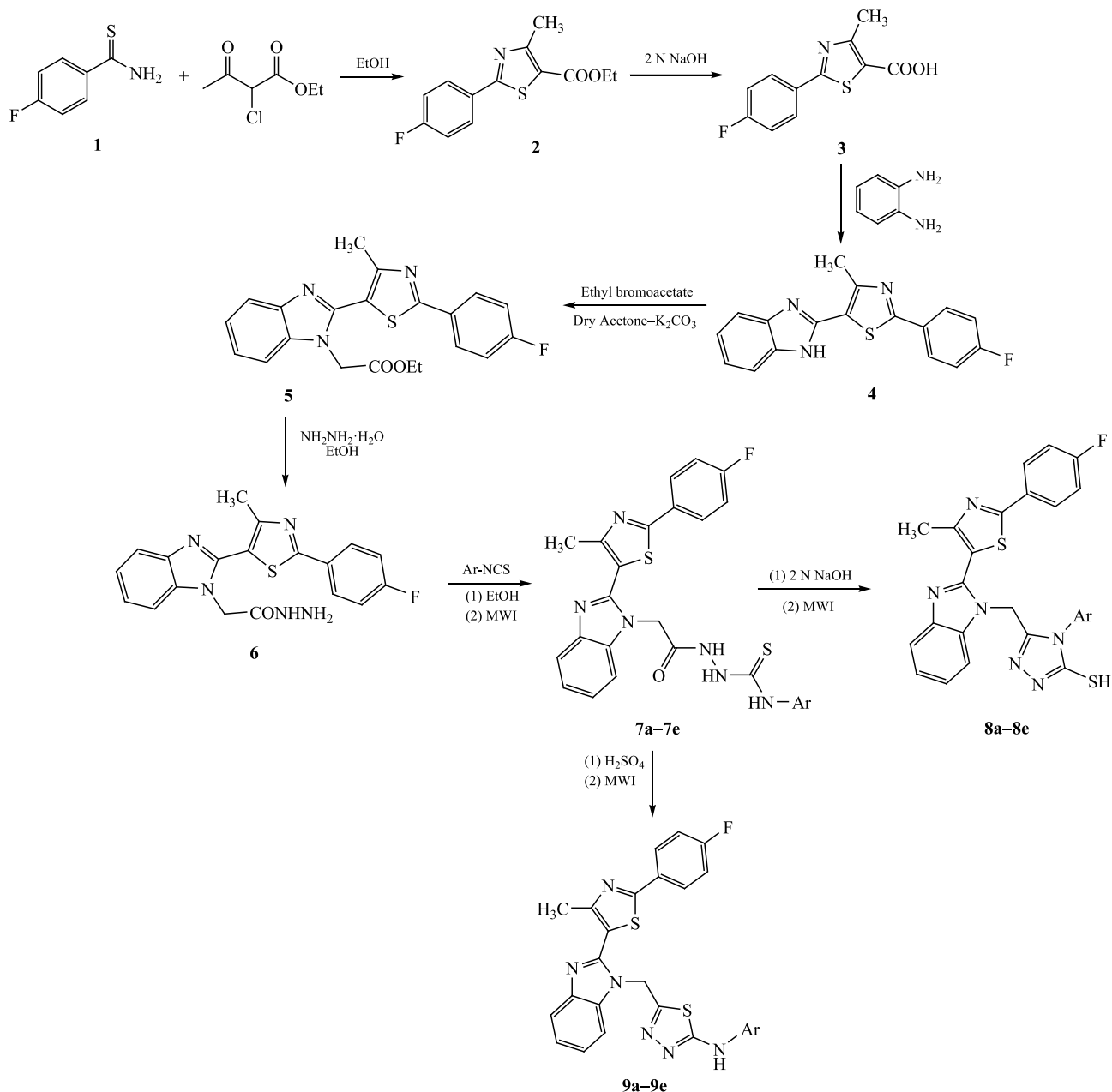
Synthesis of 2-{2-[2-(4-fluorophenyl)-4-methylthiazol-5-yl]-1*H*-benzo[*d*]imidazol-1-yl}acetohydrazide **6** was carried out by the known method (Scheme 1) [10–12].

A novel series of 1-(2-{2-[2-(4-fluorophenyl)-4-methylthiazol-5-yl]-1*H*-benzo[*d*]imidazol-1-yl}acetyl)-4-phenylthiosemicarbazide **7a–7e** was synthesized from the intermediate **6** and substituted aryl isothiocyanates by conventional method and under MW irradiation [10, 13]. Their molecular structures were supported by

IR, <sup>1</sup>H and <sup>13</sup>C NMR spectra. Reaction of compounds **7a–7e** in presence of NaOH under conventional conditions or MW irradiation gave 1,2,4-triazole derivatives **8a–8e** [10, 13]. In IR spectra of the products **8a–8e** no bands at ca. 3100 cm<sup>-1</sup> characteristic for –NH group were recorded. In <sup>1</sup>H NMR spectra of those compounds characteristic singlets of S–H were recorded at ca. 14.00 ppm. Similar reaction of compounds **7a–7e** in acidic media under conventional conditions or MW irradiation gave 1,3,4-thiadiazoles **9a–9e** [10, 13]. The NH group of compound **9a** was recorded in IR spectrum by the band at 3201 cm<sup>-1</sup> and in <sup>1</sup>H NMR spectrum by a singlet at 9.50 ppm.

The MW irradiation method proved to be more efficient in the synthesis of thiosemicarbazides **7a–7e**, 1,2,4-triazoles **8a–8e** and 1,3,4-thiadiazoles **9a–9e** derivatives than the conventional heating. It reduced the reaction time from hours to 5–10 min and increased the products yield up to 77–88% over the conventional method (60–74%) (Table 1).

**In vitro antibacterial activity.** All the synthesized compounds were tested against gram positive bacterial

**Scheme 1.** Synthesis of derivatives of thiosemicarbazide (**7a–7e**), 1,2,4-triazole (**8a–8e**), and 1,3,4-thiadiazole (**9a–9e**).

strains *Staphylococcus aureus* (NCIM 2079), *Bacillus subtilis* (NCIM 2063), and gram negative bacterial strains *Escherichia coli* (NCIM 2810), *Salmonella abony* (NCIM 2257). The zone of inhibition in mm was determined by the well diffusion method at concentration of 1 mg/mL, and Ciprofloxacin was used as the reference drug (Table 2). Compounds **7a**, **7d**, **7e**, **8d**, and **9e** demonstrated moderate activity against both gram positive and

gram negative bacteria while other compounds were characterized by low activity or none.

## EXPERIMENTAL

All organic solvents and reagents were acquired from commercial sources and used as received. The melting points were measured on a DBK melting point apparatus and are uncorrected. Microwave irradiation was carried out in a Raga's synthetic microwave oven.



**Table 1.** Synthesis data for the products

Comp. no.	Ar	Conventional method		Microwave method	
		time, min	yield, %	time, min	yield, %
7a	3-Chlorophenyl	90	74	7.0	88
7b	2-Chlorophenyl	90	70	6.5	85
7c	2,4-Dichlorophenyl	90	75	7.5	84
7d	4-Chlorophenyl	90	68	8.0	82
7e	3,4-Dichlorophenyl	90	72	9.5	87
8a	3-Chlorophenyl	150	65	8.5	80
8b	2-Chlorophenyl	150	68	9.0	78
8c	2,4-Dichlorophenyl	150	62	8.0	81
8d	4-Chlorophenyl	150	66	7.5	83
8e	3,4-Dichlorophenyl	150	70	8.5	79
9a	3-Chlorophenyl	240	68	9.0	77
9b	2-Chlorophenyl	240	62	9.5	85
9c	2,4-Dichlorophenyl	240	67	8.5	83
9d	4-Chlorophenyl	240	60	8.5	78
9e	3,4-Dichlorophenyl	240	66	8.0	81

**Table 2.** Antibacterial tests data for the synthesized compounds

Compound	Zone of inhibition, mm			
	<i>S. aureus</i>	<i>B. subtilis</i>	<i>E. coli</i>	<i>S. abony</i>
7a	16	15	14	17
7b	15	11	–	15
7c	15	14	–	13
7d	15	13	14	15
7e	16	16	17	16
8a	–	–	–	12
8b	–	–	11	10
8c	–	–	13	–
8d	15	17	13	18
8e	–	–	10	10
9a	11	12	12	16
9b	13	12	14	13
9c	12	12	14	–
9d	11	12	12	13
9e	13	15	14	16
Ciprofloxacin	23	28	26	40

FTIR spectra were recorded on a Shimadzu IR Affinity 1S (ATR) spectrophotometer.  $^1\text{H}$  and  $^{13}\text{C}$  NMR spectra were measured on a Bruker Advance 400 spectrometer using TMS as an internal standard and  $\text{DMSO}-d_6$  as a solvent. Mass spectra were measured on a Waters, Q-TOF micromass (ESI-MS) mass spectrometer.

**Synthesis of 1-(2-{2-[2-(4-fluorophenyl)-4-methylthiazol-5-yl]-1H-benzo[d]imidazol-1-yl}acetyl)-4-phenylthiosemicarbazide (7a–7e).** *Conventional method.* Equimolar amounts (0.01 mmol) of acid hydrazide **6** and aryl isothiocyanate **5** were dissolved

in 15 mL of ethanol and refluxed for 90 min. Reaction progress was monitored by TLC. Upon completion of the reaction the solid product was filtered off and crystallized from ethanol to give the corresponding pure compounds **7a–7e** (Table 1).

*Microwave method.* The mixture of equimolar amounts (0.01 mmol) of acid hydrazide **6** and aryl isothiocyanates **5** was dissolved in 15 mL of ethanol and subjected to MW irradiation for 5 to 10 min at 350 W. Reaction progress was monitored by TLC. Upon completion of the reaction the precipitated product was filtered off and crystallized

from ethanol to give the corresponding pure compounds **7a–7e** (Table 2).

**4-(3-Chlorophenyl)-1-(2-{2-[2-(4-fluorophenyl)-4-methylthiazol-5-yl]-1H-benzo[d]imidazol-1-yl}acetyl)thiosemicarbazide (7a).** White solid, mp 194–196°C. IR spectrum,  $\nu$ ,  $\text{cm}^{-1}$ : 3367 (N–H), 3277 (N–H), 3248 (N–H), 1672 (C=O), 1232 (C–F).  $^1\text{H}$  NMR spectrum,  $\delta$ , ppm: 10.51 s (1H, NH), 9.99 s (1H, NH), 9.80 s (1H, NH), 8.05 d. d (2H,  $J = 5.6$  and  $8.8$  Hz, ArH), 7.75 d (1H,  $J = 8$  Hz, ArH), 7.58 d (2H,  $J = 8$  Hz, ArH), 7.19–7.40 m (7H, ArH), 5.07 s (2H,  $\text{CH}_2$ ), 2.51 s (3H,  $\text{CH}_3$ ).  $^{13}\text{C}$  NMR spectrum,  $\delta_{\text{C}}$ , ppm: 166.22, 162.25, 155.01, 145.38, 142.48, 140.42, 135.87, 132.21, 129.76, 129.14, 128.64, 128.55, 123.14, 122.52, 119.29, 118.91, 116.50, 116.27, 110.98, 45.56, 16.47. LC-MS:  $m/z$ : 551.06  $[M + H]^+$ .

**4-(2-Chlorophenyl)-1-(2-{2-[2-(4-fluorophenyl)-4-methylthiazol-5-yl]-1H-benzo[d]imidazol-1-yl}acetyl)thiosemicarbazide (7b).** White solid, mp 226–228°C. IR spectrum,  $\nu$ ,  $\text{cm}^{-1}$ : 3365 (N–H), 3277 (N–H), 3245 (N–H), 1674 (C=O), 1231 (C–F).  $^1\text{H}$  NMR spectrum,  $\delta$ , ppm: 10.55 s (1H, NH), 9.98 s (1H, NH), 9.60 s (1H, NH), 8.05 d. d (2H,  $J = 5.2$  and  $8.8$  Hz, ArH), 7.75 d (1H,  $J = 8$  Hz, ArH), 7.29–7.57 m (9H, ArH), 5.06 s (2H,  $\text{CH}_2$ ), 2.52 s (3H,  $\text{CH}_3$ ).  $^{13}\text{C}$  NMR spectrum,  $\delta_{\text{C}}$ , ppm: 166.22, 155.01, 145.37, 142.48, 135.87, 129.39, 129.14, 128.66, 128.57, 127.21, 123.09, 122.51, 119.27, 118.94, 116.48, 116.26, 111.01, 45.50, 16.48. LC-MS:  $m/z$ : 551.06  $[M + H]^+$ .

**4-(2,4-Dichlorophenyl)-1-(2-{2-[2-(4-fluorophenyl)-4-methylthiazol-5-yl]-1H-benzo[d]imidazol-1-yl}acetyl)thiosemicarbazide (7c),** White solid, mp 220–222°C. IR spectrum,  $\nu$ ,  $\text{cm}^{-1}$ : 3366 (N–H), 3275 (N–H), 3246 (N–H), 1671 (C=O), 1232 (C–F).  $^1\text{H}$  NMR spectrum,  $\delta$ , ppm: 10.52 s (1H, NH), 10.03 s (1H, NH), 9.58 s (1H, NH), 8.01 d. d (2H,  $J = 5.6$  and  $8.4$  Hz, ArH), 7.71 d (1H,  $J = 8$  Hz, ArH), 7.66 s (1H, ArH), 7.25–7.52 m (7H, ArH), 5.02 s (2H,  $\text{CH}_2$ ), 2.48 s (3H,  $\text{CH}_3$ ). LC-MS:  $m/z$ : 585  $[M + H]^+$ .

**4-(4-Chlorophenyl)-1-(2-{2-[2-(4-fluorophenyl)-4-methylthiazol-5-yl]-1H-benzo[d]imidazol-1-yl}acetyl)thiosemicarbazide (7d).** White solid, mp 160–162°C. IR spectrum,  $\nu$ ,  $\text{cm}^{-1}$ : 3367 (N–H), 3278 (N–H), 3247 (N–H), 1672 (C=O), 1232 (C–F).  $^1\text{H}$  NMR spectrum,  $\delta$ , ppm: 10.46 s (1H, NH), 9.89 s (1H, NH), 9.74 s (1H, NH), 8.01 d. d (2H,  $J = 5.6$  and  $8.8$  Hz, ArH), 7.71 d (1H,  $J = 7.6$  Hz, ArH), 7.54 d (1H,  $J = 8$  Hz, ArH), 7.41 d (2H,  $J = 7.6$  Hz, ArH), 7.25–7.36 m (6H, ArH), 5.04 s (2H,  $\text{CH}_2$ ), 2.48 s (3H,  $\text{CH}_3$ ).  $^{13}\text{C}$  NMR spectrum,  $\delta_{\text{C}}$ , ppm:

166.25, 162.28, 155.02, 145.42, 142.49, 137.91, 135.88, 129.16, 128.67, 128.58, 128.09, 123.18, 122.54, 119.31, 118.94, 116.51, 116.29, 110.98, 45.57, 16.48. LC-MS:  $m/z$ : 551  $[M + H]^+$ .

**4-(3,4-Dichlorophenyl)-1-(2-{2-[2-(4-fluorophenyl)-4-methylthiazol-5-yl]-1H-benzo[d]imidazol-1-yl}acetyl)thiosemicarbazide (7e).** White solid, mp 188–190°C. IR spectrum,  $\nu$ ,  $\text{cm}^{-1}$ : 3367 (N–H), 3276 (N–H), 3244 (N–H), 1671 (C=O), 1231 (C–F).  $^1\text{H}$  NMR spectrum,  $\delta$ , ppm: 10.51 s (1H, NH), 10.07 s (1H, NH), 9.88 s (1H, NH), 7.29–8.05 m (11H, ArH), 5.07 s (2H,  $\text{CH}_2$ ), 2.50 s (3H,  $\text{CH}_3$ ).  $^{13}\text{C}$  NMR spectrum,  $\delta_{\text{C}}$ , ppm: 166.21, 164.73, 162.25, 154.99, 145.38, 142.48, 139.09, 135.84, 129.95, 129.10, 128.62, 128.53, 123.14, 122.52, 119.29, 118.90, 116.47, 116.25, 110.95, 45.55, 16.45. LC-MS:  $m/z$ : 585  $[M + H]^+$ .

**Synthesis of 5-({2-[2-(4-fluorophenyl)-4-methylthiazol-5-yl]-1H-benzo[d]imidazol-1-yl}methyl)-4-phenyl-4H-1,2,4-triazole-3-thiol (8a–8e).** *Conventional method.* The mixture of an appropriate thiosemicarbazide **7a–7e** (0.001 mol) with 10 mL of 2 N NaOH solution was refluxed for 2.5 h. Progress of the reaction was monitored by TLC. After completion of the reaction, the mixture was poured onto crushed ice and acidified with acetic acid. The product was filtered off and crystallized from ethanol to give the corresponding pure compound **8a–8e** (Table 1).

*Microwave method.* The mixture of an appropriate thiosemicarbazide **7a–7e** (0.01 mol) with 2 N NaOH solution was subjected to MW irradiation at 350W for 5–10 min. Progress of the reaction was monitored by TLC. After completion of the process, the mixture was poured onto crushed ice and acidified with dilute acetic acid. The product was filtered off and crystallized from DMF/water to afford the corresponding pure compound **8a–8e** (Table 1).

**4-(3-Chlorophenyl)-5-({2-[2-(4-fluorophenyl)-4-methylthiazol-5-yl]-1H-benzo[d]imidazol-1-yl}methyl)-4H-1,2,4-triazole-3-thiol (8a).** White solid, mp 230–232°C. IR spectrum,  $\nu$ ,  $\text{cm}^{-1}$ : 2939 (=C–H), 1640 (C=N), 1218 (C–F).  $^1\text{H}$  NMR spectrum,  $\delta$ , ppm: 6.99–8.01 m (12H, ArH), 5.50 s (2H,  $\text{CH}_2$ ), 2.41 s (3H,  $\text{CH}_3$ ).  $^{13}\text{C}$  NMR spectrum,  $\delta_{\text{C}}$ , ppm: 168.42, 165.99, 162.27, 154.71, 146.50, 144.53, 142.42, 135.27, 135.13, 133.19, 130.51, 128.94, 128.63, 128.54, 127.65, 126.28, 123.15, 122.51, 119.22, 118.71, 116.55, 116.32, 111.21, 40.50, 16.62. LC-MS:  $m/z$ : 533.11  $[M + H]^+$ .

**4-(2-Chlorophenyl)-5-({2-[2-(4-fluorophenyl)-4-methylthiazol-5-yl]-1H-benzo[d]imidazol-1-yl}-**

**methyl)-4H-1,2,4-triazole-3-thiol (8b).** White solid, mp 226–228°C. IR spectrum,  $\nu$ ,  $\text{cm}^{-1}$ : 2936 (=C–H), 1638 (C=N), 1219 (C–F).  $^1\text{H}$  NMR spectrum,  $\delta$ , ppm: 7.13–7.99 m (12H, ArH), 5.31 s (2H,  $\text{CH}_2$ ), 2.40 s (3H,  $\text{CH}_3$ ).  $^{13}\text{C}$  NMR spectrum,  $\delta_{\text{C}}$ , ppm: 165.87, 154.76, 142.49, 130.81, 129.92, 128.51, 127.92, 122.43, 119.16, 116.57, 116.35, 111.35, 40.12, 16.63. LC-MS:  $m/z$ : 532.98  $[M + \text{H}]^+$ .

**4-(2,4-Dichlorophenyl)-5-({2-[2-(4-fluorophenyl)-4-methylthiazol-5-yl]-1H-benzo[d]imidazol-1-yl}-methyl)-4H-1,2,4-triazole-3-thiol (8c).** White solid, mp 230–232°C. IR spectrum,  $\nu$ ,  $\text{cm}^{-1}$ : 2938 (=C–H), 1635 (C=N), 1221 (C–F).  $^1\text{H}$  NMR spectrum,  $\delta$ , ppm: 7.23–7.97 m (11H, ArH), 5.38 s (2H,  $\text{CH}_2$ ), 2.40 s (3H,  $\text{CH}_3$ ). LC-MS:  $m/z$ : 567.00  $[M + \text{H}]^+$ .

**4-(4-Chlorophenyl)-5-({2-[2-(4-fluorophenyl)-4-methylthiazol-5-yl]-1H-benzo[d]imidazol-1-yl}methyl)-4H-1,2,4-triazole-3-thiol (8d).** White solid, mp 210–212°C. IR spectrum,  $\nu$ ,  $\text{cm}^{-1}$ : 2935 (=C–H), 1639 (C=N), 1219 (C–F).  $^1\text{H}$  NMR spectrum,  $\delta$ , ppm: 14.00 s (1H, SH), 7.17–8.01 m (12H, ArH), 5.51 s (2H,  $\text{CH}_2$ ), 2.41 s (3H,  $\text{CH}_3$ ).  $^{13}\text{C}$  NMR spectrum,  $\delta_{\text{C}}$ , ppm: 168.51, 166.04, 154.75, 147.24, 144.53, 142.39, 135.16, 134.44, 131.49, 129.41, 129.31, 129.03, 128.65, 128.56, 123.29, 122.65, 119.33, 118.58, 116.59, 116.37, 111.09, 38.88, 16.57. LC-MS:  $m/z$ : 533.05  $[M + \text{H}]^+$ .

**4-(3,4-Dichlorophenyl)-5-({2-[2-(4-fluorophenyl)-4-methylthiazol-5-yl]-1H-benzo[d]imidazol-1-yl}-methyl)-4H-1,2,4-triazole-3-thiol (8e).** White solid, mp 220–222°C. IR spectrum,  $\nu$ ,  $\text{cm}^{-1}$ : 2938 (=C–H), 1637 (C=N), 1222 (C–F).  $^1\text{H}$  NMR spectrum,  $\delta$ , ppm: 14.00 s (1H, SH), 7.17–8.01 m (12H, ArH), 5.51 s (2H,  $\text{CH}_2$ ), 2.41 s (3H,  $\text{CH}_3$ ).  $^{13}\text{C}$  NMR spectrum,  $\delta_{\text{C}}$ , ppm: 168.53, 166.09, 162.30, 154.68, 146.94, 144.47, 142.35, 135.08, 132.63, 131.74, 131.15, 129.54, 129.03, 128.67, 128.59, 127.86, 123.25, 122.67, 119.32, 118.57, 116.55, 116.33, 111.09, 16.64. LC-MS:  $m/z$ : 567.05  $[M + \text{H}]^+$ .

**Synthesis of 5-({2-[2-(4-fluorophenyl)-4-methylthiazol-5-yl]-1H-benzo[d]imidazol-1-yl}-methyl)-N-phenyl-1,3,4-thiadiazol-2-amine (9a–9e).** *Conventional method.* The mixture of an appropriate thiosemicarbazide **7a–7e** (0.001 mol) with 5 mL of conc.  $\text{H}_2\text{SO}_4$  was stirred for 4 h at RT. After completion of process, the mixture was poured onto crushed ice and neutralized with liquid  $\text{NH}_3$ , a solid product was formed. It was filtered off and washed with methanol to afford the corresponding pure compound **9a–9e** (Table 1).

*Microwave method.* The mixture of an appropriate thiosemicarbazide **7a–7e** (0.01 mol) with 5 mL of conc.  $\text{H}_2\text{SO}_4$  was subjected to MW irradiation for 5 to 10 min at 350 W. After completion of the process the mixture was poured onto crushed ice and neutralized with liquid  $\text{NH}_3$ . The precipitated solid was filtered off and crystallized from water–DMF to afford the corresponding pure thiadiazole **9a–9e** (Table 1).

**N-(3-Chlorophenyl)-5-({2-[2-(4-fluorophenyl)-4-methylthiazol-5-yl]-1H-benzo[d]imidazol-1-yl}-methyl)-1,3,4-thiadiazol-2-amine (9a).** White solid, mp 130–132°C. IR spectrum,  $\nu$ ,  $\text{cm}^{-1}$ : 3201 (N–H), 3039 (=C–H), 1606 (C=N), 1232 (C–F).  $^1\text{H}$  NMR spectrum,  $\delta$ , ppm: 9.5 s (1H, NH), 7.05–8.18 m (12H, ArH), 5.85 s (2H,  $\text{CH}_2$ ), 2.40 s (3H,  $\text{CH}_3$ ).  $^{13}\text{C}$  NMR spectrum,  $\delta_{\text{C}}$ , ppm: 165.80, 165.01, 154.67, 144.15, 142.18, 134.57, 129.11, 128.54, 128.19, 127.31, 123.71, 123.02, 122.35, 121.10, 118.99, 118.11, 116.07, 115.85, 110.74, 42.31, 15.98. LC-MS:  $m/z$ : 533.15  $[M + \text{H}]^+$ .

**N-(2-Chlorophenyl)-5-({2-[2-(4-fluorophenyl)-4-methylthiazol-5-yl]-1H-benzo[d]imidazol-1-yl}methyl)-1,3,4-thiadiazol-2-amine (9b).** White solid, mp 140–142°C. IR spectrum,  $\nu$ ,  $\text{cm}^{-1}$ : 3203 (N–H), 3038 (=C–H), 1607 (C=N), 1232 (C–F).  $^1\text{H}$  NMR spectrum,  $\delta$ , ppm: 9.2 s (1H, NH), 8.17 d (1H,  $J = 8.8$  Hz, ArH), 8.01–8.02 m (2H, ArH), 7.72 d. d (2H,  $J = 13.2$  and 8 Hz, ArH), 7.26–7.44 m (6H, ArH), 7.03 t (1H,  $J = 7.2$  Hz, ArH), 5.84 s (2H,  $\text{CH}_2$ ), 2.47 s (3H,  $\text{CH}_3$ ).  $^{13}\text{C}$  NMR spectrum,  $\delta_{\text{C}}$ , ppm: 166.30, 165.51, 162.30, 155.75, 155.17, 144.65, 142.69, 136.91, 135.08, 129.61, 129.05, 128.69, 128.61, 127.81, 124.22, 123.52, 122.86, 122.70, 121.61, 119.50, 118.61, 116.57, 116.35, 111.25, 42.81, 16.48. LC-MS:  $m/z$ : 533.10  $[M + \text{H}]^+$ .

**N-(2,4-Dichlorophenyl)-5-({2-[2-(4-fluorophenyl)-4-methylthiazol-5-yl]-1H-benzo[d]imidazol-1-yl}-methyl)-1,3,4-thiadiazol-2-amine (9c).** White solid, mp 230–232°C. IR spectrum,  $\nu$ ,  $\text{cm}^{-1}$ : 3201 (N–H), 3037 (=C–H), 1608 (C=N), 1231 (C–F).  $^1\text{H}$  NMR spectrum,  $\delta$ , ppm: 9.2 s (1H, NH), 8.29 d (1H,  $J = 8.4$  Hz, ArH), 8.04 m (2H, ArH), 7.74 d. d (2H,  $J = 14.8$  and 7.2 Hz, ArH), 7.60 s (1H, ArH), 7.32–7.38 m (5H, ArH), 5.86 s (2H,  $\text{CH}_2$ ), 2.49 s (3H,  $\text{CH}_3$ ).  $^{13}\text{C}$  NMR spectrum,  $\delta_{\text{C}}$ , ppm: 166.30, 165.04, 156.19, 155.16, 144.64, 142.68, 136.09, 135.06, 128.89, 128.69, 128.61, 127.80, 126.60, 123.52, 123.02, 122.86, 122.12, 119.50, 118.59, 116.57, 116.35, 111.25, 42.78, 16.49. LC-MS:  $m/z$ : 567.05  $[M + \text{H}]^+$ .

**N-(4-Chlorophenyl)-5-({2-[2-(4-fluorophenyl)-4-methylthiazol-5-yl]-1H-benzo[d]imidazol-1-yl}-**

**methyl)-1,3,4-thiadiazol-2-amine (9d).** White solid, mp 210–212°C. IR spectrum,  $\nu$ ,  $\text{cm}^{-1}$ : 3202 (N–H), 3039 (=C–H), 1605 (C=N), 1232 (C–F).  $^1\text{H}$  NMR spectrum,  $\delta$ , ppm: 10.2 s (1H, NH), 8.04 m (1H, ArH), 7.73 d. d (2H,  $J = 17$  and 7.6 Hz, ArH), 7.56 d (1H,  $J = 8$  Hz, ArH), 7.33–7.50 m (4H, ArH), 5.86 s (2H,  $\text{CH}_2$ ), 2.49 s (3H,  $\text{CH}_3$ ).  $^{13}\text{C}$  NMR spectrum,  $\delta_{\text{C}}$ , ppm: 166.30, 164.66, 162.29, 155.16, 154.64, 144.63, 142.68, 139.13, 135.06, 129.01, 128.84, 128.68, 128.59, 125.41, 123.50, 122.84, 119.49, 118.89, 118.60, 116.55, 116.33, 111.23, 42.80, 16.48. LC-MS:  $m/z$ : 533.05 [ $M + \text{H}$ ] $^+$ .

***N*-(3,4-Dichlorophenyl)-5-({2-[2-(4-fluorophenyl)-4-methylthiazol-5-yl]-1*H*-benzo[*d*]imidazol-1-yl}-methyl)-1,3,4-thiadiazol-2-amine (9e).** White solid, mp 180–182°C. IR spectrum,  $\nu$ ,  $\text{cm}^{-1}$ : 3202 (N–H), 3035 (=C–H), 1604 (C=N), 1231 (C–F).  $^1\text{H}$  NMR spectrum,  $\delta$ , ppm: 10.5 s (1H, NH), 6.5–8.4 m (11H, ArH), 5.86 s (2H,  $\text{CH}_2$ ), 2.4 s (3H,  $\text{CH}_3$ ).  $^{13}\text{C}$  NMR spectrum,  $\delta_{\text{C}}$ , ppm: 166.29, 164.39, 162.35, 155.23, 144.65, 142.69, 140.07, 135.08, 131.25, 130.71, 128.65, 123.50, 123.13, 119.50, 118.56, 117.52, 116.51, 111.20, 42.77, 16.49. LC-MS:  $m/z$ : 567.05 [ $M + \text{H}$ ] $^+$ .

### CONCLUSIONS

The new series of derivatives of 1,2,4-triazole **8a–8e** and 1,3,4-thiadiazole **9a–9e** have been synthesized by conventional as well as MW irradiation methods from 2-{{2-[2-(4-fluorophenyl)-4-methylthiazol-5-yl]-1*H*-benzo[*d*]imidazol-1-yl}acetohydrazide. MW irradiation at 350 W reduces the reaction time from hours to 5–10 min and increases the yield of products from 60–74 to 77–88%. All the newly synthesized compounds have been tested for their antibacterial activity. Compounds **7a**, **7d**, **7e**, **8d**, and **9e** are characterized by moderate activity against both gram positive and gram negative bacterial strains.

### ACKNOWLEDGMENTS

Authors are thankful to Department of Science and Technology, New Delhi for providing financial assistance for research facilities under FIST programme.

### CONFLICT OF INTEREST

No conflict of interest was declared by the authors.

### SUPPLEMENTARY MATERIAL

Supplementary material are available for this article at <https://doi.org/10.1134/S1070363220090200> and are accessible for authorized users.

### REFERENCES

- Sirim, M.M., Krishna, V.S., Sriram, D., and Tan, O.U., *Eur. J. Med. Chem.*, 2020, vol. 188, p. 112010. <https://doi.org/10.1016/j.ejmech.2019.112010>
- Dokla, E.M.E., Abutaleb, N.S., Milik, S.N., Li, D., El-baz, K., Shalaby, M.A.W., Al-Karaki, R., Nasr, M., Klein, C.D., Abouzid, K.A.M., and Seleem, M.N., *Eur. J. Med. Chem.*, 2020, vol. 18615, p. 111850. <https://doi.org/10.1016/j.ejmech.2019.111850>
- Abdel-Galil, E., Moawad, E.B., El-Mekabaty, A., and Said, G.E., *Synth. Commun.*, 2018, vol. 48, no. 16, p. 2083. <https://doi.org/10.1080/00397911.2018.1482349>
- Shaikh, M.S., Palkar, M.B., Patel, H.M., Rane, R.A., Alwan, W.S., Shaikh, M.M., Shaikh, I.M., Hampannavar, G.A., and Karpoomath, R., *RSC Adv.*, 2014, vol. 4, p. 62308. <https://doi.org/10.1039/C4RA11752B>
- Chandra Sekhar, D., Venkata Rao, D.V., Tejeswara Rao, A., Luv kumar, U., and Jha, A., *Russ. J. Gen. Chem.*, 2019, vol. 89, p. 770. <https://doi.org/10.1134/S1070363219040224>
- Yusuf, M., Khan, R.A., Khan, M., and Ahmed, B., *Chemistry Select*, 2017, vol. 2, no. 4, p. 1323. <https://doi.org/10.1002/slct.201601137>
- Onkol, T., Dogruer, D.S., Uzun, L., Adak, S., Ozkan, S., and Şahin, M.F., *J. Enzyme Inhib. Med. Chem.*, 2008, vol. 23, no. 2, p. 277. <https://doi.org/10.1080/14756360701408697>
- Stec, A.P., Biernasiuk, A., Malm, A., and Pitucha, M., *J. Heterocycl. Chem.*, 2017, vol. 54, no. 5, p. 2867. <https://doi.org/10.1002/jhet.2893>
- Gao, F., Wang, T., Xiao, J., and Huang, G., *Eur. J. Med. Chem.*, 2019, vol. 173, p. 274. <https://doi.org/10.1016/j.ejmech.2019.04.043>
- Akolkar, H.N., Karale, B.K., Randhavane, P.V., and Dalavi, N.R., *Indian J. Chem. B*, 2017, vol. 56, p. 348. <http://nopr.niscair.res.in/handle/123456789/40728>
- Karale, B.K., Takate, S.J., Salve, S.P., Zaware, B.H., and Jadhav, S.S., *Indian J. Chem. B*, 2014, vol. 53, p. 339. <http://nopr.niscair.res.in/handle/123456789/27403>
- Phillip, M., *J. Chem. Soc. C.*, 1971, p. 1143.
- Dengale, S.G., Karale, B.K., Akolkar, H.N., Darekar, N.R., and Deshmukh, K.K., *Russ. J. Gen. Chem.*, 2019, vol. 89, p. 1535. <https://doi.org/10.1134/S1070363219070259>



## Microwave-assisted Synthesis, Characterization, and Antibacterial Screening of Some Pyrazolone Derivatives

Bhauasaheb Kisan. Karale<sup>1\*</sup>, Sarita G. Kundlikar<sup>1</sup>, Hemantkumar N. Akolkar<sup>1</sup>, Pratibha V. Randhavane<sup>1</sup>,  
Sushama J. Takate<sup>2</sup>

<sup>1</sup>Department of Chemistry, Radhabai Kale Mahila Mahavidyalaya, Ahmednagar, Maharashtra, India

<sup>2</sup>Department of Chemistry, New Arts, Science and Commerce College, Ahmednagar, Maharashtra, India

**ABSTRACT** 1-(4-(4-Chlorophenyl)thiazol-2-yl)-3-propyl-1H-pyrazol-5(4H)-one **5** was prepared by the reaction of 1-(4-(4-chlorophenyl)thiazol-2-yl)hydrazine and ethyl 3-oxohexanoate. Compound **5** was condensed with different 4-formylpyrazoles **8a-f** to give product **9a-f** through Knoevenagel condensation. The reaction was carried out by both conventional and non-conventional methods. The structures of all the newly synthesized compounds were confirmed with the help of spectral techniques. All the compounds were screened for antibacterial activity. Compounds **9a**, **9d**, and **9e** exhibited good antibacterial activity against *Bacillus subtilis*.

**KEYWORDS** Knoevenagel condensation, Pyrazolone, Thiazoles, Thiophene.

How to cite this article: Karale, B.K., Kundlikar, S.G., Akolkar, H.N., Randhavane, P.V., Takate, S.J. Microwave-assisted Synthesis, Characterization, and Antibacterial Screening of Some Pyrazolone Derivatives, *Indian J. Heterocycl. Chem.*, 2020, 30, 355-360. (DocID: <https://connectjournals.com/01951.2020.30.355>)

### INTRODUCTION

The Knoevenagel condensation reaction has been widely employed for C-C bond formation in organic synthesis<sup>[1]</sup> and their products are the key intermediates for the synthesis of various natural and therapeutic drugs, polymer, and perfumes.<sup>[2,3]</sup> Lewis bases and acids have been reported as catalysts in the Knoevenagel condensation, including Ni-SiO<sub>2</sub>,<sup>[4]</sup> synthetic phosphate Na<sub>2</sub>CaP<sub>2</sub>O<sub>7</sub>,<sup>[5]</sup> Ca<sub>2</sub>P<sub>2</sub>O<sub>7</sub>,<sup>[5]</sup> and natural phosphate ([NP]/KF or NP/NaNO<sub>3</sub>).<sup>[6]</sup> Ionic liquids<sup>[7]</sup> have been also used as catalysts in Knoevenagel condensation.

Thiazoles and their derivatives have attracted continuing interest over the years because of their varied biological activities such as anti-inflammatory,<sup>[8]</sup> antitubercular,<sup>[9]</sup> antimicrobial,<sup>[10]</sup> angiogenesis,<sup>[11]</sup> and neuroprotective.<sup>[12]</sup> Various pyrazole derivatives exhibit anti-inflammatory,<sup>[13]</sup> analgesic,<sup>[13]</sup> antiproliferative,<sup>[14]</sup> and antihepatotoxic<sup>[15]</sup> activities.

Thiophene is sulfur-containing a five-membered heterocyclic compound. Various biological activities

associated with thiophene derivatives are BACE1 inhibitors,<sup>[16]</sup> HIV protease inhibitor,<sup>[17]</sup> antibreast cancer,<sup>[18]</sup> acetylcholinesterase inhibitors,<sup>[19]</sup> and antidepressant.<sup>[20]</sup>

The pyrazolone skeleton exists in the core structure of several biologically active compounds and natural products.<sup>[21]</sup> Antipyrine<sup>[22]</sup> was the first synthetic drug containing pyrazolone ring as the main framework which has been used as an analgesic and antipyretic. Pyrazolone derivatives show a broad spectrum of biological activities such as severe acute respiratory syndrome-coronavirus 3C-like protease inhibitors,<sup>[23]</sup> cytotoxic,<sup>[24]</sup> antitubulin,<sup>[25]</sup> anaplastic lymphoma kinase inhibitors,<sup>[25]</sup> anti-inflammatory,<sup>[26]</sup> and analgesic.<sup>[26]</sup> Some of the chlorine-containing compounds exhibit anti-inflammatory,<sup>[27]</sup> analgesic,<sup>[28]</sup> antibacterial,<sup>[29]</sup> and antifungal<sup>[30]</sup> activities.

The application of microwave (MW) and ultrasound irradiation as a non-conventional energy source for the activation of reactions has now become a very popular and useful technology in organic chemistry.<sup>[31-33]</sup> These methods lead to enhanced conversion rates, higher yields, and easier work-up.

\*Corresponding author: E-mail: [bkkarale@yahoo.com](mailto:bkkarale@yahoo.com)

Journal Homepage

[www.connectjournals.com/ijhc](http://www.connectjournals.com/ijhc)

Published & Hosted by

CONNECT  
Journals

[www.connectjournals.com](http://www.connectjournals.com)



## Synthesis and Antibacterial Screening of Some New Pyrazolylchromones and Pyrazolylcoumaran-3-ones

Sushama J. Takate<sup>1</sup>, Supriya P. Salve<sup>1</sup>, Sushama B. Dare<sup>1</sup>, Bhausaheb K. Karale<sup>2</sup>, Hemantkumar N. Akolkar<sup>2</sup>, Dnyaneshwar B. Falke<sup>1</sup>, Rahul B. Ghungurde<sup>1</sup>, Sadhana D. Mhaske<sup>3\*</sup>

<sup>1</sup>Department of Chemistry, New Arts, Commerce and Science College, Ahmednagar; Affiliated to SPPU, Pune, Maharashtra, India

<sup>2</sup>Department of Chemistry, Radhabai Kale Mahila Mahavidyalaya, Ahmednagar; Affiliated to SPPU, Pune, Maharashtra, India

<sup>3</sup>Department of Chemistry, Dadapatil Rajale Arts, Science and Commerce College, Adinathnagar; Affiliated to SPPU, Pune, Maharashtra, India

**ABSTRACT** Some new pyrazolylchromones **4a-e** (flavone analogs) and pyrazolylcoumaran-3-ones **5a-e** (aurone analogs) were synthesized by refluxing chalcones **3a-e** in dimethyl sulfoxide/ $I_2$  and Pyridine/ $Hg(OAc)_2$ , respectively. Spectral techniques such as infrared, proton nuclear magnetic resonance, and mass spectrometry were used to confirm the structures of newly synthesized compounds. These compounds were studied for their antibacterial activities toward *Bacillus subtilis*, *Staphylococcus aureus*, *Escherichia coli*, and *Salmonella typhi*. Some of these compounds showed promising activity against test organisms.

**KEYWORDS:** Pyrazoles, Flavones, Aurones, Antibacterial activity.

**How to cite this article:** Takate, S.J., Salve, S.P., Dare, S.B., Karale, B.K., Akolkar, H.N., Falke, D.B., Ghungurde, R.B., Mhaske, S.D. Synthesis and Antibacterial Screening of Some New Pyrazolylchromones and Pyrazolylcoumaran-3-ones. *Indian J. Heterocycl. Chem.*, 2020, 30, 525-530. (DocID: <https://connectjournals.com/01951.2020.30.525>)

### INTRODUCTION

Treatment of various diseases is a worldwide serious issue. The emergence of newer infectious diseases, multidrug resistance developing in microbial strains, diseases due to homeostatic disturbances, toxicity associated with existing drugs have created a need of selective, potential therapeutic agents. In search of potential therapeutic agents, many natural and synthetic compounds have been investigated. Many of the natural products are heterocycles which possess medicinal properties and serve as lead molecules for drug discovery.<sup>[1]</sup> Lead modification is an important step in drug design and development.

Pyrazole containing compounds are medicinally useful because of their various therapeutic properties, including antimicrobial,<sup>[2,3]</sup> anti-inflammatory,<sup>[4]</sup> antitubercular,<sup>[5]</sup>

antitumor,<sup>[6]</sup> antidiabetic,<sup>[7]</sup> and antiviral and antioxidant<sup>[8]</sup> properties.

Flavonoids are extensively studied plant products for their biological potential. Chalcones are important intermediates in the flavonoid synthetic pathway and also have medicinal properties.<sup>[9]</sup> These are known to exhibit antibacterial,<sup>[10]</sup> antitubercular,<sup>[11]</sup> anti-inflammatory,<sup>[12,13]</sup> antimalarial,<sup>[14]</sup> antifungal,<sup>[15]</sup> and antiviral<sup>[16]</sup> activities. Synthetic chalcones with heterocyclic rings have been investigated for medicinal properties and are also used in the synthesis of various heterocycles. Pyrazole containing chalcones exhibits potential antimicrobial,<sup>[17]</sup> antioxidant,<sup>[18]</sup> and anticancer<sup>[19]</sup> activities.

Flavones and aurones are medicinally useful members of the flavonoid family. Flavones are widely known for their interesting bioactivities. As a consequence of the

\*Corresponding author: E-mail: [mhaskesadhana@gmail.com](mailto:mhaskesadhana@gmail.com)

Journal Homepage:  
[www.connectjournals.com/ijhc](http://www.connectjournals.com/ijhc)

Published & Hosted by:  
**CONNECT**  
**Journals**  
[www.connectjournals.com](http://www.connectjournals.com)

©2020 Connect Journals





ARTICLE

# Synthesis of 3-(trifluoromethyl)-1-(perfluorophenyl)-1*H*-pyrazol-5(4*H*)-one derivatives via Knoevenagel condensation and their biological evaluation

Sujata G. Dengale<sup>1</sup> | Hemantkumar N. Akolkar<sup>2</sup> | Bhausahab K. Karale<sup>2</sup> |  
Nirmala R. Darekar<sup>2</sup> | Sadhana D. Mhaske<sup>3</sup> | Mubarak H. Shaikh<sup>2</sup> |  
Dipak N. Raut<sup>4</sup> | Keshav K. Deshmukh<sup>1</sup>

<sup>1</sup>P.G. and Research, Department of Chemistry, Sangamner Nagarpalika Arts, D. J. Malpani Commerce and B. N. Sarada Science College, Sangamner, India

<sup>2</sup>P.G. and Research, Department of Chemistry, Radhabai Kale Mahila Mahavidyalaya, Ahmednagar, India

<sup>3</sup>Department of Chemistry, Dadapatil Rajale College, Pathardi, India

<sup>4</sup>Amrutvahini College of Pharmacy, Sangamner, India

## Correspondence

Hemantkumar N. Akolkar, P.G. and Research, Department of Chemistry, Radhabai Kale Mahila Mahavidyalaya, Ahmednagar, Maharashtra, India, 414001.  
Email: hemantakolkar@gmail.com

## Abstract

In search of new active molecules, a small focused library of the synthesis of 3-(trifluoromethyl)-1-(perfluorophenyl)-1*H*-pyrazol-5(4*H*)-one derivatives (**4a-d**, **5a-f**, and **6a-e**) has been efficiently prepared via the Knoevenagel condensation approach. All the derivatives were synthesized by conventional and non-conventional methods like ultrasonication and microwave irradiation, respectively. Several derivatives exhibited excellent anti-inflammatory activity compared to the standard drug. Furthermore, the synthesized compounds were found to have potential antioxidant activity. In addition, to rationalize the observed biological activity data, an *in silico* absorption, distribution, metabolism, and excretion (ADME) prediction study also been carried out. The results of the *in vitro* and *in silico* studies suggest that the 3-(trifluoromethyl)-1-(perfluorophenyl)-1*H*-pyrazol-5(4*H*)-one derivatives (**4a-d**, **5a-f**, and **6a-e**) may possess the ideal structural requirements for the further development of novel therapeutic agents.

## KEYWORDS

ADME prediction, anti-inflammatory, antioxidant, Knoevenagel, microwave, pyrazole, ultrasonication

## 1 | INTRODUCTION

The pyrazole ring is a prominent heterocyclic structural compound found in several pharmaceutically active compounds. This is because of its use in pharmacological activity and ease of synthesis. Furthermore, the selective functionalization of pyrazole with diverse substituents was also found to improve their range of action in various fields. Pyrazole containing heterocycles shows various biological activity, such as antibacterial,<sup>[1]</sup> antifungal,<sup>[2]</sup> antimicrobial,<sup>[3]</sup> anti-inflammatory,<sup>[4a]</sup> antioxidant,<sup>[4b]</sup> insecticidal,<sup>[5]</sup> antiviral,<sup>[6]</sup> anti-nitric oxide

synthase,<sup>[7]</sup> glycogen receptor antagonist,<sup>[8]</sup> anticancer,<sup>[9]</sup> anti-enzyme,<sup>[10]</sup> immunosuppressant,<sup>[11]</sup> anti-fatty acid amide hydrolase (FAAH),<sup>[12]</sup> and liver-x-receptor [LXR] partial agonist activities.<sup>[13]</sup>

Fluorine or fluorine-based compounds are of great interest in synthetic and medicinal chemistry. The position of the fluorine atom in an organic molecule plays a vital role in agrochemicals, pharmaceuticals, and materials<sup>[14]</sup> as it changes the pharmacokinetic and pharmacodynamic properties of the molecule owing to its high membrane permeability, metabolic stability, lipophilicity, and binding affinity.<sup>[15]</sup>

# Microwave Assisted Synthesis and Antibacterial Activity of New 1,3,4-Thiadiazoles and 1,2,4-Triazoles Derived from 2-{2-[2-(4-Fluorophenyl)-4-methylthiazol-5-yl]-1*H*-benzo[*d*]imidazol-1-yl}acetohydrazide

N. R. Darekar<sup>a,b</sup>, B. K. Karale<sup>a</sup>, H. N. Akolkar<sup>a</sup>, and A. S. Burungale<sup>b,\*</sup>

<sup>a</sup> P.G. and Research, Department of Chemistry, Rayat Shikshan Sanstha's Radhabai Kale Mahila Mahavidyalaya, Maharashtra, Ahmednagar, 414001 India

<sup>b</sup> P.G. and Research, Department of Chemistry, Rayat Shikshan Sanstha's S. M. Joshi College, Hadapsar, Maharashtra, Pune, 411028 India

\*e-mail: hemantakolkar@gmail.com

Received July 7, 2020; revised August 18, 2020; accepted August 31, 2020

**Abstract**—A series of novel derivatives of 1-(2-{2-[2-(4-fluorophenyl)-4-methylthiazol-5-yl]-1*H*-benzo[*d*]imidazol-1-yl}acetyl)-4-phenylthiosemicarbazide, 5-({2-[2-(4-fluorophenyl)-4-methylthiazol-5-yl]-1*H*-benzo[*d*]imidazol-1-yl}methyl)-4-phenyl-4*H*-1,2,4-triazole-3-thiol and 5-({2-[2-(4-fluorophenyl)-4-methylthiazol-5-yl]-1*H*-benzo[*d*]imidazol-1-yl}methyl)-*N*-phenyl-1,3,4-thiadiazol-2-amine have been synthesized by the conventional method as well as using MW irradiation. All newly synthesized compounds have been tested for antibacterial activity. Several products have demonstrated moderate activity against gram positive and gram negative bacterial strains.

**Keywords:** 1,3,4-thiadiazole, 1,2,4-triazole, microwave irradiation, antibacterial activity

**DOI:** 10.1134/S1070363220090200

Antimycobacterial and antimicrobial activities have been well established and studied in depth for benzimidazole [1, 2], thiazole [3, 4], 1,3,4-thiadiazole [5–7], and 1,2,4-triazole [8, 9] derivatives.

Pharmacological importance associated with those compounds inspired us to synthesize novel benzimidazole and thiazole containing 1,3,4-thiadiazoles and 1,2,4-triazoles under conventional and MW irradiation. All newly synthesized compounds were evaluated for their antibacterial activity.

## RESULTS AND DISCUSSION

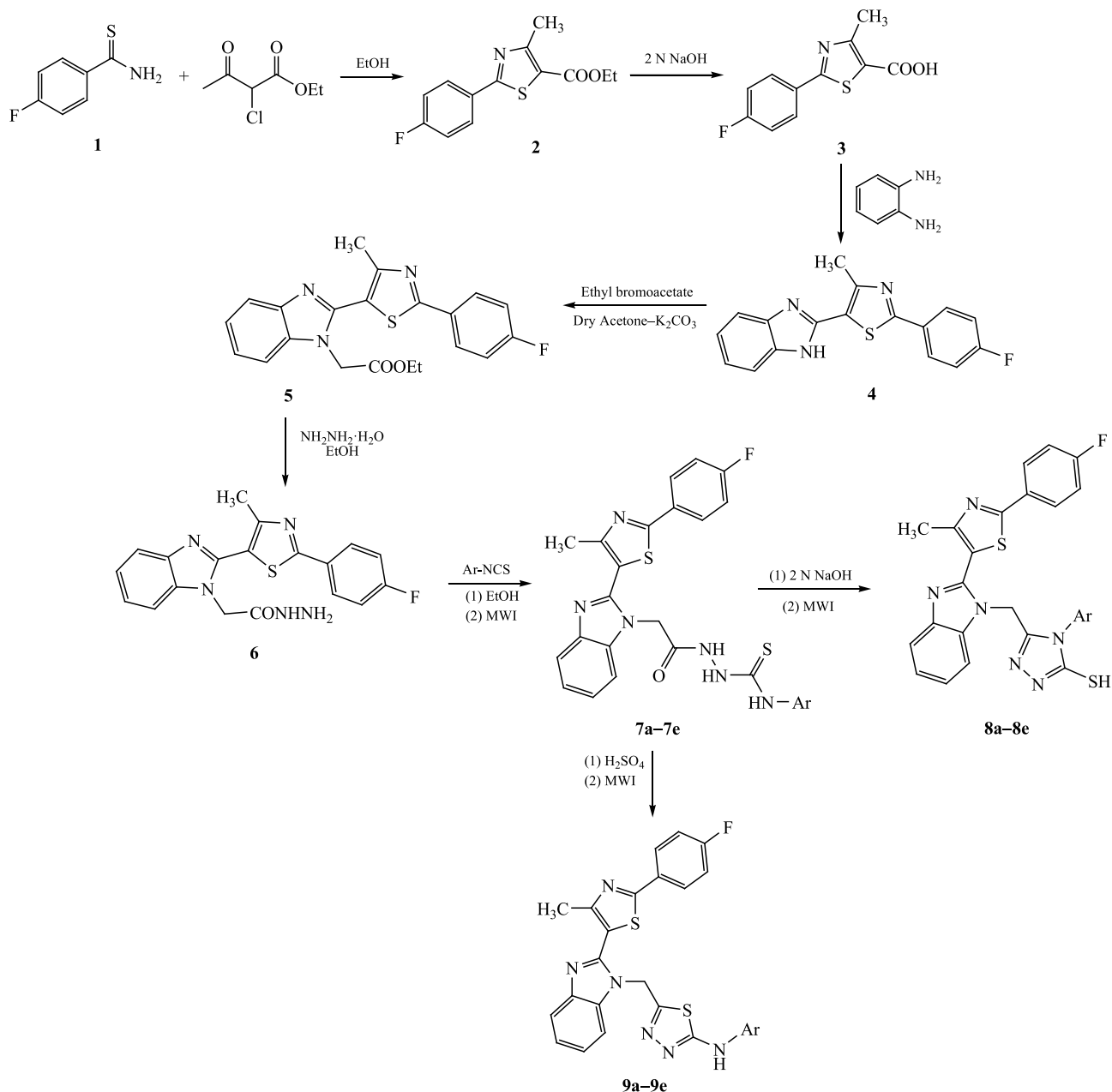
Synthesis of 2-{2-[2-(4-fluorophenyl)-4-methylthiazol-5-yl]-1*H*-benzo[*d*]imidazol-1-yl}acetohydrazide **6** was carried out by the known method (Scheme 1) [10–12].

A novel series of 1-(2-{2-[2-(4-fluorophenyl)-4-methylthiazol-5-yl]-1*H*-benzo[*d*]imidazol-1-yl}acetyl)-4-phenylthiosemicarbazide **7a–7e** was synthesized from the intermediate **6** and substituted aryl isothiocyanates by conventional method and under MW irradiation [10, 13]. Their molecular structures were supported by

IR, <sup>1</sup>H and <sup>13</sup>C NMR spectra. Reaction of compounds **7a–7e** in presence of NaOH under conventional conditions or MW irradiation gave 1,2,4-triazole derivatives **8a–8e** [10, 13]. In IR spectra of the products **8a–8e** no bands at ca. 3100 cm<sup>-1</sup> characteristic for –NH group were recorded. In <sup>1</sup>H NMR spectra of those compounds characteristic singlets of S–H were recorded at ca. 14.00 ppm. Similar reaction of compounds **7a–7e** in acidic media under conventional conditions or MW irradiation gave 1,3,4-thiadiazoles **9a–9e** [10, 13]. The NH group of compound **9a** was recorded in IR spectrum by the band at 3201 cm<sup>-1</sup> and in <sup>1</sup>H NMR spectrum by a singlet at 9.50 ppm.

The MW irradiation method proved to be more efficient in the synthesis of thiosemicarbazides **7a–7e**, 1,2,4-triazoles **8a–8e** and 1,3,4-thiadiazoles **9a–9e** derivatives than the conventional heating. It reduced the reaction time from hours to 5–10 min and increased the products yield up to 77–88% over the conventional method (60–74%) (Table 1).

**In vitro antibacterial activity.** All the synthesized compounds were tested against gram positive bacterial

**Scheme 1.** Synthesis of derivatives of thiosemicarbazide (**7a–7e**), 1,2,4-triazole (**8a–8e**), and 1,3,4-thiadiazole (**9a–9e**).

strains *Staphylococcus aureus* (NCIM 2079), *Bacillus subtilis* (NCIM 2063), and gram negative bacterial strains *Escherichia coli* (NCIM 2810), *Salmonella abony* (NCIM 2257). The zone of inhibition in mm was determined by the well diffusion method at concentration of 1 mg/mL, and Ciprofloxacin was used as the reference drug (Table 2). Compounds **7a**, **7d**, **7e**, **8d**, and **9e** demonstrated moderate activity against both gram positive and

gram negative bacteria while other compounds were characterized by low activity or none.

## EXPERIMENTAL

All organic solvents and reagents were acquired from commercial sources and used as received. The melting points were measured on a DBK melting point apparatus and are uncorrected. Microwave irradiation was carried out in a Raga's synthetic microwave oven.



**Table 1.** Synthesis data for the products

Comp. no.	Ar	Conventional method		Microwave method	
		time, min	yield, %	time, min	yield, %
7a	3-Chlorophenyl	90	74	7.0	88
7b	2-Chlorophenyl	90	70	6.5	85
7c	2,4-Dichlorophenyl	90	75	7.5	84
7d	4-Chlorophenyl	90	68	8.0	82
7e	3,4-Dichlorophenyl	90	72	9.5	87
8a	3-Chlorophenyl	150	65	8.5	80
8b	2-Chlorophenyl	150	68	9.0	78
8c	2,4-Dichlorophenyl	150	62	8.0	81
8d	4-Chlorophenyl	150	66	7.5	83
8e	3,4-Dichlorophenyl	150	70	8.5	79
9a	3-Chlorophenyl	240	68	9.0	77
9b	2-Chlorophenyl	240	62	9.5	85
9c	2,4-Dichlorophenyl	240	67	8.5	83
9d	4-Chlorophenyl	240	60	8.5	78
9e	3,4-Dichlorophenyl	240	66	8.0	81

**Table 2.** Antibacterial tests data for the synthesized compounds

Compound	Zone of inhibition, mm			
	<i>S. aureus</i>	<i>B. subtilis</i>	<i>E. coli</i>	<i>S. abony</i>
7a	16	15	14	17
7b	15	11	–	15
7c	15	14	–	13
7d	15	13	14	15
7e	16	16	17	16
8a	–	–	–	12
8b	–	–	11	10
8c	–	–	13	–
8d	15	17	13	18
8e	–	–	10	10
9a	11	12	12	16
9b	13	12	14	13
9c	12	12	14	–
9d	11	12	12	13
9e	13	15	14	16
Ciprofloxacin	23	28	26	40

FTIR spectra were recorded on a Shimadzu IR Affinity 1S (ATR) spectrophotometer.  $^1\text{H}$  and  $^{13}\text{C}$  NMR spectra were measured on a Bruker Advance 400 spectrometer using TMS as an internal standard and  $\text{DMSO-}d_6$  as a solvent. Mass spectra were measured on a Waters, Q-TOF micromass (ESI-MS) mass spectrometer.

**Synthesis of 1-(2-{2-[2-(4-fluorophenyl)-4-methylthiazol-5-yl]-1H-benzo[d]imidazol-1-yl}acetyl)-4-phenylthiosemicarbazide (7a–7e).** *Conventional method.* Equimolar amounts (0.01 mmol) of acid hydrazide **6** and aryl isothiocyanate **5** were dissolved

in 15 mL of ethanol and refluxed for 90 min. Reaction progress was monitored by TLC. Upon completion of the reaction the solid product was filtered off and crystallized from ethanol to give the corresponding pure compounds **7a–7e** (Table 1).

*Microwave method.* The mixture of equimolar amounts (0.01 mmol) of acid hydrazide **6** and aryl isothiocyanates **5** was dissolved in 15 mL of ethanol and subjected to MW irradiation for 5 to 10 min at 350 W. Reaction progress was monitored by TLC. Upon completion of the reaction the precipitated product was filtered off and crystallized

from ethanol to give the corresponding pure compounds **7a–7e** (Table 2).

**4-(3-Chlorophenyl)-1-(2-{2-[2-(4-fluorophenyl)-4-methylthiazol-5-yl]-1H-benzo[d]imidazol-1-yl}acetyl)thiosemicarbazide (7a).** White solid, mp 194–196°C. IR spectrum,  $\nu$ ,  $\text{cm}^{-1}$ : 3367 (N–H), 3277 (N–H), 3248 (N–H), 1672 (C=O), 1232 (C–F).  $^1\text{H}$  NMR spectrum,  $\delta$ , ppm: 10.51 s (1H, NH), 9.99 s (1H, NH), 9.80 s (1H, NH), 8.05 d. d (2H,  $J = 5.6$  and  $8.8$  Hz, ArH), 7.75 d (1H,  $J = 8$  Hz, ArH), 7.58 d (2H,  $J = 8$  Hz, ArH), 7.19–7.40 m (7H, ArH), 5.07 s (2H,  $\text{CH}_2$ ), 2.51 s (3H,  $\text{CH}_3$ ).  $^{13}\text{C}$  NMR spectrum,  $\delta_{\text{C}}$ , ppm: 166.22, 162.25, 155.01, 145.38, 142.48, 140.42, 135.87, 132.21, 129.76, 129.14, 128.64, 128.55, 123.14, 122.52, 119.29, 118.91, 116.50, 116.27, 110.98, 45.56, 16.47. LC-MS:  $m/z$ : 551.06 [ $M + \text{H}$ ] $^+$ .

**4-(2-Chlorophenyl)-1-(2-{2-[2-(4-fluorophenyl)-4-methylthiazol-5-yl]-1H-benzo[d]imidazol-1-yl}acetyl)thiosemicarbazide (7b).** White solid, mp 226–228°C. IR spectrum,  $\nu$ ,  $\text{cm}^{-1}$ : 3365 (N–H), 3277 (N–H), 3245 (N–H), 1674 (C=O), 1231 (C–F).  $^1\text{H}$  NMR spectrum,  $\delta$ , ppm: 10.55 s (1H, NH), 9.98 s (1H, NH), 9.60 s (1H, NH), 8.05 d. d (2H,  $J = 5.2$  and  $8.8$  Hz, ArH), 7.75 d (1H,  $J = 8$  Hz, ArH), 7.29–7.57 m (9H, ArH), 5.06 s (2H,  $\text{CH}_2$ ), 2.52 s (3H,  $\text{CH}_3$ ).  $^{13}\text{C}$  NMR spectrum,  $\delta_{\text{C}}$ , ppm: 166.22, 155.01, 145.37, 142.48, 135.87, 129.39, 129.14, 128.66, 128.57, 127.21, 123.09, 122.51, 119.27, 118.94, 116.48, 116.26, 111.01, 45.50, 16.48. LC-MS:  $m/z$ : 551.06 [ $M + \text{H}$ ] $^+$ .

**4-(2,4-Dichlorophenyl)-1-(2-{2-[2-(4-fluorophenyl)-4-methylthiazol-5-yl]-1H-benzo[d]imidazol-1-yl}acetyl)thiosemicarbazide (7c),** White solid, mp 220–222°C. IR spectrum,  $\nu$ ,  $\text{cm}^{-1}$ : 3366 (N–H), 3275 (N–H), 3246 (N–H), 1671 (C=O), 1232 (C–F).  $^1\text{H}$  NMR spectrum,  $\delta$ , ppm: 10.52 s (1H, NH), 10.03 s (1H, NH), 9.58 s (1H, NH), 8.01 d. d (2H,  $J = 5.6$  and  $8.4$  Hz, ArH), 7.71 d (1H,  $J = 8$  Hz, ArH), 7.66 s (1H, ArH), 7.25–7.52 m (7H, ArH), 5.02 s (2H,  $\text{CH}_2$ ), 2.48 s (3H,  $\text{CH}_3$ ). LC-MS:  $m/z$ : 585 [ $M + \text{H}$ ] $^+$ .

**4-(4-Chlorophenyl)-1-(2-{2-[2-(4-fluorophenyl)-4-methylthiazol-5-yl]-1H-benzo[d]imidazol-1-yl}acetyl)thiosemicarbazide (7d).** White solid, mp 160–162°C. IR spectrum,  $\nu$ ,  $\text{cm}^{-1}$ : 3367 (N–H), 3278 (N–H), 3247 (N–H), 1672 (C=O), 1232 (C–F).  $^1\text{H}$  NMR spectrum,  $\delta$ , ppm: 10.46 s (1H, NH), 9.89 s (1H, NH), 9.74 s (1H, NH), 8.01 d. d (2H,  $J = 5.6$  and  $8.8$  Hz, ArH), 7.71 d (1H,  $J = 7.6$  Hz, ArH), 7.54 d (1H,  $J = 8$  Hz, ArH), 7.41 d (2H,  $J = 7.6$  Hz, ArH), 7.25–7.36 m (6H, ArH), 5.04 s (2H,  $\text{CH}_2$ ), 2.48 s (3H,  $\text{CH}_3$ ).  $^{13}\text{C}$  NMR spectrum,  $\delta_{\text{C}}$ , ppm:

166.25, 162.28, 155.02, 145.42, 142.49, 137.91, 135.88, 129.16, 128.67, 128.58, 128.09, 123.18, 122.54, 119.31, 118.94, 116.51, 116.29, 110.98, 45.57, 16.48. LC-MS:  $m/z$ : 551 [ $M + \text{H}$ ] $^+$ .

**4-(3,4-Dichlorophenyl)-1-(2-{2-[2-(4-fluorophenyl)-4-methylthiazol-5-yl]-1H-benzo[d]imidazol-1-yl}acetyl)thiosemicarbazide (7e).** White solid, mp 188–190°C. IR spectrum,  $\nu$ ,  $\text{cm}^{-1}$ : 3367 (N–H), 3276 (N–H), 3244 (N–H), 1671 (C=O), 1231 (C–F).  $^1\text{H}$  NMR spectrum,  $\delta$ , ppm: 10.51 s (1H, NH), 10.07 s (1H, NH), 9.88 s (1H, NH), 7.29–8.05 m (11H, ArH), 5.07 s (2H,  $\text{CH}_2$ ), 2.50 s (3H,  $\text{CH}_3$ ).  $^{13}\text{C}$  NMR spectrum,  $\delta_{\text{C}}$ , ppm: 166.21, 164.73, 162.25, 154.99, 145.38, 142.48, 139.09, 135.84, 129.95, 129.10, 128.62, 128.53, 123.14, 122.52, 119.29, 118.90, 116.47, 116.25, 110.95, 45.55, 16.45. LC-MS:  $m/z$ : 585 [ $M + \text{H}$ ] $^+$ .

**Synthesis of 5-({2-[2-(4-fluorophenyl)-4-methylthiazol-5-yl]-1H-benzo[d]imidazol-1-yl}methyl)-4-phenyl-4H-1,2,4-triazole-3-thiol (8a–8e).** *Conventional method.* The mixture of an appropriate thiosemicarbazide **7a–7e** (0.001 mol) with 10 mL of 2 N NaOH solution was refluxed for 2.5 h. Progress of the reaction was monitored by TLC. After completion of the reaction, the mixture was poured onto crushed ice and acidified with acetic acid. The product was filtered off and crystallized from ethanol to give the corresponding pure compound **8a–8e** (Table 1).

*Microwave method.* The mixture of an appropriate thiosemicarbazide **7a–7e** (0.01 mol) with 2 N NaOH solution was subjected to MW irradiation at 350W for 5–10 min. Progress of the reaction was monitored by TLC. After completion of the process, the mixture was poured onto crushed ice and acidified with dilute acetic acid. The product was filtered off and crystallized from DMF/water to afford the corresponding pure compound **8a–8e** (Table 1).

**4-(3-Chlorophenyl)-5-({2-[2-(4-fluorophenyl)-4-methylthiazol-5-yl]-1H-benzo[d]imidazol-1-yl}methyl)-4H-1,2,4-triazole-3-thiol (8a).** White solid, mp 230–232°C. IR spectrum,  $\nu$ ,  $\text{cm}^{-1}$ : 2939 (=C–H), 1640 (C=N), 1218 (C–F).  $^1\text{H}$  NMR spectrum,  $\delta$ , ppm: 6.99–8.01 m (12H, ArH), 5.50 s (2H,  $\text{CH}_2$ ), 2.41 s (3H,  $\text{CH}_3$ ).  $^{13}\text{C}$  NMR spectrum,  $\delta_{\text{C}}$ , ppm: 168.42, 165.99, 162.27, 154.71, 146.50, 144.53, 142.42, 135.27, 135.13, 133.19, 130.51, 128.94, 128.63, 128.54, 127.65, 126.28, 123.15, 122.51, 119.22, 118.71, 116.55, 116.32, 111.21, 40.50, 16.62. LC-MS:  $m/z$ : 533.11 [ $M + \text{H}$ ] $^+$ .

**4-(2-Chlorophenyl)-5-({2-[2-(4-fluorophenyl)-4-methylthiazol-5-yl]-1H-benzo[d]imidazol-1-yl}-**

**methyl)-4H-1,2,4-triazole-3-thiol (8b).** White solid, mp 226–228°C. IR spectrum,  $\nu$ ,  $\text{cm}^{-1}$ : 2936 (=C–H), 1638 (C=N), 1219 (C–F).  $^1\text{H}$  NMR spectrum,  $\delta$ , ppm: 7.13–7.99 m (12H, ArH), 5.31 s (2H,  $\text{CH}_2$ ), 2.40 s (3H,  $\text{CH}_3$ ).  $^{13}\text{C}$  NMR spectrum,  $\delta_{\text{C}}$ , ppm: 165.87, 154.76, 142.49, 130.81, 129.92, 128.51, 127.92, 122.43, 119.16, 116.57, 116.35, 111.35, 40.12, 16.63. LC-MS:  $m/z$ : 532.98  $[M + \text{H}]^+$ .

**4-(2,4-Dichlorophenyl)-5-({2-[2-(4-fluorophenyl)-4-methylthiazol-5-yl]-1H-benzo[d]imidazol-1-yl}-methyl)-4H-1,2,4-triazole-3-thiol (8c).** White solid, mp 230–232°C. IR spectrum,  $\nu$ ,  $\text{cm}^{-1}$ : 2938 (=C–H), 1635 (C=N), 1221 (C–F).  $^1\text{H}$  NMR spectrum,  $\delta$ , ppm: 7.23–7.97 m (11H, ArH), 5.38 s (2H,  $\text{CH}_2$ ), 2.40 s (3H,  $\text{CH}_3$ ). LC-MS:  $m/z$ : 567.00  $[M + \text{H}]^+$ .

**4-(4-Chlorophenyl)-5-({2-[2-(4-fluorophenyl)-4-methylthiazol-5-yl]-1H-benzo[d]imidazol-1-yl}-methyl)-4H-1,2,4-triazole-3-thiol (8d).** White solid, mp 210–212°C. IR spectrum,  $\nu$ ,  $\text{cm}^{-1}$ : 2935 (=C–H), 1639 (C=N), 1219 (C–F).  $^1\text{H}$  NMR spectrum,  $\delta$ , ppm: 14.00 s (1H, SH), 7.17–8.01 m (12H, ArH), 5.51 s (2H,  $\text{CH}_2$ ), 2.41 s (3H,  $\text{CH}_3$ ).  $^{13}\text{C}$  NMR spectrum,  $\delta_{\text{C}}$ , ppm: 168.51, 166.04, 154.75, 147.24, 144.53, 142.39, 135.16, 134.44, 131.49, 129.41, 129.31, 129.03, 128.65, 128.56, 123.29, 122.65, 119.33, 118.58, 116.59, 116.37, 111.09, 38.88, 16.57. LC-MS:  $m/z$ : 533.05  $[M + \text{H}]^+$ .

**4-(3,4-Dichlorophenyl)-5-({2-[2-(4-fluorophenyl)-4-methylthiazol-5-yl]-1H-benzo[d]imidazol-1-yl}-methyl)-4H-1,2,4-triazole-3-thiol (8e).** White solid, mp 220–222°C. IR spectrum,  $\nu$ ,  $\text{cm}^{-1}$ : 2938 (=C–H), 1637 (C=N), 1222 (C–F).  $^1\text{H}$  NMR spectrum,  $\delta$ , ppm: 14.00 s (1H, SH), 7.17–8.01 m (12H, ArH), 5.51 s (2H,  $\text{CH}_2$ ), 2.41 s (3H,  $\text{CH}_3$ ).  $^{13}\text{C}$  NMR spectrum,  $\delta_{\text{C}}$ , ppm: 168.53, 166.09, 162.30, 154.68, 146.94, 144.47, 142.35, 135.08, 132.63, 131.74, 131.15, 129.54, 129.03, 128.67, 128.59, 127.86, 123.25, 122.67, 119.32, 118.57, 116.55, 116.33, 111.09, 16.64. LC-MS:  $m/z$ : 567.05  $[M + \text{H}]^+$ .

**Synthesis of 5-({2-[2-(4-fluorophenyl)-4-methylthiazol-5-yl]-1H-benzo[d]imidazol-1-yl}-methyl)-N-phenyl-1,3,4-thiadiazol-2-amine (9a–9e).**

*Conventional method.* The mixture of an appropriate thiosemicarbazide **7a–7e** (0.001 mol) with 5 mL of conc.  $\text{H}_2\text{SO}_4$  was stirred for 4 h at RT. After completion of process, the mixture was poured onto crushed ice and neutralized with liquid  $\text{NH}_3$ , a solid product was formed. It was filtered off and washed with methanol to afford the corresponding pure compound **9a–9e** (Table 1).

*Microwave method.* The mixture of an appropriate thiosemicarbazide **7a–7e** (0.01 mol) with 5 mL of conc.  $\text{H}_2\text{SO}_4$  was subjected to MW irradiation for 5 to 10 min at 350 W. After completion of the process the mixture was poured onto crushed ice and neutralized with liquid  $\text{NH}_3$ . The precipitated solid was filtered off and crystallized from water–DMF to afford the corresponding pure thiadiazole **9a–9e** (Table 1).

**N-(3-Chlorophenyl)-5-({2-[2-(4-fluorophenyl)-4-methylthiazol-5-yl]-1H-benzo[d]imidazol-1-yl}-methyl)-1,3,4-thiadiazol-2-amine (9a).** White solid, mp 130–132°C. IR spectrum,  $\nu$ ,  $\text{cm}^{-1}$ : 3201 (N–H), 3039 (=C–H), 1606 (C=N), 1232 (C–F).  $^1\text{H}$  NMR spectrum,  $\delta$ , ppm: 9.5 s (1H, NH), 7.05–8.18 m (12H, ArH), 5.85 s (2H,  $\text{CH}_2$ ), 2.40 s (3H,  $\text{CH}_3$ ).  $^{13}\text{C}$  NMR spectrum,  $\delta_{\text{C}}$ , ppm: 165.80, 165.01, 154.67, 144.15, 142.18, 134.57, 129.11, 128.54, 128.19, 127.31, 123.71, 123.02, 122.35, 121.10, 118.99, 118.11, 116.07, 115.85, 110.74, 42.31, 15.98. LC-MS:  $m/z$ : 533.15  $[M + \text{H}]^+$ .

**N-(2-Chlorophenyl)-5-({2-[2-(4-fluorophenyl)-4-methylthiazol-5-yl]-1H-benzo[d]imidazol-1-yl}-methyl)-1,3,4-thiadiazol-2-amine (9b).** White solid, mp 140–142°C. IR spectrum,  $\nu$ ,  $\text{cm}^{-1}$ : 3203 (N–H), 3038 (=C–H), 1607 (C=N), 1232 (C–F).  $^1\text{H}$  NMR spectrum,  $\delta$ , ppm: 9.2 s (1H, NH), 8.17 d (1H,  $J = 8.8$  Hz, ArH), 8.01–8.02 m (2H, ArH), 7.72 d. d (2H,  $J = 13.2$  and 8 Hz, ArH), 7.26–7.44 m (6H, ArH), 7.03 t (1H,  $J = 7.2$  Hz, ArH), 5.84 s (2H,  $\text{CH}_2$ ), 2.47 s (3H,  $\text{CH}_3$ ).  $^{13}\text{C}$  NMR spectrum,  $\delta_{\text{C}}$ , ppm: 166.30, 165.51, 162.30, 155.75, 155.17, 144.65, 142.69, 136.91, 135.08, 129.61, 129.05, 128.69, 128.61, 127.81, 124.22, 123.52, 122.86, 122.70, 121.61, 119.50, 118.61, 116.57, 116.35, 111.25, 42.81, 16.48. LC-MS:  $m/z$ : 533.10  $[M + \text{H}]^+$ .

**N-(2,4-Dichlorophenyl)-5-({2-[2-(4-fluorophenyl)-4-methylthiazol-5-yl]-1H-benzo[d]imidazol-1-yl}-methyl)-1,3,4-thiadiazol-2-amine (9c).** White solid, mp 230–232°C. IR spectrum,  $\nu$ ,  $\text{cm}^{-1}$ : 3201 (N–H), 3037 (=C–H), 1608 (C=N), 1231 (C–F).  $^1\text{H}$  NMR spectrum,  $\delta$ , ppm: 9.2 s (1H, NH), 8.29 d (1H,  $J = 8.4$  Hz, ArH), 8.04 m (2H, ArH), 7.74 d. d (2H,  $J = 14.8$  and 7.2 Hz, ArH), 7.60 s (1H, ArH), 7.32–7.38 m (5H, ArH), 5.86 s (2H,  $\text{CH}_2$ ), 2.49 s (3H,  $\text{CH}_3$ ).  $^{13}\text{C}$  NMR spectrum,  $\delta_{\text{C}}$ , ppm: 166.30, 165.04, 156.19, 155.16, 144.64, 142.68, 136.09, 135.06, 128.89, 128.69, 128.61, 127.80, 126.60, 123.52, 123.02, 122.86, 122.12, 119.50, 118.59, 116.57, 116.35, 111.25, 42.78, 16.49. LC-MS:  $m/z$ : 567.05  $[M + \text{H}]^+$ .

**N-(4-Chlorophenyl)-5-({2-[2-(4-fluorophenyl)-4-methylthiazol-5-yl]-1H-benzo[d]imidazol-1-yl}-**

**methyl)-1,3,4-thiadiazol-2-amine (9d).** White solid, mp 210–212°C. IR spectrum,  $\nu$ ,  $\text{cm}^{-1}$ : 3202 (N–H), 3039 (=C–H), 1605 (C=N), 1232 (C–F).  $^1\text{H}$  NMR spectrum,  $\delta$ , ppm: 10.2 s (1H, NH), 8.04 m (1H, ArH), 7.73 d. d (2H,  $J = 17$  and 7.6 Hz, ArH), 7.56 d (1H,  $J = 8$  Hz, ArH), 7.33–7.50 m (4H, ArH), 5.86 s (2H,  $\text{CH}_2$ ), 2.49 s (3H,  $\text{CH}_3$ ).  $^{13}\text{C}$  NMR spectrum,  $\delta_{\text{C}}$ , ppm: 166.30, 164.66, 162.29, 155.16, 154.64, 144.63, 142.68, 139.13, 135.06, 129.01, 128.84, 128.68, 128.59, 125.41, 123.50, 122.84, 119.49, 118.89, 118.60, 116.55, 116.33, 111.23, 42.80, 16.48. LC-MS:  $m/z$ : 533.05 [ $M + \text{H}$ ] $^+$ .

***N*-(3,4-Dichlorophenyl)-5-({2-[2-(4-fluorophenyl)-4-methylthiazol-5-yl]-1*H*-benzo[*d*]imidazol-1-yl}-methyl)-1,3,4-thiadiazol-2-amine (9e).** White solid, mp 180–182°C. IR spectrum,  $\nu$ ,  $\text{cm}^{-1}$ : 3202 (N–H), 3035 (=C–H), 1604 (C=N), 1231 (C–F).  $^1\text{H}$  NMR spectrum,  $\delta$ , ppm: 10.5 s (1H, NH), 6.5–8.4 m (11H, ArH), 5.86 s (2H,  $\text{CH}_2$ ), 2.4 s (3H,  $\text{CH}_3$ ).  $^{13}\text{C}$  NMR spectrum,  $\delta_{\text{C}}$ , ppm: 166.29, 164.39, 162.35, 155.23, 144.65, 142.69, 140.07, 135.08, 131.25, 130.71, 128.65, 123.50, 123.13, 119.50, 118.56, 117.52, 116.51, 111.20, 42.77, 16.49. LC-MS:  $m/z$ : 567.05 [ $M + \text{H}$ ] $^+$ .

### CONCLUSIONS

The new series of derivatives of 1,2,4-triazole **8a–8e** and 1,3,4-thiadiazole **9a–9e** have been synthesized by conventional as well as MW irradiation methods from 2-{{2-[2-(4-fluorophenyl)-4-methylthiazol-5-yl]-1*H*-benzo[*d*]imidazol-1-yl}acetohydrazide. MW irradiation at 350 W reduces the reaction time from hours to 5–10 min and increases the yield of products from 60–74 to 77–88%. All the newly synthesized compounds have been tested for their antibacterial activity. Compounds **7a**, **7d**, **7e**, **8d**, and **9e** are characterized by moderate activity against both gram positive and gram negative bacterial strains.

### ACKNOWLEDGMENTS

Authors are thankful to Department of Science and Technology, New Delhi for providing financial assistance for research facilities under FIST programme.

### CONFLICT OF INTEREST

No conflict of interest was declared by the authors.

### SUPPLEMENTARY MATERIAL

Supplementary material are available for this article at <https://doi.org/10.1134/S1070363220090200> and are accessible for authorized users.

### REFERENCES

- Sirim, M.M., Krishna, V.S., Sriram, D., and Tan, O.U., *Eur. J. Med. Chem.*, 2020, vol. 188, p. 112010. <https://doi.org/10.1016/j.ejmech.2019.112010>
- Dokla, E.M.E., Abutaleb, N.S., Milik, S.N., Li, D., El-baz, K., Shalaby, M.A.W., Al-Karaki, R., Nasr, M., Klein, C.D., Abouzid, K.A.M., and Seleem, M.N., *Eur. J. Med. Chem.*, 2020, vol. 18615, p. 111850. <https://doi.org/10.1016/j.ejmech.2019.111850>
- Abdel-Galil, E., Moawad, E.B., El-Mekabaty, A., and Said, G.E., *Synth. Commun.*, 2018, vol. 48, no. 16, p. 2083. <https://doi.org/10.1080/00397911.2018.1482349>
- Shaikh, M.S., Palkar, M.B., Patel, H.M., Rane, R.A., Alwan, W.S., Shaikh, M.M., Shaikh, I.M., Hampanavar, G.A., and Karpoornath, R., *RSC Adv.*, 2014, vol. 4, p. 62308. <https://doi.org/10.1039/C4RA11752B>
- Chandra Sekhar, D., Venkata Rao, D.V., Tejeswara Rao, A., Luv kumar, U., and Jha, A., *Russ. J. Gen. Chem.*, 2019, vol. 89, p. 770. <https://doi.org/10.1134/S1070363219040224>
- Yusuf, M., Khan, R.A., Khan, M., and Ahmed, B., *Chemistry Select*, 2017, vol. 2, no. 4, p. 1323. <https://doi.org/10.1002/slct.201601137>
- Onkol, T., Dogruer, D.S., Uzun, L., Adak, S., Ozkan, S., and Şahin, M.F., *J. Enzyme Inhib. Med. Chem.*, 2008, vol. 23, no. 2, p. 277. <https://doi.org/10.1080/14756360701408697>
- Stec, A.P., Biernasiuk, A., Malm, A., and Pitucha, M., *J. Heterocycl. Chem.*, 2017, vol. 54, no. 5, p. 2867. <https://doi.org/10.1002/jhet.2893>
- Gao, F., Wang, T., Xiao, J., and Huang, G., *Eur. J. Med. Chem.*, 2019, vol. 173, p. 274. <https://doi.org/10.1016/j.ejmech.2019.04.043>
- Akolkar, H.N., Karale, B.K., Randhavane, P.V., and Dalavi, N.R., *Indian J. Chem. B*, 2017, vol. 56, p. 348. <http://nopr.niscair.res.in/handle/123456789/40728>
- Karale, B.K., Takate, S.J., Salve, S.P., Zaware, B.H., and Jadhav, S.S., *Indian J. Chem. B*, 2014, vol. 53, p. 339. <http://nopr.niscair.res.in/handle/123456789/27403>
- Phillip, M., *J. Chem. Soc. C.*, 1971, p. 1143.
- Dengale, S.G., Karale, B.K., Akolkar, H.N., Darekar, N.R., and Deshmukh, K.K., *Russ. J. Gen. Chem.*, 2019, vol. 89, p. 1535. <https://doi.org/10.1134/S1070363219070259>





## ARTICLE

# Synthesis of 3-(trifluoromethyl)-1-(perfluorophenyl)-1*H*-pyrazol-5(4*H*)-one derivatives via Knoevenagel condensation and their biological evaluation

Sujata G. Dengale<sup>1</sup> | Hemantkumar N. Akolkar<sup>2</sup> | Bhausahab K. Karale<sup>2</sup> |  
Nirmala R. Darekar<sup>2</sup> | Sadhana D. Mhaske<sup>3</sup> | Mubarak H. Shaikh<sup>2</sup> |  
Dipak N. Raut<sup>4</sup> | Keshav K. Deshmukh<sup>1</sup>

<sup>1</sup>P.G. and Research, Department of Chemistry, Sangamner Nagarpalika Arts, D. J. Malpani Commerce and B. N. Sarada Science College, Sangamner, India

<sup>2</sup>P.G. and Research, Department of Chemistry, Radhabai Kale Mahila Mahavidyalaya, Ahmednagar, India

<sup>3</sup>Department of Chemistry, Dadapatil Rajale College, Pathardi, India

<sup>4</sup>Amrutvahini College of Pharmacy, Sangamner, India

## Correspondence

Hemantkumar N. Akolkar, P.G. and Research, Department of Chemistry, Radhabai Kale Mahila Mahavidyalaya, Ahmednagar, Maharashtra, India, 414001. Email: hemantakolkar@gmail.com

## Abstract

In search of new active molecules, a small focused library of the synthesis of 3-(trifluoromethyl)-1-(perfluorophenyl)-1*H*-pyrazol-5(4*H*)-one derivatives (**4a-d**, **5a-f**, and **6a-e**) has been efficiently prepared via the Knoevenagel condensation approach. All the derivatives were synthesized by conventional and non-conventional methods like ultrasonication and microwave irradiation, respectively. Several derivatives exhibited excellent anti-inflammatory activity compared to the standard drug. Furthermore, the synthesized compounds were found to have potential antioxidant activity. In addition, to rationalize the observed biological activity data, an *in silico* absorption, distribution, metabolism, and excretion (ADME) prediction study also been carried out. The results of the *in vitro* and *in silico* studies suggest that the 3-(trifluoromethyl)-1-(perfluorophenyl)-1*H*-pyrazol-5(4*H*)-one derivatives (**4a-d**, **5a-f**, and **6a-e**) may possess the ideal structural requirements for the further development of novel therapeutic agents.

## KEYWORDS

ADME prediction, anti-inflammatory, antioxidant, Knoevenagel, microwave, pyrazole, ultrasonication

## 1 | INTRODUCTION

The pyrazole ring is a prominent heterocyclic structural compound found in several pharmaceutically active compounds. This is because of its use in pharmacological activity and ease of synthesis. Furthermore, the selective functionalization of pyrazole with diverse substituents was also found to improve their range of action in various fields. Pyrazole containing heterocycles shows various biological activity, such as antibacterial,<sup>[1]</sup> antifungal,<sup>[2]</sup> antimicrobial,<sup>[3]</sup> anti-inflammatory,<sup>[4a]</sup> antioxidant,<sup>[4b]</sup> insecticidal,<sup>[5]</sup> antiviral,<sup>[6]</sup> anti-nitric oxide

synthase,<sup>[7]</sup> glycogen receptor antagonist,<sup>[8]</sup> anticancer,<sup>[9]</sup> antienzyme,<sup>[10]</sup> immunosuppressant,<sup>[11]</sup> anti-fatty acid amide hydrolase (FAAH),<sup>[12]</sup> and liver-x-receptor [LXR] partial agonist activities.<sup>[13]</sup>

Fluorine or fluorine-based compounds are of great interest in synthetic and medicinal chemistry. The position of the fluorine atom in an organic molecule plays a vital role in agrochemicals, pharmaceuticals, and materials<sup>[14]</sup> as it changes the pharmacokinetic and pharmacodynamic properties of the molecule owing to its high membrane permeability, metabolic stability, lipophilicity, and binding affinity.<sup>[15]</sup>

Perfluoro-alkylated and trifluoro-methylated pyrazoles represent pharmacologically related core structures that are present in many important drugs and agrochemicals, such as fluazolate (herbicide), penthiopyrad (fungicide), razaxaban (anticoagulant), deracoxib, celecoxib (anti-inflammatory), and penflufen (fungicidal) (Figure 1).<sup>[16]</sup> So, the modern trend is moving more in the direction of the synthesis of a collection of fluorine-containing molecules in order to find excellent biological activity.

Ultrasonic irradiation is a new technology that has been widely used in chemical reactions. When ultrasonic waves pass through a liquid medium, a large number of microbubbles form, grow, and collapse in very short times, about a few microseconds. The formation and violent collapse of small vacuum bubbles takes place due to the ultrasonication waves generated in alternating high pressure and low pressure in liquids, and the phenomenon is known as cavitation. It causes high-speed imposing liquid jets and strong hydrodynamic shear forces. The deagglomeration of nanometer-

sized materials was carried out using these effects. In this aspect, for high-speed mixers and agitator bead mills, ultrasonication is an alternative.<sup>[17]</sup>

In the preparative chemist's toolkit, microwave heating is a valuable technique. Due to a modern scientific microwave apparatus, it is possible to access elevated temperatures in an easy, safe, and reproducible way.<sup>[18]</sup> In recent years, microwave-assisted organic synthesis (MAOs)<sup>[19]</sup> has been emerged as a new "lead" in organic synthesis. Important advantages of this technology include a highly accelerated rate of the reaction and a decrease in reaction time, with an increase in the yield and quality of the product. The current technique is considered an important method toward green chemistry as this technique is more environmentally friendly. The conventional method of organic synthesis usually needs a longer heating time; tedious apparatus setup, which results in the higher cost of the process; and the excessive use of solvents/reagents, which leads to environmental pollution. This growth of green chemistry

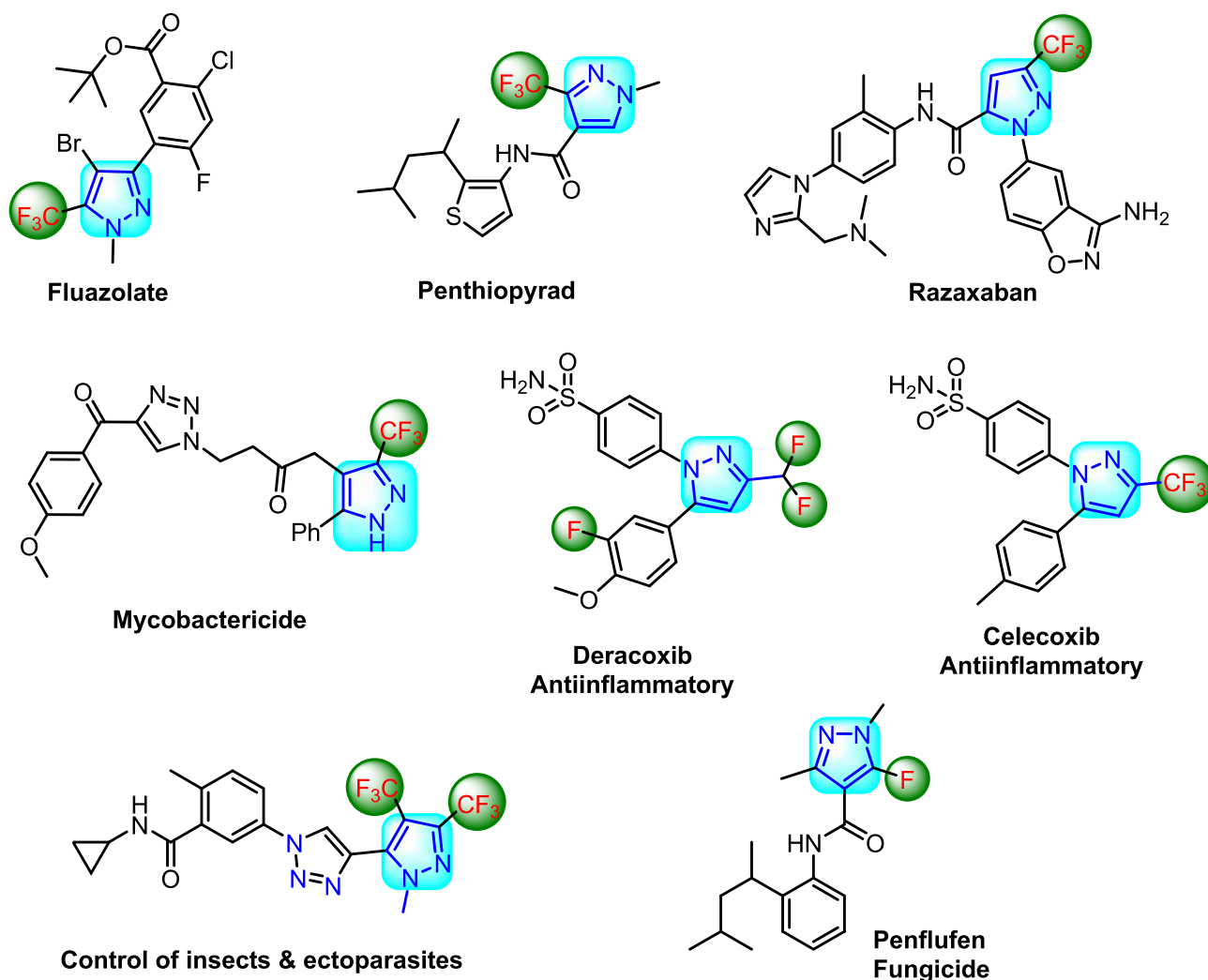


FIGURE 1 Structure of pyrazole- and fluorine-containing commercially available drugs

holds significant potential for a reduction of the byproduct, a reduction in waste production, and lowering of the energy costs. Due to its ability to couple directly with the reaction molecule and bypass thermal conductivity, leading to a rapid rise in the temperature, microwave irradiation has been used to improve many organic syntheses.<sup>[20]</sup> Knoevenagel condensation reactions are carried out by the condensation of aldehyde and the active methylene group using different catalysts such as piperidine,  $\text{InCl}_3$ ,  $\text{TiCl}_4$ ,  $\text{LiOH}$ ,  $\text{ZnCl}_2$ , and  $\text{NbCl}_5$ .<sup>[20,21]</sup> They are also carried out using  $\text{NaAlO}_2$ -promoted mesoporous catalysts,<sup>[22]</sup> ionic liquid,<sup>[23]</sup> monodisperse carbon nanotube-based NiCu nanohybrids,<sup>[24]</sup> and MAOs.<sup>[25]</sup> This is one of the most important methodologies used in synthetic organic chemistry for the formation of a C—C double bond.

From our study, the results demonstrated that green methodologies are less hazardous than classical synthesis methods, as well more efficient and economical and environmentally friendly; short reaction times and excellent yields are observed for those reactions in which conventional heating is replaced by microwave irradiation. Keeping in mind the 12 principles of green chemistry, in continuation of our research work,<sup>[26]</sup> and the advantages of microwave irradiation and activities associated with pyrazole and fluorine, we construct pyrazole and fluorine in one molecular framework as new 3-(trifluoromethyl)-1-(perfluorophenyl)-1*H*-pyrazol-5(4*H*)-one derivatives under conventional, as well as microwave, irradiation and ultrasonication and evaluated their anti-inflammatory and antioxidant activity. In addition to this, we have also performed *in silico* absorption, distribution, metabolism, and excretion (ADME) predictions for the synthesized compounds.

## 2 | RESULTS AND DISCUSSION

### 2.1 | Chemistry

A facile, economic, and green protocol for the cyclocondensation of 2-(perfluorophenyl)-5-(trifluoromethyl)-

2,4-dihydro-3*H*-pyrazol-3-one (**3**) with different aldehydes has been achieved.

The key starting material 3-(trifluoromethyl)-1-(perfluorophenyl)-1*H*-pyrazol-5(4*H*)-one (**3**) was synthesized by the condensation of 1-(perfluorophenyl)hydrazine (**1**) and ethyl 4,4,4-trifluoro-3-oxobutanoate (**2**) in ethanol<sup>[27]</sup> (Scheme 1).

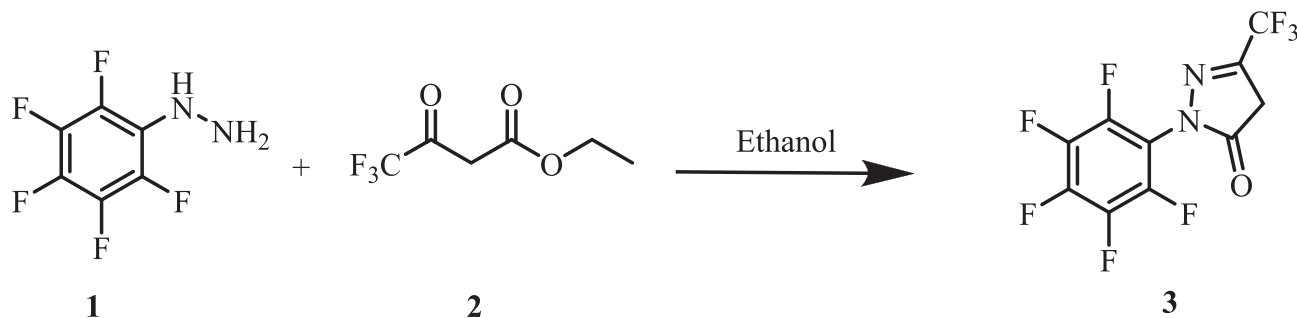
Initially, we carried out the reaction between 2-(perfluorophenyl)-5-(trifluoromethyl)-2,4-dihydro-3*H*-pyrazol-3-one (2 mmol) (**3**) and 1-phenyl-3-(thiophen-2-yl)-1*H*-pyrazole-4-carbaldehyde (2 mmol) refluxed in acetic acid as a model reaction (Scheme 2). Initially, the model reaction was carried out in ethanol without using acetic acid, and it was observed that a very low yield of product (20%) was obtained even after 2 hr. Therefore, improving the yield intervention of the catalyst was thought to be necessary. So, we decided to use acetic acid as a catalyst to promote this transformation at room temperature. At room temperature, the yield of product (45%) was found to be increased in 3 hr, so we decided to provide heating to the reaction mixture to achieve maximum product yield.

When the reaction mixture refluxed in acetic acid, product formation took place after 2 hr, and the yield of the product was 72% (Table 1).

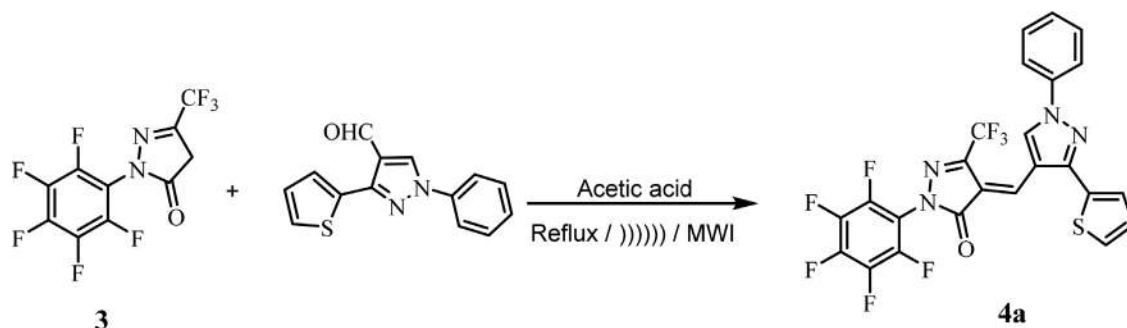
To check the ultrasonication's specific effect on this reaction, under ultrasound irradiation at 35–40°C, we carried out the model reaction using the optimized reaction conditions in hand to check whether the reaction could be accelerated with further improved product yield within a short reaction time (Scheme 2).

It was observed that, under ultrasonic conditions, the conversion rate of a reactant to product increased with less time (Table 1). Thus, when considering the basic green chemistry concept, ultrasonic irradiation was found to have a beneficial effect on the synthesis of Knoevenagel derivatives (**4a-d**, **5a-f**, and **6a-e**), which was superior to the traditional method with respect to yield and reaction time (Table 1).

To accomplish the goal and significance of green chemistry, the model reaction was carried out under



**SCHEME 1** Synthesis of 3-(trifluoromethyl)-1-(perfluorophenyl)-1*H*-pyrazol-5(4*H*)-one **3**



**SCHEME 2** Model reaction for conventional, ultrasonication, and microwave irradiation methods

**TABLE 1** Synthesis of 3-(trifluoromethyl)-1-(perfluorophenyl)-1H-pyrazol-5(4H)-one derivatives (**4a-d**, **5a-f**, and **6a-e**)

Cpd	R <sub>1</sub>	R <sub>2</sub>	R <sub>3</sub>	R <sub>4</sub>	m. p. (°C)	Conventional method <sup>a</sup>		Ultrasound method <sup>b</sup>		Microwave method <sup>c</sup>	
						Time (min)	Yield <sup>d</sup> (%)	Time (min)	Yield <sup>d</sup> (%)	Time (min)	Yield <sup>d</sup> (%)
<b>4a</b>	H	H	-	-	224–226	120	72	20	81	6.5	84
<b>4b</b>	Br	F	-	-	232–234	120	75	18	78	6.5	81
<b>4c</b>	Cl	H	-	-	216–218	120	70	20	76	6.0	80
<b>4d</b>	Br	H	-	-	230–232	120	64	16	70	6.5	76
<b>5a</b>	H	H	OMe	-	202–204	120	70	21	76	5.5	84
<b>5b</b>	H	H	H	-	186–188	120	66	17	72	6.0	80
<b>5c</b>	F	H	OMe	-	180–182	120	68	16	75	7.0	82
<b>5d</b>	H	H	Me	-	206–208	120	65	16	71	6.5	79
<b>5e</b>	H	H	OCF <sub>3</sub>	-	142–144	120	62	18	70	6.5	76
<b>5f</b>	H	Cl	Cl	-	212–214	120	70	19	80	5.5	84
<b>6a</b>	Me	Cl	Me	H	188–190	120	66	18	76	6.0	78
<b>6b</b>	H	Cl	Me	H	180–182	120	62	17	72	7.5	75
<b>6c</b>	H	Cl	H	H	176–178	120	59	18	79	7.0	80
<b>6d</b>	H	Cl	H	Cl	212–214	120	64	20	72	7.0	78
<b>6e</b>	H	H	Me	H	180–182	120	60	18	80	7.5	82

Abbreviation: Cpd, compound.

<sup>a</sup>Reaction conditions: Compound (**3**) (2 mmol) and 1-phenyl-3-(thiophen-2-yl)-1H-pyrazole-4-carbaldehyde (2 mmol) refluxed in acetic acid.

<sup>b</sup>Compound (**3**) (2 mmol) and 1-phenyl-3-(thiophen-2-yl)-1H-pyrazole-4-carbaldehyde (2 mmol) in acetic acid under ultrasound irradiation.

<sup>c</sup>Compound (**3**) (2 mmol) and 1-phenyl-3-(thiophen-2-yl)-1H-pyrazole-4-carbaldehyde (2 mmol) in acetic acid under microwave irradiation.

<sup>d</sup>Isolated yield. m.p.: melting point.

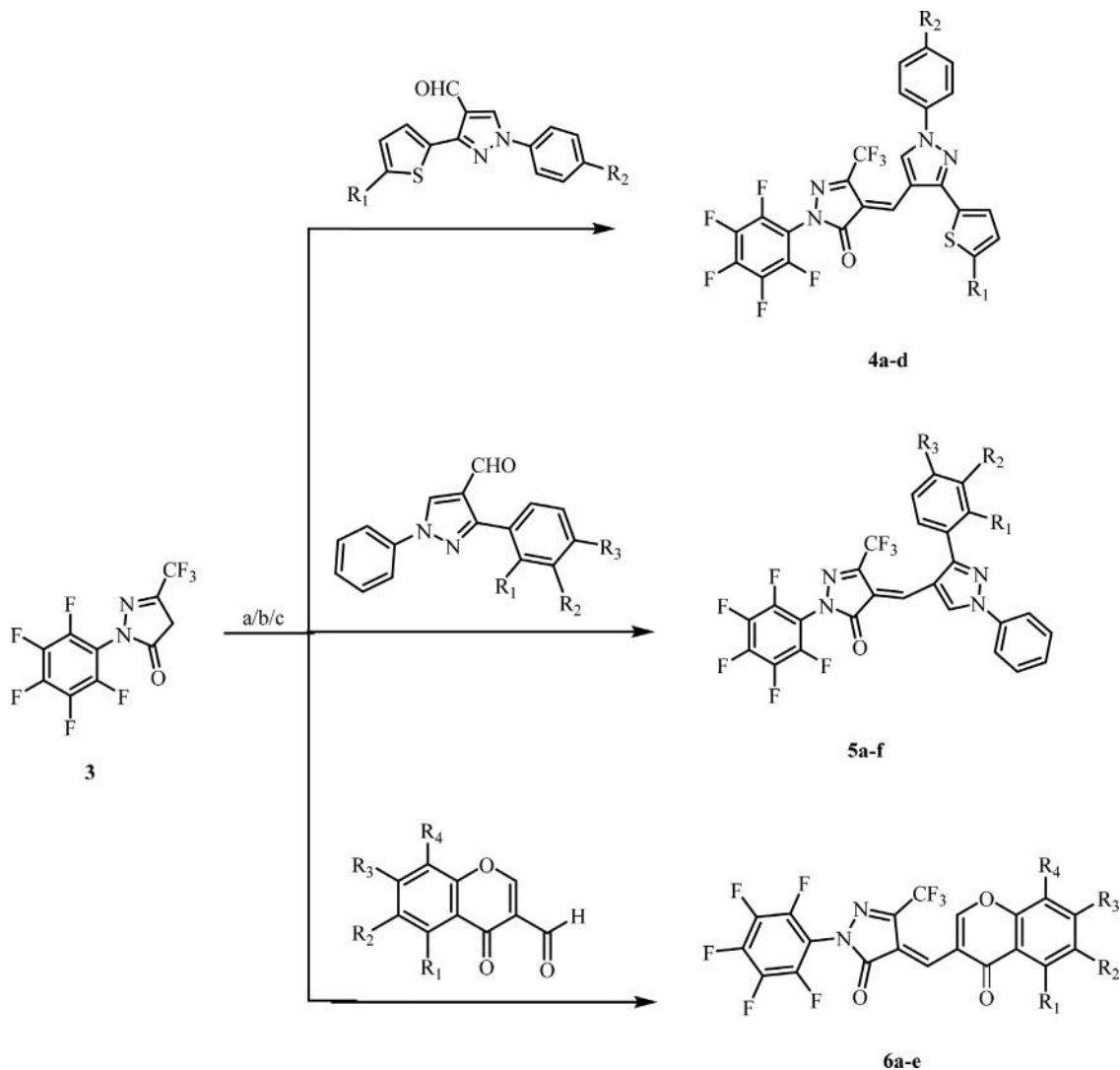
microwave irradiation for a period of time indicated in Table 1 at 350 W (Scheme 2). Fortunately, the product formation occurred in 6.5 min, with an 84% increase in yield.

So, from the above experiments, it can be concluded that, when the reaction was carried out under the conventional method, it gave comparatively low yields of products with longer reaction times, while the same reaction carried out under the influence of ultrasonic irradiation and microwave irradiation gave excellent yields of the products in short reaction times.

Finally, we assessed the scope and generality of this method for the Knoevenagel condensation between 2-(perfluorophenyl)-5-(trifluoromethyl)-2,4-dihydro-3H-pyrazol-3-one (**3**) and different aldehydes (Scheme 3), achieved under conventional and nonconventional methods like the ultrasound and microwave methods, respectively. With respect to the substituent present on the aromatic ring of aldehyde, under the optimized conditions, the corresponding products were obtained in high to excellent yields (Table 1).

More importantly, hetero aryl aldehydes were observed to be well tolerated under optimized conditions,





**SCHEME 3** Synthesis of 3-(trifluoromethyl)-1-(perfluorophenyl)-1H-pyrazol-5(4H)-one derivatives (**4a-d**, **5a-f**, and **6a-e**). Reaction conditions: **a** = Refluxed in acetic acid. **b** = Under ultrasound irradiation in acetic acid. **c** = Under microwave irradiation using acetic acid as a solvent

furnishing the product in good yields. All the synthesized compounds (**4a-d**, **5a-f**, and **6a-e**) were confirmed by IR, <sup>1</sup>H NMR, <sup>13</sup>C NMR, and mass spectra.

The formation of (4*E*)-3-(trifluoromethyl)-1-(perfluorophenyl)-4-((1-phenyl-3-(thiophen-2-yl)-1*H*-pyrazol-4-yl)methylene)-1*H*-pyrazol-5(4*H*)-one **4a-d** was confirmed by IR, <sup>1</sup>H NMR, <sup>13</sup>C NMR, and mass spectra. In the IR spectrum of compound **4a**, the peaks observed at 1,681 cm<sup>-1</sup> indicate the presence of C=O group. In the <sup>1</sup>H NMR spectrum of compound **4a**, two singlets were observed at δ 8.11 and 10.10 ppm for pyrazolyl and olefinic proton, respectively. The <sup>13</sup>C NMR spectrum of compound **4a** revealed that the peak appearing at δ 161.4 ppm is due to the presence of carbonyl carbon. The structure of compound **4a** was also confirmed by a molecular ion peak at *m/z* 555.01 (M + H)<sup>+</sup>. Similarly, the

synthesis of (4*E*)-3-(trifluoromethyl)-1-(perfluorophenyl)-4-((1,3-diphenyl-1*H*-pyrazol-4-yl)methylene)-1*H*-pyrazol-5(4*H*)-ones **5a-f** was also confirmed by spectral techniques. In the IR spectrum of compound **5a**, the peak observed at 1,701 cm<sup>-1</sup> corresponded to the C=O group. In the <sup>1</sup>H NMR spectrum of compound **5a**, the three singlets observed at δ 3.92, 8.11, and 10.10 ppm confirm the presence of -OCH<sub>3</sub>, pyrazolyl proton, and olefinic proton, respectively. The <sup>13</sup>C NMR spectrum of compound **5a** showed peaks at δ 162.5 and 55.5 ppm, confirming the presence of carbonyl carbon and methoxy carbon, respectively. Furthermore, the structure of compound **5a** was also confirmed by a molecular ion peak at *m/z* 573.21 (M + H)<sup>+</sup>.

Furthermore, the formation of (Z)-4-([4-oxo-4*H*-chromen-3-yl]methylene)-2-(perfluorophenyl)-5-(trifluoromethyl)-2,4-dihydro-3*H*-pyrazol-3-one **6a-e** was

confirmed by various spectral techniques. The IR spectrum of compound **6a** showed absorption peaks at 1,707 and 1,666  $\text{cm}^{-1}$  corresponding to two carbonyl groups present in the molecules. The  $^1\text{H}$  NMR spectrum of compound **6a** showed four singlets at  $\delta$  2.54 and  $\delta$  3.01 ppm for two  $-\text{CH}_3$ ,  $\delta$  8.50 ppm for chromone ring proton, and  $\delta$  10.54 ppm for olefinic proton. The  $^{13}\text{C}$  NMR spectrum of compound **6a** showed that two signals appear at  $\delta$  175.4 and 164.2 ppm for the carbonyl carbon of chromone and pyrazolone ring, respectively. In addition, two signals for methyl carbon appear at  $\delta$  22.2 and 18.6 ppm. The structure of compound **6a** was also confirmed by mass spectra and by a molecular ion peak observed at  $m/z$  537.11 ( $\text{M} + \text{H}$ ) $^+$ . Similarly, all the synthesized compounds were characterized by the spectral analysis. Structures of all the synthesized derivatives are shown in Figure S1 (Supporting Information).

## 2.2 | Biological activity

### 2.2.1 | Anti-inflammatory activity

The newly synthesized 3-(trifluoromethyl)-1-(perfluorophenyl)-1*H*-pyrazol-5(4*H*)-one derivatives (**4a-d**, **5a-f**, and **6a-e**) ( $\text{EC}_{50}$  range =  $0.6483 \pm 0.221$ – $0.8519 \pm 0.281$   $\mu\text{g}/\text{ml}$ ) exhibited moderate anti-inflammatory activity compared to the standard drug diclofenac sodium. Among all the synthesized compounds, except compounds **4c**, **5c**, **5e**, **6d**, and **6e**, all other compounds exhibited a minimum inhibitory concentration (MIC) of 200  $\mu\text{g}/\text{ml}$  compared to the standard drug diclofenac sodium (Table 2).

The percent inhibition of compounds in the in vitro anti-inflammatory model is shown in Figure 2. Furthermore, the comparative percent inhibition of compounds in the in vitro anti-inflammatory model is shown in Figure 3.

### 2.2.2 | Antioxidant activity

In the present study, antioxidant activity of the synthesized compounds has been assessed in vitro by the DPPH radical scavenging assay.<sup>[28]</sup> Ascorbic acid (AA) has been used as a standard drug for the comparison of antioxidant activity, and the observed results are summarized in Table 2.

According to the DPPH assay, compounds **5a**, **5d**, **5e**, **5f**, **6a**, **6b**, and **6e** ( $\text{IC}_{50}$  = <100  $\mu\text{g}/\text{ml}$ ) exhibited excellent antioxidant activity compared to the standard antioxidant drug AA ( $\text{IC}_{50}$  = <50  $\mu\text{g}/\text{ml}$ ). The remaining synthesized compounds display comparable antioxidant activity than

**TABLE 2** Anti-inflammatory and antioxidant activity of 3-(trifluoromethyl)-1-(perfluorophenyl)-1*H*-pyrazol-5(4*H*)-one derivatives (MIC in  $\mu\text{g}/\text{ml}$ )

Compound	Anti-inflammatory	Antioxidant
<b>4a</b>	200	>100
<b>4b</b>	200	>400
<b>4c</b>	400	>200
<b>4d</b>	200	>200
<b>5a</b>	200	<100
<b>5b</b>	200	>200
<b>5c</b>	NT	NT
<b>5d</b>	200	<100
<b>5e</b>	800	<100
<b>5f</b>	200	<100
<b>6a</b>	200	<100
<b>6b</b>	200	<100
<b>6c</b>	200	>200
<b>6d</b>	800	>100
<b>6e</b>	400	<100
Diclofenac sodium	50	-
Ascorbic acid	-	<50

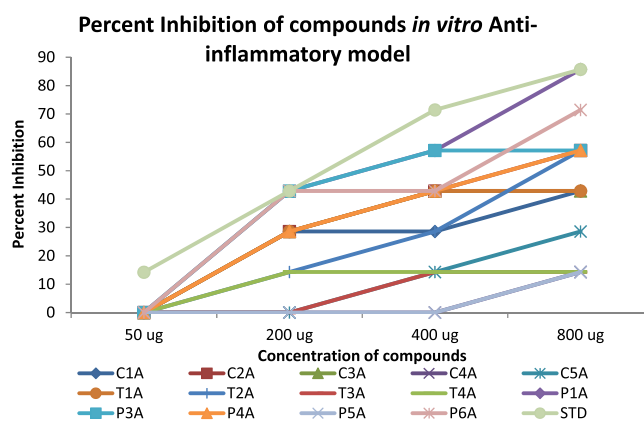


**FIGURE 2** The percent inhibition of compounds in an in vitro anti-inflammatory model

the standard drug butylated hydroxytoluene (Table 2). The percent inhibition of compounds in the in vitro antioxidant model is shown in Figure 4.

## 2.3 | Computational study

### 2.3.1 | In silico ADME

An important task for the lead compounds is early prediction of drug likeness properties as it resolves the cost

**FIGURE 3** The comparative percent inhibition of compounds in an in vitro anti-inflammatory model

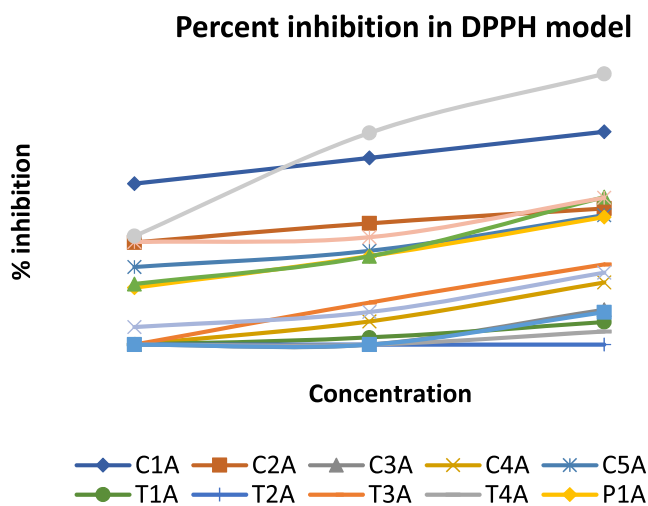
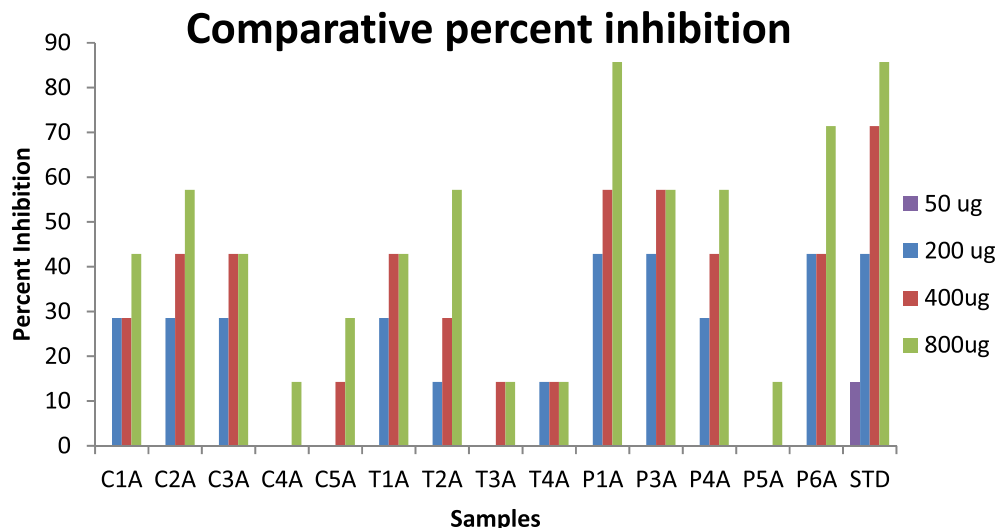


**FIGURE 4** The percent inhibition of compounds in an in vitro antioxidant model

and time issues of drug development and discovery. Due to the inadequate drug likeness properties of many active agents with a significant biological activity, these compounds have failed in clinical trials.<sup>[29]</sup> On the basis of Lipinski's rule of five, the drug likeness properties were analyzed by ADME parameters using the Molinspiration online property calculation toolkit,<sup>[30]</sup> and data are summarized in Table 3.

All the compounds exhibited noteworthy values for the various parameters analyzed and showed good drug-like characteristics based on Lipinski's rule of five and its variants, which characterized these agents to be likely orally active. For the synthesized compound **6e**, the data obtained were within the range of accepted values. Parameters such as the number of rotatable bonds and total polar surface area are linked with the intestinal absorption; results showed that all

synthesized compounds had good absorption. The in silico assessment of all the synthetic compounds has shown that they have very good pharmacokinetic properties, which are reflected in their physicochemical values, thus ultimately enhancing the pharmacological properties of these molecules.

### 3 | EXPERIMENTAL SECTION

All organic solvents were acquired from Poona Chemical Laboratory, Pune and Research-Lab Fine Chem Industries, Mumbai and were used as such without further purification. The melting points were measured on a DBK melting point apparatus and are uncorrected. Microwave irradiation was carried out in Raga's synthetic microwave oven. IR spectra were recorded on Shimadzu IR Affinity 1S (ATR) fourier transform infrared spectrophotometer. <sup>1</sup>H NMR (500 MHz) and <sup>13</sup>C NMR (125 MHz) spectra were recorded on Bruker Advance neo 500 spectrophotometers using tetramethylsilane as an internal standard, and CDCl<sub>3</sub> and dimethyl sulphoxide-*d*<sub>6</sub> as solvent and chemical shifts, respectively, were expressed as  $\delta$  ppm units. Mass spectra were obtained on Waters quadrupole time-of-flight micromass (ESI-MS) mass spectrometer.

#### 3.1 | General procedure for the synthesis of synthesize new 3-(trifluoromethyl)-1-(perfluorophenyl)-1H-pyrazol-5(4H)-one derivatives (4a-d, 5a-f and 6a-e)

**Conventional method:** An equimolar amount of 2-(perfluorophenyl)-5-(trifluoromethyl)-2,4-dihydro-3H-pyrazol-3-

TABLE 3 Pharmacokinetic parameters of (4a-d, 5a-f, and 6a-e) compounds

Entry	% ABS	TPSA (Å <sup>2</sup> )	n-ROTBT	MV	MW	miLog P	n-ON	n-OHNH	Lipinski violation	Drug likeness model score
Rule	-	-	-	-	<500	≤5	<10	<5	≤1	-
4a	90.81	52.72	5	397.75	554.42	5.83	5	0	2	-0.68
4b	90.81	52.72	5	420.56	651.31	6.92	5	0	2	-0.84
4c	90.81	52.72	5	411.28	588.87	6.63	5	0	2	-0.25
4d	90.81	52.72	5	415.63	633.32	6.76	5	0	2	-0.56
5a	87.62	61.96	6	432.58	578.42	6.10	6	0	2	-0.46
5b	90.81	52.72	5	407.04	548.39	6.04	5	0	2	-0.80
5c	87.62	61.96	6	437.51	596.41	6.19	6	0	2	-0.22
5d	90.81	52.72	5	423.60	562.42	6.49	5	0	2	-0.51
5e	87.62	61.96	7	447.32	632.39	7.01	6	0	2	-0.45
5f	90.81	52.72	5	434.11	617.28	7.33	5	0	2	-0.36
6a	86.53	65.11	3	374.21	536.76	6.25	5	0	2	-0.53
6b	86.53	65.11	3	357.65	522.74	5.87	5	0	2	-0.36
6c	86.53	65.11	3	341.09	508.71	5.49	5	0	2	-0.32
6d	86.53	65.11	3	354.62	543.15	6.10	5	0	2	-0.93
6e	86.53	65.11	3	344.11	488.29	5.26	5	0	1	-0.81

Abbreviations: % ABS, percentage absorption; TPSA, topological polar surface area; n-ROTBT, number of rotatable bonds; MV, molecular volume; MW, molecular weight; miLogP, logarithm of partition coefficient of compound between n-octanol and water; n-ON acceptors, number of hydrogen bond acceptors; n-OHNH donors, number of hydrogen bonds donors.

one (3) (0.002 mol) and substituted aldehydes (0.002 mol) was taken in a round-bottom flask using glacial acetic acid (5 ml) as a solvent and were refluxed for the period of time indicated in Table 1. The progress of the reaction was monitored by thin layer chromatography (TLC). After completion of reaction, the mixture was cooled and poured into ice-cold water. The obtained solid was filtered and washed with water and dried and purified by crystallization from ethyl acetate to obtain pure compounds (4a-d, 5a-f, and 6a-e).

**Ultrasound method:** A mixture of 2-(perfluorophenyl)-5-(trifluoromethyl)-2,4-dihydro-3H-pyrazol-3-one (3) (0.002 mol) and substituted aldehydes (0.002 mol) in acetic acid (5 ml) was taken in a 50-ml round-bottom flask. The mixture was irradiated in the water bath of an ultrasonic cleaner at 35–40°C for a period of time indicated in Table 1. After completion of the reaction (monitored by TLC), the mixture was poured into ice-cold water, and the obtained solid was collected by simple filtration and washed successively with water. The crude product was purified by crystallization from ethyl acetate to obtain pure compounds (4a-d, 5a-f, and 6a-e).

**Microwave irradiation method:** An equimolar amount of 2-(perfluorophenyl)-5-(trifluoromethyl)-

2,4-dihydro-3H-pyrazol-3-one (3) (0.002 mol) and substituted aldehydes (0.002 mol) was taken in a round-bottom flask (RBF) using glacial acetic acid (5 ml) as a solvent, and the contents of RBF were subjected to MW irradiation for the period of time indicated in Table 1 at 350 W. The progress of the reaction was monitored by TLC. After completion of reaction, the mixture was cooled and poured into ice-cold water. The obtained solid was filtered and washed with water and dried and purified by crystallization from ethyl acetate to obtain pure compounds (4a-d, 5a-f, and 6a-e).

### 3.1.1 | (4E)-3-(Trifluoromethyl)-1-(perfluorophenyl)-4-((1-phenyl-3-(thiophen-2-yl)-1H-pyrazol-4-yl)methylene)-1H-pyrazol-5(4H)-one (4a)

Orange solid; Wt. 930 mg, Yield 84%; IR( $\nu_{\max}$ /cm<sup>-1</sup>): 2,926 (=C-H), 1,681 (C=O), 1,598 (C=N), 1,519 (C=C), 1,234 (C-F); <sup>1</sup>H NMR spectrum,  $\delta$ , ppm: 7.35–7.91 (m, 8H, Ar-H), 8.11 (s, 1H, pyrazolyl-H), 10.10 (s, 1H, =C-H); <sup>13</sup>C NMR spectrum,  $\delta_c$ , ppm: 161.4 (C=O), 151.7, 140.1, 137.8, 134.9, 131.1, 130.0, 129.6, 129.1,



128.70, 128.6, 119.7, 115.7, 113.5; MS (ESI-MS):  $m/z$  555.01 (M + H)<sup>+</sup>.

### 3.1.2 | (4E)-4-((3-(5-Bromothiophen-2-yl)-1-(4-fluorophenyl)-1H-pyrazol-4-yl)methylene)-3-(trifluoromethyl)-1-(perfluorophenyl)-1H-pyrazol-5(4H)-one (4b)

Orange solid; Wt. 1.05 g; Yield 81%; IR ( $\nu_{\max}/\text{cm}^{-1}$ ): 2,927 (C–H), 1,680 (C=O), 1,598 (C=N), 1,516 (C=C), 1,231 (C–F); <sup>1</sup>H NMR spectrum,  $\delta$ , ppm: 7.16 (d, 1H,  $J$  = 3.50 Hz, Ar–H), 7.26–7.19 (m, 3H, Ar–H), 7.84 (dd, 2H,  $J$  = 5.00 Hz and 9.00 Hz, Ar–H), 8.10 (s, 1H, pyrazole-H), 10.11 (s, 1H, =C–H); MS:  $m/z$  651.03 (M + H)<sup>+</sup>.

### 3.1.3 | (4E)-4-((3-[5-Chlorothiophen-2-yl]-1-phenyl-1H-pyrazol-4-yl)methylene)-3-(trifluoromethyl)-1-(perfluorophenyl)-1H-pyrazol-5(4H)-one (4c)

Orange solid; Wt. 873 mg; Yield 80%; IR ( $\nu_{\max}/\text{cm}^{-1}$ ): 2,926 (C–H), 1,682 (C=O), 1,597 (C=N), 1,518 (C=C), 1,232 (C–F); <sup>1</sup>H NMR spectrum,  $\delta$ , ppm: 7.07 (s, 1H, Ar–H), 7.26–7.18 (s, 1H, Ar–H), 7.44 (d, 1H,  $J$  = 6.00 Hz, Ar–H), 7.52 (m, 2H, Ar–H), 7.86 (d, 2H,  $J$  = 7.00 Hz, Ar–H), 8.11 (s, 1H, pyrazole-H), 10.16 (s, 1H, =C–H); <sup>13</sup>C NMR spectrum,  $\delta_{\text{C}}$ , ppm: 162.4 (C=O), 151.3, 139.5, 138.3, 135.0, 133.5, 130.8, 130.0, 128.8, 127.6, 127.4, 120.0, 116.3, 114.6; MS:  $m/z$  547.11 (M + H)<sup>+</sup>.

### 3.1.4 | (4E)-4-((3-(5-Bromothiophen-2-yl)-1-phenyl-1H-pyrazol-4-yl)methylene)-3-(trifluoromethyl)-1-(perfluorophenyl)-1H-pyrazol-5(4H)-one (4d)

Orange solid; Wt. 960 mg; Yield 76%; IR ( $\nu_{\max}/\text{cm}^{-1}$ ): 2,926 (C–H), 1,681 (C=O), 1,597 (C=N), 1,520 (C=C), 1,235 (C–F); <sup>1</sup>H NMR spectrum,  $\delta$ , ppm: 7.16 (d, 1H,  $J$  = 4.00 Hz, Ar–H), 7.21 (d, 1H,  $J$  = 3.50 Hz, Ar–H), 7.44 (t, 1H,  $J$  = 7.50 Hz, Ar–H), 7.52 (t, 2H,  $J$  = 7.50 Hz, Ar–H), 7.75–7.86 (d, 2H,  $J$  = 7.50 Hz, Ar–H), 8.47 (s, 1H, pyrazole-H), 10.16 (s, 1H, =C–H); <sup>13</sup>C NMR spectrum,  $\delta_{\text{C}}$ , ppm: 183.2 (C=O), 162.3, 151.2, 143.2, 142.9, 139.4, 138.3, 134.9, 133.7, 133.4, 131.2, 130.6, 129.8, 129.1, 128.8, 128.5, 128.2, 120.6, 119.9, 119.6, 116.2, 115.9, 114.6; MS:  $m/z$  633.05 (M + H).

### 3.1.5 | (4Z)-3-(Trifluoromethyl)-4-((3-[4-methoxyphenyl]-1-phenyl-1H-pyrazol-4-yl)methylene)-1-(perfluorophenyl)-1H-pyrazol-5(4H)-one (5a)

Orange solid; Wt. 971 mg; Yield 84%; IR ( $\nu_{\max}/\text{cm}^{-1}$ ): 3,141 (C–H), 1,703 (C=O), 1,595 (C=N), 1,514 (C=C), 1,224 (C–F); <sup>1</sup>H NMR spectrum,  $\delta$ , ppm: 3.92 (s, 3H, –OCH<sub>3</sub>), 7.10 (d, 2H,  $J$  = 8.50 Hz, Ar–H), 7.51 (t, 2H,  $J$  = 8.50 Hz, Ar–H), 7.62 (d, 2H,  $J$  = 8.50 Hz, Ar–H), 7.90 (d, 2H,  $J$  = 9.00 Hz, Ar–H), 7.99 (s, 1H, pyrazole-H), 10.19 (s, 1H, =C–H); <sup>13</sup>C NMR spectrum,  $\delta_{\text{C}}$ , ppm: 162.5 (C=O), 161.1, 158.7, 143.3, 141.4, 138.6, 134.9, 130.7, 129.7, 128.5, 122.6, 120.1, 116.8, 114.7, 113.7, 55.5 (OCH<sub>3</sub>); MS:  $m/z$  579.21 (M + H)<sup>+</sup>.

### 3.1.6 | (4Z)-3-(Trifluoromethyl)-1-(perfluorophenyl)-4-([1,3-diphenyl-1H-pyrazol-4-yl)methylene)-1H-pyrazol-5(4H)-one (5b)

Orange solid; Wt. 876 mg; Yield 80%; IR ( $\nu_{\max}/\text{cm}^{-1}$ ): 3,142 (C–H), 1,701 (C=O), 1,595 (C=N), 1,510 (C=C), 1,223 (C–F); <sup>1</sup>H NMR spectrum,  $\delta$ , ppm: 7.42 (m, 1H, Ar–H), 7.52 (t, 2H,  $J$  = 7.50 Hz, Ar–H), 7.57–7.58 (m, 3H, Ar–H), 7.68 (dd, 2H,  $J$  = 7.50 and 2.00 Hz, Ar–H), 7.90 (d, 2H,  $J$  = 8.00 Hz, Ar–H), 8.00 (s, 1H, pyrazole-H), 10.22 (s, 1H, =C–H); <sup>13</sup>C NMR spectrum,  $\delta_{\text{C}}$ , ppm: 162.5 (C=O), 158.8, 143.0, 141.2, 138.6, 134.9, 130.3, 129.9, 129.7, 129.4, 129.2, 128.6, 120.0, 116.8, 114.0; MS:  $m/z$  549.19 (M + H)<sup>+</sup>.

### 3.1.7 | (4Z)-4-((3-[2-Fluoro-4-methoxyphenyl]-1-phenyl-1H-pyrazol-4-yl)methylene)-3-(trifluoromethyl)-1-(perfluorophenyl)-1H-pyrazol-5(4H)-one (5c)

Orange solid; Wt. 1.06 g; Yield 82%; IR ( $\nu_{\max}/\text{cm}^{-1}$ ): 3,145 (C–H), 1,702 (C=O), 1,596 (C=N), 1,512 (C=C), 1,221 (C–F); <sup>1</sup>H NMR spectrum,  $\delta$ , ppm: 3.91 (s, 3H, –OCH<sub>3</sub>), 6.82 (dd, 1H,  $J$  = 2.50 and 12.00 Hz, Ar–H), 6.91 (dd, 1H,  $J$  = 2.00 and 8.50 Hz, Ar–H), 7.42 (t, 1H,  $J$  = 7.50 Hz, Ar–H), 7.58–7.49 (m, 2H, Ar–H), 7.79 (d, 1H,  $J$  = 2.50 Hz, Ar–H), 7.88 (d, 2H,  $J$  = 7.50 Hz, Ar–H), 8.52 (s, 1H, pyrazole-H), 10.20 (s, 1H, =C–H); <sup>13</sup>C NMR spectrum,  $\delta_{\text{C}}$ , ppm: 162.7 (C=O), 162.6, 162.5, 154.1, 141.2, 138.6, 134.7, 132.5, 129.7, 128.5, 120.0, 117.6, 113.9, 111.2, 110.3, 102.2, 102.0, 55.8 (OCH<sub>3</sub>); MS:  $m/z$  653.26 (M + H)<sup>+</sup>.

### 3.1.8 | (4Z)-3-(Trifluoromethyl)-1-(perfluorophenyl)-4-([1-phenyl-3-p-tolyl-1H-pyrazol-4-yl]methylene)-1H-pyrazol-5(4H)-one (5d)

Orange solid; Wt. 887 mg; Yield 79%; IR ( $\nu_{\max}/\text{cm}^{-1}$ ): 3,143 (=C–H), 1,701 (C=O), 1,594 (C=N), 1,511 (C=C), 1,220 (C–F);  $^1\text{H}$  NMR spectrum,  $\delta$ , ppm: 2.44 (s, 3H, –CH<sub>3</sub>), 7.45 (d, 1H,  $J = 7.50$  Hz, Ar–H), 7.51 (t, 1H,  $J = 7.50$  Hz, Ar–H), 7.62 (d, 1H,  $J = 8.00$  Hz, Ar–H), 7.65 (d, 1H,  $J = 8.00$  Hz, Ar–H), 9.90 (s, 1H, pyrazole-H), 11.96 (s, 1H, =C–H); MS:  $m/z$  563.08 (M + H)<sup>+</sup>.

### 3.1.9 | (4Z)-3-(Trifluoromethyl)-1-(perfluorophenyl)-4-((1-phenyl-3-(4-[trifluoro methoxy]phenyl)-1H-pyrazol-4-yl)methylene)-1H-pyrazol-5(4H)-one (5e)

Orange solid; Wt. 960 mg; Yield 76%; IR ( $\nu_{\max}/\text{cm}^{-1}$ ): 3,145 (=C–H), 1,700 (C=O), 1,595 (C=N), 1,517 (C=C), 1,225 (C–F);  $^1\text{H}$  NMR spectrum,  $\delta$ , ppm: 7.42–7.44 (m, 3H, Ar–H), 7.51–7.54 (m, 2H, Ar–H), 7.71 (d, 1H,  $J = 2.00$  Hz, Ar–H), 7.73 (d, 1H,  $J = 2.00$  Hz, Ar–H), 7.88 (d, 1H,  $J = 2.00$  Hz, Ar–H), 7.90 (d, 1H,  $J = 3.50$  Hz, Ar–H), 7.92 (s, 1H, pyrazole-H), 10.21 (s, 1H, =C–H);  $^{13}\text{C}$  NMR spectrum,  $\delta_{\text{C}}$ , ppm: 162.4 (C=O), 157.3, 150.5, 143.2, 142.9, 140.3, 138.5, 134.9, 130.9, 129.8, 129.0, 128.7, 121.5, 120.6, 120.0, 118.4, 116.6, 114.4; MS:  $m/z$  633.23 (M + H)<sup>+</sup>.

### 3.1.10 | (4Z)-4-((3-[3,4-Dichlorophenyl]-1-phenyl-1H-pyrazol-4-yl)methylene)-3-(trifluoromethyl)-1-(perfluorophenyl)-1H-pyrazol-5(4H)-one (5f)

Orange solid; Wt. 1.03 g; Yield 84%; IR ( $\nu_{\max}/\text{cm}^{-1}$ ): 3,144 (=C–H), 1,701 (C=O), 1,596 (C=N), 1,517 (C=C), 1,227 (C–F);  $^1\text{H}$  NMR spectrum,  $\delta$ , ppm: 7.44 (m, 1H, Ar–H), 7.48 (d, 1H,  $J = 2.00$  Hz, Ar–H), 7.50 (d, 1H,  $J = 2.00$  Hz, Ar–H), 7.53 (d, 1H,  $J = 7.50$  Hz, Ar–H), 7.67 (d, 1H,  $J = 8.50$  Hz, Ar–H), 7.83 (d, 1H,  $J = 2.00$  Hz, Ar–H), 7.87–7.89 (m, 2H, Ar–H), 7.89 (s, 1H, pyrazole-H), 10.18 (s, 1H, =C–H);  $^{13}\text{C}$  NMR spectrum,  $\delta_{\text{C}}$ , ppm: 162.3 (C=O), 156.1, 143.2, 142.9, 139.7, 138.4, 135.0, 134.5, 133.7, 131.2, 131.1, 130.3, 129.8, 128.8, 128.3, 120.0, 116.4, 114.7; MS:  $m/z$  617.15 (M + H)<sup>+</sup>.

### 3.1.11 | (Z)-4-([6-Chloro-5,7-dimethyl-4-oxo-4H-chromen-3-yl]methylene)-2-(perfluorophenyl)-5-(trifluoromethyl)-2,4-dihydro-3H-pyrazol-3-one (6a)

Orange solid; Wt. 900 mg; Yield 84%; IR ( $\nu_{\max}/\text{cm}^{-1}$ ): 3,074 (=C–H), 1,707 (C=O), 1,666 (C=O), 1,624 (C=N), 1,508 (C=C), 1,192 (C–F);  $^1\text{H}$  NMR spectrum,  $\delta$ , ppm: 2.54 (s, 3H, –CH<sub>3</sub>), 3.01 (s, 3H, –CH<sub>3</sub>), 7.26 (s, 1H, Ar–H), 8.50 (s, 1H, chromone-H), 10.54 (s, 1H, =C–H);  $^{13}\text{C}$  NMR spectrum,  $\delta_{\text{C}}$ , ppm: 175.4 (C=O), 164.2 (C=O), 162.3, 155.1, 144.5, 143.4, 143.3, 139.7, 134.7, 120.9, 120.2, 119.4, 118.3, 118.2, 118.1, 22.2 (–CH<sub>3</sub>), 18.6 (–CH<sub>3</sub>); MS:  $m/z$  537.11 (M + H)<sup>+</sup>.

### 3.1.12 | (Z)-4-([6-Chloro-7-methyl-4-oxo-4H-chromen-3-yl]methylene)-2-(perfluorophenyl)-5-(trifluoromethyl)-2,4-dihydro-3H-pyrazol-3-one (6b)

Orange solid; Wt. 783 mg; Yield 75%; IR ( $\nu_{\max}/\text{cm}^{-1}$ ): 3,076 (=C–H), 1,705 (C=O), 1,664 (C=O), 1,627 (C=N), 1,508 (C=C), 1,192 (C–F);  $^1\text{H}$  NMR spectrum,  $\delta$ , ppm: 2.54 (s, 3H, –CH<sub>3</sub>), 7.47 (s, 1H, Ar–H), 8.24 (s, 1H, Ar–H), 8.48 (s, 1H, chromone-H), 10.62 (s, 1H, =C–H); MS:  $m/z$  523.08 (M + H)<sup>+</sup>.

### 3.1.13 | (Z)-4-([6-Chloro-4-oxo-4H-chromen-3-yl]methylene)-2-(perfluorophenyl)-5-(trifluoromethyl)-2,4-dihydro-3H-pyrazol-3-one (6c)

Orange solid; Wt. 812 mg; Yield 80%; IR ( $\nu_{\max}/\text{cm}^{-1}$ ): 3,074 (=C–H), 1,707 (C=O), 1,662 (C=O), 1,621 (C=N), 1,509 (C=C), 1,193 (C–F);  $^1\text{H}$  NMR spectrum,  $\delta$ , ppm: 7.55 (d, 1H,  $J = 9.00$  Hz, Ar–H), 7.73 (d, 1H,  $J = 2.50$  and  $9.00$  Hz, Ar–H), 8.26 (d, 1H,  $J = 2.50$  Hz, Ar–H), 8.47 (s, 1H, chromone-H), 10.63 (s, 1H, =C–H); MS:  $m/z$  509.08 (M + H)<sup>+</sup>.

### 3.1.14 | (Z)-4-([6,8-Dichloro-4-oxo-4H-chromen-3-yl]methylene)-2-(perfluorophenyl)-5-(trifluoromethyl)-2,4-dihydro-3H-pyrazol-3-one (6d)

Orange solid; Wt. 845 mg; Yield 78%; IR ( $\nu_{\max}/\text{cm}^{-1}$ ): 3,078 (=C–H), 1,707 (C=O), 1,665 (C=O), 1,626 (C=N), 1,506 (C=C), 1,194 (C–F);  $^1\text{H}$  NMR spectrum,  $\delta$ , ppm: 7.83 (d, 1H,  $J = 2.50$  Hz, Ar–H), 8.17 (d, 1H,  $J = 2.50$  Hz, Ar–H), 8.40 (s, 1H, chromone-H), 10.66 (s, 1H, =C–H); MS:  $m/z$  543.07 (M + H)<sup>+</sup>.

### 3.1.15 | (Z)-4-([7-Methyl-4-oxo-4H-chromen-3-yl]methylene)-2-(perfluorophenyl)-5-(trifluoromethyl)-2,4-dihydro-3H-pyrazol-3-one (6e)

Orange solid; Wt. 800 mg; Yield 82%; IR ( $\nu_{\max}/\text{cm}^{-1}$ ): 3,076 (C–H), 1,703 (C=O), 1,666 (C=O), 1,627 (C=N), 1,510 (C=C), 1,193 (C–F);  $^1\text{H}$  NMR spectrum,  $\delta$ , ppm: 2.51 (s, 3H,  $-\text{CH}_3$ ), 7.48 (d, 1H,  $J = 8.00$  Hz, Ar–H), 7.60 (dd, 1H,  $J = 8.00$  and 2.00 Hz, Ar–H), 8.08 (d, 1H,  $J = 1.50$  Hz), 8.54 (s, 1H, chromone-H), 10.64 (s, 1H, =C–H);  $^{13}\text{C}$  NMR spectrum,  $\delta_{\text{C}}$ , ppm: 174.5 (C=O), 165.5 (C=O), 162.4, 154.2, 143.4, 142.4, 137.5, 136.3, 126.2, 120.9, 123.3, 120.2, 118.6, 118.5, 118.2, 118.1, 21.1 ( $-\text{CH}_3$ ); MS:  $m/z$  489.14 (M + H) $^+$ .

## 3.2 | Anti-inflammatory activity

All the synthesized compounds were screened for their in vitro anti-inflammatory activities against the standard drug diclofenac sodium. The minimum inhibitory concentration was determined by the well diffusion method at 1 mg/ml of concentration. (Table 2). A volume of 1 ml of diclofenac sodium at different concentrations (50, 100, 200, 400, 800, and 1,000  $\mu\text{g}/\text{ml}$ ) was homogenized with 1 ml of aqueous solution of bovine serum albumin (5%) and incubated at 27°C for 15 minutes. The mixture of distilled water and bismuth sulphite agar constituted the control tube. Denaturation of the proteins was caused by placing the mixture in a water bath for 10 minutes at 70°C. The mixture was cooled within the ambient room temperature, and the activity of each mixture was measured at 255 nm. Each test was conducted thrice. The following formula was used to calculate inhibition percentage:

$$\% \text{inhibition} = \frac{\text{absorbance of control} - \text{absorbance of sample}}{\text{absorbance of control}} \times 100.$$

## 3.3 | In silico ADME

In the present study, we have calculated molecular volume (MV), molecular weight (MW), logarithm of partition coefficient ( $\text{miLog } P$ ), number of hydrogen bond acceptors (n-ON), number of hydrogen bonds donors (n-OHNH), topological polar surface area (TPSA), number of rotatable bonds (n-ROTB), and Lipinski's rule of five<sup>[31]</sup> using the Molinspiration online property calculation toolkit.<sup>[30]</sup> Absorption (% ABS) was calculated by: %

ABS =  $109 - (0.345 \times \text{TPSA})$ .<sup>[32]</sup> Drug likeness model score (a collective property of physicochemical properties, pharmacokinetics, and pharmacodynamics of a compound that is represented by a numerical value) was computed by MolSoft software.<sup>[33]</sup>

## 4 | CONCLUSIONS

In conclusion, we have constructed pyrazole and fluorine in one molecular framework as new 3-(trifluoromethyl)-1-(perfluorophenyl)-1H-pyrazol-5(4H)-one derivatives under conventional and nonconventional methods like microwave irradiation and ultrasonication, respectively, via Knoevenagel condensation and evaluated their biological activity. Ultrasonication and microwave irradiation can shorten the reaction time from a few hours to a few minutes and increases the product yield (74–84%) compared to the conventional method (59–75%). The synthesized compounds exhibited promising anti-inflammatory activity compared to the standard drug diclofenac sodium. Similarly, the synthesized compound displayed promising antioxidant activity compared to the standard drug. Furthermore, an analysis of the ADME parameters for synthesized compounds showed good drug-like properties and can be developed as an oral drug candidate, thus suggesting that compounds from the present series can be further optimized and developed as a lead molecule.

## ACKNOWLEDGMENT

The authors are thankful to the Department of Science and Technology, New Delhi for providing research facilities under FIST scheme and to CIF, Savitribai Phule Pune University, Pune and SAIF, Panjab University, Chandigarh for providing spectral facilities.

## CONFLICT OF INTEREST

The authors declare no conflict of interest, financial or otherwise.

## REFERENCES

- [1] M. Bhat, G. K. Nagaraja, R. Kayarmar, S. K. Peethamber, M. Shefeeulla, *RSC Adv.* **2016**, 6, 59375.
- [2] A. L. Luz, C. D. Kassotis, H. M. Stapleton, J. N. Meyer, *Toxicology* **2018**, 393, 150.
- [3] P. Khloya, S. Kumar, P. Kaushik, P. Surain, D. Kaushik, P. K. Sharma, *Bioorg. Med. Chem. Lett.* **2015**, 25, 1177.
- [4] (a) Y. R. Li, C. Li, J. C. Liu, M. Guo, T. Y. Zhang, L. P. Sun, C. J. Zheng, H. R. Piao, *Bioorg. Med. Chem. Lett.* **2015**, 25, 5052. (b) S. A. Ali, S. M. Awad, A. M. Said, S. Mahgouba, H. Tahaa, N. M. Ahmed, *J. Enzyme Inhib. Med. Chem.* **2020**, 35, 847.
- [5] X. L. Deng, J. Xie, Y. Q. Li, D. K. Yuan, X. P. Hu, L. Zhang, Q. M. Wang, M. Chi, X. L. Yang, *Chin. Chem. Lett.* **2016**, 27, 566.

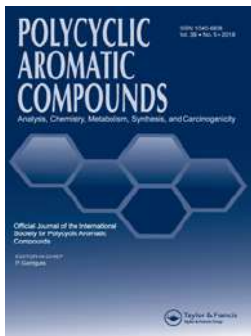
- [6] H. Jia, F. Bai, N. Liu, X. Liang, P. Zhan, C. Ma, X. Jiang, X. Liu, *Eur. J. Med. Chem.* **2016**, *123*, 202.
- [7] C. I. Nieto, M. P. Cabildo, M. P. Cornago, D. Sanz, R. M. Claramunt, I. Alkorta, J. Elguero, J. A. Garcia, A. Lopez, D. A. Castroviejo, *J. Mol. Struct.* **2015**, *1100*, 518.
- [8] S. Shu, X. Cai, J. Li, Y. Feng, A. Dai, J. Wang, D. Yang, M. W. Wang, H. Liu, *Bioorg. Med. Chem.* **2016**, *24*, 2852.
- [9] R. Dummer, P. A. Ascierto, H. J. Gogas, A. Arance, M. Mandala, G. Liskay, C. Garbe, D. Schadendorf, L. Krajsova, R. Gutzmer, V. C. Sileni, C. Dutriaux, J. W. Groot, N. Yamazaki, C. Loquai, L. A. M. D. Parseval, M. D. Pickard, V. Sandor, C. Robert, K. T. Flaherty, *Lancet Oncol.* **2018**, *19*, 6035.
- [10] E. Therrien, G. Larouche, N. Nguyen, J. Rahil, A. M. Lemieux, Z. Li, M. Fournel, T. P. Yan, A. J. Landry, S. Lefebvre, J. J. Wang, K. Macbeth, C. Heise, A. Nguyen, J. M. Besterman, R. Deziel, A. Wahhab, *Bioorg. Med. Chem. Lett.* **2015**, *25*, 2514.
- [11] X. H. Lv, Q. S. Li, Z. L. Ren, M. J. Chu, J. Sun, X. Zhang, M. Xing, H. L. Zhu, H. Q. Cao, *Eur. J. Med. Chem.* **2016**, *108*, 586.
- [12] M. A. Tabrizi, P. G. Baraldi, E. Ruggiero, G. Saponaro, S. Baraldi, R. Romagnoli, A. Martinelli, T. Tuccinardi, *Eur. J. Med. Chem.* **2015**, *97*, 289.
- [13] E. Kick, R. Martin, Y. Xie, B. Flatt, E. Schweiger, T. L. Wang, B. Busch, M. Nyman, X. H. Gu, G. Yan, B. Wagner, M. Nanao, L. Nguyen, T. Stout, A. Plonowski, I. Schulman, J. Ostrowski, T. Kirchgessner, R. Wexler, R. Mohan, *Bioorg. Med. Chem. Lett.* **2015**, *25*, 372.
- [14] a) K. Muller, C. Faeh, F. Diederich, *Science* **2007**, *317*, 1881. b) W. K. Hagmann, *J. Med. Chem.* **2008**, *51*, 4359. c) R. E. Banks, B. E. Smart, J. C. Tatlow, *Organo Fluorine Chemistry. Principles and Commercial Applications*, Plenum, New York **1994**. d) S. Purser, P. R. Moore, S. Swallow, V. Gouverneur, *Chem. Soc. Rev.* **2008**, *37*, 320. e) P. Jeschke, *ChemBioChem* **2004**, *5*, 570.
- [15] a) D. O'Hagan, *Chem. Soc. Rev.* **2008**, *37*, 308. b) H. J. Bohm, D. Banner, S. Bendels, M. Kansy, B. Kuhn, K. Muller, U. ObstSander, M. Stahl, *ChemBioChem* **2004**, *5*, 637. (c) P. Nagender, D. Pulakesh, G. Gouverneur, N. Shibata, *Org. Lett.* **2018**, *20*, 1526. (d) D. Pulakesh, G. Satoshi, P. Nagender, U. Hiroto, T. Etsuko, N. Shibata, *Chem. Sci.* **2018**, *9*, 3276. (e) P. Nagender, S. Takuya, K. Mikhail, T. Etsuko, S. Yuji, N. Shibata, *Chem. Commun.* **2018**, *54*, 4294. (f) D. K. Swaroop, N. Ravi Kumar, P. Nagender, G. Jitender Dev, N. Jagadeesh Babu, B. Narsaiah, *Eur. J. Org. Chem.* **2019**, *2019*, 3654. <https://doi.org/10.1002/ejoc.201900482>. (g) P. Nagender, H. Kyosuke, N. Shibata, *Chem. Commun.* **2018**, *54*, 7171.
- [16] (a) I. I. Gerus, R. X. Mironetz, I. S. Kondratov, A. V. Bezdudny, Y. V. Dmytriv, O. V. Shishkin, V. S. Starova, O. A. Zaporozhets, A. A. Tolmachev, P. K. Mykhailiuk, *J. Org. Chem.* **2012**, *77*, 47. (b) B. D. Maxwell, *J. Labell. Compd. Radiopharm.* **2000**, *43*, 645.
- [17] T. G. Leighton, *The acoustic bubble*, Academic Press, London **1994**, p. 531.
- [18] C. O. Kappe, A. Stadler, D. Dallinger, *Microwaves in Organic and Medicinal Chemistry*, 2nd ed., Wiley-VCH, Weinheim **2012**.
- [19] (a) A. S. William, F. B. Aleksel, C. Ron, Organic synthesis: The science behind art. in *Royal Society of Chemistry (Great Britain)*, RSC publications, Cambridge, **1998**. (b) *Organic Synthesis Co. II vol*; **1935**. (c) *Comprehensive Organic Synthesis Book Volumes*, John Wiley & Sons, Hoboken, NJ, **1991**.
- [20] (a) T. Syed, A. Yahya, J. A. Alsheri, *Lett. Org. Chem.* **2020**, *17*, 157. (b) S. Mallouk, K. Bougrin, A. Laghzizil, R. Benhida, *Molecules* **2010**, *15*, 813. (c) J. S. Biradar, B. S. Sasidhar, *Eur. J. Med. Chem.* **2011**, *46*, 6112. (d) M. B. Ansari, H. Jin, M. N. Parvin, S. E. Park, *Catal. Today* **2012**, *185*, 211.
- [21] (a) M. A. Pasha, K. Manjula, J. Saudi, *Chem. Soc.* **2011**, *15*, 283. (b) Y. Ogiwara, K. Takahashi, T. Kitazawa, N. Sakai, *J. Org. Chem.* **2015**, *80*, 3101. (c) P. Leelavathi, S. R. Kumar, *J. Mol. Catal. A Chem.* **2005**, *240*, 99. (d) J. V. Schijndel, A. C. Luiz, D. Molendijk, J. Meuldijk, *Green Chem. Lett. Rev.* **2017**, *10*, 404.
- [22] S. Ramesh, F. Devred, D. P. Debecker, *ChemistrySelect* **2020**, *5*, 300.
- [23] R. B. Ardakani, N. Safaeian, M. Oftadeh, M. F. Mehrjardi, *Theor. Chem. Acc.* **2020**, *139*, 45.
- [24] N. Zengin, H. Burhan, A. Savk, H. Goksu, F. Sen, *Scie. Rep.* **2020**, *10*, 12758.
- [25] A. R. Bhat, M. H. Najjar, R. S. Dongre, M. S. Akhter, *Res. Green Sust. Chem.*, **2020**, *3*, 100008. <https://doi.org/10.1016/j.jrgsc.2020.06.001>.
- [26] (a) K. S. Hon, H. N. Akolkar, B. K. Karale, *J. Het. Chem.* **2020**, *57*, 1692. (b) S. P. Kunde, K. G. Kanade, B. K. Karale, H. N. Akolkar, S. S. Arbuj, P. V. Randhavane, S. T. Shinde, M. H. Shaikh, A. K. Kulkarni, *RSC Adv.* **2020**, *10*, 26997. (c) S. J. Takate, A. D. Shinde, B. K. Karale, H. Akolkar, L. Nawale, D. Sarkar, P. C. Mhaske, *Bioorg. Med. Chem. Lett.* **2019**, *29*, 1999. (d) S. P. Kunde, K. G. Kanade, B. K. Karale, H. N. Akolkar, P. V. Randhavane, S. T. Shinde, *Res. Chem. Intermed.* **2017**, *43*, 7277. (e) R. S. Endait, B. K. Karale, H. N. Akolkar, P. V. Randhavane, *Indian J. Het. Chem.* **2016**, *26*, 141.
- [27] B. S. Furniss, A. J. Hannaford, P. W. G. Smith, A. R. Tatchell, *Vogel's Text Book of Practical Organic Chemistry*, 5th ed., Addison Wesley Longman Limited, England **1998**.
- [28] S. Kandia, A. L. Charles, *Food Chem.* **2019**, *287*, 338.
- [29] S. Zhang, Y. Luo, L. Q. He, Z. J. Liu, A. Q. Jiang, Y. H. Yang, H. L. Zhu, *Bioorg. Med. Chem.* **2013**, *21*, 3723.
- [30] Molinspiration Chemoinformatics Brastislava, Slovak Republic. <http://www.molinspiration.com/cgi-bin/properties>; **2014**.
- [31] C. A. Lipinski, L. Lombardo, B. W. Dominy, P. J. Feeney, *Adv. Drug Del. Rev.* **2001**, *46*, 3.
- [32] Y. Zhao, M. H. Abraham, J. Lee, A. Hersey, N. C. Luscombe, G. Beck, B. Sherborne, I. Cooper, *Pharm. Res.* **2002**, *19*, 1446.
- [33] Drug-Likeness and Molecular Property Prediction. <http://www.molsoft.com/mprop/>.

## SUPPORTING INFORMATION

Additional supporting information may be found online in the Supporting Information section at the end of this article.

**How to cite this article:** Dengale SG, Akolkar HN, Karale BK, et al. Synthesis of 3-(trifluoromethyl)-1-(perfluorophenyl)-1H-pyrazol-5 (4H)-one derivatives via Knoevenagel condensation and their biological evaluation. *J Chin Chem Soc.* 2020;1–12. <https://doi.org/10.1002/jccs.202000357>






## Design, Synthesis and Biological Evaluation of Novel Furan & Thiophene Containing Pyrazolyl Pyrazolines as Antimalarial Agents

Hemantkumar N. Akolkar , Sujata G. Dengale , Keshav K. Deshmukh ,  
Bhausahab K. Karale , **Nirmala R. Darekar** , Vijay M. Khedkar & Mubarak H.  
Shaikh

To cite this article: Hemantkumar N. Akolkar , Sujata G. Dengale , Keshav K. Deshmukh ,  
Bhausahab K. Karale , Nirmala R. Darekar , Vijay M. Khedkar & Mubarak H. Shaikh (2020): Design,  
Synthesis and Biological Evaluation of Novel Furan & Thiophene Containing Pyrazolyl Pyrazolines  
as Antimalarial Agents, Polycyclic Aromatic Compounds, DOI: [10.1080/10406638.2020.1821231](https://doi.org/10.1080/10406638.2020.1821231)

To link to this article: <https://doi.org/10.1080/10406638.2020.1821231>

 View supplementary material 

 Published online: 14 Sep 2020.

 Submit your article to this journal 

 Article views: 9

 View related articles 

 View Crossmark data 



# Design, Synthesis and Biological Evaluation of Novel Furan & Thiophene Containing Pyrazolyl Pyrazolines as Antimalarial Agents

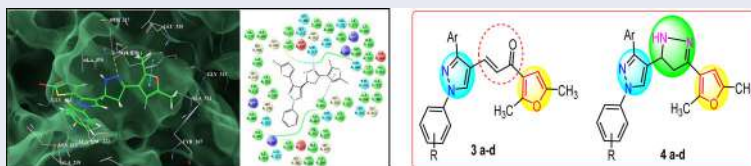
Hemantkumar N. Akolkar<sup>a</sup>, Sujata G. Dengale<sup>b</sup>, Keshav K. Deshmukh<sup>b</sup>, Bhausaheb K. Karale<sup>a</sup>, Nirmala R. Darekar<sup>a</sup>, Vijay M. Khedkar<sup>c</sup>, and Mubarak H. Shaikh<sup>a</sup>

<sup>a</sup>P.G. and Research, Department of Chemistry, Radhabai Kale Mahila Mahavidyalaya, Ahmednagar, India;

<sup>b</sup>P.G. and Research, Department of Chemistry, Sangamner Nagarpalika Arts, D. J. Malpani Commerce, B.N. Sarada Science College, Sangamner, India; <sup>c</sup>Department of Pharmaceutical Chemistry, School of Pharmacy, Vishwakarma University, Pune, India

## ABSTRACT

In search for novel compounds targeting Malaria, based on the *in silico* molecular docking binding affinity data, the novel furans containing pyrazolyl chalcones (**3a-d**) and pyrazoline derivatives (**4a-d**) were synthesized. The formation of the synthesized compound were confirmed by spectral analysis like IR, <sup>1</sup>H NMR, <sup>13</sup>C NMR and mass spectrometry. Compounds with thiophene and pyrazoline ring **4b** (0.47  $\mu$ M), **4c** (0.47  $\mu$ M) and **4d** (0.21  $\mu$ M) exhibited excellent anti-malarial activity against *Plasmodium falciparum* compared with standard antimalarial drug Quinine (0.83  $\mu$ M). To check the selectivity furthermore, compounds were tested for antimicrobial activity and none of the synthesized compound exhibited significant potency compared with the standard antibacterial drug Chloramphenicol and antifungal drug Nystatin respectively. So, it can be resolved that the produced compounds show selectively toward antimalarial activity and have the potential to be explored further.



## ARTICLE HISTORY

Received 7 August 2020

Accepted 5 September 2020


## KEYWORDS

Antimalarial; antimicrobial; chalcones; pfENR inhibitor; pyrazole-pyrazolines; thiophene

## Introduction

Life-threatening disease Malaria is caused by *Plasmodium* parasites that are spread to people through the bites of infected female Anopheles mosquitoes. Out of five *Plasmodium* Parasites *Plasmodium falciparum* produces high levels of blood-stage parasites that sequester in critical organs in all age groups.<sup>1</sup> As per the World Health Organization report in 2018, in sub Saharan Africa 11 million pregnant women were infected with malaria and 872 000 children were born with a low birth weight. Around 24 million children estimated to be infected with the *P. falciparum* parasite in the region; out of these, 1.8 million had severe anemia and 12 million had

**CONTACT** Hemantkumar N. Akolkar  hemantakolkar@gmail.com  P.G. and Research, Department of Chemistry, Radhabai Kale Mahila Mahavidyalaya, Ahmednagar, Maharashtra 414001, India.

 Supplemental data for this article is available online at <https://doi.org/10.1080/10406638.2020.1821231>.

moderate anemia.<sup>2</sup> Mortality and morbidity caused by malaria are continually increasing. This subject is the consequence of the ever-increasing development of parasite resistance to drugs and also increased mosquito resistance to insecticides which is one of the most critical complications in controlling malaria over recent years.<sup>3</sup>

*P. falciparum* enoyl-acyl carrier protein (ACP) reductase (ENR) is an enzyme in type II fatty acid synthesis (FAS II) pathway which catalyzes the NADH-dependent reduction of trans-2-enoyl-ACP to acyl-ACP and plays important role in completion of the fatty acid elongation cycles. Due to its role in the parasite's fatty acid pathway, PfENR has been known as one of the most promising antimalarial targets for structure-based drug design.<sup>4-6</sup> Triclosan, a broadly used antibiotic, is effective inhibitor of PfENR enzyme activity. Several efforts have been taken in the recent past in the direction of the identification of new antimalarials using pharmacophore modeling, molecular docking and MD simulations.<sup>7-12</sup>

Pyrazole is a well-known class of nitrogen containing heterocyclic compounds and play important role in agricultural and medicinal field. Pyrazole and its derivatives are known to possess antibacterial,<sup>13</sup> antipyretic,<sup>14</sup> fungistatic,<sup>15</sup> anticonvulsant,<sup>16</sup> antitubercular,<sup>17</sup> antipyretic,<sup>18</sup> insecticides,<sup>19</sup> and anti-inflammatory<sup>20</sup> activities. Pyrazoline containing compounds are recognized to possess various pharmacological activities like antimalarial,<sup>21,22</sup> anticancer,<sup>23</sup> anti-inflammatory,<sup>24</sup> analgesic,<sup>24</sup> antitumor,<sup>25</sup> antimicrobial<sup>26</sup> and antidepressant activities.<sup>27</sup> Furan containing compounds possess lipoxygenase inhibitor,<sup>28</sup> urotensin-II receptor antagonists,<sup>29</sup> fungicidal,<sup>30</sup> epidermal growth factor receptor inhibitors and anticancer<sup>31</sup> etc. activities. Chalcone is a natural pigment found in plant and is an important intermediate for the synthesis of flavonoids. Varieties of biological activities are associated with chalcones and their derivatives such as antiplasmodial,<sup>32</sup> nematicide,<sup>33</sup> antiallergenic,<sup>34</sup> antimalarial,<sup>35</sup> anti-HIV,<sup>36</sup> anti-cancer,<sup>37</sup> anti-inflammatory<sup>38</sup> and anti-tuberculosis.<sup>39</sup>

So, considering the biological importance of pyrazoles, furan and chalcone, herein we report the design of a small library of furan containing pyrazolyl pyrazoline derivatives by molecular hybridization approach targeting PfENR using the *in silico* molecular docking technique. The promising results obtained from this *in silico* study served the basis for the synthesis of these molecules followed by evaluation of their antimalarial potential.

Molecular docking technique plays significant role in lead identification/optimization and in the mechanistic study by predicting the binding affinity and the thermodynamic interactions leading the binding of a ligand to its biological receptor. Thus, with the objective to identify novel leads targeting the crucial antimalarial target *Plasmodium falciparum* enoyl-ACP reductase (PfENR or FabI) (pdb code: 1NHG), molecular docking was carried out using the GLIDE (Grid-based LIgand Docking with Energetics) program of the Schrodinger Molecular modeling package.<sup>40-42</sup> A small library of 8 molecules comprising furan containing pyrazolyl pyrazoline derivatives (**3a-3d**, **4a-4d**) was docked against PfENR. The ensuing docking conformation revealed that these molecules changed a binding mode which is corresponding with the active site of pfENR and were found to be involved in a series of bonded and non-bonded interactions with the residues lining the active site. Their docking scores varied from -6.979 to -8.222 with an average docking score of -7.563 signifying a potent binding affinity to PfENR. In order to get a quantitative insight into the most significantly interacting residues and their associated thermodynamic interactions, a detailed per-residue interaction analysis was carried out (Table S1, Supporting Information). This analysis showed that the furan containing pyrazolyl chalcones (**3a-d**) (Figure 1) were deeply embedded into the active site of PfENR engaging in a sequence of favorable *van der Waals* interactions observed with Ile:C369, Phe:C368, IleA323, Ala:A320, Ala:A319, Arg:A318, Ser:A317, Leu:A315, Pro:A314, Gly:A313, Ala:A312, Lys:A285, Met:A281, Tyr:A277, Tyr:A267, Thr:A266, Leu:A265, Gly:A112, Tyr:A111, Gly:A110 and Asp:A107 residues through the 1,3-substituted-1*H*-pyrazol-4-yl scaffold while the 1-(2,5-Dimethylfuran-3-yl) prop-2-en-1-one

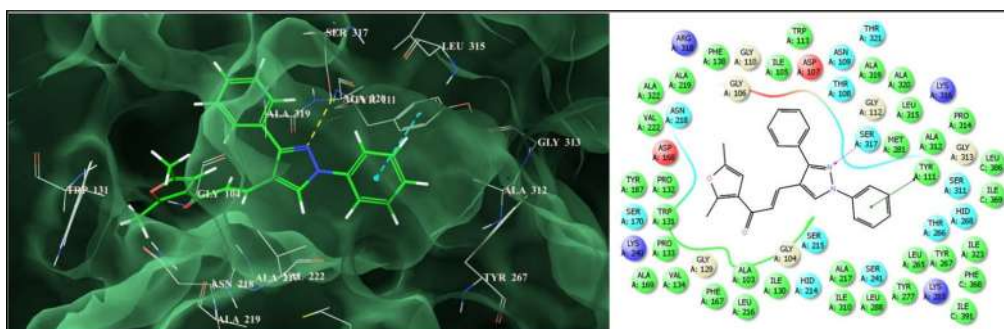


**Figure 1.** Binding mode of **3a** into the active site of *Plasmodium falciparum* enoyl-ACP reductase (on right side: pink lines represent the hydrogen bond while green lines signify  $\pi$ - $\pi$  stacking interactions).

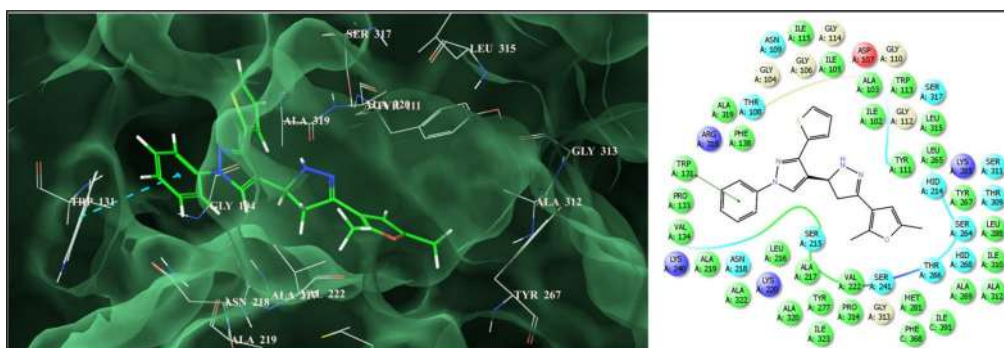


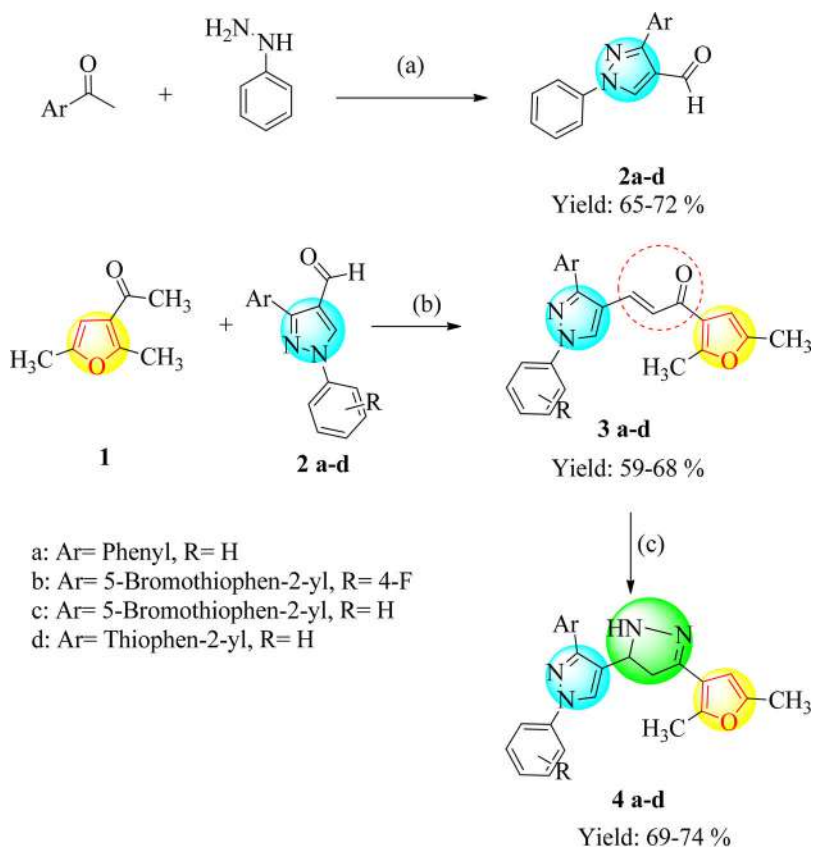
**Figure 2.** Binding mode of **4d** into the active site of *Plasmodium falciparum* enoyl-ACP reductase (on right side: pink lines represent the hydrogen bond while green lines signify  $\pi$ - $\pi$  stacking interactions).

component of the molecules was seen to be involved in similar interactions with Asn:A218, Ala:A217, Leu:A216, Ser:A215, Trp:A131, Gly:A106, Ile:A105, Gly:A104 residues of the active site.

Furthermore the enhanced binding affinity of these molecule is also attributed to significant electrostatic interactions observed with Arg:A318, Ser:A317, Lys:A285, Asp:A236, Asn:A218, Ala:A217, Ser:A215, Tyr:A111, Gly:A110, Asp:A107, Gly:A104 residues lining the active site. On the other hand, the furan containing pyrazoline derivatives (**4a-d**) (Figure 2) were also seen to be stabilized into the active of *Pf*ENR through a network of significant *van der Waals* interactions observed with (2,5-dimethylfuran-3-yl)-1*H*-pyrazolyl scaffold *via* Ile:C369, Phe:C368, Ala:A320, Ser:A317, Leu:A315, Pro:A314, Gly:A313, Ala:A312, Lys:A285, Tyr:A267, Thr:A266, Leu:A265, Gly:A112, Tyr:A111, Gly:A110, Gly:A106 and Ile:A105 while other half of the molecule i.e., 2-thiophenyl-1-phenyl-1*H*-pyrazole showed similar type of interactions with Ile:A323, Ala:A319, Arg:A318, Met:A281, Tyr:A277, Val:A222, Ala:A219, Asn:A218, Ala:A217, Leu:A216, Ser:A215, Trp:A131, Ile:A130, Trp:A113, Asp:A107, Gly:A104 residues.

Further the enhanced binding affinity of the molecules is also attributed to favorable electrostatic interactions observed with Arg:A318, Ser:A317, Glu:A289, Lys:A285, Asp:A236, Asn:A218, Ala:A217, Ser:A215, Tyr:A111, Gly:A110, Asp:A107 and Gly:A104. While these non-bonded interactions (*van der Waals* and electrostatic) were observed to be the major driving force for the mechanical interlocking of these novel furan containing pyrazolyl pyrazoline derivatives into the active site *Pf*ENR, the enhanced binding affinity of these molecules is also contributed by very prominent hydrogen bonding interaction observed for **3a** (Ser:A317(2.708 Å)), **4a** (Ser:A317(2.783 Å)), **4b** (Ser:A317(2.462 Å)) and **4c** (Ser:A317(2.462 Å)). Furthermore these





**Reagents and conditions:** (a): i) EtOH, reflux, 2 hr ii) DMF/POCl<sub>3</sub>, 0-10° C;  
 (b) 10 % aq. KOH, EtOH, RT, 14hr; (c) NH<sub>2</sub>NH<sub>2</sub>·H<sub>2</sub>O, EtOH, AcOH, 6hr

**Scheme 1.** Synthesis of pyrazolyl chalcones (**3a-d**) and pyrazolyl pyrazolines (**4a-d**).

molecules were also engaged in a very close  $\pi$ - $\pi$  stacking interactions: **3a**: Tyr: A111(2.669 Å), **3b**: Tyr:A267(2.529 Å), **3c**: Tyr:A267(2.541 Å), **3d**: Tyr:A267(2.335 Å), **4a**: Tyr:A111(2.602 Å), **4b**: Trp:A131(2.073 Å), **4c**: TyrA:111(2.073 Å) and **4d**: TrpA131(2.538 Å) (Figures S1-S6, Supporting Information).

This type of bonded interactions i.e., hydrogen bonding and  $\pi$ - $\pi$  stacking are known to serve as an “anchor” to guide the alignment of a molecule into the 3D space of enzyme’s active site and facilitate the non-bonded interactions (*Van der Waals* and electrostatic) as well. Overall, the in-silico binding affinity data suggested that these furans containing pyrazolyl pyrazoline derivatives (**3a-d**, **4a-d**) could be developed as novel scaffold to arrive at compounds with high selectivity and potency *Plasmodium falciparum*.

## Results and discussion

### Chemistry

The novel series of furan containing pyrazolyl chalcones (**3a-d**) and pyrazoline derivatives (**4a-d**) were synthesized from commercially available starting materials (Scheme 1). Initially, pyrazole aldehyde **2a-d** was formed by the condensation between substituted acetophenone and phenyl

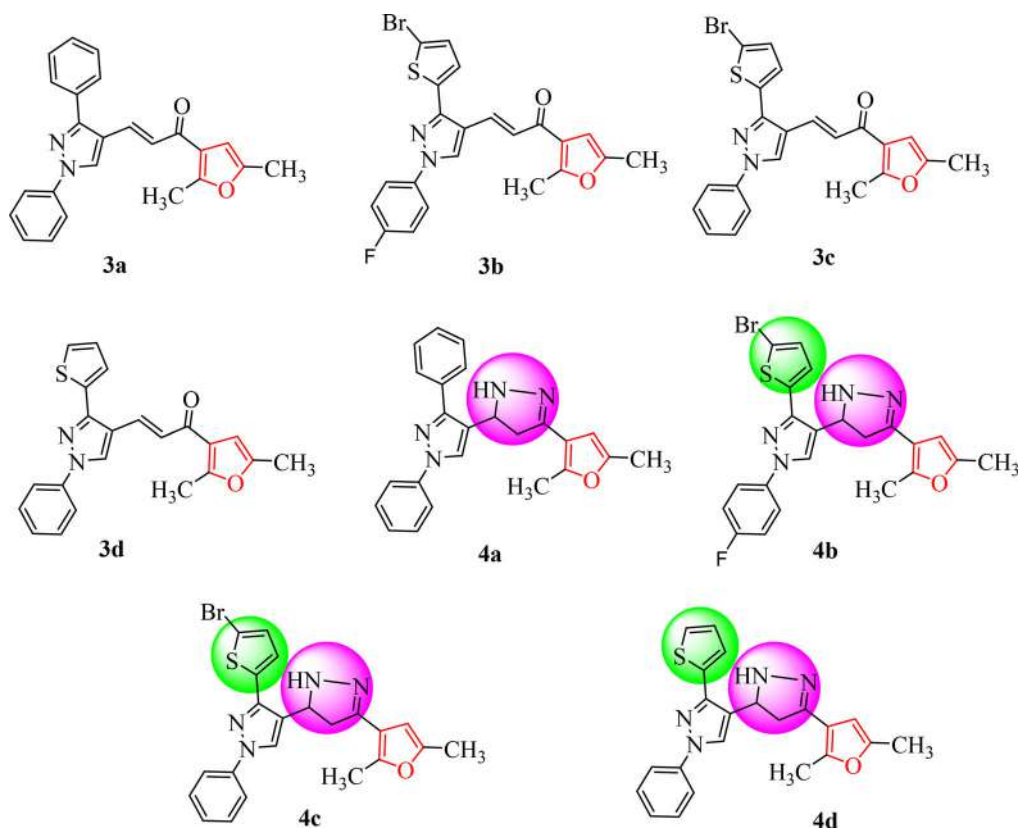


**Figure 3.** The newly synthesized compounds structure **3a-d** & **4a-d**.

hydrazine followed by Vilsmeier-Haack formylation reaction (Scheme 1). Then furan containing pyrazolyl chalcones **3a-d** were synthesized by base-catalyzed Claisen-Schmidt condensation of 1-(2,5-dimethylfuran-3-yl)ethanone **1** and substituted pyrazole aldehyde **2a-d**.<sup>43</sup> Finally, the furan containing pyrazolyl chalcones **3a-d** and hydrazine hydrate in ethanol solvent using catalytic amount of acetic acid at reflux condition for 6 hr afforded the corresponding pyrazolyl pyrazolines (**4a-d**) in quantitative isolated yield (69–74%) (Scheme 1).

The newly synthesized compounds structures were shown in Figure 3. The newly synthesized compound's structures were confirmed by IR, <sup>1</sup>H NMR, <sup>13</sup>C NMR, mass spectral data. For compound **3a**, in IR spectrum the stretching band for C=O was detected at 1657 cm<sup>-1</sup>. In the <sup>1</sup>H NMR spectrum of compound **3a**, the proton of pyrazole and furan ring resonate as a singlet at  $\delta$  9.31 and  $\delta$  6.60 ppm respectively. Also, singlet for two -CH<sub>3</sub> were observed at  $\delta$  2.27 and  $\delta$  2.50 ppm. The <sup>13</sup>C NMR spectrum of compound **3a** showed signal at  $\delta$  184.41 ppm due to C=O and  $\delta$  12.89 and  $\delta$  13.93 ppm is due to two -CH<sub>3</sub>. Mass spectrum confirms the formation of compound **3a** showed  $m/z = 369$  (M + H)<sup>+</sup>.

Secondly, in the IR spectrum of compound **4a**, -N-H stretching band observed at 3252 cm<sup>-1</sup>. The <sup>1</sup>H NMR spectrum of compound **4a**, the CH<sub>2</sub> protons of the pyrazoline ring resonated as a pair of doublets of doublets at  $\delta$  2.88 ppm and 3.35 ppm. The CH proton appeared as triplet at  $\delta$  4.87 ppm due to vicinal coupling with two protons of the methylene group. In the <sup>13</sup>C NMR spectra of the compound **4a** carbons of the pyrazoline ring were observed at  $\delta$  41.97 ppm and 54.67 ppm. All the other aromatic and aliphatic protons and carbons were observed at expected regions. Mass spectrum confirms the formation of compound **4a** showed  $m/z = 383$  (M + H)<sup>+</sup>.

**Table 1.** Antimalarial ( $\mu\text{M}$ ), Antibacterial (MIC in  $\mu\text{g/mL}$ ) & Antifungal (MIC in  $\mu\text{g/mL}$ ) activity.

Cpd	Antimalarial activity Plasmodium falciparum	Antibacterial activity				Antifungal activity			Molecular Docking Score
		EC	PA	SA	SP	CA	AN	AC	
<b>3a</b>	1.46	200	200	250	250	500	500	500	-7.814
<b>3b</b>	3.93	100	250	250	200	1000	500	500	-7.032
<b>3c</b>	2.16	62.5	200	125	250	500	>1000	>1000	-7.192
<b>3d</b>	3.07	100	100	200	200	1000	500	500	-7.118
<b>4a</b>	6.31	125	100	100	100	500	500	500	-6.979
<b>4b</b>	0.47	100	200	100	100	250	500	500	-8.157
<b>4c</b>	0.47	125	125	200	200	1000	>1000	>1000	-8.222
<b>4d</b>	0.21	200	100	125	100	500	500	500	-7.988
Chloroquine	0.06	-	-	-	-	-	-	-	-
Quinine	0.83	-	-	-	-	-	-	-	-
CP	-	50	50	50	50	-	-	-	-
NS	-	-	-	-	-	100	100	100	-

Cpd: Compound; EC: *Escherichia coli*; PA: *Pseudomonas aeruginosa*; SA: *Staphylococcus aureus*; SP: *Streptococcus pyogenes*; CA: *Candida albicans*; AN: *Aspergillus niger*; AC: *Aspergillus clavatus*; CP: Chloramphenicol; NS: Nystatin.

## Biological evaluation

### *In vitro* antimalarial screening

All the synthesized novel compounds were tested for antimalarial activities. The *in vitro* antimalarial assay was carried out according to the micro assay protocol of Rieckmann and coworkers with minor modifications.<sup>44–47</sup> The results were recorded as the minimum inhibitory concentrations ( $\mu\text{M}$  MIC) chloroquine and quinine were used as the reference drug (Table 1).

Herein, we have synthesized four chalcone and pyrazoline derivatives respectively. Structure activity relationship (SAR) plays very important role while displaying the antimalarial activity. All the synthesized chalcone derivatives (**3a–d**) exhibited less potency compared to the standard drug. But pyrazoline derivatives exhibited excellent antimalarial activity compared to the standard drug. In compound **4a**, thiophene ring was absent and pyrazoline ring is present, so, the compound **4a** exhibited less potency compared to the standard drug. Now, in compound **4b**, bromo substituted thiophene and pyrazoline rings are present along with the fluorine at the para position on benzene ring. Interestingly, this compound **4b** (0.47  $\mu\text{M}$ ), exhibited excellent activity compared to the standard drug quinine (0.83  $\mu\text{M}$ ). Again, in compound **4c**, bromo substituted thiophene and pyrazoline rings are present but no fluorine at the para position of benzene ring. Though fluorine is absent on benzene ring in compound **4c** (0.47  $\mu\text{M}$ ), it exhibited same potency as that of compound **4b** compared to the standard drug quinine (0.83  $\mu\text{M}$ ). Finally, in compound **4d**, there were no substitution on the thiophene and benzene ring. In compound **4d** plane thiophene, plane benzene ring and pyrazoline ring constructed in a single molecular framework. Compound **4d** (0.21  $\mu\text{M}$ ), exhibited four-fold more antimalarial activity compared to the standard drug quinine (0.83  $\mu\text{M}$ ). From SAR, we can conclude that for the antimalarial activity thiophene, pyrazoline and benzene ring were very important in a single molecular framework.

### Antimicrobial activities

Further, all the novel synthesized compounds were also screened for antimicrobial activities against the bacterial strains *Escherichia coli* (MTCC 443), *Staphylococcus aureus* (MTCC 96), *Pseudomonas aeruginosa* (MTCC 1688), *Streptococcus pyogenes* (MTCC 442) and fungal strains *Aspergillus clavatus* (MTCC 1323), *Candida albicans* (MTCC 227) and *Aspergillus niger* (MTCC 282). The minimum inhibitory concentration (MIC) was determined by the broth dilution method. Chloramphenicol and Nystatin were used as reference drugs for antibacterial and antifungal activity, respectively. The results of antibacterial and antifungal activity were given in Table 1.

The results given in Table 1 indicated that none of the synthesized compound exhibited significant potency toward the standard antibacterial drug Chloramphenicol and antifungal drug Nystatin. Hence, from above result we can conclude that the synthesized compounds show selectively antimalarial activity and negligible antimicrobial activity.

## Conclusion

In conclusion, Considering the importance of enoyl-ACP reductase (*Pf*ENR) in *Plasmodium*, a small library of 8 molecules comprising furan containing pyrazolyl pyrazoline derivatives (**3a-d**, **4a-d**) was designed and docked against *Pf*ENR. Based on the *in silico* binding affinity data, synthesis was carried out for these novel furans containing pyrazolyl pyrazoline derivatives (**3a-d**, **4a-d**) and was evaluated for activity against *Plasmodium falciparum*. The synthesized compounds shown selectively antimalarial activity with minimal antimicrobial activity. Compounds (**3a-d**) exhibited less antimalarial activity compared to the standard drug. From the series of compounds (**4a-d**), compound **4b** (0.47  $\mu$ M), **4c** (0.47  $\mu$ M) and **4d** (0.21  $\mu$ M) exhibited more antimalarial activity compared to the standard drug quinine (0.83  $\mu$ M). Compound **4d** shows four-fold more activity compared to the standard drug quinine. From the SAR, we have distinguished areas of the pyrazolyl chalcones and pyrazolyl pyrazolines framework where variations can be made to expand the pharmacokinetic profile as well as features required to improve inhibitor effectiveness. This innovative molecular scaffold presents breakthrough for optimization to develop effective *Pf*ENR inhibitors.

## Experimental

### General

All the reagents, solvents and chemicals were taken from commercial sources found to be and used as such without purification. The physical constant like melting points were measured on a DBK melting point apparatus and are uncorrected. IR spectra were recorded on Shimadzu IR Affinity 1S (ATR) FTIR spectrophotometer.  $^1\text{H}$  NMR (400 MHz) and  $^{13}\text{C}$  NMR (100 MHz) spectra were recorded on Bruker Advance II 400 spectrophotometer using TMS as an internal standard and DMSO- $d_6$  as solvent and chemical shifts were expressed as  $\delta$  ppm units. Mass spectra were obtained on Waters, Q-TOF micro mass (ESI-MS) mass spectrometer.

### General procedure for the synthesis of pyrazolyl chalcones (**3a-d**)

A mixture of 1-(2,5-dimethylfuran-3-yl)ethanone **1** (0.05 mol), substituted pyrazole aldehyde **2** (0.05 mol) and 10% aqueous potassium hydroxide (10 mL) in ethanol (50 mL) was stirred at room temperature for 14 h. The progress of the reaction was monitored by TLC. After completion of the reaction, the reaction mixture was transferred into crushed ice and neutralized by dil. HCl. The precipitation observed, filtered it, washed with water and dried. The crystallization of product carried out in ethanol.

### (*E*)-1-(2,5-Dimethylfuran-3-yl)-3-(1,3-diphenyl-1H-pyrazol-4-yl)prop-2-en-1-one (**3a**)

Yield: 61%, yellow solid; mp: 80–82  $^{\circ}\text{C}$ ; IR ( $\nu_{\text{max}}$ ,  $\text{cm}^{-1}$ ): 2921 (=C-H), 2855 (C-H), 1657 (C=O), 1454 (C=N);  $^1\text{H}$ -NMR (400 MHz, DMSO- $d_6$ ,  $\delta$ , ppm): 9.31 (s, 1H, Pyrazole-H), 7.93 (d, 2H,  $J=7.9$  Hz), 7.38–7.68 (m, 10H, Ar-H), 6.60 (s, 1H, Furan-H), 2.53 (s, 3H,  $-\text{CH}_3$ ), 2.27 (s, 3H,  $-\text{CH}_3$ );  $^{13}\text{C}$  NMR (100 MHz, DMSO- $d_6$ ,  $\delta$ , ppm): 184.4 (C=O), 159.9, 152.8, 149.7, 138.9, 132.2, 132.0, 129.6, 128.8, 128.5, 128.6, 128.4, 127.1, 123.8, 122.1, 118.6, 117.6, 105.9, 13.9 ( $\text{CH}_3$ ), 12.9 ( $\text{CH}_3$ ); MS(ESI-MS):  $m/z$  369.11 (M + H).<sup>+</sup>



***(E)-3-(3-(5-Bromothiophen-2-yl)-1-(4-fluorophenyl)-1H-pyrazol-4-yl)-1-(2,5-dimethylfuran-3-yl)prop-2-en-1-one (3b)***

Yield: 59%, yellow solid, mp: 112–114 °C; IR ( $\nu_{\max}$ ,  $\text{cm}^{-1}$ ): 2923 (=C–H), 2856 (C–H), 1656 (C=O), 1455 (C=N);  $^1\text{H-NMR}$  (400 MHz, DMSO- $d_6$ ,  $\delta$ , ppm): 9.25 (s, 1H, Pyrazole-H), 7.90 (dd, 2H,  $J=4.7$  & 9.0 Hz, Ar–H), 7.64 (d, 1H,  $J=15.4$  Hz, olefinic-H), 7.39–7.45 (m, 3H, Ar–H), 7.34 (d, 1H,  $J=3.8$  Hz, Ar–H), 7.25 (d, 1H,  $J=3.8$  Hz, Ar–H), 6.61 (s, 1H, Furan-H), 2.55 (s, 3H,  $-\text{CH}_3$ ), 2.28 (s, 3H,  $-\text{CH}_3$ );  $^{13}\text{C NMR}$  (100 MHz, DMSO- $d_6$ ,  $\delta$ , ppm): 184.2, 162.0, 159.6, 157.1, 149.7, 145.7, 135.4, 135.1, 131.4, 130.8, 128.9, 127.3, 124.6, 122.0, 120.7, 120.6, 117.3, 116.6, 116.3, 112.5, 105.9, 13.9, 12.9; MS (ESI-MS):  $m/z$  472.89 (M + H).<sup>+</sup>

***(E)-3-(3-(5-Bromothiophen-2-yl)-1-phenyl-1H-pyrazol-4-yl)-1-(2,5-dimethylfuran-3-yl)prop-2-en-1-one (3c)***

Yield: 68%, yellow solid, mp 120–114 °C; IR ( $\nu_{\max}$ ,  $\text{cm}^{-1}$ ): 2921 (=C–H), 2855 (C–H), 1699 (C=O), 1454 (C=N);  $^1\text{H-NMR}$  (400 MHz, DMSO- $d_6$ ,  $\delta$ , ppm): 9.14 (s, 1H, Pyrazole-H), 7.87 (d, 2H,  $J=7.8$  Hz, Ar–H), 7.70 (d, 1H,  $J=15$  Hz, olefinic-H), 7.52 (t, 2H,  $J=8$  Hz, Ar–H), 7.36–7.40 (m, 2H, Ar–H), 7.20 (s, 2H, Ar–H), 6.55 (s, 1H, Furan-H), 2.57 (s, 3H,  $-\text{CH}_3$ ), 2.29 (s, 3H,  $-\text{CH}_3$ );  $^{13}\text{C NMR}$  (100 MHz, DMSO- $d_6$ ,  $\delta$ , ppm): 184.3, 157.1, 149.7, 145.7, 138.6, 135.5, 131.4, 130.9, 129.7, 128.8, 127.3, 127.3, 124.6, 122.0, 118.6, 117.4, 112.5, 105.9, 13.9, 12.9; MS(ESI-MS):  $m/z$  454.57 (M + H).<sup>+</sup>

***(E)-1-(2,5-Dimethylfuran-3-yl)-3-(1-phenyl-3-(thiophen-2-yl)-1H-pyrazol-4-yl)prop-2-en-1-one (3d)***

Yield: 62%, yellow solid, mp 124–126 °C; IR ( $\nu_{\max}$ ,  $\text{cm}^{-1}$ ): 2921 (=C–H), 2715 (C–H), 1652 (C=O), 1456 (C=N);  $^1\text{H-NMR}$  (400 MHz, DMSO- $d_6$ ,  $\delta$ , ppm): 8.56 (s, 1H, Pyrazole-H), 7.91 (d, 2H,  $J=7.8$  Hz, Ar–H), 7.76 (d, 1H,  $J=15.4$  Hz, olefinic-H), 7.60 (d, 1H,  $J=5.1$  Hz, Ar–H), 7.54 (t, 2H,  $J=8.2$  Hz, Ar–H), 7.35–7.44 (m, 3H, Ar–H), 7.21 (dd, 1H,  $J=5.0$  & 3.7 Hz, Ar–H), 6.59 (s, 1H, Furan-H), 2.57 (s, 3H,  $-\text{CH}_3$ ), 2.29 (s, 3H,  $-\text{CH}_3$ );  $^{13}\text{C NMR}$  (100 MHz, DMSO- $d_6$ ,  $\delta$ , ppm): 184.4, 157.0, 149.7, 146.8, 138.7, 133.5, 131.5, 129.7, 128.7, 128.1, 127.3, 127.2, 126.8, 124.3, 122.1, 118.6, 117.4, 105.9, 13.9, 12.9; MS(ESI-MS):  $m/z$  375.10 (M + H).<sup>+</sup>

***General procedure for synthesis of pyrazolyl-pyrazoline (4a-d)***

A mixture of chalcone **3a-d** (0.001 mol) and hydrazine hydrate (0.004 mol) in solvent ethanol (10 ml) was refluxed in presence of catalytic amount of glacial acetic acid for 6 h. The progress of the reaction was monitored by TLC. After completion of the reaction, the reaction mixture was transferred into crushed ice. The precipitation observed, filtered it, washed with water and dried. The crystallization of product carried out in ethanol to get pure pyrazolines.

***4-(4,5-Dihydro-3-(2,5-dimethylfuran-3-yl)-1H-pyrazol-5-yl)-1,3-diphenyl-1H-pyrazole (4a)***

Yield: 74%, white solid, mp 102–104 °C; IR ( $\nu_{\max}$ ,  $\text{cm}^{-1}$ ): 3306 (N–H), 3049 (Ar–H), 1592 (C=N);  $^1\text{H-NMR}$  (400 MHz, DMSO- $d_6$ ,  $\delta$ , ppm): 8.56 (s, 1H, pyrazole-H), 7.90 (d, 2H,  $J=7.8$  Hz, Ar–H), 7.76 (d, 2H,  $J=8.3$  Hz, Ar–H), 7.47–7.52 (m, 4H, Ar–H), 7.41 (t, 1H,  $J=7.3$  Hz, Ar–H), 7.31 (t, 1H,  $J=7.4$  Hz, Ar–H), 7.20 (s, 1H, N–H), 6.19 (s, 1H, furan-H), 4.87 (t, 1H,  $J=10.7$  Hz, pyrazoline-H), 3.34 (dd, 1H,  $J=10.5$  & 15.6 Hz, pyrazoline-H), 2.88 (dd, 1H,  $J=11.1$  & 16.1 Hz, pyrazoline-H), 2.38 (s, 3H,  $\text{CH}_3$ ), 2.20 (s, 3H,  $\text{CH}_3$ );  $^{13}\text{C NMR}$  (100 MHz, DMSO- $d_6$ ,  $\delta$ , ppm): 150.4, 149.3, 147.6, 145.1, 139.5, 132.9, 129.5, 128.6, 127.9, 127.2, 126.2, 123.2, 118.1, 115.2, 105.9, 54.7, 41.9, 13.3, 12.9; MS (ESI-MS):  $m/z$  383.04 (M + H).<sup>+</sup>

**3-(5-Bromothiophen-2-yl)-1-(4-fluorophenyl)-4-(4,5-dihydro-3-(2,5-dimethylfuran-3-yl)-1H-pyrazol-5-yl)-1H-pyrazole (4b)**

Yield: 69%, white solid, mp 98–100 °C; IR ( $\nu_{\max}$ ,  $\text{cm}^{-1}$ ): 3310 (N–H), 3046 (Ar–H), 1594 (C=N);  $^1\text{H}$  NMR (400 MHz, DMSO- $d_6$ ,  $\delta$ , ppm): 8.54 (s, 1H, pyrazole-H), 7.88 (m, 2H, Ar–H), 7.35 (t, 2H,  $J=8.7$  Hz, Ar–H), 7.28 (dd, 2H,  $J=3.8$  Hz, Ar–H), 7.21 (s, 1H, N–H), 6.20 (s, 1H, furan-H), 4.93 (t, 1H,  $J=10.68$  Hz, pyrazoline-H), 3.37 (dd, 1H,  $J=10.7$  & 16.5 Hz, pyrazoline-H), 2.86 (dd, 1H,  $J=10.9$  & 16.1 Hz, pyrazoline-H), 2.38 (s, 3H,  $\text{CH}_3$ ), 2.20 (s, 3H,  $\text{CH}_3$ );  $^{13}\text{C}$  NMR (100 MHz, DMSO- $d_6$ ,  $\delta$ , ppm): 161.6, 159.1, 149.3, 147.7, 145.3, 144.1, 136.9, 135.6, 131.2, 128.0, 126.6, 122.6, 120.2, 120.2, 116.4, 116.2, 115.1, 111.5, 105.9, 54.3, 41.1, 13.3, 12.9; MS (ESI-MS):  $m/z$  486.93 (M + H).<sup>+</sup>

**3-(5-Bromothiophen-2-yl)-4-(4,5-dihydro-3-(2,5-dimethylfuran-3-yl)-1H-pyrazol-5-yl)-1-phenyl-1H-pyrazole (4c)**

Yield: 72%, white solid, mp 122–124 °C; IR ( $\nu_{\max}$ ,  $\text{cm}^{-1}$ ): 3303 (N–H), 3096 (Ar–H), 1593 (C=N),  $^1\text{H}$  NMR (400 MHz, DMSO- $d_6$ ,  $\delta$ , ppm): 8.55 (s, 1H, pyrazole-H), 7.84 (d, 2H,  $J=7.9$  Hz, Ar–H), 7.51 (t, 2H,  $J=7.6$  Hz, Ar–H), 7.22–7.34 (m, 4H, Ar–H), 6.20 (s, 1H, furan-H), 4.94 (t, 1H,  $J=10.6$  Hz, pyrazoline-H), 3.38 (m, 1H, pyrazoline-H), 2.88 (dd, 1H,  $J=12.1$  & 16.1 Hz, pyrazoline-H), 2.39 (s, 3H,  $\text{CH}_3$ ), 2.20 (s, 3H,  $\text{CH}_3$ );  $^{13}\text{C}$  NMR (100 MHz, DMSO- $d_6$ ,  $\delta$ , ppm): 149.3, 147.7, 145.2, 144.0, 139.0, 137.0, 131.2, 129.6, 127.8, 126.6, 126.5, 122.5, 118.0, 115.1, 111.4, 105.9, 54.4, 41.1, 13.3, 12.9; MS (ESI-MS):  $m/z$  468.95 (M + H).<sup>+</sup>

**4-(4,5-Dihydro-3-(2,5-dimethylfuran-3-yl)-1H-pyrazol-5-yl)-1-phenyl-3-(thiophen-2-yl)-1H-pyrazole (4d)**

Yield: 70%, white solid, mp 96–98 °C; IR ( $\nu_{\max}$ ,  $\text{cm}^{-1}$ ): 3336 (N–H), 3067 (Ar–H), 1501 (C=N);  $^1\text{H}$  NMR (400 MHz, DMSO- $d_6$ ,  $\delta$ , ppm): 8.53 (s, 1H, pyrazole-H), 7.86 (d, 1H,  $J=8$  Hz, Ar–H), 7.58 (d, 1H,  $J=4.9$  Hz, Ar–H), 7.47–7.52 (m, 3H, Ar–H), 7.31 (t, 1H,  $J=7.3$  Hz, Ar–H), 7.15–7.20 (m, 2H, Ar–H), 6.21 (s, 1H, furan-H), 4.98 (t, 1H,  $J=10.5$  Hz, pyrazoline-H), 3.42 (m, 1H, pyrazoline-H), 2.89 (dd, 1H,  $J=10.7$  & 16.1 Hz, pyrazoline-H), 2.39 (s, 3H,  $\text{CH}_3$ ), 2.20 (s, 3H,  $\text{CH}_3$ );  $^{13}\text{C}$  NMR (100 MHz, DMSO- $d_6$ ,  $\delta$ , ppm): 149.3, 147.7, 145.1, 144.9, 139.2, 135.0, 129.6, 127.9, 127.4, 126.3, 126.0, 125.8, 122.6, 118.1, 115.1, 105.9, 54.5, 41.3, 13.3, 12.9; MS (ESI-MS):  $m/z$  389.03 (M + H).<sup>+</sup>

**Experimental protocol for biological activity****Antimalarial assay**

The antimalarial activity of the synthesized compounds was carried out in the Microcare laboratory & TRC, Surat, Gujarat. According to the micro assay protocol of Rieckmann and coworkers the *in vitro* antimalarial assay was carried out in 96 well microtiter plates. To maintain *P. falciparum* strain culture in medium Roswell Park Memorial Institute (RPMI) 1640 supplemented with 25 mM (4-(2-hydroxyethyl)-1-piperazineethanesulfonic acid) (HEPES), 1% D-glucose, 0.23% sodium bicarbonate and 10% heat inactivated human serum. To obtain only the ring stage parasitized cells, 5% D-sorbitol treatment required to synchronized the asynchronous parasites of *P. falciparum*. To determine the percent parasitaemia (rings) and uniformly maintained with 50% RBCs ( $\text{O}^+$ ) an initial ring stage parasitaemia of 0.8 to 1.5% at 3% hematocrit in a total volume of 200  $\mu\text{l}$  of medium RPMI-1640 was carried out for the assay. A stock solution of 5 mg/ml of each of the test samples was prepared in DMSO and subsequent dilutions were prepared with culture medium. To the test wells to obtain final concentrations (at five-fold dilutions) ranging between 0.4  $\mu\text{g/ml}$  to 100  $\mu\text{g/ml}$  in duplicate well containing parasitized cell preparation the diluted samples in 20  $\mu\text{l}$  volume were added. In a candle jar, the culture plates were incubated at 37 °C. Thin

blood smears from each well were prepared and stained with Jaswant Singh-Bhattacharji (JSB) stain after 36 to 40 h incubation. To record maturation of ring stage parasites into trophozoites and schizonts in presence of different concentrations of the test agents the slides were microscopically observed. The minimum inhibitory concentrations (MIC) was recorded as the test concentration which inhibited the complete maturation into schizonts. Chloroquine was used as the reference drug.

After incubation for 38 hours, and percent maturation inhibition with respect to control group, the mean number of rings, trophozoites and schizonts recorded per 100 parasites from duplicate wells.

### **Molecular docking**

The crystal structure of *Plasmodium Falciparum* Enoyl-Acyl-Carrier-Protein Reductase (*Pf*ENR or FabI) in complex with its inhibitor Triclosan was retrieved from the protein data bank (PDB) (pdb code: 1NHG) and refined using the protein preparation wizard. It involves eliminating all crystallographically observed water (as no conserved interaction is reported with co-crystallized water molecules), addition of missing side chain/hydrogen atoms. Considering the appropriate ionization states for the acidic as well as basic amino acid residues, the appropriate charge and protonation state were assigned to the protein structure corresponding to pH 7.0 followed by thorough minimization, using OPLS-2005 force-field, of the obtained structure to relieve the steric clashes due to addition of hydrogen atoms. The 3D structures of the furan containing pyrazolyl chalcones (**3a-d**) were sketched using the build panel in Maestro and were optimized using the Ligand Preparation module followed by energy minimization using OPLS-2005 force-field until their average root mean square deviation (RMSD) reached 0.001 Å. The active site of *Pf*ENR was defined using receptor grid generation panel to include residues within a 10 Å radius around the co-crystallized ligand. Using this setup, flexible docking was carried using the extra precision (XP) Glide scoring function to gauge the binding affinities of these molecules and to identify binding mode within the target. The obtained results as docking poses were visualized and analyzed quantitatively for the thermodynamic elements of interactions with the residues lining the active site of the enzyme using the Maestro's Pose Viewer utility.

### **Acknowledgements**

Authors are thankful to Microcare laboratory and TRC, Surat, Gujarat for providing antimicrobial and antimalarial activities and Director, SAIF, Panjab University, Chandigarh for providing spectral data; Schrodinger Inc. for providing the software to perform the *in silico* study.

### **Disclosure statement**

No potential conflict of interest was reported by the author(s).

### **Funding**

Authors are thankful to Department of Science and Technology, New Delhi for providing financial assistance for research facilities under DST-FIST programme.

### **References**

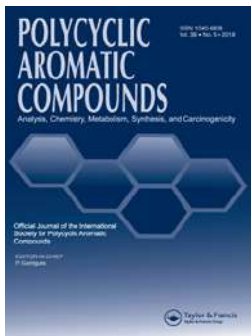
1. E. A. Ashley, A. Pyae Phyo, and C. J. Woodrow, "Malaria," *The Lancet* 391, no. 10130 (2018): 1608–21.
2. World Health Organization. "World Malaria Report 2019" (World Health Organization, Geneva, 2019). Licence: CC BY-NC-SA 3.0 IGO.

3. J. Talapko, I. Skrlec, T. Alebic, M. Jukic, and A. Vcev, "Malaria: The Past and the Present," *Microorganisms* 7 (2019): 179.
4. R. J. Heath, and C. O. Rock, "Enoyl-Acyl Carrier Protein Reductase (fabI) Plays a Determinant Role in Completing Cycles of Fatty Acid Elongation in Escherichia coli," *The Journal of Biological Chemistry* 270, no. 44 (1995): 26538–42.
5. R. F. Waller, S. A. Ralph, M. B. Reed, V. Su, J. D. Douglas, D. E. Minnikin, A. F. Cowman, G. S. Besra, and G. I. McFadden, "A Type II Pathway for Fatty Acid Biosynthesis Presents Drug Targets in Plasmodium falciparum," *Antimicrobial Agents and Chemotherapy* 47, no. 1 (2003): 297–301.
6. G. Nicola, C. A. Smith, E. Lucumi, M. R. Kuo, L. Karagyzov, D. A. Fidock, J. C. Sacchettini, and R. Abagyan, "Discovery of Novel Inhibitors Targeting Enoyl-Acyl Carrier Protein Reductase in Plasmodium falciparum by Structure-Based Virtual Screening," *Biochemical and Biophysical Research Communications* 358, no. 3 (2007): 686–91.
7. N. Surolia, and A. Surolia, "Triclosan Offers Protection against Blood Stages of Malaria by Inhibiting enoyl-ACP Reductase of Plasmodium falciparum," *Nature Medicine* 7, no. 2 (2001): 167–73.
8. S. Sharma, T. N. C. Ramya, A. Surolia, and N. Surolia, "Triclosan as a Systemic Antibacterial Agent in a Mouse Model of Acute Bacterial Challenge," *Antimicrobial Agents and Chemotherapy* 47, no. 12 (2003): 3859–66.
9. R. P. Samal, V. M. Khedkar, R. R. S. Pissurlenkar, A. G. Bwalya, D. Tasdemir, R. A. Joshi, P. R. Rajamohan, V. G. Puranik, and E. C. Coutinho, "Design, Synthesis, Structural Characterization by IR, (1) H, (13) C, (15) N, 2D-NMR, X-Ray Diffraction and Evaluation of a New Class of Phenylaminoacetic Acid Benzylidene Hydrazines as pFENR Inhibitors," *Chemical Biology & Drug Design* 81, no. 6 (2013): 715–29.
10. M. Chhibber, G. Kumar, P. Parasuraman, T. N. C. Ramya, N. Surolia, and A. Surolia, "Novel Diphenyl Ethers: Design, Docking Studies, Synthesis and Inhibition of Enoyl ACP Reductase of Plasmodium falciparum and Escherichia coli," *Bioorganic & Medicinal Chemistry* 14, no. 23 (2006): 8086–98.
11. V. A. Morde, M. S. Shaikh, R. R. S. Pissurlenkar, and E. C. Coutinho, "Molecular Modeling Studies, Synthesis, and Biological Evaluation of Plasmodium falciparum Enoyl-Acyl Carrier Protein Reductase (PfENR) Inhibitors," *Molecular Diversity* 13, no. 4 (2009): 501–17.
12. A. Manhas, A. Patel, M. Y. Lone, P. K. Jha, and P. C. Jha, "Identification of PfENR Inhibitors: A Hybrid Structure-Based Approach in Conjunction with Molecular Dynamics Simulations," *Journal of Cellular Biochemistry* 119, no. 10 (2018): 8490–500.
13. M. A. Berghot, and E. B. Moawad, "Convergent Synthesis and Antibacterial Activity of Pyrazole and Pyrazoline Derivatives of Diazepam," *European Journal of Pharmaceutical Sciences: Official Journal of the European Federation for Pharmaceutical Sciences* 20, no. 2 (2003): 173–9.
14. J. N. Dominguez, J. E. Charris, M. Caparelli, and F. Riggione, "Synthesis and Antimalarial Activity of Substituted Pyrazole Derivatives," *Arzneimittel-Forschung* 52, no. 6 (2002): 482–8.
15. R. Sridhar, P. T. Perumal, S. Etti, G. Shanmugam, M. N. Ponnuswamy, V. R. Prabavathy, and N. Mathivanan, "Design, Synthesis and anti-Microbial Activity of 1H-Pyrazole Carboxylates," *Bioorganic & Medicinal Chemistry Letters* 14, no. 24 (2004): 6035–40.
16. Shivapura Viveka, Dinesha Dinesha, Prasanna Shama, Shivalingegowda Naveen, Neratur Krishnappagowda Lokanath, and Gundibasappa Karikannar Nagaraja, "Design, Synthesis, Anticonvulsant and Analgesic Studies of New Pyrazole Analogues: A Knoevenagel Reaction Approach," *RSC Advances* 5no. 115 (2015): 94786–95.
17. Z. Xu, C. Gao, Q. C. Ren, X. F. Song, L. S. Feng, and Z. S. Lv, "Recent Advances of Pyrazole-Containing Derivatives as Anti-Tubercular Agents," *European Journal of Medicinal Chemistry* 139, (2017): 429–40.
18. R. S. Fabiane, T. S. Vanessa, R. Viviane, P. B. Lysandro, R. O. Marli, G. B. Helio, Z. Nilo, A. P. M. Marcos, and F. M. Carlos, "Hypothermic and Antipyretic Effects of 3-Methyl- and 3-Phenyl-5-Hydroxy-5-Trichloromethyl-4,5-Dihydro-1H-Pyrazole-1-Carboxyamides in Mice," *European Journal of Pharmacology* 451 (2002): 141–7.
19. A. Ana, R. C. Jose, P. C. Fernando, D. O. Agel, J. G. Maria, H. Antonio, L. Fernando, and M. Andres, "Efficient Tautomerization Hydrazone-Azomethine Imine under Microwave Irradiation. Synthesis of [4,3] and [5,3]Bipyrazoles," *Tetrahedron* 54 (1998): 13167–80.
20. K. O. Mohammed, and Y. M. Nissan, "Synthesis, Molecular Docking, and Biological Evaluation of Some Novel Hydrazones and Pyrazole Derivatives as Anti-Inflammatory Agents," *Chemical Biology & Drug Design* 84, no. 4 (2014): 473–88.
21. B. Insuasty, A. Montoya, D. Becerra, J. Quiroga, R. Abonia, S. Robledo, I. D. Velez, Y. Upegui, M. Noguera, and J. Cobo, "Synthesis of Novel Analogs of 2-pyrazoline Obtained from [(7-Chloroquinolin-4-yl)Amino]Chalcones and Hydrazine as Potential Antitumor and Antimalarial Agents," *European Journal of Medicinal Chemistry* 67 (2013): 252–62.
22. G. Kumar, O. Tanwar, J. Kumar, M. Akhter, S. Sharma, C. R. Pillai, M. M. Alam, and M. S. Zama, "Pyrazole-Pyrazoline as Promising Novel Antimalarial Agents: A Mechanistic Study," *European Journal of Medicinal Chemistry* 149 (2018): 139–47.



23. R. Alam, A. Alam, and A. K. Panda Rahisuddin, "Design, Synthesis and Cytotoxicity Evaluation of Pyrazolyl Pyrazoline and Pyrazolyl Aminopyrimidine Derivatives as Potential Anticancer Agents," *Medicinal Chemistry Research* 27 (2018): 560–70.
24. S. Viveka, D. P. Shama, G. K. Nagaraja, S. Ballav, and S. Kerkar, "Design and Synthesis of Some New Pyrazolyl-Pyrazolines as Potential Anti-Inflammatory, Analgesic and Antibacterial Agents," *European Journal of Medicinal Chemistry* 101 (2015): 442–51.
25. H. Khanam, A. Mashrai, A. Sherwani, M. Owais, and N. Siddiqui, "Synthesis and Anti-Tumor Evaluation of B-Ring Substituted Steroidal Pyrazoline Derivatives," *Steroids* 78, (2013): 1263–72.
26. S. K. Sahu, M. Banerjee, A. Samantray, C. Behera, and M. A. Azam, "Synthesis, Analgesic, anti-Inflammatory and Antimicrobial Activities of Some Novel Pyrazoline Derivatives," *Tropical Journal of Pharmaceutical Research* 7, no. 2 (2008): 961–8.
27. M. Johnson, B. Younglove, L. Lee, R. LeBlanc, H. Holt, Jr, P. Hills, H. Mackay, T. Brown, S. L. Mooberry, and M. Lee, "Design, Synthesis, and Biological Testing of Pyrazoline Derivatives of combretastatin-A4," *Bioorganic & Medicinal Chemistry Letters* 17, no. 21 (2007): 5897–901.
28. J. Vinayagam, R. L. Gajbhiye, L. Mandal, M. Arumugam, A. Achari, and P. Jaisankar, "Substituted Furans as Potent Lipoxigenase Inhibitors: Synthesis, in Vitro and Molecular Docking Studies," *Bioorganic Chemistry* 71 (2017): 97–101.
29. C. J. Lim, N. H. Kim, H. J. Park, B. H. Lee, K. S. Oh, and K. Y. Yi, "Synthesis and SAR of 5-Aryl-Furan-2-Carboxamide Derivatives as Potent urotensin-II Receptor Antagonists," *Bioorganic & Medicinal Chemistry Letters* 29, no. 4 (2019): 577–80.
30. B. Wang, Y. Shi, Y. Zhan, L. Zhang, Y. Zhang, L. Wang, X. Zhang, Y. Li, Z. Li, and B. Li, "Synthesis and Biological Activity of Novel Furan/Thiophene and Piperazine-Containing (Bis)1,2,4-Triazole Mannich Bases," *Chinese Journal of Chemistry* 33, no. 10 (2015): 1124–34.
31. Z. Lan, D. Xinshan, W. Jiaofeng, M. Guangpeng, L. Congchong, C. Guzhou, Z. Qingchun, and H. Chun, "Design, Synthesis and Biological Activities of N-(Furan-2-Ylmethyl)-1H-Indole-3-Carboxamide Derivatives as Epidermal Growth Factor Receptor Inhibitors and Anticancer Agents," *Chemical Research in Chinese Universities* 33, no. 3 (2017): 365–72.
32. M. L. Go, M. Liu, P. Wilairat, P. J. Rosenthal, K. J. Saliba, and K. Kirk, "Anti-plasmodial Chalcones Inhibit Sorbitol-Induced Hemolysis of Plasmodium falciparum-Infected Erythrocytes," *Antimicrobial Agents and Chemotherapy* 48, no. 9 (2004): 3241–5.
33. J. A. Gonzalez, and A. Estevez-Braun, "Effect of (E)-Chalcone on Potato-Cyst Nematodes *Globodera pallida* and *G. rostochiensis*," *Journal of Agricultural and Food Chemistry* 46 (1998): 1163–5.
34. M. Yoshimura, A. Sano, J. L. Kamei, and A. Obata, "Identification and Quantification of Metabolites of Orally Administered Naringenin Chalcone in Rats," *Journal of Agricultural and Food Chemistry* 57, no. 14 (2009): 6432–7.
35. M. Chen, T. G. Theander, S. B. Christensen, L. Hviid, L. Zhai, and A. Kharazmi, "Licochalcone A, a New Antimalarial Agent, Inhibits in Vitro Growth of the Human Malaria Parasite *Plasmodium falciparum* and Protects Mice from *P. yoelii* Infection," *Antimicrobial Agents and Chemotherapy* 38, no. 7 (1994): 1470–5.
36. L. Mishra, R. Sinha, H. Itokawa, K. F. Bastow, Y. Tachibana, Y. Nakanishi, N. Kilgore, and K. H. Lee, "Anti-HIV and Cytotoxic Activities of Ru(II)/Ru(III) Polypyridyl Complexes Containing 2,6-(2'-Benzimidazolyl)-Pyridine/Chalcone as Co-Ligand," *Bioorganic & Medicinal Chemistry* 9, no. 7 (2001): 1667–71.
37. C. Jin, Y. J. Liang, H. He, and L. Fu, "Synthesis and Antitumor Activity of Novel Chalcone Derivatives," *Biomedicine & Pharmacotherapy = Biomedecine & Pharmacotherapie* 67, no. 3 (2013): 215–7.
38. F. Herencia, M. L. Ferrándiz, A. Ubeda, J. N. Domínguez, J. E. Charris, G. M. Lobo, and M. J. Alcaraz, "Synthesis and anti-Inflammatory Activity of Chalcone Derivatives," *Bioorganic & Medicinal Chemistry Letters* 8, no. 10 (1998): 1169–74.
39. Y. Qian, G. Y. Ma, Y. Yang, K. Cheng, Q. Z. Zheng, W. J. Mao, L. Shi, J. Zhao, and H. L. Zhu, "Synthesis, Molecular Modeling and Biological Evaluation of Dithiocarbamates as Novel Antitubulin Agents," *Bioorganic & Medicinal Chemistry* 18, no. 12 (2010): 4310–6.
40. R. A. Friesner, J. L. Banks, R. B. Murphy, T. A. Halgren, J. J. Klicic, D. T. Mainz, M. P. Repasky, E. H. Knoll, M. Shelley, J. K. Perry, et al. "Glide: A New Approach for Rapid, Accurate Docking and Scoring. 1. Method and Assessment of Docking accuracy," *Journal of Medicinal Chemistry* 47, no. 7 (2004): 1739–49.
41. R. A. Friesner, R. B. Murphy, M. P. Repasky, L. L. Frye, J. R. Greenwood, T. A. Halgren, P. C. Sanschagrin, and D. T. Mainz, "Extra Precision Glide: Docking and Scoring Incorporating a Model of Hydrophobic Enclosure for Protein-Ligand Complexes," *Journal of Medicinal Chemistry* 49, no. 21 (2006): 6177–96.
42. T. A. Halgren, R. B. Murphy, R. A. Friesner, H. S. Beard, L. L. Frye, W. T. Pollard, and J. L. Banks, "Glide: A New Approach for Rapid, Accurate Docking and Scoring. 2. Enrichment Factors in Database Screening," *Journal of Medicinal Chemistry* 47, no. 7 (2004): 1750–9.

43. S. J. Takate, A. D. Shinde, B. K. Karale, H. Akolkar, L. Nawale, D. Sarkar, and P. C. Mhaske, "Thiazolyl-Pyrazole Derivatives as Potential Antimycobacterial Agents," *Bioorganic & Medicinal Chemistry Letters* 29, no. 10 (2019): 1199–202.
44. K. H. Rieckmann, G. H. Campbell, L. J. Sax, and J. E. Ema, "Drug Sensitivity of plasmodium falciparum. An In-Vitro Micro Technique," *The Lancet* 311, no. 8054 (1978): 22–3.
45. R. Panjarathinam, *Text Book of Medical Parasitology*, 2nd ed. (Chennai: Orient Longman Pvt. Ltd., 2007), 329–331.
46. C. Lambros, and J. P. Vanderberg, "Synchronization of Plasmodium falciparum Erythrocytic Stages in Culture," *The Journal of Parasitology* 65, no. 3 (1979): 418–20.
47. J. S. B. Singh, "Stain; a Review," *Indian Journal of Malariology* 10 (1956): 117–29.




## Tetrazoloquinoline-1,2,3-Triazole Derivatives as Antimicrobial Agents: Synthesis, Biological Evaluation and Molecular Docking Study

**Mubarak H. Shaikh**, Dnyaneshwar D. Subhedar, Satish V. Akolkar, Amol A. Nagargoje, Vijay M. Khedkar, Dhiman Sarkar & Bapurao B. Shingate

To cite this article: Mubarak H. Shaikh, Dnyaneshwar D. Subhedar, Satish V. Akolkar, Amol A. Nagargoje, Vijay M. Khedkar, Dhiman Sarkar & Bapurao B. Shingate (2020): Tetrazoloquinoline-1,2,3-Triazole Derivatives as Antimicrobial Agents: Synthesis, Biological Evaluation and Molecular Docking Study, Polycyclic Aromatic Compounds, DOI: [10.1080/10406638.2020.1821229](https://doi.org/10.1080/10406638.2020.1821229)


To link to this article: <https://doi.org/10.1080/10406638.2020.1821229>

 View supplementary material 

 Published online: 16 Sep 2020.

 Submit your article to this journal 

 Article views: 6

 View related articles 

 View Crossmark data 



# Tetrazoloquinoline-1,2,3-Triazole Derivatives as Antimicrobial Agents: Synthesis, Biological Evaluation and Molecular Docking Study

Mubarak H. Shaikh<sup>a,b</sup>, Dnyaneshwar D. Subhedar<sup>a</sup>, Satish V. Akolkar<sup>a</sup>,  
Amol A. Nagargoje<sup>a,c</sup>, Vijay M. Khedkar<sup>d</sup>, Dhiman Sarkar<sup>e</sup>, and Bapurao B. Shingate<sup>a</sup>

<sup>a</sup>Department of Chemistry, Dr. Babasaheb Ambedkar Marathwada University, Aurangabad, India; <sup>b</sup>Department of Chemistry, Radhabai Kale Mahila Mahavidyalaya, Ahmednagar, India; <sup>c</sup>Department of Chemistry, Khopoli Municipal Council College, Khopoli, India; <sup>d</sup>Department of Pharmaceutical Chemistry, School of Pharmacy, Vishwakarma University, Pune, India; <sup>e</sup>Combi-Chem Resource Centre, CSIR-National Chemical Laboratory, Pune, India

## ABSTRACT

In search of new active molecules, a small focused library of tetrazoloquinoline-based 1,2,3-triazoles has been efficiently prepared *via* click chemistry approach. Several derivatives were found to be exhibiting promising antimicrobial and antioxidant activity characterized by their lower minimum inhibitory concentration values. All the synthesized compounds exhibited excellent antibacterial activity against Gram negative bacteria *E. coli* and *F. devorans* and antifungal activity against *C. albicans* and *A. niger*. Further, these compounds were tested for their antitubercular activity against dormant *MTB H37Ra* and dormant *M. bovis BCG* using XRMA assay protocol and showed no significant activity. Also, the synthesized compounds were found to have potential antioxidant activity with  $IC_{50}$  range = 12.48–50.20  $\mu$ g/mL. Furthermore, to rationalize the observed biological activity data, the molecular docking study also been carried out against the active site of fungal *C. albicans* enzyme P450 cytochrome lanosterol 14 $\alpha$ -demethylase, which revealed a significant correlation between the binding score and biological activity for these compounds. The results of the *in vitro* and *in silico* study suggest that the triazole-incorporated tetrazoloquinolines may possess the ideal structural requirements for further development of novel therapeutic agents.

## ARTICLE HISTORY

Received 21 June 2020  
Accepted 5 September 2020


## KEYWORDS

1,2,3-Triazole; antimicrobial; antioxidant; docking study; ADME prediction

## Introduction

In recent years, life threatening systemic fungal infections have become increasingly common, especially in immunocompromised hosts suffering from tuberculosis, cancer, or AIDS and in organ transplant cases. Development of resistance against available antifungal agents (generally azoles) is also an alarming factor. Commonly used azole antifungal agents are fluconazole, itraconazole, miconazole, and voriconazole displayed broad spectrum antifungal activity.<sup>1</sup> Azoles have broad spectrum activities against most yeasts and filamentous fungi and are the drug of choice for antifungal chemotherapy.<sup>2</sup> These antifungal drugs inhibiting CYP51 in the process of biosynthesis of ergosterol through a mechanism in which the heterocyclic nitrogen atom (*N*-4

**CONTACT** Bapurao B. Shingate  [bapushingate@gmail.com](mailto:bapushingate@gmail.com)  Department of Chemistry, Dr. Babasaheb Ambedkar Marathwada University, Aurangabad 431 004, India.

 Supplemental data for this article is available online at <https://doi.org/10.1080/10406638.2020.1821229>.



of triazole) binds to the heme iron atom.<sup>3</sup> However, increasing use of these antifungal drugs has led to increase in resistance to these drugs.<sup>4-6</sup>

Heterocyclic compounds play an important role in designing new class of structural entities for medicinal applications. Quinoline and their derivatives are pharmacologically important heterocyclic compounds because of their wide existence in alkaloids, therapeutics, and synthetic analogues with interesting biological activities such as antimalarial,<sup>7</sup> analgesic,<sup>8</sup> anticancer,<sup>9</sup> anti-inflammatory,<sup>10</sup> antiviral,<sup>11</sup> antihelmintic,<sup>12</sup> anti-protozoal,<sup>13</sup> cardiovascular,<sup>14</sup> hypoglycemic,<sup>15</sup> and antimicrobial activity.<sup>16</sup>

Triazoles are stable to acidic/basic hydrolysis and also reductive/oxidative conditions, indicative of a high aromatic stabilization. This moiety is relatively resistant to metabolic degradation. Over the past two decades 1,2,3-triazole and its derivatives have attracted continued interest in the medicinal field and are reported to possess a wide range of biological activities such as antifungal,<sup>17</sup> antitubercular,<sup>18</sup> antiallergic,<sup>19</sup> a anti-HIV,<sup>19</sup> a antibacterial,<sup>19</sup> b  $\alpha$ -glycosidase inhibitor,<sup>20</sup> antimicrobial,<sup>21</sup> anticoccidiostats,<sup>22</sup> anticonvulsant,<sup>23</sup> antimalarial,<sup>24</sup> antiviral,<sup>25</sup> and antimycobacterial.<sup>26</sup> Triazole has been used to improve the pharmacokinetic properties of the desired drug.<sup>27</sup>

Click chemistry is a newer approach for the synthesis of drug-like molecules that can accelerate the drug discovery process by utilizing a few practical and reliable reactions. Sharpless<sup>28</sup> and Meldal<sup>29</sup> groups have reported the dramatic rate enhancement (up to 10<sup>7</sup> times) and improved regio-selectivity of the Huisgen 1,3-dipolar cycloaddition reaction of an organic azide and terminal acetylene to afford, regio-specifically, the 1,4-disubstituted-1,2,3-triazole in the presence of Cu (I) catalyst. The Cu (I)-catalyzed azide alkyne cycloaddition (CuAAC) reaction has successfully fulfilled the requirement of "click chemistry" as prescribed by Sharpless and within the past few years has become a premier component of synthetic organic chemistry.<sup>30</sup>

Tetrazoles can act as pharmacophore for the carboxylate group, increasing their utility. Angiotensin II blocker often contain tetrazoles, as Losartan and candesartan. Tetrazoles and its derivatives displays various biological activities such as antibacterial,<sup>31</sup> a,b anti-inflammatory,<sup>31</sup> a,b antinociceptive,<sup>31</sup> a,b hypoglycemic,<sup>31</sup> a,b anticancer<sup>31</sup> a,b antifungal,<sup>31</sup> c antiviral,<sup>31</sup> a antitubercular & antimalarial,<sup>31</sup> d and cyclo-oxygenase inhibitors activities.<sup>31</sup> e They are used as catalyst in the synthesis of phosphonates.<sup>31</sup> a

In recent years, a library of quinoline derivatives conjugated with 1,2,3-triazole were synthesized and proved to possess different bioactivity such as antimicrobial activity<sup>32</sup> (Figure 1, A),  $\beta$ -haematin inhibitor<sup>33</sup> (Figure 1, B), antimalarial agent<sup>33</sup> (Figure 1, C), antifungal agent<sup>16</sup> (Figure 1, D), antimalarial and cytotoxic activity<sup>34</sup> (Figure 1, E), DNA binding and photonuclease activity<sup>35</sup> (Figure 1, F).

In continuation of our earlier work<sup>16,36</sup> on synthesis and biological properties of heterocyclic moieties and the importance of tetrazoloquinoline-1,2,3-triazole moieties as a single molecular scaffold, herein we would like to report the design and syntheses of new tetrazoloquinoline-linked triazole hybrids and their evaluation for antimicrobial and antioxidant activities. The computational parameters like docking study for antimicrobial activity and ADME prediction of synthesized tetrazoloquinoline-triazole conjugates **5a-i** were also performed.

## Results and discussion

### Chemistry

We have described a protocol for the syntheses of a series of new derivatives of 8-methoxy-4-((4-(phenoxyethyl)-1H-1,2,3-triazol-1-yl)methyl)tetrazolo[1,5-*a*]quinoline **5a-i** as a potential antimicrobial, antioxidant, and antitubercular agents from commercially available starting materials. These compounds were formed by the fusion of substituted (prop-2-yn-1-yloxy)benzenes **4a-h**,

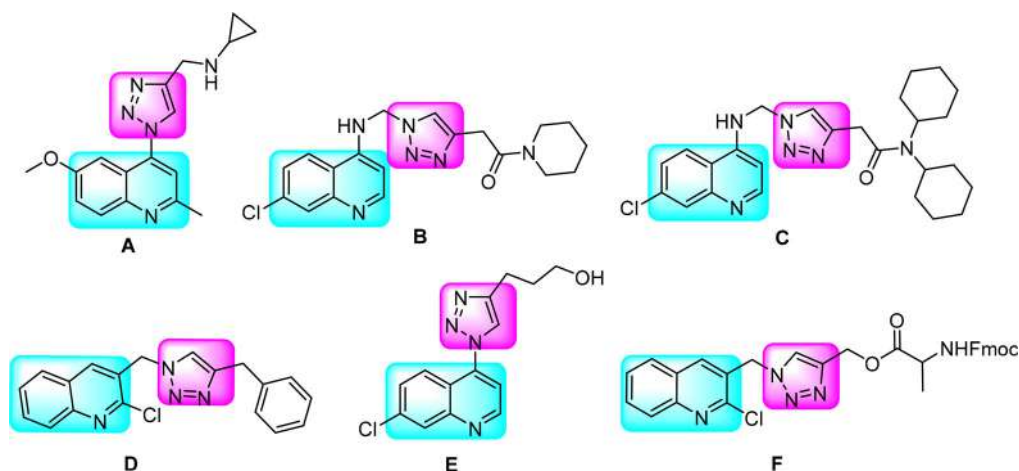
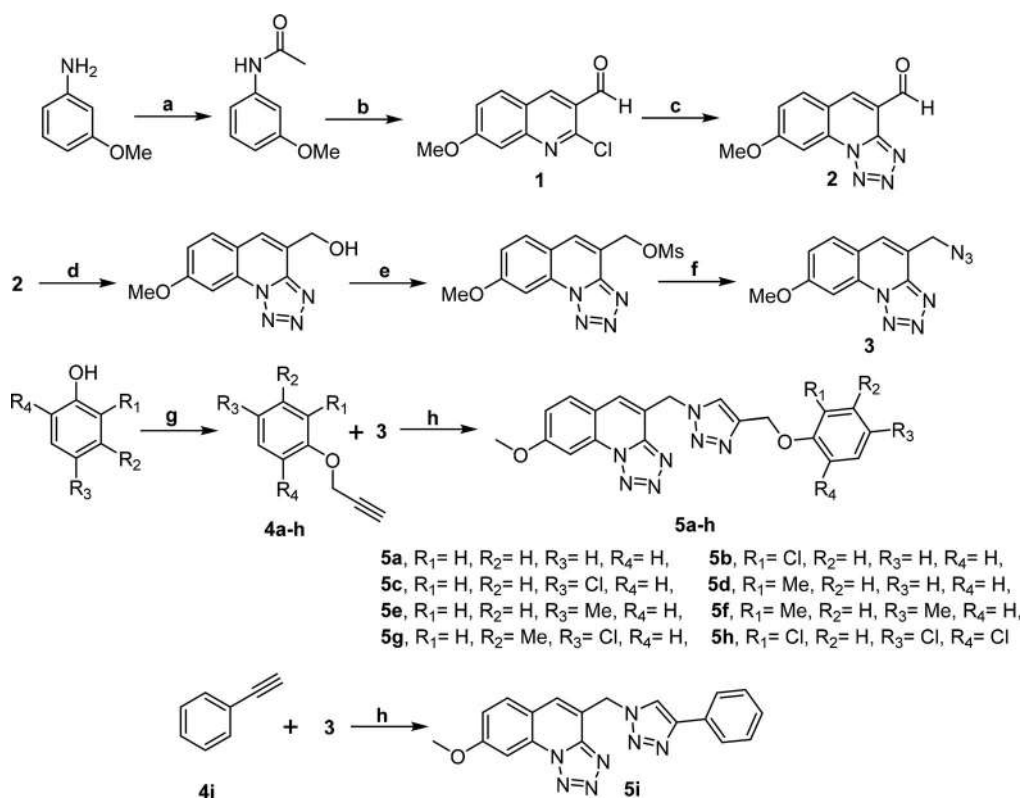


**Figure 1.** Triazole incorporated quinoline derivatives A–F.

phenyl acetylene **4i** and 4-(azidomethyl)-8-methoxytetrazolo[1,5-*a*]quinoline **3** via click chemistry approach (Scheme 1). The synthesis of starting material 4-(azidomethyl)-8-methoxytetrazolo[1,5-*a*]quinoline **3** was prepared from 8-methoxytetrazolo[1,5-*a*]quinoline-4-carbaldehyde **2** via  $\text{NaBH}_4$  reduction, mesylation followed by nucleophilic substitution reaction of sodium azide (Scheme 1).

The synthesis of methoxytetrazolo[1,5-*a*]quinoline-4-carbaldehyde **2** was prepared from 3-methoxyaniline (*m*-anisidine) which on acylation followed by Vilsmeier-Haack formylation at  $80^\circ\text{C}$  for 8 hr to generate 2-chloro-7-methoxyquinoline-3-carbaldehyde **1**, which on further reaction with sodium azide in DMF at  $80^\circ\text{C}$  for 6 hr produces tetrazoloquinoline aldehyde **2** in good yield. The commercially available phenols have been alkylated with propargyl bromide in the presence of  $\text{K}_2\text{CO}_3$  as a base in *N,N*-dimethylformamide (DMF) afforded the corresponding (prop-2-yn-1-yloxy)benzene derivatives **4a–h** in good to excellent yield (Supporting Information). Finally, the Huisgen's CuAAC reaction has been performed on 4-(azidomethyl)-8-methoxytetrazolo[1,5-*a*]quinoline **3** and (prop-2-yn-1-yloxy)benzene derivatives **4a–h** and phenylacetylene **4i** in the presence of  $\text{Cu}(\text{OAc})_2$  in *t*-BuOH- $\text{H}_2\text{O}$  (3:1) at room temperature for 16–22 hr gives the corresponding 1,4-disubstituted-1,2,3-triazole based tetrazoloquinoline derivatives **5a–h** and **5i**, respectively, in quantitative isolated yield (86–90%) (Scheme 1). The formation of compounds **3** and **5a–i** were confirmed by  $^1\text{H}$  NMR,  $^{13}\text{C}$  NMR, and HRMS spectral analysis. In the  $^1\text{H}$  NMR spectrum of the compound **5a**, the two methylene groups attached to nitrogen and oxygen showed singlet at  $\delta$  5.16 and 6.09 ppm, respectively. In addition to this, the signal observed at  $\delta$  4.06 ppm indicates the  $-\text{OCH}_3$  proton present on the quinoline ring. Similarly signal observed at  $\delta$  8.01 ppm indicates the proton present on the triazole ring. In the  $^{13}\text{C}$  NMR spectrum for compound **5a**, the signals at  $\delta$  61.5 and 66.2 ppm indicates the presence of methylene carbon attached to the nitrogen of triazole ring and oxygen to phenyl ring, respectively, and signal at  $\delta$  54 ppm indicates the presence of methoxy carbon.

For compound **5a**, the calculated mass for  $[\text{M} + \text{H}]^+$  is 388.1516 and in HRMS, the  $[\text{M} + \text{H}]^+$  peak observed at 388.1513. Furthermore, to expand the series, 1,4-disubstituted-1,2,3-triazole tetrazoloquinoline derivatives **5b–i** with various substituent has been prepared by the cycloaddition reaction of 4-(azidomethyl)-8-methoxytetrazolo[1,5-*a*]quinoline **3** and alkynes (prop-2-yn-1-yloxy)benzene derivatives **4b–h** and phenylacetylene **6** (Scheme 1) under similar reaction condition in good to excellent yields.



**Scheme 1.** Reagents and conditions: (a) acetic acid, 110–120 °C, 6 hr; (b) DMF, POCl<sub>3</sub>, 0–80 °C, 8 hr, (c) NaN<sub>3</sub>, DMF, 80 °C, 6 hr; (d) NaBH<sub>4</sub>, methanol, 0 °C to rt, 2 hr; (e) MsCl, DCM, 0 °C to rt, 4 hr; (f) NaN<sub>3</sub>, DMF, 80 °C, 2 hr; (g) propargyl bromide, K<sub>2</sub>CO<sub>3</sub>, DMF; (h) Cu(OAc)<sub>2</sub> (20 mol%), *t*-BuOH-H<sub>2</sub>O (3:1), rt.

## Biological evaluation

### Antibacterial activity

Minimum inhibitory concentration (MIC) values for bacteria determined according to the two-fold broth micro-dilution method using Muller-Hinton broth in 96-well micro-test plates recommended by National Committee for Clinical Laboratory Standards (NCCLS) guidelines.<sup>37</sup> All the tested tetrazoloquinoline-1,4-disubstituted 1,2,3-triazole based derivatives **5a–i** shows significant antibacterial activity (Table 1). For bacterial strain *S. aureus*, it can be seen that, the compounds **5b**, **5d**, **5e**, **5f**, and **5g** shows excellent inhibitory activity with MIC value 8 µg/mL, which is two-fold more potent than the clinical drug ampicillin and kanamycin (MIC 16 µg/mL) and equivalent to the chloramphenicol (8 µg/mL). However, the compounds **5a**, **5c**, **5h**, and **5i** also possess equivalent antibacterial effect against *S. aureus* with MIC value 16 µg/mL compared to the ampicillin and kanamycin. Compounds **5b**, **5c**, **5d**, **5f**, **5h**, and **5i** with MIC value 16 µg/mL exhibit equivalent antibacterial activity for *M. luteus* compared to the standard drug ampicillin. All the synthesized compounds show considerable activity against *B. cereus*, especially compounds **5e**, **5f**, **5g**, and **5i** with MIC value 4 µg/mL exhibited four-fold more activity compared to the ampicillin and two-fold more potent than kanamycin and chloramphenicol. Compound **5h** shows equivalent activity compared to the standard drug kanamycin and chloramphenicol. Compounds **5b** and **5c** show good activity against *B. cereus* compared to the ampicillin. It can be seen that, all the synthesized tetrazoloquinoline-1,2,3-triazole-based derivatives **5a–i** possess comparable activity against *E. coli* as compared to ampicillin, kanamycin, and chloramphenicol.

**Table 1.** *In vitro* antimicrobial evaluation of synthesized compounds **3** and **5a-i** MIC values ( $\mu\text{g/mL}$ ).

Entry	Antibacterial activity											CN
	Gram +ve bacteria			Gram -ve bacteria			Antifungal activity					
	SA	ML	BC	EC	PF	FD	CA	AN	CL	PC	AF	
<b>3</b>	128	128	256	256	256	256	128	128	256	256	256	256
<b>5a</b>	16	32	32	16	16	8	8	8	8	32	32	128
<b>5b</b>	8	16	16	8	8	32	16	16	32	64	16	32
<b>5c</b>	16	16	16	4	8	4	4	8	8	16	16	16
<b>5d</b>	8	16	32	4	128	16	16	32	16	32	16	128
<b>5e</b>	8	32	4	16	16	16	8	8	8	64	16	16
<b>5f</b>	8	16	4	4	16	8	16	8	16	64	32	32
<b>5g</b>	8	32	4	4	4	4	4	8	8	32	8	128
<b>5h</b>	16	16	8	4	4	4	4	8	8	32	128	256
<b>5i</b>	16	16	4	4	128	4	8	16	32	128	256	256
AP	16	16	16	16	16	16	–	–	–	–	–	–
KM	16	8	8	16	16	16	–	–	–	–	–	–
CP	8	8	8	8	8	8	–	–	–	–	–	–
MA	–	–	–	–	–	–	16	16	16	16	16	16
AB	–	–	–	–	–	–	16	8	16	16	8	16
FA	–	–	–	–	–	–	8	8	8	8	8	8

SA, *Staphylococcus aureus*; ML, *Micrococcus luteus*; BC, *Bacillus cereus*; EC, *Escherichia coli*; PF, *Pseudomonas fluorescens*; FD, *Flavobacterium devorans*; AN, *Aspergillus niger*; PC, *Penicillium chrysogenum*; CL, *Curvularia lunata*; CA, *Candida albicans*; AF, *Aspergillus flavus*; CN, *Cryptococcus neoformans*; AP, Ampicillin; KM, Kanamycin; CP, Chloramphenicol; MA, Miconazole; AB; Amphotericin B; FA, Fluconazole.

Compounds **5c**, **5d**, **5f**, **5g**, **5h**, and **5i** with MIC value  $4\ \mu\text{g/mL}$  shows four-fold more activity compared to the ampicillin, kanamycin, and two-fold more activity compared to the chloramphenicol against *E. coli*. Compound **5b** with MIC value  $8\ \mu\text{g/mL}$ , possesses equivalent activity compared to the standard drug chloramphenicol. Compounds **5g** and **5h** with MIC value  $4\ \mu\text{g/mL}$  show four-fold more activity compared to the ampicillin, kanamycin, and two-fold more activity compared to the chloramphenicol against bacterial strain *P. fluorescens*. Compounds **5b** and **5c** shows two-fold more activity compared to the standard ampicillin, kanamycin, and show equivalent activity compared to the chloramphenicol. Compounds **5a**, **5e**, and **5f** show equivalent activity compared to the standard drug ampicillin and chloramphenicol with MIC value  $16\ \mu\text{g/mL}$ . Compounds **5c**, **5g**, **5h**, and **5i** with MIC value  $4\ \mu\text{g/mL}$  show four-fold more activity compared to the ampicillin, kanamycin, and two-fold more activity compared to the chloramphenicol against bacterial strain *F. devorans*.

Compounds **5a** and **5f** (MIC =  $8\ \mu\text{g/mL}$ ) show two-fold more activity compared to the standard ampicillin, kanamycin, and shows equivalent activity compared to the chloramphenicol. Compounds **5d** and **5e** show equivalent activity compared to the ampicillin and chloramphenicol with MIC value  $16\ \mu\text{g/mL}$ . In general, for Gram positive bacteria, among all the synthesized compounds **3** and **5a-i**, compounds **5e**, **5f**, **5g**, and **5i** show promising antibacterial activity against bacterial strain *B. cereus* and all the synthesized compounds exhibited excellent antibacterial activity against Gram negative bacteria *E. coli* and *F. devorans* compared to the standard drugs.

### Antifungal activity

Fungi were subcultured in potato dextrose broth medium. MIC of the synthesized compounds was determined using potato dextrose broth in 96-well micro-test plates recommended by NCCLS guidelines.<sup>37</sup> In case of antifungal activity, all the synthesized 1,4-disubstituted 1,2,3-triazole-based tetrazoloquinoline derivatives **5a-i** show good to moderate activity against *C. albicans*, *A. niger*, *C. lunata*, *P. chrysogenum*, *A. flavus*, and *C. neoformans* strains (Table 1). Compounds **5c**, **5g**, and **5h** with MIC value  $4\ \mu\text{g/mL}$ , exhibited four-fold more activity compared to the standard drug miconazole, amphotericin B and two-fold more activity compared to the fluconazole against the fungicidal strain *C. albicans*. Compounds **5a**, **5e**, and **5i** with MIC values  $8\ \mu\text{g/mL}$ ,

exhibited two-fold more activity compared to the standard drug miconazole, amphotericin B and equivalent potency compared to the standard fluconazole. Compounds **5b**, **5d**, and **5f** with MIC values 16  $\mu\text{g}/\text{mL}$ , exhibited equivalent activity compared to the standard drug miconazole and amphotericin B against the fungal strain *C. albicans*. Compounds **5a**, **5c**, **5e**, **5f**, **5g**, and **5h** with MIC values 8  $\mu\text{g}/\text{mL}$ , exhibited two-fold more activity compared to the standard drug miconazole, amphotericin B and equivalent activity compared to the fluconazole against the fungicidal strain *A. niger*. Compounds **5b** and **5i** with MIC values 16  $\mu\text{g}/\text{mL}$ , exhibited equivalent potency compared to the standard drug miconazole against the fungal strain *A. niger*. Compounds **5a**, **5c**, and **5e** with MIC values 8  $\mu\text{g}/\text{mL}$ , exhibited two-fold more activity compared to the standard drug miconazole, amphotericin B and equivalent activity compared to the fluconazole against the fungicidal strain *C. lunata*. Compounds **5d** and **5f** with MIC values 16  $\mu\text{g}/\text{mL}$ , exhibited equivalent potency compared to the standard drug miconazole and amphotericin B against the fungal strain *C. lunata*. Compound **5c** with MIC values 16  $\mu\text{g}/\text{mL}$ , exhibited equivalent potency compared to the standard drug miconazole and amphotericin B against the fungal strain *P. chrysogenum*. Compound **5g** with MIC values 8  $\mu\text{g}/\text{mL}$ , exhibited two-fold more activity compared to the standard drug miconazole and equivalent potency compared to the amphotericin B and fluconazole against the fungal strain *A. flavus*. Compounds **5b**, **5c**, **5d**, and **5e** with MIC value 16  $\mu\text{g}/\text{mL}$  exhibited equivalent activity as compared to standard drug miconazole for fungal strain *A. flavus*. Compounds **5c** and **5e** with MIC value of 16  $\mu\text{g}/\text{mL}$ , show equivalent antifungal activity against *C. neoformans* as compared to standard drug miconazole and fluconazole. Overall, the starting material 4-(azidomethyl)-8-methoxytetrazolo[1,5-*a*]quinoline **3** exhibited very less antifungal activity but the 1,2,3-triazoles derived from the azide **3** shows excellent antifungal activity compared to the standard antifungal drugs miconazole, amphotericin B and fluconazole.

### Antitubercular activity

All the synthesized compounds **5a-i** showed antibacterial activity against both Gram positive and Gram negative bacteria, especially against the Gram negative bacteria. As these compounds have shown significant antibacterial activities, we extended our study for evaluation of antitubercular activity. The newly synthesized 1,4-disubstituted-1,2,3-triazole containing tetrazoloquinoline derivatives **5a-i** were screened for *in vitro* antitubercular activity against *MTB H37Ra* (ATCC 25177) and *M. bovis BCG* (ATCC 35743) in liquid medium. In a preliminary screening (Supporting Information, Table S1), the antimycobacterial activity of these compounds was assessed at concentrations of 30, 10, and 3  $\mu\text{g}/\text{mL}$  using an established XTT Reduction Menadione assay (XRMA) anti-tubercular screening protocol<sup>38</sup> using first-line antitubercular drugs rifampicin and isoniazid as reference standards and the MIC and  $\text{IC}_{50}$  values are presented in Table 2. The MIC, that is, concentration of compounds required to completely inhibit MTB growth, were recorded. The MIC was calculated from a dose response curve. The compounds with more than 90% inhibition of initial primary screening were further assayed for secondary screening, that is, determination of MIC against dormant *MTB H37Ra* and dormant *M. bovis BCG* clinical isolates (drug sensitive and resistant). The tetrazoloquinoline-1,2,3-triazole conjugates **5a-i** (MIC range > 30  $\mu\text{g}/\text{mL}$ ) were found to be particularly inactive against dormant *MTB H37Ra*, dormant *M. bovis BCG*.

### Antioxidant activity

In the present study, antioxidant activity of the synthesized compounds has been assessed *in vitro* by the 1,1-diphenyl-2-picrylhydrazyl (DPPH) radical scavenging assay<sup>39</sup> and all the synthesized compounds **5a-i** show good to moderate antioxidant activity as compared to the standard drug BHT (Butylated Hydroxy Toluene) (Table 2). Compounds **5b** and **5d** having *chloro*-substituent at *ortho*- and *para*-position of phenyl ring, respectively, shows potent activity ( $\text{IC}_{50}$  12.48 and 16.30  $\mu\text{g}/\text{mL}$ , respectively) as compared to the standard drug BHT. However, the compound **5g**



**Table 2.** *In vitro* antitubercular activity against dormant *MTB H37Ra*, dormant *M. bovis BCG* and DPPH radical scavenging activity of compound **3** and **5a-i**.

Compounds	MTB H37Ra dormant		<i>M. bovis</i> BCG dormant		DPPH IC <sub>50</sub> (µg/mL)
	MIC	IC <sub>50</sub>	MIC	IC <sub>50</sub>	
<b>3</b>	>30	>30	>30	>30	50.20
<b>5a</b>	>30	>30	>30	>30	29.43
<b>5b</b>	>30	>30	>30	>30	12.48
<b>5c</b>	>30	>30	>30	>30	16.30
<b>5d</b>	>30	>30	>30	>30	40.41
<b>5e</b>	>30	>30	>30	>30	26.78
<b>5f</b>	>30	>30	>30	>30	32.55
<b>5g</b>	>30	>30	>30	>30	15.19
<b>5h</b>	>30	>30	>30	>30	19.20
<b>5i</b>	>30	>30	>30	>30	33.82
<b>RP</b>	0.043 ± 0.15	0.0018 ± 0.009	0.041 ± 0.01	0.0016 ± 0.002	NT
<b>INH</b>	0.075 ± 0.25	0.0025 ± 0.0007	0.045 ± 0.02	0.0023 ± 0.001	NT
<b>BHT</b>	NT	NT	NT	NT	16.47

RP: Rifampicin; INH: Isoniazid; BHT: Butylated hydroxy toluene; NT: Not tested.

(15.19 µg/mL) with *methyl*-group at *meta*- and *chloro*-group at *para*-position of phenyl ring shows excellent antioxidant activity as compared to the BHT. The starting material 4-(azidomethyl)-8-methoxytetrazolo[1,5-*a*]quinoline **3** exhibited very less antioxidant activity as compared to standard drugs.

## Computational study

### Molecular docking

Molecular docking is now an established approach in drug discovery for predicting the binding mode of a specified compound within the active site of the protein target of interest and the types of thermodynamic interactions governing the protein-inhibitor complexation especially in the absence of available resources to carry out the enzymatic assays. Thus, with the aim of rationalizing the promising antifungal activity portrayed by the title compounds tetrazoloquinoline-1,2,3-triazole derivatives (**5a-i**) and to gain an insight into the molecular basis of their interactions, a molecular docking study was carried out against the fungal sterol 14 $\alpha$ -demethylase (CYP51) as the target enzyme. Sterol 14 $\alpha$ -demethylase (CYP51) is an ancestral activity of the cytochrome P450 superfamily. It converts lanosterol into 4,4'-dimethyl cholesta-8,14,24-triene-3- $\beta$ -ol-a step required for ergosterol biosynthesis which is an essential component of the fungal cytoplasmic membrane. Inhibition of CYP51 causes depletion of ergosterol coupled with an accumulation of 14-methyl sterols resulting in impaired cell growth in fungi. This crucial role of CYP51 in fungi makes it an important target for drug design. A perusal of the docking poses obtained for all these tetrazoloquinoline-1,2,3-triazole derivatives revealed that they could snugly fit into the active site of CYP51 with varying degree of binding affinities adopting a very homologous orientation and at co-ordinates very close to that of the native ligand-fluconazole (Figure 2). The resulting enzyme-inhibitor complexation was stabilized through a network of steric and electrostatic interactions with the active site residues.

To gauge the accuracy and reliability of the docking protocol, the co-crystallized ligand (fluconazole) was extracted from the crystal structure and again subjected to dock into the same binding pocket defining the above-mentioned parameters. The docked conformation of fluconazole comparing with the experimental binding mode as in X-ray is shown in Figure 3. The result show that the docking protocol could reproduce the X-ray bound conformation of fluconazole with an RMSD of less than 1.0 Å indicating the reliability of the docking protocol in accurately predicting the binding mode for the title molecules.

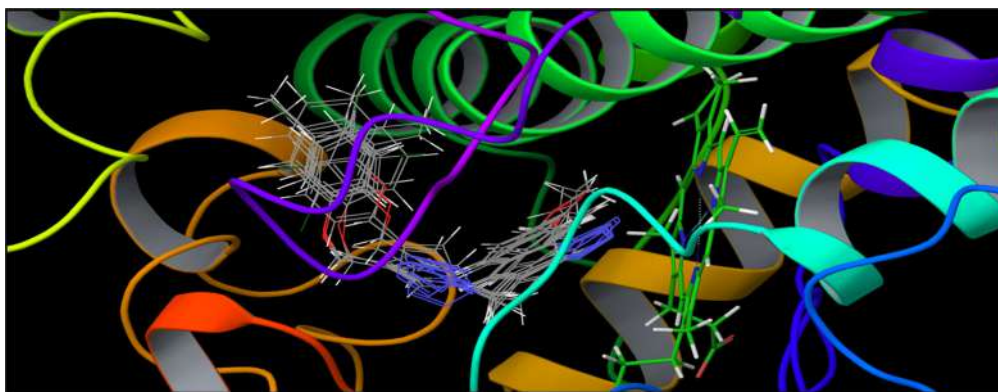


**Figure 2.** Docking-based binding mode of tetrazoloquinoline-1,2,3-triazole derivatives (**5a-i**) into the active site of fungal sterol 14 $\alpha$ -demethylase (CYP51).

The minimum energy (Glide energy) for each of these complexes was observed to be negative ranging from  $-58.54$  kcal/mol to  $-49.70$  kcal/mol while the docking scores ranged from  $-7.79$  to  $-7.14$  with a significant correlation between their docking score and the experimentally observed MIC values—the active compounds possessing higher scores while those with relatively lower activity were also predicted to have lower docking scores. The binding energy for the reference ligand-fluconazole was found to be  $-52.92$  kcal/mol with a docking score of  $-7.34$ . The binding energy signifies the energy required for a ligand to cover the entire enzyme surface and its putative interactions with the amino acid residues. A higher negative value for the binding energy (and docking score) signifies a good binding affinity for the ligand toward the target enzyme and vice versa. Furthermore, a detailed analysis of the per-residue interactions between the enzyme and these compounds was carried out to identify the most significantly interacting residues and the type of thermodynamic elements (bonded and non-bonded interactions) governing the binding of these molecules to the target. This analysis is elucidated in the next section for one of the most active compound **5g** while the results for the remaining compounds are summarized in [Table 3](#) and their binding modes are provided in the Supporting Information as [Figure 4](#).

The lowest energy docked conformation of **5g** into the active site of CYP51 showed that the inhibitor binds at the same co-ordinates as the native ligand with a significantly higher binding affinity resulting in a docking score of  $-7.79$  and a binding energy  $-58.54$  kcal/mol ([Figure 4](#)). The higher binding affinity can be explained in terms of the specific bonded and non-bonded per-residue interactions with the residues lining the active site.

The complexation of **5g** with CYP51 is observed to be stabilized through an extensive network of van der Waals interactions with Ala291 ( $-3.08$  kcal/mol), Ala288 ( $-1.55$  kcal/mol), Ala287 ( $-1.99$  kcal/mol), Tyr116 ( $-3.54$  kcal/mol), Phe110 ( $-1.94$  kcal/mol), and Tyr103 ( $-3.54$  kcal/mol) through quinoline-tetrazole backbone while 1,2,3-triazole heterocycle was engaged in similar interactions through Val461 ( $-3.28$  kcal/mol), Met460 ( $-2.52$  kcal/mol), Thr459 ( $-1.28$  kcal/mol), Leu356 ( $-2.46$  kcal/mol), and Met106 ( $-4.00$  kcal/mol) residues in the active site. Furthermore, the substituted aromatic ring connected to 1,2,3-triazole heterocycle also showed favorable van der Waals interactions through His294 ( $-1.40$  kcal/mol), Phe290 ( $-3.98$  kcal/mol), Leu208 ( $-3.02$  kcal/mol), and Glu205 ( $-1.96$  kcal/mol) residues. The compound was also involved in a set of relatively few but significant electrostatic interactions as well through Met106 ( $-1.50$  kcal/mol) and Tyr103 ( $-1.18$  kcal/mol) residues in the active site CYP51. The excellent binding affinity of **5g** toward CYP51 can also be attributed to a very strong van der Waals ( $-10.62$  kcal/mol) as well as electrostatic ( $-9.425$  kcal/mol) interactions with heme moiety in the active site. Furthermore, a prominent  $\pi$ - $\pi$  stacking interaction was observed through the aromatic ring of quinoline-tetrazole backbone with the Phe110 having a bonding distance of  $2.451$  Å which as well contributed significantly to the stability of the **5g** in the active site of the

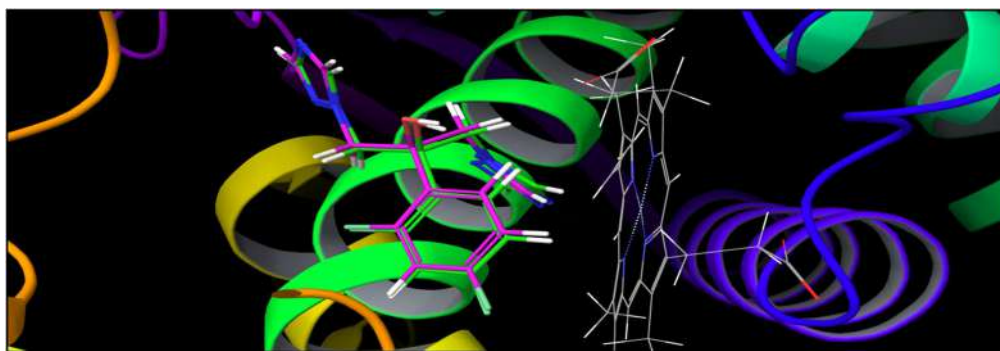


**Figure 3.** Validation of the molecular docking protocol: super-imposed image of the structures of fluconazole from the crystal structure (orange carbon chain) and the docked conformation (purple carbon chain).

enzyme. Such  $\pi$ - $\pi$  stacking interactions serve as an “anchor” for channelizing the 3D orientation of the ligand in its active site and also facilitate the steric and electrostatic interactions thereby contributing to the stability of the enzyme-inhibitor complex.

A similar network of interaction was observed for the other quinoline-tetrazole-1,2,3-triazole derivatives as well but decreasing gradually with their observed antifungal activity. The per-residue interaction analysis revealed that the primary driving forces for mechanical interlocking is the steric complementarity between the ligand and the active site of CYP51 which is evident from the relatively higher number of van der Waals interactions over other components contributing to the binding scores. Interestingly, all the quinoline-tetrazole-1,2,3-triazole derivatives investigated herein were found coordinated to the iron of the heme group present in the active site. This is a very important observation as the native ligand-fluconazole is also coordinated with the metal ion in the active site of CYP51. Thus, these quinoline-tetrazole-1,2,3-triazoles may as well share the same inhibition mechanism as fluconazole making them pertinent starting points for structure-based drug design.

### *In silico* ADME prediction

The success of a drug is determined not only by good efficacy but also by an acceptable ADME (absorption, distribution, metabolism, and excretion) profile. In the present study, we have calculated molecular volume (MV), molecular weight (MW), logarithm of partition coefficient (miLog  $P$ ), number of hydrogen bond acceptors (n-ON), number of hydrogen bonds donors (n-OH/NH), topological polar surface area (TPSA), number of rotatable bonds (n-ROTB), and Lipinski's rule of five<sup>40</sup> using Molinspiration online property calculation toolkit.<sup>41</sup> Absorption (% ABS) was calculated by: % ABS =  $109 - (0.345 \times \text{TPSA})$ .<sup>42</sup> Drug-likeness model score (a collective property of physic-chemical properties, pharmacokinetics, and pharmacodynamics of a compound is represented by a numerical value) was computed by MolSoft software.<sup>43</sup>

A computational study of all the synthesized **5a-i** was performed for prediction of ADME properties and the value obtained is presented in Table 4.

It is observed that, the compounds exhibited a good % ABS (% absorption) ranging from 77.16 to 80.35%. Furthermore, none of the synthesized compounds **5a-i** violated Lipinski's rule of five (miLog  $P \leq 5$ ). A molecule likely to be developed as an orally active drug candidate should not show more than one violation of the following four criteria: miLog  $P$  (octanol-water partition coefficient)  $\leq 5$ , molecular weight  $\leq 500$ , number of hydrogen bond acceptors  $\leq 10$  and number of hydrogen bond donors  $\leq 5$ .<sup>44</sup> The larger the value of the drug likeness model score, the higher is also probability that the particular molecule will be active. All the tested compounds followed the criteria for orally active drug and therefore, these compounds may have a good potential for eventual development as oral agents.

**Table 3.** Quantitative estimate of the per-residue interactions for the tetrazoloquinoline-1,2,3-triazole derivative (**5a-i**) with the fungal sterol *14 $\alpha$* -demethylase (*CYP51*) enzyme.

Cpd	Docking score	Binding energy	Per-residue interaction energy analysis		
			van der Waals (kcal/mol)	Electrostatic (kcal/mol)	$\pi$ - $\pi$ stacking (Å)
<b>5a</b>	-7.40	-53.57	500(-10.79), Val461(-2.92), Met460(-2.41), Thr459(-1.19), Leu356(-2.21), Ala291(-2.31), Phe290(-2.30), Ala288(-1.24), Ala287(-1.59), Leu208(-1.26), Tyr116(-2.45), Phe110(-1.52), Met106(-3.16), Tyr103(-2.92)	500(-7.37), Met106(-1.25), Tyr103(-1.09)	Tyr116(2.07)
<b>5b</b>	-7.1	-50.77	500(-10.72), Val461(-2.41), Met460(-1.78), Thr459(-1.08), Leu356(-2.10), Ala291(-2.03), Phe290(-2.19), Ala288(-1.14), Ala287(-1.11), Leu208(-1.14), Leu127(-1.04), Tyr116(-1.98), Phe110(-1.27), Met106(-2.92), Tyr103(-3.75)	500(-6.75), Tyr116(-1.32), Met106(-1.10), Tyr103(-1.017)	Tyr116(2.06)
<b>5c</b>	-7.78	-57.71	500(-10.85), Val461(-3.18), Met460(-3.11), Thr459(-1.42), Leu356(-2.10), His294(-1.40), Ala291(-2.91), Phe290(-3.51), Ala288(-1.43), Ala287(-1.96), Leu208(-2.96), Glu205(-1.85), Tyr116(-3.55), Phe110(-1.77), Met106(-3.83), Ile105(-2.63), Tyr103(-3.05)	500(-9.67), Met106(-1.43), Tyr103(-1.19)	Phe110(2.39)
<b>5d</b>	-7.14	-49.70	500(-10.52), Val461(-2.50), Met460(-1.71), Thr459(-1.00), Leu356(-2.16), Ala291(-2.04), Phe290(-2.09), Ala288(-1.14), Ala287(-1.05), Leu208(-1.18), Leu127(-1.00), Tyr116(-1.95), Phe110(-1.25), Met106(-2.59), Tyr103(-2.61)	500(-6.76), Tyr116(-1.11), Met106(-1.19)	Tyr116(2.066)
<b>5e</b>	-7.33	-53.50	500(-10.42), Val461(-2.70), Met460(-2.35), Thr459(-1.13), Leu356(-2.27), His294(-1.11), Ala291(-2.21), Phe290(-2.25), Ala288(-1.24), Ala287(-1.57), Leu208(-1.33), Tyr116(-2.25), Phe110(-1.42), Met106(-3.03), Tyr103(-3.14)	500(-7.29), Tyr116(-0.86), Met106(-1.24), Tyr103(-1.09)	Tr116(2.07)
<b>5f</b>	-7.26	-50.74	500(-10.44), Val461(-2.40), Met460(-1.41), Thr459(-1.07), Leu356(-2.17), His294(-1.34), Ala291(-2.18), Phe290(-2.16), Ala288(-1.06), Ala287(-1.05), Leu208(-1.04), Glu205(-1.67), Tyr116(-1.35), Phe110(-1.15), Met106(-2.29), Tyr103(-2.83)	500(-7.05), Tyr116(-1.22), Met106(-1.12)	Tyr116(1.97)
<b>5g</b>	-7.79	-58.54	500(-10.62), Val461(-3.28), Met460(-2.52), Thr459(-1.28), Leu356(-2.46), His294(-1.40), Ala291(-3.08), Phe290(-3.98), Ala288(-1.55), Ala287(-1.99), Leu208(-3.02), Glu205(-1.96), Tyr116(-3.54), Phe110(-1.94), Met106(-4.00), Tyr103(-3.54)	500(-9.42), Met106(-1.5), Tyr103(-1.18)	Phe110(2.45)
<b>5h</b>	-7.72	-57.51	500(-10.87), Val461(-3.13), Met460(-2.29), Thr459(-1.58), Leu356(-2.58), His294(-1.37), Ala291(-2.94), Phe290(-3.29), Ala288(-1.45), Ala287(-1.84), Leu208(-3.40), Glu205(-1.98), Tyr116(-3.42), Phe110(-1.81), Met106(-3.72), Tyr103(-3.01)	500(-9.41), Tyr116(-1.31), Tyr103(-1.13)	Tyr116(2.07)
<b>5i</b>	-7.42	-51.64	500(-10.26), Val461(-2.78), Met460(-2.53), Thr459(-1.14), Leu356(-2.26), Ala291(-2.33), Phe290(-2.29), Ala288(-1.28), Ala287(-1.67), Leu208(-1.49), Tyr116(-2.29), Phe110(-1.40), Met106(-3.01), Tyr103(-2.81)	500(-7.97), Tyr116(-1.18), Tyr103(-1.016)	Tyr103(2.92), Tyr116(2.01)

## Conclusion

We have synthesized new 1,4-disubstituted 1,2,3-triazole-based tetrazoloquinoline derivatives *via* click chemistry approach and evaluated for biological activity. The synthesized compound displays promising antibacterial, antifungal, and antioxidant activity as compared to the respective standard drugs and unfortunately does not show antitubercular activity. Compounds **5g** and **5h** displayed significant antibacterial activity as compared to the standard antibacterial drug. Compounds **5c**, **5g**, and **5h** displayed significant antifungal activity as compared to the standard



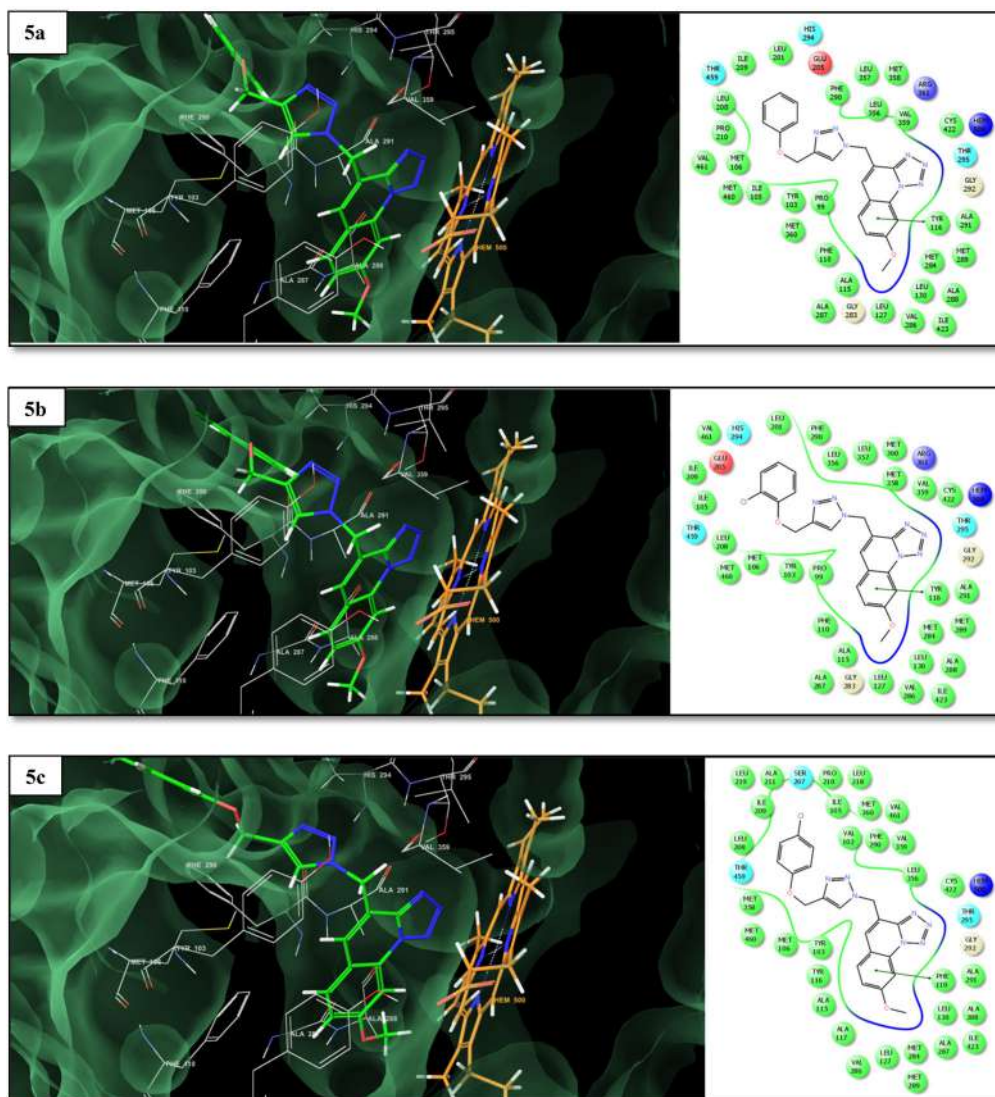


**Figure 4.** Docking-based binding mode of **5a**, **5b**, **5c**, **5d**, **5e**, **5f**, **5g**, **5h**, and **5i** into the active site of sterol 14 $\alpha$ -demethylase (CYP51) (the  $\pi$ - $\pi$  stacking interaction is represented using the green line).

antifungal drug. Compounds **5b**, **5d**, and **5g** shows potential antioxidant activity when compared with standard BHT. The trend observed in the antifungal activity for these tetrazoloquinoline-1,2,3-triazole derivatives was further rationalized by molecular docking studies with respect to their binding energy toward target enzyme sterol 14 $\alpha$ -demethylase (CYP51). The theoretical predictions from molecular docking studies were found to be in agreement with the experimental antifungal data. Furthermore, the quantitative estimation of the per-residue interactions between these tetrazoloquinoline-1,2,3-triazoles and CYP51 enzyme helps to speculate regarding the detailed binding patterns in the cavity and the most significantly interacting the residues as well as the type of thermodynamic interactions governing the binding of these molecules which can provide an ample opportunity for medicinal chemist to design more specific and potent analogues targeting CYP51. Furthermore, analysis of the ADME parameters for synthesized compounds predicted good drug like properties and





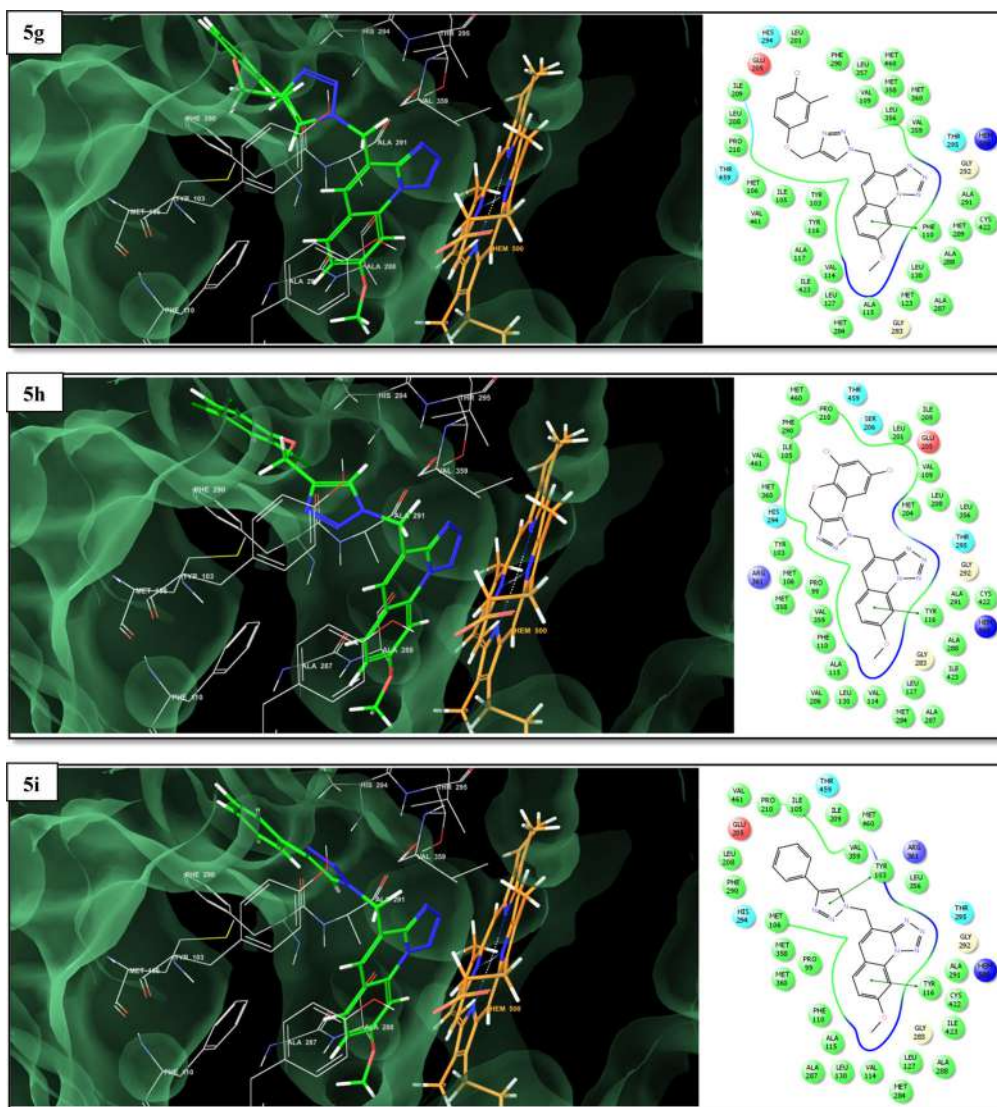


Figure 4. Continued.

In case of solid product, it was filtered and the obtained crude solid product was crystallized using ethanol. The crystallized products were taken for next step. When the products are liquid, it has been extracted in ethyl acetate (20 mL  $\times$  3). The combined organic layers were dried over  $\text{MgSO}_4$ . The solvent was removed under a reduced pressure and used for further reaction without purification.

#### **General procedure for the synthesis of 8-methoxy-4-((4-(phenoxy)methyl)-1H-1,2,3-triazol-1-yl)methyl)tetrazolo[1,5-a]quinoline 5a-i**

To the solution of 1-(prop-2-ynoxy)benzene and phenyl acetylene (**4a-i**) (0.5 mmol), 4-(azido-methyl)-8-methoxytetrazolo[1,5-a]quinoline **3** (0.5 mmol) and copper diacetate ( $\text{Cu}(\text{OAc})_2$ ) (20 mole %) in *t*-BuOH- $\text{H}_2\text{O}$  (3:1, 8 mL) and the resulting mixture was stirred at room temperature for 16–22 hr. The progress of the reaction was monitored by TLC using ethyl acetate:hexane

**Table 4.** Pharmacokinetic parameters important for good oral bioavailability and its drug likeness model score.

Entry	% ABS	TPSA (Å <sup>2</sup> )	n-ROTB	MV	MW	miLog <i>P</i>	n-ON	n-OHND	Lipinski violation	Drug-likeness model score
Rule	–	–	–	–	<500	≤5	<10	<5	≤1	–
5a	77.16	92.28	6	332.93	387.40	3.01	9	0	0	–0.24
5b	77.16	92.28	6	346.47	421.85	3.64	9	0	0	0.18
5c	77.16	92.28	6	346.47	421.85	3.69	9	0	0	0.21
5d	77.16	92.28	6	349.49	401.43	3.42	9	0	0	0.14
5e	77.16	92.28	6	349.49	401.43	3.46	9	0	0	–0.24
5f	77.16	92.28	6	366.05	415.46	3.84	9	0	0	–0.10
5g	77.16	92.28	6	363.03	435.88	4.07	9	0	0	0.32
5h	77.16	92.28	6	373.54	490.74	4.90	9	0	0	0.10
5i	80.35	83.04	4	307.14	357.38	2.80	8	0	0	–0.03

% ABS: Percentage absorption, TPSA: Topological polar surface area, n-ROTB: Number of rotatable bonds, MV: Molecular volume, MW: Molecular weight, miLog *P*: Logarithm of partition coefficient of compound between n-octanol and water, n-ON Acceptors: Number of hydrogen bond acceptors, n-OHND donors: Number of hydrogen bonds donors.

as a solvent system. The reaction mixture was quenched with crushed ice and extracted with ethyl acetate (2 × 25 mL). The organic extracts were washed with brine solution (2 × 25 mL) and dried over anhydrous sodium sulfate. The solvent was evaporated under reduced pressure to afford the corresponding crude compounds. The obtained crude compounds were crystallized using ethanol and ethyl acetate.

### Synthesis of 2-chloro-7-methoxyquinoline-3-carbaldehyde<sup>45</sup>

To a solution of *N*-(3-methoxyphenyl)acetamide (5 mmol) in dry DMF (15 mmol) at 0–5 °C with stirring POCl<sub>3</sub> (60 mmol) was added drop wise and the mixture stirred at 80–90 °C for time 8 hr. After the completion of reaction (checked by TLC), the mixture was poured into crushed ice, stirred for 5 min and the resulting solid filtered, washed well with water and dried. The compounds were purified by recrystallization from ethyl acetate.

### Synthesis of 8-methoxytetrazolo[1,5-*a*]quinoline-4-carbaldehyde

2-Chloro-7-methoxyquinoline-3-carbaldehyde (5 mmol), sodium azide (10 mmol), and DMF (10 mL) were taken in round bottom flask as per reported procedure.<sup>46</sup> The reaction mixture was slowly heated at 80 °C for 2 hr. After the completion of reaction (checked by TLC), the product was filtered and washed with ethanol. The crude product was purified by crystallization in DMF. Melting point is 240–242 °C.

### Synthesis of (8-methoxytetrazolo[1,5-*a*]quinolin-4-yl)methanol

8-methoxytetrazolo[1,5-*a*]quinoline-4-carbaldehyde (1 equiv) were taken in round bottom flask, methanol used as a solvent and allowed reaction mixture for stirring below 0 °C. Then, NaBH<sub>4</sub> (3 equiv.) were added slowly with constant stirring and maintaining the temperature below 0 °C for 2 hr. The progress of the reaction was monitored by thin layer chromatography (TLC) using ethyl acetate:hexane as a solvent system. After completion of the reaction as indicated by TLC, the reaction mixture was then poured on crushed ice and extracted in ethylacetate (3 × 10 mL). The combined organic layer was dried over MgSO<sub>4</sub>. Solvent was removed under reduced pressure and the (8-methoxytetrazolo[1,5-*a*]quinolin-4-yl)methanol were sufficiently pure to use without further work up.

### Synthesis of (8-methoxytetrazolo[1,5-*a*]quinolin-4-yl)methyl methanesulfonate

To a mixture of (2-chloro quinolin-3-yl)methanol **1** (1 equiv) in acetone, triethyl amine (2 equiv) was added at 0 °C. Methane sulfonyl chloride (1.5 equiv) in acetone was added dropwise in 10 min at 0 °C, and stirred for 4 hr. The progress of the reaction was monitored on TLC. After completion of the reaction, reaction mixture was poured on crushed ice. The solid obtained was extracted with ethylacetate (2 × 20 mL) and washed with brine (2 × 20 mL). Thus, organic layer was separated, dried over anhydrous Na<sub>2</sub>SO<sub>4</sub>. The solvent was removed under reduced pressure. The obtained crude product was crystallized using ethanol/ethylacetate obtain pure compound (8-methoxytetrazolo[1,5-*a*]quinolin-4-yl)methyl methanesulfonate.

### Synthesis of 4-(azidomethyl)-8-methoxytetrazolo[1,5-*a*]quinoline (**3**)

To a solution of (8-methoxytetrazolo[1,5-*a*]quinolin-4-yl)methyl methanesulfonate (1 equiv) in dry DMF, sodium azide (2 equiv) was added and stirred at 80 °C for 2 hr. The progress of the reaction was monitored on TLC. After completion of reaction, reaction mixture was poured on crushed ice. The solid obtained was extracted with EtOAc (2 × 25 mL). The organic extract was washed with water and brine. The solvent was removed under reduced pressure to afford crude product **3**, which was purified by crystallization using ethanol/ethylacetate with 92% yield. Mp 133–135 °C. <sup>1</sup>H NMR (400 MHz, DMSO-*d*<sub>6</sub>, δ ppm): 4.05 (s, 3H, -OMe), 4.95 (s, N-CH<sub>2</sub>), 7.40–7.46 (m, 1H), 7.98–7.99 (d, 1H), and 8.15–8.25 (m, 2H). HRMS calculated [M + H]<sup>+</sup> for C<sub>11</sub>H<sub>10</sub>N<sub>7</sub>O: 256.0941, found: 256.0935.

### 8-Methoxy-4-((4-(phenoxy)methyl)-1H-1,2,3-triazol-1-yl)methyl)tetrazolo[1,5-*a*]quinoline (**5a**)

The compound **5a** as a pale pink solid and was obtained *via* 1,3-dipolar cycloaddition reaction between 4-(azidomethyl)-8-methoxytetrazolo[1,5-*a*]quinoline **3** and (prop-2-yn-1-yloxy)benzene **4a** in 17 hr with 90% yield. Mp 150 °C. <sup>1</sup>H NMR (200 MHz, DMSO-*d*<sub>6</sub>, δ ppm): 4.06 (s, 3H, -OMe), 5.16 (s, N-CH<sub>2</sub>), 6.09 (s, O-CH<sub>2</sub>), 6.92–7.06 (m, 3H), 7.27–7.35 (m, 2H), 7.43–7.47 (d, 1H), 8.01 (s, 1H), 8.16 (s, 1H), 8.20 (s, 1H) and 8.44 (s, 1H). <sup>13</sup>C NMR (50 MHz, CDCl<sub>3</sub>, δ ppm): 49.3, 56.8, 61.8, 99, 117, 117.6, 118.6, 125.1, 126, 129.7, 131.8, 131.9, 133.6, 143, 147.3, 157.4 and 162.3. HRMS calculated [M + H]<sup>+</sup> for C<sub>20</sub>H<sub>17</sub>N<sub>7</sub>O<sub>2</sub>: 388.1516, found: 388.1513.

### 4-(((4-(2-Chlorophenoxy)methyl)-1H-1,2,3-triazol-1-yl)methyl)-8-methoxytetrazolo[1,5-*a*]quinoline (**5b**)

The compound **5b** as a off white solid and was obtained *via* 1,3-dipolar cycloaddition reaction between 4-(azidomethyl)-8-methoxytetrazolo[1,5-*a*]quinoline **3** and 1-chloro-2-(prop-2-yn-1-yloxy)benzene **4b** in 19 hr with 88% yield. Mp 139–140 °C. <sup>1</sup>H NMR (200 MHz, DMSO-*d*<sub>6</sub>, δ ppm): 4.03 (s, 3H, -OMe), 5.14 (s, N-CH<sub>2</sub>), 6.06 (s, O-CH<sub>2</sub>), 7.02–7.06 (m, 2H), 7.29–7.45 (m, 3H), 7.98–7.99 (d, 1H), 8.13 (s, 1H), 8.17 (s, 1H), and 8.41 (s, 1H).

### 4-(((4-(4-Chlorophenoxy)methyl)-1H-1,2,3-triazol-1-yl)methyl)-8-methoxytetrazolo[1,5-*a*]quinoline (**5c**)

The compound **5c** as a off white solid and was obtained *via* 1,3-dipolar cycloaddition reaction between 4-(azidomethyl)-8-methoxytetrazolo[1,5-*a*]quinoline **3** and 1-chloro-4-(prop-2-yn-1-yloxy)benzene **4c** in 20 hr with 87% yield. Mp 180 °C. <sup>1</sup>H NMR (200 MHz, DMSO-*d*<sub>6</sub>, δ ppm): 4.06 (s, 3H, -OMe), 5.17 (s, N-CH<sub>2</sub>), 6.09 (s, O-CH<sub>2</sub>), 7.05–7.09 (m, 2H), 7.32–7.37 (m, 2H), 7.43–7.48 (3, 1H), 8.01–8.02 (d, 1H), 8.16 (s, 1H), 8.20 (s, 1H), and 8.44 (s, 1H). <sup>13</sup>C NMR (50 MHz,



CDCl<sub>3</sub>,  $\delta$  ppm): 48.8, 56.3, 61.3, 98.4, 116.5, 117, 118.1, 124.6, 125.5, 129.2, 131.2, 131.3, 133.1, 142.5, 146.8, 156.8, and 161.8. HRMS calculated  $[M + H]^+$  for C<sub>20</sub>H<sub>17</sub>N<sub>7</sub>O<sub>2</sub>Cl: 422.1127, found: 422.1123.

#### **8-Methoxy-4-((4-((o-tolyloxy)methyl)-1H-1,2,3-triazol-1-yl)methyl)tetrazolo[1,5-a]quinoline (5d)**

The compound **5d** as a pale pink solid and was obtained *via* 1,3-dipolar cycloaddition reaction between 4-(azidomethyl)-8-methoxytetrazolo[1,5-*a*]quinoline **3** and 1-methyl-2-(prop-2-yn-1-yloxy)benzene **4d** in 17 hr with 89% yield. Mp 145 °C.

#### **8-Methoxy-4-((4-((p-tolyloxy)methyl)-1H-1,2,3-triazol-1-yl)methyl)tetrazolo[1,5-a]quinoline (5e)**

The compound **5a** as a pale pink solid and was obtained *via* 1,3-dipolar cycloaddition reaction between 4-(azidomethyl)-8-methoxytetrazolo[1,5-*a*]quinoline **3** and 1-methyl-4-(prop-2-yn-1-yloxy)benzene **4e** in 16 hr with 90% yield. Mp 152–153 °C.

#### **4-((4-((2,4-Dimethylphenoxy)methyl)-1H-1,2,3-triazol-1-yl)methyl)-8-methoxytetrazolo[1,5-a]quinoline (5f)**

The compound **5f** as a off white solid and was obtained *via* 1,3-dipolar cycloaddition reaction between 4-(azidomethyl)-8-methoxytetrazolo[1,5-*a*]quinoline **3** and 2,4-dimethyl-1-(prop-2-yn-1-yloxy)benzene **4f** in 18 hr with 90% yield. Mp 135 °C. <sup>1</sup>H NMR (200 MHz, DMSO-*d*<sub>6</sub>,  $\delta$  ppm): 2.06 (*s*, 3H), 2.18 (*s*, 3H), 4.04 (*s*, 3H, -OMe), 5.10 (*s*, N-CH<sub>2</sub>), 6.07 (*s*, O-CH<sub>2</sub>), 6.93–6.96 (*m*, 3H), 7.39–7.45 (*m*, 1H), 7.99–8.00 (*d*, 1H), 8.13–8.17 (*m*, 2H), and 8.39 (*s*, 1H). HRMS calculated  $[M + H]^+$  for C<sub>22</sub>H<sub>22</sub>N<sub>7</sub>O<sub>2</sub>: 416.1829, found: 416.1825.

#### **4-((4-((4-Chloro-3-methylphenoxy)methyl)-1H-1,2,3-triazol-1-yl)methyl)-8-methoxytetrazolo[1,5-a]quinoline (5g)**

The compound **5f** as a pale pink solid and was obtained *via* 1,3-dipolar cycloaddition reaction between 4-(azidomethyl)-8-methoxytetrazolo[1,5-*a*]quinoline **3** and 1-chloro-2-methyl-4-(prop-2-yn-1-yloxy)benzene **4g** in 21 hr with 86% yield. Mp 150 °C. <sup>1</sup>H NMR (200 MHz, DMSO-*d*<sub>6</sub>,  $\delta$  ppm): 2.27 (*s*, 3H), 4.04 (*s*, 3H, -OMe), 5.13 (*s*, N-CH<sub>2</sub>), 6.07 (*s*, O-CH<sub>2</sub>), 6.85–7.03 (*m*, 2H), 7.26–7.46 (*m*, 2H), 7.99–8.00 (*d*, 1H), 8.14 (*s*, 1H), 8.18 (*s*, 1H), and 8.41 (*s*, 1H). HRMS calculated  $[M + H]^+$  for C<sub>21</sub>H<sub>19</sub>N<sub>7</sub>O<sub>2</sub>Cl: 436.1283, found: 436.1283.

#### **8-Methoxy-4-((4-((2,4,6-trichlorophenoxy)methyl)-1H-1,2,3-triazol-1-yl)methyl)tetrazolo [1,5-a]quinoline (5h)**

The compound **5h** as a off white solid and was obtained *via* 1,3-dipolar cycloaddition reaction between 4-(azidomethyl)-8-methoxytetrazolo[1,5-*a*]quinoline **3** and 1,3,5-trichloro-2-(prop-2-yn-1-yloxy)benzene **4h** in 22 hr with 86% yield. Mp 143–145 °C.

#### **8-Methoxy-4-((4-phenyl-1H-1,2,3-triazol-1-yl)methyl)tetrazolo[1,5-a]quinoline (5i)**

The compound **5i** as a pale pink solid and was obtained *via* 1,3-dipolar cycloaddition reaction between 4-(azidomethyl)-8-methoxytetrazolo[1,5-*a*]quinoline **3** and phenyl acetylene **4i** in 19 hr



with 88% yield. Mp 175–177 °C.  $^1\text{H}$  NMR (200 MHz, DMSO- $d_6$ ,  $\delta$  ppm): 4.07 (s, 3H, -OMe), 6.12 (s, N-CH $_2$ ), 7.34–7.47 (m, 4H), 7.84–7.88 (m, 2H), 8.04–8.05 (d, 1H), 8.21–8.26 (m, 2H), and 8.72 (s, 1H).  $^{13}\text{C}$  NMR (50 MHz, CDCl $_3$ ,  $\delta$  ppm): 48.9, 56.3, 98.5, 117, 117.5, 118.1, 122.2, 125.2, 127.9, 128.9, 130.8, 131.3, 131.4, 133.1, 146.4, 146.9, and 161.8.

## Experimental protocol for biological activity

### Antibacterial activity

The antimicrobial susceptibility testing of newly synthesized compounds were performed *in vitro* against bacterial strains *viz.*, Gram positive *Staphylococcus aureus* (ATCC No. 29737), *Micrococcus luteus* (ATCC No. 398), *Bacillus cereus* (ATCC No. 6630), and Gram negative *Escherichia coli* (NCIM No. 2256), *Pseudomonas fluorescens* (NCIM No. 2173), and *Flavobacterium devorans* (ATCC No. 10829), respectively, to find out MIC. The MIC ( $\mu\text{g}/\text{mL}$ ) were defined as the lowest concentrations of compound that completely inhibit the growth of each strain. Serial two-fold dilutions of all samples were prepared in triplicate in micro titer plates and inoculated with suitably prepared cell suspension to achieve the required initial concentration. Serial dilutions were prepared for screening. Dimethyl sulfoxide (DMSO) was used as solvent control. Ampicillin, kanamycin, and chloramphenicol were used as a standard antibacterial drug. The concentration range of tested compounds and standard was 256–0.5  $\mu\text{g}/\text{mL}$ . The plates were incubated at 37 °C for all micro-organisms; absorbance at 595 nm was recorded to assess the inhibition of cell growth after 24 hr. The compounds which are showing promising antibacterial activity were selected for MIC studies. The MIC was determined by assaying at 256, 128, 64, 32, 16, 8, 4, 2, 1, and 0.5  $\mu\text{g}/\text{mL}$  concentrations along with standards at the same concentrations.

### Antifungal activity

The antifungal activity was evaluated against different fungal strains such as *Aspergillus niger* (NCIM No. 1196), *Penicillium chrysogenum* (NCIM No. 723), *Curvularia lunata* (NCIM No. 1131), *Candida albicans* (NCIM No. 3471), *Aspergillus flavus* (NCIM No. 539), and *Cryptococcus neoformans* (NCIM No. 3378). Fluconazole, miconazole, and amphotericin B were used as standard drugs for the comparison of antifungal activity. The plates were incubated at 37 °C for all micro-organisms; absorbance at 410 nm was recorded to assess the inhibition of cell growth after 48 hr. The lowest concentration inhibiting growth of the organisms was recorded as the MIC. DMSO was used as a solvent or negative control. In order to clarify any effect of DMSO on the biological screening, separate studies were carried out with solutions alone of DMSO and showed no activity against any microbial strains. The compounds which are showing promising antifungal activity were selected for MIC studies. The MIC was determined by assaying at 256, 128, 64, 32, 16, 8, 4, 2, 1, and 0.5  $\mu\text{g}/\text{mL}$  concentrations along with standards at the same concentrations.

### Antitubercular activity protocol

Compounds were tested for their *in vitro* effects against *MTB H37Ra* (ATCC 25177) which is susceptible to control drugs (Rifampicin, Isoniazid, Ethambutol, and Pyrazinamide). Compounds were screened for their inhibitory effect on MTB by *in vitro* according to standard XTT Reduction Menadione Assay (XRMA) protocol as described previously.<sup>38</sup> Dimethyl Sulfoxide (DMSO) was used as a solvent or negative control. In order to clarify any effect of DMSO on the biological screening, separate studies were carried out with solutions alone of DMSO and showed no activity against any mycobacteria. Rifampicin and Isoniazide was used as positive control for assay. Primary screening was done against MTB at 30, 10, and 3  $\mu\text{g}/\text{mL}$  concentration of

compound. Those compounds were shown more than 90% inhibition at 30 µg/mL which were selected for dose response. The MIC (in µg/mL) was recorded as the lowest concentration/highest dilution of the compounds/control drugs that completely inhibited the growth of MTB cultures.

The *in vitro* effect of compounds against *M. bovis* BCG (ATCC 35743) was done according to standard NR assay protocol as described previously.<sup>38</sup> Briefly in NR assay, take 80 µL of culture from incubated 96 well plate into another 96 well plate, then add 80 µL of 1% sulfanilic acid in 20% of conc. HCl, incubate it for 10 min at room temperature then add 80 µL of 0.1% NEDD solution in D/W. Finally, the optical density of the suspension was measured at 540 nm using micro plate reader. MIC and IC<sub>50</sub> values were calculated using origin9 software. The % inhibition of bacilli was measured using following formula,

$$\% \text{ Inhibition} = \frac{[(\text{Abs of control}) - (\text{Abs of test sample}) / (\text{Abs of control}) - (\text{Abs of blank})]}{\times 100.}$$

Control: cell growth in medium without compound, with DMSO

Test: cell growth in presence of compound

Blank: culture medium without cells.

### **DPPH radical scavenging activity**

The hydrogen atom or electron donation ability of the compounds was measured from the bleaching of the purple-colored methanol solution of 1,1-diphenyl-1-picrylhydrazyl (DPPH).<sup>39</sup> The spectrophotometric assay uses the stable radical DPPH as a reagent. One milliliter of various concentrations of the test compounds (5, 10, 25, 50, and 100 µg/mL) in methanol was added to 4 mL of 0.004% (w/v) methanol solution of DPPH. After a 30-min incubation period at room temperature, the absorbance was measured against blank at 517 nm. The percent inhibition (I %) of free radical production from DPPH was calculated by the following equation.

$$\% \text{ of scavenging} = \frac{[(A \text{ control} - A \text{ sample}) / A \text{ blank}] \times 100}$$

Where “A control” is the absorbance of the control reaction (containing all reagents except the test compound) and “A sample” is the absorbance of the test compound. Tests were carried at in triplicate.

### **Molecular docking**

To gain an insight into the binding mode of quinoline-tetrazole-1,2,3-triazole derivatives into the active site of fungal sterol 14 $\alpha$ -demethylase (CYP51) enzyme and to increase the understanding of their action as antifungal agents, the molecular docking study was performed using the *Glide* (Grid-Based Ligand Docking with Energetics) program of Schrodinger molecular modeling suite.<sup>47</sup> *Glide* is an interactive molecular graphics program for analyzing the enzyme-inhibitor interactions and identifying potential binding site of the bio-macromolecular targets. The algorithm carries out a systematic search for favorable interactions between the ligand(s) and the target enzyme through a complete search of the conformational, orientation, and positional space of the docked ligand by adopting a funnel type approach and eliminates unwanted conformations using a scoring function followed by energy optimization. With this purpose, the starting coordinates of the sterol 14 $\alpha$ -demethylase (CYP51) in complex with its inhibitor-fluconazole were retrieved from the Protein Data Bank (PDB) ([www.rcsb.org](http://www.rcsb.org)) (PDB code: 3KHM) and further modified to be used for *Glide* docking. The crystal structure was preprocessed the *Protein Preparation Wizard in Glide* which involved eliminating the crystallographically observed water molecules (as none of them were observed to be conserved), assigning the correct bond orders

followed by addition of missing hydrogen atoms corresponding to pH 7.0 (considering the appropriate ionization states for the acidic as well as basic amino acid residues). Following the assignment of appropriate charge and protonation state, the enzyme-inhibitor complex was subjected to energy minimization (until the average root-mean-square deviation (RMSD) of the non-hydrogen atoms reached 0.3 Å) using Optimized Potentials for Liquid Simulations-2005 (OPLS-2005) force field in order to relieve the steric clashes among the residues due to addition of hydrogen atoms. After ensuring that enzyme-inhibitor complex is in the correct form, the shape and properties of the active site of the enzyme was characterized and setup for the docking study using the *receptor grid generation* panel in *Glide*. With the non-covalently bound native ligand-fluconazole in place, the active site grid was defined by a box of 10X10X10Å dimensions centered on the centroid of fluconazole in the crystal complex which was sufficiently large to explore a bigger surface of the enzyme. The co-crystallized ligand serves as the reference co-ordinate signifying the active site of a ligand with respect to the target.

The 3D-structures of all the tetrazoloquinoline-1,2,3-triazole derivatives (**3**, **5a-i**) were sketched using the *build* panel within *Maestro* and were optimized using the *LigPrep* module which involved addition of hydrogens, adjusting realistic bond lengths and angles, correcting the chiralities, ionization states and ring conformations, and generation of tautomers. The partial atomic charges were ascribed for these structures using the OPLS-2005 force-field and finally each of these structures was subjected to energy minimization until energy gradient of 0.001 kcal/mol/Å is reached. The optimized enzyme and ligand structures were then used as input for carrying out docking study utilizing the *extra precision* (XP) *Glide* scoring function to rank the docking poses and to estimate the binding affinities of these ligands to the target. This scoring function is equipped with force field-based parameters accounting for contributions from van der Waals and coulombic interaction energies along with terms for solvation, repulsive, hydrophobic, hydrogen bonding, and metal-ligand interactions all integrated in an empirical energy functions. The output files in terms of the docking poses of the ligands were visualized and analyzed for the key elements of interaction with the enzyme using the *Pose Viewer* utility in *Maestro*.

## Acknowledgement

Authors are also thankful to the Head, Department of Chemistry, Dr. Babasaheb Ambedkar Marathwada University, Aurangabad-431 004, India for providing laboratory facility. We also thank Schrodinger Inc. for providing the Demo license of Schrodinger Suite and especially Craig Coel for the valuable technical support that has tremendously helped in this study.

## Disclosure statement

There are no conflicts of interest.

## Funding

The authors MHS, DDS, and SVA are very much grateful to the Council for Scientific and Industrial Research (CSIR), New Delhi for the award research fellowship.

## References

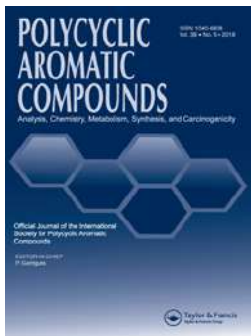
1. D. J. Sheehan, C. A. Hitchcock, and C. M. Sibley, "Current and Emerging Azole Antifungal Agents," *Clinical Microbiology Reviews* 12, no. 1 (1999): 40–79.
2. R. Cha, and J. D. Sobel, "Fluconazole for the Treatment of Candidiasis: 15 Years Experience," *Expert Review of Anti-Infective Therapy* 2, no. 3 (2004): 357–66.

3. N. H. Georgopapadakou and T. J. Walsh, "Antifungal Agents: Chemotherapeutic Targets and Immunologic Strategies," *Antimicrobial Agents and Chemotherapy* 40, no. 2 (1996): 279–91.
4. M. A. Pfaller, S. A. Messer, R. J. Hollis, and R. N. Jones, "In Vitro Activities of Posaconazole (Sch 56592) Compared with Those of Itraconazole and Fluconazole against 3685 Clinical Isolates of *Candida* Spp. and *Cryptococcus neoformans*," *Antimicrobial Agents and Chemotherapy* 45, no. 10 (2001): 2862–4.
5. L. Jeu, F. J. Piacenti, A. G. Lyakhovetskiy, and H. B. Fung, "Voriconazole," *Clinical Therapeutics* 25, no. 5 (2003): 1321–81.
6. G. I. Lepesheva, N. G. Zaitseva, W. D. Nes, W. Zhou, M. Arase, J. Liu, G. C. Hill, and M. R. Waterman, "CYP51 from *Trypanosoma cruzi*: A Phyla-Specific Residue in the B' Helix Defines Substrate Preferences of Sterol 14 $\alpha$ -Demethylase," *The Journal of Biological Chemistry* 281, no. 6 (2006): 3577–85.
7. H. Shiraki, M. P. Kozar, V. Melendez, T. H. Hudson, C. Ohrt, A. J. Magill, and A. J. Lin, "Antimalarial Activity of Novel 5-Aryl-8-Aminoquinoline Derivatives," *Journal of Medicinal Chemistry* 54, no. 1 (2011): 131–42.
8. C. Manera, M. G. Cascio, V. Benetti, M. Allara, T. Tuccinardi, A. Martinelli, G. Saccomanni, E. Vivoli, C. Ghelardini, V. D. Marzo, et al. "New 1,8-Naphthyridine and Quinoline Derivatives as CB2 Selective Agonists," *Bioorganic & Medicinal Chemistry Letters* 17, no. 23 (2007): 6505–10.
9. S. B. Marganakop, R. R. Kamble, T. Taj, and M. Y. Kariduraganvar, "An Efficient One-Pot Cyclization of Quinoline Thiosemicarbazones to Quinolines Derivatized with 1,3,4-Thiadiazole as Anticancer and Anti-Tubercular Agents," *Medicinal Chemistry Research* 21, no. 2 (2012): 185–91.
10. A. M. Gilbert, M. G. Bursavich, S. Lombardi, K. E. Georgiadis, E. Reifenberg, C. Flannery, and E. A. Morris, "N-((8-Hydroxy-5-Substituted-Quinolin-7-yl)(Phenyl)methyl)-2-Phenylxyloxy/Amino-Acetamide Inhibitors of ADAMTS-5 (Aggrecanase-2)," *Bioorganic & Medicinal Chemistry Letters* 18, no. 24 (2008): 6454–7.
11. S. Chen, R. Chen, M. He, R. Pang, Z. Tan, and M. Yang, "Design, Synthesis, and Biological Evaluation of Novel Quinoline Derivatives as HIV-1 Tat-TAR Interaction Inhibitors," *Bioorganic & Medicinal Chemistry* 17 (2009): 1948–56.
12. S. Rossiter, J.-M. Péron, P. J. Whitfield, and K. Jones, "Synthesis and Anthelmintic Properties of Arylquinolines with Activity against Drug-Resistant Nematodes," *Bioorganic & Medicinal Chemistry Letters* 15, no. 21 (2005): 4806–8.
13. X. Ma, W. Zhou, and R. Brun, "Synthesis, In Vitro Antitrypanosomal and Antibacterial Activity of Phenoxy, Phenylthio or Benzylxyloxy Substituted Quinolones," *Bioorganic & Medicinal Chemistry Letters* 19, no. 3 (2009): 986–9.
14. T. A. Rano, E. S. McMaster, P. D. Pelton, M. Yang, K. T. Demarest, and G. H. Kuo, "Design and Synthesis of Potent Inhibitors of Cholesteryl Ester Transfer Protein (CETP) Exploiting a 1,2,3,4-Tetrahydroquinoline Platform," *Bioorganic & Medicinal Chemistry Letters* 19, no. 9 (2009): 2456–60.
15. D. Edmont, R. Rocher, C. Plisson, and J. Chenault, "Synthesis and Evaluation of Quinoline Carboxyguanidines as Antidiabetic Agents," *Bioorganic & Medicinal Chemistry Letters* 10, no. 16 (2000): 1831–4.
16. A. H. Kategaonkar, P. V. Shinde, A. H. Kategaonkar, S. K. Pasale, B. B. Shingate, and M. S. Shingare, "Synthesis and Biological Evaluation of New 2-Chloro-3-((4-Phenyl-1H-1,2,3-Triazol-1-yl)methyl)Quinoline Derivatives via Click Chemistry Approach," *European Journal of Medicinal Chemistry* 45, no. 7 (2010): 3142–6.
17. (a) R. C. Venkata, V. D. Mukund, G. T. Santosh, and K. Yadagiri, "Novel 1,2,3 triazole antifungal agents and preparation thereof" (US Patent US 9,981,923B2);(b) K. N. Venugopala, M. A. Khedr, Y. R. Girish, S. Bhandary, D. Chopra, M. A. Morsy, B. E. Aldhubiab, P. K. Deb, M. Attimarad, A. B. Nair, et al., "Crystallography, *In Silico* Studies, and *In Vitro* Antifungal Studies of 2, 4, 5 Trisubstituted 1, 2, 3-Triazole Analogues," *Antibiotics* 9 (2020): 350.
18. K. N. Venugopala, G. B. Dharma Rao, S. Bhandary, M. Pillay, D. Chopra, B. E. Aldhubiab, M. Attimarad, O. I. Alwassil, S. Harsha, and K. Mlisana, "Design, Synthesis, and Characterization of (1-(4-Aryl)-1H-1,2,3-Triazol-4-yl)methyl, Substituted Phenyl-6-Methyl-2-Oxo-1,2,3,4-Tetrahydropyrimidine-5-Carboxylates against *Mycobacterium tuberculosis*," *Drug Design, Development and Therapy* 10 (2016): 2681–90.
19. (a) S. G. Agalave, R. S. Maujan, and V. S. Pore, "Click Chemistry: 1,2,3-Triazoles as Pharmacophores," *Chemistry - An Asian Journal* 6 (2011): 2696–2718 and references cited therein;(b) M. Hussain, T. Qadri, Z. Hussain, A. Saeed, P. A. Channar, S. A. Shehzadi, M. Hassan, F. A. Larik, T. Mahmood, and A. Malik, "Synthesis, Antibacterial Activity and Molecular Docking Study of Vanillin Derived 1,4-Disubstituted 1,2,3-Triazoles as Inhibitors of Bacterial DNA Synthesis," *Heliyon* 5 (2019): e02812.
20. M. R. Senger, L. C. Gomes, S. B. Ferreira, C. R. Kaiser, V. F. Ferreira, and F. P. Silva, "Kinetics Studies on the Inhibition Mechanism of Pancreatic  $\alpha$ -Amylase by Glycoconjugated 1H-1,2,3-Triazoles: A New Class of Inhibitors with Hypoglycemic Activity," *ChemBioChem: A European Journal of Chemical Biology* 13, no. 11 (2012): 1584–93.

21. T. El. Malah, H. F. Nour, A. A. E. Satti, B. A. Hemdan, and W. A. El-Sayed, "Design, Synthesis, and Antimicrobial Activities of 1,2,3-Triazole Glycoside Clickamers," *Molecules* 25, no. 4 (2020): 790.
22. M. J. Genin, D. A. Allwine, D. J. Anderson, M. R. Barbachyn, D. Edward Emmert, S. A. Garmon, D. R. Graber, K. C. Grega, J. B. Hester, D. K. Hutchinson, et al. "Substituent Effects on the Antibacterial Activity of Nitrogen-Carbon-Linked (Azolyphenyl)Oxazolidinones with Expanded Activity against the Fastidious Gram-Negative Organisms *Haemophilus influenzae* and *Moraxella catarrhalis*," *Journal of Medicinal Chemistry* 43, no. 5 (2000): 953–70.
23. R. J. Bochis, J. C. Chabala, E. Harris, L. H. Peterson, L. Barash, T. Beattie, J. E. Brown, D. W. Graham, F. S. Waksmunski, M. Tischler, et al. "Benzylated 1,2,3-Triazoles as Anticocciostats," *Journal of Medicinal Chemistry* 34, no. 9 (1991): 2843–52.
24. J. L. Kelley, C. S. Koble, R. G. Davis, E. W. Mclean, F. E. Soroko, and B. R. Cooper, "1-(Fluorobenzyl)-4-Amino-1H-1,2,3-Triazolo[4,5-c]Pyridines: Synthesis and Anticonvulsant Activity," *Journal of Medicinal Chemistry* 38, no. 20 (1995): 4131–4.
25. R. Raj, P. Singh, P. Singh, J. Gut, P. J. Rosenthal, and V. Kumar, "Azide-Alkyne Cycloaddition en Route to 1H-1,2,3-Triazole-Tethered 7-Chloroquinoline-Isatin Chimeras: Synthesis and Antimalarial Evaluation," *European Journal of Medicinal Chemistry* 62 (2013): 590–6.
26. M. H. Shaikh, D. D. Subhedar, M. Arkile, V. M. Khedkar, N. Jadhav, D. Sarkar, and B. B. Shingate, "Synthesis and Bioactivity of Novel Triazole Incorporated Benzothiazinone Derivatives as Antitubercular and Antioxidant Agent," *Bioorganic & Medicinal Chemistry Letters* 26, no. 2 (2016): 561–9.
27. B. L. Wilkinson, H. Long, E. Sim, and A. J. Fairbanks, "Synthesis of Arabino Glycosyl Triazoles as Potential Inhibitors of Mycobacterial Cell Wall Biosynthesis," *Bioorganic & Medicinal Chemistry Letters* 18, no. 23 (2008): 6265–7.
28. V. V. Rostovtsev, L. G. Green, V. V. Fokin, and K. B. Sharpless, "A Stepwise Huisgen Cycloaddition Process: Copper(I)-Catalyzed Regioselective "Ligation" of Azides and Terminal Alkynes," *Angewandte Chemie International Edition* 41, no. 14 (2002): 2596–9.
29. C. W. Tornøe, C. Christensen, and M. Meldal, "Peptidotriazoles on Solid Phase: [1,2,3]-Triazoles by Regiospecific Copper(I)-Catalyzed 1,3-Dipolar Cycloadditions of Terminal Alkynes to Azides," *The Journal of Organic Chemistry* 67, no. 9 (2002): 3057–64.
30. H. C. Kolb, M. G. Finn, and K. B. Sharpless, "Click Chemistry: Diverse Chemical Function from a Few Good Reactions," *Angewandte Chemie International Edition* 40, no. 11 (2001): 2004–21.
31. (a) V. A. Ostrovskii, R. E. Trifonov, and E. A. Popova, "Medicinal Chemistry of Tetrazoles," *Russian Chemical Bulletin* 61 (2012): 768–80 and references cited therein;(b) P. B. Mohite and V. H. Bhaskar, "Potential Pharmacological Activities of Tetrazoles in the New Millennium," *International Journal of PharmTech Research* 3 (2011): 1557–66 and references cited therein;(c) S. Q. Wang, Y. F. Wang, and Z. Xu, "Tetrazole Hybrids and Their Antifungal Activities," *European Journal of Medicinal Chemistry* 170 (2019): 225–34;(d) C. Gao, L. Chang, Z. Xu, X. F. Yan, C. Ding, F. Zhao, X. Wu, and L. S. Feng, "Recent Advances of Tetrazole Derivatives as Potential Anti-Tubercular and Anti-Malarial Agents," *European Journal of Medicinal Chemistry* 163 (2018): 404–12;(e) P. F. Lamie, J. N. Philoppes, A. A. Azouz, and N. M. Safwat, "Novel Tetrazole and Cyanamide Derivatives as Inhibitors of Cyclooxygenase-2 Enzyme: Design, Synthesis, Anti-Inflammatory Evaluation, Ulcerogenic Liability and Docking Study," *Journal of Enzyme Inhibition and Medicinal Chemistry* 32 (2017): 805–20.
32. K. D. Thomas, A. V. Adhikari, and N. S. Shetty, "Design, Synthesis and Antimicrobial Activities of Some New Quinoline Derivatives Carrying 1,2,3-Triazole Moiety," *European Journal of Medicinal Chemistry* 45, no. 9 (2010): 3803–10.
33. M. C. Joshi, K. J. Wicht, D. Taylor, R. Hunter, P. J. Smith, and T. J. Egan, "In Vitro Antimalarial Activity,  $\beta$ -Haematin Inhibition and Structure-Activity Relationships in a Series of Quinoline Triazoles," *European Journal of Medicinal Chemistry* 69 (2013): 338–47.
34. G. R. Pereira, G. C. Brandao, L. M. Arantes, H. A. de Oliveira, Jr., R. C. de Paula, M. F. A. do Nascimento, F. M. dos Santos, R. K. da Rocha, J. C. D. Lopes, and A. B. de Oliveira, "7-Chloroquinolinotriazoles: Synthesis by the Azide-Alkyne Cycloaddition Click Chemistry, Antimalarial Activity, Cytotoxicity and SAR Studies," *European Journal of Medicinal Chemistry* 73 (2014): 295–309.
35. T. Aravinda, H. S. Bhojya Naik, and H. R. Prakash Naik, "1,2,3-Triazole Fused Quinoline-Peptidomimetics: Studies on Synthesis, DNA Binding and Photocleavage Activity," *International Journal of Peptide Research and Therapeutics* 15, no. 4 (2009): 273–9.
36. (a) D. D. Subhedar, M. H. Shaikh, M. A. Arkile, A. Yeware, D. Sarkar, and B. B. Shingate, "Facile Synthesis of 1,3-Thiazolidin-4-Ones as Antitubercular Agents," *Bioorganic & Medicinal Chemistry Letters* 26 (2016): 1704–8;(b) D. D. Subhedar, M. H. Shaikh, L. Nawale, A. Yeware, D. Sarkar, F. A. K. Khan, J. N. Sangshetti, and B. B. Shingate, "Novel Tetrazoloquinoline-Rhodanine Conjugates: Highly Efficient Synthesis and Biological Evaluation," *Bioorganic Medicinal & Chemistry Letters* 26 (2016): 2278–83;(c) M. H. Shaikh, D. D. Subhedar, F. A. K. Khan, J. N. Sangshetti, and B. B. Shingate, "1,2,3-Triazole Incorporated Coumarin



- Derivatives as a Potential Antifungal and Antioxidant Agents,” *Chinese Chemical Letters* 27 (2016): 295–301;
- (d) M. H. Shaikh, D. D. Subhedar, L. Nawale, D. Sarkar, F. A. K. Khan, J. N. Sangshetti, and B. B. Shingate, “1,2,3-Triazole Derivatives as Antitubercular Agents; Synthesis, Biological Evaluation and Molecular Docking Study,” *Medicinal Chemistry Communications* 6 (2015): 1104–16.
37. (a) National Committee for Clinical Laboratory Standard, “Reference Method for Broth Dilution Antifungal Susceptibility Testing of Yeast Approved Standard” (Document M27-A, National Committee for Clinical Laboratory Standards, Wayne, PA, 1997);(b) National Committee for Clinical Laboratory Standard, “Reference Method for Broth Dilution Antifungal Susceptibility Testing of Conidium Forming Filamentous Fungi Proposed Standard” (Document M38-P, National Committee for Clinical Laboratory Standard, Wayne, PA, 1998);(c) National Committee for Clinical Laboratory Standards, “Methods for Dilution Antimicrobial Susceptibility Tests for Bacteria that Grow Aerobically Approved Standard”, 5th ed. (M7-A5, NCCLS, Villanova, PA, 2000).
38. (a) A. Khan, S. Sarkar, and D. Sarkar, “Bactericidal Activity of 2-Nitroimidazole against the Active Replicating Stage of *Mycobacterium bovis* BCG and *Mycobacterium tuberculosis* with Intracellular Efficacy in THP-1 Macrophages,” *International Journal of Antimicrobial Agents* 32 (2008): 40–5;(b) U. Singh, S. Akhtar, A. Mishra, and D. Sarkar, “A Novel Screening Method Based on Menadione Mediated Rapid Reduction of Tetrazolium Salt for Testing of Anti-Mycobacterial Agents,” *Journal of Microbiological Methods* 84 (2011): 202–7;(c) S. Sarkar and D. Sarkar, “Potential Use of Nitrate Reductase as a Biomarker for the Identification of Active and Dormant Inhibitors of *Mycobacterium tuberculosis* in a THP-1 Infection Model,” *Journal of Biomolecular Screening* 17 (2012): 966–73.
39. M. Burits and F. Bucar, “Antioxidant Activity of *Nigella sativa* Essential Oil,” *Phytotherapy Research* 14, no. 5 (2000): 323–8.
40. C. A. Lipinski, L. Lombardo, B. W. Dominy, and P. J. Feeney, “Experimental and Computational Approaches to Estimate Solubility and Permeability in Drug Discovery and Development Settings,” *Advanced Drug Delivery Reviews* 46, no. 1–3 (2001): 3–26.
41. Molinspiration Chemoinformatics, Brastislava, Slovak Republic, 2014, <http://www.molinspiration.com/cgi-bin/properties>.
42. Y. H. Zhao, M. H. Abraham, J. Le, A. Hersey, C. N. Luscombe, G. Beck, B. Sherborne, and I. Cooper, “Rate Limited Steps of Human Oral Absorption and QSAR Studies,” *Pharmaceutical Research* 19, no. 10 (2002): 1446–57.
43. “Drug-Likeness and Molecular Property Prediction,” <http://www.molsoft.com/mprop/>.
44. P. Ertl, B. Rohde, and P. Selzer, “Fast Calculation of Molecular Polar Surface Area as a Sum of Fragment-Based Contributions and Its Application to the Prediction of Drug Transport Properties,” *Journal of Medicinal Chemistry* 43, no. 20 (2000): 3714–7.
45. R. M. Singh and A. Srivastava, “Vilsmeier-Haack Reagent: A Facile Synthesis of 2-Chloro-3-Formylquinolines from N-Acetamides and Transformation into Different Functionalities,” *Indian Journal of Chemistry* 44B (2005): 1868–75.
46. N. K. Ladani, M. P. Patel, and R. G. Patel, “An Efficient Three Component One-Pot Synthesis of Some New Octahydroquinazolinone Derivatives and Investigation of Their Antimicrobial Activities,” *Arkivoc* vii (2009): 292–302.
47. (a) Schrodinger Suite 2015-4 QM-Polarized Ligand Docking Protocol; Glide Version 6.9 (New York, NY: Schrodinger, LLC, 2015); Jaguar Version 9.0 (New York, NY: Schrodinger, LLC, 2015); QSite Version 6.9 (New York, NY: Schrodinger, LLC, 2015);(b) R. A. Friesner, R. B. Murphy, M. P. Repasky, L. L. Frye, J. R. Greenwood, T. A. Halgren, P. C. Sanschagrin, and D. T. Mainz, “Extra Precision Glide: Docking and Scoring Incorporating a Model of Hydrophobic Enclosure for Protein-Ligand Complexes,” *Journal of Medicinal Chemistry* 49 (2006): 6177–96 and related references cited therein.





## Amide-Linked Monocarbonyl Curcumin Analogues: Efficient Synthesis, Antitubercular Activity and Molecular Docking Study

Dnyaneshwar D. Subhedar , **Mubarak H. Shaikh** , Amol A. Nagargoje , Satish V. Akolkar , Sujit G. Bhansali , Dhiman Sarkar & Bapurao B. Shingate


To cite this article: Dnyaneshwar D. Subhedar , Mubarak H. Shaikh , Amol A. Nagargoje , Satish V. Akolkar , Sujit G. Bhansali , Dhiman Sarkar & Bapurao B. Shingate (2020): Amide-Linked Monocarbonyl Curcumin Analogues: Efficient Synthesis, Antitubercular Activity and Molecular Docking Study, Polycyclic Aromatic Compounds, DOI: [10.1080/10406638.2020.1852288](https://doi.org/10.1080/10406638.2020.1852288)

To link to this article: <https://doi.org/10.1080/10406638.2020.1852288>

 View supplementary material 

 Published online: 09 Dec 2020.

 Submit your article to this journal 

 View related articles 

 View Crossmark data 



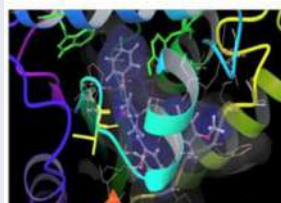
# Amide-Linked Monocarbonyl Curcumin Analogues: Efficient Synthesis, Antitubercular Activity and Molecular Docking Study

Dnyaneshwar D. Subhedar<sup>a</sup>, Mubarak H. Shaikh<sup>a,b</sup>, Amol A. Nagargoje<sup>a,c</sup>,  
Satish V. Akolkar<sup>a</sup>, Sujit G. Bhansali<sup>d</sup>, Dhiman Sarkar<sup>d</sup>, and Bapurao B. Shingate<sup>a</sup>

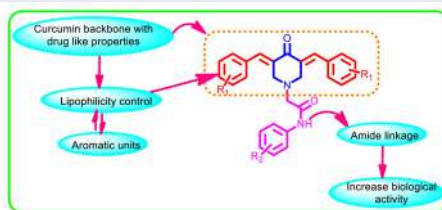
<sup>a</sup>Department of Chemistry, Dr. Babasaheb Ambedkar Marathwada University, Aurangabad, India; <sup>b</sup>Department of Chemistry, Radhabai Kale Mahila Mahavidyalaya, Ahmednagar, India; <sup>c</sup>Department of Chemistry, Khopoli Municipal Council College, Khopoli, India; <sup>d</sup>Combichem Bioresource Centre, Organic Chemistry Division, CSIR-National Chemical Laboratory, Pune, India

## ABSTRACT

An approach toward the synthesis of novel conjugates of 3,5-bis (arylidene)-4-piperidones (DAP) pharmacophore with amide-linkage has been developed *via* one-pot multicomponent reaction of aryl aldehydes, piperidinone and 2-chloro-*N*-phenylacetamide using [Et<sub>3</sub>NH][HSO<sub>4</sub>] as a catalyst/medium. Both substitutions on arylidene rings and piperidinone nitrogen (substituted 2-chloro-*N*-phenylacetamide) were varied. The synthesized conjugates were evaluated for their *in vitro* antitubercular activity against *M. tuberculosis* H<sub>37</sub>Ra (*MTB*) and *M. bovis* BCG strains. Among the series, compounds **4f**, **4g**, **4i** and **4j** showed remarkable broad spectrum antitubercular activity with low IC<sub>50</sub> values. Furthermore, computer docking simulations, for the most active conjugates were performed with the active site of mycobacterial enoyl-acyl carrier protein reductase (InhA) support the antitubercular activity. Lower cytotoxicity, high potency and promising activity against *MTB* and *M. Bovis* BCG suggest that amide linked DAP could serve as good leads for further modifications and development.



3D view of binding of compound **4f**



## ARTICLE HISTORY

Received 14 September 2020  
Accepted 25 October 2020


## KEYWORDS

Bis (arylidene)-4-piperidones; Ionic liquid; Antimycobacterial activity; Cytotoxicity; Molecular docking Study

## Introduction

Tuberculosis is the ninth leading cause of death worldwide from a single infectious agent ranking above HIV/AIDS. It is fatal airborne disease caused by *Mycobacterium tuberculosis* (*Mtb*) which affects the lung and also responsible for infection in others sites of body.<sup>1</sup> Global tuberculosis report of 2017 given by World Health Organization (WHO), shows that TB is the leading cause of deaths due to antimicrobial resistance and among people with HIV.<sup>2</sup> Over 6.3 million new TB

**CONTACT** Bapurao B. Shingate  [bapushingate@gmail.com](mailto:bapushingate@gmail.com)  Department of Chemistry, Dr. Babasaheb Ambedkar Marathwada University, Aurangabad, 431004, India.

 Supplemental data for this article can be accessed online at <https://doi.org/10.1080/10406638.2020.1852288>.

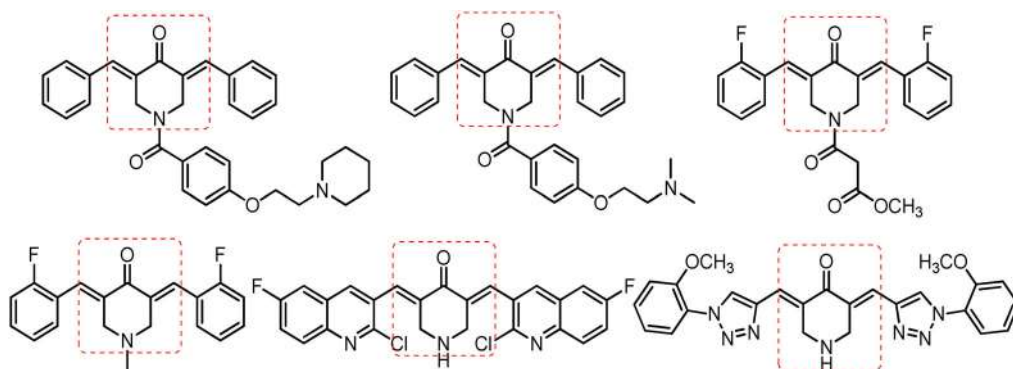


**Figure 1.** Known MACs as an antimycobacterial agents.

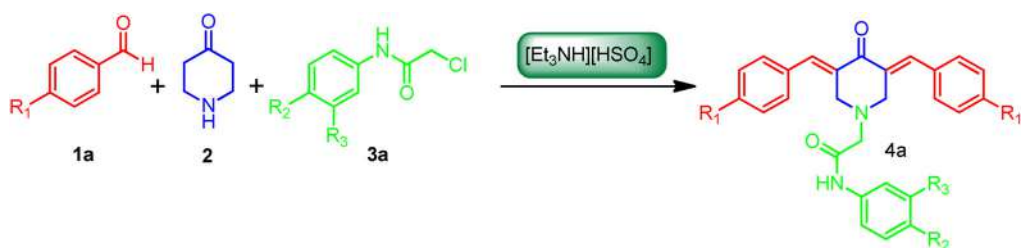
cases were notified to WHO by national authorities. In 2016 WHO estimates that there have been emergence and increasing evidences of extensively drug resistance and multiple drug resistance TB cases which results in global epidemic. Also, 4.9 lacs of new multidrug resistance TB cases were reported as per global tuberculosis report given by WHO. It was also reported that about 6 lacs new TB cases were found to exhibit resistance to most of the front-line drug against TB like rifampicin.<sup>3</sup> Hence, development of new therapeutic agents against TB is the urgent need of time.

In recent years enormous efforts have made by organic chemists across the globe in the development of structurally modified, therapeutically active curcumin analogues/derivatives.<sup>4</sup> Monocarbonyl analogue of curcumin is one of the class of structurally modified and potentially active curcuminoids obtained by removing  $\beta$ -diketone moiety and active methylene group from curcumin.<sup>5,6</sup> Monocarbonyl curcumin analogues exhibit a wide array of biological activities,<sup>7</sup> such as antileishmanial,<sup>8</sup> antiparasitic,<sup>9</sup> anti-inflammatory,<sup>10</sup> antitumor and antioxidant,<sup>11</sup> alzheimer's disease,<sup>12</sup> antibacterial,<sup>13</sup> anticancer<sup>14</sup> and antitubercular activity are well reported<sup>15</sup> (Figure 1).

Owing to the potential importance of curcumin derivatives as a key moieties in life sciences, pharmaceuticals, agriculture, world-wide efforts have made in the last few decades by researchers and various protocols have been developed for their synthesis<sup>16</sup> a using catalysts, such as NaOH/EtOH,<sup>16b</sup> EtOH/KOH,<sup>16c</sup> piperidine/HCl,<sup>16d</sup> AcOH/HCl gas,<sup>16e</sup> piperidine, L-Proline/EtOH<sup>16f</sup> and MgBr<sub>2</sub>.Et<sub>2</sub>O/Et<sub>3</sub>NH.<sup>16g</sup> The above methods suffer from one or more limitations such as the use of excess or stoichiometric quantity, corrosive, which are non-recoverable and/or recoverable with tedious separation procedures involving lots of toxic waste generation besides a long reaction time and low yield for the desired product.

Ionic Liquids (ILs) have attracted interest because of alternative green reaction media due to their unique chemical and physical properties such as low vapor pressure, high thermal and chemical stability, good solvating ability, ease of recyclability, and controlled miscibility.<sup>17</sup> Thus, ILs are considered to be a safer alternative to original organic solvents as they are cleaner and safer to use and reuse.<sup>18</sup> The utility of Acidic Bronsted Ionic Liquid (ABIL), particularly [Et<sub>3</sub>NH][HSO<sub>4</sub>]<sup>19</sup> has received considerable attention because, it is an inexpensive, nontoxic catalyst as well as solvent for many organic transformations in excellent yields. Multicomponent reactions (MCRs) are important class of organic transformations and increasing attention due to their, efficiency, atom economy, short reaction times and diversity in organic synthesis.<sup>20</sup> Moreover, use of solvent-free methods in MCRs makes the process safer, cleaner and easier to perform.<sup>21</sup> Thus, the utilization of MCRs coupled with environmentally benign solvent-free condition is highly desirable.

Monocarbonyl analogues of curcumin (MACs) are key constituent and structural backbone of many pharmaceutical and agricultural compounds and the development of more general and cost



**Scheme 1.** Model reaction.

**Table 1.** Optimization of solvent and temperature.

Entry	Solvent	Temp	Time (h)	Yield(%) <sup>a</sup>
1	EtOH	rt	6	60
2	MeOH	rt	6	65
3	DMF	rt	6	70
4	THF	rt	6	55
5	CH <sub>3</sub> CN	rt	6	50
6	Toluene	rt	6	71
7	Solvent-free	rt	2.5	82

Reaction conditions: **1a** (1 mmol), **2** (1 mmol), **3a** (1 mmol) and 25 mol%. [Et<sub>3</sub>NH][HSO<sub>4</sub>].

<sup>a</sup>Isolated yield.

effective, one-pot multi-component protocols for their synthesis under more efficient, environment friendly conditions using recyclable, ecofriendly catalysts is still a possibility to explore. Hence keeping in view the potential of MACs as an antitubercular agents and as part of our continuous efforts for the development of bioactive molecules<sup>22</sup> using highly efficient, safer as cost effective protocols,<sup>23,24</sup> we would like to report herein, synthesis and antimycobacterial evaluation of novel MACs by using [Et<sub>3</sub>NH][HSO<sub>4</sub>] as a medium/catalyst *via* one-pot multicomponent approach.

## Results and discussion

### Chemistry

In a preliminary experimental investigation of the optimum reaction conditions regarding the solvent, amount of catalyst and temperature. For this, benzaldehyde **1a** (1 mmol), piperidone **2** (1 mmol) and 2-chloro-*N*-phenyl acetamide **3a** (1 mmol) were chosen as standard model substrates for the synthesis of representative compound **4a** *via* Clasien-Schmidt reaction-alkylation as shown in Scheme 1.

The model reaction was carried out with 25 mol% of [Et<sub>3</sub>NH][HSO<sub>4</sub>] as a catalyst in different solvents (Table 1) at room temperature. In methanol (MeOH) and ethanol (EtOH), the reaction took a longer time (6h) with a moderate yield of the products (Table 1, entries 1 and 2). In *N,N*-Dimethylformamide (DMF), a better yield of the product was obtained (Table 1, entry 3). Further, the reaction carried out in tetrahydrofuran (THF) and acetonitrile (CH<sub>3</sub>CN), but again a lower yield of the product (Table 1, entries 4, 5) obtained In Toluene, a good yield of the product was obtained in 6h (Table1, entry 6). However, when the model reaction was carried out under a solvent-free condition, there is a significant increase in the yield of the product in a shorter period (Table1, entry 7). Thus, solvent-free is the best condition for this Clasien-Schmidt reaction.

To optimize the concentration of catalyst, we further examined the influence of catalyst concentration on the reaction time and percentage yield. So, the model reaction was performed using different concentration of catalyst 5, 10, 15, 20, 25 and 30 mol% of [Et<sub>3</sub>NH][HSO<sub>4</sub>] at room



**Table 2.** The effect of catalyst loading on model reaction **4a**.<sup>a</sup>

Entry	Catalyst (mol %)	Yield (%) <sup>b</sup>
1	5	40
2	10	59
3	15	69
4	20	73
5	25	82
6	30	82

<sup>a</sup>Reaction conditions: **1a** (1 mmol), **2** (1 mmol), **3a** (1 mmol) and 25 mol%. [Et<sub>3</sub>NH][HSO<sub>4</sub>].

<sup>b</sup>Isolated yield.

**Table 3.** Reusability of [Et<sub>3</sub>NH][HSO<sub>4</sub>] in the synthesis of **4a**.<sup>a</sup>

Entry	Reaction cycle	Isolated yield (%) <sup>b</sup>
1	1st (fresh run)	82
2	2nd cycle	80
3	3rd cycle	78
4	4th cycle	78
5	5th cycle	74

<sup>a</sup>Reaction conditions: **1a** (1 mmol), **2** (1 mmol), **3a** (1 mmol) and 25 mol%. [Et<sub>3</sub>NH][HSO<sub>4</sub>], rt.

<sup>b</sup>Isolated yield of products.

temperature under solvent-free conditions and the product **4a** was obtained in 40, 59, 69, 73, 82 and 82% yields, respectively.

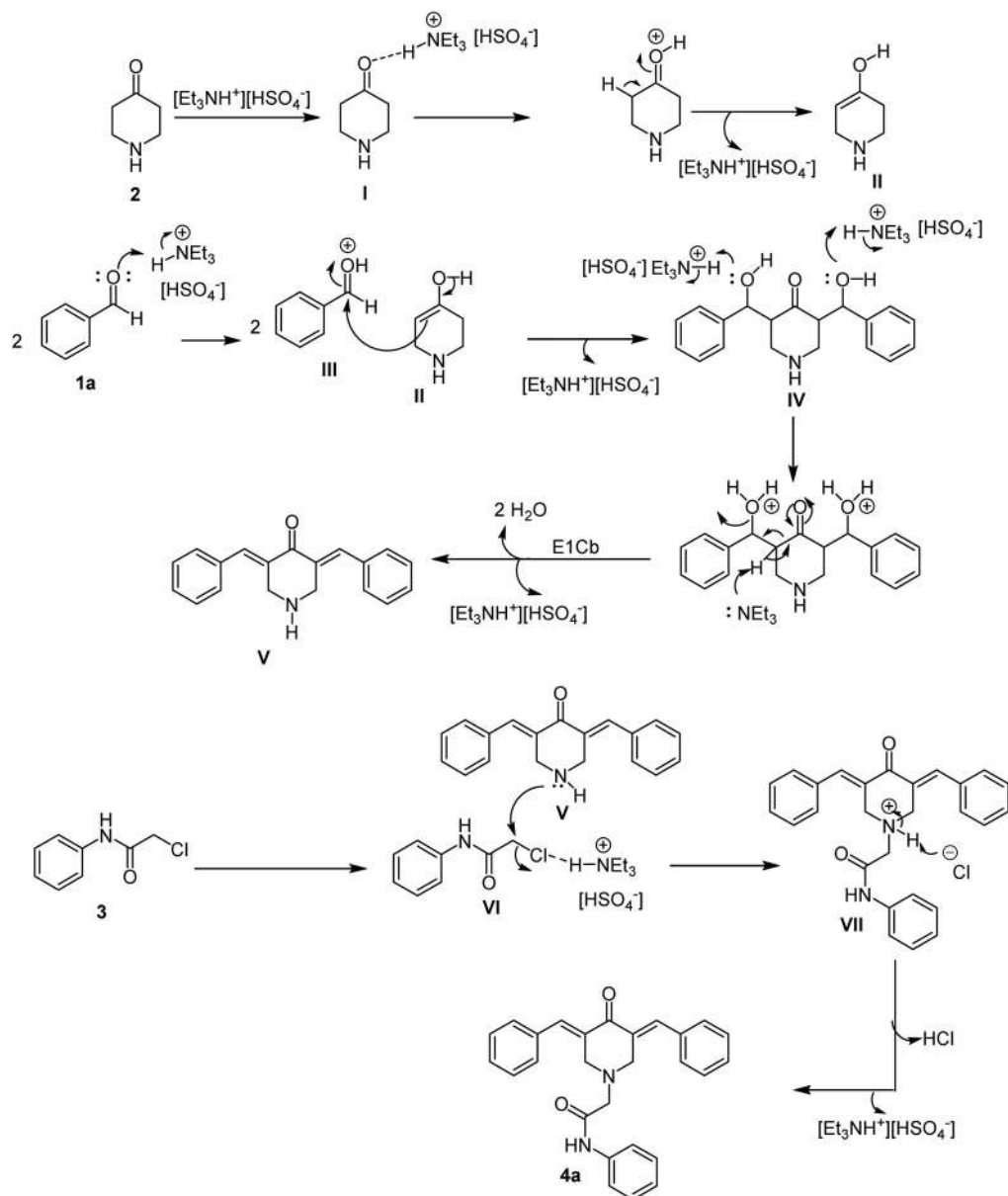
Further, the yield of the product did not improve as the concentration of catalyst increased (Table 2, entry 6). It was therefore concluded that the optimum concentration of catalyst was 25 mol % (Table 2, entry 5). Thus, it is concluded that 25 mol % of [Et<sub>3</sub>NH][HSO<sub>4</sub>] is sufficient for the best result.

Further, the recyclability of the ionic liquid [Et<sub>3</sub>NH][HSO<sub>4</sub>] was then studied and the results are shown in Table 3. After completion of the reaction, the reaction mixture was poured on ice cold water and the product was extracted using ethyl acetate solvent. The filtrate was subjected for evaporation of water to get viscous liquid, which on cooling afforded ionic liquid. Further, the residual ionic liquid was washed with diethyl ether, dried under vacuum at 60 °C and reused for subsequent reactions. It was then reused at least four consecutive cycles without much appreciable loss in its catalytic activity (Table 3, entries 1–5).

The formation of compound **4a** has been confirmed by IR, <sup>1</sup>H NMR, <sup>13</sup>C NMR and HRMS spectral study. IR spectrum of **4a** displayed characteristic signals for C=O at 1707 and 1656 cm<sup>-1</sup>. In the <sup>1</sup>H NMR spectrum of compound **4a**, a sharp singlet resonating at around δ 4.47 ppm for four protons, assigned to methylene groups of the piperidine ring. The peak observed at δ 4.12 ppm for the CH<sub>2</sub> group attached to the *N*-phenylacetamide. <sup>13</sup>C NMR spectrum was also in agreement with the proposed structure displaying characteristic signals for carbonyl at around δ 187.2 and 169.5 ppm. Similarly, signals resonating at around δ 57.5 and 50.5 have been assigned to methylene carbons of the piperidine and *N*-phenylacetamide ring. The HRMS spectral analysis of the **4a** was also conformity with the proposed structure. Similarly, the structure of other derivatives was confirmed by physical and spectral data (Supplementary information).

A plausible mechanistic pathway is proposed to illustrate the synthesis of monocarbonyl curcumin analogues catalyzed by [Et<sub>3</sub>NH][HSO<sub>4</sub>] (Scheme 2).

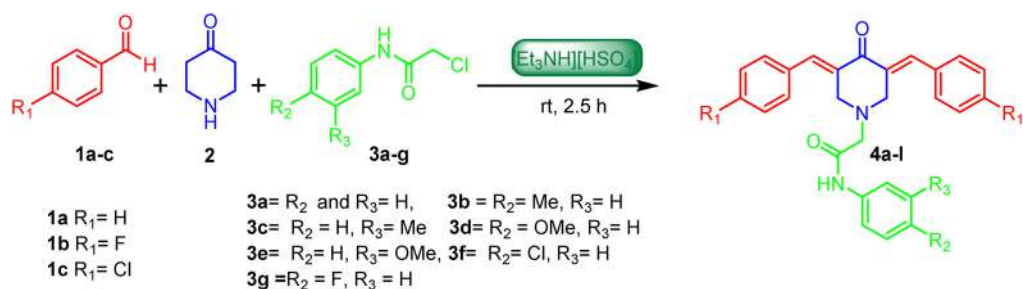
The initial step is believed to be the protonation of the carbonyl carbon of aldehyde **1a** by ionic liquid [Et<sub>3</sub>NH][HSO<sub>4</sub>] to form intermediate **III** and enolate formation of piperidinone **II** which facilitates the nucleophilic attack of piperidinone to promote the formation of C-C bond to yield intermediate **IV**. The subsequent protonation and elimination of H<sub>2</sub>O molecule *via* E<sub>1</sub>CB



**Scheme 2.** Plausible mechanistic catalytic cycle for the synthesis of compound 4a.

mechanism leads to the formation of intermediate V. Ionic liquid increases the electrophilicity of 2-chloro-*N*-phenylacetamide C-Cl carbon shown in structure VI. Then nucleophilic substitution of 2-chloro-*N*-phenylacetamide by compound V expedite the formation of C-N bond to yield compound VII. The final step involves deprotonation of intermediate VII leads to regeneration of ionic to yield compound 4a.

So, having the optimized reaction conditions in hand, the scope and efficiency of this approach were explored for the synthesis of highly functionalized amide linked 3,5-bis(arylidene)-4-piperidones (Scheme 3) and the structures are given in Figure 2. The structures of all the synthesized conjugates were confirmed by their physical data and spectral analysis.



**Scheme 3.** Synthetic pathway for 3,5-bis(arylidene)-4-piperidones.

## Biological activity

### Antitubercular activity

In a standard primary screening, all the newly synthesized 3,5-bis(arylidene)-4-piperidones **4a-l** were evaluated for their *in vitro* antitubercular activity against *M. tuberculosis* H<sub>37</sub>Ra and

*M. bovis* BCG at concentrations of 30, 10 and 3  $\mu\text{g}/\text{mL}$  using an established XTT Reduction Menadione assay (XRMA) method.<sup>25</sup> The drug rifampicin was used as reference.

In general, compounds which showed more than 90% inhibition (SI, Table S1, S2) at 30  $\mu\text{g}/\text{mL}$  were confirmed by carrying out dose dependent effect using a range from 50 to 0.39  $\mu\text{g}/\text{mL}$  to determine IC<sub>50</sub> and MIC with serial dilution in DMSO (Table 4).

Among all the prepared xanthene conjugates, compounds **4f**, **4h**, **4i**, **4j**, **4k** and **4l** are found prominent antimycobacterial activities against *MTB* and *M. bovis* BCG strain with MIC values 1.89–26.37 and 2.69–29.14  $\mu\text{g}/\text{mL}$ , respectively. However, rest of the xanthene conjugates **4a**, **4b**, **4c**, **4d**, **4e** and **4g** are inactive against *MTB* and *M. bovis* BCG strain with MIC = >30  $\mu\text{g}/\text{mL}$ .

### Cytotoxic activity

The most active conjugates **4f**, **4h**, **4i**, **4j**, **4k** and **4l** were further evaluated against human cancer cell lines (MCF-7, A549 and HCT 116) for toxicity and results are given in Table 5. The GI<sub>50</sub>/GI<sub>90</sub> (>250  $\mu\text{g}/\text{mL}$ ) values of all the compounds (except **4k**) indicate that the compounds are potent and specific inhibitors against *MTB*. The primary cytotoxic study information is given in supporting information (SI S3, S4 and S5).

### Selectivity index (SI)

The selectivity index reflects the concentration of the compound at which it is active against *mycobacteria* but not toxic toward host cells. A higher selectivity index of compounds indicates that they can be used as a therapeutic agent. The compound **4f** (SI > 12) showed very high SI, which is actually good inhibitor of *MTB* and *M. bovis* BCG and the results are shown in Table 6.

Although the selectivity index of rifampicin is very high, it is important to consider the significance of this study with respect to the developing resistance among microorganisms against available antibiotics. According to a study of Hartkoorn et al.<sup>26</sup> on the drug susceptibility of TB, antimycobacterial activity was considered to be specific when the selectivity index was >10. In the current study compound **4f** exhibited highest selectivity index of >10, indicating their potential as an antitubercular agent and should be investigated further.

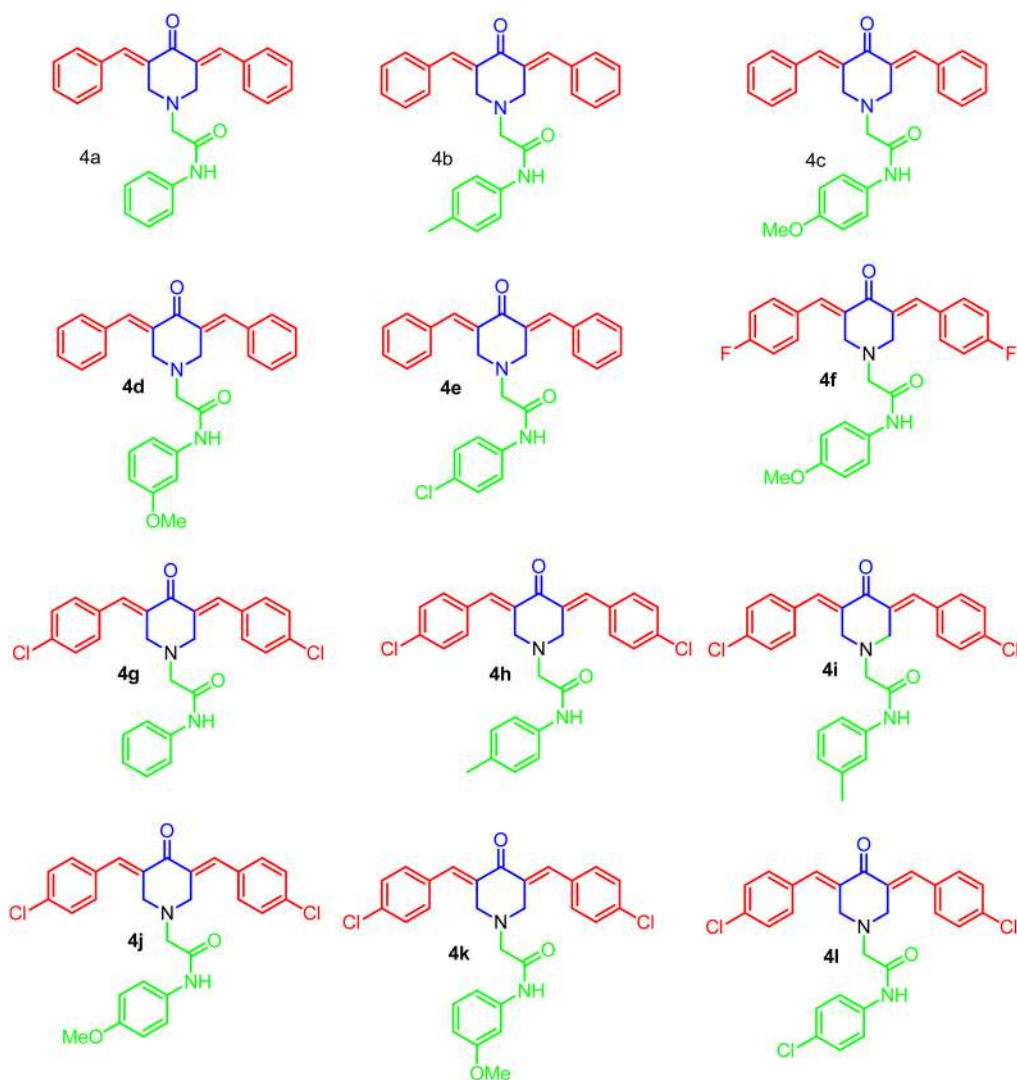


**Figure 2.** Structures of synthesized MACs.

**Table 4.** Antitubercular screening results of compounds 4a-l ( $\mu\text{g/mL}$ )<sup>a</sup>.

Compound	MTB H37Ra		<i>M. bovis</i> BCG	
	MIC	IC <sub>50</sub>	MIC	IC <sub>50</sub>
4a	>30	>30	>30	>30
4b	>30	>30	>30	>30
4c	>30	>30	>30	>30
4d	>30	>30	>30	>30
4e	>30	>30	>30	>30
4f	20.57	1.89	22.33	2.69
4g	>30	6.85	>30	7.33
4h	>30	>30	>30	>30
4i	>30	18.33	>30	6.94
4j	28.46	2.37	29.42	2.85
4k	>30	26.37	>30	29.14
4l	>30	27.64	>30	23.4
<sup>b</sup> Rifampicin	0.045	0.0017	0.017	0.0015

<sup>a</sup>MIC in  $\mu\text{g/mL}$ . Antitubercular activity of all agents was firm by serial dose dependent dilutions method.

<sup>b</sup>Standard antitubercular drug rifampicin as a positive control. Data were expressed as the means of triplication. SD ( $\pm$ ): Standard Deviation.

**Table 5.** Cytotoxicity activity.

Compound	MCF-7		A549		HCT-116	
	GI <sub>50</sub>	GI <sub>90</sub>	GI <sub>50</sub>	GI <sub>90</sub>	GI <sub>50</sub>	GI <sub>90</sub>
4f	>250	>250	>250	>250	>250	>250
4h	>250	>250	>250	>250	>250	>250
4i	>250	>250	>250	>250	>250	>250
4j	>250	>250	>250	>250	>250	>250
4k	188.58	>250	225.51	>250	219.11	>250
4l	>250	>250	>250	>250	>250	>250
Rifampicin	>100	>100	>100	>100	>100	>100
Paclitaxel	0.0048	0.075	0.0035	0.0706	0.1279	5.715

The GI<sub>50</sub> (cytotoxicity) values were calculated as the concentration of compounds resulting in 50% reduction of absorbance compared to untreated cells.

**Table 6.** SI of selected 3,5-bis (arylidene)-4-piperidones.

Compound	MCF-7		A549		HCT 116	
	MTB	BCG	MTB	BCG	MTB	BCG
4f	>12	>11	>12	>11	>12	>11
4h	>8	>8	>8	>8	>8	>8
4i	>8	>8	>8	>8	>8	>8
4j	>6	>6	>8	>8	>7	>7
4k	>9	>8	>9	>8	>9	>8
4l	>8	>8	>8	>8	>8	>8
Rifampicin	>133	>123	>133	>123	>133	>123

**Table 7.** Antibacterial activity of curcumin derivatives (MIC in µg/mL).

Compound	Gram-negative		Gram-positive	
	<i>E. coli</i>	<i>P. fluorescens</i>	<i>S. aureus</i>	<i>B. subtilis</i>
4f	>100	>100	>100	>100
4h	>100	>100	>100	>100
4i	18.54	20.99	20.61	22.48
4j	>100	>100	>100	>100
4k	>100	>100	>100	>100
4l	28.32	22.87	26.57	26.65
Ampicillin	1.46	4.36	1	10.32
Kanamycin	1.62	0.49	>30	1.35

### Antibacterial activity

For investigating the specificity of conjugates **4f**, **4h**, **4i**, **4j**, **4k** and **4l** were further screened for their anti-bacterial activity against four bacterial strains. All the compounds (except **4i** and **4l**) showed higher specificity toward *MTB*, because they display no anti-bacterial activity upto 100 µg/mL (Tables 6 and 7).

### Computational study

#### Molecular docking

Studies of whole genome sequence of *MTB* H37Ra showed the presence of genes which encodes the components of the FAS-II system along with enzyme enoyl-acyl carrier protein reductase (InhA) aids in elongation and synthesis of mycolic acids.<sup>27</sup> We have carried out the docking study of benzylidene-4-oxopiperidin-1-yl-*N*-phenylacetamide derivatives against mycobacterial enoyl-acyl carrier protein reductase (InhA) which could give the important leads for treatment of TB.



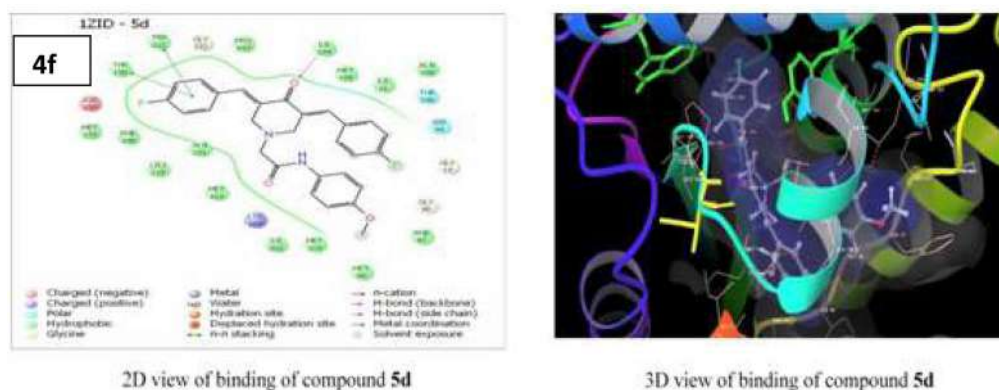


Figure 3. 2D and 3D view of binding of compound **4f** with the active site of InhA.

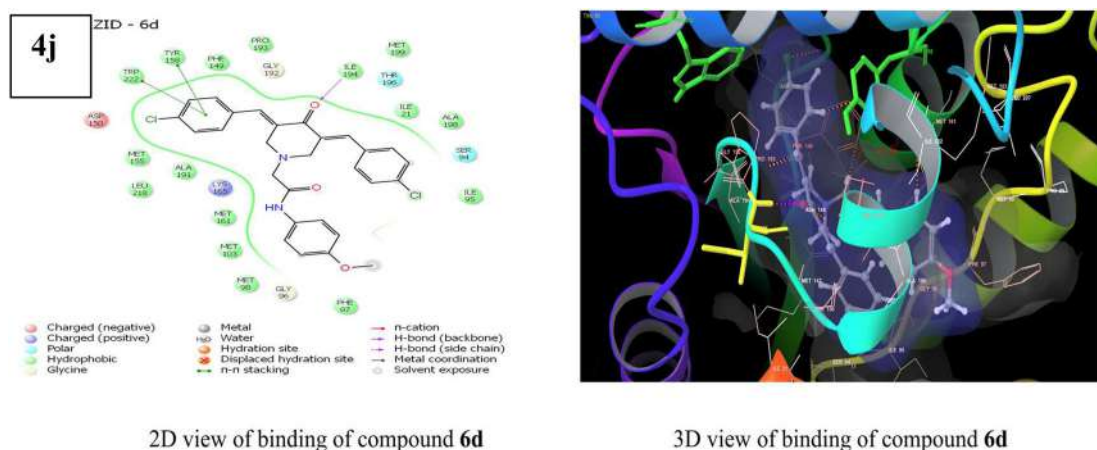
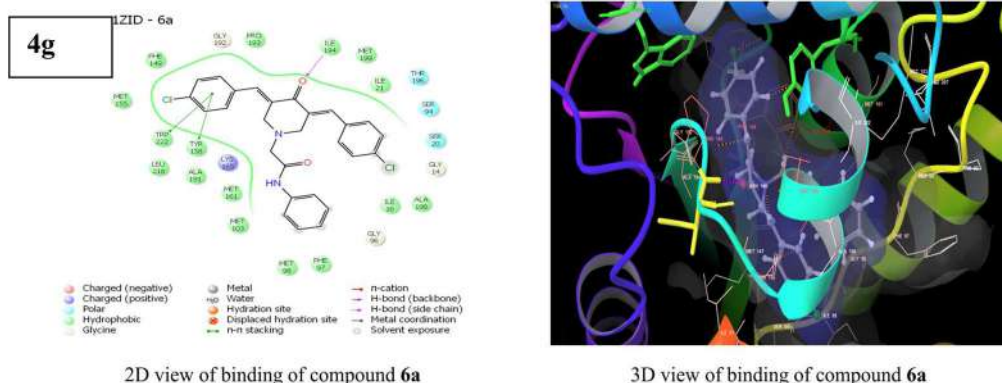


Figure 4. 2D and 3D view of binding of compound **4j** with the active site of InhA.

All the conjugates were successfully docked into the active site of mycobacterial InhA. The docking score of most active compounds **4f**, **4g** and **4j** were found to be  $-8.102$ ,  $-7.960$  and  $-7.816$ , respectively. The interactions of these molecules with the active site of mycobacterial InhA is shown in Figures 3–5, respectively. The lowest energy docking pose for **4f**, **4g** and **4j** revealed the presence of hydrogen bonding interactions between 4-oxo group of piperidine ring and Ile194 with a distance of  $1.966 \text{ \AA}$ ,  $2.086 \text{ \AA}$  and  $1.900 \text{ \AA}$  as observed in Figures 3–5, respectively. These firm hydrogen bonding interactions helps in 3D orientation of these ligands within the active site which increases the steric and electrostatic interactions of ligands with the amino acid residues present within the active site of mycobacterial InhA.

The per residue interaction analysis showed that several strong van der Waals and electrostatic interactions which played an important role for binding of benzylidene-4-oxopiperidin-1-yl-*N*-phenylacetamide derivatives with the active site of mycobacterial InhA. (Data represented in Table S6 in SI.) In addition, one of the 4-fluoro phenyl ring of compound **4f** and 4-chloro phenyl ring of compound **4g** and **4j** showed the two  $\pi$ - $\pi$  stacking interactions with amino acid Tyr158 and Trp222 which were enclosed in the hydrophobic pocket of the active site of mycobacterial InhA formed by the amino acids Pro193, Trp222, Met155 and Phe149 as observed in Figures 3–5.

Further, the other 4-fluoro phenyl ring of compound **4f** and 4-chloro phenyl ring of compound **4g** and **4j** fits into the hydrophobic pocket formed by the amino acid residues Ile21,



2D view of binding of compound 6a

3D view of binding of compound 6a

**Figure 5.** 2D and 3D view of binding of compound **4g** with the active site of InhA.

Ala198, Ile95 and Ile16 present within the active site of mycobacterial InhA. Also, the phenyl ring attached to acetamide group is embedded in the hydrophobic pocket formed by the Met103, Mett98 and Phe97 amino acid residues present within the active site of mycobacterial InhA. Therefore, from the docking studies, it is clear that these compounds have significant binding with the active site of mycobacterial InhA. The hydrophobic substituents on aromatic rings attached to piperidin-4-one ring are necessary for firm binding through  $\pi$ - $\pi$  stacking interactions with the active site of mycobacterial InhA. The  $-C=O$  group attached to the piperidine is essential for firm binding with the active site through strong hydrogen bonding interactions with the Ile194 amino acid residue present within the active site of mycobacterial InhA. Also, the phenyl ring attached to the acetamide group is essential for binding since it perfectly fits into hydrophobic pocket formed by the amino acid residues of active site which helps in the firm binding of these compounds with the active site of mycobacterial InhA. Hence, the mode of action of antitubercular activity for these compounds might be through the inhibition of active site of mycobacterial InhA.

## Conclusions

In conclusion, a novel, highly efficient, one-pot multi-component protocol has been developed for the synthesis of 3,5-bis (arylidene)-4-piperidones in excellent yields using  $[Et_3NH][HSO_4]$  as a catalyst at room temperature in a short reaction time. These analogues were evaluated for the first time for antitubercular activity against the *MTB* H37Ra and *M. Bovis* BCG strains. However, the compounds **4f**, **4g** and **4j** exhibited  $IC_{50}$  values of 1.89, 6.85 and 2.37  $\mu\text{g/ml}$  against *MTB* H37Ra, respectively. Compounds **4f**, **4g**, **4i** and **4j** showing excellent antitubercular activity against *M. Bovis* BCG strain with  $IC_{50}$  values of 2.69, 7.33, 6.94 and 2.85  $\mu\text{g/mL}$ , respectively. From the docking studies, the most active conjugates **4f**, **4g** and **4j** showed hydrogen binding with the amino acid residue Ile194 and two  $\pi$ - $\pi$  stacking hydrophobic interactions with the amino acid residue Tyr158 and Trp222 present in the active site of *MTB* InhA. Furthermore, evaluation of the data on the cytotoxicity, antimicrobial activity and docking studies shows that the conjugates **4f**, **4g**, **4i** and **4j** are highly selective toward the *MTB* H37Ra and *M. Bovis* BCG strain.

## Experimental section

### Materials and methods

All chemicals and reagents were procured from Sigma Aldrich, S.D. Fine chemical and commercial suppliers and used without further purification. The completion of the reactions was

monitored by thin-layer chromatography (TLC) on aluminum plates coated with silica gel 60 F<sub>254</sub>, 0.25 mm thickness (Merck). The detection of the components was made by exposure to iodine vapors or UV light. Melting points were determined by open capillary methods and are uncorrected. The products were characterized using <sup>1</sup>H NMR, <sup>13</sup>C NMR spectra and HRMS. The NMR spectra of the product were obtained using a Bruker AC-400MHz spectrometer with TMS as the internal standard. High-resolution mass spectra (HRMS) were recorded on Agilent 6520 (QTOF) mass spectrometer.

#### **Experimental procedure for the synthesis of [Et<sub>3</sub>NH][HSO<sub>4</sub>]**

The synthesis of ionic liquid was carried out in a 100 mL round-bottom flask, which was immersed in a recirculating heated water-bath and fitted with a reflux condenser. Sulfuric acid (98%) (1.96 g, 0.02 mol) was added drop wise from triethylamine (2.02 g, 0.02 mol) stirring at 60 °C for 1 h. After the addition, the reaction mixture was stirred for an additional period of 1 h at 70 °C to ensure the reaction had proceeded to completion. The traces of water were removed by heating the residue at 80 °C in high vacuum until the weight of the residue remains constant.

#### **Triethylammonium hydrogen sulfate [Et<sub>3</sub>NH][HSO<sub>4</sub>]**

<sup>1</sup>H NMR (400 MHz, DMSO-*d*<sub>6</sub>): δ ppm = 1.16–1.23 (t, 9H, 3 × CH<sub>3</sub>), 3.04–3.15 (q, 6H, 3 × CH<sub>2</sub>) and 8.85 (s, 1H, NH); <sup>13</sup>C NMR (100 MHz, DMSO-*d*<sub>6</sub>): δ ppm = 11.03 (CH<sub>3</sub>) and 52.6 (CH<sub>2</sub>); FT-IR cm<sup>-1</sup> 3024 (for N-H stretch), 2815.74 (for C-H stretch), 1231.96 (for C-N stretch).

#### **General procedure for one-pot synthesis of 2-((3*E*,5*E*)-3,5-dibenzylidene-4-oxopiperidin-1-yl)-*N*-phenylacetamide (4a-l)**

A mixture of the substituted aldehyde (**1a-c**) (1 mmol), piperidinone (**2**) (1 mmol) and various 2-chloro-*N*-phenyl acetamides (**3a-g**) (1 mmol) in 25 mol% [Et<sub>3</sub>NH][HSO<sub>4</sub>] catalyst was stirred at room temperature for 2.5 h. The progress of the reaction was monitored by TLC. After the completion of reaction confirmed by the TLC using *n*-hexane: ethyl acetate (8:2) as solvent system. After completion of the reaction, the reaction mixture was poured on ice cold water and the product was extracted using ethyl acetate solvent. The organic layer evaporated under vacuum on rotavapor to get crude solid which further crystallized from ethanol to obtain a pure solid product (**4a-l**). The aqueous filtrate was subjected for evaporation of water to get viscous liquid, which on cooling afforded ionic liquid. Further, the residual ionic liquid was washed with diethyl ether, dried under vacuum at 60 °C and reused for subsequent reactions. It was then reused at least four consecutive cycles without much appreciable loss in its catalytic activity.

**2-((3*E*,5*E*)-3,5-Dibenzylidene-4-oxopiperidin-1-yl)-*N*-phenylacetamide (4a):** The compound **4a** was obtained from **1a**, **2** and **3a** as yellow solid; Yield: 82%; Mp: 182–184 °C; IR (cm<sup>-1</sup>): 3030, 2985, 1707, 1656, 1591, 1555 and 1493; <sup>1</sup>H NMR (400 MHz, DMSO-*d*<sub>6</sub>, δppm): 9.76 (s, 1H, NH), 7.83 (s, 2H, -C=H), 7.67–7.65 (m, 4H, Ar-H), 7.59–7.30 (m, 10H, Ar-H), 4.47 (s, 4H, -CH<sub>2</sub>) and 4.12 (s, 2H, -CH<sub>2</sub>); <sup>13</sup>C NMR (100 MHz, DMSO-*d*<sub>6</sub>, δppm): 187.2, 169.5, 145.8, 137.0, 136.6, 132.3, 131.5, 131.0, 130.9, 127.5, 126.7, 125.0, 123.3, 121.9, 119.7, 57.5 and 50.5; HRMS (ESI-qTOF): Calcd for C<sub>27</sub>H<sub>25</sub>N<sub>2</sub>O<sub>2</sub> [M + H]<sup>+</sup>, 409.2838, found: 409.2842.

**2-((3*E*,5*E*)-3,5-Dibenzylidene-4-oxopiperidin-1-yl)-*N*-(*p*-tolyl)acetamide (4b):** The compound **4b** was obtained from **1a**, **2** and **3b** as pale yellow solid; Yield: 75%; Mp: 205–207 °C; <sup>1</sup>H NMR (400 MHz, DMSO-*d*<sub>6</sub>, δppm): 7.75 (s, 2H, -C=H), 7.59–7.48 (m, 10H, Ar-H), 7.46–7.29 (m, 4H, Ar-H), 4.48 (s, 4H, -CH<sub>2</sub>), 4.11 (s, 2H, -CH<sub>2</sub>) and 2.42 (s, 3H, CH<sub>3</sub>); <sup>13</sup>C NMR (100 MHz, DMSO-*d*<sub>6</sub>, δppm): 183.8, 162.2, 142.2, 134.9, 131.7, 129.9, 129.8, 128.3, 124.2, 123.1, 115.2, 115.0, 114.6, 55.2, 51.3 and 21.1.

**2-((3E,5E)-3,5-Dibenzylidene-4-oxopiperidin-1-yl)-N-(4-methoxyphenyl) acetamide (4c):** The compound **4c** was obtained from **1a**, **2** and **3c** as yellow solid; Yield: 76%; Mp: 181–183 °C; <sup>1</sup>H NMR (400 MHz, DMSO-*d*<sub>6</sub>, δppm): 7.69 (s, 2H, -C=H), 7.54–7.36 (m, 12H, Ar-H), 7.04–7.03 (m, 2H, Ar-H), 4.57 (s, 4H, -CH<sub>2</sub>), 4.37 (s, 2H, -CH<sub>2</sub>) and 3.84 (s, 3H, OCH<sub>3</sub>); <sup>13</sup>C NMR (100 MHz, DMSO-*d*<sub>6</sub>, δppm): 184.9, 155.7, 136.5, 135.2, 132.2, 128.6, 125.6, 125.5, 123.5, 121.8, 121.3, 119.7, 119.1, 111.1, 57.3, 54.5 and 49.9; HRMS (ESI-qTOF): Calcd for C<sub>28</sub>H<sub>27</sub>N<sub>2</sub>O<sub>3</sub> [M + H]<sup>+</sup>, 439.1555, found: 439.1586.

**2-((3E,5E)-3,5-Dibenzylidene-4-oxopiperidin-1-yl)-N-(3-methoxyphenyl) acetamide (4d):** The compound **4d** was obtained from **1a**, **2** and **3d** as yellow solid; Yield: 71%; Mp: 198–200 °C; <sup>1</sup>H NMR (400 MHz, DMSO-*d*<sub>6</sub>, δppm): 7.84 (s, 2H, -C=H), 7.56–7.08 (m, 11H, Ar-H), 7.02–6.73 (m, 3H, Ar-H), 4.79 (s, 4H, -CH<sub>2</sub>), 4.46 (s, 2H, -CH<sub>2</sub>) and 3.89 (s, 3H, OCH<sub>3</sub>); <sup>13</sup>C NMR (100 MHz, DMSO-*d*<sub>6</sub>, δppm): 185.1, 160.0, 140.3, 137.8, 135.3, 131.5, 129.4, 129.1, 127.8, 127.5, 127.1, 126.2, 124.3, 123.4, 122.6, 119.9, 56.4, 53.7 and 49.2.

**N-(4-Chlorophenyl)-2-((3E,5E)-3,5-dibenzylidene-4-oxopiperidin-1-yl) acetamide (4e):** The compound **4e** was obtained from **1a**, **2** and **3f** as pale yellow solid; Yield: 76%; Mp: 207–209 °C; <sup>1</sup>H NMR (400 MHz, DMSO-*d*<sub>6</sub>, δppm): 7.77 (s, 2H, -C=H), 7.61–7.46 (m, 12H, Ar-H), 7.38–7.36 (m, 2H, Ar-H), 4.53 (s, 4H, -CH<sub>2</sub>) and 4.16 (s, 2H, -CH<sub>2</sub>); <sup>13</sup>C NMR (100 MHz, DMSO-*d*<sub>6</sub>, δppm): 184.3, 168.1, 141.1, 136.7, 132.5, 131.6, 130.9, 137.3, 126.7, 126.3, 122.6, 122.3, 122.0, 121.8, 119.5, 55.3 and 49.6; HRMS (ESI-qTOF): Calcd for C<sub>27</sub>H<sub>24</sub>ClN<sub>2</sub>O<sub>2</sub> [M + H]<sup>+</sup>, 443.2032, found: 443.2005

**2-((3E,5E)-3,5-Bis(4-fluorobenzylidene)-4-oxopiperidin-1-yl)-N-(4-methoxyphenyl)acetamide (4f):** The compound **4f** was obtained from **1b**, **2** and **3f** as yellow solid; Yield: 78%; Mp: 232–234 °C; <sup>1</sup>H NMR (400 MHz, DMSO-*d*<sub>6</sub>, δppm): 7.83 (s, 2H, -C=H), 7.60–7.58 (m, 4H, Ar-H), 7.39–7.04 (m, 8H, Ar-H), 4.59 (s, 4H, -CH<sub>2</sub>), 4.03 (s, 2H, -CH<sub>2</sub>) and 3.91 (s, 3H, OCH<sub>3</sub>); <sup>13</sup>C NMR (101 MHz, DMSO) δ 183.9, 163.4, 162.1, 160.4, 136.1, 132.4, 130.9, 129.5, 127.5, 125.5, 122.1, 115.83, 57.3, 52.78, 46.58; HRMS (ESI-qTOF): Calcd for C<sub>28</sub>H<sub>25</sub>F<sub>2</sub>N<sub>2</sub>O<sub>3</sub> [M + H]<sup>+</sup>, 475.2342, found: 475.2364

**2-((3E,5E)-3,5-Bis(4-chlorobenzylidene)-4-oxopiperidin-1-yl)-N-phenylacetamide (4g):** The compound **4g** was obtained from **1c**, **2** and **3g** as pale yellow solid; Yield: 80%; Mp: 186–188 °C; <sup>1</sup>H NMR (400 MHz, DMSO-*d*<sub>6</sub>, δppm): 7.79 (s, 2H, -C=H), 7.53–7.46 (m, 4H, Ar-H), 7.44–7.16 (m, 9H, Ar-H), 4.40 (s, 4H, -CH<sub>2</sub>) and 4.08 (s, 2H, -CH<sub>2</sub>); <sup>13</sup>C NMR (100 MHz, DMSO-*d*<sub>6</sub>, δppm): 184.1, 166.7, 160.8, 148.8, 148.2, 142.2, 138.7, 129.9, 129.8, 128.6, 128.4, 124.2, 123.1, 115.2, 115.0, 114.0, 57.4 and 51.5; ESI-MS: Calcd for C<sub>27</sub>H<sub>23</sub>Cl<sub>2</sub>N<sub>2</sub>O<sub>2</sub> [M + H]<sup>+</sup>, 478.1, found: 478.0.

**2-((3E,5E)-3,5-Bis(4-chlorobenzylidene)-4-oxopiperidin-1-yl)-N-(p-tolyl)acetamide (4h):** The compound **4h** was obtained from **1c**, **2** and **3b** as pale yellow solid; Yield: 82%; Mp: 175–177 °C; <sup>1</sup>H NMR (400 MHz, DMSO-*d*<sub>6</sub>, δppm): 7.77 (s, 2H, -C=H), 7.49–7.43 (m, 8H, Ar-H), 7.30–7.25 (m, 4H, Ar-H), 4.50 (s, 4H, -CH<sub>2</sub>), 3.98 (s, 2H, -CH<sub>2</sub>) and 2.37 (s, 3H, CH<sub>3</sub>); 184.4, 143.1, 139.5, 135.1, 134.5, 133.5, 130.5, 129.7, 128.4, 125.3, 124.4, 115.3, 57.3, 49.6 and 21.5; ESI-MS: Calcd for C<sub>28</sub>H<sub>25</sub>Cl<sub>2</sub>N<sub>2</sub>O<sub>2</sub> [M + H]<sup>+</sup>, 492.2, found: 492.0.

**2-((3E,5E)-3,5-Bis(4-chlorobenzylidene)-4-oxopiperidin-1-yl)-N-(m-tolyl)acetamide (4i):** The compound **4i** was obtained from **1c**, **2** and **3c** as pale yellow solid; Yield: 75%; Mp: 201–203 °C; <sup>1</sup>H NMR (400 MHz, DMSO-*d*<sub>6</sub>, δppm): 7.81 (s, 2H, -C=H), 7.47–7.43 (m, 8H, Ar-H), 7.30–7.02 (m, 4H, Ar-H), 4.48 (s, 4H, -CH<sub>2</sub>), 3.90 (s, 2H, -CH<sub>2</sub>) and 2.40 (s, 3H, CH<sub>3</sub>); <sup>13</sup>C NMR (100 MHz, DMSO-*d*<sub>6</sub>, δppm): 185.8, 167.8, 144.8, 143.6, 139.5, 134.1, 129.3, 120.3, 119.2, 57.9, 55.8 and 21.2; ESI-MS: Calcd for C<sub>28</sub>H<sub>25</sub>Cl<sub>2</sub>N<sub>2</sub>O<sub>2</sub> [M + H]<sup>+</sup>, 492.4, found: 492.0.

**2-((3E,5E)-3,5-Bis(4-chlorobenzylidene)-4-oxopiperidin-1-yl)-N-(4-methoxyphenyl)acetamide (4j):** The compound **4j** was obtained from **1c**, **2** and **3d** as yellow solid; Yield: 74%; Mp: 217–219 °C; <sup>1</sup>H NMR (400 MHz, DMSO-*d*<sub>6</sub>, δppm): 7.78 (s, 2H, -C=H), 7.49–7.43 (m, 10H, Ar-H), 7.00–6.99 (m, 2H, Ar-H), 4.48 (s, 4H, -CH<sub>2</sub>), 3.96 (s, 2H, -CH<sub>2</sub>) and 3.86 (s, 3H, OCH<sub>3</sub>); <sup>13</sup>C

NMR (100 MHz, DMSO- $d_6$ ,  $\delta$ ppm): 186.4, 161.3, 137.6, 136.7, 132.7, 129.0, 126.2, 126.1, 124.9, 124.8, 124.0, 122.4, 121.7, 120.1, 56.8, 52.7 and 47.4; HRMS (ESI-qTOF): Calcd for  $C_{28}H_{25}Cl_2N_2O_3$   $[M + H]^+$ , 508.2652, found: 508.2629

**2-((3E,5E)-3,5-Bis(4-chlorobenzylidene)-4-oxopiperidin-1-yl)-N-(3-methoxyphenyl)acetamide (4k):** The compound **4k** was obtained from **1c**, **2** and **3e** as yellow solid; Yield: 76%; Mp: 221–223 °C;  $^1H$  NMR (400 MHz, DMSO- $d_6$ ,  $\delta$ ppm): 7.95 (s, 2H, -C=H), 7.65–7.53 (m, 9H, Ar-H), 7.11–6.85 (m, 3H, Ar-H), 4.53 (s, 4H, -CH<sub>2</sub>), 3.93 (s, 2H, -CH<sub>2</sub>) and 3.88 (s, 3H, OCH<sub>3</sub>);  $^{13}C$  NMR (100 MHz, DMSO- $d_6$ ,  $\delta$ ppm): 185.1, 161.7, 136.5, 134.6, 129.7, 129.3, 126.3, 126.0, 125.6, 125.3, 122.9, 122.5, 122.0, 121.2, 120.4, 120.2, 119.8, 119.3, 56.1, 52.4 and 49.0.

**2-((3E,5E)-3,5-Bis(4-chlorobenzylidene)-4-oxopiperidin-1-yl)-N-(4-chlorophenyl)acetamide (4l):** The compound **4l** was obtained from **1c**, **2** and **3f** as yellow solid; Yield: 78%; Mp: 190–192 °C;  $^1H$  NMR (400 MHz, DMSO- $d_6$ ,  $\delta$ ppm): 8.05 (s, 2H, -C=H), 7.84–7.80 (m, 9H, Ar-H), 7.76–7.64 (m, 3H, Ar-H), 4.52 (s, 4H, -CH<sub>2</sub>) and 4.26 (s, 2H, -CH<sub>2</sub>);  $^{13}C$  NMR (100 MHz, DMSO- $d_6$ ,  $\delta$ ppm): 187.0, 168.9, 146.0, 144.8, 137.7, 136.7, 135.3, 130.4, 129.8, 132.4, 59.1 and 57.0; HRMS (ESI-qTOF): Calcd for  $C_{27}H_{22}Cl_3N_2O_2$   $[M + H]^+$ , 512.4762, found: 512.4727.

## Biological assay

### Antitubercular activity

All the chemicals such as sodium salt XTT, DMSO, sulfanilic acid, sodium nitrate, NEED and rifampicin were purchased from Sigma-Aldrich, USA. Dubos medium was purchased from DIFCO, USA. Compounds were dissolved in DMSO and used as stock solution for further antimycobacterial testing. Microbial strains such as *Mycobacterium bovis* BCG (ATCC 35734) and *Mycobacterium tuberculosis* H<sub>37</sub>Ra (ATCC 25177) were obtained from AstraZeneca, India. The stock culture was maintained at –80 °C and sub cultured once in a liquid medium before inoculation into an experimental culture. Cultures were grown in Dubos media (enrichment media). *Mycobacterium pheli* medium (minimal essential medium) was used for antimycobacterial assay. It contains 0.5 g KH<sub>2</sub>PO<sub>4</sub>, 0.25 g trisodium citrate, 60 mg MgSO<sub>4</sub>, 0.5 g asparagine and 2 mL glycerol in distilled water (100 mL) followed by pH adjustment to 6.6. All the newly synthesized compounds were screened *in vitro* against two *Mycobacterium* species such as *Mycobacterium tuberculosis* H<sub>37</sub>Ra and *Mycobacterium bovis* BCG. Both species of *Mycobacterium* were grown in *Mycobacterium pheli* medium. Screening of *Mycobacterium tuberculosis* H<sub>37</sub>Ra was done by using XTT reduction menadione assay (XRMA) and *Mycobacterium Bovis* BCG screening was done by using NR (Nitrate reductase) assay, both of them were developed earlier in our lab.<sup>25</sup> Briefly, 2.5  $\mu$ l of these inhibitor solutions were added in a total volume of 250  $\mu$ l of *Mycobacterium pheli* medium consisting of bacilli. The incubation was terminated on the 8th day for Active and 12 days for Dormant MTB culture. The XRMA and NR was then carried out to estimate viable cells present in different wells of the assay plate. The optical density was read on a micro plate reader (Spectramax plus384 plate reader, Molecular Devices Inc) at 470 nm filter for XTT and at 540 nm filter for NR against a blank prepared from cell-free wells. Absorbance given by cells treated with the vehicle alone was taken as 100% cell growth. Primary screening was done at 30, 10 and 3  $\mu$ g/mL. Compounds showing 90% inhibition of bacilli, at or lower than 30  $\mu$ g/mL were selected for further dose response curve. All experiments were performed in triplicates and the quantitative value was expressed as the average  $\pm$  standard deviation. MIC and IC<sub>50</sub> values of selected compound were calculated from their dose response curves by using Origin 6 software. % Inhibition was calculated by using following formula: % Inhibition = [(absorbance of compound – absorbance of Test)/(absorbance of Control – absorbance of Blank)]  $\times$  100, where control is the medium with bacilli along with vehicle and blank is cell free medium.



### Cytotoxicity activity

Three human cancer cell lines, HeLa (human cervical cancer cell line), A549 (human lung adenocarcinoma cell line) and PANC-1 (human pancreas carcinoma cell line) were used to check the cytotoxicity of compounds. The cell lines were obtained from the American Type Culture Collection (ATCC) and maintained in T 25 flasks with 10% (v/v) fetal bovine serum (FBS) containing Dulbecco's Modified Eagle Medium (DMEM). Cell line containing T 25 flasks were maintained at 37 °C under 5% CO<sub>2</sub> and 95% air in a humidified atmosphere. Medium were replaced twice a week. All the compounds were tested for their cytotoxicity against HeLa, A549 and PANC-1 cell line by using modified MTT assay.<sup>28</sup> Briefly, cells were seeded as,  $1.5 \times 10^4$  cells/ml for HeLa,  $1 \times 10^4$ -cells/well for A549 and PANC-1 in a 96 well plate. The plates were incubated for 24 h into CO<sub>2</sub> incubator (37 °C under 5% CO<sub>2</sub> and 95% air in a humidified atmosphere) to adhere the cells. After incubation, compound was added in such a way that final concentration becomes 30, 10, and 3 µg/ml in the test well. Concentrations ranges of compound were selected as 30, 10 and 3 µg/ml of each. Again, plates were incubated for additional 72 h for HeLa and 48 h for A549 and PANC-1 to see the effect of compound on cells. After that, cell medium was replaced with 100 µl of Glucose-MTT (0.5 mg/ml)-PBS medium and kept the plate for 2–4 h to form the reduced MTT or Formazan crystals. This reduced MTT or Formazan crystals were solubilized by addition of acidified isopropanol. The optical density was read on a micro plate reader (Spectramax plus 384 plate reader, Molecular Devices Inc) at 470 nm filter against a blank prepared from cell-free wells. Absorbance given by cells treated with the vehicle alone was taken as 100% cell growth. All the experiments were performed in triplicates and the quantitative value was expressed as the average  $\pm$  standard deviation. GI<sub>50</sub> and MIC values were calculated by plotting the graphs, by using Origin Pro software. The viability and growth in the presence of test material is calculated by using the following formula: % cytotoxicity = [(average absorbance of control-absorbance of compound)/(absorbance of control-absorbance of blank)]  $\times$  100, where control is the culture medium with cells and DMSO and blank is the culture medium without cells.

### Selectivity index

The selectivity index (SI) was calculated by dividing the 50% growth inhibition concentration (GI<sub>50</sub>) for cell lines (HeLa, A549 and PANC-1) by the MIC for *in vitro* activity against active/dormant MTB and BCG.<sup>29</sup>

### Anti-bacterial activity

All bacterial cultures were first grown in LB media at 37 °C at 180 RPM. Once the culture reaches 1 O.D, it is used for antibacterial assay. Bacterial strains *E. coli* (NCIM 2688), *P. fluorescens* (NCIM 2036) as Gram-negative and *B. subtilis* (NCIM 2079), *S. aureus* (NCIM 2010) as Gram-positive were obtained from NCIM (NCL, Pune) and were grown in Luria Burtony medium from Himedia, India. The assay was performed in 96 well plates after 8 and 12 h. for Gram-negative and Gram-positive bacteria, respectively. 0.1% of 1 OD culture at 620 nm was used for screening.<sup>30</sup> 0.1% inoculated culture was added in to each well of 96 well plate containing the compounds to be tested. Optical density for each plate was measured at 620 nm after 8 h for Gram negative bacteria and after 12 h for Gram-positive bacteria.

### Computational study

#### Molecular docking study

To understand mode of action for antitubercular activity of the synthesized benzylidene-4-oxopiperidin-1-yl-*N*-phenylacetamide derivatives, molecular modeling and docking studies were

performed. Glide 5.8<sup>31</sup> was used to perform docking studies using crystal structure of mycobacterium tuberculosis enoyl-acyl carrier protein reductase (InhA) (PDB id:1ZID).

The structures of the compounds were drawn using 2D-sketcher present in Maestro 9.3<sup>32</sup> and were converted from 2D into 3D representations and saved in maestro format. For further computational studies, compounds were prepared using LigPrep 2.5<sup>33</sup> which gives the low-energy conformers, 3D structures with correct chiralities for each successfully processed input structure. The protein was purified using the protein preparation wizard present in Maestro 9.3. All the water molecules were deleted. Bond order was assigned and H-atoms were added to the protein, including the protons necessary to define the correct ionization and tautomeric states of the amino acid residues. Missing residues of the side chain were added using Prime 3.1.<sup>34</sup> Protein refinement was done in two steps. Initially, orientation of polar hydrogens, flip terminal amides and histidines was optimized and the protonation states were adjusted. Further, steric clashes potentially existing in the protein were relaxed using the OPLS-2005 force field present in the impact refinement module. Minimization was terminated when the energy converged or the root mean square deviation reached a maximum cut off of 0.30 Å.<sup>35</sup> To predict the active site of the receptor, a grid was generated using grid generation panel of glide with the default settings. Grid is generated to define the binding site of co-crystallized ligand in the receptor. The ligand was selected to define the position of active site and size of the enclosing box was set to 20 Å to include the significant part of 1ZID.

## Acknowledgments

DDS and MHS are very much grateful to the Council of Scientific and Industrial Research (CSIR), New Delhi, India for the award of research fellowship. Authors are also thankful to the Head, Department of Chemistry, Dr. Babasaheb Ambedkar Marathwada University, for providing laboratory facility and University Grants Commission, Department of Science and Technology, New Delhi for financial support under DST-FIST and UGC-SAP Schemes.

## Disclosure statement

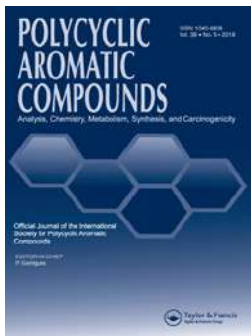
There are no conflicts of interest.

## References

1. R. Rappuoli, "Changing Route: Aerosol Vaccine against Tuberculosis," *The Lancet Infectious Diseases* 14, no. 10 (2014): 901–2.
2. "Global Tuberculosis Report." [http://www.who.int/tb/publications/global\\_report/en/](http://www.who.int/tb/publications/global_report/en/).
3. B. D. Kana, P. C. Karakousis, T. Parish, and T. Dick, "Future Target-Based Drug Discovery for Tuberculosis?," *Tuberculosis (Edinburgh, Scotland)* 94, no. 6 (2014): 551–6.
4. S. A. Noureddin, R. M. El-Shishtawy, and K. O. Al-Footy, "Curcumin Analogues and Their Hybrid Molecules as Multifunctional Drugs," *European Journal of Medicinal Chemistry* 182, (2019): 111631.
5. T. P. Robinson, T. Ehlers, R. B. Hubbard IV, X. Bai, J. L. Arbiser, D. J. Goldsmith, and J. P. Bowen, "Design, Synthesis, and Biological Evaluation of Angiogenesis Inhibitors: Aromatic Enone and Dienone Analogues of curcumin," *Bioorganic & Medicinal Chemistry Letters* 13, no. 1 (2003): 115–7.
6. H. Ohtsu, Z. Xiao, J. Ishida, M. Nagai, H.-K. Wang, H. Itokawa, C.-Y. Su, C. Shih, T. Chiang, E. Chang, et al. "Antitumor Agents. 217. Curcumin Analogues as Novel Androgen Receptor Antagonists with Potential as anti-Prostate Cancer Agents," *Journal of Medicinal Chemistry* 45, no. 23 (2002): 5037–42.
7. K. Bairwa, J. Grover, M. Kania, and S. M. Jachak, "Recent Developments in Chemistry and Biology of Curcumin Analogues," *RSC Advances* 4, no. 27 (2014): 13946–78; and references cited therein.
8. A. Tiwari, S. Kumar, R. Shivahare, P. Kant, S. Gupta, and S. N. Suryawanshi, "Chemotherapy of Leishmaniasis Part XIII: Design and Synthesis of Novel Heteroretinoid-Bisbenzylidene Ketone Hybrids as Antileishmanial Agents," *Bioorganic & Medicinal Chemistry Letters* 25, no. 2 (2015): 410–3.
9. S. F. P. Braga, E. V. P. Alves, R. S. Ferreira, J. R. B. Fradico, P. S. Lage, M. C. Duarte, T. G. Ribeiro, P. A. S. Junior, A. J. Romanha, M. L. Tonini, et al. "Synthesis and Evaluation of the Antiparasitic Activity of Bis-(Arylmethylidene) Cycloalkanones," *European Journal of Medicinal Chemistry* 71 (2014): 282–9.

10. P. Yu, L. Dong, Y. Zhang, W. Chen, S. Xu, Z. Wang, X. Shan, J. Zhou, Z. Liu, and G. Liang, "Design, Synthesis and Biological Activity of Novel Asymmetric C66 Analogs as anti-Inflammatory Agents for the Treatment of Acute Lung Injury," *European Journal of Medicinal Chemistry* 94 (2015): 436–46.
11. T. Kalai, M. L. Kuppusamy, M. Balog, K. Selvendiran, B. K. Rivera, P. Kuppusamy, and K. Hideg, "Synthesis of N-Substituted 3,5-Bis(arylidene)-4-piperidones with High Antitumor and Antioxidant Activity," *Journal of Medicinal Chemistry* 54, no. 15 (2011): 5414–21.
12. S. Y. Chen, Y. Chen, Y. P. Li, S. H. Chen, J. H. Tan, T. M. Ou, L. Q. Gu, and Z. S. Huang, "Design, Synthesis, and Biological Evaluation of Curcumin Analogues as Multifunctional Agents for the Treatment of Alzheimer's disease," *Bioorganic & Medicinal Chemistry* 19, no. 18 (2011): 5596–604.
13. S. Kaur, N. H. Modi, D. Panda, and N. Roy, "Probing the Binding Site of Curcumin in Escherichia coli and Bacillus subtilis FtsZ-A Structural Insight to Unveil Antibacterial Activity of Curcumin," *European Journal of Medicinal Chemistry* 45, no. 9 (2010): 4209–14.
14. K. Kandi, S. Manohar, C. E. Gerena, B. Zayas, S. V. Malhotra, and D. S. Rawat, "C<sub>5</sub>-Curcuminoid-4-Aminoquinoline Based Molecular Hybrids: Design, Synthesis and Mechanistic Investigation of Anticancer Activity," *New Journal of Chemistry* 39, no. 1 (2015): 224–34.
15. P. R. Baldwin, A. Z. Reeves, K. R. Powell, R. J. Napier, A. I. Swimm, A. Sun, K. Giesler, B. Bommarius, T. M. Shinnick, J. P. Snyder, et al., "Monocarbonyl Analogs of Curcumin Inhibit Growth of Antibiotic Sensitive and Resistant Strains of Mycobacterium tuberculosis," *European Journal of Medicinal Chemistry* 92 (2015): 693–9; (b) N. Singh, J. Pandey, A. Yadav, V. Chaturvedi, S. Bhatnagar, A. N. Gaikwad, S. K. Sinha, A. Kumar, P. K. Shukla, and R. P. Tripathi, "A Facile Synthesis of Alpha, alpha'-(EE)-bis(benzylidene)-Cycloalkanones and Their Antitubercular Evaluations," *European Journal of Medicinal Chemistry* 44 (2009): 1705–9; (c) U. Das, S. Das, B. Bandy, J. P. Stables, and J. R. Dimmoc, "N-Aroyl-3,5-Bis(benzylidene)-4-Piperidones: A Novel Class of Antimycobacterial Agents," *Bioorganic & Medicinal Chemistry* 16 (2008): 3602–7.
16. Methods for the synthesis of curcumin analogues see: (a) S. A. Nouredin, R. M. El-Shishtawy, and K. O. Al-Footy, "Synthesis of New Symmetric Cyclic and Acyclic Halocurcumin Analogues Typical Precursors for Hybridization," *Research on Chemical Intermediates* 46 (2020): 5307–5323; (b) H. Lin, G. X. Hua, J. Guo, Y. Ge, G. Liang, Q. Q. Lian, Y. Chu, X. Yuan, P. Huang, and R. S. Ge, "Mono-Carbonyl Curcumin Analogues as 11 $\beta$ -Hydroxysteroid Dehydrogenase 1 Inhibitors," *Bioorganic & Medicinal Chemistry Letters* 23 (2013): 4362–6; (c) X. Yuan, H. Li, H. Bai, Z. Su, Q. Xiang, C. Wang, B. Zhao, Y. Zhang, Q. Zhang, Y. Chu, et al., "Synthesis of Novel Curcumin Analogues for Inhibition of 11 $\beta$ -Hydroxysteroid Dehydrogenase Type 1 with Anti-Diabetic Properties," *European Journal of Medicinal Chemistry* 77 (2014): 223–30; (d) I. M. Fawzy, K. M. Youssef, N. S. M. Ismail, J. Gullbo, and K. A. M. Abouzid, "Design and Synthesis and Biological Evaluation of Novel Curcumin Analogs with Anticipated Anticancer Activity," *Future Journal of Pharmaceutical Sciences* 1 (2015): 22; (e) N. K. Paul, M. Jha, K. S. Bhullar, H. P. V. Rupasinghe, J. Balzarini, and A. Jha, "All Trans 1-(3-arylacryloyl)-3,5-bis(pyridin-4-ylmethylene)piperidin-4-ones as Curcumin-Inspired Antineoplastics," *European Journal of Medicinal Chemistry* 87 (2014): 461–70; (f) A. Tiwari, S. Kumar, R. Shivahare, P. Kant, S. Gupta, and S. N. Suryawanshi, "Chemotherapy of leishmaniasis part XIII: Design and synthesis of novel heteroretinoid-bisbenzylidene ketone hybrids as antileishmanial agents," *Bioorganic & Medicinal Chemistry Letters* 25 (2015): 410; (g) M. V. Makarov, E. S. Leonova, E. Y. Rybalkina, P. Tongwa, V. N. Khrustalev, T. V. Timofeeva, and I. L. Odinet, "Synthesis, Characterization and Structure-Activity Relationship of Novel N-Phosphorylated E,E-3,5-bis(thienylidene)piperid-4-ones," *European Journal of Medicinal Chemistry* 45 (2010): 992–1000.
17. (a) P. Wasserscheid, and T. Welton, Eds. (Weinheim, Germany: Wiley-VCH, Verlag GmbH & Co., 2002); (b) C. Yue, D. Fang, L. Liu, and T. F. Yi, "Synthesis and Application of Task-Specific Ionic Liquids Used as Catalysts and/or Solvents in Organic Unit Reactions," *Journal of Molecular Liquids* 163 (2011): 99–121.
18. N. Samaan, Q. Zhong, J. Fernandez, G. Chen, A. M. Hussain, S. Zheng, G. Wang, and Q. H. Chen, "Design, Synthesis, and Evaluation of Novel Heteroaromatic Analogs of Curcumin as anti-Cancer Agents," *European Journal of Medicinal Chemistry* 75 (2014): 123–31.
19. C. Wang, W. Zhao, H. Li, and L. Guo, "Solvent-Free Synthesis of Unsaturated Ketones by the Saucy–Marbet Reaction Using Simple Ammonium Ionic Liquid as a Catalyst," *Green Chemistry* 11, no. 6 (2009): 843–7.
20. R. C. Cioc, E. Ruijter, and R. V. A. Orru, "Multicomponent Reactions: Advanced Tools for Sustainable Organic Synthesis," *Green Chemistry* 16, no. 6 (2014): 2958–75.
21. N. Isambert, M. M. S. Duque, J. C. Plaquevent, Y. Genisson, J. Rodriguez, and T. Constantieux, "Multicomponent Reactions and Ionic Liquids: A Perfect Synergy for Eco-Compatible Heterocyclic Synthesis," *Chemical Society Reviews* 40, no. 3 (2011): 1347–57.
22. (a) D. D. Subhedar, M. H. Shaikh, L. Nawale, A. Yeware, D. Sarkar, and B. B. Shingate, "[Et<sub>3</sub>NH][HSO<sub>4</sub>] Catalyzed Efficient Synthesis of 5-Arylidene-Rhodanine Conjugates and Their Antitubercular Activity," *Research on Chemical Intermediates* 42 (2016): 6607–26; (b) D. D. Subhedar, M. H. Shaikh, L. Nawale, A. Yeware, D. Sarkar, F. A. K. Khan, J. N. Sangshetti, and B. B. Shingate, "Novel Tetrazoloquinoline-Rhodanine

- Conjugates: Highly Efficient Synthesis and Biological Evaluation,” *Bioorganic & Medicinal Chemistry Letters* 26 (2016): 2278–83; (c) M. H. Shaikh, D. D. Subhedar, F. A. K. Khan, J. N. Sangshetti, and B. B. Shingate, “[Et<sub>3</sub>NH][HSO<sub>4</sub>]-Catalyzed One-Pot, Solvent-Free Synthesis and Biological Evaluation of  $\alpha$ -Amino Phosphonates,” *Research on Chemical Intermediates* 42 (2016): 5115–31; (d) D. D. Subhedar, M. H. Shaikh, M. Arkile, A. Yeware, D. Sarkar, and B. B. Shingate, *Bioorganic & Medicinal Chemistry Letters* 26 (2016): 1704; (e) A. A. Nagargoje, S. V. Akolkar, and M. M. Siddiqui, “Synthesis and Evaluation of Pyrazole Incorporated Monocarbonyl Curcumin Analogues as Antiproliferative and Antioxidant Agents,” *Journal of the Chinese Chemical Society* 66 (2019): 1658–65; (f) A. A. Nagargoje, S. V. Akolkar, and D. D. Subhedar, “Propargylated Monocarbonyl Curcumin Analogues: Synthesis, Bioevaluation and Molecular Docking Study,” *Medicinal Chemistry Research* 29 (2020): 1902–13.
23. J. Weng, C. Wang, H. Li, and Y. Wang, “Novel Quaternary Ammonium Ionic Liquids and Their Use as Dual Solvent-Catalysts in the Hydrolytic Reaction,” *Green Chemistry* 8, no. 1 (2006): 96–9.
  24. Z. N. Siddiqui, and K. Khan, “[Et<sub>3</sub>NH][HSO<sub>4</sub>]-Catalyzed Efficient, Eco-Friendly, and Sustainable Synthesis of Quinoline Derivatives via Knoevenagel Condensation,” *ACS Sustainable Chemistry & Engineering* 2, no. 5 (2014): 1187–94; and references cited therein.
  25. A. Khan, S. Sarkar, and D. Sarkar, “Bactericidal Activity of 2-Nitroimidazole against the Active Replicating Stage of Mycobacterium bovis BCG and Mycobacterium tuberculosis with Intracellular Efficacy in THP-1 Macrophages,” *International Journal of Antimicrobial Agents* 32, no. 1 (2008): 40–5.
  26. R. C. Hartkoorn, B. Chandler, A. Owen, S. A. Ward, S. Bertel Squire, D. J. Back, and S. H. Khoo, “Differential Drug Susceptibility of Intracellular and Extracellular Tuberculosis, and the Impact of P-Glycoprotein,” *Tuberculosis* 87, no. 3 (2007): 248–55.
  27. S. T. Cole, R. Brosch, J. Parkhill, T. Garnier, C. Churcher, D. Harris, S. V. Gordon, K. Eiglmeier, S. Gas, C. E. Barry, et al. “Deciphering the Biology of Mycobacterium tuberculosis from the Complete Genome Sequence,” *Nature* 393, no. 6685 (1998): 537–44.
  28. D. Sreekanth, A. Syed, S. Sarkar, D. Sarkar, B. Santhakumari, A. Ahmad, and I. Khan, “Production, Purification and Characterization of Taxol and 10DAB III from a New Endophytic Fungus Gliocladium sp. isolated from the Indian Yew Tree,” *Journal of Microbiology and Biotechnology* 19 (2009): 1342–7.
  29. L. L. Gundersen, J. N. Meyer, and B. Spilsberg, “Synthesis and Antimycobacterial Activity of 6-Arylpurines: The Requirements for the N-9 Substituent in Active Antimycobacterial Purines,” *Journal of Medicinal Chemistry* 45, no. 6 (2002): 1383–6.
  30. R. Singh, L. U. Nawale, M. Arkile, U. U. Shedbalkar, S. A. Wadhvani, D. Sarkar, and B. A. Chopade, “Chemical and Biological Metal Nanoparticles as Antimycobacterial Agents: A Comparative Study,” *International Journal of Antimicrobial Agents* 46, no. 2 (2015): 183–8.
  31. *Glide* (version 5.8) (New York, NY: Schrodinger, LLC, 2012).
  32. *Maestro* (version 9.3) (New York, NY: Schrodinger, LLC, 2012).
  33. *LigPrep* (version 2.5) (New York, NY: Schrodinger, LLC, 2012).
  34. *Prime* (version 3.1) (New York, NY: Schrodinger, LLC, 2012).
  35. R. A. Friesner, J. L. Banks, R. B. Murphy, T. A. Halgren, J. J. Klicic, D. T. Mainz, M. P. Repasky, E. H. Knoll, M. Shelley, J. K. Perry, et al. “Glide: A New Approach for Rapid, Accurate Docking and Scoring. 1. Method and Assessment of Docking Accuracy,” *Journal of Medicinal Chemistry* 47, no. 7 (2004): 1739–49.




## Design, Synthesis and Biological Evaluation of Novel Furan & Thiophene Containing Pyrazolyl Pyrazolines as Antimalarial Agents

Hemantkumar N. Akolkar , Sujata G. Dengale , Keshav K. Deshmukh ,  
Bhausahab K. Karale , Nirmala R. Darekar , Vijay M. Khedkar & **Mubarak H. Shaikh**

To cite this article: Hemantkumar N. Akolkar , Sujata G. Dengale , Keshav K. Deshmukh , Bhausahab K. Karale , Nirmala R. Darekar , Vijay M. Khedkar & Mubarak H. Shaikh (2020): Design, Synthesis and Biological Evaluation of Novel Furan & Thiophene Containing Pyrazolyl Pyrazolines as Antimalarial Agents, Polycyclic Aromatic Compounds, DOI: [10.1080/10406638.2020.1821231](https://doi.org/10.1080/10406638.2020.1821231)

To link to this article: <https://doi.org/10.1080/10406638.2020.1821231>

 View supplementary material 

 Published online: 14 Sep 2020.

 Submit your article to this journal 

 Article views: 9

 View related articles 

 View Crossmark data 





# Design, Synthesis and Biological Evaluation of Novel Furan & Thiophene Containing Pyrazolyl Pyrazolines as Antimalarial Agents

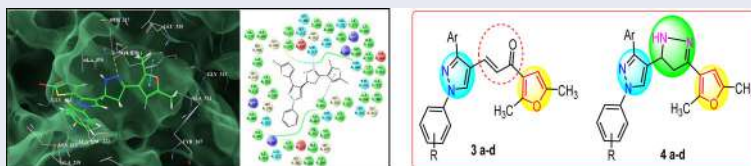
Hemantkumar N. Akolkar<sup>a</sup>, Sujata G. Dengale<sup>b</sup>, Keshav K. Deshmukh<sup>b</sup>, Bhausaheb K. Karale<sup>a</sup>, Nirmala R. Darekar<sup>a</sup>, Vijay M. Khedkar<sup>c</sup>, and Mubarak H. Shaikh<sup>a</sup>

<sup>a</sup>P.G. and Research, Department of Chemistry, Radhabai Kale Mahila Mahavidyalaya, Ahmednagar, India;

<sup>b</sup>P.G. and Research, Department of Chemistry, Sangamner Nagarpalika Arts, D. J. Malpani Commerce, B.N. Sarada Science College, Sangamner, India; <sup>c</sup>Department of Pharmaceutical Chemistry, School of Pharmacy, Vishwakarma University, Pune, India

## ABSTRACT

In search for novel compounds targeting Malaria, based on the *in silico* molecular docking binding affinity data, the novel furans containing pyrazolyl chalcones (**3a-d**) and pyrazoline derivatives (**4a-d**) were synthesized. The formation of the synthesized compound were confirmed by spectral analysis like IR, <sup>1</sup>H NMR, <sup>13</sup>C NMR and mass spectrometry. Compounds with thiophene and pyrazoline ring **4b** (0.47  $\mu$ M), **4c** (0.47  $\mu$ M) and **4d** (0.21  $\mu$ M) exhibited excellent anti-malarial activity against *Plasmodium falciparum* compared with standard antimalarial drug Quinine (0.83  $\mu$ M). To check the selectivity furthermore, compounds were tested for antimicrobial activity and none of the synthesized compound exhibited significant potency compared with the standard antibacterial drug Chloramphenicol and antifungal drug Nystatin respectively. So, it can be resolved that the produced compounds show selectively toward antimalarial activity and have the potential to be explored further.



## ARTICLE HISTORY

Received 7 August 2020

Accepted 5 September 2020


## KEYWORDS

Antimalarial; antimicrobial; chalcones; pfENR inhibitor; pyrazole-pyrazolines; thiophene

## Introduction

Life-threatening disease Malaria is caused by *Plasmodium* parasites that are spread to people through the bites of infected female Anopheles mosquitoes. Out of five *Plasmodium* Parasites *Plasmodium falciparum* produces high levels of blood-stage parasites that sequester in critical organs in all age groups.<sup>1</sup> As per the World Health Organization report in 2018, in sub Saharan Africa 11 million pregnant women were infected with malaria and 872 000 children were born with a low birth weight. Around 24 million children estimated to be infected with the *P. falciparum* parasite in the region; out of these, 1.8 million had severe anemia and 12 million had

**CONTACT** Hemantkumar N. Akolkar  hemantakolkar@gmail.com  P.G. and Research, Department of Chemistry, Radhabai Kale Mahila Mahavidyalaya, Ahmednagar, Maharashtra 414001, India.

 Supplemental data for this article is available online at <https://doi.org/10.1080/10406638.2020.1821231>.

© 2020 Taylor & Francis Group, LLC

moderate anemia.<sup>2</sup> Mortality and morbidity caused by malaria are continually increasing. This subject is the consequence of the ever-increasing development of parasite resistance to drugs and also increased mosquito resistance to insecticides which is one of the most critical complications in controlling malaria over recent years.<sup>3</sup>

*P. falciparum* enoyl-acyl carrier protein (ACP) reductase (ENR) is an enzyme in type II fatty acid synthesis (FAS II) pathway which catalyzes the NADH-dependent reduction of trans-2-enoyl-ACP to acyl-ACP and plays important role in completion of the fatty acid elongation cycles. Due to its role in the parasite's fatty acid pathway, *Pf*ENR has been known as one of the most promising antimalarial targets for structure-based drug design.<sup>4-6</sup> Triclosan, a broadly used antibiotic, is effective inhibitor of *Pf*ENR enzyme activity. Several efforts have been taken in the recent past in the direction of the identification of new antimalarials using pharmacophore modeling, molecular docking and MD simulations.<sup>7-12</sup>

Pyrazole is a well-known class of nitrogen containing heterocyclic compounds and play important role in agricultural and medicinal field. Pyrazole and its derivatives are known to possess antibacterial,<sup>13</sup> antipyretic,<sup>14</sup> fungistatic,<sup>15</sup> anticonvulsant,<sup>16</sup> antitubercular,<sup>17</sup> antipyretic,<sup>18</sup> insecticides,<sup>19</sup> and anti-inflammatory<sup>20</sup> activities. Pyrazoline containing compounds are recognized to possess various pharmacological activities like antimalarial,<sup>21,22</sup> anticancer,<sup>23</sup> anti-inflammatory,<sup>24</sup> analgesic,<sup>24</sup> antitumor,<sup>25</sup> antimicrobial<sup>26</sup> and antidepressant activities.<sup>27</sup> Furan containing compounds possess lipoxygenase inhibitor,<sup>28</sup> urotensin-II receptor antagonists,<sup>29</sup> fungicidal,<sup>30</sup> epidermal growth factor receptor inhibitors and anticancer<sup>31</sup> etc. activities. Chalcone is a natural pigment found in plant and is an important intermediate for the synthesis of flavonoids. Varieties of biological activities are associated with chalcones and their derivatives such as antiplasmodial,<sup>32</sup> nematicide,<sup>33</sup> antiallergenic,<sup>34</sup> antimalarial,<sup>35</sup> anti-HIV,<sup>36</sup> anti-cancer,<sup>37</sup> anti-inflammatory<sup>38</sup> and anti-tuberculosis.<sup>39</sup>

So, considering the biological importance of pyrazoles, furan and chalcone, herein we report the design of a small library of furan containing pyrazolyl pyrazoline derivatives by molecular hybridization approach targeting *Pf*ENR using the *in silico* molecular docking technique. The promising results obtained from this *in silico* study served the basis for the synthesis of these molecules followed by evaluation of their antimalarial potential.

Molecular docking technique plays significant role in lead identification/optimization and in the mechanistic study by predicting the binding affinity and the thermodynamic interactions leading the binding of a ligand to its biological receptor. Thus, with the objective to identify novel leads targeting the crucial antimalarial target *Plasmodium falciparum* enoyl-ACP reductase (*Pf*ENR or FabI) (pdb code: 1NHG), molecular docking was carried out using the GLIDE (Grid-based LIgand Docking with Energetics) program of the Schrodinger Molecular modeling package.<sup>40-42</sup> A small library of 8 molecules comprising furan containing pyrazolyl pyrazoline derivatives (**3a-3d**, **4a-4d**) was docked against *Pf*ENR. The ensuing docking conformation revealed that these molecules changed a binding mode which is corresponding with the active site of *Pf*ENR and were found to be involved in a series of bonded and non-bonded interactions with the residues lining the active site. Their docking scores varied from -6.979 to -8.222 with an average docking score of -7.563 signifying a potent binding affinity to *Pf*ENR. In order to get a quantitative insight into the most significantly interacting residues and their associated thermodynamic interactions, a detailed per-residue interaction analysis was carried out (Table S1, Supporting Information). This analysis showed that the furan containing pyrazolyl chalcones (**3a-d**) (Figure 1) were deeply embedded into the active site of *Pf*ENR engaging in a sequence of favorable *van der Waals* interactions observed with Ile:C369, Phe:C368, IleA323, Ala:A320, Ala:A319, Arg:A318, Ser:A317, Leu:A315, Pro:A314, Gly:A313, Ala:A312, Lys:A285, Met:A281, Tyr:A277, Tyr:A267, Thr:A266, Leu:A265, Gly:A112, Tyr:A111, Gly:A110 and Asp:A107 residues through the 1,3-substituted-1*H*-pyrazol-4-yl scaffold while the 1-(2,5-Dimethylfuran-3-yl) prop-2-en-1-one

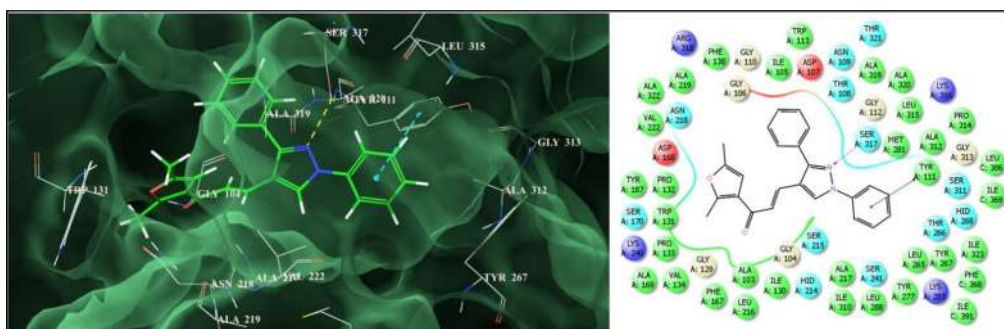


**Figure 1.** Binding mode of **3a** into the active site of *Plasmodium falciparum* enoyl-ACP reductase (on right side: pink lines represent the hydrogen bond while green lines signify  $\pi$ - $\pi$  stacking interactions).

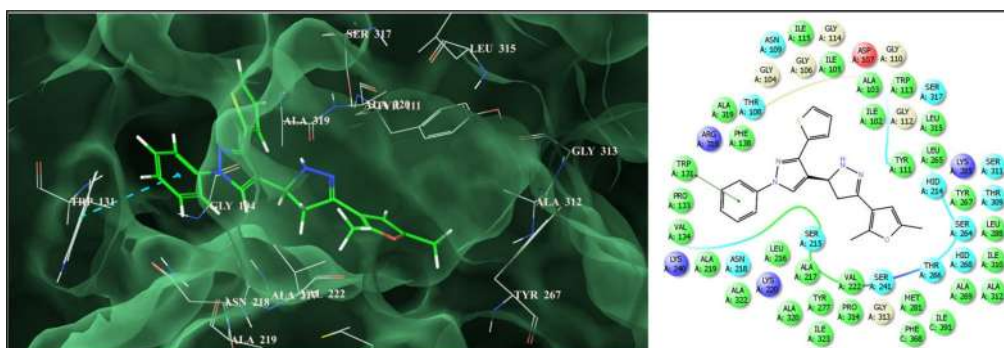
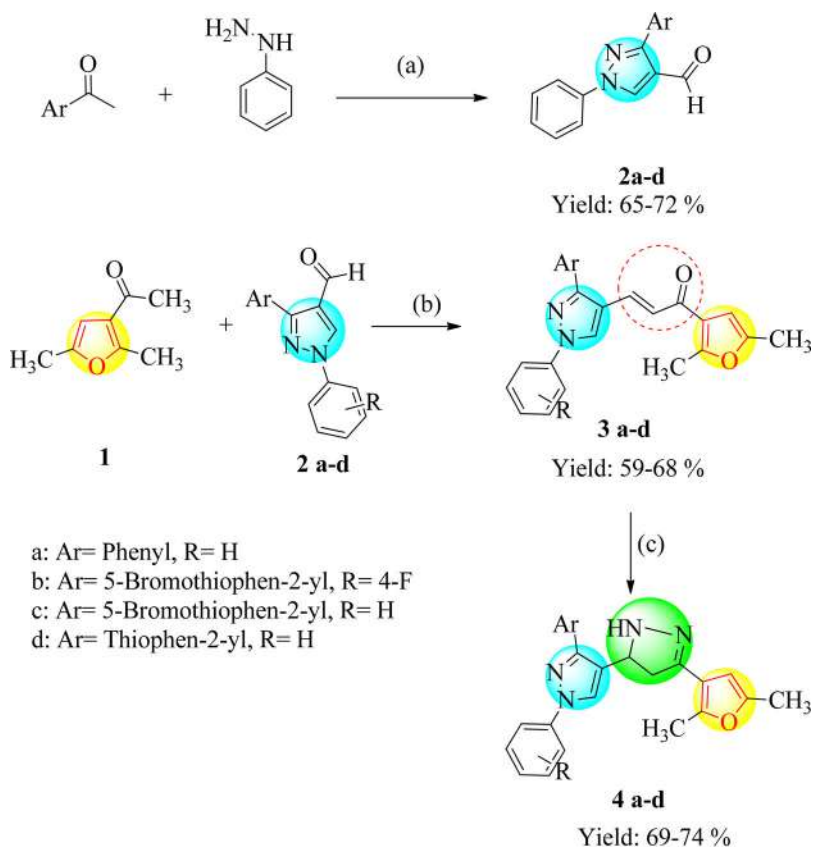


**Figure 2.** Binding mode of **4d** into the active site of *Plasmodium falciparum* enoyl-ACP reductase (on right side: pink lines represent the hydrogen bond while green lines signify  $\pi$ - $\pi$  stacking interactions).

component of the molecules was seen to be involved in similar interactions with Asn:A218, Ala:A217, Leu:A216, Ser:A215, Trp:A131, Gly:A106, Ile:A105, Gly:A104 residues of the active site.

Furthermore the enhanced binding affinity of these molecule is also attributed to significant electrostatic interactions observed with Arg:A318, Ser:A317, Lys:A285, Asp:A236, Asn:A218, Ala:A217, Ser:A215, Tyr:A111, Gly:A110, Asp:A107, Gly:A104 residues lining the active site. On the other hand, the furan containing pyrazoline derivatives (**4a-d**) (Figure 2) were also seen to be stabilized into the active of *Pf*ENR through a network of significant *van der Waals* interactions observed with (2,5-dimethylfuran-3-yl)-1*H*-pyrazolyl scaffold *via* Ile:C369, Phe:C368, Ala:A320, Ser:A317, Leu:A315, Pro:A314, Gly:A313, Ala:A312, Lys:A285, Tyr:A267, Thr:A266, Leu:A265, Gly:A112, Tyr:A111, Gly:A110, Gly:A106 and Ile:A105 while other half of the molecule i.e., 2-thiophenyl-1-phenyl-1*H*-pyrazole showed similar type of interactions with Ile:A323, Ala:A319, Arg:A318, Met:A281, Tyr:A277, Val:A222, Ala:A219, Asn:A218, Ala:A217, Leu:A216, Ser:A215, Trp:A131, Ile:A130, Trp:A113, Asp:A107, Gly:A104 residues.

Further the enhanced binding affinity of the molecules is also attributed to favorable electrostatic interactions observed with Arg:A318, Ser:A317, Glu:A289, Lys:A285, Asp:A236, Asn:A218, Ala:A217, Ser:A215, Tyr:A111, Gly:A110, Asp:A107 and Gly:A104. While these non-bonded interactions (*van der Waals* and electrostatic) were observed to be the major driving force for the mechanical interlocking of these novel furan containing pyrazolyl pyrazoline derivatives into the active site *Pf*ENR, the enhanced binding affinity of these molecules is also contributed by very prominent hydrogen bonding interaction observed for **3a** (Ser:A317(2.708 Å)), **4a** (Ser:A317(2.783 Å)), **4b** (Ser:A317(2.462 Å)) and **4c** (Ser:A317(2.462 Å)). Furthermore these



**Reagents and conditions:** (a): i) EtOH, reflux, 2 hr ii) DMF/POCl<sub>3</sub>, 0-10° C;  
 (b) 10 % aq. KOH, EtOH, RT, 14hr; (c) NH<sub>2</sub>NH<sub>2</sub>·H<sub>2</sub>O, EtOH, AcOH, 6hr

**Scheme 1.** Synthesis of pyrazolyl chalcones (3a-d) and pyrazolyl pyrazolines (4a-d).

molecules were also engaged in a very close  $\pi$ - $\pi$  stacking interactions: **3a**: Tyr: A111(2.669 Å), **3b**: Tyr:A267(2.529 Å), **3c**: Tyr:A267(2.541 Å), **3d**: Tyr:A267(2.335 Å), **4a**: Tyr:A111(2.602 Å), **4b**: Trp:A131(2.073 Å), **4c**: TyrA:111(2.073 Å) and **4d**: TrpA131(2.538 Å) (Figures S1-S6, Supporting Information).

This type of bonded interactions i.e., hydrogen bonding and  $\pi$ - $\pi$  stacking are known to serve as an “anchor” to guide the alignment of a molecule into the 3D space of enzyme’s active site and facilitate the non-bonded interactions (*Van der Waals* and electrostatic) as well. Overall, the in-silico binding affinity data suggested that these furans containing pyrazolyl pyrazoline derivatives (**3a-d**, **4a-d**) could be developed as novel scaffold to arrive at compounds with high selectivity and potency *Plasmodium falciparum*.

## Results and discussion

### Chemistry

The novel series of furan containing pyrazolyl chalcones (**3a-d**) and pyrazoline derivatives (**4a-d**) were synthesized from commercially available starting materials (Scheme 1). Initially, pyrazole aldehyde **2a-d** was formed by the condensation between substituted acetophenone and phenyl

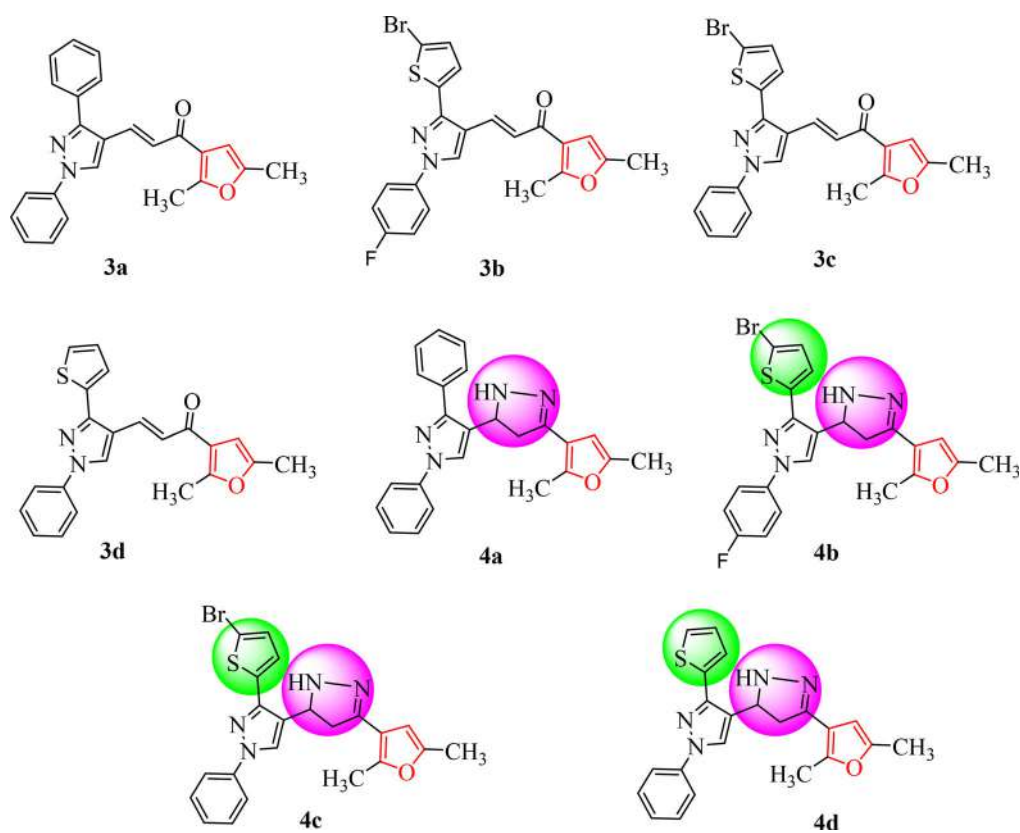


**Figure 3.** The newly synthesized compounds structure **3a-d** & **4a-d**.

hydrazine followed by Vilsmeier-Haack formylation reaction (Scheme 1). Then furan containing pyrazolyl chalcones **3a-d** were synthesized by base-catalyzed Claisen-Schmidt condensation of 1-(2,5-dimethylfuran-3-yl)ethanone **1** and substituted pyrazole aldehyde **2a-d**.<sup>43</sup> Finally, the furan containing pyrazolyl chalcones **3a-d** and hydrazine hydrate in ethanol solvent using catalytic amount of acetic acid at reflux condition for 6 hr afforded the corresponding pyrazolyl pyrazolines (**4a-d**) in quantitative isolated yield (69–74%) (Scheme 1).

The newly synthesized compounds structures were shown in Figure 3. The newly synthesized compound's structures were confirmed by IR, <sup>1</sup>H NMR, <sup>13</sup>C NMR, mass spectral data. For compound **3a**, in IR spectrum the stretching band for C=O was detected at 1657 cm<sup>-1</sup>. In the <sup>1</sup>H NMR spectrum of compound **3a**, the proton of pyrazole and furan ring resonate as a singlet at  $\delta$  9.31 and  $\delta$  6.60 ppm respectively. Also, singlet for two -CH<sub>3</sub> were observed at  $\delta$  2.27 and  $\delta$  2.50 ppm. The <sup>13</sup>C NMR spectrum of compound **3a** showed signal at  $\delta$  184.41 ppm due to C=O and  $\delta$  12.89 and  $\delta$  13.93 ppm is due to two -CH<sub>3</sub>. Mass spectrum confirms the formation of compound **3a** showed  $m/z = 369$  (M + H)<sup>+</sup>.

Secondly, in the IR spectrum of compound **4a**, -N-H stretching band observed at 3252 cm<sup>-1</sup>. The <sup>1</sup>H NMR spectrum of compound **4a**, the CH<sub>2</sub> protons of the pyrazoline ring resonated as a pair of doublets of doublets at  $\delta$  2.88 ppm and 3.35 ppm. The CH proton appeared as triplet at  $\delta$  4.87 ppm due to vicinal coupling with two protons of the methylene group. In the <sup>13</sup>C NMR spectra of the compound **4a** carbons of the pyrazoline ring were observed at  $\delta$  41.97 ppm and 54.67 ppm. All the other aromatic and aliphatic protons and carbons were observed at expected regions. Mass spectrum confirms the formation of compound **4a** showed  $m/z = 383$  (M + H)<sup>+</sup>.



**Table 1.** Antimalarial ( $\mu\text{M}$ ), Antibacterial (MIC in  $\mu\text{g/mL}$ ) & Antifungal (MIC in  $\mu\text{g/mL}$ ) activity.

Cpd	Antimalarial activity Plasmodium falciparum	Antibacterial activity				Antifungal activity			Molecular Docking Score
		EC	PA	SA	SP	CA	AN	AC	
<b>3a</b>	1.46	200	200	250	250	500	500	500	-7.814
<b>3b</b>	3.93	100	250	250	200	1000	500	500	-7.032
<b>3c</b>	2.16	62.5	200	125	250	500	>1000	>1000	-7.192
<b>3d</b>	3.07	100	100	200	200	1000	500	500	-7.118
<b>4a</b>	6.31	125	100	100	100	500	500	500	-6.979
<b>4b</b>	0.47	100	200	100	100	250	500	500	-8.157
<b>4c</b>	0.47	125	125	200	200	1000	>1000	>1000	-8.222
<b>4d</b>	0.21	200	100	125	100	500	500	500	-7.988
Chloroquine	0.06	-	-	-	-	-	-	-	-
Quinine	0.83	-	-	-	-	-	-	-	-
CP	-	50	50	50	50	-	-	-	-
NS	-	-	-	-	-	100	100	100	-

Cpd: Compound; EC: *Escherichia coli*; PA: *Pseudomonas aeruginosa*; SA: *Staphylococcus aureus*; SP: *Streptococcus pyogenes*; CA: *Candida albicans*; AN: *Aspergillus niger*; AC: *Aspergillus clavatus*; CP: Chloramphenicol; NS: Nystatin.

## Biological evaluation

### *In vitro* antimalarial screening

All the synthesized novel compounds were tested for antimalarial activities. The *in vitro* antimalarial assay was carried out according to the micro assay protocol of Rieckmann and coworkers with minor modifications.<sup>44–47</sup> The results were recorded as the minimum inhibitory concentrations ( $\mu\text{M}$  MIC) chloroquine and quinine were used as the reference drug (Table 1).

Herein, we have synthesized four chalcone and pyrazoline derivatives respectively. Structure activity relationship (SAR) plays very important role while displaying the antimalarial activity. All the synthesized chalcone derivatives (**3a–d**) exhibited less potency compared to the standard drug. But pyrazoline derivatives exhibited excellent antimalarial activity compared to the standard drug. In compound **4a**, thiophene ring was absent and pyrazoline ring is present, so, the compound **4a** exhibited less potency compared to the standard drug. Now, in compound **4b**, bromo substituted thiophene and pyrazoline rings are present along with the fluorine at the para position on benzene ring. Interestingly, this compound **4b** (0.47  $\mu\text{M}$ ), exhibited excellent activity compared to the standard drug quinine (0.83  $\mu\text{M}$ ). Again, in compound **4c**, bromo substituted thiophene and pyrazoline rings are present but no fluorine at the para position of benzene ring. Though fluorine is absent on benzene ring in compound **4c** (0.47  $\mu\text{M}$ ), it exhibited same potency as that of compound **4b** compared to the standard drug quinine (0.83  $\mu\text{M}$ ). Finally, in compound **4d**, there were no substitution on the thiophene and benzene ring. In compound **4d** plane thiophene, plane benzene ring and pyrazoline ring constructed in a single molecular framework. Compound **4d** (0.21  $\mu\text{M}$ ), exhibited four-fold more antimalarial activity compared to the standard drug quinine (0.83  $\mu\text{M}$ ). From SAR, we can conclude that for the antimalarial activity thiophene, pyrazoline and benzene ring were very important in a single molecular framework.

### Antimicrobial activities

Further, all the novel synthesized compounds were also screened for antimicrobial activities against the bacterial strains *Escherichia coli* (MTCC 443), *Staphylococcus aureus* (MTCC 96), *Pseudomonas aeruginosa* (MTCC 1688), *Streptococcus pyogenes* (MTCC 442) and fungal strains *Aspergillus clavatus* (MTCC 1323), *Candida albicans* (MTCC 227) and *Aspergillus niger* (MTCC 282). The minimum inhibitory concentration (MIC) was determined by the broth dilution method. Chloramphenicol and Nystatin were used as reference drugs for antibacterial and antifungal activity, respectively. The results of antibacterial and antifungal activity were given in Table 1.

The results given in Table 1 indicated that none of the synthesized compound exhibited significant potency toward the standard antibacterial drug Chloramphenicol and antifungal drug Nystatin. Hence, from above result we can conclude that the synthesized compounds show selectively antimalarial activity and negligible antimicrobial activity.

## Conclusion

In conclusion, Considering the importance of enoyl-ACP reductase (*Pf*ENR) in *Plasmodium*, a small library of 8 molecules comprising furan containing pyrazolyl pyrazoline derivatives (**3a-d**, **4a-d**) was designed and docked against *Pf*ENR. Based on the *in silico* binding affinity data, synthesis was carried out for these novel furans containing pyrazolyl pyrazoline derivatives (**3a-d**, **4a-d**) and was evaluated for activity against *Plasmodium falciparum*. The synthesized compounds shown selectively antimalarial activity with minimal antimicrobial activity. Compounds (**3a-d**) exhibited less antimalarial activity compared to the standard drug. From the series of compounds (**4a-d**), compound **4b** (0.47  $\mu$ M), **4c** (0.47  $\mu$ M) and **4d** (0.21  $\mu$ M) exhibited more antimalarial activity compared to the standard drug quinine (0.83  $\mu$ M). Compound **4d** shows four-fold more activity compared to the standard drug quinine. From the SAR, we have distinguished areas of the pyrazolyl chalcones and pyrazolyl pyrazolines framework where variations can be made to expand the pharmacokinetic profile as well as features required to improve inhibitor effectiveness. This innovative molecular scaffold presents breakthrough for optimization to develop effective *Pf*ENR inhibitors.

## Experimental

### General

All the reagents, solvents and chemicals were taken from commercial sources found to be and used as such without purification. The physical constant like melting points were measured on a DBK melting point apparatus and are uncorrected. IR spectra were recorded on Shimadzu IR Affinity 1S (ATR) FTIR spectrophotometer.  $^1\text{H}$  NMR (400 MHz) and  $^{13}\text{C}$  NMR (100 MHz) spectra were recorded on Bruker Advance II 400 spectrophotometer using TMS as an internal standard and DMSO- $d_6$  as solvent and chemical shifts were expressed as  $\delta$  ppm units. Mass spectra were obtained on Waters, Q-TOF micro mass (ESI-MS) mass spectrometer.

### General procedure for the synthesis of pyrazolyl chalcones (**3a-d**)

A mixture of 1-(2,5-dimethylfuran-3-yl)ethanone **1** (0.05 mol), substituted pyrazole aldehyde **2** (0.05 mol) and 10% aqueous potassium hydroxide (10 mL) in ethanol (50 mL) was stirred at room temperature for 14 h. The progress of the reaction was monitored by TLC. After completion of the reaction, the reaction mixture was transferred into crushed ice and neutralized by dil. HCl. The precipitation observed, filtered it, washed with water and dried. The crystallization of product carried out in ethanol.

### (*E*)-1-(2,5-Dimethylfuran-3-yl)-3-(1,3-diphenyl-1H-pyrazol-4-yl)prop-2-en-1-one (**3a**)

Yield: 61%, yellow solid; mp: 80–82  $^{\circ}\text{C}$ ; IR ( $\nu_{\text{max}}$ ,  $\text{cm}^{-1}$ ): 2921 (=C-H), 2855 (C-H), 1657 (C=O), 1454 (C=N);  $^1\text{H}$ -NMR (400 MHz, DMSO- $d_6$ ,  $\delta$ , ppm): 9.31 (s, 1H, Pyrazole-H), 7.93 (d, 2H,  $J=7.9$  Hz), 7.38–7.68 (m, 10H, Ar-H), 6.60 (s, 1H, Furan-H), 2.53 (s, 3H,  $-\text{CH}_3$ ), 2.27 (s, 3H,  $-\text{CH}_3$ );  $^{13}\text{C}$  NMR (100 MHz, DMSO- $d_6$ ,  $\delta$ , ppm): 184.4 (C=O), 159.9, 152.8, 149.7, 138.9, 132.2, 132.0, 129.6, 128.8, 128.5, 128.6, 128.4, 127.1, 123.8, 122.1, 118.6, 117.6, 105.9, 13.9 ( $\text{CH}_3$ ), 12.9 ( $\text{CH}_3$ ); MS(ESI-MS):  $m/z$  369.11 (M + H).<sup>+</sup>

***(E)-3-(3-(5-Bromothiophen-2-yl)-1-(4-fluorophenyl)-1H-pyrazol-4-yl)-1-(2,5-dimethylfuran-3-yl)prop-2-en-1-one (3b)***

Yield: 59%, yellow solid, mp: 112–114 °C; IR ( $\nu_{\max}$ ,  $\text{cm}^{-1}$ ): 2923 (=C–H), 2856 (C–H), 1656 (C=O), 1455 (C=N);  $^1\text{H-NMR}$  (400 MHz, DMSO- $d_6$ ,  $\delta$ , ppm): 9.25 (s, 1H, Pyrazole-H), 7.90 (dd, 2H,  $J=4.7$  & 9.0 Hz, Ar–H), 7.64 (d, 1H,  $J=15.4$  Hz, olefinic-H), 7.39–7.45 (m, 3H, Ar–H), 7.34 (d, 1H,  $J=3.8$  Hz, Ar–H), 7.25 (d, 1H,  $J=3.8$  Hz, Ar–H), 6.61 (s, 1H, Furan-H), 2.55 (s, 3H, –CH<sub>3</sub>), 2.28 (s, 3H, –CH<sub>3</sub>);  $^{13}\text{C NMR}$  (100 MHz, DMSO- $d_6$ ,  $\delta$ , ppm): 184.2, 162.0, 159.6, 157.1, 149.7, 145.7, 135.4, 135.1, 131.4, 130.8, 128.9, 127.3, 124.6, 122.0, 120.7, 120.6, 117.3, 116.6, 116.3, 112.5, 105.9, 13.9, 12.9; MS (ESI-MS):  $m/z$  472.89 (M + H).<sup>+</sup>

***(E)-3-(3-(5-Bromothiophen-2-yl)-1-phenyl-1H-pyrazol-4-yl)-1-(2,5-dimethylfuran-3-yl)prop-2-en-1-one (3c)***

Yield: 68%, yellow solid, mp 120–114 °C; IR ( $\nu_{\max}$ ,  $\text{cm}^{-1}$ ): 2921 (=C–H), 2855 (C–H), 1699 (C=O), 1454 (C=N);  $^1\text{H-NMR}$  (400 MHz, DMSO- $d_6$ ,  $\delta$ , ppm): 9.14 (s, 1H, Pyrazole-H), 7.87 (d, 2H,  $J=7.8$  Hz, Ar–H), 7.70 (d, 1H,  $J=15$  Hz, olefinic-H), 7.52 (t, 2H,  $J=8$  Hz, Ar–H), 7.36–7.40 (m, 2H, Ar–H), 7.20 (s, 2H, Ar–H), 6.55 (s, 1H, Furan-H), 2.57 (s, 3H, –CH<sub>3</sub>), 2.29 (s, 3H, –CH<sub>3</sub>);  $^{13}\text{C NMR}$  (100 MHz, DMSO- $d_6$ ,  $\delta$ , ppm): 184.3, 157.1, 149.7, 145.7, 138.6, 135.5, 131.4, 130.9, 129.7, 128.8, 127.3, 127.3, 124.6, 122.0, 118.6, 117.4, 112.5, 105.9, 13.9, 12.9; MS(ESI-MS):  $m/z$  454.57 (M + H).<sup>+</sup>

***(E)-1-(2,5-Dimethylfuran-3-yl)-3-(1-phenyl-3-(thiophen-2-yl)-1H-pyrazol-4-yl)prop-2-en-1-one (3d)***

Yield: 62%, yellow solid, mp 124–126 °C; IR ( $\nu_{\max}$ ,  $\text{cm}^{-1}$ ): 2921 (=C–H), 2715 (C–H), 1652 (C=O), 1456 (C=N);  $^1\text{H-NMR}$  (400 MHz, DMSO- $d_6$ ,  $\delta$ , ppm): 8.56 (s, 1H, Pyrazole-H), 7.91 (d, 2H,  $J=7.8$  Hz, Ar–H), 7.76 (d, 1H,  $J=15.4$  Hz, olefinic-H), 7.60 (d, 1H,  $J=5.1$  Hz, Ar–H), 7.54 (t, 2H,  $J=8.2$  Hz, Ar–H), 7.35–7.44 (m, 3H, Ar–H), 7.21 (dd, 1H,  $J=5.0$  & 3.7 Hz, Ar–H), 6.59 (s, 1H, Furan-H), 2.57 (s, 3H, –CH<sub>3</sub>), 2.29 (s, 3H, –CH<sub>3</sub>);  $^{13}\text{C NMR}$  (100 MHz, DMSO- $d_6$ ,  $\delta$ , ppm): 184.4, 157.0, 149.7, 146.8, 138.7, 133.5, 131.5, 129.7, 128.7, 128.1, 127.3, 127.2, 126.8, 124.3, 122.1, 118.6, 117.4, 105.9, 13.9, 12.9; MS(ESI-MS):  $m/z$  375.10 (M + H).<sup>+</sup>

***General procedure for synthesis of pyrazolyl-pyrazoline (4a-d)***

A mixture of chalcone **3a-d** (0.001 mol) and hydrazine hydrate (0.004 mol) in solvent ethanol (10 ml) was refluxed in presence of catalytic amount of glacial acetic acid for 6 h. The progress of the reaction was monitored by TLC. After completion of the reaction, the reaction mixture was transferred into crushed ice. The precipitation observed, filtered it, washed with water and dried. The crystallization of product carried out in ethanol to get pure pyrazolines.

***4-(4,5-Dihydro-3-(2,5-dimethylfuran-3-yl)-1H-pyrazol-5-yl)-1,3-diphenyl-1H-pyrazole (4a)***

Yield: 74%, white solid, mp 102–104 °C; IR ( $\nu_{\max}$ ,  $\text{cm}^{-1}$ ): 3306 (N–H), 3049 (Ar–H), 1592 (C=N);  $^1\text{H-NMR}$  (400 MHz, DMSO- $d_6$ ,  $\delta$ , ppm): 8.56 (s, 1H, pyrazole-H), 7.90 (d, 2H,  $J=7.8$  Hz, Ar–H), 7.76 (d, 2H,  $J=8.3$  Hz, Ar–H), 7.47–7.52 (m, 4H, Ar–H), 7.41 (t, 1H,  $J=7.3$  Hz, Ar–H), 7.31 (t, 1H,  $J=7.4$  Hz, Ar–H), 7.20 (s, 1H, N–H), 6.19 (s, 1H, furan-H), 4.87 (t, 1H,  $J=10.7$  Hz, pyrazoline-H), 3.34 (dd, 1H,  $J=10.5$  & 15.6 Hz, pyrazoline-H), 2.88 (dd, 1H,  $J=11.1$  & 16.1 Hz, pyrazoline-H), 2.38 (s, 3H, CH<sub>3</sub>), 2.20 (s, 3H, CH<sub>3</sub>);  $^{13}\text{C NMR}$  (100 MHz, DMSO- $d_6$ ,  $\delta$ , ppm): 150.4, 149.3, 147.6, 145.1, 139.5, 132.9, 129.5, 128.6, 127.9, 127.2, 126.2, 123.2, 118.1, 115.2, 105.9, 54.7, 41.9, 13.3, 12.9; MS (ESI-MS):  $m/z$  383.04 (M + H).<sup>+</sup>

**3-(5-Bromothiophen-2-yl)-1-(4-fluorophenyl)-4-(4,5-dihydro-3-(2,5-dimethylfuran-3-yl)-1H-pyrazol-5-yl)-1H-pyrazole (4b)**

Yield: 69%, white solid, mp 98–100 °C; IR ( $\nu_{\max}$ ,  $\text{cm}^{-1}$ ): 3310 (N–H), 3046 (Ar–H), 1594 (C=N);  $^1\text{H}$  NMR (400 MHz, DMSO- $d_6$ ,  $\delta$ , ppm): 8.54 (s, 1H, pyrazole-H), 7.88 (m, 2H, Ar–H), 7.35 (t, 2H,  $J=8.7$  Hz, Ar–H), 7.28 (dd, 2H,  $J=3.8$  Hz, Ar–H), 7.21 (s, 1H, N–H), 6.20 (s, 1H, furan-H), 4.93 (t, 1H,  $J=10.68$  Hz, pyrazoline-H), 3.37 (dd, 1H,  $J=10.7$  & 16.5 Hz, pyrazoline-H), 2.86 (dd, 1H,  $J=10.9$  & 16.1 Hz, pyrazoline-H), 2.38 (s, 3H,  $\text{CH}_3$ ), 2.20 (s, 3H,  $\text{CH}_3$ );  $^{13}\text{C}$  NMR (100 MHz, DMSO- $d_6$ ,  $\delta$ , ppm): 161.6, 159.1, 149.3, 147.7, 145.3, 144.1, 136.9, 135.6, 131.2, 128.0, 126.6, 122.6, 120.2, 120.2, 116.4, 116.2, 115.1, 111.5, 105.9, 54.3, 41.1, 13.3, 12.9; MS (ESI-MS):  $m/z$  486.93 (M + H).<sup>+</sup>

**3-(5-Bromothiophen-2-yl)-4-(4,5-dihydro-3-(2,5-dimethylfuran-3-yl)-1H-pyrazol-5-yl)-1-phenyl-1H-pyrazole (4c)**

Yield: 72%, white solid, mp 122–124 °C; IR ( $\nu_{\max}$ ,  $\text{cm}^{-1}$ ): 3303 (N–H), 3096 (Ar–H), 1593 (C=N),  $^1\text{H}$  NMR (400 MHz, DMSO- $d_6$ ,  $\delta$ , ppm): 8.55 (s, 1H, pyrazole-H), 7.84 (d, 2H,  $J=7.9$  Hz, Ar–H), 7.51 (t, 2H,  $J=7.6$  Hz, Ar–H), 7.22–7.34 (m, 4H, Ar–H), 6.20 (s, 1H, furan-H), 4.94 (t, 1H,  $J=10.6$  Hz, pyrazoline-H), 3.38 (m, 1H, pyrazoline-H), 2.88 (dd, 1H,  $J=12.1$  & 16.1 Hz, pyrazoline-H), 2.39 (s, 3H,  $\text{CH}_3$ ), 2.20 (s, 3H,  $\text{CH}_3$ );  $^{13}\text{C}$  NMR (100 MHz, DMSO- $d_6$ ,  $\delta$ , ppm): 149.3, 147.7, 145.2, 144.0, 139.0, 137.0, 131.2, 129.6, 127.8, 126.6, 126.5, 122.5, 118.0, 115.1, 111.4, 105.9, 54.4, 41.1, 13.3, 12.9; MS (ESI-MS):  $m/z$  468.95 (M + H).<sup>+</sup>

**4-(4,5-Dihydro-3-(2,5-dimethylfuran-3-yl)-1H-pyrazol-5-yl)-1-phenyl-3-(thiophen-2-yl)-1H-pyrazole (4d)**

Yield: 70%, white solid, mp 96–98 °C; IR ( $\nu_{\max}$ ,  $\text{cm}^{-1}$ ): 3336 (N–H), 3067 (Ar–H), 1501 (C=N);  $^1\text{H}$  NMR (400 MHz, DMSO- $d_6$ ,  $\delta$ , ppm): 8.53 (s, 1H, pyrazole-H), 7.86 (d, 1H,  $J=8$  Hz, Ar–H), 7.58 (d, 1H,  $J=4.9$  Hz, Ar–H), 7.47–7.52 (m, 3H, Ar–H), 7.31 (t, 1H,  $J=7.3$  Hz, Ar–H), 7.15–7.20 (m, 2H, Ar–H), 6.21 (s, 1H, furan-H), 4.98 (t, 1H,  $J=10.5$  Hz, pyrazoline-H), 3.42 (m, 1H, pyrazoline-H), 2.89 (dd, 1H,  $J=10.7$  & 16.1 Hz, pyrazoline-H), 2.39 (s, 3H,  $\text{CH}_3$ ), 2.20 (s, 3H,  $\text{CH}_3$ );  $^{13}\text{C}$  NMR (100 MHz, DMSO- $d_6$ ,  $\delta$ , ppm): 149.3, 147.7, 145.1, 144.9, 139.2, 135.0, 129.6, 127.9, 127.4, 126.3, 126.0, 125.8, 122.6, 118.1, 115.1, 105.9, 54.5, 41.3, 13.3, 12.9; MS (ESI-MS):  $m/z$  389.03 (M + H).<sup>+</sup>

**Experimental protocol for biological activity****Antimalarial assay**

The antimalarial activity of the synthesized compounds was carried out in the Microcare laboratory & TRC, Surat, Gujarat. According to the micro assay protocol of Rieckmann and coworkers the *in vitro* antimalarial assay was carried out in 96 well microtiter plates. To maintain *P. falciparum* strain culture in medium Roswell Park Memorial Institute (RPMI) 1640 supplemented with 25 mM (4-(2-hydroxyethyl)-1-piperazineethanesulfonic acid) (HEPES), 1% D-glucose, 0.23% sodium bicarbonate and 10% heat inactivated human serum. To obtain only the ring stage parasitized cells, 5% D-sorbitol treatment required to synchronized the asynchronous parasites of *P. falciparum*. To determine the percent parasitaemia (rings) and uniformly maintained with 50% RBCs ( $\text{O}^+$ ) an initial ring stage parasitaemia of 0.8 to 1.5% at 3% hematocrit in a total volume of 200  $\mu\text{l}$  of medium RPMI-1640 was carried out for the assay. A stock solution of 5 mg/ml of each of the test samples was prepared in DMSO and subsequent dilutions were prepared with culture medium. To the test wells to obtain final concentrations (at five-fold dilutions) ranging between 0.4  $\mu\text{g/ml}$  to 100  $\mu\text{g/ml}$  in duplicate well containing parasitized cell preparation the diluted samples in 20  $\mu\text{l}$  volume were added. In a candle jar, the culture plates were incubated at 37 °C. Thin

blood smears from each well were prepared and stained with Jaswant Singh-Bhattacharji (JSB) stain after 36 to 40 h incubation. To record maturation of ring stage parasites into trophozoites and schizonts in presence of different concentrations of the test agents the slides were microscopically observed. The minimum inhibitory concentrations (MIC) was recorded as the test concentration which inhibited the complete maturation into schizonts. Chloroquine was used as the reference drug.

After incubation for 38 hours, and percent maturation inhibition with respect to control group, the mean number of rings, trophozoites and schizonts recorded per 100 parasites from duplicate wells.

### **Molecular docking**

The crystal structure of *Plasmodium Falciparum* Enoyl-Acyl-Carrier-Protein Reductase (*Pf*ENR or FabI) in complex with its inhibitor Triclosan was retrieved from the protein data bank (PDB) (pdb code: 1NHG) and refined using the protein preparation wizard. It involves eliminating all crystallographically observed water (as no conserved interaction is reported with co-crystallized water molecules), addition of missing side chain/hydrogen atoms. Considering the appropriate ionization states for the acidic as well as basic amino acid residues, the appropriate charge and protonation state were assigned to the protein structure corresponding to pH 7.0 followed by thorough minimization, using OPLS-2005 force-field, of the obtained structure to relieve the steric clashes due to addition of hydrogen atoms. The 3D structures of the furan containing pyrazolyl chalcones (**3a-d**) were sketched using the build panel in Maestro and were optimized using the Ligand Preparation module followed by energy minimization using OPLS-2005 force-field until their average root mean square deviation (RMSD) reached 0.001 Å. The active site of *Pf*ENR was defined using receptor grid generation panel to include residues within a 10 Å radius around the co-crystallized ligand. Using this setup, flexible docking was carried using the extra precision (XP) Glide scoring function to gauge the binding affinities of these molecules and to identify binding mode within the target. The obtained results as docking poses were visualized and analyzed quantitatively for the thermodynamic elements of interactions with the residues lining the active site of the enzyme using the Maestro's Pose Viewer utility.

### **Acknowledgements**

Authors are thankful to Microcare laboratory and TRC, Surat, Gujarat for providing antimicrobial and antimalarial activities and Director, SAIF, Panjab University, Chandigarh for providing spectral data; Schrodinger Inc. for providing the software to perform the *in silico* study.

### **Disclosure statement**

No potential conflict of interest was reported by the author(s).

### **Funding**

Authors are thankful to Department of Science and Technology, New Delhi for providing financial assistance for research facilities under DST-FIST programme.

### **References**

1. E. A. Ashley, A. Pyae Phyo, and C. J. Woodrow, "Malaria," *The Lancet* 391, no. 10130 (2018): 1608–21.
2. World Health Organization. "World Malaria Report 2019" (World Health Organization, Geneva, 2019). Licence: CC BY-NC-SA 3.0 IGO.



3. J. Talapko, I. Skrlec, T. Alebic, M. Jukic, and A. Vcev, "Malaria: The Past and the Present," *Microorganisms* 7 (2019): 179.
4. R. J. Heath, and C. O. Rock, "Enoyl-Acyl Carrier Protein Reductase (fabI) Plays a Determinant Role in Completing Cycles of Fatty Acid Elongation in Escherichia coli," *The Journal of Biological Chemistry* 270, no. 44 (1995): 26538–42.
5. R. F. Waller, S. A. Ralph, M. B. Reed, V. Su, J. D. Douglas, D. E. Minnikin, A. F. Cowman, G. S. Besra, and G. I. McFadden, "A Type II Pathway for Fatty Acid Biosynthesis Presents Drug Targets in Plasmodium falciparum," *Antimicrobial Agents and Chemotherapy* 47, no. 1 (2003): 297–301.
6. G. Nicola, C. A. Smith, E. Lucumi, M. R. Kuo, L. Karagyzov, D. A. Fidock, J. C. Sacchettini, and R. Abagyan, "Discovery of Novel Inhibitors Targeting Enoyl-Acyl Carrier Protein Reductase in Plasmodium falciparum by Structure-Based Virtual Screening," *Biochemical and Biophysical Research Communications* 358, no. 3 (2007): 686–91.
7. N. Surolia, and A. Surolia, "Triclosan Offers Protection against Blood Stages of Malaria by Inhibiting enoyl-ACP Reductase of Plasmodium falciparum," *Nature Medicine* 7, no. 2 (2001): 167–73.
8. S. Sharma, T. N. C. Ramya, A. Surolia, and N. Surolia, "Triclosan as a Systemic Antibacterial Agent in a Mouse Model of Acute Bacterial Challenge," *Antimicrobial Agents and Chemotherapy* 47, no. 12 (2003): 3859–66.
9. R. P. Samal, V. M. Khedkar, R. R. S. Pissurlenkar, A. G. Bwalya, D. Tasdemir, R. A. Joshi, P. R. Rajamohan, V. G. Puranik, and E. C. Coutinho, "Design, Synthesis, Structural Characterization by IR, (1) H, (13) C, (15) N, 2D-NMR, X-Ray Diffraction and Evaluation of a New Class of Phenylaminoacetic Acid Benzylidene Hydrazines as pFENR Inhibitors," *Chemical Biology & Drug Design* 81, no. 6 (2013): 715–29.
10. M. Chhibber, G. Kumar, P. Parasuraman, T. N. C. Ramya, N. Surolia, and A. Surolia, "Novel Diphenyl Ethers: Design, Docking Studies, Synthesis and Inhibition of Enoyl ACP Reductase of Plasmodium falciparum and Escherichia coli," *Bioorganic & Medicinal Chemistry* 14, no. 23 (2006): 8086–98.
11. V. A. Morde, M. S. Shaikh, R. R. S. Pissurlenkar, and E. C. Coutinho, "Molecular Modeling Studies, Synthesis, and Biological Evaluation of Plasmodium falciparum Enoyl-Acyl Carrier Protein Reductase (PfENR) Inhibitors," *Molecular Diversity* 13, no. 4 (2009): 501–17.
12. A. Manhas, A. Patel, M. Y. Lone, P. K. Jha, and P. C. Jha, "Identification of PfENR Inhibitors: A Hybrid Structure-Based Approach in Conjunction with Molecular Dynamics Simulations," *Journal of Cellular Biochemistry* 119, no. 10 (2018): 8490–500.
13. M. A. Berghot, and E. B. Moawad, "Convergent Synthesis and Antibacterial Activity of Pyrazole and Pyrazoline Derivatives of Diazepam," *European Journal of Pharmaceutical Sciences: Official Journal of the European Federation for Pharmaceutical Sciences* 20, no. 2 (2003): 173–9.
14. J. N. Dominguez, J. E. Charris, M. Caparelli, and F. Riggione, "Synthesis and Antimalarial Activity of Substituted Pyrazole Derivatives," *Arzneimittel-Forschung* 52, no. 6 (2002): 482–8.
15. R. Sridhar, P. T. Perumal, S. Etti, G. Shanmugam, M. N. Ponnuswamy, V. R. Prabavathy, and N. Mathivanan, "Design, Synthesis and anti-Microbial Activity of 1H-Pyrazole Carboxylates," *Bioorganic & Medicinal Chemistry Letters* 14, no. 24 (2004): 6035–40.
16. Shivapura Viveka, Dinesha Dinesha, Prasanna Shama, Shivalingegowda Naveen, Neratur Krishnappagowda Lokanath, and Gundibasappa Karikannar Nagaraja, "Design, Synthesis, Anticonvulsant and Analgesic Studies of New Pyrazole Analogues: A Knoevenagel Reaction Approach," *RSC Advances* 5no. 115 (2015): 94786–95.
17. Z. Xu, C. Gao, Q. C. Ren, X. F. Song, L. S. Feng, and Z. S. Lv, "Recent Advances of Pyrazole-Containing Derivatives as Anti-Tubercular Agents," *European Journal of Medicinal Chemistry* 139, (2017): 429–40.
18. R. S. Fabiane, T. S. Vanessa, R. Viviane, P. B. Lysandro, R. O. Marli, G. B. Helio, Z. Nilo, A. P. M. Marcos, and F. M. Carlos, "Hypothermic and Antipyretic Effects of 3-Methyl- and 3-Phenyl-5-Hydroxy-5-Trichloromethyl-4,5-Dihydro-1H-Pyrazole-1-Carboxyamides in Mice," *European Journal of Pharmacology* 451 (2002): 141–7.
19. A. Ana, R. C. Jose, P. C. Fernando, D. O. Agel, J. G. Maria, H. Antonio, L. Fernando, and M. Andres, "Efficient Tautomerization Hydrazone-Azomethine Imine under Microwave Irradiation. Synthesis of [4,3] and [5,3]Bipyrazoles," *Tetrahedron* 54 (1998): 13167–80.
20. K. O. Mohammed, and Y. M. Nissan, "Synthesis, Molecular Docking, and Biological Evaluation of Some Novel Hydrazones and Pyrazole Derivatives as Anti-Inflammatory Agents," *Chemical Biology & Drug Design* 84, no. 4 (2014): 473–88.
21. B. Insuasty, A. Montoya, D. Becerra, J. Quiroga, R. Abonia, S. Robledo, I. D. Velez, Y. Upegui, M. Noguera, and J. Cobo, "Synthesis of Novel Analogs of 2-pyrazoline Obtained from [(7-Chloroquinolin-4-yl)Amino]Chalcones and Hydrazine as Potential Antitumor and Antimalarial Agents," *European Journal of Medicinal Chemistry* 67 (2013): 252–62.
22. G. Kumar, O. Tanwar, J. Kumar, M. Akhter, S. Sharma, C. R. Pillai, M. M. Alam, and M. S. Zama, "Pyrazole-Pyrazoline as Promising Novel Antimalarial Agents: A Mechanistic Study," *European Journal of Medicinal Chemistry* 149 (2018): 139–47.

23. R. Alam, A. Alam, and A. K. Panda Rahisuddin, "Design, Synthesis and Cytotoxicity Evaluation of Pyrazolyl Pyrazoline and Pyrazolyl Aminopyrimidine Derivatives as Potential Anticancer Agents," *Medicinal Chemistry Research* 27 (2018): 560–70.
24. S. Viveka, D. P. Shama, G. K. Nagaraja, S. Ballav, and S. Kerkar, "Design and Synthesis of Some New Pyrazolyl-Pyrazolines as Potential Anti-Inflammatory, Analgesic and Antibacterial Agents," *European Journal of Medicinal Chemistry* 101 (2015): 442–51.
25. H. Khanam, A. Mashrai, A. Sherwani, M. Owais, and N. Siddiqui, "Synthesis and Anti-Tumor Evaluation of B-Ring Substituted Steroidal Pyrazoline Derivatives," *Steroids* 78, (2013): 1263–72.
26. S. K. Sahu, M. Banerjee, A. Samantray, C. Behera, and M. A. Azam, "Synthesis, Analgesic, anti-Inflammatory and Antimicrobial Activities of Some Novel Pyrazoline Derivatives," *Tropical Journal of Pharmaceutical Research* 7, no. 2 (2008): 961–8.
27. M. Johnson, B. Younglove, L. Lee, R. LeBlanc, H. Holt, Jr, P. Hills, H. Mackay, T. Brown, S. L. Mooberry, and M. Lee, "Design, Synthesis, and Biological Testing of Pyrazoline Derivatives of combretastatin-A4," *Bioorganic & Medicinal Chemistry Letters* 17, no. 21 (2007): 5897–901.
28. J. Vinayagam, R. L. Gajbhiye, L. Mandal, M. Arumugam, A. Achari, and P. Jaisankar, "Substituted Furans as Potent Lipoxigenase Inhibitors: Synthesis, in Vitro and Molecular Docking Studies," *Bioorganic Chemistry* 71 (2017): 97–101.
29. C. J. Lim, N. H. Kim, H. J. Park, B. H. Lee, K. S. Oh, and K. Y. Yi, "Synthesis and SAR of 5-Aryl-Furan-2-Carboxamide Derivatives as Potent urotensin-II Receptor Antagonists," *Bioorganic & Medicinal Chemistry Letters* 29, no. 4 (2019): 577–80.
30. B. Wang, Y. Shi, Y. Zhan, L. Zhang, Y. Zhang, L. Wang, X. Zhang, Y. Li, Z. Li, and B. Li, "Synthesis and Biological Activity of Novel Furan/Thiophene and Piperazine-Containing (Bis)1,2,4-Triazole Mannich Bases," *Chinese Journal of Chemistry* 33, no. 10 (2015): 1124–34.
31. Z. Lan, D. Xinshan, W. Jiaofeng, M. Guangpeng, L. Congchong, C. Guzhou, Z. Qingchun, and H. Chun, "Design, Synthesis and Biological Activities of N-(Furan-2-Ylmethyl)-1H-Indole-3-Carboxamide Derivatives as Epidermal Growth Factor Receptor Inhibitors and Anticancer Agents," *Chemical Research in Chinese Universities* 33, no. 3 (2017): 365–72.
32. M. L. Go, M. Liu, P. Wilairat, P. J. Rosenthal, K. J. Saliba, and K. Kirk, "Anti-plasmodial Chalcones Inhibit Sorbitol-Induced Hemolysis of Plasmodium falciparum-Infected Erythrocytes," *Antimicrobial Agents and Chemotherapy* 48, no. 9 (2004): 3241–5.
33. J. A. Gonzalez, and A. Estevez-Braun, "Effect of (E)-Chalcone on Potato-Cyst Nematodes *Globodera pallida* and *G. rostochiensis*," *Journal of Agricultural and Food Chemistry* 46 (1998): 1163–5.
34. M. Yoshimura, A. Sano, J. L. Kamei, and A. Obata, "Identification and Quantification of Metabolites of Orally Administered Naringenin Chalcone in Rats," *Journal of Agricultural and Food Chemistry* 57, no. 14 (2009): 6432–7.
35. M. Chen, T. G. Theander, S. B. Christensen, L. Hviid, L. Zhai, and A. Kharazmi, "Licochalcone A, a New Antimalarial Agent, Inhibits in Vitro Growth of the Human Malaria Parasite *Plasmodium falciparum* and Protects Mice from *P. yoelii* Infection," *Antimicrobial Agents and Chemotherapy* 38, no. 7 (1994): 1470–5.
36. L. Mishra, R. Sinha, H. Itokawa, K. F. Bastow, Y. Tachibana, Y. Nakanishi, N. Kilgore, and K. H. Lee, "Anti-HIV and Cytotoxic Activities of Ru(II)/Ru(III) Polypyridyl Complexes Containing 2,6-(2'-Benzimidazolyl)-Pyridine/Chalcone as Co-Ligand," *Bioorganic & Medicinal Chemistry* 9, no. 7 (2001): 1667–71.
37. C. Jin, Y. J. Liang, H. He, and L. Fu, "Synthesis and Antitumor Activity of Novel Chalcone Derivatives," *Biomedicine & Pharmacotherapy = Biomedecine & Pharmacotherapie* 67, no. 3 (2013): 215–7.
38. F. Herencia, M. L. Ferrándiz, A. Ubeda, J. N. Domínguez, J. E. Charris, G. M. Lobo, and M. J. Alcaraz, "Synthesis and anti-Inflammatory Activity of Chalcone Derivatives," *Bioorganic & Medicinal Chemistry Letters* 8, no. 10 (1998): 1169–74.
39. Y. Qian, G. Y. Ma, Y. Yang, K. Cheng, Q. Z. Zheng, W. J. Mao, L. Shi, J. Zhao, and H. L. Zhu, "Synthesis, Molecular Modeling and Biological Evaluation of Dithiocarbamates as Novel Antitubulin Agents," *Bioorganic & Medicinal Chemistry* 18, no. 12 (2010): 4310–6.
40. R. A. Friesner, J. L. Banks, R. B. Murphy, T. A. Halgren, J. J. Klicic, D. T. Mainz, M. P. Repasky, E. H. Knoll, M. Shelley, J. K. Perry, et al. "Glide: A New Approach for Rapid, Accurate Docking and Scoring. 1. Method and Assessment of Docking accuracy," *Journal of Medicinal Chemistry* 47, no. 7 (2004): 1739–49.
41. R. A. Friesner, R. B. Murphy, M. P. Repasky, L. L. Frye, J. R. Greenwood, T. A. Halgren, P. C. Sanschagrin, and D. T. Mainz, "Extra Precision Glide: Docking and Scoring Incorporating a Model of Hydrophobic Enclosure for Protein-Ligand Complexes," *Journal of Medicinal Chemistry* 49, no. 21 (2006): 6177–96.
42. T. A. Halgren, R. B. Murphy, R. A. Friesner, H. S. Beard, L. L. Frye, W. T. Pollard, and J. L. Banks, "Glide: A New Approach for Rapid, Accurate Docking and Scoring. 2. Enrichment Factors in Database Screening," *Journal of Medicinal Chemistry* 47, no. 7 (2004): 1750–9.

43. S. J. Takate, A. D. Shinde, B. K. Karale, H. Akolkar, L. Nawale, D. Sarkar, and P. C. Mhaske, "Thiazolyl-Pyrazole Derivatives as Potential Antimycobacterial Agents," *Bioorganic & Medicinal Chemistry Letters* 29, no. 10 (2019): 1199–202.
44. K. H. Rieckmann, G. H. Campbell, L. J. Sax, and J. E. Ema, "Drug Sensitivity of plasmodium falciparum. An In-Vitro Micro Technique," *The Lancet* 311, no. 8054 (1978): 22–3.
45. R. Panjarathinam, *Text Book of Medical Parasitology*, 2nd ed. (Chennai: Orient Longman Pvt. Ltd., 2007), 329–331.
46. C. Lambros, and J. P. Vanderberg, "Synchronization of Plasmodium falciparum Erythrocytic Stages in Culture," *The Journal of Parasitology* 65, no. 3 (1979): 418–20.
47. J. S. B. Singh, "Stain; a Review," *Indian Journal of Malariology* 10 (1956): 117–29.


 Cite this: *RSC Adv.*, 2020, 10, 26997

# Nanostructured N doped TiO<sub>2</sub> efficient stable catalyst for Kabachnik–Fields reaction under microwave irradiation†

 Sachin P. Kunde,<sup>ab</sup> Kaluram G. Kanade,<sup>id\*ac</sup> Bhausheb K. Karale,<sup>a</sup> Hemant N. Akolkar,<sup>a</sup> Sudhir S. Arbuj,<sup>id d</sup> Pratibha V. Randhavane,<sup>a</sup> Santosh T. Shinde,<sup>a</sup> Mubarak H. Shaikh<sup>a</sup> and Aniruddha K. Kulkarni<sup>e</sup>

Herein, we report nitrogen-doped TiO<sub>2</sub> (N-TiO<sub>2</sub>) solid-acid nanocatalysts with heterogeneous structure employed for the solvent-free synthesis of  $\alpha$ -aminophosphonates through Kabachnik–Fields reaction. N-TiO<sub>2</sub> were synthesized by direct amination using triethylamine as a source of nitrogen at low temperature and optimized by varying the volume ratios of TiCl<sub>4</sub>, methanol, water, and triethylamine, under identical conditions. An X-ray diffraction (XRD) study showed the formation of a rutile phase and the crystalline size is 10 nm. The nanostructural features of N-TiO<sub>2</sub> were examined by HR-TEM analysis, which showed they had rod-like morphology with a diameter of  $\sim$ 7 to 10 nm. Diffuse reflectance spectra show the extended absorbance in the visible region with a narrowing in the band gap of 2.85 eV, and the high resolution XPS spectrum of the N 1s region confirmed successful doping of N in the TiO<sub>2</sub> lattice. More significantly, we found that as-synthesized N-TiO<sub>2</sub> showed significantly higher catalytic activity than commercially available TiO<sub>2</sub> for the synthesis of a novel series of  $\alpha$ -amino phosphonates via Kabachnik–Fields reaction under microwave irradiation conditions. The improved catalytic activity is due to the presence of strong and Bronsted acid sites on a porous nanorod surface. This work signifies N-TiO<sub>2</sub> is an efficient stable catalyst for the synthesis of  $\alpha$ -aminophosphonate derivatives.

Received 21st May 2020

Accepted 7th July 2020

DOI: 10.1039/d0ra04533k

[rsc.li/rsc-advances](http://rsc.li/rsc-advances)

## 1 Introduction

In recent years, organophosphorus compounds have received much attention due to their widespread applications in medicinal and agriculture industries.<sup>1,2</sup>  $\alpha$ -Aminophosphonates are one such biological important framework that are structural mimics of amino acids. For example, glyphosate (*N*-(phosphonomethyl)glycine) is extensively utilized in agriculture as a systemic herbicide and Alafosfalin is used as an antibacterial agent<sup>3</sup> (Fig. 1). The bioactivity of these molecules such as antimicrobial,<sup>4</sup> antioxidant,<sup>5</sup> anti-inflammatory,<sup>6</sup> enzyme inhibitors<sup>7</sup> and antibacterial<sup>8</sup> is one of the reasons for them to be of

immense interest in synthetic organic chemistry. It has been demonstrated that on incorporation of heterocycles such as thiophene,<sup>9</sup> benzothiazoles,<sup>10</sup> thiadiazoles,<sup>11</sup> and pyrazole<sup>12</sup> into the  $\alpha$ -aminophosphonates scaffold, the resulting compounds exhibited interesting biological activities. Pyrazole derivatives of  $\alpha$ -aminophosphonates have been rarely reported in the literature,<sup>13,14</sup> thus synthesis of novel pyrazole derivatives of  $\alpha$ -aminophosphonates is important to research.

Although several protocols for the synthesis of  $\alpha$ -aminophosphonates are reported, one of the most important is the Kabachnik–Fields reaction.<sup>15,16</sup> This involves a one-pot three-component coupling of a carbonyl compound, an amine and alkylphosphite. These protocols has been accomplished in presence of a variety of catalyst such as TiCl<sub>4</sub>,<sup>17</sup> CuI,<sup>18</sup> hexanesulphonic sodium salt,<sup>19</sup> trifluoroacetic acid (TFA),<sup>20</sup> In(OTf)<sub>3</sub>,<sup>21</sup> BiCl<sub>3</sub>,<sup>22</sup> Cu(OTf)<sub>2</sub>,<sup>23</sup> SbCl<sub>3</sub>/Al<sub>2</sub>O<sub>3</sub>,<sup>24</sup> InCl<sub>3</sub>,<sup>25</sup> LiClO<sub>4</sub>,<sup>26</sup> ZrOCl<sub>2</sub>,<sup>27</sup> TsCl,<sup>28</sup> Mg(ClO<sub>4</sub>)<sub>2</sub>,<sup>29</sup> and Na<sub>2</sub>CaP<sub>2</sub>O<sub>3</sub><sup>30</sup> in presence or

<sup>a</sup>PG and Research Centre, Radhabai Kale Mahila Mahavidyalaya, Ahmednagar, 414 001 India. E-mail: kgkanade@yahoo.co.in

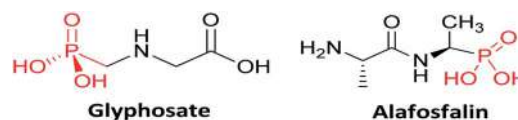
<sup>b</sup>PG and Research Centre, Mahatma Phule Arts, Science and Commerce College, Panvel, 410 206, India

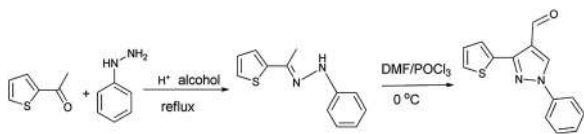
<sup>c</sup>PG and Research Centre, Yashwantrao Chavan Institute of Science, Satara, 415 001 India

<sup>d</sup>Centre for Materials for Electronics Technology (C-MET), Department of Electronics and Information Technology (DeitY), Government of India, Panchavati, Off Pashan Road, Pune-411 008, India

<sup>e</sup>Dr. John Barnabas School for Biological Studies, Department of Chemistry, Ahmednagar College, Ahmednagar-414 001, India

† Electronic supplementary information (ESI) available. See DOI: 10.1039/d0ra04533k


 Fig. 1 Some biological active  $\alpha$ -aminophosphonate.

Scheme 1 Synthesis of 1-phenyl-5-(thiophen-2-yl)-1H-pyrrole-3-carbaldehyde.

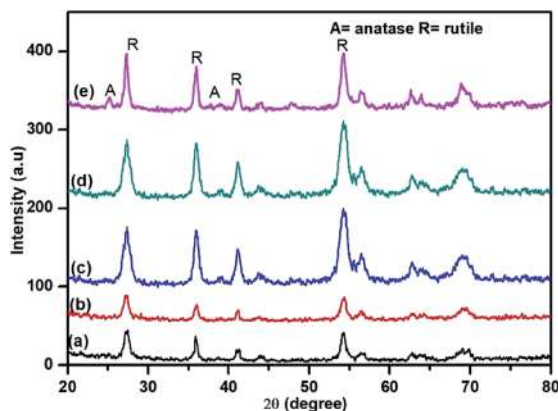


Fig. 2 X-ray diffraction patterns of (a) TN0 (TiO<sub>2</sub>), (b) TN1, (c) TN2, (d) TN3 (e) TN4.

even in the absence of a solvent. However, most of these existing procedures are sluggish, require long reaction times, use of strong acidic conditions, give unsatisfactory yields and also suffer from the formation of many side products. Moreover, in all alternatives microwave reaction proved to be a kind of promising medium for such reaction.<sup>31</sup>

In the last few years, the application of transition metal oxides gained particular interest as a heterogeneous catalyst for various organic synthesis.<sup>32</sup> Among all transition metal oxides the use of nanocrystalline titania (TiO<sub>2</sub>) has been grown extensively owing to their outstanding physiochemical properties, which furnished their wide applications in sensors,<sup>33</sup> pigments,<sup>34</sup> photovoltaic cells,<sup>35</sup> and catalysis.<sup>36</sup> Also, the use of potential titania catalyst attracted in organic synthesis due to its environmental compatibility, inexpensive, safe, stable, reusable and earth-abundant. It has been proven the desired property of TiO<sub>2</sub> was attained by fulfilling requirements in terms of unique morphology, high crystallinity and mixed-phase composition,

Table 1 Phase composition and crystallite size of as-prepared samples from analysis of XRD

Sample	Rutile	Anatase	Crystallite size (nm)
TN0	100	0	25
TN1	98	2	19
TN2	94	6	16
TN3	95	5	12
TN4	91	9	9

the ability of oxidizing and reducing ability under suitable irradiation makes promising greener alternative approach towards important organic transformations compared to other expensive, toxic, transition metal oxides. Moreover, the phase composition and the degree of crystallinity of the titania sample plays an important role in catalytic activity.<sup>8</sup> In the past several organic transformations such as oxidation of primary alcohols,<sup>37</sup> synthesis of xanthenes,<sup>38</sup> Friedel-Crafts alkylation,<sup>39</sup> Beckmann rearrangement<sup>40</sup> efficiently utilizes TiO<sub>2</sub> as a heterogeneous reusable catalyst. In the literature several reports have been debated to influence nitrogen doping on photocatalytic activity of nanocrystalline TiO<sub>2</sub>. However, the effect is unrevealed for catalytic applications in organic synthesis. Recently, Hosseini-Sarvari explored the use of commercial TiO<sub>2</sub> in the synthesis of  $\alpha$ -aminophosphonates *via* Kabachnik-Fields reactions.<sup>41</sup>

In present investigation, we have prepared nanostructured N doped TiO<sub>2</sub> and also investigation emphasis was given on the synthesis of a series of a novel diethyl(1-phenyl-3-(thiophen-2-yl)-1H-pyrazol-4-yl)(phenylamino) methylphosphonates under microwave irradiation.

## 2 Experimental sections

### 2.1 Synthesis of N doped TiO<sub>2</sub> nanorods

The nanostructured N-TiO<sub>2</sub> were synthesized by previously reported method with some modification.<sup>42,43</sup> In a typical procedure, 0.5 mL of titanium tetrachloride (TiCl<sub>4</sub>) was added in absolute methanol (25 mL) with constant stirring at room temperature. To this solution requisite quantity a 0.1–2 M aqueous triethylamine solution is injected rapidly. The resulting solution was refluxed for 24 h with constant stirring. The white precipitate formed was collected and washed with ethanol several times followed by centrifugation (10 000 rpm for 20 min). The precipitate was dried at 473 K for 24 h. To control the final morphologies of samples, the sample were synthesized as function of volume ratio of TiCl<sub>4</sub>, methanol, water, and triethylamine. The sample prepared in volume ratio 1 : 10 : 50 : 0, 1 : 10 : 50 : 1, 1 : 10 : 50 : 2, 2 : 10 : 50 : 2, and 2 : 10 : 50 : 4 were denoted as TN0 (pure TiO<sub>2</sub>), TN1, TN2, TN3 and TN4 respectively.

### 2.2 Synthesis of 1-phenyl-5-(thiophen-2-yl)-1H-pyrrole-3-carbaldehyde

1-Phenyl-5-(thiophene-2-yl)-1H-pyrrole-3-carbaldehyde were obtained *via* the Vilsmeier-Haack reaction of the appropriate phenylhydrazones, derived from the reaction of 2-acetyl thiophene with phenylhydrazine<sup>44</sup> (Scheme 1).

### 2.3 Synthesis of diethyl(1-phenyl-3-(thiophene-2-yl)-1H-pyrazole-4-yl)(phenylamino)methylphosphonates

In a typical procedure, the pyrazolealdehyde **1** (1 mmol), aniline **2** (1 mmol), triethyl phosphite **3** (1.1 mmol) and N-TiO<sub>2</sub> (12 mol%) were taken in a round bottom flask equipped with a condenser and subjected to microwave irradiation for (10–15 min) using 420 W (RAGA's Microwave system) (Scheme 3). The





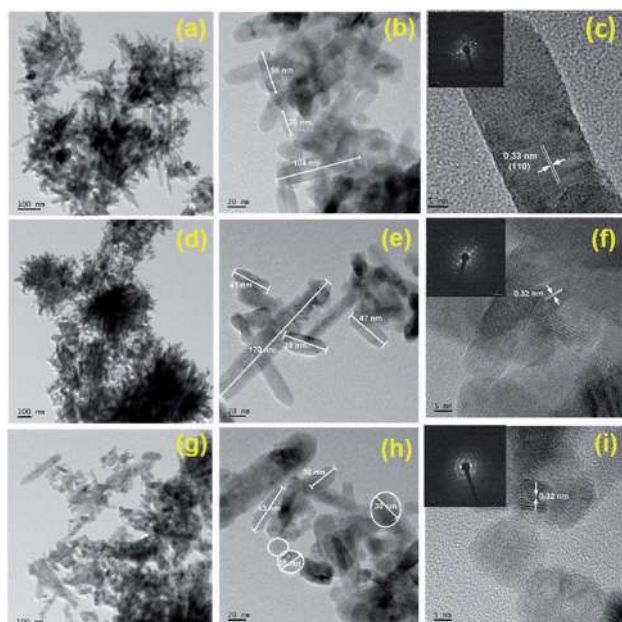


Fig. 3 HR-TEM images of (a–c) TN0, (d–f) TN1, and (g–i) TN2; inset c, f and h SAED pattern of TN0, TN1 and TN2 respectively.

progress of the reaction was monitored by TLC. After the reaction was completed, the reaction mixture extracted using ethyl acetate and insoluble catalyst separated by filtration. The crude product was purified by silica gel column chromatography using *n*-hexane/ethyl acetate as eluent. The product structure was determined by FTIR,  $^1\text{H}$  NMR, and LS-MS.

## 2.4 Samples characterization

The phase purity and crystallinity were examined by X-ray diffraction (XRD) technique (Advance, Bruker AXS D8) using  $\text{Cu K}\alpha 1$  (1.5406 Å) radiation with scanning  $2\theta$  range from 20 to 80°. For FE-TEM analysis samples were prepared by evaporating dilute solution on carbon-coated grids. FE-TEM measurements were carried using the JEOL SS2200 instrument operated at an

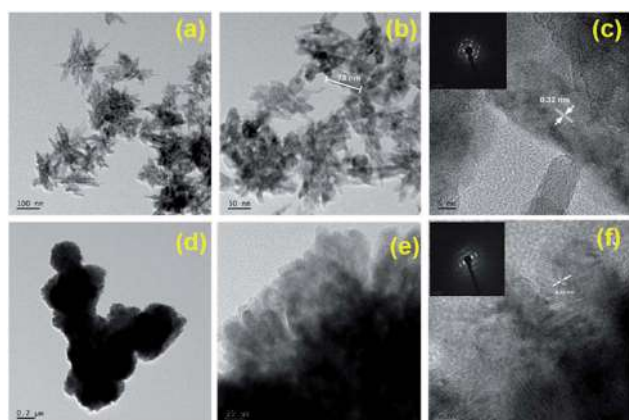


Fig. 4 HR-TEM images of (a–c) TN3 and (d–f) TN4; inset c, and f SAED pattern of TN3, and TN4 respectively.

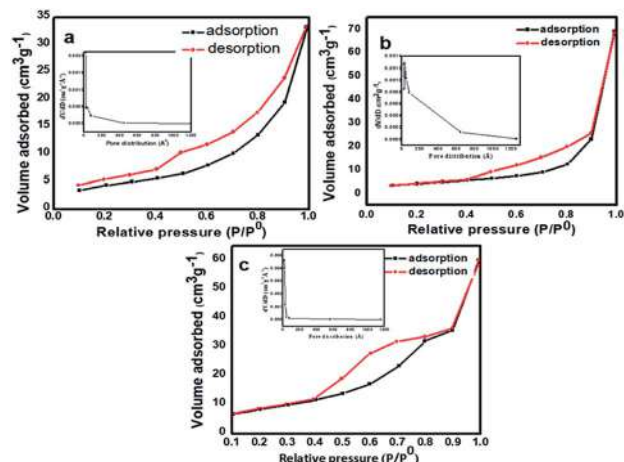


Fig. 5 Nitrogen ( $\text{N}_2$ ) adsorption–desorption isotherms of (a) TN0 ( $\text{TiO}_2$ ), (b) TN2 ( $\text{N-TiO}_2$ ), (c) TN4 ( $\text{N-TiO}_2$ ). Insets show their corresponding pore size distributions.

accelerating voltage of 300 kV. The Brunauer–Emmett–Teller (BET) surface area of nanocatalysts was examined using the Quantachrome v 11.02 nitrogen instrument. The optical properties of the powder samples were studied using UV-vis diffuse reflectance absorption spectra (UV-DRS) were recorded on the Perkin-Elmer Lambda-950 spectrophotometer in the wavelength range of 200–800 nm. Powder samples were used for XPS measurements. The XPS measurements of powdered samples were carried out on a VG Microtech ESCA3000 instrument. Fourier transform infrared (FTIR) spectra of prepared samples were recorded on a Shimadzu Affinity 1-S spectrophotometer in over a range of 400–4000  $\text{cm}^{-1}$ .  $^1\text{H}$  NMR was recorded in  $\text{DMSO-}d_6$  solvent on a Bruker Advance-400 spectrometer with tetramethylsilane (TMS) as an internal reference.

## 3 Results and discussions

### 3.1 Structural study

Nanostructured  $\text{TiO}_2$  and N doped  $\text{TiO}_2$  were synthesized by a simple refluxing method. The phase purity and phase formation of as-synthesized material were analysed by powder X-ray diffraction pattern. Fig. 2 compares powder XRD patterns of  $\text{TiO}_2$  and N doped  $\text{TiO}_2$  samples. The peak position and peak intensity of the pure  $\text{TiO}_2$  powder can be indexed into rutile phases (Fig. 2). Further, it is observed that an increase in the amount N-dopant (triethylamine) the intensity of the diffraction

Table 2 BET specific surface area and pore size distribution of  $\text{TiO}_2$  and N- $\text{TiO}_2$

Sample	Surface area ( $\text{m}^2 \text{g}^{-1}$ )	Pore volume ( $\text{cm}^3 \text{g}^{-1}$ )	Pore radius (Å)
TN0	21.956	0.051	18.108
TN2	40.359	0.215	30.811
TN4	53.589	0.101	18.041



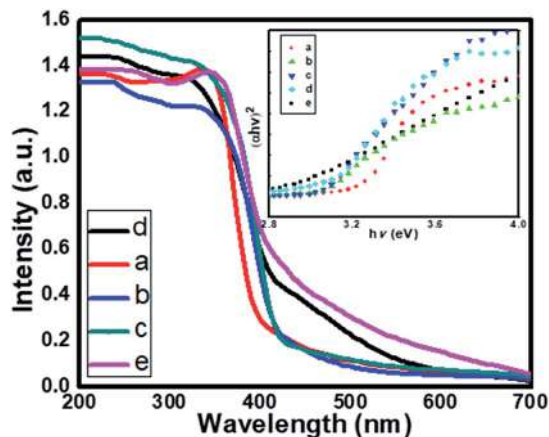


Fig. 6 UV-DRS spectra of (a) TN0 (TiO<sub>2</sub>), (b) TN1 (N-TiO<sub>2</sub>), (c) TN2 (N-TiO<sub>2</sub>), (d) TN3 (N-TiO<sub>2</sub>), (e) TN4. Inset shows Tauc plot of TiO<sub>2</sub> and N-TiO<sub>2</sub> samples.

peaks of the rutile phase decreases, while that of anatase phase increases, indicating that the fraction of the anatase phase gradually increases at the expense of the rutile phase during this condition (sample TN2–TN4). The phase composition of rutile and anatase phase of TiO<sub>2</sub> evaluated from the peak intensity using the following equation,

$$f_A = \frac{1}{1 + \frac{I_R}{K I_A}} \quad K = 0 : 79; f_A > 0.2; K_{1/4} = 0 : 68; f_A \leq 0.2$$

where  $f_A$  is the fraction of the anatase phase, and  $I_A$  and  $I_R$  are the intensities of the anatase (1 0 1) and rutile (1 1 0) diffraction peaks, respectively. The higher molar concentration of triethylamine is favourable for the transformation from rutile to anatase.<sup>45,46</sup> Therefore, the phase composition of TiO<sub>2</sub> samples, *i.e.* the fraction of anatase and rutile, can be facilely controlled through adjusting the concentration of triethylamine. The slight shift of rutile (1 1 0) diffraction peaks towards a higher angle with an increase in the amount of N dopant suggesting

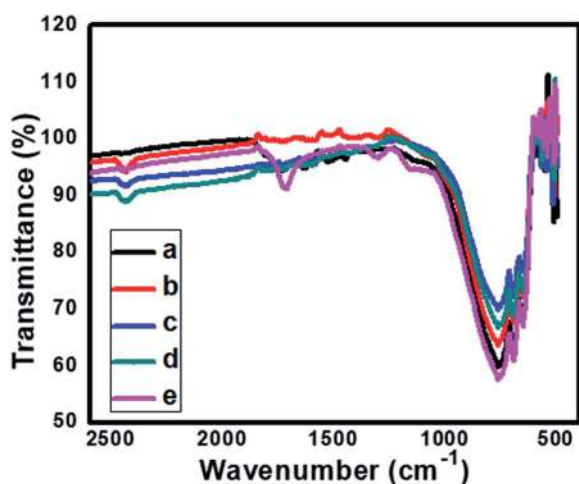


Fig. 7 FTIR spectra of (a) TN0 pure (TiO<sub>2</sub>), (b) TN1 (N-TiO<sub>2</sub>), (c) TN2, (d) TN3 and (e) TN4.

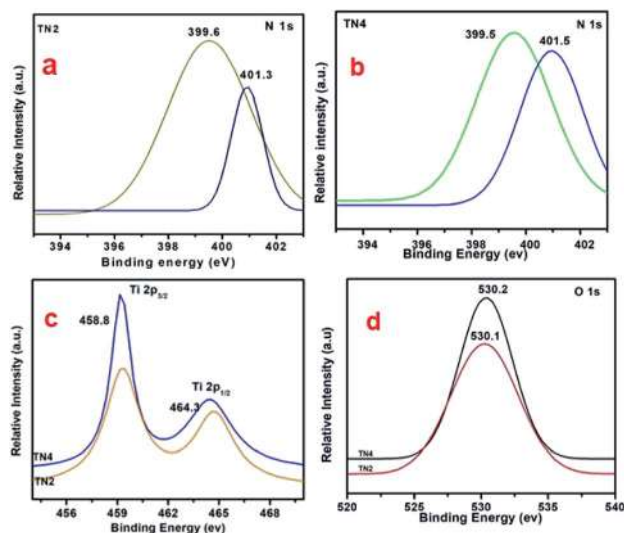
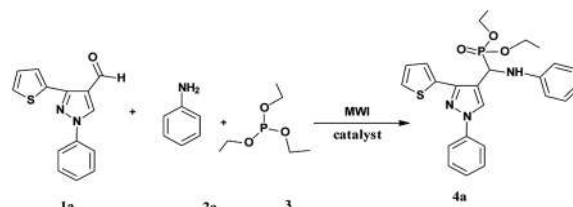


Fig. 8 (a and b) High resolution spectrum of N 1s region (c) high resolution spectrum of Ti 2p region (d) high resolution spectrum of O 1s region.

the incorporation of nitrogen in the TiO<sub>2</sub> crystal structure. The crystallite size is calculated from each (1 1 0) peak in the XRD pattern using the Sherrer formula.<sup>39</sup> The average crystalline size are 25, 19, 16, 12 and 9 nm for TN0, TN1, TN2, TN3, and TN4 respectively (Table 1). From XRD analysis it is clear that with an increase in the concentration of nitrogen in TiO<sub>2</sub>, fraction of anatase increases and crystalline size decreases.

### 3.2 Surface and morphological study

Transmission electron microscopy (TEM) and high-resolution transmission electron microscopy (HRTEM) analysis were performed to study morphology and crystallinity of as-synthesized pure and N doped TiO<sub>2</sub> materials (Fig. 3). The pure TiO<sub>2</sub> (TN0) sample seems flowerlike nanostructures (Fig. 3a). At high-resolution it reveals that each flower microstructure consisting several nanorods. The length of nanorods are in the range of 50–70 nm and diameter is about 10–15 nm (Fig. 3b). Fig. 3c shows the lattice fringes of the material with interplanar spacing  $d$  spacing 0.33 nm matches well (1 0 0) plane of rutile TiO<sub>2</sub>. Fig. 3c inset shows a selected area diffraction pattern in which bright spots observed that confirm the TiO<sub>2</sub> nanorods are in nanocrystalline nature. It was observed that addition of N dopant, resulting sample TN1 and TN2 grows into new superstructure consisting nanorods of length 30–50 nm and spheres



Scheme 2 Standard model reaction.



**Table 3** Comparative study of catalysts used for the synthesis of  $\alpha$ -aminophosphonate<sup>a</sup>

Entry	Catalyst	Time (minutes)	Yield <sup>b</sup> (%)
1	—	20	Trace
2	Acetic acid	20	30
3	Commercial ZnO	15	20
4	Commercial TiO <sub>2</sub>	15	30
5	TN0	10	72
6	TN1	10	73
7	TN2	10	76
8	TN3	10	85
9	TN4	10	95

<sup>a</sup> Reaction condition: aldehyde (**1a**) (1 mmol), aniline (1 mmol), triethylphosphite (1.1 mmol), catalyst, MW power 420 watt. <sup>b</sup> Isolated yield.

of diameter 20–30 nm, particles size is obviously smaller than TN0 (Fig. 3d and h). HRTEM results are consistent with XRD results. The *d*-spacing is about 0.325 Å between adjacent lattice planes of the N doped TiO<sub>2</sub>.

It was revealed that with doubling concentration of TiCl<sub>4</sub>, sample TN3 and TN4 were grown into very fine agglomerated nanorods (Fig. 4). Further, it is observed that these nanorods having size in length 30–40 nm and diameter is around 7–10 nm which is lower than pure TiO<sub>2</sub>. Fig. 4f inset shows selected area diffraction pattern shows, surprisingly, ring-like pattern unlike TiO<sub>2</sub>, indicates N-TiO<sub>2</sub> nanorods are in polycrystalline nature. From HR-TEM results it is concluded that increase in concentration of TiCl<sub>4</sub> and triethylamine reduces the size of the nanorods.

The specific surface area of as-prepared samples was studied by (N<sub>2</sub>) nitrogen gas adsorption–desorption measurement at 77 K using the Brunauer–Emmett–Teller (BET) method. The N<sub>2</sub> adsorption–desorption isotherm of N-TiO<sub>2</sub> nanoparticles is shown in Fig. 5. The pure TiO<sub>2</sub> shows type IV isotherm according to IUPAC classification,<sup>47</sup> which are typical characteristics of a material with pore size in the range of 1.5–100 nm Fig. 5a. The shape of the hysteresis loop is H<sub>3</sub> type may associates due to the agglomeration of nanoparticles forming slit-like pores, reflected in TEM images. At higher relative pressure (*p/p*<sup>0</sup>) the slope shows increased uptake of adsorbate as pores become filled; inflection point typically occurs near

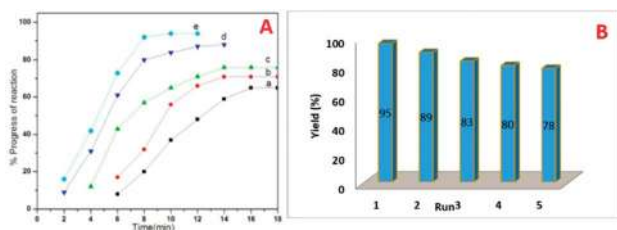


**Fig. 9** (A) Progress of reaction (a) TN0 (b) TN1 (c) TN2 (d) TN3 and (e) TN4. (B) Reusability of catalyst TN4; reaction condition: aldehyde (**1a**) (1 mmol), aniline (**2a**) (1 mmol), triethylphosphite **3** (1.1 mmol), N-TiO<sub>2</sub> (12 mol%), MW power 420 watt.

**Table 4** Optimization of the concentration of catalyst<sup>a</sup>

Sr. no.	Concentration of catalyst (mol%)	Yield <sup>b</sup> (%)
1	3	69
2	6	76
3	9	86
4	12	95
5	15	95

<sup>a</sup> Reaction condition: aldehyde (**1a**) (1 mmol), aniline (1 mmol), triethylphosphite (1.1 mmol), N-TiO<sub>2</sub> catalyst, MW power 420 watt. <sup>b</sup> Isolated yield.

completion of the first monolayer. The BET surface area of pure TiO<sub>2</sub> is found to be 21.956 m<sup>2</sup> g<sup>-1</sup>. The pore size distribution of prepared samples was investigated by Barrett–Joyner–Halenda (BJH) method Fig. 5(a)–(c) insets. The average pore diameter of pure TiO<sub>2</sub> nanoparticles is 18 nm which demonstrates the material is mesoporous nature. Further, it is observed that the incorporation of nitrogen in TiO<sub>2</sub> nanoparticles the surface area shifts towards higher values. The adsorption–desorption isotherms of nitrogen-doped TiO<sub>2</sub> samples display the type II isotherm according to IUPAC classification.<sup>46</sup> The specific BET surface area of samples TN<sub>2</sub> and TN<sub>4</sub> are 40.359 m<sup>2</sup> g<sup>-1</sup> and 53.589 m<sup>2</sup> g<sup>-1</sup> respectively (Fig. 5b and 4c). This observation specifies a decrease in the particle size of TiO<sub>2</sub> nanoparticles specific surface area increases which are in consisting of XRD and TEM results. The Brunauer–Emmett–Teller (BET) specific surface areas, pore volumes and mean pore and mean pore diameters of samples TN0, TN2, and TN4 are summarized in Table 2.

### 3.3 Optical and electronic property studies

The optical property of the as-synthesized material was analyzed by UV-Vis diffuse absorbance spectra as shown in Fig. 6. Fig. 6 displays the comparative UV-DRS spectra of pristine TiO<sub>2</sub> and a series of N doped TiO<sub>2</sub> samples. The absorption edge for the pure TiO<sub>2</sub> (TN0) is observed at around 410 nm (Fig. 6a), which is consistent with the band gap of the rutile phase.<sup>45</sup> The N doped TiO<sub>2</sub> nanostructures show strong absorption in the visible region (410–600 nm). The redshift clearly indicates the

**Table 5** Screening of solvents<sup>a</sup>

Entry	Solvent	Yield (%) <sup>b</sup>
1	Ethanol	85
2	Methanol	87
3	Dichloromethane	55
4	THF	58
6	Toluene	60
7	Neat	95

<sup>a</sup> Reaction condition: aldehyde (**1a**) (1 mmol), aniline (1 mmol), triethylphosphite (1.1 mmol), N-TiO<sub>2</sub> catalyst, solvent, MW power 420 watt. <sup>b</sup> Isolated yield.





successful doping of N in the lattice of TiO<sub>2</sub>. Moreover, as the concentration of triethylamine increases redshift of N-TiO<sub>2</sub> also increases which confirms higher nitrogen doping and a higher fraction of absorption of photons from the visible region. The band gap of as-synthesized material calculated by using the Tauc plot shown in Fig. 6 (insets). The band gap ( $E_g$ ) for the sample TN0, TN1, TN2, TN3, and TN4, were observed to 3.15, 3.09, 3.07, 3.03 and 2.85 eV respectively. The decrease in the band gap is attributed to higher mixing of the (O/N) 2p level is developed in the Ti-3d level falls at the top of the VB, therefore, band gap reduced compared to the pristine TiO<sub>2</sub> nanostructure.

### 3.4 FT-IR spectroscopy

Fig. 7 shows comparative FTIR spectra for pure and N doped TiO<sub>2</sub>. The absorption peak signal in the range of 400–1100 cm<sup>-1</sup> is characteristic of the formation of O-Ti-O lattice. The absorption at 668 cm<sup>-1</sup>, 601 cm<sup>-1</sup>, 546 cm<sup>-1</sup> and 419 cm<sup>-1</sup> corresponds to Ti-O vibrations.<sup>48,49</sup> Further, for the sample TN1–TN3 the IR bands centred at 1400–1435 cm<sup>-1</sup> indicates nitrogen doping in the TiO<sub>2</sub> sample. The band located at 1070 cm<sup>-1</sup> is attributed to Ti-N bond vibrations. Also, it is observed that the band at 1335 cm<sup>-1</sup> for pure TiO<sub>2</sub> is shifted towards longer wavenumber 1430 cm<sup>-1</sup> supports for the claim of N doping in TiO<sub>2</sub> lattice. Further it is also observed that some of the minor the peaks of pure TiO<sub>2</sub> are rather different than the N-doped TiO<sub>2</sub>, this indicates the incorporation of nitrogen in TiO<sub>2</sub> lattices. The peak centered at 1600–2180 cm<sup>-1</sup> is ascribed due to -OH stretching frequency. From, IR spectra it is clear that N<sub>2</sub> is successfully incorporated in the lattice of TiO<sub>2</sub>.

### 3.5 X-ray photoelectron spectroscopy

The XPS were used for chemical identification and electronic state of dopant nitrogen in sample TN2 and TN4. The high resolution XPS spectra of N 1s on deconvolution shows two different peaks at 399.6 and 401.5 eV indicates nitrogen present in two different electronic state (Fig. 8a and b). The peak at 399.6 is attributed to presence of interstitial N or N-Ti-O linkage. The result is consistent with previous reports.<sup>43</sup> The peak at 401.5 is attributed to presence of N in oxidized state as NO or NO<sub>2</sub>. The concentration of nitrogen on surface of TN2 and TN4 are 2.8% and 3.4% respectively. Fig. 8c shows the peak at 458.8 and 458.3 is attributed to Ti 2p<sub>3/2</sub> and Ti 2p<sub>1/2</sub>, in good agreement the presence of Ti(IV) in TiO<sub>2</sub>. The peak at binding energy 530.1 and 530.2 eV of sample are attributed to O 1s (Fig. 8d).

### 3.6 Catalytic study in synthesis of $\alpha$ -aminophosphonates

In order to find out the best experimental condition, the reaction of pyrazolaldehyde **1a**, aniline **2a** and triethylphosphite **3** under microwave irradiation is considered as standard model reaction (Scheme 2).

In the absence of a catalyst, the standard model reaction gave a small amount of product (Table 3 entry 1). These results specify catalyst is required to occur reaction. In order to check the catalytic utility, the model reaction carried out in the presence of a variety of catalysts (Table 3 entry 2–9). The N-TiO<sub>2</sub> NRs

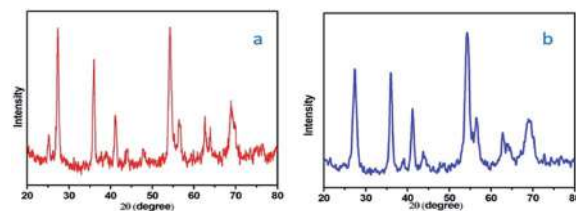


Fig. 10 XRD of sample TN4 (a) before reaction (b) after reaction.

gave better results than acetic acid, commercial ZnO and commercial TiO<sub>2</sub>.

Inspiring these results, we further studied the progress of reaction at different time intervals, we observed the sample N-doped TiO<sub>2</sub> catalyzes efficiently than undoped TiO<sub>2</sub>, and this may be attributed to the higher surface area (Fig. 9A).

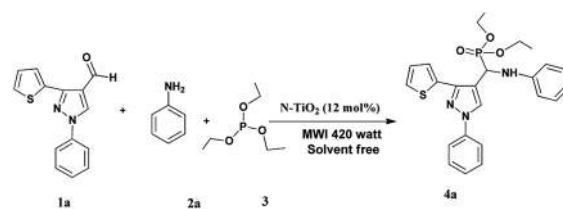
The optimum concentration of the catalyst was investigated by performing the model reaction at different concentrations such as 3, 6, 9, 12 and 15 mol%. The reaction yielded in 69, 76, 86, 95 and 95% yields respectively (Table 4). This shows that 12 mol% of TN<sub>4</sub> is adequate for the reaction by considering the yield of the product.

To evaluate the effect of solvents, different solvents such as ethanol, methanol, dichloromethane, THF, 1,4-dioxane and toluene were used for the model reaction in presence of N-TiO<sub>2</sub> catalyst. The reaction proceed with better yield in polar protic solvent (Table 5, entries 1, 2). However it was observed that the usage of solvents slows down the rate of reaction and gives the desired product in lower yields than that for neat condition (Table 5, entries 1–6).

The recyclability of the catalyst was then examined and the outcomes are shown in Fig. 9B. After the completion of reaction, the reaction mixture was extracted with ethyl acetate. The residual catalyst was washed with acetone, dried under vacuum at 100 °C and reused for consequent reactions. The recovered catalyst could be used for 5 times without obvious loss of catalytic activity.

The difference between the XRD of fresh catalyst and reused catalyst shown in Fig. 10.

The usefulness of optimized reaction condition for model reaction (12 mmol % of catalyst, solvent-free, MWI) was extended for the synthesis of a series of novel  $\alpha$ -amino-phosphonates (**4a–l**) by reacting pyrazolaldehyde (**1a–c**), anilines (**2a–d**) and triethylphosphite (**3**) in excellent yields (Scheme 3).



Scheme 3 Optimized reaction condition for synthesis of diethyl(1-phenyl-3-(thiophen-2-yl)-1H-pyrazol-4-yl)(phenylamino)methylphosphonates



Table 6 Microwave assisted synthesis of novel diethyl(1-phenyl-3-(thiophen-2-yl)-1H-pyrazol-4-yl)(phenylamino)methylphosphonates<sup>a</sup>

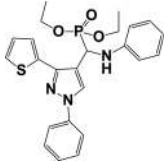
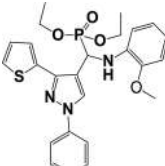
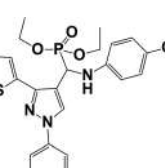
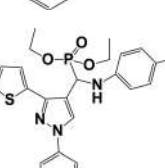
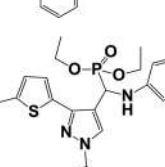
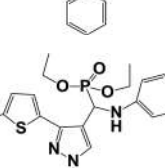
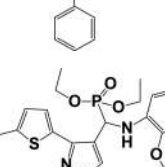
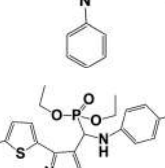
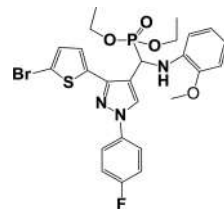
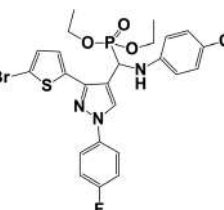
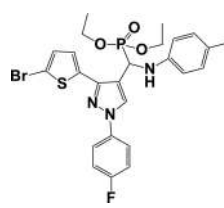
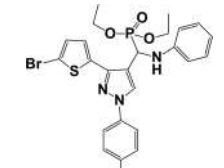
Entry	Product	M.P. (°C)	Yield <sup>b</sup> (%)
4a		218	95
4b		220	79
4c		208	92
4d		216	79
4e		180	86
4f		200	82
4g		162	85
4h		190	71

Table 6 (Contd.)

Entry	Product	M.P. (°C)	Yield <sup>b</sup> (%)
4i		195	81
4j		120	76
4k		210	89
4l		190	75

<sup>a</sup> Reaction condition: aldehyde (1 mmol), aniline (1 mmol), triethylphosphite (1.1 mmol), N-TiO<sub>2</sub> (12 mol%), MW power 420 watt.  
<sup>b</sup> Isolated yield.

The obtained product **4a–l** was characterized by spectroscopic techniques (Table 6).

The spectroscopic data of synthesized compounds are given in ESI (S-2 to S-26).†

## 4 Conclusions

In summary, we have prepared N doped TiO<sub>2</sub> nanorods by thermal hydrolysis method using triethylamine as the source of nitrogen at relatively low temperatures. The XRD analysis showed that with varying composition molar ratios of TiCl<sub>4</sub>, CH<sub>3</sub>OH, H<sub>2</sub>O, and (C<sub>2</sub>H<sub>5</sub>)<sub>3</sub>N, phase composition of rutile to anatase also tunes. FTIR spectra show the chemical environment of doping by the formation of the N-Ti-O and Ti-O-Ti bond. The morphological study performed by the FE-TEM technique shows the formation of well-developed nanorods of size in length 30–40 nm and diameter is around 7–10 nm, which is lower than pure TiO<sub>2</sub>. Further, BET analysis N-TiO<sub>2</sub> shows the maximum specific surface area 53.4 m<sup>2</sup> g<sup>-1</sup> which is 2.5 times





higher than pure TiO<sub>2</sub>. The as-synthesized materials were employed for the synthesis of  $\alpha$ -aminophosphonates via Kabachnik–Fields reaction under microwave irradiation. The N-TiO<sub>2</sub> shows remarkable catalytic activity for aminophosphonate derivatives compared with TiO<sub>2</sub> and other similar nanocatalysts.

## Conflicts of interest

There are no conflicts to declare.

## Acknowledgements

SPK is gratefully acknowledged UGC New Delhi for the award of Senior Research Fellowship (F.11-16/2013(SA-I)). The authors are thankful to parent institute Rayat Shikshan Sanstha, Satara.

## Notes and references

- L. G. Costa, *Toxicol. Sci.*, 2018, **162**(1), 24–35.
- M. Eto, *Organophosphorus pesticides*, CRC press, 2018.
- A. Mucha, P. Kafarski and L. Berlicki, *J. Med. Chem.*, 2011, **54**(17), 5955–5980.
- M. K. Awad, M. F. Abdel-Aal, F. M. Atlam and H. A. Hekal, *Spectrochim. Acta, Part A*, 2018, **206**, 78–88.
- M. M. Azaam, E. R. Kenawy, A. S. El-din, A. A. Khamis and M. A. El-Magd, *J. Saudi Chem. Soc.*, 2018, **22**(1), 34–41.
- R. Damiche and S. Chafaa, *J. Mol. Struct.*, 2017, **1130**, 1009–1017.
- Z. Chen, P. Marce, R. Resende, P. M. Alzari, A. C. Frasch, J. M. Van den Elsen, S. J. Crennell and A. G. Watts, *Eur. J. Med.*, 2018, **158**, 25–33.
- A. Hellal, S. Chafaa, N. Chafai and L. Touafri, *J. Mol. Struct.*, 2017, **1134**, 217–225.
- D. Rogacz, J. Lewkowski, M. Siedlarek, R. Karpowicz, A. Kowalczyk and P. Rychter, *Materials*, 2019, **12**(12), 2018.
- L. Jin, B. Song, G. Zhang, R. Xu, S. Zhang, X. Gao and S. Yang, *Bioorg. Med. Chem. Lett.*, 2006, **16**(6), 537–1543.
- S. M. Lu and R. Y. Chen, *Org. Prep. Proced. Int.*, 2000, **32**(3), 302–306.
- A. G. Nikalje, P. A. Gawhane, S. V. Tiwari, J. N. Sangshetti and M. G. Damale, *Anti-Cancer Agents Med. Chem.*, 2018, **18**(9), 1267–1280.
- C. W. Guo, S. H. Wu, F. L. Chen, Z. Y. Han, X. H. Fu and R. Wan, *Phosphorus, Sulfur Silicon Relat. Elem.*, 2016, **191**(9), 1250–1255.
- L. Wu, B. Song, P. S. Bhadury, S. Yang, D. Hu and L. Jin, *J. Heterocycl. Chem.*, 2011, **48**, 389–396.
- W. Fan, Y. Queneau and F. Popowycz, *RSC Adv.*, 2018, **8**, 31496–31501.
- B. Rajendra Prasad Reddy, P. Vasu Govardhana Reddy and B. N. Reddy, *New J. Chem.*, 2015, **39**, 9605–9610.
- Y. T. Reddy, P. N. Reddy, B. S. Kumar, P. Rajput, N. Sreenivasulu and B. Rajitha, *Phosphorus, Sulfur Silicon Relat. Elem.*, 2007, **182**(1), 161–165.
- H. Fang, X. Xie, B. Hong, Y. Zhao and M. Fang, *Phosphorus, Sulfur Silicon Relat. Elem.*, 2011, **186**(11), 2145–2155.
- K. S. Niralwad, B. B. Shingate and M. S. Shingare, *Ultrason. Sonochem.*, 2010, **17**(5), 760–763.
- T. Akiyama, M. Sanada and K. Fuchibe, *Synlett*, 2003, **10**, 1463–1464.
- R. Ghosh, S. Maiti, A. Chakraborty and D. K. Maiti, *J. Mol. Catal. A: Chem.*, 2004, **210**(1–2), 53–57.
- Z. P. Zhan and J. P. Li, *Synth. Commun.*, 2005, **35**(19), 2501–2508.
- A. S. Paraskar and A. Sudalai, *ARKIVOC*, 2006, 183–189.
- K. S. Ambica, S. C. Taneja, M. S. Hundal and K. K. Kapoor, *Tetrahedron Lett.*, 2008, **49**, 2208–2212.
- B. C. Ranu, A. Hajraa and U. Jana, *Org. Lett.*, 1999, **1**, 1141–1143.
- N. Azizi, F. Rajabi and M. R. Saidi, *Tetrahedron Lett.*, 2004, **45**, 9233–9236.
- S. Bhagat and A. K. Chakraborti, *J. Org. Chem.*, 2008, **73**, 6029–6032.
- B. Kaboudin and E. Jafari, *Synlett*, 2008, **12**, 1837–1839.
- S. Bhagat and A. K. Chakraborti, *J. Org. Chem.*, 2007, **72**, 1263–1266.
- A. Elmakssoudi, M. Zahouily, A. Mezdar, A. Rayadh and S. Sebti, *C. R. Chim.*, 2005, **8**, 1954–1959.
- A. Tajti, E. Szatmári, F. Perdih, G. Keglevich and E. Balint, *Molecules*, 2019, **24**(8), 1640.
- S. P. Kunde, K. G. Kanade, B. K. Karale, H. N. Akolkar, P. V. Randhavane and S. T. Shinde, *Arabian J. Chem.*, 2019, **12**, 5212–5222.
- S. Ardizzone, C. L. Bianchi, G. Cappelletti, S. Gialanella, C. Pirola and V. Ragaini, *J. Phys. Chem. C*, 2007, **111**(35), 13222–13231.
- J. P. Jalava, *Part. Part. Syst. Charact.*, 2006, **23**(2), 159–164.
- M. Pelaez, N. T. Nolan, S. C. Pillai, M. K. Seery, P. Falaras, A. G. Kontos, P. S. Dunlop, J. W. Hamilton, J. A. Byrne, K. O'shea and M. H. Entezari, *Appl. Catal. B*, 2012, **125**, 331–349.
- G. C. Nakhate, V. S. Nikam, K. G. Kanade, S. S. Arbut, B. B. Kale and J. O. Baeg, *Mater. Chem. Phys.*, 2010, **124**(2–3), 976–981.
- D. I. Enache, J. K. Edwards, P. Landon, B. Solsona-Espriu, A. F. Carley, A. A. Herzing, M. Watanabe, C. J. Kiely, D. W. Knight and G. J. Hutchings, *Science*, 2006, **311**, 362–365.
- B. F. Mirjalilia, A. Bamoniri, A. Akbari and N. Taghavinia, *J. Iran. Chem. Soc.*, 2011, **8**, S129–S134.
- L. Kantam, S. Laha, J. Yadav and B. Sreedhar, *Tetrahedron Lett.*, 2006, **47**, 6213–6216.
- H. S. Sarvar and M. H. Sarvari, *J. Chem. Res.*, 2003, **2**, 176–178.
- M. Hosseini-Sarvari, *Tetrahedron*, 2008, **64**(23), 5459–5466.
- Y. Wang, L. Zhang, K. Deng, X. Chen and Z. Zou, *J. Phys. Chem. C*, 2007, **111**, 2709–2714.
- L. Hu, J. Wang, J. Zhang, Q. Zhang and Z. Liu, *RSC Adv.*, 2014, **4**, 420–427.
- B. F. Abdel-wahab, R. E. Khidre and A. A. Farahat, *ARKIVOC*, 2011, (i), 196–245.
- J. Senthilnathan and L. Philip, *Chem. Eng. J.*, 2010, **16**(1–2), 83–92.



## Paper

- 46 T. C. Jagadale, S. P. Takale, R. S. Sonawane, H. M. Joshi, S. I. Patil, B. B. Kale and S. B. Ogale, *J. Phys. Chem. C*, 2008, **11293**, 14595–14602.
- 47 S. Y. Choi, M. Mamak, N. Coombs, N. Chopra and G. A. Ozin, *Adv. Funct. Mater.*, 2004, **14**(4), 335–344.
- 48 X. Chen, X. Wang, Y. Hou, J. Huang, L. Wu and X. Fu, *J. Catal.*, 2008, **255**(1), 59–67.
- 49 M. Hema, A. Y. Arasi, P. Tamilselvi and R. Anbarasan, *Chem. Sci. Trans.*, 2012, **2**, 239–245.





# CHEMISTRY & BIOLOGY INTERFACE

An official Journal of ISCB, Journal homepage; [www.cbijournal.com](http://www.cbijournal.com)

## Synthesis, evaluation and molecular docking of 1,2,3-triazolyl chalcones as potential antifungal and antioxidant agents

Amol A. Nagargoje<sup>1,2</sup>, Satish V. Akolkar<sup>1</sup>, Mubarak H. Shaikh<sup>1,3</sup>, Dnyaneshwar D. Subhedar<sup>1</sup>, Jaiprakash N. Sangshetti<sup>4</sup>, Vijay M. Khedkar<sup>5</sup>, Bapurao B. Shingate\*<sup>1</sup>

<sup>1</sup>Department of Chemistry, Dr Babasaheb Ambedkar Marathwada University, Aurangabad, 431004, India

<sup>2</sup>Department of Chemistry, Khopoli Municipal Council College, Khopoli, 410203, India

<sup>3</sup>Department of Chemistry, Radhabai Kale Mahila Mahavidyalaya, Ahmednagar, 414001, India

<sup>4</sup>Department of Pharmaceutical Chemistry, Y. B. Chavan College of Pharmacy, Rafiq Zakaria Campus, Aurangabad, 431001, India

<sup>5</sup>Department of Pharmaceutical Chemistry, School of Pharmacy, Vishwakarma University, Pune, 411048, India

E-mail: \* [bapushingate@gmail.com](mailto:bapushingate@gmail.com) (B. B. Shingate)

\*Corresponding author. Tel.: (91-0240-2403312)

Received 15 June 2020, Accepted 30 June 2020

**Abstract:** A series of new 1,2,3-triazolyl chalcones were efficiently synthesized and screened for *in vitro* antifungal activity against five different fungal strains such as *Candida albicans*, *Fusarium oxysporum*, *Aspergillus flavus*, *Aspergillus niger* and *Cryptococcus neoformans*. All the synthesized chalcones displayed potential antifungal activity against most of the tested fungal strains. Especially, compounds **9b**, **9c**, **9d** and **9g** are the most active chalcones and displayed excellent MIC values as compared to standard antifungal drug Miconazole. Based on the structural similarity to known triazole inhibitors of sterol 14 $\alpha$ -demethylase (CYP51), molecular docking study was performed to gauge the binding affinity of these chalcones and gains an insight into the plausible mechanism of antifungal action. The synthesized chalcones were also evaluated for *in vitro* antioxidant activity. All compounds exhibited moderate to excellent antioxidant activity, particularly compounds **9e**, **9f**, **9g** and **9h** exhibited excellent antioxidant activity in comparison with standard butylated hydroxytoluene (BHT). Furthermore, the synthesized chalcones were analyzed for ADME properties and showed the potential to build up as good oral drug candidates.

**Keywords:** 1,2,3-triazole, Chalcone, Antifungal activity, Antioxidant activity, Molecular docking study, ADME prediction.

### 1. Introduction

The incidences of multidrug-resistant fungal

infections in recent years have increased dramatically and commonly seen in patients with weak immune systems<sup>[1]</sup>. An increasing number

of infections with stem cell transplantation, organ transplantation, chemotherapy, and human immunodeficiency virus increases invasive fungal infections [2]. The major pathogenic strains responsible for systematic fungal infections are *Candida albicans*, *Cryptococcus neoformans* and *Aspergillus fumigates* [3]. Fluconazole, Voriconazole, Itraconazole and Miconazole are some of the widely used azole based broad-spectrum antifungal drugs [4] (Figure 1). They displayed broad-spectrum antifungal potential against most of the filamentous fungi, however, some of them are not effective against invasive aspergillosis and also suffered from severe drug resistance [5]. Moreover, the broad use of existing antifungal drugs has caused severe drug resistance. Therefore, it is urgent to develop new antifungal agents with excellent activity against a variety of clinical fungal strains.

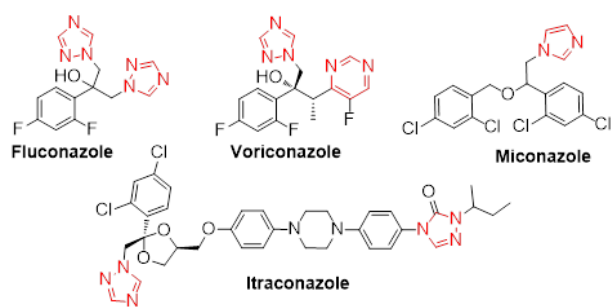


**Figure 1.** Known azole containing antifungal drugs

Many natural enzymatic and non-enzymatic antioxidants present in the human body that counteract the harmful effect of free radicals and other oxidants [6]. Although reactive oxygen species (ROS) are essential for various complex mechanisms of the organism's body in various diseases, the excessive production of ROS causes various diseases and oxidative stress. Antioxidant protects the cell from oxidative injury by neutralizing free radicals. Recently, it has been observed that reactive oxygen species participates in the mechanism of action of triazole containing antifungals [7]. It is important to elucidate possible association

among oxidative stress response and antifungal mechanism of action for developing new targets for novel antifungal agents by rational development of antifungal drugs.

Chalcones i.e.  $\alpha$ - $\beta$  unsaturated ketones are important pharmacophore in many natural and synthetic biologically active compounds [8-12]. It is used as an effective template in medicinal chemistry and drug discovery process [13,14]. The double bond in conjugation to carbonyl group is considered as responsible for the pharmacological effect in chalcones. Literature revealed that chalcones exhibited broad spectrum of biological activities like anticancer [15], antimalarial [16], antimicrobial [17], antioxidant [18], anti-inflammatory [13] etc.

1,2,3-triazole based natural and synthetic compounds are privileged scaffold in the drug discovery process with a broad spectrum of biological activities [19-25]. Molecular hybridization of chalcones with 1,2,3-triazole can be an efficient strategy to synthesize chemically diverse and biologically active conjugates. Recent literature revealed that 1,2,3-triazolyl chalcones displayed a broad spectrum of pharmacological activities [17,22,26-31] (Figure 2).

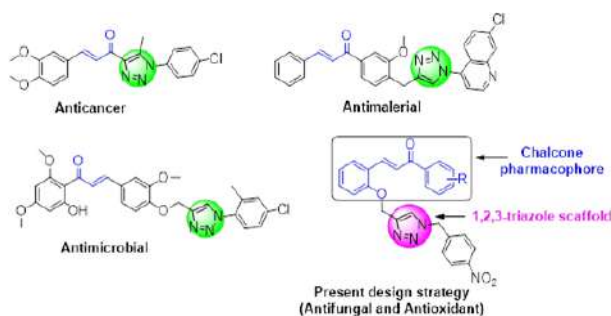


**Figure 2.** Known 1,2,3-triazolyl-chalcones and our design strategy

In search of the development of new active antifungal and antioxidant agents, combinatorial synthesis of 1,2,3-triazolyl chalcones has

been efficiently carried out by click chemistry and Aldol type condensation reaction. We were encouraged to design and synthesize 1,2,3-triazolyl chalcones from commercially available starting materials with high overall yield and evaluation of their antifungal and antioxidant activities.

Hence, keeping in view the urgent need of potential antifungal and antioxidant agents and in continuation to our earlier work on 1,2,3-triazole based bioactive compounds [21,23,24] and  $\alpha,\beta$ -unsaturated compounds [32–34], we report herein design, synthesis, molecular docking, ADME prediction and bio evaluation of some new 1,2,3-triazolyl chalcones as potential antifungal and antioxidant agents.

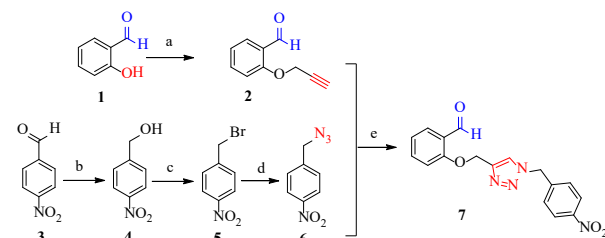
## 2 Result and discussion

### 2.1 Chemistry

In present work, we have described the syntheses of new substituted 1,2,3-triazolyl chalcones **9a-i** from commercially available starting materials (**Scheme 2**). 1,2,3-triazole based benzaldehyde **7** was formed by the fusion of benzyl azide and the terminal alkyne group of substituted benzaldehyde *via* the click chemistry approach (**Scheme 1**).

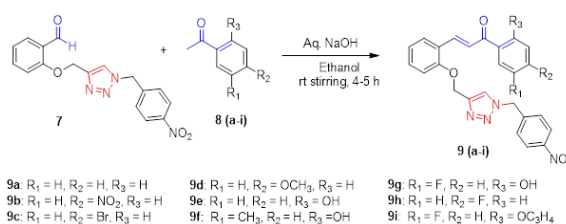
The treatment of *o*-hydroxy benzaldehyde **1** with propargyl bromide in the presence of  $K_2CO_3$  as a base in *N,N*-dimethylformamide (DMF) at room temperature afforded 2-(prop-2-yn-1-yloxy)benzaldehyde **2** in 89% yield (**Scheme 1**). The *p*-nitrobenzyl azide **6** was prepared from the *p*-nitrobenzaldehyde *via*  $NaBH_4$  reduction, bromination, and nucleophilic substitution reaction of sodium azide, according to the reported procedure [35]. (**Scheme 1**). Furthermore, 1,3-dipolar cycloaddition reaction of benzyl azide **6** and terminal alkyne group of benzaldehyde **2** using a catalytic amount of copper diacetate  $Cu(OAc)_2$  in *t*-BuOH- $H_2O$

(3:1) at room temperature for 20 h afforded regioselective 1,4-disubstituted-1,2,3-triazole incorporated benzaldehyde **7** in 88% yield (**Scheme 1**).



**Scheme 1.** Reagents and conditions: (a) Propargyl bromide,  $K_2CO_3$ , DMF, r.t., 2.5 h; (b)  $NaBH_4$ , methanol, 0 °C to r.t., 2 h; (c)  $PBr_3$ ,  $CH_2Cl_2$ , 0 °C, 0.5 h; (d)  $NaN_3$ , acetone: $H_2O$  (3:1), r.t., 24 h; (e)  $Cu(OAc)_2$  (20 mol%), *t*-BuOH/ $H_2O$  (3:1), r.t., 19-27 h.

Finally, newly synthesized 1,2,3-triazole based benzaldehyde **7** was condensed with various substituted acetophenone (**8a-i**) in aqueous NaOH, resulted into the corresponding 1,2,3-triazolyl chalcones (**9a-i**) in quantitative isolated yield (85-90%) (**Scheme 2**).



**Scheme 2.** Synthesis of 1,2,3-triazolyl-chalcones

The structures of 1,2,3-triazolyl-chalcones **9a-i** were confirmed by FT-IR,  $^1H$  NMR,  $^{13}C$  NMR and LC/ESI-MS analysis. Structures of the synthesized 1,2,3-triazolyl-chalcones are given below in **Figure 3**.



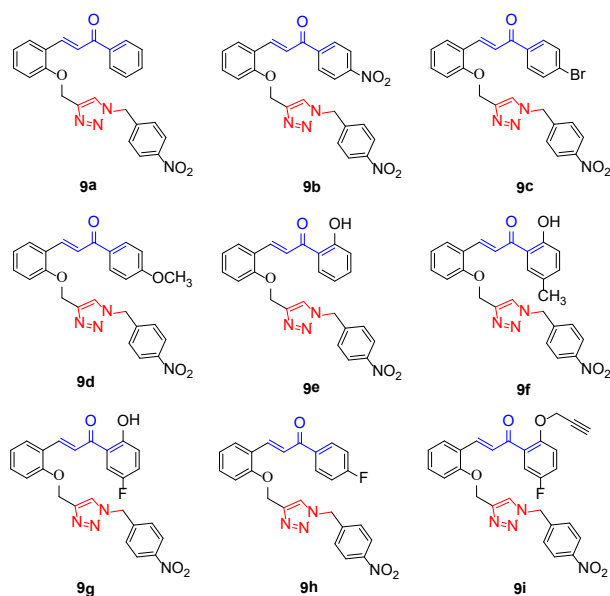


**Figure 3.** Structures of 1,2,3-triazolyl chalcones

## 2.2 Antifungal activity

All the synthesized 1,2,3-triazolyl-chalcones were screened for their *in vitro* antifungal activity. The antifungal activity was evaluated against five different pathogenic fungal strains such as *Candida albicans*, *Fusarium oxysporum*, *Aspergillus flavus*, *Aspergillus niger*, and *Cryptococcus neoformans*. Minimum inhibitory concentration (MIC) values were determined using a standard agar plate method [36,37]. MIC value of an antimicrobial compound is its lowest concentration that prevents visible growth of the microorganism. It is a measure of the effective ability of the antimicrobial against the concerned microbe. Miconazole was used as a standard for the comparison of antifungal activity. Dimethyl sulfoxide was used as solvent control.

**Table 1.** *In vitro* antifungal, antioxidant data and *in silico* molecular docking score of 1,2,3-triazolyl chalcones (9a-i).

Entry	Antifungal Activity MIC ( $\mu\text{g/mL}$ )					Antioxidant activity IC <sub>50</sub> ( $\mu\text{g/mL}$ )	Molecular Docking Score
	CA	FO	AF	AN	CN		
9a	25	25	25	25	6.25	50.17 $\pm$ 0.35	-7.944
9b	6.25	12.5	12.5	25	12.5	40.32 $\pm$ 0.46	-8.947
9c	12.5	50	12.5	50	12.5	27.11 $\pm$ 0.25	-8.154
9d	12.5	12.5	25	25	12.5	21.12 $\pm$ 0.19	-8.447
9e	25	12.5	50	50	12.5	16.34 $\pm$ 0.91	-7.902
9f	12.5	25	50	75	12.5	15.66 $\pm$ 0.45	-8.015
9g	25	25	50	50	50	16.37 $\pm$ 0.87	-7.458
9h	25	25	75	50	100	16.06 $\pm$ 0.18	-7.263
9i	75	50	75	50	50	31.46 $\pm$ 0.88	-7.039
MA	25	25	12.5	25	25	-	-
BHT	-	-	-	-	-	16.47 $\pm$ 0.18	-

CA-*Candida albicans*, FO-*Fusarium oxysporum*, AF-*Aspergillus flavus*, AN-*Aspergillus Niger*, CN-*Cryptococcus neoformans*, MA- Miconazole, BHT- Butoxy hydroxy toluene, Values are the average of three readings (n=3)  $\pm$  standard deviation

MIC values of the tested compounds are presented in **Table 1**. Most of the newly synthesized 1,2,3-triazolyl chalcones were found to show excellent antifungal activity as compared to standard antifungal drug Miconazole. From the antifungal activity data (**Table 1**), it is observed that almost all the synthesized chalcones were displayed promising antifungal activity against fungal strain *C. Albicans*. Particularly, chalcones **9b**, **9c**, **9d**, and **9g** are the most active among all tested compounds against most of the fungal strains. Structure-activity relationship revealed that introduction of nitro (-NO<sub>2</sub>) group at *para*- position of acetophenone moiety in compound **9b** showed a significant rise in activity as compared to **9a** (activity increases by two-fold as reflected in lowered MIC value). Compound **9a** is equipotent to Miconazole against *C. albicans* (MIC value 25  $\mu\text{g/mL}$ ), *A. Niger* (MIC value 25  $\mu\text{g/mL}$ ), *F. oxysporum* (MIC value 25  $\mu\text{g/mL}$ ), *A. flavus* (MIC value 25  $\mu\text{g/mL}$ ) and most active than Miconazole in case of fungal strain *C. neoformans* (MIC value 12.5

$\mu\text{g/mL}$ ). Introduction of alkyne group in case of **9i** reduces the antifungal activity compared to other tested compounds. Introduction of electron-withdrawing groups and halogens on acetophenone shows a significant enhancement in an activity. Graphical representation of antifungal activity data of the synthesized compounds is represented in **figure 4**.

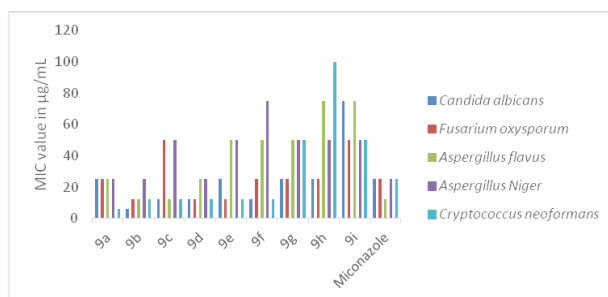


**Figure 4.** Antifungal activity of synthesized analogues as compared to standard Miconazole

### 2.3 Antioxidant activity

All the synthesized chalcones displayed good to moderate radical scavenging activity when compared with the standard drug BHT (**Table 1**). Particularly compounds **9e**, **9f**, **9g** and **9h** exhibit significant  $\text{IC}_{50}$  values ( $\text{IC}_{50} = 16.34 \pm 0.91$ ,  $15.66 \pm 0.45$ ,  $16.37 \pm 0.87$ ,  $16.06 \pm 0.18$  in  $\mu\text{g/mL}$  respectively) as compared to standard antioxidant BHT. Structure-activity data revealed that the hydroxy group is important for the enhancement of antioxidant potential as reflected in  $\text{IC}_{50}$  values. Also, the substitution of electron-donating groups on acetophenone increases the antioxidant activity of 1,2,3-triazole substituted chalcones as compared to standard antioxidant BHT. The antioxidant activity of these compounds may be related to their redox properties, which allow them to act as reducing agents or hydrogen atom donors and scavenge-free radicals.

### 2.4 Molecular docking

Molecular docking study revealed the binding

orientations of 1,2,3-triazolyl-chalcones in the active sites of CYP51. It was observed that all the synthesized chalcones could snugly fit into the active site of CYP51 with varying degrees of affinities at co-ordinates close to a native ligand. Their docking scores varied from -8.947 for the most active analogue to -7.039 for moderately active with average docking score of -7.907 signifying a promising binding affinity towards CYP51 (**Table 2**, **Fig 5** and **Fig 6-13**). To gain a better understanding on the potency and types of interactions contributing to the enhanced binding affinity towards the target, a detailed investigation of the per-residue interactions for the most active analogues (**9b**, **9c**, **9d** and **9f**) was carried out which is elaborated in detail for one of the most active compound **9b** while it summarized in **Table 2** for other active compounds (**9c-Fig 6**, **9d- Fig 7** and **9f- Fig 9**).

The best-docked conformation of **9b** was seen to be deeply embedded into the active pocket of sterol 14 $\alpha$ -demethylase (CYP51). The lower interaction energy (Glide binding energy -62.896 kcal/mol, Glide score of from -8.947) rationalizes the tighter binding of this chalcone analogue (**Figure. 5**) into the CYP51 active site.

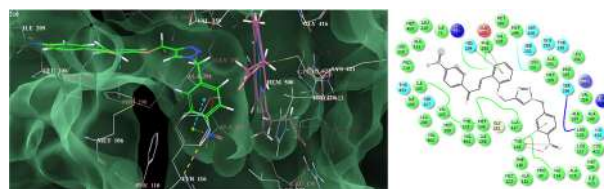


**Figure 5:** Binding mode of **9b** into the active site of sterol 14 $\alpha$ -demethylase (CYP51) (on the right side: the pink lines signify hydrogen bonding interaction, green lines signify  $\pi$ - $\pi$  stacking while red line represent cation- $\pi$  stacking interactions)

The per-residue interaction analysis revealed that the enzyme-inhibitor complex was stabilized by a series of favourable van der Waals interactions observed with Hem500 (-6.776 kcal/mol), Val461 (-2.929 kcal/mol), Val359 (-2.431 kcal/

**Table 2.** The per-residue interaction analysis based on molecular docking for 1,2,3-triazolyl-chalcones with sterol 14 $\alpha$ -demethylase (CYP51).

Code	Docking Score	Glide Interaction Energy (kcal/mole)	Per-Residues interactions			$\pi$ - $\pi$ / Cation- $\pi$ Stacking
			Van der Waals (kcal/mol)	Columbic (kcal/mol)	H-bond (Å)	
<b>9b</b>	-8.947	-62.896	Hem 500(-6.776), Val461 (-2.929), Met460 (-3.151), Thr459 (-2.898), His458 (-2.543), Met360 (-3.233), Val359 (-2.431), Met358 (-2.981), Leu356 (-2.779), Thr295 (-2.358), His294 (-2.277), Ala291 (-3.531), Phe290 (-3.236), Ala287 (-2.528), Pro210 (-2.614), Ile209 (-2.643), Leu208 (-3.157), Glu205 (-2.827), Leu127 (-2.789), Tyr116 (-3.788), Phe110 (-2.735), Met106 (-3.434), Ile105 (-2.742), Tyr103 (-2.39), Val102 (-2.825)	Hem500 (-3.959), Arg361 (-2.414), Phe290 (-2.362), Leu208 (-2.522), Glu205 (-3.569), Arg124 (-2.223), Ile105 (-2.293), Val102 (-3.201)	Tyr116 (2.65)	$\pi$ - $\pi$ Stacking: His294 (2.168), Phe290 (2.374), Tyr116 (2.651) Cation- $\pi$ Stacking: Tyr116 (2.651)
<b>9c</b>	-8.154	-60.358	Hem500 (-6.458), Val461 (-2.463), Met460 (-2.793), Thr459 (-2.264), His458 (-2.129), Met360 (-2.233), Val359 (-2.143), Met358 (-2.280), Leu356 (-2.261), Thr295 (-2.157), His294 (-2.082), Ala291 (-2.191), Phe290 (-2.467), Ala287 (-2.269), Pro210 (-2.600), Ile209 (-2.204), Leu208 (-3.072), Glu205 (-2.523), Leu127 (-2.114), Tyr116 (-2.878), Phe110 (-2.034), Met106 (-3.247), Ile105 (-2.558), Tyr103 (-2.095), Val102 (-2.216)	Hem500 (-3.548), Arg361 (-2.239), Phe290 (-2.203), Leu208 (-2.136), Glu205 (-3.122), Arg124 (-2.183), Ile105 (-2.150), Val102 (-2.872)	Tyr116 (2.50)	$\pi$ - $\pi$ Stacking: His294 (2.271), Phe290 (2.303), Tyr116 (2.498) Cation- $\pi$ Stacking: Tyr116 (2.498)
<b>9d</b>	-8.447	-61.216	Hem500 (-6.702), Val461 (-2.751), Met460 (-2.901), Thr459 (-2.727), His458 (-2.241), Met360 (-2.929), Val359 (-2.230), Met358 (-2.328), Leu356 (-2.388), Thr295 (-2.377), His294 (-2.191), Ala291 (-2.796), Phe290 (-2.866), Ala287 (-2.324), Pro210 (-2.628), Ile209 (-2.315), Leu208 (-3.096), Glu205 (-2.617), Leu127 (-2.187), Tyr116 (-2.892), Phe110 (-2.128), Met106 (-3.338), Ile105 (-2.729), Tyr103 (-2.123), Val102 (-2.221)	Hem500 (-3.667), Arg361 (-2.548), Phe290 (-2.226), Leu208 (-2.254), Glu205 (-3.417), Arg124 (-1.110), Ile105 (-2.025), Val102 (-2.442)	Tyr116 (2.63)	$\pi$ - $\pi$ Stacking: His294 (2.175), Phe290 (2.369), Tyr116 (2.632) Cation- $\pi$ Stacking: Tyr116 (2.632)
<b>9f</b>	-8.015	-59.091	Hem500 (-5.137), Val461 (-2.644), Met460 (-2.481), Thr459 (-2.282), His458 (-2.230), Met360 (-2.233), Val359 (-1.834), Met358 (-1.928), Leu356 (-2.037), Thr295 (-2.171), His294 (-1.871), Ala291 (-1.897), Phe290 (-2.569), Ala287 (-2.022), Pro210 (-1.911), Ile209 (-1.798), Leu208 (-2.316), Glu205 (-1.899), Leu127 (-2.017), Tyr116 (-2.838), Phe110 (-1.969), Met106 (-2.010), Ile105 (-2.167), Tyr103 (-2.154), Val102 (-2.111)	Hem500 (-2.299), Arg361 (-1.324), Phe290 (-1.732), Leu208 (-2.001), Glu205 (-2.970), Arg124 (-1.537), Ile105 (-2.023), Val102 (-2.219)	--	$\pi$ - $\pi$ Stacking: His294 (2.126), Phe290 (2.549), Tyr116 (3.176) Cation- $\pi$ Stacking: Tyr116 (3.176)

mol), Leu356 (-2.779 kcal/mol), Thr295 (-2.358 kcal/mol), Ala291 (-3.531 kcal/mol), Ala287 (-2.528 kcal/mol), Leu127 (-2.789 kcal/mol), Tyr116 (-3.788 kcal/mol), Phe110 (-2.735 kcal/mol) and Met106 (-3.434 kcal/mol) residues through 1-(4-nitrobenzyl)-1*H*-1,2,3-triazole core while the other half of the molecule i.e. 4-nitro-phenylprop-2-en-1-one was seen to be engaged significant van der Waals interactions with Met460 (-3.151 kcal/mol), Thr459 (-2.898 kcal/mol), His458 (-2.543 kcal/mol), Pro210 (-2.614 kcal/mol), Ile209 (-2.643 kcal/mol), Leu208 (-3.157 kcal/mol), Ile105 (-2.742 kcal/mol), Tyr103 (-2.39 kcal/mol) and Val102 (-2.825 kcal/mol) residues. The central phenyl ring linking these two halves of the molecule also showed very favourable van der Waals interactions with Met360 (-3.233), Met358 (-2.981), His294 (-2.277), Phe290 (-3.236) and Glu205 (-2.827) residues. The enhanced binding affinity observed for **9b** is also attributed to significant electrostatic interactions observed with Hem500 (-3.959 kcal/mol), Arg361 (-2.414 kcal/mol), Phe290 (-2.362 kcal/mol), Leu208 (-2.522 kcal/mol), Glu205 (-3.569 kcal/mol), Arg124 (-2.223 kcal/mol), Ile105 (-2.293 kcal/mol) and Val102 (-3.201 kcal/mol) residues of active site. Since CYP51 is a Heme enzyme, it is expected for a ligand to show significant steric and electrostatic interactions with Heme moiety and in the present study, it was consistently observed for all the chalcone analogues investigated. Furthermore, **9b** showed a very prominent hydrogen bonding interactions via the nitro (-NO<sub>2</sub>) functional group with Tyr116 residue having a bonding distance of 2.65Å. The compound was also seen to be engaged in very close pi stacking interactions, firstly a pi-pi stacking interaction was observed between the central phenyl ring and His294 (2.168Å), Phe290 (2.374Å) residues and secondly through the 4-nitro phenyl ring and Tyr116 (2.651Å) residue. A Cation-Pi stacking type of interaction was also observed through the same nitro functional group and Tyr116 (2.651Å) residue.

While the non-bonded interactions (steric and electrostatic) were observed to be the major driving force for mechanical interlocking of the chalcone analogues, the high binding affinity was strongly facilitated by these hydrogen bonding and Pi-stacking interactions which serve as an "anchor" to guide the orientation of inhibitor into the 3D space of enzyme's active site.

Overall, the binding affinity data derived from the docking study suggest that the 1,2,3-triazolyl chalcones possess a promising affinity for the fungal CYP51 enzyme qualifying them as a pertinent starting point for structure-based lead optimization to generate compounds with high selectivity and potency against CYP51.

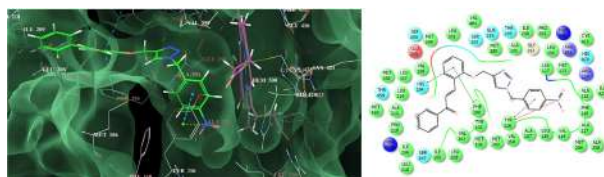


**Figure 6:** Binding mode of **9a** into the active site of sterol 14 $\alpha$ -demethylase (CYP51) (on the right side: the pink lines signify hydrogen bonding interaction, green lines signify  $\pi$ - $\pi$  stacking while red line represent cation-pi stacking interactions)

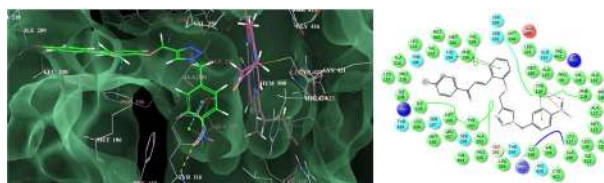


**Figure 7:** Binding mode of **9c** into the active site of sterol 14 $\alpha$ -demethylase (CYP51) (on the right side: the pink lines signify hydrogen bonding interaction, green lines signify  $\pi$ - $\pi$  stacking while red line represent cation-pi stacking interactions)



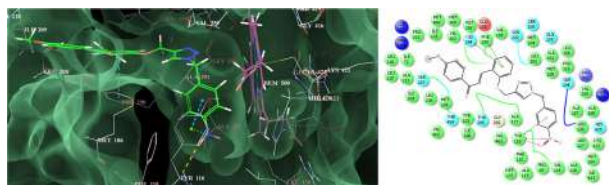


**Figure 8:** Binding mode of **9d** into the active site of sterol 14 $\alpha$ -demethylase (CYP51) (on the right side: the pink lines signify hydrogen bonding interaction, green lines signify  $\pi$ - $\pi$  stacking while red line represent cation- $\pi$  stacking interactions)

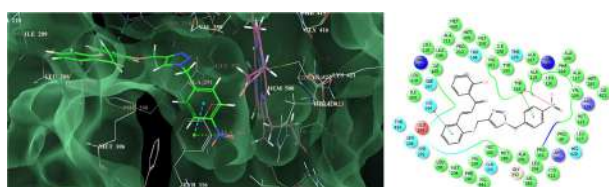


**Figure 9:** Binding mode of **9e** into the active site of sterol 14 $\alpha$ -demethylase (CYP51) (on the right side: the pink lines signify hydrogen bonding interaction, green lines signify  $\pi$ - $\pi$  stacking while red line represent cation- $\pi$  stacking interactions)

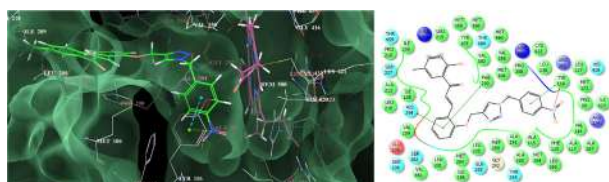


**Figure 10:** Binding mode of **9f** into the active site of sterol 14 $\alpha$ -demethylase (CYP51) (on the right side: the pink lines signify hydrogen bonding interaction, green lines signify  $\pi$ - $\pi$  stacking while red line represent cation- $\pi$  stacking interactions)

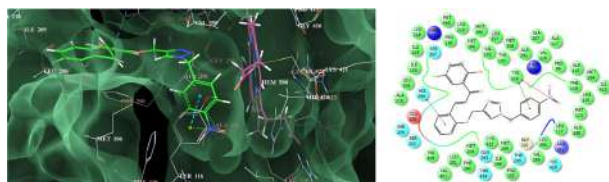


**Figure 11:** Binding mode of **9g** into the active site of sterol 14 $\alpha$ -demethylase (CYP51) (on the right side: the pink lines signify hydrogen

bonding interaction, green lines signify  $\pi$ - $\pi$  stacking while red line represent cation- $\pi$  stacking interactions)



**Figure 12:** Binding mode of **9h** into the active site of sterol 14 $\alpha$ -demethylase (CYP51) (on the right side: the pink lines signify hydrogen bonding interaction, green lines signify  $\pi$ - $\pi$  stacking while red line represent cation- $\pi$  stacking interactions)

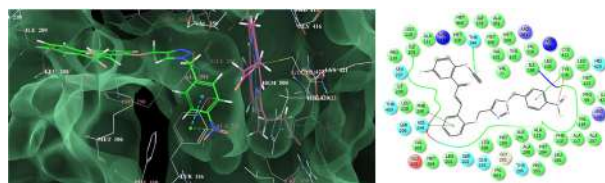


**Figure 13:** Binding mode of **9i** into the active site of sterol 14 $\alpha$ -demethylase (CYP51) (on the right side: the pink lines signify hydrogen bonding interaction, green lines signify  $\pi$ - $\pi$  stacking while red line represent cation- $\pi$  stacking interactions)

## 2.5 ADME Properties

Pharmacokinetic parameters of the synthesized 1,2,3-triazolyl-chalcones are summarised in **table 3**. It is observed that only compounds **9c** and **9i** violated Lipinski's rule of five ( $\text{miLogP} \leq 5$ ), remaining all other compounds did not show more than one violation of Lipinski's rule of five. Also, compounds exhibited a good % ABS (% absorption) ranging from 57.70% to 73.51%. Hence, All the tested compounds except **9c** and **9i** followed the criteria for orally active drug and therefore, these newly synthesized 1,2,3-triazolyl-chalcones may have a good potential to develop as good oral active drug candidates.



**Table 3.** Pharmacokinetic parameters important for good oral bioavailability

Entry	%ABS	n-atoms	TPSA (A <sup>2</sup> )	n-ROTB	MV	MW	mllog p	n-ON	n-OHNH	Lipinski's violations	Drug-likeness model score
Rule	-	-	-	-	-	<500	≤5	<10	<5	≤1	-
<b>9a</b>	73.51	33	102.85	09	387.65	440.46	4.94	8	0	0	-0.50
<b>9b</b>	57.70	36	148.67	10	410.98	485.46	4.90	11	0	1	-0.44
<b>9c</b>	73.51	34	102.85	09	405.53	519.36	5.75	08	0	2	-0.35
<b>9d</b>	70.33	35	112.08	10	413.19	470.49	5.00	09	0	1	-0.35
<b>9e</b>	66.54	34	123.08	09	395.66	456.46	4.88	09	1	0	+0.25
<b>9f</b>	66.54	35	123.08	09	412.23	470.49	5.31	09	1	1	+0.00
<b>9g</b>	66.54	35	123.08	09	400.60	474.45	5.02	09	1	1	+0.16
<b>9h</b>	73.51	34	102.85	09	392.58	458.45	5.11	08	0	1	-0.19
<b>9i</b>	70.33	38	112.08	11	440.62	512.50	5.23	09	0	2	-0.03

ABS: absorption; TPSA: topological polar surface area; n-ROTB: number of rotatable bonds; MV: molecular volume; MW: molecular weight; lmiLog P: logarithm of partition coefficient; n-ON: number of hydrogen bond acceptors; n-OHNH: number of hydrogen bonds donors.

### 3 Conclusion

In conclusion, we have synthesized some new 1,2,3-triazolyl-chalcones and subsequently screened for their *in vitro* antifungal and antioxidant activity. Most of the synthesized chalcones were displayed potential antifungal activity against most of the fungal strain used in the experiment which indicates the broad-spectrum antifungal activity of the synthesized chalcones. Molecular docking studies further supported the strong inhibitory activity which was further enriched using per-residue interaction analysis that could provide a deeper insight into the specific residues and their associated type of thermodynamic interactions influencing the binding affinity for the crucial fungal enzyme CYP51. Also, synthesized 1,2,3-triazolyl-chalcones showed potential antioxidant properties. Furthermore, ADME

prediction shows better chances of these derivatives to evolve as a potential antifungal and antioxidant drug candidates. This inference derived from the *in vitro*/*in silico* experiments is now fruitfully utilized to carry out site-specific modifications around the scaffold to improve the selectivity and potency of the 1,2,3-triazolyl-chalcones.

### 4 Experimental

#### 4.1 Analytical methods

All chemicals and reagents used were of analytical grade. The progress of the reactions was monitored by thin-layer chromatography (TLC) on aluminium plates coated with silica gel 60 F<sub>254</sub>, 0.25 mm thickness (Merck). The detection of the components was made by exposure to iodine vapours or UV light. Melting points were determined by an open capillary method and are uncorrected. <sup>1</sup>H-NMR spectra were recorded in DMSO-*d*<sub>6</sub> on a Bruker DRX-200 MHz spectrometer. <sup>13</sup>C NMR spectra were recorded in DMSO-*d*<sub>6</sub> on a Bruker DRX-100 MHz instrument. IR spectra were recorded using a Bruker ALPHA ECO-ATR FTIR spectrometer. Mass spectra were recorded on

LC/ESI-MS spectrometer.

## 4.2 Chemistry

### General procedure for the preparation of 1,2,3-triazolyl-chalcones:

A mixture of 1,2,3-triazole incorporated benzaldehyde **7** (1 mmol) and various substituted acetophenone (**8a-i**) (1 mmol) in ethanolic NaOH was taken in a 50 mL round bottom flask, equipped with a mechanical stirrer. The reaction mixture was stirred at room temperature for 4-5hrs. The progress of the reaction was monitored by TLC. The reaction mixture was poured into 50 mL ice-water and the obtained solid was filtered, dried and recrystallized from ethanol-DMF to obtain a dark brown solid product (**Scheme 2, 9a-i**).

### Spectral data of synthesized compounds:

#### 4.2.1 (*E*)-3-(2-((1-(4-Nitrobenzyl)-1H-1,2,3-triazol-4-yl)methoxy)phenyl)-1-phenylprop-2-en-1-one (**9a**):

Yellow colored solid, Yield: 86%, mp. 178-180 °C; IR (cm<sup>-1</sup>): 1655 (C=O), 1588 (C=C), 1506 (C=C Ar), 1341 (N-O), 999 (N-N); <sup>1</sup>H NMR (200 MHz, DMSO-*d*<sub>6</sub> ppm): 8.83 (s, 1H), 8.66 (d, *J* = 8.0 Hz, 2H), 8.30 (d, *J* = 8.0 Hz, 5H), 7.96 (d, *J* = 8.0 Hz, 4H), 7.66 (d, *J* = 8.0 Hz, 4H), 6.24 (s, 2H), 5.72 (s, 2H); <sup>13</sup>C NMR (100 MHz, DMSO-*d*<sub>6</sub> ppm): 191.0, 158.3, 148.3, 144.9, 143.7, 140.9, 138.3, 133.0, 130.4, 128.8, 128.5, 124.5, 125.0, 122.3, 122.2, 121.9, 115.7, 58.0 and 50.2; ESI-MS: Calcd for C<sub>25</sub>H<sub>20</sub>N<sub>4</sub>NaO<sub>4</sub> [M+Na]<sup>+</sup>, 463.4, found: 463.0

#### 4.2.2 (*E*)-3-(2-((1-(4-Nitrobenzyl)-1H-1,2,3-triazol-4-yl)methoxy)phenyl)-1-(4-nitrophenyl)prop-2-en-1-one (**9b**):

Yellow colored solid, Yield: 85%, mp. 182-184 °C; IR (cm<sup>-1</sup>): 1592 (C=O), 1511 (C=C), 1392 (C=C Ar), 1339 (N-O), 1009 (N-N); <sup>1</sup>H NMR (200 MHz, DMSO-*d*<sub>6</sub> ppm): 8.88 (s, 1H), 8.72

(d, *J* = 8.0 Hz, 3H), 8.35 (d, *J* = 8.0 Hz, 4H), 8.01 (d, *J* = 8.0 Hz, 3H), 7.70 (d, *J* = 8.0 Hz, 4H), 6.28 (s, 2H), 5.76 (s, 2H); <sup>13</sup>C NMR (100 MHz, DMSO-*d*<sub>6</sub> ppm): 191.6, 158.9, 151.3, 148.9, 145.5, 144.3, 143.8, 141.5, 129.7, 129.4, 129.2, 125.1, 124.6, 122.8, 116.3, 58.6 and 50.8; LC-MS: Calcd for C<sub>25</sub>H<sub>20</sub>N<sub>5</sub>O<sub>6</sub> [M+H]<sup>+</sup>, 486.5, found: 486.2

#### 4.2.3 (*E*)-1-(4-Bromophenyl)-3-(2-((1-(4-nitrobenzyl)-1H-1,2,3-triazol-4-yl)methoxy)phenyl)prop-2-en-1-one (**9c**):

Yellow colored solid, Yield: 85%, mp. 190-193 °C; IR (cm<sup>-1</sup>): 1655 (C=O), 1587 (C=C), 1407 (C=C Ar), 1343 (N-O), 998 (N-N); <sup>1</sup>H NMR (200 MHz, DMSO-*d*<sub>6</sub> ppm): 8.79 (s, 1H), 8.43 - 8.35 (m, 4H), 7.93-7.73 (m, 9H), 7.48 (t, *J* = 8.0 Hz, 1H) 6.08 (s, 2H), 5.72 (s, 2H); <sup>13</sup>C NMR (100 MHz, DMSO-*d*<sub>6</sub> ppm): 188.0, 155.3, 137.9, 133.6, 129.1, 127.4, 126.7, 125.8, 125.7, 125.6, 125.4, 121.5, 119.4, 119.2, 118.9, 112.7, 55.0 and 47.2; ESI-MS: Calcd for C<sub>25</sub>H<sub>19</sub>BrN<sub>4</sub>NaO<sub>4</sub> [M+Na]<sup>+</sup>, 542.3, found: 542.0

#### 4.2.4 (*E*)-1-(4-Methoxyphenyl)-3-(2-((1-(4-nitrobenzyl)-1H-1,2,3-triazol-4-yl)methoxy)phenyl)prop-2-en-1-one (**9d**):

Yellow colored solid, Yield: 87%, mp. 175-178 °C; IR (cm<sup>-1</sup>): 1655 (C=O), 1588 (C=C), 1477 (C=C Ar), 1340 (N-O), 1014 (N-N); <sup>13</sup>C NMR (100 MHz, DMSO-*d*<sub>6</sub> ppm): 187.8, 160.5, 155.1, 145.1, 141.7, 140.5, 137.7, 127.6, 125.6, 125.4, 121.3, 119.2, 119.0, 112.5, 110.7, 54.8, 52.8 and 47.0; LC-MS: Calcd for C<sub>26</sub>H<sub>23</sub>N<sub>4</sub>O<sub>5</sub> [M+H]<sup>+</sup>, 471.5, found: 471.2

#### 4.2.5 (*E*)-1-(2-Hydroxyphenyl)-3-(2-((1-(4-nitrobenzyl)-1H-1,2,3-triazol-4-yl)methoxy)phenyl)prop-2-en-1-one (**9e**):

Yellow colored solid, Yield: 86%, mp. 198-200 °C; IR (cm<sup>-1</sup>): 1766 (C=O), 1594 (C=C), 1402 (C=C Ar), 1343 (N-O), 1008 (N-N); <sup>1</sup>H NMR (200 MHz, DMSO-*d*<sub>6</sub> ppm): 8.83 (s, 1H), 8.67 (d, *J* = 8.0 Hz, 2H), 8.30 (d, *J* = 8.0 Hz, 2H), 7.96 (d, *J* = 8.0 Hz, 4H), 7.65 (d, *J* = 8.0 Hz, 6H),

6.23 (s, 2H), 5.71 (s, 2H);  $^{13}\text{C}$  NMR (100 MHz, DMSO- $d_6$  ppm): 190.0, 158.7, 155.1, 145.1, 141.7, 140.5, 136.7, 132.3, 127.2, 126.8, 125.6, 125.5, 125.3, 121.3, 119.8, 119.1, 119.0, 116.6, 114.7, 112.5, 54.7 and 47.0; LC-MS: Calcd for  $\text{C}_{25}\text{H}_{21}\text{N}_4\text{O}_5$   $[\text{M}+\text{H}]^+$ , 457.5, found: 457.2

**4.2.6 (E)-1-(2-Hydroxy-5-methylphenyl)-3-(2-((1-(4-nitrobenzyl)-1H-1,2,3-triazol-4-yl)methoxy)phenyl)prop-2-en-1-one (9f):**

Yellow coloured solid, Yield: 88%, mp. 188-192 °C; IR ( $\text{cm}^{-1}$ ): 1660 (C=O), 1515 (C=C), 1433 (C=C Ar), 1344 (N-O), 1044 (N-N);  $^1\text{H}$  NMR (200 MHz, DMSO- $d_6$  ppm): 8.41 (s, 1 H), 8.25 (d,  $J = 8.0$  Hz, 3H), 7.88 (d,  $J = 8.0$  Hz, 4H), 7.54 (d,  $J = 8.0$  Hz, 3H), 7.24 (d,  $J = 8.0$  Hz, 3H), 5.81 (s, 2H), 5.29 (s, 2H), 1.90 (s, 3H);  $^{13}\text{C}$  NMR (100 MHz, DMSO- $d_6$  ppm): 186.4, 153.0, 152.2, 142.2, 138.8, 137.6, 133.8, 128.9, 124.9, 124.3, 123.3, 122.7, 122.6, 122.5, 118.4, 117.4, 116.9, 116.3, 116.1, 112.5, 109.6, 51.9, 44.1 and 15.1; LC-MS: Calcd for  $\text{C}_{26}\text{H}_{23}\text{N}_4\text{O}_5$   $[\text{M}+\text{H}]^+$ , 471.5, found: 471.2

**4.2.7 (E)-1-(5-Fluoro-2-hydroxyphenyl)-3-(2-((1-(4-nitrobenzyl)-1H-1,2,3-triazol-4-yl)methoxy)phenyl)prop-2-en-1-one (9g):**

Yellow coloured solid, Yield: 87%, mp. 177-180 °C; IR ( $\text{cm}^{-1}$ ): 1659 (C=O), 1593 (C=C), 1440 (C=C Ar), 1337 (N-O), 1026 (N-N);  $^1\text{H}$  NMR (400 MHz, DMSO- $d_6$  ppm): 8.60 (d,  $J = 8.0$  Hz, 3H), 8.34-8.21 (m, 4H), 7.90 (d,  $J = 8.0$  Hz, 4H), 7.51 (d,  $J = 8.0$  Hz, 3H), 6.15 (s, 2H), 5.68 (s, 2H);  $^{13}\text{C}$  NMR (100 MHz, DMSO- $d_6$  ppm): 192.5, 158.3, 157.8, 155.5, 148.3, 144.9, 143.7, 139.9, 130.4, 128.8, 128.5, 124.5, 123.0, 122.3, 121.8, 120.7, 119.7, 118.3, 115.7, 58.0 and 50.2; ESI-MS: Calcd for  $\text{C}_{25}\text{H}_{20}\text{FN}_4\text{O}_5$   $[\text{M}+\text{H}]^+$ , 475.4, found: 476.0

**4.2.8 (E)-1-(4-Fluorophenyl)-3-(2-((1-(4-nitrobenzyl)-1H-1,2,3-triazol-4-yl)methoxy)phenyl)prop-2-en-1-one (9h):**

Yellow colored solid, Yield: 90%, mp. 197-200 °C; IR ( $\text{cm}^{-1}$ ): 1655 (C=O), 1597 (C=C), 1445

(C=C Ar), 1333 (N-O), 1008 (N-N);  $^{13}\text{C}$  NMR (100 MHz, DMSO- $d_6$  ppm): 191.0, 165.9, 163.8, 158.3, 148.3, 144.9, 143.7, 140.9, 134.9, 131.0, 130.4, 128.8, 128.5, 124.5, 122.3, 121.9, 116.0, 115.7, 58.0 and 50.2; LC-MS: Calcd for  $\text{C}_{25}\text{H}_{19}\text{FN}_4\text{O}_4$   $[\text{M}]^+$ , 458.4, found: 458.1

**4.2.9 (E)-1-(5-Fluoro-2-(prop-2-yn-1-yloxy)phenyl)-3-(2-((1-(4-nitrobenzyl)-1H-1,2,3-triazol-4-yl)methoxy)phenyl)prop-2-en-1-one (9i):**

Yellow colored solid, Yield: 86%, mp. 200-204 °C; IR ( $\text{cm}^{-1}$ ): 1674 (C=O), 1564 (C=C), 1412 (C=C Ar), 1341 (N-O), 1008 (N-N);  $^{13}\text{C}$  NMR (100 MHz, DMSO- $d_6$  ppm): 190.6, 160.9, 158.8, 158.3, 154.0, 148.3, 144.9, 143.7, 139.9, 130.4, 128.8, 128.5, 126.8, 124.5, 123.0, 122.3, 120.1, 119.6, 118.6, 115.7, 80.0, 78.8, 59.7, 58.0 and 50.2; ESI-MS: Calcd for  $\text{C}_{28}\text{H}_{21}\text{FN}_4\text{NaO}_5$   $[\text{M}+\text{Na}]^+$ , 535.5, found: 535.0

**4.3 Antifungal activity assay**

Antifungal activity was determined by standard agar dilution method as per CLSI (formerly, NCCLS) guidelines<sup>[38]</sup>. The synthesized compounds and standard Miconazole were dissolved in DMSO solvent. The medium yeast nitrogen base was dissolved in phosphate buffer pH 7 and it was autoclaved at 110°C for 10 min. With each set a growth control without the antifungal agent and solvent control DMSO were included. The fungal strains were freshly sub cultured onto Sabouraud dextrose agar (SDA) and incubated at 25°C for 72 h. The fungal cells were suspended in sterile distilled water and diluted to get 10<sup>5</sup> cells/mL. Ten microliters of standardized suspension was inoculated onto the control plates and the media incorporated with the antifungal agents. The inoculated plates were incubated at 25°C for 48 h. The readings were taken at the end of 48 and 72 h. The MIC was the lowest concentration of drug preventing growth of macroscopically visible colonies on drug containing plates when there was visible

growth on the drug free control plates.

#### 4.4 Antioxidant activity assay

Antioxidant activity of the synthesized compounds has been assessed *in vitro* by the 1, 1-diphenyl-2-picrylhydrazyl (DPPH) radical scavenging assay [39]. Results were compared with standard antioxidant BHT (Butylated Hydroxy Toluene). The hydrogen atom or electron donation ability of the compounds was measured from the bleaching of the purple coloured methanol solution of 1, 1-diphenyl-1-picrylhydrazyl (DPPH). The spectrophotometric assay uses the stable radical DPPH as a reagent. 1mL of various concentrations of the test compounds (5, 10, 25, 50 and 100 mg/mL) in methanol was added to 4 mL of 0.004% (w/v) methanol solution of DPPH. After a 30 min incubation period at room temperature, the absorbance was measured against blank at 517 nm. The per cent inhibition (I %) of free radical production from DPPH was calculated by the following equation.

$$\% \text{ of scavenging} = [(A \text{ control} - A \text{ sample}) / A \text{ blank}] \times 100$$

Where 'A control' is the absorbance of the control reaction (containing all reagents except the test compound) and 'A sample' is the absorbance of the test compound. Tests were carried at in triplicate.

#### 4.5 Molecular docking

To gain insight into the plausible mechanism of action by which the 1,2,3-triazolyl-chalcones studied herein could exhibit the antifungal activity and guide further SAR based on our experimental studies, molecular docking against sterol 14 $\alpha$ -demethylase (CYP51) was performed. Molecular docking has emerged as a reliable tool to identify the biological target for the bioactive molecules and gain an insight

into crucial ligand-protein thermodynamic interactions. Especially in the absence of available resources to perform enzyme-based assays, molecular docking is considered as complementary to the *in vivo* and *in vitro* biological study for understanding the ligand-receptor interactions at the atomic level. With this purpose, the 3D X-ray crystal structure of sterol 14 $\alpha$ -demethylase (CYP51) enzyme complexed with its inhibitor-Miconazole (pdb code: 3KHM) was retrieved from the Protein Data Bank (PDB) (<http://www.rcsb.org/pdb>). Sterol 14 $\alpha$ -demethylase (CYP51) is a crucial fungal enzyme that catalyses the conversion of lanosterol to ergosterol in the cell and thus its inhibition could lead to accumulation of 14 $\alpha$ -methyl sterols in the cell causing impaired cell growth. The GLIDE (Grid-based Ligand Docking with Energetics) program integrated into the Schrödinger Molecular modelling package (Schrodinger, LLC, New York, NY, 2018) [40-43] was used to perform the docking study. The preliminary crystal structure of CYP51 was refined using with the protein preparation wizard to remove the experimental errors in the structure. This involved eliminating the crystallographic water molecules since no conserved interactions with the enzyme are reported; adding the missing hydrogen/side-chain atoms corresponding to pH 7.0, assignment of appropriate charge and protonation state followed by energy minimization (applying the OPLS-2005 force field) of the obtained structure to relieve the steric clashes among the amino acid residues till RMSD for the heavy atoms reached 0.30Å. The 3D structures of the 1,2,3-triazole incorporated chalcone were sketched using the build panel and optimized using Ligand Preparation tool in Maestro which involves adjusting realistic bond lengths and angles, ascribing the partial charges using OPLS-2005 force-field followed by energy minimization until its average RMSD reached 0.001Å. The active site of CYP51 enzyme for docking was defined using Receptor Grid Generation panel



wherein a grid box of 10X10X10Å dimensions centred on centroid of the co-crystallized ligand was generated. With this automatic setup, the lowest energy conformation of each ligand was docked against defined active site of CYP51 using extra precision (XP) Glide scoring function to gauge the binding affinities of triazole analogues towards CYP51. For each compound, the most stable docking pose was selected according to best-scored conformation and analysed quantitatively for the most significant interactions with residues lining the active site using Maestro's Pose Viewer utility.

#### 4.6 ADME Prediction

All the synthesized 1,2,3-triazolyl-chalcones were tested for Lipinski's rule of five. According to this rule, a molecule likely to be developed as an orally active drug should not exhibit more than one violation of following four criteria: molecular weight  $\leq 500$ , number of hydrogen bond donors  $\leq 5$ , miLogP (octanol-water partition coefficient)  $\leq 5$ , number of hydrogen bond acceptors  $\leq 10$ . ADME properties were predicted by using molinspiration online property calculation toolkit. A collective property of physicochemical properties, pharmacokinetics and pharmacodynamics of a compound is represented by a numerical value known as the drug-likeness model score was computed by using MolSoft software.

#### Conflict of interest

The authors declare that they have no conflict of interest.

#### Acknowledgement

One of the author AAN is thankful to Principal, K. M. C. College Khopoli, for providing necessary help and DST-FIST funded research laboratory to conduct this work. Also, author SVA is very much grateful to the Council for

Scientific and Industrial Research (CSIR), New Delhi for the award of the research fellowship. Authors acknowledge Schrodinger Inc. for providing the Schrodinger molecular Modeling software to perform the molecular modelling studies. Authors are also thankful to the Head, Department of Chemistry, Dr Babasaheb Ambedkar Marathwada University Aurangabad for providing laboratory facility.

#### References

1. P. Vandeputte, S. Ferrari, A. T. Coste, *Int. J. Microbiol.* **2012**, DOI 10.1155/2012/713687.
2. D. A. Enoch, H. A. Ludlam, N. M. Brown, *J. Med. Microbiol.* **2006**, *55*, 809.
3. J. N. Steenbergen, A. Casadevall, *J. Clin. Microbiol.* **2000**, *38*, 1974.
4. D. J. Sheehan, C. A. Hitchcock, C. M. Sibley, *Clin. Microbiol. Rev.* **1999**, *12*, 40.
5. R. Seufert, L. Sedlacek, B. Kahl, M. Hogardt, A. Hamprecht, G. Haase, F. Gunzer, A. Haas, S. Grauling-Halama, C. R. MacKenzie, et al., *J. Antimicrob. Chemother.* **2018**, *73*, 2047.
6. F. Azam, in *Handbook of Free Radicals: Formation, Types and Effects* (Eds: D. Kozyrev, V. Slutsky), Nova science Publishers, **2010**, *1*, 2, 57.
7. C. R. Da Silva, J. B. De Andrade Neto, R. De Sousa Campos, N. S. Figueiredo, L. S. Sampaio, H. I. F. Magalhães, B. C. Cavalcanti, D. M. Gaspar, G. M. De Andrade, I. S. P. Lima, et al., *Antimicrob. Agents Chemother.* **2014**, *58*(3), 1468.
8. V. Sharma, G. Singh, H. Kaur, A. K. Saxena, M. P. S. Ishar, *Bioorganic Med. Chem. Lett.* **2012**, *22*, 6343.
9. P. Singh, A. Anand, V. Kumar, *Eur. J. Med. Chem.* **2014**, *85*, 758.
10. W. Chen, X. Ge, F. Xu, Y. Zhang, Z. Liu, J. Pan, J. Song, Y. Dai, J. Zhou, J. Feng, et al., *Bioorg. Med. Chem. Lett.* **2015**, *25*, 2998.
11. H. L. Qin, Z. P. Shang, I. Jantan, O. U. Tan, M. A. Hussain, M. Sher, S. N. A. Bukhari, *RSC Adv.* **2015**, *5*, 46330.
12. Y. Zuo, Y. Yu, S. Wang, W. Shao, B. Zhou, L. Lin, Z. Luo, R. Huang, J. Du, X. Bu, *Eur. J. Med. Chem.* **2012**, *50*, 393.
13. C. Zhuang, W. Zhang, C. Sheng, W. Zhang, C. Xing, Z. Miao, *Chem. Rev.* **2017**, *117*, 7762.
14. A. Rammohan, J. S. Reddy, G. Sravya, C. N. Rao, G. V. Zyryanov, *Environ. Chem. Lett.* **2020**, *18*, 433.
15. R. Abonia, D. Insuasty, J. Castillo, B. Insuasty, J. Quiroga, M. Nogueras, J. Cobo, *Eur. J. Med. Chem.* **2012**, *57*, 29.
16. E. M. Guantai, K. Ncokazi, T. J. Egan, J. Gut, P. J. Rosenthal, P. J. Smith, K. Chibale, *Bioorg. Med. Chem.* **2010**, *18*, 8243.
17. R. Kant, D. Kumar, D. Agarwal, R. D. Gupta, R. Tilak, S.



- K. Awasthi, A. Agarwal, *Eur. J. Med. Chem.* **2016**, *113*, 34.
18. J. Chu, C. L. Guo, *Arch. Pharm. (Weinheim)*. **2016**, *349*, 63.
19. K. B. Mishra, V. K. Tiwari, *J. Org. Chem.* **2014**, *79*, 5752.
20. N. Kerru, P. Singh, N. Koorbanally, R. Raj, V. Kumar, *Eur. J. Med. Chem.* **2017**, *142*, 179.
21. M. H. Shaikh, D. D. Subhedar, F. A. K. Khan, J. N. Sangshetti, B. B. Shingate, *Chin. Chem. Lett.* **2016**, *27*, 295.
22. L. Zhao, L. Mao, G. Hong, X. Yang, T. Liu, *Bioorg. Med. Chem. Lett.* **2015**, *25*, 2540.
23. M. H. Shaikh, D. D. Subhedar, M. Arkile, V. M. Khedkar, N. Jadhav, D. Sarkar, B. B. Shingate, *Bioorg. Med. Chem. Lett.* **2016**, *26*, 561.
24. M. H. Shaikh, D. D. Subhedar, L. Nawale, D. Sarkar, F. A. Kalam Khan, J. N. Sangshetti, B. B. Shingate, *Med. chem. comm.* **2015**, *6*, 1104.
25. S. V. Akolkar, A. A. Nagargoje, V. S. Krishna, D. Sriram, J. N. Sangshetti, M. Damale, B. B. Shingate, *RSC Adv.* **2019**, *9*, 22080.
26. K. Lal, P. Yadav, A. Kumar, A. Kumar, A. K. Paul, *Bioorg. Chem.* **2018**, *77*, 236.
27. S. Y. Zhang, D. J. Fu, X. X. Yue, Y. C. Liu, J. Song, H. H. Sun, H. M. Liu, Y. B. Zhang, *Molecules* **2016**, *21(5)*, 653.
28. R. Santosh, M. K. Selvam, S. U. Kanekar, G. K. Nagaraja, *ChemistrySelect* **2018**, *3*, 6338.
29. H. F. Ashour, L. A. Abou-zeid, M. A. A. El-Sayed, K. B. Selim, *Eur. J. Med. Chem.* **2020**, *189*, 112062.
30. S. M. A. Hussaini, P. Yedla, K. S. Babu, T. B. Shaik, G. K. Chityal, A. Kamal, *Chem. Biol. Drug Des.* **2016**, *4*, 97.
31. D. J. Fu, J. Song, R. H. Zhao, Y. C. Liu, Y. B. Zhang, H. M. Liu, *J. Chem. Res.* **2016**, *40*, 674.
32. A. A. Nagargoje, S. V. Akolkar, M. M. Siddiqui, A. V. Bagade, K. M. Kodam, J. N. Sangshetti, M. G. Damale, B. B. Shingate, *J. Chinese Chem. Soc.* **2019**, *66*, 1658.
33. A. A. Nagargoje, S. V. Akolkar, M. M. Siddiqui, D. D. Subhedar, J. N. Sangshetti, V. M. Khedkar, B. B. Shingate, *Chem. Biodiversity* **2020**, *17*, e1900624.
34. D. D. Subhedar, M. H. Shaikh, L. Nawale, D. Sarkar, V. M. Khedkar, B. B. Shingate, *Bioorg. Med. Chem. Lett.* **2017**, *27*, 922.
35. S. G. Alvarez, M. T. Alvarez, *Synthesis.* **1997**, *4*, 413.
36. B. Duraiswamy, S. Mishra, V. Subhashini, S. Dhanraj, B. Suresh, *Indian J. Pharm. Sci.* **2009**, *68*, 389.
37. K. L. Therese, R. Bagyalakshmi, H. N. Madhavan, P. Deepa, *Indian J. Med. Microbiol.* **2006**, *24*, 273.
38. Collins CH, *Microbiological methods.* Butterworth-Heinemann, London, **1967**.
39. M. Burits, F. Bucar, *Phyther. Res.* **2000**, *14*, 323.
40. R. A. Friesner, R. B. Murphy, M. P. Repasky, L. L. Frye, J. R. Greenwood, T. A. Halgren, P. C. Sanschagrin, D. T. Mainz, *J. Med. Chem.* **2006**, *49*, 6177.
41. T. A. Halgren, R. B. Murphy, R. A. Friesner, H. S. Beard, L. L. Frye, W. T. Pollard, J. L. Banks, *J. Med. Chem.* **2004**, *47*, 1750.
42. R. A. Friesner, J. L. Banks, R. B. Murphy, T. A. Halgren, J. J. Klicic, D. T. Mainz, M. P. Repasky, E. H. Knoll, M. Shelley, J. K. Perry, et al., *J. Med. Chem.* **2004**, *47*, 1739.
43. T. A. Halgren, R. B. Murphy, R. A. Friesner, H. S. Beard, L. L. Frye, W. T. Pollard, J. L. Banks, *J. Med. Chem.* **2004**, *47*, 1750.



# Propargylated monocarbonyl curcumin analogues: synthesis, bioevaluation and molecular docking study

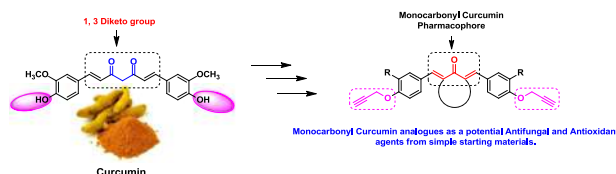
Amol A. Nagargoje<sup>1,2</sup> · Satish V. Akolkar<sup>1</sup> · Dnyaneshwar D. Subhedar<sup>1</sup> · Mubarak H. Shaikh<sup>1,3</sup> · Jaiprakash N. Sangshetti<sup>4</sup> · Vijay M. Khedkar<sup>5</sup> · Bapurao B. Shingate<sup>1</sup>

Received: 21 April 2020 / Accepted: 31 July 2020  
© Springer Science+Business Media, LLC, part of Springer Nature 2020

## Abstract

In the current experimental study, we have synthesised new monocarbonyl curcumin analogues bearing propargyl ether moiety in their structure and evaluated for in vitro antifungal and radical scavenging activity. The antifungal activity was carried out against five human pathogenic fungal strains such as *Candida albicans*, *Fusarium oxysporum*, *Aspergillus flavus*, *Aspergillus niger* and *Cryptococcus neoformans*. Most of the curcumin analogues displayed excellent to moderate fungicidal activity when compared with standard drug Miconazole. Also, synthesised analogues exhibited potential radical scavenging activity as compared with standard antioxidant Butylated hydroxyl toluene (BHT). Based on biological data, structure-activity relationship (SAR) were also discussed. Furthermore, in silico computational study was carried out to know binding interactions of synthesised analogues in the active sites of enzyme sterol 14 $\alpha$ -demethylase (CYP51).

## Graphical Abstract



**Keywords** Monocarbonyl curcumin analogues · Antifungal activity · Antioxidant activity · SAR · Molecular docking study

## Introduction

Curcumin is the principal curcuminoid of the turmeric plant of the family *Zingiberaceae*. It has been used to treat many health conditions in India and other parts of Asia since

ancient times. According to recent literature, curcumin is the multi-target pleiotropic agent displaying a wide spectrum of biological activities (Goel et al. 2008; Marchiani et al. 2013; Bairwa et al. 2014; Shetty et al. 2015). Curcumin has been evaluated in clinical trials for the treatment of various diseases like cancer, liver diseases, infectious diseases and rheumatoid arthritis (Hatcher et al. 2008; Bairwa et al. 2014). However, clinical use of the curcumin is restricted due to poor bioavailability, poor

**Supplementary information** The online version of this article (<https://doi.org/10.1007/s00044-020-02611-7>) contains supplementary material, which is available to authorized users.

✉ Bapurao B. Shingate  
bapushingate@gmail.com

<sup>1</sup> Department of Chemistry, Dr Babasaheb Ambedkar Marathwada University, Aurangabad 431004, India

<sup>2</sup> Department of Chemistry, Khopoli Municipal Council College, Khopoli 410203, India

<sup>3</sup> Department of Chemistry, Radhabai Kale Mahila Mahavidyalaya, Ahmednagar 414001, India

<sup>4</sup> Department of Pharmaceutical Chemistry, Y. B. Chavan College of Pharmacy, Rafiq Zakaria Campus, Aurangabad 431001, India

<sup>5</sup> Department of Pharmaceutical Chemistry, School of Pharmacy, Vishwakarma University, Pune 411048, India

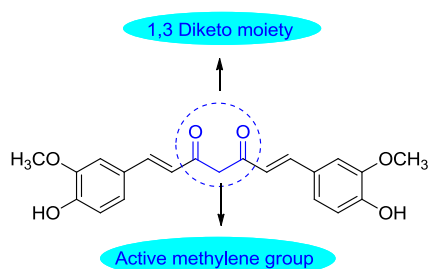


**Fig. 1** Curcumin and groups responsible for the instability

pharmacokinetics and rapid in vivo metabolism (Anand et al. 2008). It was observed that, presence of the  $\beta$ -diketone and active methylene groups are responsible for the instability of curcumin (Anand et al. 2007; Wang et al. 1997) (Fig. 1).

Structural modification on curcumin by replacing  $\beta$ -diketone moiety as well as an active methylene group with single keto-functionality leads to the formation of therapeutically active, stable monocarbonyl analogues of curcumin (MACs) (Shetty et al. 2015). The literature survey revealed that, MACs were displayed a wide spectrum of biological activities which are found to be superior to curcumin itself. MACs shows potential anticancer (Kerru et al. 2017), anti-inflammatory (Wang et al. 2017), antioxidant (Zheng et al. 2017), antibacterial (Sanabria-Rios et al. 2015), anti-Alzheimer's activity (Chen et al. 2011), anti-parasitic (Carapina da Silva et al. 2019), antileishmanial (Tiwari et al. 2015), topoisomerase II alpha inhibitors (Paul et al. 2014), antiobesity (Buduma et al. 2016), anti-tubulin (Singh et al. 2016), anti-invasive chemotypes (Roman et al. 2015), lipoxygenase and proinflammatory cytokines (Ahmad et al. 2014), anti-tubercular (Subhedar et al. 2017), antifungal activity (Sahu et al. 2012) etc.

In recent years, invasive fungal infections are a major concern due to an increase in organ transplantation, stem cell transplantation, chemotherapy and human immunodeficiency virus. Candidosis, aspergillosis and cryptococcosis, are three major fungal infections responsible for clinical infections in patients having a weak immune system. Although, there are several drugs available to treat fungal diseases, multidrug-resistant strain development among the fungal species against existing amphotericin B, triazoles, and echinocandins based antifungal drugs (Pappas et al. 2015) become a critical problem for therapeutic strategies (Seufert et al. 2018). Also, existing antifungal drugs have many side effects. Long term use of the existing antifungal drugs can induce many side effects such as cough, bad taste, nausea, hepatotoxicity, liver toxicity, hypokalemia, fever, gastrointestinal, endocrinologic, metabolic, carcinogenic, chills and drug-drug interactions between azole and other drug classes that are metabolised *via* similar pathways in the liver (Bodey 1992; Shehaan et al. 1999).

These limitations emphasise the need to develop new and more effective antifungal agents. Martins et al. (Martins et al. 2009) evaluated the potential of curcumin against various fungal strains as an effective antifungal as compared with commercial drug fluconazole. Very recently, anti-infective properties of curcumin have been reviewed (Praditya et al. 2019). Hence, curcumin and its analogues can be the new scaffold in the search of new antifungal agents. Covalent modification by prenylation have been recognised as a mechanism for promoting membrane interactions and biological activity of a variety of cellular proteins (Casey 1992).

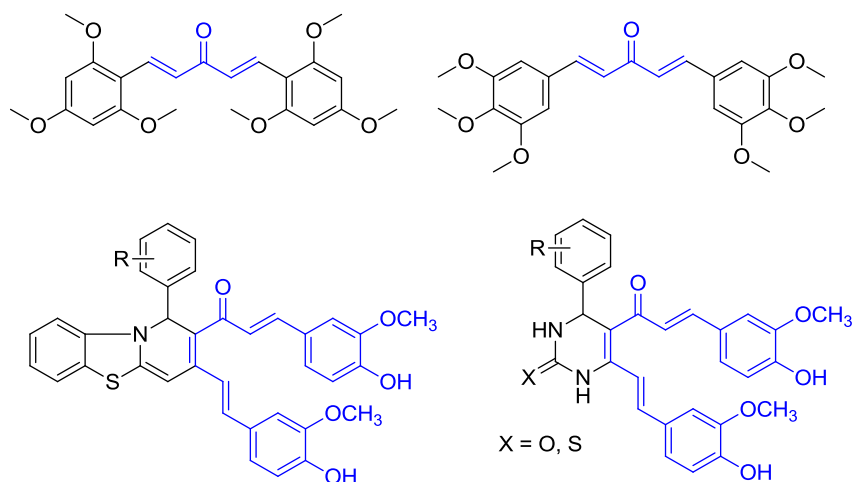
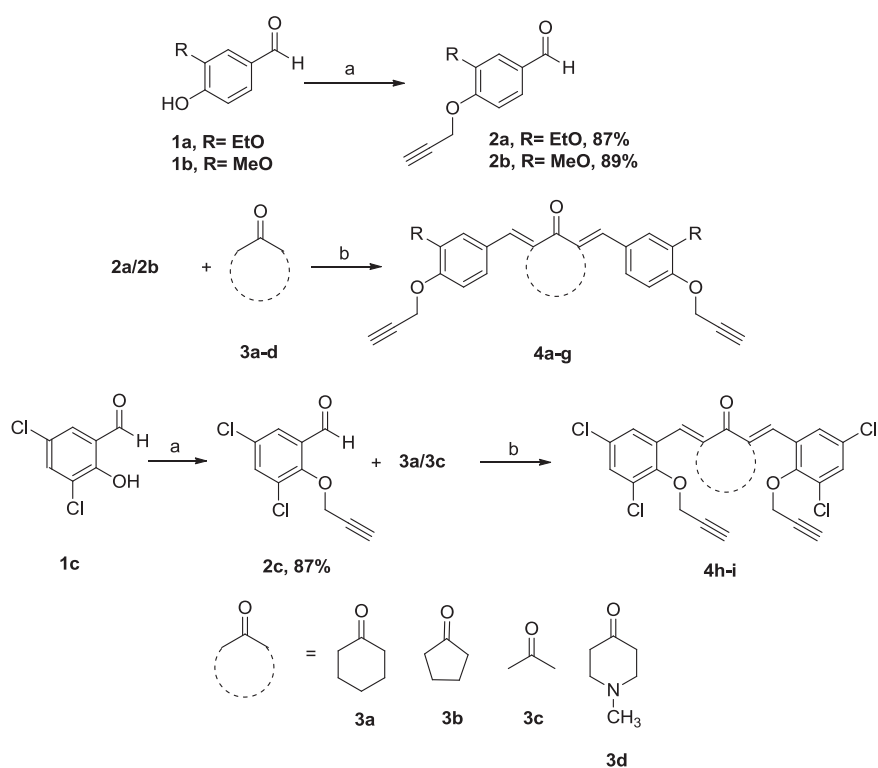
It was observed that, reactive oxygen species were involved in the mechanism of action of antifungal drugs (Da Silva et al. 2014). Therefore, new antifungals with antioxidant potential can be a good choice. Literature revealed that, curcumin moiety is responsible for antioxidant activity (Masuda et al. 2001; Sokmen, Khan 2016). Considering the antioxidant activity of curcumin analogues (Li et al. 2015; Sahu et al. 2016a, b; Lal et al. 2016; Zheng et al. 2017), many attempts were made to develop new curcumin based molecules as an antioxidant agents. Some of the representative structures of the molecules as an antioxidant agents were shown in Fig. 2.

Under this context and as a part of our ongoing research in the synthesis and biological evaluation of monocarbonyl curcumin analogues (Deshmukh et al. 2020; Subhedar et al. 2017; Nagargoje et al. 2019, 2020), we report herein, synthesis, antifungal and antioxidant evaluation of new propargylated monocarbonyl curcumin analogues. Furthermore, to understand the binding mechanism of newly synthesised analogues into the active sites of cytochrome P450, molecular docking study was also performed.

## Results and discussion

### Chemistry

In the present work, we have described the synthesis of new propargylated monocarbonyl curcumin analogues by the Claisen-Schmidt type condensation (Fine, Pulaski 1973; Ziani et al. 2013) of propargylated benzaldehydes with monoketone linkers like cyclohexanone, cyclopentanone, acetone and 4-methyl piperidone by literature method. The reaction of benzaldehyde **1a–c** with propargyl bromide in the presence of an alkaline condition resulted in the corresponding substituted prop-2-yn-1-yloxy-benzaldehydes **2a–c** in excellent yields (Scheme 1). The condensation of these benzaldehydes **2a–c** with respective monoketone **3a–d** using aq. NaOH and ethanol at room temperature resulted into corresponding propargylated monocarbonyl curcumin analogues **4a–i** in a good yield. (Scheme 1).

**Fig. 2** Known MACs with antioxidant activity**Scheme 1** Synthesis of propargylated monocarbonyl curcumin analogues. Reagent and conditions: (a) Propargyl bromide,  $K_2CO_3$ , DMF, rt, 3–4 h; (b) Aq. NaOH, EtOH, rt, 4–5 h

The formation of propargylated monocarbonyl curcumin analogues **4a–i** has been confirmed by physical data and spectroscopic methods such as FT-IR,  $^1H$  NMR,  $^{13}C$  NMR and LC/ESI-MS. According to the FT-IR spectrum of compound **4a**, the peaks observed at  $3262\text{ cm}^{-1}$ ,  $2120\text{ cm}^{-1}$  indicate the presence of the alkyne group and  $1660\text{ cm}^{-1}$  for the presence of a carbonyl group. In the  $^1H$  NMR spectrum of compound **4a**, the triplet at 1.47 ppm is observed for methyl group adjacent to a methylene group present on the benzene ring, multiple ranging in between 1.84 and 1.78 ppm, and triplet at 2.93 ppm is observed for methylene groups of cyclohexanone ring, triplet at 2.53 ppm with coupling constant 2.4 Hz for two alkyne protons (This

indicates coupling of acetylenic proton with methylene protons adjacent to oxygen and alkyne group), the quartet at 4.12 ppm for four methylene protons adjacent to oxygen and methyl group on benzene rings, a doublet at 4.81 ppm with coupling constant 2.4 Hz (This indicates coupling of these protons with terminal acetylene protons) for the presence of two methylene protons adjacent to oxygen and alkyne group on a benzene ring. In addition to this, the signal appeared at 7.03 and 7.08 ppm for six aromatic protons of benzene rings. The signal appeared at 7.73 ppm is for two alkene protons. These alkene protons are benzyldine protons, and also in  $\beta$  position to the carbonyl group, hence due to resonance effect and  $-I$  effect of the

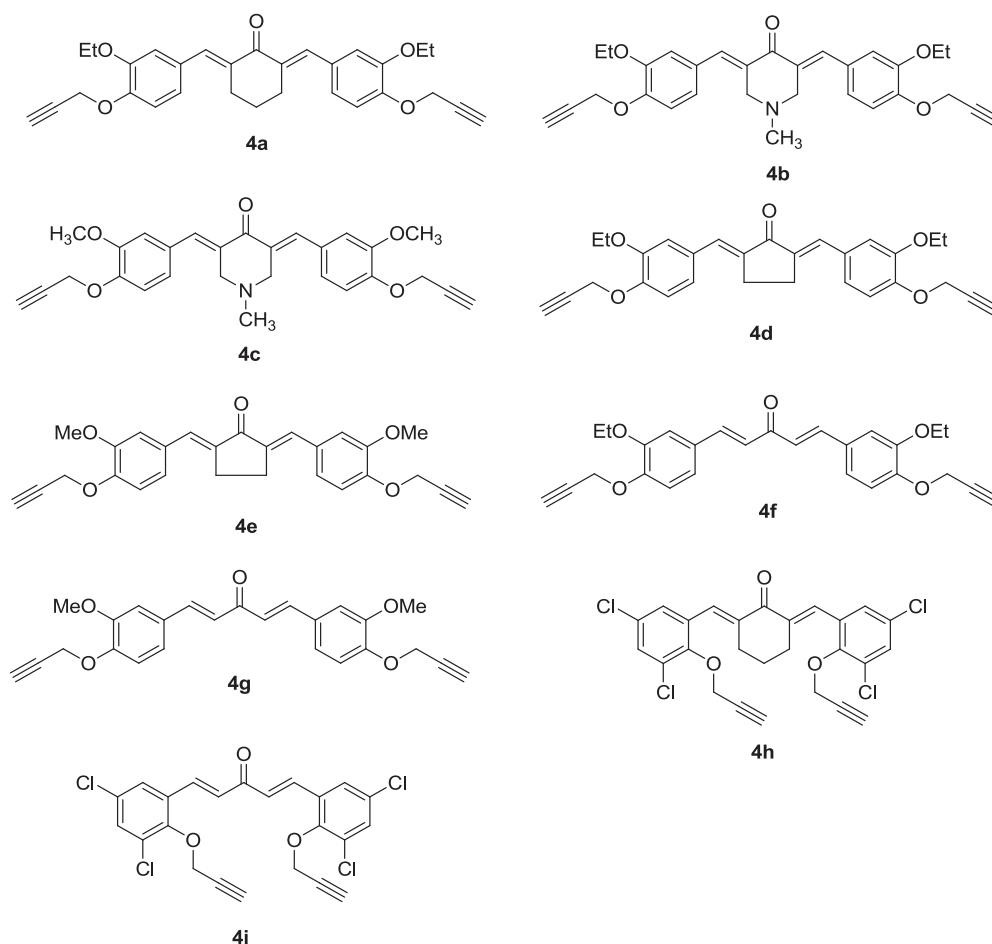


**Fig. 3** Structures of synthesised monocarbonyl curcumin analogues

carbonyl group and benzene ring this signal is shifted to downfield region. In the  $^{13}\text{C}$  NMR spectrum of compound **4a**, the signal at 14.8 ppm is observed for the methyl carbon and the signals at 23.0 and 28.5 ppm indicate the presence of two methylene carbon of cyclohexanone ring. The signals at 56.8 and 64.6 ppm indicate the presence of methylene carbons adjacent to oxygen. The signal at 76.0 and 78.4 ppm shows the presence of alkyne carbons. Furthermore, the peak observed at 190.1 ppm for carbonyl carbon. The formation of compound **4a** has been further confirmed by mass spectrometry. The calculated  $[\text{M}-\text{H}]^+$  for compound **4a** is 469.2093 and observed  $[\text{M}-\text{H}]^+$  in the mass spectrum at 469.2143. Similarly compounds **4b–i** were characterised by the spectral analysis. The structures of all the synthesised MACs are given in Fig. 3.

### In vitro antifungal activity

The synthesised MACs were evaluated for in vitro antifungal activity against various fungal strains like *Cryptococcus neoformans*, *Aspergillus niger*, *Aspergillus flavus*,

*Candida albicans*, *Fusarium oxysporum* etc. The minimum inhibitory potential of synthesised analogues were compared against the standard antifungal drug Miconazole. The MIC values in  $\mu\text{g}/\text{mL}$  were estimated and the results are summarised in Table 1.

Most of the synthesised MACs exhibited excellent to moderate antifungal potential against most of the pathogenic fungal strains, which is reflected by their MIC values. Antifungal activity of synthesised MACs compare to standard Miconazole is represented graphically in Fig. 4. Among the series, compound **4a** displayed equivalent or two/three fold more potency as compared with positive control Miconazole, which reflects its broad-spectrum nature. Compound **4a** demonstrates excellent inhibitory activity against *Candida albicans*, *Fusarium oxysporum* and *Cryptococcus neoformans* (MIC 12.5  $\mu\text{g}/\text{mL}$ , MIC 12.5  $\mu\text{g}/\text{mL}$  and MIC 12.5  $\mu\text{g}/\text{mL}$ , respectively) with compared with Miconazole. Also, **4a** is equipotent against *Aspergillus flavus* and *Aspergillus niger* (MIC 25  $\mu\text{g}/\text{mL}$  each) with compared with Miconazole. Furthermore, compound **4b** and **4c** exhibited almost equal potency as



**Table 1** In vitro antifungal and antioxidant evaluation of propargylated monocarbonyl curcumin analogues

Entry	Antifungal activity (MIC in $\mu\text{g}/\text{mL}$ )					Molecular docking score	Antioxidant activity ( $\text{IC}_{50}$ in $\mu\text{g}/\text{mL}$ )
	CA <sup>[a]</sup>	FO <sup>[b]</sup>	AF <sup>[c]</sup>	AN <sup>[d]</sup>	CN <sup>[e]</sup>		
<b>4a</b>	12.5	12.5	25	25	12.5	-8.939	24.28 $\pm$ 0.45
<b>4b</b>	25	12.5	25	25	50	-8.559	16.17 $\pm$ 0.11
<b>4c</b>	62.5	25	37.5	12.5	25	-8.097	15.78 $\pm$ 0.47
<b>4d</b>	37.5	87.5	25	50	62.5	-8.534	40.34 $\pm$ 0.14
<b>4e</b>	25	25	75	50	100	-7.490	13.18 $\pm$ 0.34
<b>4f</b>	75	75	12.5	25	75	-7.762	28.36 $\pm$ 0.43
<b>4g</b>	100	75	75	100	175	-7.338	27.81 $\pm$ 0.05
<b>4h</b>	12.5	25	75	100	25	-7.637	41.42 $\pm$ 0.67
<b>4i</b>	150	125	150	175	100	-7.088	12.78 $\pm$ 0.71
<b>MA</b>	25	25	12.5	25	25	-	-
<b>BHT</b>	-	-	-	-	-	-	16.47 $\pm$ 0.18

MA miconazole, BHT butoxy hydroxy toluene

<sup>a</sup>Candida albicans

<sup>b</sup>Fusarium oxysporum

<sup>c</sup>Aspergillus flavus

<sup>d</sup>Aspergillus niger

<sup>e</sup>Cryptococcus neoformans

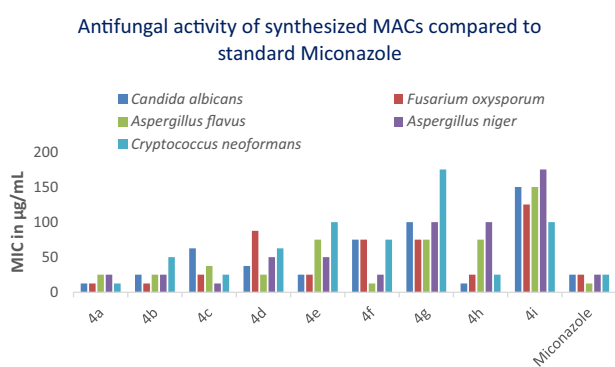


**Fig. 4** Antifungal activity of synthesised MACs compared with Miconazole

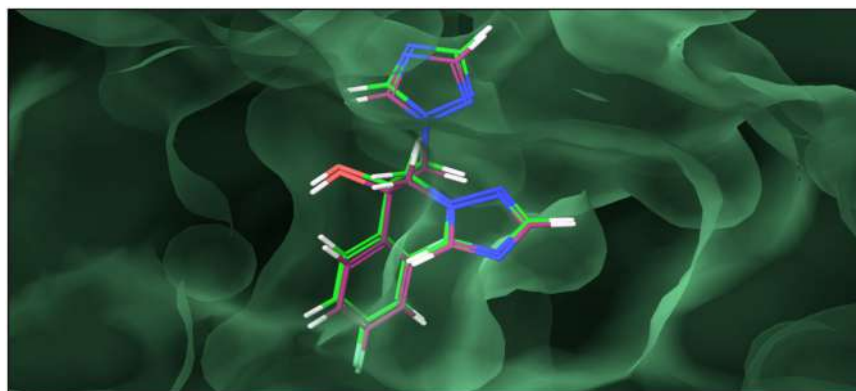
compared with standard. Compound **4e**, **4f** and **4h** displayed moderate potential to act as an antifungal agent. Also, antifungal activity data showed that **4a**, **4b** and **4f** were the most active against *Aspergillus flavus*. The trends in the MIC values of the synthesised analogues help to establish some sort of structure-activity relationship (SAR). From the minimum inhibitory concentration values of the synthesised propargylated monocarbonyl curcumin analogues against different fungal strains, it was observed that curcumin analogues with cyclic linkers like cyclohexanone and *N*-methyl piperidone enhances antifungal potential. To be more specific, analogues with cyclohexanone linker displayed better antifungal activity. Comparing MIC values of compound **4a** and **4h** it was observed that cyclohexanone

linker played an important role in enhancing antifungal activity. Analogues with ethoxy (-OEt) group on the aromatic side-chain have better antifungal potential than other analogues having a methoxy (-OMe) and chloro (-Cl) group. Furthermore, antifungal potential is found to decrease when cyclopentanone and acetone were used as a linker molecule. Also, it was observed that most of the curcumin analogues showed strong potential against all fungal strains except *Cryptococcus neoformans*. In contrast, curcumin analogues **4g** and **4i** do not show significant antifungal activity against any tested pathogenic fungal strains, which also revealed that open space linker like acetone found to decrease antifungal activity.

### In vitro antioxidant activity

All synthesised propargylated monocarbonyl curcumin analogues were further evaluated for in vitro radical scavenging activity. It was observed that the compound **4i** with acetone linker and 3,5-chloro substitution on the aromatic ring displayed potential antioxidant activity ( $\text{IC}_{50} = 12.78 \pm 0.71$ ) when compared with the standard drug BHT ( $\text{IC}_{50} = 16.47 \pm 0.18$ ) (Table 1). Furthermore, analogues **4b**, **4c** and **4e** displays almost greater or equal antioxidant potential as compared with BHT. Trends in antioxidant and antifungal activity data revealed that analogues **4b**, **4c** and **4e** exhibited potential antifungal and antioxidant activity as reflected in their MIC and  $\text{IC}_{50}$  values. Also, analogue **4i** which was inactive against fungal strains were found to exhibit strong antioxidant activity. It was observed that

**Fig. 5** Superimposition of the best scoring pose for Fluconazole obtained from docking (green carbon) against the X-ray bound conformation (pink carbon)



acetone linker enhances antioxidant activity than cyclic linker.

### Molecular docking study

Promising levels of activities demonstrated by the propargylated monocarbonyl curcumin analogues investigated herein against the various fungal strains prompted us to carry out molecular docking studies against the crucial sterol 14 $\alpha$ -demethylase (CYP51) enzyme (PDB code: 3KHM) to elucidate their plausible mechanism of antifungal activity. Within the framework of *in silico* structure-based drug design approaches, molecular docking has evolved an inevitable tool to predict the potential biological target with a substantial degree of accuracy especially in the absence of available resources to do the experimental enzyme assay. Sterol 14 $\alpha$ -demethylase (CYP51) is an ancestral activity of the cytochrome P450 superfamily and is essential for ergosterol biosynthesis in fungi where it catalyzes the conversion of lanosterol to ergosterol. Inhibition of CYP51 leads to accumulation of 14 $\alpha$ -methyl sterols and depletion of ergosterol in the fungal cell wall, resulting in altered cell membrane properties and function with subsequently increased permeability and inhibition of cell growth and replication.

Molecular docking protocol was validated by extracting the co-crystallised ligand (Fluconazole) and re-docking using the experimental set up described in the experimental part of docking analysis (Fig. 5).

From the ensuing docked conformations, it is revealed that all the propargylated monocarbonyl curcumin analogues could bind to the active site of CYP51 with varying degrees of affinities at co-ordinates close to the native structure by formation of a network of close interactions. The docking scores for the series varied from  $-8.939$  for the most active to  $-7.088$  for moderately active with an average docking score of  $-7.963$  signifying a promising binding affinity towards CYP51. Furthermore, a detailed per-residue interaction analysis was carried out to identify the most

significantly interacting residues and their associated thermodynamic interactions. This analysis is discussed in detail for one of the most active molecule **4a** and summarised in Table 2 for other active compounds **4b**, **4c**, **4f** and **4h** as well (SI-1 to SI-4, Supplementary Information).

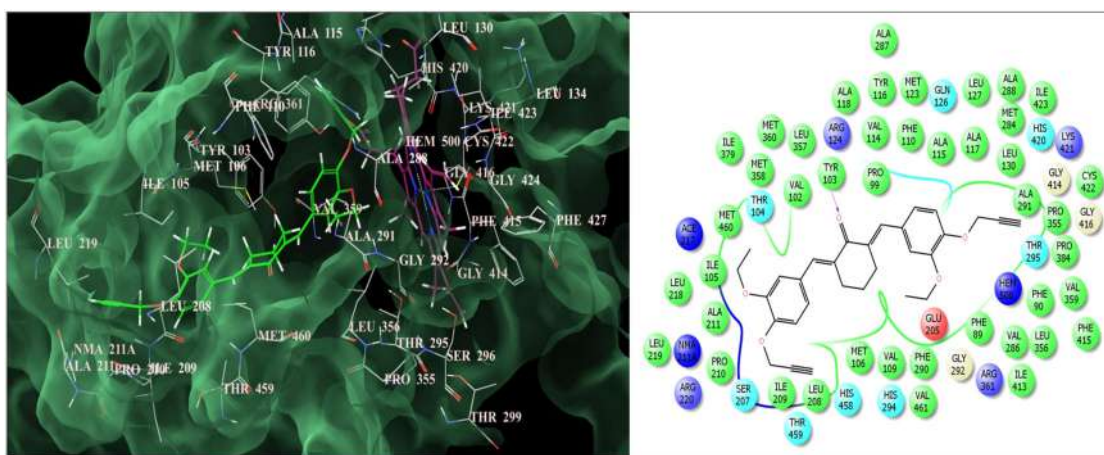
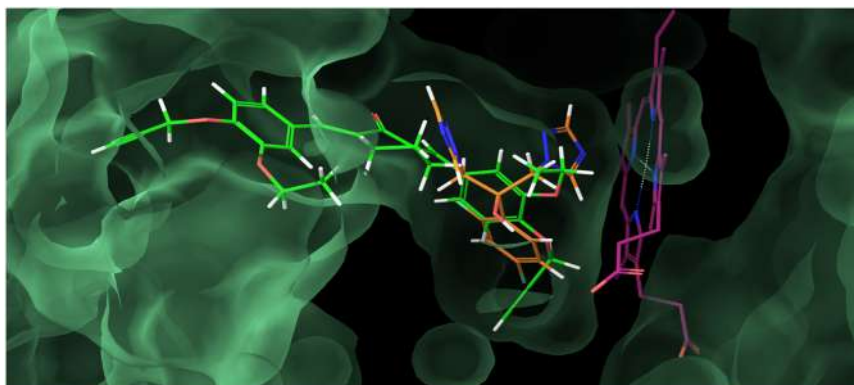
The lowest energy docked conformation of **4a** (Fig. 6) revealed that it could snugly fit into the active site of CYP450 at co-ordinates similar to native ligand (Fig. 7) engaging in a network of bonded and non-bonded (steric and electrostatic) interactions.

The compound was found to be stabilised through most significant van der Waals interactions observed with Val461 ( $-3.246$  kcal/mol), Phe290 ( $-2.953$  kcal/mol), Ala287 ( $-2.954$  kcal/mol), Glu205 ( $-2.741$  kcal/mol), Tyr116 ( $-4.431$  kcal/mol), Phe110 ( $-2.871$  kcal/mol), Met106 ( $-3.155$  kcal/mol), Tyr103 ( $-3.098$  kcal/mol) residues *via* the central cyclohexanone nucleus while the 3-ethoxy-4-(prop-2-yn-1-yloxy) benzylidene side chains flanking both side of the nucleus engaged in similar van der Waals interactions with Hem500 ( $-5.738$  kcal/mol), Met460 ( $-4.355$  kcal/mol), Thr459 ( $-3.486$  kcal/mol), Leu356 ( $-3.261$  kcal/mol), Thr295 ( $-2.918$  kcal/mol), Ala291 ( $-2.972$  kcal/mol), Pro210 ( $-3.197$  kcal/mol), Ile209 ( $-2.977$  kcal/mol), Leu208 ( $-3.232$  kcal/mol) and Ile105 ( $-3.288$  kcal/mol) residues lining the active site. The enhanced binding affinity of **4a** is also attributed to very significant electrostatic interactions observed through Hem500 ( $-3.185$  kcal/mol), Ile209 ( $-2.896$  kcal/mol), Glu205 ( $-2.867$  kcal/mol) and Tyr103 ( $-2.712$  kcal/mol) residues.

Furthermore, **4a** also exhibited a very close hydrogen-bonding interactions with Tyr103 ( $1.989$  Å) residue through the ketone function of the central cyclohexanone nucleus which serve as an "anchor" to stabilise the 3D orientation of a ligand into the active site and also guide the steric and electrostatic (non-bonded) interactions. A similar network of bonded (H-bond) and non-bonded (steric and electrostatic) interactions were observed for other active analogues. It is noteworthy that all the active molecules,

**Table 2** The per-residue interaction analysis based on docking study for propargylated monocarbonyl curcumin analogues with sterol 14 $\alpha$ -demethylase (CYP51)

Code	Docking score	Glide interaction energy (kcal/mole)	Per-residues interactions	
			Coulombic (kcal/mol)	H-bond ( $\text{\AA}$ )
<b>4a</b>	-8.939	-49.907	Hem500 (-3.185), Ile209 (-2.896), Glu205 (-2.867), Tyr103 (-2.712)	Tyr103 (1.989)
<b>4b</b>	-8.559	-48.324	Hem500 (-3.077), Ile209 (-2.596), Glu205 (-2.367), Tyr103 (-2.429)	-
<b>4c</b>	-8.097	-46.877	Hem500 (-2.939), Ile209 (-2.292), Glu205 (-2.349), Tyr103 (-2.392)	Tyr103 (2.088)
<b>4f</b>	-7.762	-47.954	Hem500 (-2.850), Ile209 (-2.196), Glu205 (-2.267), Tyr103 (-2.128)	Tyr103 (1.899)
<b>4h</b>	-7.637	-45.814	Hem500 (-2.739), Ile209 (-1.432), Glu205 (-2.139), Tyr103 (-2.092)	-
Fluconazole	-7.34	-52.92	Hem500 (-5.862), Ile209 (-2.896), Glu205 (-2.929), Tyr103 (-2.35)	Tyr116 (2.11)

**Fig. 6** Binding mode of **4a** into the active site of sterol 14 $\alpha$ -demethylase (CYP51) (on the right side: the pink lines signify hydrogen-bonding interaction)**Fig. 7** Superimposition of the **4a** against the X-ray bound conformation of Fluconazole (Green backbone: **4a**, Orange backbone: Fluconazole; Pink backbone: Hem)

including **4a**, showed a very strong steric as well as electrostatic interaction with the Hem moiety (iron metal) of CYP51 which is crucial for antifungal activity knowing the experimental evidence that Miconazole is also coordinated

with CYP51 through this Hem moiety. This suggests that the propargylated monocarbonyl curcumin analogues investigated herein may also exhibit their antifungal activity through CYP51 inhibition.

## Materials and methods

### General

All chemicals and reagents were procured from Sigma Aldrich, S.D. Fine chemical and commercial suppliers and used without further purification. TLC was performed on 0.25 mm E. Merck pre-coated silica gel plates (60 F<sub>254</sub>). The components were identified by exposure to iodine vapours or UV light. The melting point was decided by using an open capillary technique and are uncorrected. The products were characterised using <sup>1</sup>H NMR, <sup>13</sup>C NMR spectra and MS. <sup>1</sup>H-NMR spectra were recorded in CDCl<sub>3</sub> on a Bruker DRX-400 MHz spectrometer. <sup>13</sup>C NMR spectra were recorded in CDCl<sub>3</sub> on a Bruker DRX-100 MHz instrument. TMS was used as the internal standard. IR spectra were recorded using a Bruker ALPHA ECO-ATR FTIR spectrometer. Mass spectra were recorded on LC/ESI-MS spectrometer.

### General procedure for the preparation of prop-2-yn-1-yloxy benzaldehydes (2a–c)

An appropriate mixture of hydroxybenzaldehyde **1a–c** (1 mmol), propargyl bromide (1 mmol) and K<sub>2</sub>CO<sub>3</sub> (2 mmol) in DMF (9–10 mL) was stirred at room temperature for 2–3 h. The progress of the reaction was monitored using TLC. After completion of the reaction, the reaction mixture was poured in ice-cold water. The separated solid was filtered washed with water, dried and recrystallised from ethanol resulted in the corresponding propargylated benzaldehydes in good yields (87–89%).

### General procedure for the preparation of propargylated monocarbonyl curcumin analogues (4a–i)

A mixture of appropriate propargylated benzaldehydes **2a–c** (1 mmol), appropriate monoketone linker (1 mmol) and aq. NaOH in ethanol (10 mL) was stirred at room temperature for about 3–4 h. The progress of the reaction was monitored using TLC. The precipitate was washed with water, dried and recrystallised using ethyl acetate-chloroform as a solvent.

#### (2E,6E)-2,6-Bis(3-ethoxy-4-(prop-2-yn-1-yloxy)benzylidene)cyclohexanone (4a)

Yellow coloured crystal; yield 82%; mp: 150–153 °C; IR (KBr)  $\nu_{\max}$  3262, 2120, 1660, 1589, 1503 cm<sup>-1</sup>; <sup>1</sup>H NMR (CDCl<sub>3</sub>, 400 MHz):  $\delta$  = 7.73 (2H, s, Ar-CH=C-, H-3, H-3'), 7.08 (4H, s, Ar-H, H-5, H-5', H-9, H-9'), 7.03 (2H, s, Ar-H, H-8, H-8'), 4.81 (4H, d,  $J$  = 2.4 Hz, Ar-OCH<sub>2</sub>), 4.12

(4H, q,  $J$  = 8.0 Hz, -OCH<sub>2</sub>CH<sub>3</sub>), 2.93 (4H, t,  $J$  = 8.0 Hz, -CH<sub>2</sub>-CH<sub>2</sub>-CH<sub>2</sub>), 2.53 (2H, d,  $J$  = 2.4 Hz, -C≡CH), 1.84–1.78 (2H, m, -CH<sub>2</sub>-CH<sub>2</sub>-CH<sub>2</sub>), 1.47 (6H, t,  $J$  = 8.0 Hz, -OCH<sub>2</sub>-CH<sub>3</sub>); <sup>13</sup>C NMR (CDCl<sub>3</sub>, 100 MHz):  $\delta$  = 190.1 (C = O, C-1), 148.6 (Ar-C, C-7, C-7'), 147.6 (Ar-C, C-6, C-6'), 136.7 (Ar-CH=C-, C-3, C-3'), 134.8 (Ar-CH=C-, C-2, C-2'), 130.2 (Ar-C, C-4, C-4'), 123.5 (Ar-C, C-9, C-9'), 115.7 (Ar-C, C-8, C-8'), 114.2 (Ar-C, C-5, C-5'), 78.4 (-C≡CH-), 76.0 (-C≡CH-), 64.6 (-OCH<sub>2</sub>), 56.8 (-OCH<sub>2</sub>CH<sub>3</sub>), 28.5 (-CH<sub>2</sub>), 23.0 (-CH<sub>2</sub>) and 14.8 (OCH<sub>2</sub>-CH<sub>3</sub>); HRMS: Calcd for C<sub>30</sub>H<sub>29</sub>O<sub>5</sub> [M-H]<sup>+</sup>, 469.2093, found: 469.2143

#### (3E,5E)-3,5-Bis(3-ethoxy-4-(prop-2-yn-1-yloxy)benzylidene)-1-methylpiperidin-4-one (4b)

Yellow coloured crystal; yield 84%; mp: 152–154 °C; IR (KBr)  $\nu_{\max}$  3241, 2117, 1660, 1574, 1502 cm<sup>-1</sup>; <sup>1</sup>H NMR (CDCl<sub>3</sub>, 400 MHz):  $\delta$  = 7.76 (2H, s, Ar-CH=C-, H-3, H-3'), 7.11 (2H, d,  $J$  = 8.4 Hz, Ar-H, H-9, H-9'), 7.02 (2H, d,  $J$  = 1.6 Hz, Ar-H, H-5, H-5'), 6.99 (2H, d,  $J$  = 8.4 Hz, Ar-H, H-8, H-8'), 4.83 (4H, d,  $J$  = 2.4 Hz, Ar-OCH<sub>2</sub>), 4.14 (4H, q,  $J$  = 8.0 Hz, -OCH<sub>2</sub>CH<sub>3</sub>), 3.80 (4H, s, -CH<sub>2</sub>-N-CH<sub>2</sub>-), 2.56 (2H, d,  $J$  = 2.4 Hz, -C≡CH), 2.5 (3H, s, -N-CH<sub>3</sub>), 1.50 (6H, t,  $J$  = 8.0 Hz, -OCH<sub>2</sub>-CH<sub>3</sub>); <sup>13</sup>C NMR (CDCl<sub>3</sub>, 100 MHz):  $\delta$  = 186.7 (C = O, C-1), 148.8 (Ar-C, C-7, C-7'), 148.0 (Ar-C, C-6, C-6'), 136.3 (Ar-CH=C-, C-3, C-3'), 131.8 (Ar-CH=C-, C-2, C-2'), 129.5 (Ar-C, C-4, C-4'), 123.4 (Ar-C, C-9, C-9'), 115.8 (Ar-C, C-8, C-8'), 114.3 (Ar-C, C-5, C-5'), 78.4 (-C≡CH-), 76.1 (-C≡CH-), 64.6 (OCH<sub>2</sub>-CH<sub>3</sub>), 56.8 (Ar-OCH<sub>2</sub>), 45.8 (-CH<sub>2</sub>-N-CH<sub>2</sub>), 29.7 (-N-CH<sub>3</sub>), 14.8 (OCH<sub>2</sub>-CH<sub>3</sub>); LC-MS: Calcd for C<sub>30</sub>H<sub>32</sub>NO<sub>5</sub> [M + H]<sup>+</sup>, 486.2, found: 486.2

#### (3E,5E)-3,5-Bis(3-methoxy-4-(prop-2-yn-1-yloxy)benzylidene)-1-methylpiperidin-4-one (4c)

Yellow coloured crystal; yield 80%; mp: 159–161 °C; IR (KBr)  $\nu_{\max}$  3227, 2117, 1660, 1569, 1503 cm<sup>-1</sup>; <sup>1</sup>H NMR (CDCl<sub>3</sub>, 400 MHz):  $\delta$  = 7.75 (2H, s, Ar-CH=C-, H-3, H-3'), 7.08 (2H, d,  $J$  = 8.4 Hz, Ar-H, H-9, H-9'), 7.01 (2H, d,  $J$  = 1.2 Hz, Ar-H, H-5, H-5'), 6.97 (2H, d,  $J$  = 8.4 Hz, Ar-H, H-8, H-8'), 4.81 (4H, d,  $J$  = 2.4 Hz, Ar-OCH<sub>2</sub>), 3.90 (6H, s, -OCH<sub>3</sub>), 3.78 (4H, s, -CH<sub>2</sub>-N-CH<sub>2</sub>-), 2.54 (2H, d,  $J$  = 2.4 Hz, -C≡CH), 2.48 (3H, s, -N-CH<sub>3</sub>); <sup>13</sup>C NMR (CDCl<sub>3</sub>, 100 MHz):  $\delta$  = 186.7 (C = O, C-1), 149.3 (Ar-C, C-7, C-7'), 147.7 (Ar-C, C-6, C-6'), 136.2 (Ar-CH=C-, C-3, C-3'), 131.9 (Ar-CH=C-, C-2, C-2'), 129.4 (Ar-C, C-4, C-4'), 123.3 (Ar-C, C-9, C-9'), 114.3 (Ar-C, C-8, C-8'), 113.6 (Ar-C, C-5, C-5'), 78.1 (-C≡CH-), 76.2 (-C≡CH-), 57.1 (Ar-OCH<sub>2</sub>), 56.6 (OCH<sub>3</sub>), 56.0 (-CH<sub>2</sub>-N-CH<sub>2</sub>), 45.8 (-N-CH<sub>3</sub>); LC-MS: Calcd for C<sub>28</sub>H<sub>28</sub>NO<sub>5</sub> [M + H]<sup>+</sup>, 458.5, found: 458.5



**(2E,5E)-2,5-Bis(3-ethoxy-4-(prop-2-yn-1-yloxy)benzylidene)cyclopentanone (4d)**

Yellow coloured crystal; yield 81%; mp: 177–179 °C; IR (KBr)  $\nu_{\max}$  3253, 2119, 1672, 1581, 1505  $\text{cm}^{-1}$ ;  $^1\text{H}$  NMR ( $\text{CDCl}_3$ , 400 MHz):  $\delta$  = 7.53 (2H, s, Ar-CH = C-, H-3, H-3'), 7.23 (2H, dd,  $J$  = 8.4 Hz and 1.6 Hz, Ar-H, H-9, H-9'), 7.15 (2H, d,  $J$  = 1.6 Hz, Ar-H), 7.11 (2H, d,  $J$  = 8.4 Hz, Ar-H), 4.83 (4H, d,  $J$  = 2.4 Hz, Ar-OCH<sub>2</sub>), 4.15 (4H, q,  $J$  = 7.2 Hz, -OCH<sub>2</sub>CH<sub>3</sub>), 3.10 (4H, s, -CH<sub>2</sub>), 2.53 (2H, d,  $J$  = 2.4 Hz, -C  $\equiv$  CH), 1.49 (6H, t,  $J$  = 7.2 Hz, -OCH<sub>2</sub>-CH<sub>3</sub>);  $^{13}\text{C}$  NMR ( $\text{CDCl}_3$ , 100 MHz):  $\delta$  = 196.1 (C = O, C-1), 148.9 (Ar-C, C-7, C-7'), 148.3 (Ar-C, C-6, C-6'), 135.8 (Ar-CH = C-, C-3, C-3'), 133.6 (Ar-CH = C-, C-2, C-2'), 130.2 (Ar-C, C-4, C-4'), 124.0 (Ar-C, C-9, C-9'), 115.6 (Ar-C, C-8, C-8'), 114.4 (Ar-C, C-5, C-5'), 78.3 (-C  $\equiv$  CH-), 76.1 (-C  $\equiv$  CH-), 64.7 (OCH<sub>2</sub>-CH<sub>3</sub>), 56.7 (Ar-OCH<sub>2</sub>), 26.5 (-CH<sub>2</sub>), 14.8 (OCH<sub>2</sub>-CH<sub>3</sub>); LC-MS: Calcd for C<sub>29</sub>H<sub>29</sub>O<sub>5</sub> [M + H]<sup>+</sup>, 457.5, found: 457.2.

**(2E,5E)-2,5-Bis(3-methoxy-4-(prop-2-yn-1-yloxy)benzylidene)cyclopentanone (4e)**

Yellow coloured crystal; yield 83%; mp: 178–180 °C; IR (KBr)  $\nu_{\max}$  3251, 2117, 1671, 1580, 1503  $\text{cm}^{-1}$ ;  $^1\text{H}$  NMR ( $\text{CDCl}_3$ , 400 MHz):  $\delta$  = 7.78 (2H, s, Ar-CH = C-, H-3, H-3'), 7.10 (2H, d,  $J$  = 8.4 Hz, Ar-H, H-9, H-9'), 7.03 – 6.98 (4H, m, Ar-H, H-5, H-5', H-8, H-8'), 4.84 (4H, d,  $J$  = 2.4 Hz, Ar-OCH<sub>2</sub>), 3.93 (6H, s, -OCH<sub>3</sub>), 2.57 (2H, d,  $J$  = 2.4 Hz, -C  $\equiv$  CH), 2.50 (4H, s, -CH<sub>2</sub>);  $^{13}\text{C}$  NMR ( $\text{CDCl}_3$ , 100 MHz):  $\delta$  = 196.4 (C = O, C-1), 149.1 (Ar-C, C-7, C-7'), 148.5 (Ar-C, C-6, C-6'), 136.0 (Ar-CH = C-, C-3, C-3'), 133.9 (Ar-CH = C-, C-2, C-2'), 130.4 (Ar-C, C-4, C-4'), 124.3 (Ar-C, C-9, C-9'), 115.8 (Ar-C, C-8, C-8'), 114.6 (Ar-C, C-5, C-5'), 78.5 (-C  $\equiv$  CH-), 76.4 (-C  $\equiv$  CH-), 64.8 (Ar-OCH<sub>2</sub>), 56.8 (-OCH<sub>3</sub>), 26.5 (-CH<sub>2</sub>); ESI-MS: Calcd for C<sub>27</sub>H<sub>25</sub>O<sub>5</sub> [M + H]<sup>+</sup>, 429.5, found: 430.0.

**(1E,4E)-1,5-Bis(3-ethoxy-4-(prop-2-yn-1-yloxy)phenyl)penta-1,4-dien-3-one (4f)**

Yellow coloured crystal; yield 85%; mp: 144–146 °C; IR (KBr)  $\nu_{\max}$  3263, 2120, 1645, 1579, 1502  $\text{cm}^{-1}$ ;  $^1\text{H}$  NMR ( $\text{CDCl}_3$ , 400 MHz):  $\delta$  = 7.67 (2H, d,  $J$  = 16 Hz, Ar-CH = C-, H-3, H-3'), 7.20 (2H, dd,  $J$  = 8.4 Hz and 2 Hz, Ar-H, H-9, H-9'), 7.16 (2H, d,  $J$  = 2 Hz, Ar-H, H-5, H-5'), 7.06 (2H, d,  $J$  = 8.4 Hz, Ar-H, H-8, H-8'), 6.95 (2H, d,  $J$  = 16 Hz, Ar-CH = CH-, H-2, H-2'), 4.82 (4H, d,  $J$  = 2.4 Hz, Ar-OCH<sub>2</sub>), 4.15 (4H, q,  $J$  = 7.2 Hz, -OCH<sub>2</sub>CH<sub>3</sub>), 2.54 (2H, d,  $J$  = 2.4 Hz, -C  $\equiv$  CH), 1.50 (6H, t,  $J$  = 7.2 Hz, -OCH<sub>2</sub>-CH<sub>3</sub>);  $^{13}\text{C}$  NMR ( $\text{CDCl}_3$ , 100 MHz):  $\delta$  = 188.8 (C = O, C-1), 149.3 (Ar-C, C-7, C-7'), 149.2 (Ar-C, C-6, C-6'), 143.0 (Ar-CH = CH-, C-3, C-3'), 129.0 (Ar-C, C-4, C-4'), 124.0 (Ar-CH

= CH-, C-2, C-2'), 122.5 (Ar-C, C-9, C-9'), 114.4 (Ar-C, C-8, C-8'), 112.2 (Ar-C, C-5, C-5'), 78.3 (-C  $\equiv$  CH-), 76.3 (-C  $\equiv$  CH-), 64.7 (OCH<sub>2</sub>-CH<sub>3</sub>), 56.8 (Ar-OCH<sub>2</sub>), 14.9 (OCH<sub>2</sub>-CH<sub>3</sub>); LC-MS: Calcd for C<sub>27</sub>H<sub>27</sub>O<sub>5</sub> [M + H]<sup>+</sup>, 431.5, found: 431.1.

**(1E,4E)-1,5-Bis(3-methoxy-4-(prop-2-yn-1-yloxy)phenyl)penta-1,4-dien-3-one (4g)**

Yellow coloured crystal; yield 82%; mp: 155–157 °C; IR (KBr)  $\nu_{\max}$  3253, 2109, 1660, 1571, 1495  $\text{cm}^{-1}$ ;  $^1\text{H}$  NMR ( $\text{CDCl}_3$ , 400 MHz):  $\delta$  = 7.71 (2H, d,  $J$  = 16 Hz, Ar-CH = C-, H-3, H-3'), 7.22 (2H, d,  $J$  = 8.4 Hz, Ar-H, H-9, H-9'), 7.17 (2H, s, Ar-H, H-5, H-5'), 7.07 (2H, d,  $J$  = 8 Hz, Ar-H, H-8, H-8'), 6.98 (2H, d,  $J$  = 16 Hz, Ar-CH = CH-, H-2, H-2'), 4.84 (4H, d,  $J$  = 2.4 Hz, Ar-OCH<sub>2</sub>), 3.96 (6H, s, -OCH<sub>3</sub>), 2.57 (2H, t,  $J$  = 2.4 Hz, -C  $\equiv$  CH);  $^{13}\text{C}$  NMR ( $\text{CDCl}_3$ , 100 MHz):  $\delta$  = 188.6 (C = O, C-1), 149.8 (Ar-C, C-7, C-7'), 149.0 (Ar-C, C-6, C-6'), 143.0 (Ar-CH = CH-, C-3, C-3'), 129.0 (Ar-C, C-4, C-4'), 124.0 (Ar-CH = CH-, C-2, C-2'), 122.5 (Ar-C, C-9, C-9'), 113.7 (Ar-C, C-8, C-8'), 110.5 (Ar-C, C-5, C-5'), 78.0 (-C  $\equiv$  CH-), 76.3 (-C  $\equiv$  CH-), 56.6 (Ar-OCH<sub>2</sub>), 56.0 (OCH<sub>3</sub>); LC-MS: Calcd for C<sub>25</sub>H<sub>23</sub>O<sub>5</sub> [M + H]<sup>+</sup>, 403.4, found: 403.1.

**(2E,6E)-2,6-Bis(3,5-dichloro-2-(prop-2-yn-1-yloxy)benzylidene)cyclohexanone (4h)**

Yellow coloured crystal; yield 84%; mp: 146–148 °C; IR (KBr)  $\nu_{\max}$  3243, 2109, 1661, 1560, 1423  $\text{cm}^{-1}$ ;  $^1\text{H}$  NMR ( $\text{CDCl}_3$ , 400 MHz):  $\delta$  = 7.87 (2H, s, Ar-CH = C-, H-3, H-3'), 7.42 (2H, d,  $J$  = 2.4 Hz, Ar-H, H-7, H-7'), 7.22 (2H, d,  $J$  = 2.4 Hz, Ar-H, H-5, H-5'), 4.71 (4H, d,  $J$  = 2.4 Hz, Ar-OCH<sub>2</sub>), 2.78 (4H, t,  $J$  = 8.0 Hz, -CH<sub>2</sub>-CH<sub>2</sub>-CH<sub>2</sub>), 2.54 (2H, t,  $J$  = 2.4 Hz, -C  $\equiv$  CH), 1.82–1.76 (2H, m, -CH<sub>2</sub>-CH<sub>2</sub>-CH<sub>2</sub>);  $^{13}\text{C}$  NMR ( $\text{CDCl}_3$ , 100 MHz):  $\delta$  = 189.0 (C = O, C-1), 151.3 (Ar-C, C-9, C-9'), 138.8 (Ar-CH = C-, C-3, C-3'), 133.3 (Ar-CH = C-, C-2, C-2'), 131.3 (Ar-C, C-7, C-7'), 130.2 (Ar-C, C-6, C-6'), 129.7 (Ar-C, C-5, C-5'), 129.5 (Ar-C, C-8, C-8'), 128.5 (Ar-C, C-4, C-4'), 77.8 (-C  $\equiv$  CH-), 61.0 (Ar-OCH<sub>2</sub>), 28.5 (-CH<sub>2</sub>), 22.7 (-CH<sub>2</sub>); LC-MS: Calcd for C<sub>26</sub>H<sub>18</sub>Cl<sub>4</sub>O<sub>3</sub> [M]<sup>+</sup>, 520.2, found: 520.0.

**(1E,4E)-1,5-Bis(3,5-dichloro-2-(prop-2-yn-1-yloxy)phenyl)penta-1,4-dien-3-one (4i)**

Yellow coloured crystal; yield 80%; mp: 181–183 °C; IR (KBr)  $\nu_{\max}$  3285, 2126, 1664, 1599, 1554  $\text{cm}^{-1}$ ;  $^1\text{H}$  NMR ( $\text{CDCl}_3$ , 400 MHz):  $\delta$  = 8.03 (2H, d,  $J$  = 16 Hz, Ar-CH = C-, H-3, H-3'), 7.57 (2H, d,  $J$  = 2.4 Hz, Ar-H, H-7, H-7'), 7.45 (2H, d,  $J$  = 2.4 Hz, Ar-H, H-5, H-5'), 7.12 (2H, d,  $J$  = 16 Hz, Ar-CH = CH-, H-2, H-2'), 4.78 (4H, d,  $J$  = 2.4 Hz, Ar-OCH<sub>2</sub>), 2.57 (2H, t,  $J$  = 2.4 Hz, -C  $\equiv$  CH);  $^{13}\text{C}$  NMR



(CDCl<sub>3</sub>, 100 MHz):  $\delta$  = 188.4 (C = O, C-1), 151.8 (Ar-C, C-9, C-9'), 136.9 (Ar-CH = CH-, C-3, C-3'), 132.3 (Ar-CH = CH-, C-2, C-2'), 131.7 (Ar-C, C-7, C-7'), 130.7 (Ar-C, C-6, C-6'), 129.8 (Ar-C, C-5, C-5'), 127.9 (Ar-C, C-8, C-8'), 125.9 (Ar-C, C-4, C-4'), 77.6 (-C  $\equiv$  CH-), 61.5 (Ar-OCH<sub>2</sub>); ESI-MS: Calcd for C<sub>23</sub>H<sub>14</sub>Cl<sub>4</sub>KO<sub>3</sub> [M + K]<sup>+</sup>, 519.3, found: 520.0

## Bioactivity assay

### Antifungal activity assay

Standard agar dilution method as per CLSI (formerly, NCCLS) was used to determine in vitro antifungal activity of synthesised analogues (Collins 1967; Duraiswamy et al. 2009). Synthesised analogues and standard drug Miconazole were dissolved in DMSO solvent. A phosphate buffer solution of pH 7 was used to dissolve medium yeast nitrogen base furthermore, it was autoclaved at 110 °C for 10 min. A growth control without an antifungal agent and solvent control DMSO were included with each set. On Sabouraud dextrose agar, fungal strains were freshly sub-cultured and incubated at 25 °C for 72 h. Fungal cells were suspended and diluted to get 10<sup>5</sup> cells/mL in sterile distilled water. Ten microliters of standardised suspension were inoculated onto the control plates and the antifungal agents were integrated with the media. The inoculated plates were incubated at 25 °C for 48 h. At the end of 48 and 72 h readings were taken. The MIC values (Minimum inhibitory concentration of drugs preventing the growth of macroscopically visible colonies on drug-containing plates when there was visible growth on the drug-free control plates) was calculated.

### Antioxidant activity assay

Synthesised curcumin analogues were screened for in vitro antioxidant activity by using 1, 1-diphenyl-2-picrylhydrazyl (DPPH) radical scavenging assay. The results were compared with standard antioxidant drug BHT (Butylated Hydroxy Toluene).

Radical scavenging activity of the synthesised compounds has been carried out in vitro by the 1, 1-diphenyl-2-picrylhydrazyl (DPPH) radical scavenging assay (Burits and Bucar 2000). The obtained results were compared with standard antioxidant BHT (Butylated Hydroxy Toluene). The hydrogen atom or electron donation ability of the compounds was calculated from the bleaching of the purple-coloured methanol solution of 1, 1-diphenyl-1-picrylhydrazyl (DPPH). The spectrophotometric assay uses the stable radical DPPH as a reagent. 1 mL of various concentrations of the test compounds (5, 10, 25, 50 and 100 mg/mL) in methanol was added to 4 mL of 0.004% (w/v)

methanol solution of DPPH. After a 30 min incubation period at room temperature, the absorbance was measured against blank at 517 nm. The percent inhibition (I %) of free radical production from DPPH was calculated by the following equation.

$$\% \text{ of scavenging} = [(A \text{ control} - A \text{ sample}) / A \text{ blank}] \times 100,$$

where 'A control' is the absorbance of the control reaction (containing all reagents except the test compound) and 'A sample' is the absorbance of the test compound. Tests were carried at in triplicate.

## Molecular docking

To gauge the binding affinity and the mode of interaction of the new propargylated monocarbonyl curcumin analogues to the critical fungal enzyme sterol 14 $\alpha$ -demethylase (CYP51), molecular docking study has been performed using the GLIDE (Grid-based Ligand Docking with Energetics) module of the Schrodinger Molecular modelling package (Schrodinger, LLC, New York, NY, 2015) (Halgren et al. 2004; Friesner et al. 2006). The 3D X-ray crystal structure of sterol 14 $\alpha$ -demethylase (CYP51) complexed with its inhibitor-fluconazole (pdb code: 3KHM) was obtained from the Protein Data Bank (PDB) (<http://www.rcsb.org/pdb>) and cleaned using with the *protein preparation wizard* applying the OPLS-2005 force field. This includes deletion of the crystallographic water molecules as there are no conserved interactions with receptor; addition of the missing protons/side-chain atoms corresponding to pH 7.0 and assignment of the appropriate charge and protonation state. The refined structure thus obtained was subjected to energy minimisation to relieve the steric clashes among the amino acid residues till RMSD for the heavy atoms reached 0.30 Å. The 3D structures of the curcumin analogues were sketched using the *build* panel in *Maestro* and further optimised using *Ligand Preparation* tool. This involves adjusting realistic bond lengths and angles, assignment of the partial charges using the OPLS-2005 force-field followed by energy minimisation until the RMSD of heavy atoms reached 0.001 Å. Next, using the *Receptor Grid Generation* panel, shape and properties of the active site of the CYP51 enzyme were defined for which a grid box of 10  $\times$  10  $\times$  10 Å dimensions centred on the centroid of the co-crystallised ligand was generated. Before submitting the calculations for the synthesised dataset, the molecular docking protocol was validated by extracting the co-crystallised ligand (Fluconazole) and re-docking using the above setup which could produce an RMSD of <0.29 Å (Fig. 7).

With this setup, molecular docking was performed to determine the binding affinities and modes of binding of

the propargylated monocarbonyl curcumin analogues towards CYP51 using the extra precision Glide scoring function. The outputs files i.e. docking poses were visualised and investigated for the most significant elements of thermodynamic interactions using the Maestro's Pose Viewer utility.

## Conclusion

In conclusion, we have synthesised a small, focused library of propargylated monocarbonyl curcumin analogues and screened for their *in vitro* antifungal and antioxidant activity. Most of the synthesised analogues especially **4a**, **4b** and **4c** were found to display excellent antifungal potential and can be further developed as lead molecules in search of new antifungal agents. Furthermore, the antioxidant activity of synthesised analogues was studied using DPPH assay and BHT as a positive control. Compound **4b**, **4c**, **4e** and **4i** displayed stronger antioxidant potential as compared with BHT. Furthermore, molecular docking study could provide valuable insight into the binding affinity and the mode of interactions of these compounds into the active site of crucial fungal enzyme CYP51. The per-residue interaction analysis could highlight the bonded (hydrogen bonding) and non-bonded (steric and electrostatic) interactions that influence their binding affinity towards the target. This information is being fruitfully utilised to optimise these propargylated monocarbonyl curcumin analogues to identify and optimise new antifungal and antioxidant agents.

**Acknowledgements** Author AAN is thankful to Principal, K. M. C. College Khopoli, for providing DST-FIST funded laboratory for this research work. Author SVA is very thankful to the Council of Scientific and Industrial Research (CSIR), New Delhi for providing a research fellowship. The authors are also grateful for providing laboratory facilities to the Head, Department of Chemistry, Dr Babasaheb Ambedkar Marathwada University, Aurangabad. We are also grateful to Schrodinger Inc. for GLIDE software to perform the molecular docking studies.

## Compliance with ethical standards

**Conflict of interest** The authors declare that they have no conflict of interest.

**Publisher's note** Springer Nature remains neutral with regard to jurisdictional claims in published maps and institutional affiliations.

## References

Ahmad W, Kumolosasi E, Jantan I et al. (2014) Effects of novel diarylpentanoid analogues of curcumin on secretory phospholipase A2, cyclooxygenases, lipo-oxygenase, and microsomal prostaglandin e synthase-1. *Chem Biol Drug Des* 83:670–681

- Anand P, Kunnumakkara AB, Newman RA et al. (2007) Bioavailability of curcumin: problems and promises. *Mol Pharm* 4:807–818
- Anand P, Thomas SG, Kunnumakkara AB et al. (2008) Biological activities of curcumin and its analogues (Congeners) made by man and mother nature. *Biochem Pharmacol* 76:1590–1611
- Bairwa K, Grover J, Kania M, Jachak SM (2014) Recent developments in chemistry and biology of curcumin analogues. *RSC Adv* 4:13946–13978
- Bodey GP (1992) Azole antifungal agents. *Clin Infect Dis* 14: S161–S169
- Buduma K, Chinde S, Dommati AK et al. (2016) Synthesis and evaluation of anticancer and antiobesity activity of 1-ethoxy carbonyl-3,5-bis (3'-indolyl methylene)-4-piperidone analogs. *Bioorg Med Chem Lett* 26:1633–1638
- Burits M, Bucar F (2000) Antioxidant activity of *Nigella sativa* essential oil. *Phyther Res* 14:323–328
- Carapina da Silva C, Pacheco BS, das Neves RN et al. (2019) Antiparasitic activity of synthetic curcumin monocarbonyl analogues against *Trichomonas vaginalis*. *Biomed Pharmacother* 111:367–377
- Casey PJ (1992) Biochemistry of protein prenylation. *J Lipid Res* 33:1731–1740
- Chen SY, Chen Y, Li YP et al. (2011) Design, synthesis, and biological evaluation of curcumin analogues as multifunctional agents for the treatment of Alzheimer's disease. *Bioorg Med Chem* 19:5596–5604
- Collins CH (1967) *Microbiological methods*. Butterworth-Heinemann, London
- Da Silva CR, De Andrade Neto JB, De Sousa, Campos R et al. (2014) Synergistic effect of the flavonoid catechin, quercetin, or epigallocatechin gallate with fluconazole induces apoptosis in *Candida tropicalis* resistant to fluconazole. *Antimicrob Agents Chemother* 58:1468–1478
- Deshmukh TR, Krishna VS, Sriram D et al. (2020) Synthesis and bioevaluation of  $\alpha, \alpha'$ -bis(1*H*-1,2,3-triazol-5-ylmethylene) ketones. *Chem Pap* 74:809–820
- Duraiswamy B, Mishra S, Subhashini V et al. (2009) Studies on the antimicrobial potential of *Mahonia leschenaultii* Takeda root and root bark. *Indian J Pharm Sci* 68:389
- Fine SA, Pulaski PD (1973) Reexamination of the Claisen-Schmidt condensation of phenylacetone with aromatic aldehydes. *J Org Chem* 38:1747–1749
- Friesner RA, Murphy RB, Repasky MP et al. (2006) Extra precision glide: docking and scoring incorporating a model of hydrophobic enclosure for protein-ligand complexes. *J Med Chem* 49:6177–6196
- Goel A, Kunnumakkara AB, Aggarwal BB (2008) Curcumin as "Curecumin": from kitchen to clinic. *Biochem Pharmacol* 75:787–809
- Halgren TA, Murphy RB, Friesner RA et al. (2004) Glide: a new approach for rapid, accurate docking and scoring. 2. Enrichment factors in database screening. *J Med Chem* 47:1750–1759
- Hatcher H, Planalp R, Cho J et al. (2008) Curcumin: from ancient medicine to current clinical trials. *Cell Mol Life Sci* 65:1631–1652
- Kerru N, Singh P, Koorbanally N et al. (2017) Recent advances (2015–2016) in anticancer hybrids. *Eur J Med Chem* 142:179–212
- Lal J, Gupta S, Thavaselvam D et al. (2016) Synthesis and pharmacological activity evaluation of curcumin derivatives. *Chin Chem Lett* 27:1067–1072
- Li Y, Zhang LP, Dai F et al. (2015) Hexamethoxylated monocarbonyl analogues of curcumin cause G2/M cell cycle arrest in NCI-H460 cells via Michael acceptor-dependent redox intervention. *J Agric Food Chem* 63:7731–7742

- Marchiani A, Rozzo C, Fadda A et al. (2013) Curcumin and curcumin-like molecules: from spice to drugs. *Curr Med Chem* 21:204–222
- Martins CVB, Da Silva DL, Neres ATM et al. (2009) Curcumin as a promising antifungal of clinical interest. *J Antimicrob Chemother* 63:337–339
- Masuda T, Maekawa T, Hidaka K, Bando H et al. (2001) Chemical studies on antioxidant mechanism of curcumin: analysis of oxidative coupling products from curcumin and linoleate. *J Agric Food Chem* 49:2539–2547
- Nagargoje AA, Akolkar SV, Siddiqui MM et al. (2019) Synthesis and evaluation of pyrazole-incorporated monocarbonyl curcumin analogues as antiproliferative and antioxidant agents. *J Chin Chem Soc* 66:1658–1665
- Nagargoje AA, Akolkar SV, Siddiqui MM et al. (2020) Quinoline based monocarbonyl curcumin analogs as potential antifungal and antioxidant agents: synthesis, bioevaluation and molecular docking study. *Chem Biodivers* 17(2):e1900624
- Pappas PG, Kauffman CA, Andes DR et al. (2015) Clinical practice guideline for the management of candidiasis: 2016 update by the infectious diseases society of America. *Clin Infect Dis* 62:e1–e50
- Paul NK, Jha M, Bhullar KS et al. (2014) All trans 1-(3-arylacryloyl)-3,5-bis (pyridin-4-ylmethylene)piperidin-4-ones as curcumin-inspired antineoplastics. *Eur J Med Chem* 87:461–470
- Praditya D, Kirchhoff L, Bruning J et al. (2019) Anti-infective properties of the golden spice curcumin. *Front Microbiol* 10:912
- Roman BI, De Ryck T, Verhasselt S et al. (2015) Further studies on anti-invasive chemotypes: an excursion from chalcones to curcuminoids. *Bioorg Med Chem Lett* 25:1021–1025
- Sahu PK (2016a) Design, structure activity relationship, cytotoxicity and evaluation of antioxidant activity of curcumin derivatives/analogues. *Eur J Med Chem* 121:510–516
- Sahu PK, Gupta SK et al. (2012) Synthesis and evaluation of antimicrobial activity of 4H-pyrimido[2,1-b] benzothiazole, pyrazole and benzylidene derivatives of curcumin. *Eur J Med Chem* 54:366–378
- Sahu PK, Sahu PL, Agarwal DD et al. (2016b) Structure activity relationship, cytotoxicity and evaluation of antioxidant activity of curcumin derivatives. *Bioorg Med Chem Lett* 26:1342–1347
- Sanabria-Rios DJ, Rivera-Torres Y, Rosario J et al. (2015) Chemical conjugation of 2-hexadecyanoic acid to C5-curcumin enhances its antibacterial activity against multi-drug resistant bacteria. *Bioorg Med Chem Lett* 25:5067–5071
- Seufert R, Sedlacek L, Kahl B et al. (2018) Prevalence and characterization of azole-resistant *Aspergillus fumigatus* in patients with cystic fibrosis: a prospective multicentre study in Germany. *J Antimicrob Chemother* 73:2047–2053
- Shehaan DJ, Hitchcock CA, Sibley CA et al. (1999) Current and emerging azole antifungal agents. *Clin Microbiol Rev* 12:40–79
- Shetty D, Kim YJ, Shim H, Snyder JP (2015) Eliminating the heart from the curcumin molecule: monocarbonyl curcumin mimics (MACs). *Molecules* 20:249–292
- Singh H, Kumar M, Nepali K et al. (2016) Triazole tethered C 5 -curcuminoid-coumarin based molecular hybrids as novel anti-tubulin agents: design, synthesis, biological investigation and docking studies. *Eur J Med Chem* 116:102–115
- Sokmen M, Khan A (2016) The antioxidant activity of some curcuminoids and chalcones. *Inflammopharmacol* 24:81–86
- Subhedar DD, Shaikh MH, Nawale L et al. (2017) Quinolidene based monocarbonyl curcumin analogues as promising antimycobacterial agents: synthesis and molecular docking study. *Bioorg Med Chem Lett* 27:922–928
- Tiwari A, Kumar S, Shivahare R et al. (2015) Chemotherapy of leishmaniasis part XIII: design and synthesis of novel heteroretinoid-bisbenzylidene ketone hybrids as antileishmanial agents. *Bioorg Med Chem Lett* 25:410–413
- Wang YJ, Pan MH, Cheng AL, Lin LI, Ho YS, Hsieh CY et al. (1997) Stability of curcumin in buffer solutions and characterization of its degradation products. *J Pharm Biomed Anal* 15:1867–1876
- Wang ZSen, Chen LZ, Liu XH, Chen FH (2017) Diarylpentadienone derivatives (curcumin analogues): synthesis and anti-inflammatory activity. *Bioorg Med Chem Lett* 27:1803–1807
- Zheng QT, Yang ZH, Yu LY et al. (2017) Synthesis and antioxidant activity of curcumin analogs. *J Asian Nat Prod Res* 19:489–503
- Ziani N, Sid A, Demonceau A et al. (2013) Synthesis of new curcumin analogues from Claisen-Schmidt condensation. *Eur J Chem* 4:146–148



## FULL PAPER

# New *N*-phenylacetamide-linked 1,2,3-triazole-tethered coumarin conjugates: Synthesis, bioevaluation, and molecular docking study

Satish V. Akolkar<sup>1</sup> | Amol A. Nagargoje<sup>1,2</sup> | Mubarak H. Shaikh<sup>1,3</sup> |  
Murad Z. A. Warshagha<sup>1</sup> | Jaiprakash N. Sangshetti<sup>4</sup> | Manoj G. Damale<sup>5</sup> |  
Bapurao B. Shingate<sup>1</sup>

<sup>1</sup>Department of Chemistry, Dr. Babasaheb Ambedkar Marathwada University, Aurangabad, India

<sup>2</sup>Department of Chemistry, Khopoli Municipal Council College, Khopoli, India

<sup>3</sup>Department of Chemistry, Radhabai Kale Mahila Mahavidyalaya, Ahmednagar, India

<sup>4</sup>Department of Pharmaceutical Chemistry, Y. B. Chavan College of Pharmacy, Dr. Rafiq Zakaria Campus, Aurangabad, India

<sup>5</sup>Department of Pharmaceutical Chemistry, Srinath College of Pharmacy, Aurangabad, India

## Correspondence

Bapurao B. Shingate, Department of Chemistry, Dr. Babasaheb Ambedkar Marathwada University, Aurangabad 431 004, India.  
Email: [bapushingate@gmail.com](mailto:bapushingate@gmail.com)

## Abstract

A series of new 1,2,3-triazole-tethered coumarin conjugates linked by *N*-phenylacetamide was efficiently synthesized via the click chemistry approach in excellent yields. The synthesized conjugates were evaluated for their in vitro antifungal and antioxidant activities. Antifungal activity determination was carried out against fungal strains such as *Candida albicans*, *Fusarium oxysporum*, *Aspergillus flavus*, *Aspergillus niger* and *Cryptococcus neoformans*. Compounds **7b**, **7d**, **7e**, **8b** and **8e** displayed higher potency than the standard drug miconazole, with lower minimum inhibitory concentration values. Also, compound **7a** exhibited potential radical scavenging activity as compared with the standard antioxidant butylated hydroxytoluene. In addition, a molecular docking study of the newly synthesized compounds was carried out, and the results showed a good binding mode at the active site of the fungal (*C. albicans*) P450 cytochrome lanosterol 14 $\alpha$ -demethylase enzyme. Furthermore, the synthesized compounds were also tested for ADME properties, and they demonstrated potential as good candidates for oral drugs.

## KEYWORDS

ADME properties, antifungal activity, antioxidant activity, molecular docking, triazole-coumarin conjugates

## 1 | INTRODUCTION

The incidence of systemic fungal infection has increased dramatically in recent years due to an increase in the number of patients undergoing anticancer chemotherapy and organ transplantation, and AIDS patients.<sup>[1]</sup> Fungi are vital opportunistic human pathogens that have become drug-resistant to many approved compounds, especially *Cryptococcus neoformans*, *Candida*, and *Aspergillus* species, with serious potential consequences. The commonly used azole-based antifungal agents are miconazole, fluconazole, voriconazole, and itraconazole, which showed a wide range of antifungal activity.<sup>[2]</sup> Azoles, especially triazole-based antifungal agents (e.g., voriconazole, fluconazole, and posaconazole) are

widely used for the prevention and treatment of fungal infections (Figure 1). These antifungal drugs inhibit CYP51 (P450 cytochrome lanosterol 14 $\alpha$ -demethylase), a key enzyme in ergosterol biosynthesis.<sup>[3]</sup> However, extensive use of these drugs has resulted in severe drug resistance.<sup>[4]</sup> Therefore, the development of more potent, broad-spectrum antifungal agents with fewer side effects and improved efficiency to cure fungal infections is urgently required.

To counteract the harmful effects of free radicals and other oxidants, the human body has a complex system of natural enzymatic and nonenzymatic antioxidants. Free radicals are unstable chemical species having unpaired electrons that are extremely reactive toward other species. The action of reactive oxygen species (ROS) results in

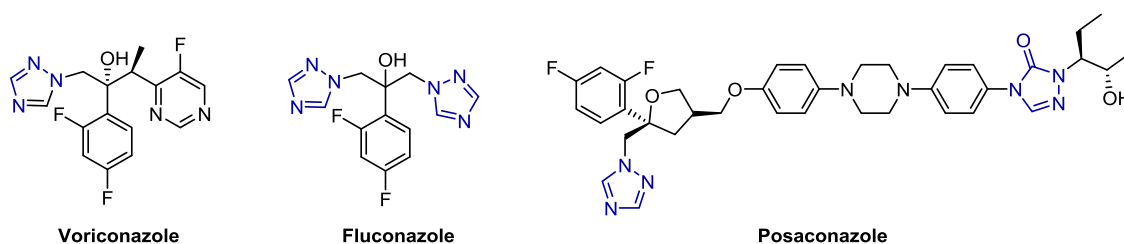


**FIGURE 1** 1,2,4-Triazole-based antifungal drugs

key biomolecules being altered and modulated in function. There is a delicate balance between producing and removing free radicals in healthy organisms. Triazole–coumarin conjugates have unique potential to scavenge ROS such as hydroxyl and superoxide radicals.<sup>[9]</sup> Therefore, the synthesis and development of new antioxidants having the triazole–coumarin pharmacophore have enormous significance in medicinal chemistry.

Diversely functionalized 1,2,3-triazole derivatives have attracted great attention due to their extensive biological properties such as antioxidant,<sup>[5]</sup> antifungal,<sup>[6,7]</sup> antitubercular,<sup>[8]</sup> antibacterial,<sup>[9]</sup> anticancer,<sup>[10]</sup> anti-HIV,<sup>[11]</sup> antimicrobial,<sup>[12]</sup> and antimalarial activity.<sup>[13]</sup> The 1,4-disubstituted-1,2,3-triazoles were synthesized *via* copper-catalyzed azide–alkyne cycloaddition reaction, well known as a click chemistry reaction.<sup>[14]</sup> In the field of medicinal chemistry and drug discovery, 1,2,3-triazoles have received<sup>[15–19]</sup> increasing attention since Sharpless group introduced the “click chemistry” concept. The promising properties of the 1,2,3-triazole ring, such as hydrogen bonding capability, rigidity, stability under *in vivo* conditions, and moderate dipole character, could be helpful for binding of biomolecular targets and increasing solubility.<sup>[15,20,21]</sup> Moreover, 1,2,3-triazoles have become increasingly useful and important in the construction of bioactive and functional molecules as attractive linker units that could connect two pharmacophores to provide innovative bifunctional drugs.<sup>[22–24]</sup> Many drugs available in the market contain 1,2,3-triazole core in their structure, such as cefatrizine (antibiotic), carboxyamidotriazole (anticancer agent), rufinamide (anticonvulsant) and tazobactam (antibacterial agent; Figure 2).

Synthesis of new heterocycles with multiple biological activities remains an interest of the researchers. Among the oxygen heterocycles, coumarins are the privileged structural motifs commonly found in many natural products. Literature reveals that coumarin and its derivatives are isolated from plant-associated endophytes and

display potential biological activities.<sup>[25–29]</sup> In recent years, coumarin-based hybrid molecules have attracted intense interest due to their diverse biological properties.<sup>[30,31]</sup> Different nitrogen-containing heterocycles (e.g., triazole, thiazolidine, thiazole, etc.) in conjunction with coumarin backbone significantly increase the antimicrobial efficiency and also broaden antimicrobial spectrum of these compounds.<sup>[32–34]</sup>

Due to the rapid and effective distribution of privileged systems with relatively improved biological properties as compared with individual entities, the molecular hybridization approach has established eminence over the past few years.<sup>[35]</sup> With strong drug-like properties and desirable binding interactions, these hybrid molecules have emerged for further chemical modifications as structurally novel chemotypes with several exploitable sites. In recent years, a library of coumarin–triazole conjugates was synthesized and proved to enhance biological activity.<sup>[36–39]</sup> There are various reports on the synthesis of coumarin–triazole conjugates with antifungal activity.<sup>[32,38,40,41]</sup> Therefore, the design and synthesis of coumarin–triazole conjugates is crucial for the enhancement of activity.

In continuation of our previous works<sup>[40,42–51]</sup> on the synthesis and biological evaluation of heterocycles, and the significance of coumarin and 1,2,3-triazole moieties in a single molecular framework, herein, we would like to report the design and syntheses of new *N*-phenylacetamide-linked coumarin–triazole conjugates by using the molecular hybridization approach (Figure 3).

The 1,2,3-triazole moiety is good for antifungal activity, and coumarin derivatives have been well reported for the antioxidant activity. Thus, we have evaluated the synthesized compounds for their antifungal and antioxidant activities. The computational parameters like docking study for antifungal activity and ADME (absorption, distribution, metabolism, and elimination) prediction of synthesized coumarin–triazole conjugates were also performed.

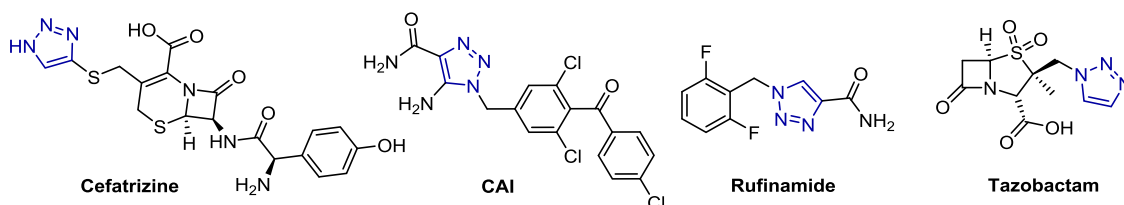


**FIGURE 2** Marketed drugs containing the 1,2,3-triazole unit



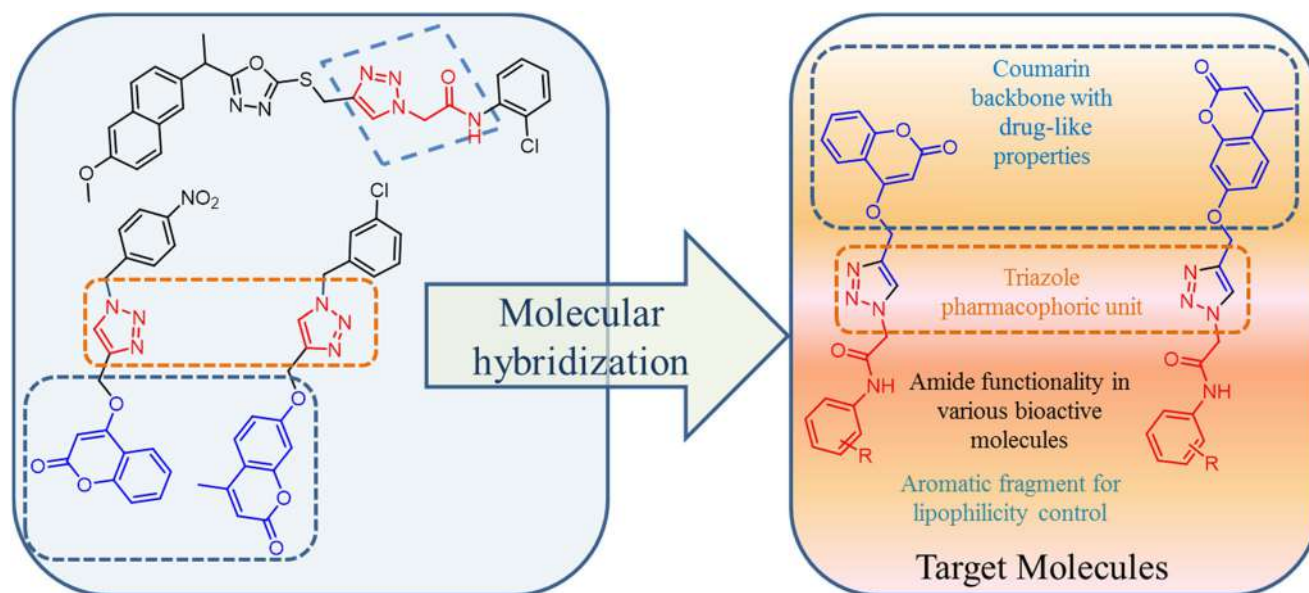


**FIGURE 3** The design strategy for the synthesis of new *N*-phenylacetamide-linked 1,2,3-triazole-coumarin conjugates

## 2 | RESULTS AND DISCUSSION

### 2.1 | Chemistry

1,4-Disubstituted-1,2,3-triazoles bearing amide functionality displayed several biological activities.<sup>[52–55]</sup> On the basis of these reports and molecular hybridization concept, we have designed and synthesized coumarin-triazole conjugates with amide linkage in their structures. A library of substituted 2-(4-[[[4-methyl-2-oxo-2*H*-chromen-7-yl]oxy]methyl]-1*H*-1,2,3-triazol-1-yl)-*N*-phenylacetamides **7a–g** and substituted 2-(4-[[[2-oxo-2*H*-chromen-4-yl]oxy]methyl]-1*H*-1,2,3-triazol-1-yl)-*N*-phenylacetamides **8a–g** was synthesized from commercially available starting materials. These compounds were constructed by the fusion of coumarin-based alkynes and substituted 2-azido-*N*-phenylacetamides *via* the click chemistry approach (Scheme 1).

The starting materials, 2-azido-*N*-phenylacetamides **3a–g**, were prepared by a previously reported method<sup>[45,51]</sup> from corresponding anilines in excellent yields (Scheme 1). The 7-hydroxy-4-methyl coumarin **5a** has been synthesized *via* acid-catalyzed Pechmann condensation between resorcinol and ethyl acetoacetate in 80% yield (Scheme 1). Compounds **6a** and **6b** were prepared by a previously reported method.<sup>[44]</sup> Compounds **5a** and **5b** were treated with propargyl bromide in the presence of  $K_2CO_3$  as a base in *N,N*-dimethylformamide (DMF) at room temperature, resulting in 4-methyl-7-(prop-2-yn-1-yloxy)-2*H*-chromen-2-one **6a** and 4-(prop-2-yn-1-yloxy)-2*H*-chromen-2-one **6b**, respectively, in excellent yields (Scheme 1).

Finally, the click reaction of compounds **6a,b** with azides **3a–g** in the presence of  $Cu(OAc)_2$  in *t*-BuOH- $H_2O$  (3:1) at room temperature for 8–10 hr gave the corresponding 1,4-disubstituted-1,2,3-triazole-coumarin conjugates **7a–g** and **8a–g**, respectively, in good-to-excellent yield (88–94%; Scheme 1).

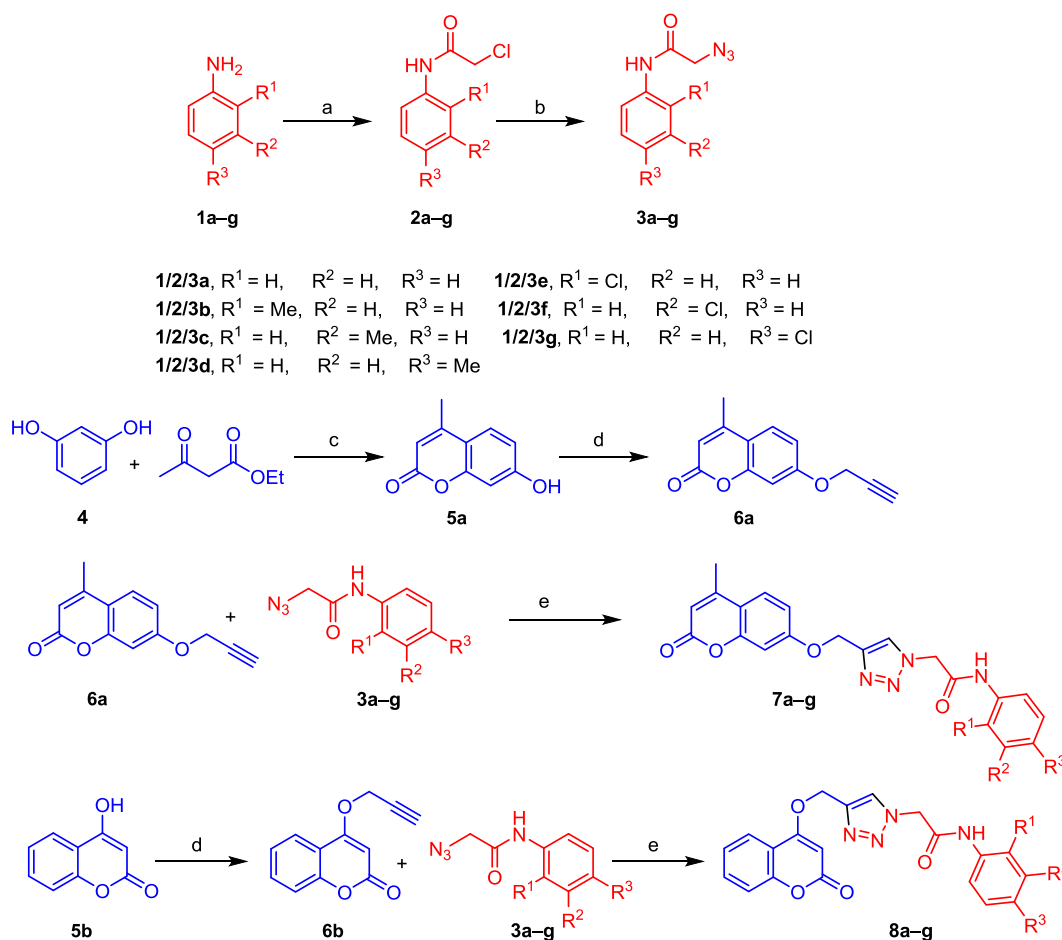
Regioselective formation of 1,4-disubstituted 1,2,3-triazole-coumarin conjugates **7a–g** and **8a–g** has been confirmed by physical

data and spectroscopic techniques such as Fourier-transform infrared spectroscopy (FTIR),  $^1H$  nuclear magnetic resonance (NMR),  $^{13}C$  NMR, and high-resolution mass spectra (HRMS). According to the FTIR spectrum of compound **7a**, the peaks observed at  $3,275\text{ cm}^{-1}$  indicate the presence of N-H group, and the peaks observed at  $1,698$  and  $1,670\text{ cm}^{-1}$  indicate the presence of two carbonyl groups. In the  $^1H$  NMR spectrum of compound **7a**, the signal at 2.41 ppm indicates the methyl group present on the coumarin ring, and signals at 5.32 and 5.37 ppm are for two protons each and they indicate the presence of two methylene groups attached with nitrogen and oxygen heteroatom, respectively. In addition to this, the signal appearing at 8.32 ppm for one proton clearly indicates the formation of the 1,4-disubstituted 1,2,3-triazole ring. In the  $^{13}C$  NMR spectrum of compound **7a**, the signal at 18.6 ppm indicates methyl carbon, and the signals at 52.7 and 62.1 ppm indicate the presence of two methylene groups attached to the nitrogen of triazole and oxygen attached to the coumarin ring, respectively. Furthermore, the peak observed at 161.6 ppm indicates amide carbonyl carbon and the peak at 164.6 ppm indicates the presence of carbonyl carbon (lactone carbon) in the coumarin ring. The formation of compound **7a** has been further confirmed by mass spectrometry. The calculated  $[M+Na]^+$  for compound **7a** is at 413.1226, and observed  $[M+Na]^+$  in mass spectrum is at 413.1171. Similarly, compounds **7b–g** and **8a–g** were characterized by the spectral analysis. The structures of synthesized triazole-coumarin conjugates are represented in Figure 4.

### 2.2 | Biological activity

#### 2.2.1 | Antifungal activity

The synthesized compounds were screened for their *in vitro* antifungal activities against five different fungal strains such as *Candida*



**SCHEME 1** The synthesis of coumarin-triazole conjugates. Reagents and conditions: (a) Chloroacetyl chloride, NEt<sub>3</sub>, CH<sub>2</sub>Cl<sub>2</sub>, 0°C at room temperature (rt), 3–5 hr, 85–95%; (b) NaN<sub>3</sub>, toluene, reflux, 5–7 hr, 88–96%; (c) H<sub>2</sub>SO<sub>4</sub>, 0°C, 80%; (d) propargyl bromide, K<sub>2</sub>CO<sub>3</sub>, N,N-dimethylformamide, 2 hr, 93–95%; (e) Cu(OAc)<sub>2</sub> (10 mol%), t-BuOH/H<sub>2</sub>O (3:1), rt, 8–10 hr, 88–94%

*albicans*, *Fusarium oxysporum*, *Aspergillus flavus*, *Aspergillus niger* and *C. neoformans*. The minimum inhibitory concentration (MIC, µg/ml) values of all the newly synthesized compounds were determined by the standard agar dilution method as per the Clinical & Laboratory Standards Institute (CLSI; formerly NCCLS) guidelines.<sup>[56]</sup> Miconazole was used as the standard antifungal drug for the comparison of antifungal activities and dimethyl sulfoxide (DMSO) was used as negative control. The data on the antifungal activity are presented in Table 1. Most of the compounds from the series exhibited a good-to-excellent antifungal activity against all the fungal strains with MIC values ranging from 12.5 to 25 µg/ml.

Without substitution on the phenyl ring, compound 7a exhibited a two fold antifungal activity against *A. niger* and an equipotent activity against *C. albicans* and *F. oxysporum*, with MIC values of 12.5, 25, and 25 µg/ml, respectively, as compared with the standard antifungal drug miconazole. Compound 7b having methyl group at *ortho* position of the phenyl ring was two fold more potent than the standard miconazole against *F. oxysporum*, *A. niger* and *C. neoformans*, with an MIC value of 12.5 µg/ml; it was also equipotent against the fungal strain *C. albicans* with an MIC value of

25 µg/ml. Compound 7c with methyl substituent at *meta* position of the phenyl ring is equipotent to miconazole against fungal strains *A. niger* and *C. neoformans*, with an MIC value of 25 µg/ml, and it is two fold more potent than miconazole against *C. albicans*, with an MIC value of 12.5 µg/ml. Compound 7d with methyl group at *para* position shows two fold potency than the miconazole against *A. niger*, with an MIC value of 12.5 µg/ml, and it is equipotent against *C. albicans* (MIC: 25 µg/ml), *F. oxysporum* (MIC: 25 µg/ml), *A. flavus* (MIC: 12.5 µg/ml), and *C. neoformans* (MIC: 25 µg/ml). Compound 7e (chloro group at *ortho* position) exhibited a two fold activity against *C. albicans* and *A. niger* (MIC: 12.5 µg/ml). Compound 7e also displayed an equivalent activity against *F. oxysporum* and *C. neoformans*, with an MIC value of 25 µg/ml. Compounds 7f and 7g displayed an equipotent activity against *A. niger*, *C. neoformans*, *C. albicans* and *F. oxysporum*, with an MIC value of 25 µg/ml. In addition, compounds 8a–g are equivalent or more potent than the standard miconazole. Among the compounds, 8b, 8c, 8e, and 8f showed an equivalent or two fold activity against all the fungal strains, with MIC values of 12.5–25 µg/ml. The activity results clearly indicate that most of the triazole-coumarin conjugates are

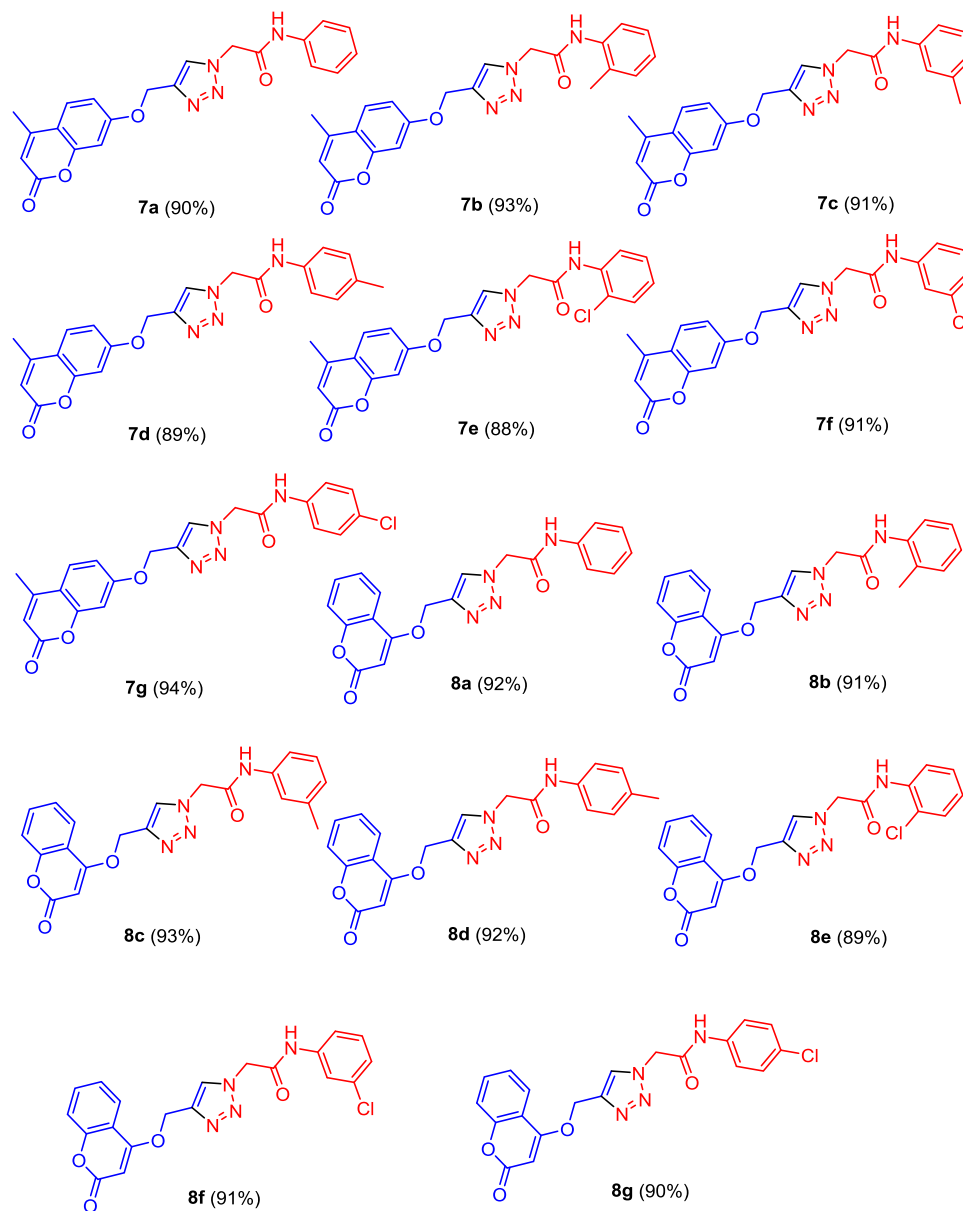


**FIGURE 4** Structures of triazole-coumarin conjugates

more potent or equipotent as compared with the miconazole, as shown in the graphical representation (Figure 5).

## 2.2.2 | Antioxidant activity

The 2,2-diphenyl-1-picrylhydrazyl (DPPH) radical scavenging assay was used to screen the antioxidant activities of the synthesized compounds 7a–g and 8a–g. The DPPH radical scavenging assay is the most widely used tool for screening the antioxidant activity of various natural and synthetic compounds. A lower  $IC_{50}$  value indicates more activity against antioxidants. The  $IC_{50}$  (concentration required to scavenge 50% of the radicals) values were calculated to assess the potential antioxidant activities. Butylated hydroxytoluene (BHT) has been used as the standard drug to compare antioxidant activities; the

findings obtained are summarized in Table 1. In comparison to the synthetic antioxidant BHT, compound 7a exhibited excellent radical scavenging activities, with an  $IC_{50}$  value of 15.01  $\mu\text{g/ml}$ , and remaining compounds showed good-to-moderate activities.

## 2.3 | Computational study

### 2.3.1 | Comparative modeling

The sequence identity and atomic resolution are two key parameters while selection of the template structure, which were 44% and 2.8 Å, respectively, which satisfy the basic criterion for comparative modeling. The final model was subjected to structure validation tool such as Procheck, ProSA, SPDBV and were found that 99.7 percent of the

Compound	Antifungal activity (MIC in $\mu\text{g/ml}$ )					DPPH IC <sub>50</sub> ( $\mu\text{g/ml}$ )	Molecular docking score
	CA	FO	AF	AN	CN		
7a	25	25	25	12.5	50	15.01 $\pm$ 0.26	-7.0932
7b	25	12.5	50	12.5	12.5	19.24 $\pm$ 0.19	-7.3901
7c	12.5	50	25	25	25	21.14 $\pm$ 0.97	-6.8629
7d	25	25	12.5	12.5	25	24.37 $\pm$ 0.34	-7.7256
7e	12.5	25	25	12.5	25	38.25 $\pm$ 0.24	-7.9245
7f	50	50	37.5	25	25	29.34 $\pm$ 0.19	-6.8669
7g	25	25	75	75	50	38.18 $\pm$ 0.54	-6.7934
8a	37.5	25	25	37.5	25	36.59 $\pm$ 0.64	-6.2456
8b	12.5	25	12.5	12.5	12.5	27.44 $\pm$ 0.31	-7.1950
8c	25	12.5	25	12.5	25	67.30 $\pm$ 0.05	-6.2411
8d	37.5	25	12.5	75	25	44.31 $\pm$ 0.99	-7.4214
8e	12.5	12.5	12.5	12.5	25	89.32 $\pm$ 0.76	-7.2302
8f	25	12.5	12.5	12.5	25	71.08 $\pm$ 0.26	-6.6233
8g	37.5	50	62.5	37.5	12.5	57.16 $\pm$ 0.79	-6.7248
MA	25	25	12.5	25	25	NA	-5.26
BHT	NA	NA	NA	NA	NA	16.47 $\pm$ 0.18	NA

Abbreviations: AF, *Aspergillus flavus*; AN, *Aspergillus niger*; BHT, butylated hydroxytoluene; CA, *Candida albicans*; CN, *Cryptococcus neoformans*; DPPH, 2,2-diphenyl-1-picrylhydrazyl; FO, *Fusarium oxysporum*; MA, miconazole; MIC, minimum inhibitory concentration; NA, not applicable.

residue followed in the allowed region. Also, overall model quality was assessed using Prosa where Z score is -3.2 and C $\alpha$  deviation is 0.45 Å, respectively. The validation study of the model suggested that it was perfect for further computation study.

### 2.3.2 | Molecular docking study

The molecular docking study of all synthesized triazole-coumarin conjugates, 7a-g and 8a-g, was performed against modeled

three-dimensional structure of cytochrome P450 lanosterol 14 $\alpha$ -demethylase of *C. albicans* to understand the binding affinity and binding interactions of enzyme and synthesized derivatives. The synthesized triazole-coumarin conjugates (7a-g, 8a-g) and the standard drug miconazole were docked in the active site of modeled CACYP51 using the AutoDock Vina docking tool. The results of docking are shown in Table 1. The analysis of docking interaction revealed that the triazole ring was mainly responsible for the interaction.

The triazole-coumarin conjugates 7b, 7d, 7e, 8b and 8e reproduced a similar result as that of in vitro activity data. All active

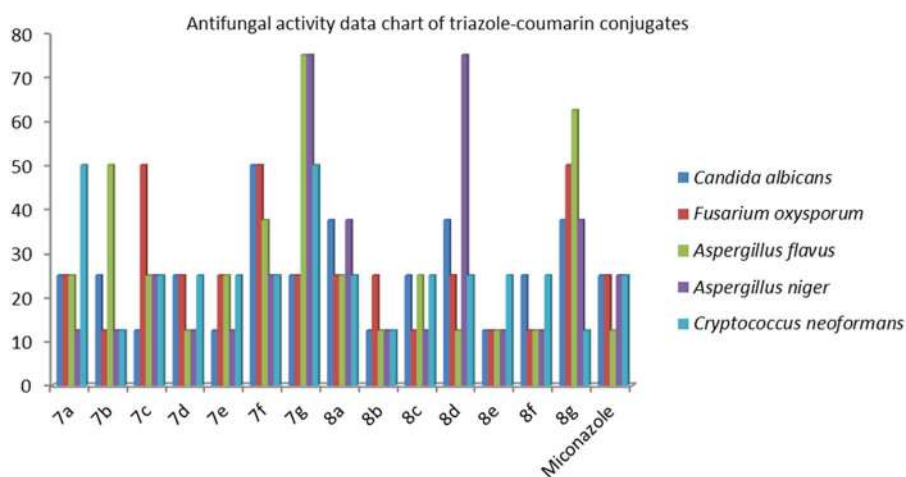


**TABLE 1** In vitro biological evaluation of the synthesized triazole-coumarin conjugates 7a-g and 8a-g

**FIGURE 5** A comparison of the antifungal activities of triazole-coumarin conjugates with miconazole

compounds efficiently interact with the active-site residues like Tyr105, Phe108, Phe121, Val130, Tyr168, Tyr154, Phe162, Leu412, Phe246, Met342, Ala343, Cys439, Ser414, Leu412 and Met544. The triazole-coumarin conjugates having *ortho* substitution on the phenyl ring partially replicate in vitro antifungal results, that is, **8b** and **8e**.

The *ortho*-substituted ( $-CH_3$ ) phenyl ring derivative **8b** (-7.19) interacts with polar and nonpolar amino acids of the active site. The polar amino acid Ser414 interacts with the nitrogen atom of the triazole ring to form conventional hydrogen bond interactions with a distance of 2.37 Å. The sulfur atom of polar amino acid Cys439 interacts with  $\pi$  electron cloud of the phenyl ring to form  $\pi$ -sulfur interactions. The aliphatic and hydrophobic amino acids Leu412, Tyr105, Phe108, Phe121, and Val130 interact with  $\pi$  electron cloud of aromatic ring to form  $\pi$ - $\pi$  T-shaped,  $\pi$ - $\pi$  stacked, and  $\pi$ -sulfur interactions with various distance values shown in Figure 6a.

The *ortho*-substituted ( $-Cl$ ) phenyl ring derivative **8e** (-7.23) interacts with aliphatic and hydrophobic amino acid residues Ala342 and Tyr168, where it interacts with carbonyl oxygen atom and nitrogen atom of the triazole ring with a distance of 2.21 and 2.08 Å to form conventional hydrogen bond interactions. The polar amino acid residue Met342 and hydrophobic amino acid Phe264 form a carbon-hydrogen bond and  $\pi$  interaction with *ortho*-substituted

chlorine atom with a distance of 2.08 and 3.77 Å. However, aliphatic and hydrophobic amino acids Leu412, Phe264, Phe162, Tyr154, and Met342 interact with  $\pi$  electron cloud of aromatic phenyl rings to form  $\pi$ - $\pi$  stacked, amide- $\pi$  stacked, alkyl and  $\pi$ -alkyl interactions shown in Figure 6b.

### 2.3.3 | In silico ADME prediction

Early prediction of druglikeness properties of lead compounds is an important task, as it decides the time and cost of drug discovery and development. Many of the active agents with a significant biological activity have failed in clinical trials due to inadequate druglikeness properties.<sup>[57]</sup> The druglikeness properties were predicted by analyzing ADME parameters based on Lipinski's rule of five. We had calculated and analyzed various physical descriptors and pharmaceutical relevant properties for ADMET prediction by using FAFDrugs2, and data are summarized in Table 2.

All the compounds showed significant values for the various parameters analyzed and showed good drug-like characteristics based on Lipinski's rule of five and its variants that characterized these agents to be likely orally active. The data obtained for all the

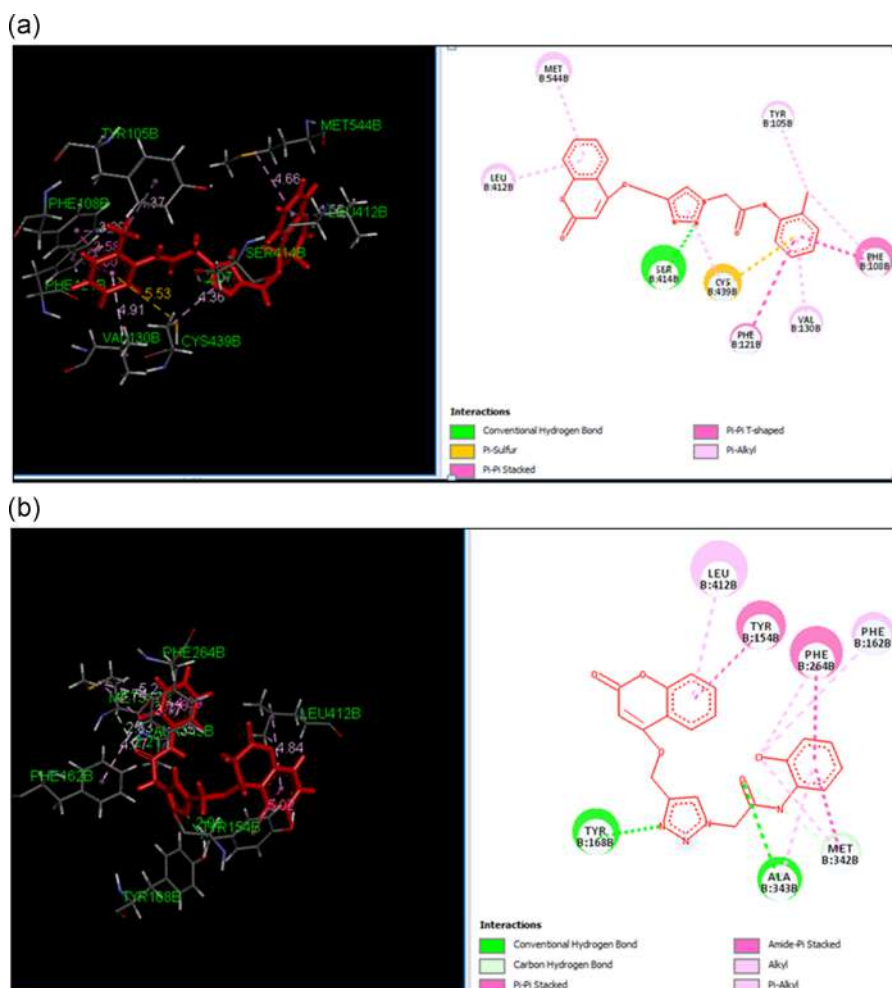


**FIGURE 6** Binding pose and molecular interactions of (a) **8b** and (b) **8e** in the active site of cytochrome P450 lanosterol 14 $\alpha$ -demethylase (CYP51)



**TABLE 2** Pharmacokinetic parameters of triazole–coumarin conjugates (**7a–g** and **8a–g**)

Entry	%ABS	MW	LogP	PSA	RotB	RigidB	HBD	HBA	Ratio H/C	Lipinski violation	Toxicity
<b>7a</b>	74.76	390.39	2.98	99.25	6	25	1	6	0.4	0	Nontoxic
<b>7b</b>	74.76	404.42	3.29	99.25	6	25	1	6	0.4	0	Nontoxic
<b>7c</b>	74.76	404.42	3.29	99.25	6	25	1	6	0.4	0	Nontoxic
<b>7d</b>	74.76	404.42	3.29	99.25	6	25	1	6	0.4	0	Nontoxic
<b>7e</b>	74.76	424.84	3.64	99.25	6	25	1	6	0.4	0	Nontoxic
<b>7f</b>	74.76	424.84	3.64	99.25	6	25	1	6	0.4	0	Nontoxic
<b>7g</b>	74.76	424.84	3.64	99.25	6	25	1	6	0.4	0	Nontoxic
<b>8a</b>	76.11	378.38	2.56	95.34	6	25	1	6	0.4	0	Nontoxic
<b>8b</b>	76.11	392.41	2.87	95.34	6	25	1	6	0.4	0	Nontoxic
<b>8c</b>	76.11	392.41	2.87	95.34	6	25	1	6	0.4	0	Nontoxic
<b>8d</b>	76.11	392.41	2.87	95.34	6	25	1	6	0.4	0	Nontoxic
<b>8e</b>	76.11	412.83	3.21	95.34	6	25	1	6	0.5	0	Nontoxic
<b>8f</b>	76.11	412.83	3.21	95.34	6	25	1	6	0.5	0	Nontoxic
<b>8g</b>	76.11	412.83	3.21	95.34	6	25	1	6	0.5	0	Nontoxic

Abbreviations: HBA, hydrogen bond acceptor; HBD, hydrogen bond donor; MW, molecular weight; PSA, polar surface area; RotB, rotatable bonds; RigidB, rigid bonds; %ABS, percentage absorption.

synthesized compounds were within the range of accepted values. None of the synthesized compounds had violated the Lipinski's rule of five. The value of polar surface area, logP, and H/C ratio of synthesized compounds **7a–g** and **8a–g** indicated good oral bioavailability. The parameters like the number of rotatable bonds and number of rigid bonds are linked with the intestinal absorption; results showed that all synthesized compounds had good absorption. All the synthesized compounds were found to be nontoxic. The in silico assessment of all the synthetic compounds has shown that they have very good pharmacokinetic properties, which is reflected in their physicochemical values, thus ultimately enhancing pharmacological properties of these molecules.

### 3 | CONCLUSIONS

In conclusion, we have synthesized new triazole–coumarin conjugates via the click chemistry approach, which were evaluated for their in vitro antifungal and antioxidant activity. The synthesized compounds displayed a promising antifungal activity as compared with the standard drug miconazole. Compounds **7b**, **7d**, **7e**, **8b**, and **8e** displayed an excellent antifungal activity as compared with the standard antifungal drug miconazole. Compound **7a** displayed a potential antioxidant activity when compared with standard BHT. In addition, molecular docking study of these synthesized triazole–coumarin conjugates reveals that they have a high affinity toward the active site of enzyme P450 cytochrome lanosterol 14 $\alpha$ -demethylase, which offers a strong platform for new structure-based design efforts. Furthermore, the analysis of the ADME parameters for the synthesized compounds predicted good drug-like properties and potential for development as

oral drug candidates. Thus, we suggest that compounds **7a** (antioxidant activity), **7b**, **7d**, **7e**, **8b** and **8e** (antifungal activity) can be developed as an important lead moiety, as they replicate in vitro activity in the inhibition assay and in silico molecular docking study. They can be used in scaffolds, hoping for the design and development of new lead compounds as antifungal agents.

## 4 | EXPERIMENTAL

### 4.1 | Chemistry

#### 4.1.1 | General

All the solvents and reagents were purchased from commercial suppliers, Sigma-Aldrich, Rankem India Ltd., and Spectrochem Pvt. Ltd., and were used without further purification. The completion of the reactions was monitored by thin-layer chromatography (TLC) on aluminum plates coated with silica gel 60 F<sub>254</sub>, with 0.25 mm thickness (Merck). The detection of the components was done by exposure to iodine vapors or UV light. Melting points were determined by open capillary methods and were uncorrected. <sup>1</sup>H NMR and <sup>13</sup>C NMR spectra were recorded in DMSO-*d*<sub>6</sub> on a Bruker DRX-400 and 500-MHz spectrometer. Infrared (IR) spectra were recorded using a Bruker ALPHA Eco-ATR FTIR spectrometer. High-resolution mass spectra (HRMS) were recorded on an Agilent 6520 (QTOF) mass spectrometer.

The original spectra of the investigated compounds, together with their InChI codes and some biological activity data, are provided as Supporting Information Data.

#### 4.1.2 | General procedure for the synthesis of substituted 2-(4-[[4-methyl-2-oxo-2H-chromen-7-yl]oxy]methyl)-1H-1,2,3-triazol-1-yl)-N-phenylacetamide derivatives 7a–g and 8a–g

To the stirred solution of alkyne **6** (1 mmol), azide **3** (1 mmol) and copper diacetate ( $\text{Cu}(\text{OAc})_2$ ; 10 mol%) in  $t\text{-BuOH-H}_2\text{O}$  (3:1) were added, and the resulting mixture was stirred at room temperature for 8–10 hr. The progress of the reaction was monitored by TLC using ethyl acetate/hexane as a solvent system. The reaction mixture was quenched with crushed ice, and the obtained solid was filtered and washed with water. The crude solid was crystallized in ethanol to afford the corresponding pure product. The synthesized compounds **7a–g** and **8a–g** were characterized by IR,  $^1\text{H}$  NMR,  $^{13}\text{C}$  NMR, and mass spectroscopy.

##### 2-(4-[[4-Methyl-2-oxo-2H-chromen-7-yl]oxy]methyl)-1H-1,2,3-triazol-1-yl)-N-phenylacetamide (**7a**)

Compound **7a** was obtained via the 1,3-dipolar cycloaddition reaction between azide **3a** and alkyne **6a** in 8.5 hr as a white solid, mp: 149–151°C; FTIR ( $\text{cm}^{-1}$ ): 3,275 (N–H stretching), 1,698 and 1,670 ( $\text{C}=\text{O}$  stretching);  $^1\text{H}$  NMR (500 MHz,  $\text{DMSO-}d_6$ ,  $\delta$  ppm): 2.41 (s, 3H,  $-\text{CH}_3$ ), 5.32 (s, 2H,  $-\text{NCH}_2\text{CO-}$ ), 5.37 (s, 2H,  $-\text{OCH}_2$ ), 6.23 (s, 1H, Ar-H), 7.07 (dd,  $J = 8.0, 3.0$  Hz, 1H, Ar-H), 7.10 (d,  $J = 8.0$  Hz, 1H, Ar-H), 7.18 (s, 1H, Ar-H), 7.34 (t,  $J = 8.0$  Hz, 2H, Ar-H), 7.58 (d,  $J = 8.0$  Hz, 2H, Ar-H), 7.71 (d,  $J = 8.0$  Hz, 1H, Ar-H), 8.32 (s, 1H, triazole), and 10.48 (s, 1H, NH);  $^{13}\text{C}$  NMR (125 MHz,  $\text{DMSO-}d_6$ ,  $\delta$  ppm): 18.6, 52.7, 62.1, 102.1, 111.8, 113.1, 113.9, 119.7, 124.3, 127.0, 127.1, 129.4, 138.9, 142.3, 153.9, 155.2, 160.6, 161.6, and 164.6; mass calculated for  $\text{C}_{21}\text{H}_{18}\text{N}_4\text{O}_4\text{Na}$  [ $\text{M}+\text{Na}$ ] $^+$ : 413.1226 and found: 413.1171.

##### 2-(4-[[4-Methyl-2-oxo-2H-chromen-7-yl]oxy]methyl)-1H-1,2,3-triazol-1-yl)-N-(o-tolyl)acetamide (**7b**)

Compound **7b** was obtained via the 1,3-dipolar cycloaddition reaction between azide **3b** and alkyne **6a** in 9.5 hr as an orange solid, mp: 195–197°C; FTIR ( $\text{cm}^{-1}$ ): 3,276 (N–H stretching), 1,690 and 1,670 ( $\text{C}=\text{O}$  stretching);  $^1\text{H}$  NMR (400 MHz,  $\text{DMSO-}d_6$ ,  $\delta$  ppm): 1.95 (s, 3H,  $-\text{CH}_3$ ), 2.12 (s, 3H,  $-\text{CH}_3$ ), 5.04 (s, 4H,  $-\text{NCH}_2\text{CO-}$  and  $-\text{OCH}_2$ ), 5.84 (s, 1H, Ar-H), 6.67–6.68 (m, 4H, Ar-H), 7.25 (s, 3H, Ar-H), 7.75 (s, 1H, triazole), and 9.07 (s, 1H, NH); mass calculated for  $\text{C}_{22}\text{H}_{20}\text{N}_4\text{O}_4\text{Na}$  [ $\text{M}+\text{Na}$ ] $^+$ : 427.1382 and found: 427.1334.

##### 2-(4-[[4-Methyl-2-oxo-2H-chromen-7-yl]oxy]methyl)-1H-1,2,3-triazol-1-yl)-N-(m-tolyl)acetamide (**7c**)

Compound **7c** was obtained via the 1,3-dipolar cycloaddition reaction between azide **3c** and alkyne **6a** in 8 hr as a white solid, mp: 190–192°C; FTIR ( $\text{cm}^{-1}$ ): 3,291 (N–H stretching), 1,678 ( $\text{C}=\text{O}$  stretching);  $^1\text{H}$  NMR (500 MHz,  $\text{DMSO-}d_6$ ,  $\delta$  ppm): 2.27 (s, 3H,  $-\text{CH}_3$ ), 2.39 (s, 3H,  $-\text{CH}_3$ ), 5.31 (s, 2H,  $-\text{NCH}_2\text{CO-}$ ), 5.36 (s, 2H,  $-\text{OCH}_2$ ), 6.21 (s, 1H, Ar-H), 6.91 (d,  $J = 8.0$  Hz, 1H, Ar-H), 7.05 (dd,  $J = 8.0, 4.0$  Hz, 1H, Ar-H), 7.17 (d,  $J = 4.0$  Hz, 1H, Ar-H), 7.21 (t,  $J = 8.0$  Hz, 1H, Ar-H), 7.37 (d,  $J = 8.0$  Hz, 1H, Ar-H), 7.42 (s, 1H, Ar-H), 7.69 (d,  $J = 8.0$  Hz, 1H, Ar-H), 8.31 (s, 1H, triazole) and 10.40 (s, 1H, NH);  $^{13}\text{C}$  NMR (125 MHz,  $\text{DMSO-}d_6$ ,  $\delta$  ppm): 17.9, 20.9, 52.1, 61.4, 101.4,

111.1, 112.4, 113.2, 116.3, 119.6, 124.3, 126.3, 126.4, 128.6, 138.0, 138.1, 141.6, 153.2, 154.5, 160.0, 160.9, and 163.9; HRMS calculated for  $\text{C}_{22}\text{H}_{21}\text{N}_4\text{O}_4$  [ $\text{M}+\text{H}$ ] $^+$ : 405.1563 and found: 405.1571.

##### 2-(4-[[4-Methyl-2-oxo-2H-chromen-7-yl]oxy]methyl)-1H-1,2,3-triazol-1-yl)-N-(p-tolyl)acetamide (**7d**)

Compound **7d** was obtained via the 1,3-dipolar cycloaddition reaction between azide **3d** and alkyne **6a** in 9 hr as a red solid, mp: 216–218°C; FTIR ( $\text{cm}^{-1}$ ): 3,248 (N–H stretching), 1,698 and 1,659 ( $\text{C}=\text{O}$  stretching);  $^1\text{H}$  NMR (400 MHz,  $\text{DMSO-}d_6$ ,  $\delta$  ppm): 2.25 (s, 3H,  $-\text{CH}_3$ ), 2.40 (s, 3H,  $-\text{CH}_3$ ), 5.31 (s, 2H,  $-\text{NCH}_2\text{CO-}$ ), 5.34 (s, 2H,  $-\text{OCH}_2$ ), 6.22 (s, 1H, Ar-H), 7.06 (dd,  $J = 8.0, 4.0$  Hz, 1H, Ar-H), 7.13 (d,  $J = 8.0$  Hz, 2H, Ar-H), 7.17 (d,  $J = 4.0$  Hz, 1H, Ar-H), 7.46 (d,  $J = 8.0$  Hz, 2H, Ar-H), 7.70 (d,  $J = 8.0$  Hz, 1H, Ar-H), 8.31 (s, 1H, triazole), and 10.40 (s, 1H, NH);  $^{13}\text{C}$  NMR (100 MHz,  $\text{DMSO-}d_6$ ,  $\delta$  ppm): 18.5, 20.8, 52.5, 61.9, 101.9, 111.6, 113.0, 113.7, 119.6, 126.9, 127.0, 129.6, 133.1, 136.2, 142.1, 153.8, 155.0, 160.5, 161.4, and 164.2; HRMS calculated for  $\text{C}_{22}\text{H}_{19}\text{N}_4\text{O}_4$  [ $\text{M-H}$ ] $^+$ : 403.1412 and found: 403.1424.

##### N-(2-Chlorophenyl)-2-(4-[[4-methyl-2-oxo-2H-chromen-7-yl]oxy]methyl)-1H-1,2,3-triazol-1-yl)acetamide (**7e**)

Compound **7e** was obtained via the 1,3-dipolar cycloaddition reaction between azide **3e** and alkyne **6a** in 9.5 hr as a white solid, mp: 206–208°C; FTIR ( $\text{cm}^{-1}$ ): 3,118 (N–H stretching), 1,664 and 1,600 ( $\text{C}=\text{O}$  stretching);  $^1\text{H}$  NMR (400 MHz,  $\text{DMSO-}d_6$ ,  $\delta$  ppm): 2.40 (s, 3H,  $-\text{CH}_3$ ), 5.31 (s, 2H,  $-\text{NCH}_2\text{CO-}$ ), 5.48 (s, 2H,  $-\text{OCH}_2$ ), 6.22 (s, 1H, Ar-H), 7.05 (d,  $J = 8.0$  Hz, 1H, Ar-H), 7.17 (s, 1H, Ar-H), 7.22 (t,  $J = 8.0$  Hz, 1H, Ar-H), 7.34 (t,  $J = 8.0$  Hz, 1H, Ar-H), 7.52 (d,  $J = 8.0$  Hz, 1H, Ar-H), 7.69 (d,  $J = 8.0$  Hz, 1H, Ar-H), 7.74 (d,  $J = 8.0$  Hz, 1H, Ar-H), 8.32 (s, 1H, triazole), and 10.09 (s, 1H, NH);  $^{13}\text{C}$  NMR (100 MHz,  $\text{DMSO-}d_6$ ,  $\delta$  ppm): 18.1, 52.0, 61.6, 101.6, 111.3, 112.6, 113.4, 125.9, 126.3, 126.5, 126.7, 126.8, 127.6, 129.6, 134.1, 141.8, 153.4, 154.7, 160.1, 161.1, and 164.9; HRMS calculated for  $\text{C}_{21}\text{H}_{16}\text{ClN}_4\text{O}_4$  [ $\text{M-H}$ ] $^+$ : 423.0866 and found: 423.0880.

##### N-(3-Chlorophenyl)-2-(4-[[4-methyl-2-oxo-2H-chromen-7-yl]oxy]methyl)-1H-1,2,3-triazol-1-yl)acetamide (**7f**)

Compound **7f** was obtained via the 1,3-dipolar cycloaddition reaction between azide **3f** and alkyne **6a** in 10 hr as a yellow solid, mp: 218–220°C;  $^1\text{H}$  NMR (400 MHz,  $\text{DMSO-}d_6$ ,  $\delta$  ppm): 2.39 (s, 3H,  $-\text{CH}_3$ ), 5.31 (s, 2H,  $-\text{NCH}_2\text{CO-}$ ), 5.38 (s, 2H,  $-\text{OCH}_2$ ), 6.21 (s, 1H, Ar-H), 7.05 (dd,  $J = 8.0, 4.0$  Hz, 1H, Ar-H), 7.15 (d,  $J = 8.0$  Hz, 2H, Ar-H), 7.36 (t,  $J = 8.0$  Hz, 1H, Ar-H), 7.44 (d,  $J = 8.0$  Hz, 1H, Ar-H), 7.69 (d,  $J = 8.0$  Hz, 1H, Ar-H), 7.77 (s, 1H, Ar-H), 8.31 (s, 1H, triazole), and 10.68 (s, 1H, NH);  $^{13}\text{C}$  NMR (100 MHz,  $\text{DMSO-}d_6$ ,  $\delta$  ppm): 18.2, 52.2, 61.6, 101.6, 111.3, 112.6, 113.4, 117.7, 118.8, 123.6, 126.5, 126.7, 130.7, 133.2, 139.8, 141.8, 154.7, 160.2, 161.1, and 164.7; HRMS calculated for  $\text{C}_{21}\text{H}_{16}\text{ClN}_4\text{O}_4$  [ $\text{M-H}$ ] $^+$ : 423.0866 and found: 423.0872.

##### N-(4-Chlorophenyl)-2-(4-[[4-methyl-2-oxo-2H-chromen-7-yl]oxy]methyl)-1H-1,2,3-triazol-1-yl)acetamide (**7g**)

Compound **7g** was obtained via the 1,3-dipolar cycloaddition reaction between azide **3g** and alkyne **6a** in 8.5 hr as a yellow solid,

mp: 210–212°C;  $^1\text{H}$  NMR (400 MHz, DMSO- $d_6$ ,  $\delta$  ppm): 2.40 (s, 3H,  $-\text{CH}_3$ ), 5.30 (s, 2H,  $-\text{NCH}_2\text{CO}-$ ), 5.36 (s, 2H,  $-\text{OCH}_2$ ), 6.23 (s, 1H, Ar-H), 7.05 (dd,  $J = 8.0, 4.0$  Hz, 1H, Ar-H), 7.17 (d,  $J = 4.0$  Hz, 1H, Ar-H), 7.39 (d,  $J = 8.0$  Hz, 2H, Ar-H), 7.60 (d,  $J = 8.0$  Hz, 2H, Ar-H), 7.70 (d,  $J = 8.0$  Hz, 1H, Ar-H), 8.31 (s, 1H, triazole), and 10.63 (s, 1H, NH); HRMS calculated for  $\text{C}_{21}\text{H}_{16}\text{ClN}_4\text{O}_4$   $[\text{M}-\text{H}]^+$ : 423.0866 and found: 423.0878.

2-(4-[[[2-Oxo-2H-chromen-4-yl]oxy]methyl]-1H-1,2,3-triazol-1-yl)-N-phenylacetamide (**8a**)

Compound **8a** was obtained via the 1,3-dipolar cycloaddition reaction between azide **3a** and alkyne **6b** in 10 hr as a white solid, mp: 216–218°C;  $^1\text{H}$  NMR (400 MHz, DMSO- $d_6$ ,  $\delta$  ppm): 5.40 (s, 2H,  $-\text{NCH}_2\text{CO}-$ ), 5.47 (s, 2H,  $-\text{OCH}_2$ ), 6.20 (s, 1H, Ar-H), 7.09 (t,  $J = 8.0$  Hz, 1H, Ar-H), 7.33 (t,  $J = 8.0$  Hz, 3H, Ar-H), 7.40 (d,  $J = 8.0$  Hz, 1H, Ar-H), 7.59 (d,  $J = 8.0$  Hz, 2H, Ar-H), 7.65 (t,  $J = 8.0$  Hz, 1H, Ar-H), 7.74 (d,  $J = 8.0$  Hz, 1H, Ar-H), 8.43 (s, 1H, triazole), and 10.51 (s, 1H, NH);  $^{13}\text{C}$  NMR (100 MHz, DMSO- $d_6$ ,  $\delta$  ppm): 52.3, 62.8, 91.4, 115.1, 116.5, 119.3, 122.8, 123.8, 124.3, 127.1, 128.9, 132.8, 138.4, 152.8, 164.2, and 164.4; HRMS calculated for  $\text{C}_{20}\text{H}_{15}\text{N}_4\text{O}_4$   $[\text{M}-\text{H}]^+$ : 375.1099 and found: 375.1080.

2-(4-[[[2-Oxo-2H-chromen-4-yl]oxy]methyl]-1H-1,2,3-triazol-1-yl)-N-(o-tolyl)acetamide (**8b**)

Compound **8b** was obtained via the 1,3-dipolar cycloaddition reaction between azide **3b** and alkyne **6b** in 8.5 hr as a white solid, mp: 170–172°C; FTIR ( $\text{cm}^{-1}$ ): 3,248 (N–H stretching), 1,698 and 1,659 ( $\text{C}=\text{O}$  stretching);  $^1\text{H}$  NMR (400 MHz, DMSO- $d_6$ ,  $\delta$  ppm): 2.24 (s, 3H,  $-\text{CH}_3$ ), 5.45 (s, 2H,  $-\text{NCH}_2\text{CO}-$ ), 5.47 (s, 2H,  $-\text{OCH}_2$ ), 6.20 (s, 1H, Ar-H), 7.11 (t,  $J = 8.0$  Hz, 1H, Ar-H), 7.17 (t,  $J = 8.0$  Hz, 1H, Ar-H), 7.23 (d,  $J = 8.0$  Hz, 1H, Ar-H), 7.33 (t,  $J = 8.0$  Hz, 1H, Ar-H), 7.42 (d,  $J = 8.0$  Hz, 2H, Ar-H), 7.65 (t,  $J = 8.0$  Hz, 1H, Ar-H), 7.73 (d,  $J = 8.0$  Hz, 1H, Ar-H), 8.43 (s, 1H, triazole), and 9.83 (s, 1H, NH);  $^{13}\text{C}$  NMR (100 MHz, DMSO- $d_6$ ,  $\delta$  ppm): 17.8, 52.0, 62.8, 91.4, 115.1, 116.5, 122.8, 124.2, 124.8, 125.6, 126.1, 127.0, 130.5, 131.6, 132.8, 135.5, 152.8, 161.6, 164.3, and 164.4; HRMS calculated for  $\text{C}_{21}\text{H}_{17}\text{N}_4\text{O}_4$   $[\text{M}-\text{H}]^+$ : 389.1255 and found: 389.1311.

2-(4-[[[2-Oxo-2H-chromen-4-yl]oxy]methyl]-1H-1,2,3-triazol-1-yl)-N-(m-tolyl)acetamide (**8c**)

Compound **8c** was obtained via the 1,3-dipolar cycloaddition reaction between azide **3c** and alkyne **6b** in 9 hr as a yellow solid, mp: 211–213°C; FTIR ( $\text{cm}^{-1}$ ): 3,307 (N–H stretching), 1,703 and 1,666 ( $\text{C}=\text{O}$  stretching);  $^1\text{H}$  NMR (400 MHz, DMSO- $d_6$ ,  $\delta$  ppm): 2.27 (s, 3H,  $-\text{CH}_3$ ), 5.40 (s, 2H,  $-\text{NCH}_2\text{CO}-$ ), 5.47 (s, 2H,  $-\text{OCH}_2$ ), 6.20 (s, 1H, Ar-H), 6.90 (d,  $J = 8.0$  Hz, 1H, Ar-H), 7.21 (t,  $J = 8.0$  Hz, 1H, Ar-H), 7.30–7.44 (m, 4H, Ar-H), 7.65 (t,  $J = 8.0$  Hz, 1H, Ar-H), 7.73 (d,  $J = 8.0$  Hz, 1H, Ar-H), 8.43 (s, 1H, triazole) and 10.44 (s, 1H, NH);  $^{13}\text{C}$  NMR (125 MHz, DMSO- $d_6$ ,  $\delta$  ppm): 21.4, 52.5, 63.0, 91.6, 115.3, 116.6, 116.7, 120.0, 123.3, 124.4, 124.7, 127.3, 129.0, 133.0, 138.4, 138.5, 153.0, 161.8, 164.3, and 164.6; HRMS calculated for  $\text{C}_{21}\text{H}_{17}\text{N}_4\text{O}_4$   $[\text{M}-\text{H}]^+$ : 389.1255 and found: 389.1346.

2-(4-[[[2-Oxo-2H-chromen-4-yl]oxy]methyl]-1H-1,2,3-triazol-1-yl)-N-(p-tolyl)acetamide (**8d**)

Compound **8d** was obtained via the 1,3-dipolar cycloaddition reaction between azide **3d** and alkyne **6b** in 8.5 hr as a white solid, mp: 247–249°C;  $^1\text{H}$  NMR (400 MHz, DMSO- $d_6$ ,  $\delta$  ppm): 2.25 (s, 3H,  $-\text{CH}_3$ ), 5.38 (s, 2H,  $-\text{NCH}_2\text{CO}-$ ), 5.47 (s, 2H,  $-\text{OCH}_2$ ), 6.20 (s, 1H, Ar-H), 7.13 (d,  $J = 8.0$  Hz, 2H, Ar-H), 7.34 (t,  $J = 8.0$  Hz, 1H, Ar-H), 7.41 (d,  $J = 8.0$  Hz, 1H, Ar-H), 7.47 (d,  $J = 8.0$  Hz, 2H, Ar-H), 7.66 (t,  $J = 8.0$  Hz, 1H, Ar-H), 7.74 (d,  $J = 8.0$  Hz, 1H, Ar-H), 8.41 (s, 1H, triazole), and 10.41 (s, 1H, NH);  $^{13}\text{C}$  NMR (100 MHz, DMSO- $d_6$ ,  $\delta$  ppm): 20.5, 52.3, 62.8, 91.4, 116.5, 119.2, 122.8, 124.2, 127.0, 129.3, 132.8, 135.9, 140.6, 152.8, 161.6, 163.9, and 164.4; HRMS calculated for  $\text{C}_{21}\text{H}_{17}\text{N}_4\text{O}_4$   $[\text{M}-\text{H}]^+$ : 389.1255 and found: 389.1314.

N-(2-Chlorophenyl)-2-(4-[[[2-oxo-2H-chromen-4-yl]oxy]methyl]-1H-1,2,3-triazol-1-yl)acetamide (**8e**)

Compound **8e** was obtained via the 1,3-dipolar cycloaddition reaction between azide **3e** and alkyne **6b** in 9.5 hr as a brown solid, mp: 217–219°C; FTIR ( $\text{cm}^{-1}$ ): 3,254 (N–H stretching), 1,709 and 1,673 ( $\text{C}=\text{O}$  stretching);  $^1\text{H}$  NMR (400 MHz, DMSO- $d_6$ ,  $\delta$  ppm): 5.47 (s, 2H,  $-\text{NCH}_2\text{CO}-$ ), 5.51 (s, 2H,  $-\text{OCH}_2$ ), 6.19 (s, 1H, Ar-H), 7.20–7.76 (m, 8H, Ar-H), 8.43 (s, 1H, triazole), and 10.12 (s, 1H, NH);  $^{13}\text{C}$  NMR (100 MHz, DMSO- $d_6$ ,  $\delta$  ppm): 52.0, 62.7, 91.4, 115.0, 116.5, 122.8, 124.2, 125.9, 126.3, 126.8, 127.1, 127.6, 129.6, 132.8, 134.1, 152.8, 161.5, 164.3, and 164.8; HRMS calculated for  $\text{C}_{20}\text{H}_{14}\text{ClN}_4\text{O}_4$   $[\text{M}-\text{H}]^+$ : 409.0709 and found: 409.0722.

N-(3-Chlorophenyl)-2-(4-[[[2-oxo-2H-chromen-4-yl]oxy]methyl]-1H-1,2,3-triazol-1-yl)acetamide (**8f**)

Compound **8f** was obtained via the 1,3-dipolar cycloaddition reaction between azide **3f** and alkyne **6b** in 10 hr as a red solid, mp: 218–220°C;  $^1\text{H}$  NMR (400 MHz, DMSO- $d_6$ ,  $\delta$  ppm): 5.42 (s, 2H,  $-\text{NCH}_2\text{CO}-$ ), 5.47 (s, 2H,  $-\text{OCH}_2$ ), 6.20 (s, 1H, Ar-H), 7.15 (d,  $J = 8.0$  Hz, 1H, Ar-H), 7.32–7.41 (m, 3H, Ar-H), 7.45 (d,  $J = 8.0$  Hz, 1H, Ar-H), 7.65 (t,  $J = 8.0$  Hz, 1H, Ar-H), 7.73 (d,  $J = 8.0$  Hz, 1H, Ar-H), 7.78 (s, 1H, Ar-H), 8.43 (s, 1H, triazole), and 10.71 (s, 1H, NH);  $^{13}\text{C}$  NMR (100 MHz, DMSO- $d_6$ ,  $\delta$  ppm): 52.3, 62.8, 91.4, 115.1, 116.5, 117.7, 118.8, 122.8, 123.6, 124.2, 127.0, 130.7, 132.8, 133.2, 139.8, 140.8, 152.8, 161.6, 164.4, and 164.6; HRMS calculated for  $\text{C}_{20}\text{H}_{14}\text{ClN}_4\text{O}_4$   $[\text{M}-\text{H}]^+$ : 409.0709 and found: 409.0724.

N-(4-Chlorophenyl)-2-(4-[[[2-oxo-2H-chromen-4-yl]oxy]methyl]-1H-1,2,3-triazol-1-yl)acetamide (**8g**)

Compound **8g** was obtained via the 1,3-dipolar cycloaddition reaction between azide **3g** and alkyne **6b** in 8 hr as a white solid, mp: 240–242°C;  $^1\text{H}$  NMR (400 MHz, DMSO- $d_6$ ,  $\delta$  ppm): 5.40 (s, 2H,  $-\text{NCH}_2\text{CO}-$ ), 5.46 (s, 2H,  $-\text{OCH}_2$ ), 6.19 (s, 1H, Ar-H), 7.30–7.44 (m, 4H, Ar-H), 7.57–7.68 (m, 3H, Ar-H), 7.74 (d,  $J = 8.0$  Hz, 1H, Ar-H), 8.41 (s, 1H, triazole), and 10.64 (s, 1H, NH);  $^{13}\text{C}$  NMR (100 MHz, DMSO- $d_6$ ,  $\delta$  ppm): 52.8, 63.2, 91.8, 115.6, 117.0, 121.3, 123.3, 124.7, 127.5, 127.9, 129.3, 133.3, 137.8, 141.3, 153.3, 162.0, and 164.8; HRMS calculated for  $\text{C}_{20}\text{H}_{14}\text{ClN}_4\text{O}_4$   $[\text{M}-\text{H}]^+$ : 409.0709 and found: 409.0715.

## 4.2 | Biological activity assays

### 4.2.1 | Antifungal activity

The antifungal activity was determined by the standard agar dilution method as per the CLSI (formerly NCCLS) guidelines.<sup>[56]</sup> The newly synthesized compounds were screened against five human pathogenic fungal strains, including *C. albicans* (NCIM 3471), *F. oxysporum* (NCIM 1332), *A. flavus* (NCIM 539), *A. niger* (NCIM 1196), and *C. neoformans* (NCIM 576). The standard miconazole and synthesized compounds were dissolved in DMSO. In phosphate buffer of pH 7, the medium yeast nitrogen base was dissolved and autoclaved for a duration of 10 min at 110°C. With each set, a growth control without the antifungal agent and solvent control DMSO were included. The fungal strains were freshly subcultured on Sabouraud dextrose agar and incubated at 25°C for 72 hr. The fungal cells were suspended in sterile distilled water and diluted to get 10<sup>5</sup> cells/ml. Then, 10 ml of the standardized suspension was inoculated on the control plates and the media were incorporated with the antifungal agents. The inoculated plates were incubated at 25°C for 48 hr. The readings were taken at the end of 48 and 72 hr. MIC is the lowest concentration of the drug preventing the growth of macroscopically visible colonies on the drug-containing plates when there is visible growth on the drug-free control plates.

### 4.2.2 | Antioxidant activity

Synthesized triazole-coumarin conjugates were screened for in vitro radical scavenging potential by using the DPPH radical scavenging assay. The results were compared with the standard synthetic antioxidant BHT.

The antioxidant activity of the synthesized compounds was assessed in vitro by the DPPH radical scavenging assay.<sup>[58]</sup> Results were compared with the standard antioxidant BHT. The hydrogen atom or electron-donating ability of the compounds was measured from the bleaching of the purple-colored methanol solution of DPPH. The spectrophotometric assay uses the stable radical DPPH as a reagent. Furthermore, 1 ml of various concentrations of the test compounds (5, 10, 25, 50, and 100 mg/ml) in methanol was added to 4 ml of 0.004% (w/v) methanol solution of DPPH. After a 30-min incubation period at room temperature, the absorbance was measured against blank at 517 nm. The percent inhibition (%) of free radical production from DPPH was calculated by the following equation:

$$\% \text{ scavenging} = [(A_{\text{control}} - A_{\text{sample}})/A_{\text{blank}}] \times 100,$$

where  $A_{\text{control}}$  is the absorbance of the control reaction (containing all reagents except the test compound) and  $A_{\text{sample}}$  is the absorbance of the test compound. Tests were carried out in triplicate.

## 4.3 | Molecular modeling study

### 4.3.1 | Homology modeling

The homology modeling technique was employed to build a 3D model structure of cytochrome P450 lanosterol 14 $\alpha$ -demethylase of *C. albicans* with the help of VLifeMDS 4.3 Promodel molecular modeling tool. The protein sequence was retrieved from UniprotKB database (accession number: P10613). The homologs' template sequence search was carried out against the protein structure database (<http://www.rcsb.org/>) by using BlastP. The appropriate template crystal structure of human lanosterol 14 $\alpha$ -demethylase (CYP51) complexes with miconazole (3LD6 B) which was based on default parameters, identity and positive criteria. The secondary structure assignment and sequence realignment were carried out to build the final modeled structure of fungal CYP51.

### 4.3.2 | Molecular docking study

The model protein structure and 3D structure of sketched synthesized compound were prepared for molecular docking using AutoDock Vina docking tool. The molecular docking study of synthesized compounds **7a-g** and **8a-g** was carried out using the final modeled structure of fungal CYP51. To understand this mechanism of action of inhibitors, molecular interactions were analyzed.

### 4.3.3 | ADMET testing

The ADMET properties of synthesized compounds **7a-g** and **8a-g** and standard drug were tested using FAFDrug2 tool, which is run on the Linux operating system.<sup>[59]</sup> The FAFDrug2 tool works on assumptions of Lipinski's rule of five and Veber's rule, which was widely followed in filtering lead compounds that would likely be further developed in drug design programs.<sup>[60]</sup> In addition to this, some other parameters were also considered to test ADMET properties, such as the number of rotatable bonds (>10), the number of rigid bonds, and percentage absorption (%ABS), which significantly contribute to good oral bioavailability and good intestinal absorption.<sup>[61]</sup>

## ACKNOWLEDGMENTS

S. V. A. is very grateful to the Council of Scientific and Industrial Research (CSIR), New Delhi, for providing a research fellowship. The authors are also grateful for providing laboratory facilities to the Head, Department of Chemistry, Dr. Babasaheb Ambedkar Marathwada University, Aurangabad.

## CONFLICTS OF INTERESTS

The authors declare that there are no conflicts of interests.



**ORCID**

 Satish V. Akolkar  <http://orcid.org/0000-0002-5467-4962>

 Jaiprakash N. Sangshetti  <http://orcid.org/0000-0002-9064-4111>

 Bapurao B. Shingate  <http://orcid.org/0000-0001-7207-0794>
**REFERENCES**

- [1] D. A. Enoch, H. A. Ludlam, N. M. Brown, *J. Med. Microbiol.* **2006**, 55, 809.
- [2] D. J. Sheehan, C. A. Hitchcock, C. M. Sibley, *Clin. Microbiol. Rev.* **1999**, 12, 40.
- [3] N. H. Georgopapadakou, T. J. Walsh, *Antimicrob. Agents Chemother.* **1996**, 40, 279.
- [4] M. A. Pfaller, *Am. J. Med.* **2012**, 125, S3.
- [5] A. Bistrovic, N. Stipanicev, T. Opacak-Bernardi, M. Jukic, S. Martinez, L. Glavas-Obrovac, S. Raic-Malic, *New J. Chem.* **2017**, 41, 7531.
- [6] Z. C. Dai, Y. F. Chen, M. Zhang, S. K. Li, T. T. Yang, L. Shen, J. X. Wang, S. S. Qian, H. L. Zhu, Y. H. Ye, *Org. Biomol. Chem.* **2015**, 13, 477.
- [7] N. Fu, S. Wang, Y. Zhang, C. Zhang, D. Yang, L. Weng, B. Zhao, L. Wang, *Eur. J. Med. Chem.* **2017**, 136, 596.
- [8] S. Zhang, Z. Xu, C. Gao, Q.-C. Ren, L. Chang, Z.-S. Lv, L.-S. Feng, *Eur. J. Med. Chem.* **2017**, 138, 501.
- [9] H. M. Faidallah, A. S. Girgis, A. D. Tiwari, H. H. Honkanadavar, S. J. Thomas, A. Samir, A. Kalmouch, K. A. Alamry, K. A. Khan, T. S. Ibrahim, A. Al-Mahmoudy, A. M. Asiri, S. S. Panda, *Eur. J. Med. Chem.* **2018**, 143, 1524.
- [10] Z. Xu, S.-J. Zhao, Y. Liu, *Eur. J. Med. Chem.* **2019**, 183, 111700.
- [11] Y. Tian, Z. Liu, J. Liu, B. Huang, D. Kang, H. Zhang, E. De Clercq, D. Daelemans, C. Pannecouque, K.-H. Lee, C. H. Chen, P. Zhan, X. Liu, *Eur. J. Med. Chem.* **2018**, 151, 339.
- [12] P. Yadav, J. K. Yadav, A. Agarwal, S. K. Awasthi, *RSC Adv.* **2019**, 9, 31969.
- [13] D. Dheer, V. Singh, R. Shankar, *Bioorg. Chem.* **2017**, 71, 30.
- [14] V. V. Rostovtsev, L. G. Green, V. V. Fokin, K. B. Sharpless, *Angew. Chem., Int. Ed.* **2002**, 41, 2596.
- [15] H. C. Kolb, K. B. Sharpless, *Drug Discov. Today* **2003**, 8, 1128.
- [16] G. C. Tron, T. Pirali, R. A. Billington, P. L. Canonico, G. Sorba, A. A. Genazzani, *Med. Res. Rev.* **2008**, 28, 278.
- [17] S. G. Agalave, S. R. Maujan, V. S. Pore, *Chem.-Asian J.* **2011**, 6, 2696.
- [18] N. M. Meghani, H. H. Amin, B.-J. Lee, *Drug Discov. Today* **2017**, 22, 1604.
- [19] K. Bozorov, J. Zhao, H. A. Aisa, *Bioorg. Med. Chem.* **2019**, 27, 3511.
- [20] N. S. Vatmurge, B. G. Hazra, V. S. Pore, F. Shirazi, P. S. Chavan, M. V. Deshpande, *Bioorg. Med. Chem. Lett.* **2008**, 18, 2043.
- [21] Y. C. Duan, Y. C. Ma, E. Zhang, X. J. Shi, M. M. Wang, X. W. Ye, H. M. Liu, *Eur. J. Med. Chem.* **2013**, 62, 11.
- [22] J. Zhang, H. Zhang, W. Cai, L. Yu, X. Zhen, A. Zhang, *Bioorg. Med. Chem.* **2009**, 17, 4873.
- [23] D. Huber, H. Hubner, P. Gmeiner, *J. Med. Chem.* **2009**, 52, 6860.
- [24] T. V. Soumya, C. M. Ajmal, D. Bahulayan, *Bioorg. Med. Chem. Lett.* **2017**, 27, 450.
- [25] J. Xiao, L. B. Lin, J. Y. Hu, D. Z. Duan, W. Shi, Q. Zhang, W. B. Han, L. Wang, X. L. Wang, *Tetrahedron Lett.* **2018**, 59, 1772.
- [26] Z. Xu, X. Wu, G. Li, Z. Feng, J. Xu, *Nat. Prod. Res.* **2019**, 34, 1002.
- [27] M. Zhao, L. Y. Yuan, D. Y. Guo, *Phytochemistry* **2018**, 148, 97.
- [28] R. Cai, Y. Wu, S. Chen, H. Cui, Z. Liu, C. Li, Z. She, *J. Nat. Prod.* **2018**, 81, 1376.
- [29] N. Rustamova, K. Bozorov, T. Efferth, A. Yili, *Phytochem. Rev.* **2020**, 19, 425.
- [30] H. Singh, J. V. Singh, K. Bhagat, H. K. Gulati, M. Sanduja, N. Kumar, N. Kinarivala, S. Sharma, *Bioorg. Med. Chem.* **2019**, 27, 3477.
- [31] P. O. Patil, S. B. Bari, S. D. Firke, P. K. Deshmukh, S. T. Donda, D. A. Patil, *Bioorg. Med. Chem.* **2013**, 21, 2434.
- [32] Y. Shi, C. Zhou, *Bioorg. Med. Chem. Lett.* **2011**, 21, 956.
- [33] P. M. Ronad, M. N. Noolvi, S. Sapkal, S. Dharbhamulla, V. S. Maddi, *Eur. J. Med. Chem.* **2010**, 45, 85.
- [34] R. Aggarwal, S. Kumar, P. Kaushik, D. Kaushik, G. K. Gupta, *Eur. J. Med. Chem.* **2013**, 62, 508.
- [35] T. Gregoric, M. Sedic, P. Grbcic, A. Tomljenovic Paravic, S. Kraljevic Pavelic, M. Cetina, R. Vianello, S. Raic-Malic, *Eur. J. Med. Chem.* **2017**, 125, 1247.
- [36] Y. C. Zheng, Y. C. Duan, J. L. Ma, R. M. Xu, X. Zi, W. L. Lv, M. M. Wang, X. W. Ye, S. Zhu, D. Mobley, Y. Y. Zhu, J. W. Wang, J. F. Li, Z. R. Wang, W. Zhao, H. M. Liu, *J. Med. Chem.* **2013**, 56, 8543.
- [37] J. Dandriyal, R. Singla, M. Kumar, V. Jaitak, *Eur. J. Med. Chem.* **2016**, 119, 141.
- [38] S. Z. Ferreira, H. C. Carneiro, H. A. Lara, R. B. Alves, J. M. Resende, H. M. Oliveira, L. M. Silva, D. A. Santos, R. P. Freitas, *ACS Med. Chem. Lett.* **2015**, 6, 271.
- [39] Y.-L. Fan, X. Ke, M. Liu, *J. Heterocycl. Chem.* **2018**, 55, 791.
- [40] M. H. Shaikh, D. D. Subhedar, F. A. K. Khan, J. N. Sangshetti, B. B. Shingate, *Chin. Chem. Lett.* **2016**, 27, 295.
- [41] K. Kushwaha, N. Kaushik, Lata, S. C. Jain, *Bioorg. Med. Chem. Lett.* **2014**, 24, 1795.
- [42] M. H. Shaikh, D. D. Subhedar, L. Nawale, D. Sarkar, F. A. K. Khan, J. N. Sangshetti, B. B. Shingate, *Mini-Rev. Med. Chem.* **2019**, 19, 1178.
- [43] S. P. Khare, T. R. Deshmukh, J. N. Sangshetti, V. S. Krishna, D. Sriram, V. M. Khedkar, B. B. Shingate, *ChemistrySelect* **2018**, 3, 13113.
- [44] M. H. Shaikh, D. D. Subhedar, B. B. Shingate, F. A. Kalam Khan, J. N. Sangshetti, V. M. Khedkar, L. Nawale, D. Sarkar, G. R. Navale, S. S. Shinde, *Med. Chem. Res.* **2016**, 25, 790.
- [45] S. V. Akolkar, A. A. Nagargoje, V. S. Krishna, D. Sriram, J. N. Sangshetti, M. Damale, B. B. Shingate, *RSC Adv.* **2019**, 9, 22080.
- [46] A. A. Nagargoje, S. V. Akolkar, M. M. Siddiqui, A. V. Bagade, K. M. Kodam, J. N. Sangshetti, M. G. Damale, B. B. Shingate, *J. Chin. Chem. Soc.* **2019**, 66, 1658.
- [47] D. D. Subhedar, M. H. Shaikh, B. B. Shingate, L. Nawale, D. Sarkar, V. M. Khedkar, F. A. Kalam Khan, J. N. Sangshetti, *Eur. J. Med. Chem.* **2017**, 125, 385.
- [48] M. H. Shaikh, D. D. Subhedar, M. Arkile, V. M. Khedkar, N. Jadhav, D. Sarkar, B. B. Shingate, *Bioorg. Med. Chem. Lett.* **2016**, 26, 561.
- [49] A. B. Danne, A. S. Choudhari, S. Chakraborty, D. Sarkar, V. M. Khedkar, B. B. Shingate, *MedChemComm* **2018**, 9, 1114.
- [50] M. H. Shaikh, D. D. Subhedar, L. Nawale, D. Sarkar, F. A. Kalam Khan, J. N. Sangshetti, B. B. Shingate, *MedChemComm* **2015**, 6, 1104.
- [51] T. R. Deshmukh, A. P. Sarkate, D. K. Lokwani, S. V. Tiwari, R. Azad, B. B. Shingate, *Bioorg. Med. Chem. Lett.* **2019**, 29, 126618.
- [52] G. Wang, Z. Peng, J. Wang, X. Li, J. Li, *Eur. J. Med. Chem.* **2017**, 125, 423.
- [53] P. Neeraja, S. Srinivas, K. Mukkanti, P. K. Dubey, S. Pal, *Bioorg. Med. Chem. Lett.* **2016**, 26, 5212.
- [54] G. Wang, Z. Peng, J. Wang, J. Li, X. Li, *Bioorg. Med. Chem. Lett.* **2016**, 26, 5719.
- [55] C. Ferroni, A. Pepe, Y. S. Kim, S. Lee, A. Guerrini, M. D. Parenti, A. Tesse, A. Zamagni, M. Cortesi, N. Zaffaroni, M. De Cesare, G. L. Beretta, J. B. Trepel, S. V. Malhotra, G. Varchi, *J. Med. Chem.* **2017**, 60, 3082.
- [56] Z. K. Khan, Proc. Int. Work. UNIDO-CDRI, 1997, pp. 210–211.
- [57] S. Zhang, Y. Luo, L.-Q. He, Z.-J. Liu, A.-Q. Jiang, Y.-H. Yang, H.-L. Zhu, *Bioorg. Med. Chem.* **2013**, 21, 3723.
- [58] M. Burits, F. Bucar, *Phyther. Res.* **2000**, 14, 323.
- [59] D. Lagorce, O. Sperandio, H. Galons, M. A. Miteva, B. O. Villoutreix, *BMC Bioinf.* **2008**, 9, 396.



- [60] C. A. Lipinski, F. Lombardo, B. W. Dominy, P. J. Feeney, *Adv. Drug Deliv. Rev.* **2001**, *46*, 3.
- [61] P. Ertl, B. Rohde, P. Selzer, *J. Med. Chem.* **2000**, *43*, 3714.

#### SUPPORTING INFORMATION

Additional supporting information may be found online in the Supporting Information section.

**How to cite this article:** Akolkar SV, Nagargoje AA, Shaikh MH, et al. New N-phenylacetamide-linked 1,2,3-triazole-tethered coumarin conjugates: Synthesis, bioevaluation, and molecular docking study. *Arch Pharm.* 2020;e2000164.

<https://doi.org/10.1002/ardp.202000164>



## ARTICLE

# Synthesis of 3-(trifluoromethyl)-1-(perfluorophenyl)-1*H*-pyrazol-5(4*H*)-one derivatives via Knoevenagel condensation and their biological evaluation

Sujata G. Dengale<sup>1</sup> | Hemantkumar N. Akolkar<sup>2</sup> | Bhausahab K. Karale<sup>2</sup> |  
Nirmala R. Darekar<sup>2</sup> | Sadhana D. Mhaske<sup>3</sup> | Mubarak H. Shaikh<sup>2</sup> |  
Dipak N. Raut<sup>4</sup> | Keshav K. Deshmukh<sup>1</sup>

<sup>1</sup>P.G. and Research, Department of Chemistry, Sangamner Nagarpalika Arts, D. J. Malpani Commerce and B. N. Sarada Science College, Sangamner, India

<sup>2</sup>P.G. and Research, Department of Chemistry, Radhabai Kale Mahila Mahavidyalaya, Ahmednagar, India

<sup>3</sup>Department of Chemistry, Dadapatil Rajale College, Pathardi, India

<sup>4</sup>Amrutvahini College of Pharmacy, Sangamner, India

## Correspondence

Hemantkumar N. Akolkar, P.G. and Research, Department of Chemistry, Radhabai Kale Mahila Mahavidyalaya, Ahmednagar, Maharashtra, India, 414001. Email: hemantakolkar@gmail.com

## Abstract

In search of new active molecules, a small focused library of the synthesis of 3-(trifluoromethyl)-1-(perfluorophenyl)-1*H*-pyrazol-5(4*H*)-one derivatives (**4a-d**, **5a-f**, and **6a-e**) has been efficiently prepared via the Knoevenagel condensation approach. All the derivatives were synthesized by conventional and non-conventional methods like ultrasonication and microwave irradiation, respectively. Several derivatives exhibited excellent anti-inflammatory activity compared to the standard drug. Furthermore, the synthesized compounds were found to have potential antioxidant activity. In addition, to rationalize the observed biological activity data, an *in silico* absorption, distribution, metabolism, and excretion (ADME) prediction study also been carried out. The results of the *in vitro* and *in silico* studies suggest that the 3-(trifluoromethyl)-1-(perfluorophenyl)-1*H*-pyrazol-5(4*H*)-one derivatives (**4a-d**, **5a-f**, and **6a-e**) may possess the ideal structural requirements for the further development of novel therapeutic agents.

## KEYWORDS

ADME prediction, anti-inflammatory, antioxidant, Knoevenagel, microwave, pyrazole, ultrasonication

## 1 | INTRODUCTION

The pyrazole ring is a prominent heterocyclic structural compound found in several pharmaceutically active compounds. This is because of its use in pharmacological activity and ease of synthesis. Furthermore, the selective functionalization of pyrazole with diverse substituents was also found to improve their range of action in various fields. Pyrazole containing heterocycles shows various biological activity, such as antibacterial,<sup>[1]</sup> antifungal,<sup>[2]</sup> antimicrobial,<sup>[3]</sup> anti-inflammatory,<sup>[4a]</sup> antioxidant,<sup>[4b]</sup> insecticidal,<sup>[5]</sup> antiviral,<sup>[6]</sup> anti-nitric oxide

synthase,<sup>[7]</sup> glycogen receptor antagonist,<sup>[8]</sup> anticancer,<sup>[9]</sup> antienzyme,<sup>[10]</sup> immunosuppressant,<sup>[11]</sup> anti-fatty acid amide hydrolase (FAAH),<sup>[12]</sup> and liver-x-receptor [LXR] partial agonist activities.<sup>[13]</sup>

Fluorine or fluorine-based compounds are of great interest in synthetic and medicinal chemistry. The position of the fluorine atom in an organic molecule plays a vital role in agrochemicals, pharmaceuticals, and materials<sup>[14]</sup> as it changes the pharmacokinetic and pharmacodynamic properties of the molecule owing to its high membrane permeability, metabolic stability, lipophilicity, and binding affinity.<sup>[15]</sup>

Perfluoro-alkylated and trifluoro-methylated pyrazoles represent pharmacologically related core structures that are present in many important drugs and agrochemicals, such as fluazolate (herbicide), penthiopyrad (fungicide), razaxaban (anticoagulant), deracoxib, celecoxib (anti-inflammatory), and penflufen (fungicidal) (Figure 1).<sup>[16]</sup> So, the modern trend is moving more in the direction of the synthesis of a collection of fluorine-containing molecules in order to find excellent biological activity.

Ultrasonic irradiation is a new technology that has been widely used in chemical reactions. When ultrasonic waves pass through a liquid medium, a large number of micro-bubbles form, grow, and collapse in very short times, about a few microseconds. The formation and violent collapse of small vacuum bubbles takes place due to the ultrasonication waves generated in alternating high pressure and low pressure in liquids, and the phenomenon is known as cavitation. It causes high-speed imposing liquid jets and strong hydrodynamic shear forces. The deagglomeration of nanometer-

sized materials was carried out using these effects. In this aspect, for high-speed mixers and agitator bead mills, ultrasonication is an alternative.<sup>[17]</sup>

In the preparative chemist's toolkit, microwave heating is a valuable technique. Due to a modern scientific microwave apparatus, it is possible to access elevated temperatures in an easy, safe, and reproducible way.<sup>[18]</sup> In recent years, microwave-assisted organic synthesis (MAOs)<sup>[19]</sup> has been emerged as a new "lead" in organic synthesis. Important advantages of this technology include a highly accelerated rate of the reaction and a decrease in reaction time, with an increase in the yield and quality of the product. The current technique is considered an important method toward green chemistry as this technique is more environmentally friendly. The conventional method of organic synthesis usually needs a longer heating time; tedious apparatus setup, which results in the higher cost of the process; and the excessive use of solvents/reagents, which leads to environmental pollution. This growth of green chemistry

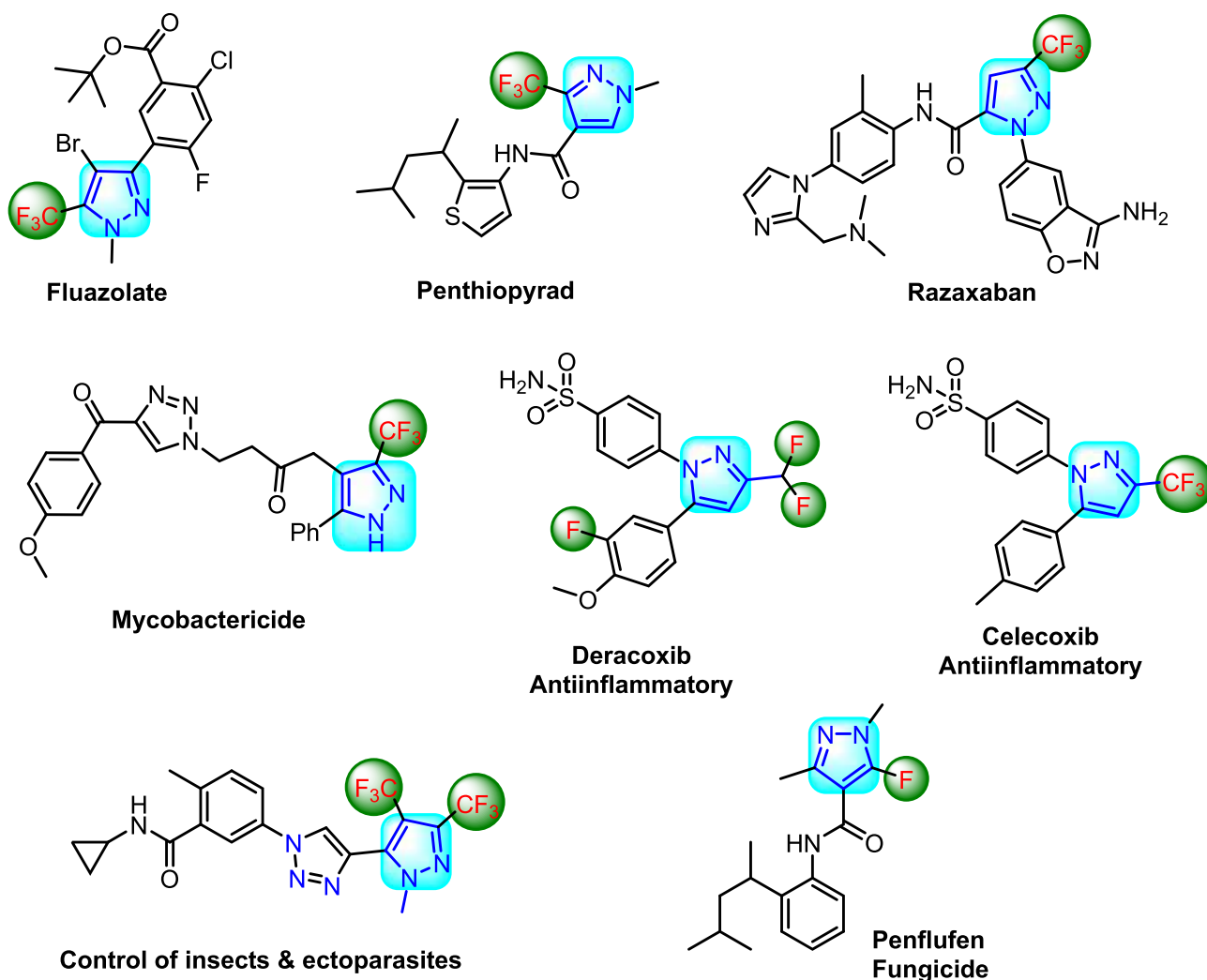


FIGURE 1 Structure of pyrazole- and fluorine-containing commercially available drugs

holds significant potential for a reduction of the byproduct, a reduction in waste production, and lowering of the energy costs. Due to its ability to couple directly with the reaction molecule and bypass thermal conductivity, leading to a rapid rise in the temperature, microwave irradiation has been used to improve many organic syntheses.<sup>[20]</sup> Knoevenagel condensation reactions are carried out by the condensation of aldehyde and the active methylene group using different catalysts such as piperidine,  $\text{InCl}_3$ ,  $\text{TiCl}_4$ ,  $\text{LiOH}$ ,  $\text{ZnCl}_2$ , and  $\text{NbCl}_5$ .<sup>[20,21]</sup> They are also carried out using  $\text{NaAlO}_2$ -promoted mesoporous catalysts,<sup>[22]</sup> ionic liquid,<sup>[23]</sup> monodisperse carbon nanotube-based NiCu nanohybrids,<sup>[24]</sup> and MAOs.<sup>[25]</sup> This is one of the most important methodologies used in synthetic organic chemistry for the formation of a C—C double bond.

From our study, the results demonstrated that green methodologies are less hazardous than classical synthesis methods, as well more efficient and economical and environmentally friendly; short reaction times and excellent yields are observed for those reactions in which conventional heating is replaced by microwave irradiation. Keeping in mind the 12 principles of green chemistry, in continuation of our research work,<sup>[26]</sup> and the advantages of microwave irradiation and activities associated with pyrazole and fluorine, we construct pyrazole and fluorine in one molecular framework as new 3-(trifluoromethyl)-1-(perfluorophenyl)-1*H*-pyrazol-5(4*H*)-one derivatives under conventional, as well as microwave, irradiation and ultrasonication and evaluated their anti-inflammatory and antioxidant activity. In addition to this, we have also performed *in silico* absorption, distribution, metabolism, and excretion (ADME) predictions for the synthesized compounds.

## 2 | RESULTS AND DISCUSSION

### 2.1 | Chemistry

A facile, economic, and green protocol for the cyclocondensation of 2-(perfluorophenyl)-5-(trifluoromethyl)-

2,4-dihydro-3*H*-pyrazol-3-one (**3**) with different aldehydes has been achieved.

The key starting material 3-(trifluoromethyl)-1-(perfluorophenyl)-1*H*-pyrazol-5(4*H*)-one (**3**) was synthesized by the condensation of 1-(perfluorophenyl)hydrazine (**1**) and ethyl 4,4,4-trifluoro-3-oxobutanoate (**2**) in ethanol<sup>[27]</sup> (Scheme 1).

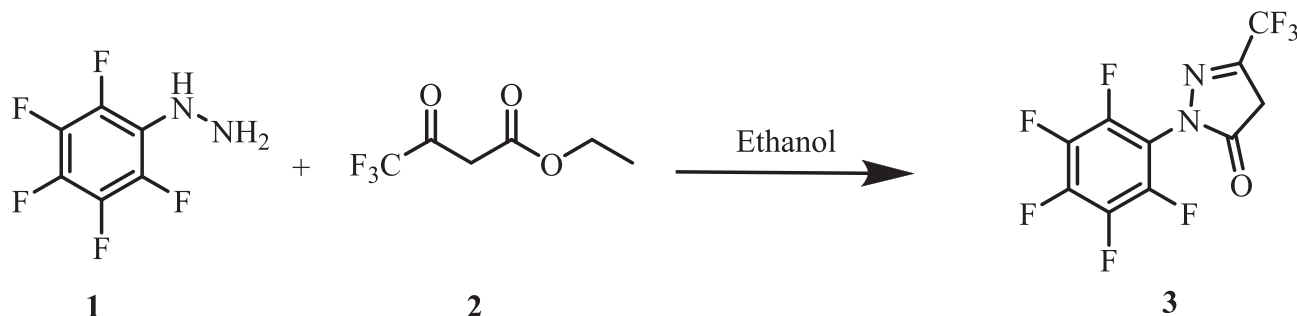
Initially, we carried out the reaction between 2-(perfluorophenyl)-5-(trifluoromethyl)-2,4-dihydro-3*H*-pyrazol-3-one (2 mmol) (**3**) and 1-phenyl-3-(thiophen-2-yl)-1*H*-pyrazole-4-carbaldehyde (2 mmol) refluxed in acetic acid as a model reaction (Scheme 2). Initially, the model reaction was carried out in ethanol without using acetic acid, and it was observed that a very low yield of product (20%) was obtained even after 2 hr. Therefore, improving the yield intervention of the catalyst was thought to be necessary. So, we decided to use acetic acid as a catalyst to promote this transformation at room temperature. At room temperature, the yield of product (45%) was found to be increased in 3 hr, so we decided to provide heating to the reaction mixture to achieve maximum product yield.

When the reaction mixture refluxed in acetic acid, product formation took place after 2 hr, and the yield of the product was 72% (Table 1).

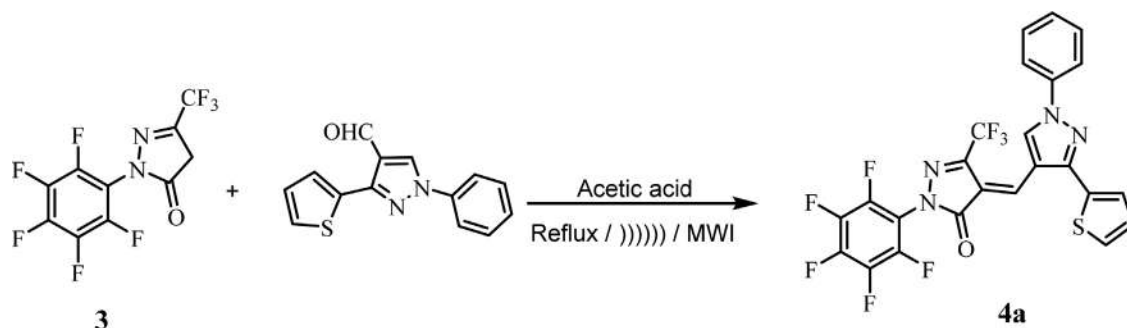
To check the ultrasonication's specific effect on this reaction, under ultrasound irradiation at 35–40°C, we carried out the model reaction using the optimized reaction conditions in hand to check whether the reaction could be accelerated with further improved product yield within a short reaction time (Scheme 2).

It was observed that, under ultrasonic conditions, the conversion rate of a reactant to product increased with less time (Table 1). Thus, when considering the basic green chemistry concept, ultrasonic irradiation was found to have a beneficial effect on the synthesis of Knoevenagel derivatives (**4a-d**, **5a-f**, and **6a-e**), which was superior to the traditional method with respect to yield and reaction time (Table 1).

To accomplish the goal and significance of green chemistry, the model reaction was carried out under



**SCHEME 1** Synthesis of 3-(trifluoromethyl)-1-(perfluorophenyl)-1*H*-pyrazol-5(4*H*)-one **3**



**SCHEME 2** Model reaction for conventional, ultrasonication, and microwave irradiation methods

**TABLE 1** Synthesis of 3-(trifluoromethyl)-1-(perfluorophenyl)-1H-pyrazol-5(4H)-one derivatives (**4a-d**, **5a-f**, and **6a-e**)

Cpd	R <sub>1</sub>	R <sub>2</sub>	R <sub>3</sub>	R <sub>4</sub>	m. p. (°C)	Conventional method <sup>a</sup>		Ultrasound method <sup>b</sup>		Microwave method <sup>c</sup>	
						Time (min)	Yield <sup>d</sup> (%)	Time (min)	Yield <sup>d</sup> (%)	Time (min)	Yield <sup>d</sup> (%)
<b>4a</b>	H	H	-	-	224–226	120	72	20	81	6.5	84
<b>4b</b>	Br	F	-	-	232–234	120	75	18	78	6.5	81
<b>4c</b>	Cl	H	-	-	216–218	120	70	20	76	6.0	80
<b>4d</b>	Br	H	-	-	230–232	120	64	16	70	6.5	76
<b>5a</b>	H	H	OMe	-	202–204	120	70	21	76	5.5	84
<b>5b</b>	H	H	H	-	186–188	120	66	17	72	6.0	80
<b>5c</b>	F	H	OMe	-	180–182	120	68	16	75	7.0	82
<b>5d</b>	H	H	Me	-	206–208	120	65	16	71	6.5	79
<b>5e</b>	H	H	OCF <sub>3</sub>	-	142–144	120	62	18	70	6.5	76
<b>5f</b>	H	Cl	Cl	-	212–214	120	70	19	80	5.5	84
<b>6a</b>	Me	Cl	Me	H	188–190	120	66	18	76	6.0	78
<b>6b</b>	H	Cl	Me	H	180–182	120	62	17	72	7.5	75
<b>6c</b>	H	Cl	H	H	176–178	120	59	18	79	7.0	80
<b>6d</b>	H	Cl	H	Cl	212–214	120	64	20	72	7.0	78
<b>6e</b>	H	H	Me	H	180–182	120	60	18	80	7.5	82

Abbreviation: Cpd, compound.

<sup>a</sup>Reaction conditions: Compound (**3**) (2 mmol) and 1-phenyl-3-(thiophen-2-yl)-1H-pyrazole-4-carbaldehyde (2 mmol) refluxed in acetic acid.

<sup>b</sup>Compound (**3**) (2 mmol) and 1-phenyl-3-(thiophen-2-yl)-1H-pyrazole-4-carbaldehyde (2 mmol) in acetic acid under ultrasound irradiation.

<sup>c</sup>Compound (**3**) (2 mmol) and 1-phenyl-3-(thiophen-2-yl)-1H-pyrazole-4-carbaldehyde (2 mmol) in acetic acid under microwave irradiation.

<sup>d</sup>Isolated yield. m.p.: melting point.

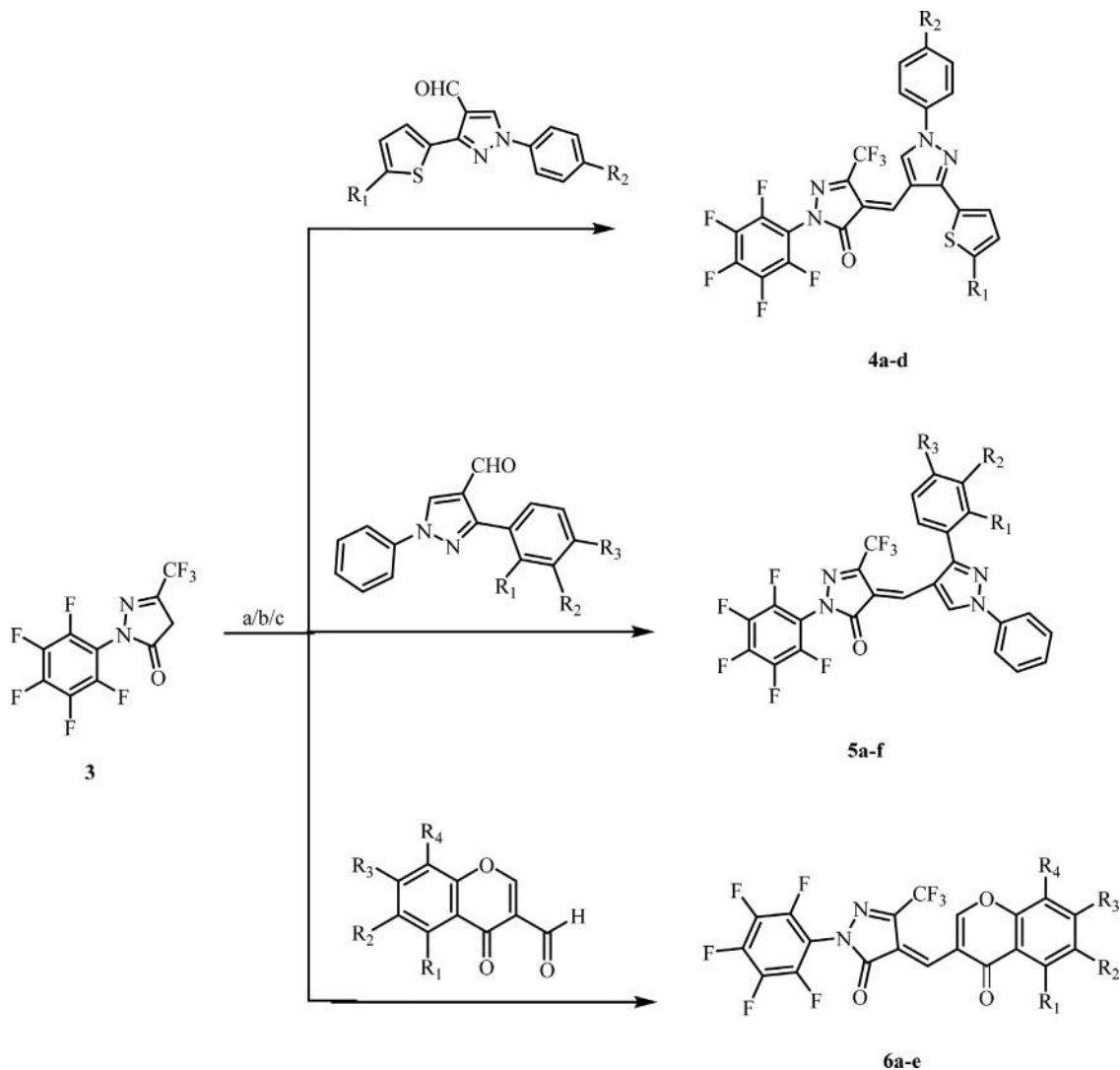
microwave irradiation for a period of time indicated in Table 1 at 350 W (Scheme 2). Fortunately, the product formation occurred in 6.5 min, with an 84% increase in yield.

So, from the above experiments, it can be concluded that, when the reaction was carried out under the conventional method, it gave comparatively low yields of products with longer reaction times, while the same reaction carried out under the influence of ultrasonic irradiation and microwave irradiation gave excellent yields of the products in short reaction times.

Finally, we assessed the scope and generality of this method for the Knoevenagel condensation between 2-(perfluorophenyl)-5-(trifluoromethyl)-2,4-dihydro-3H-pyrazol-3-one (**3**) and different aldehydes (Scheme 3), achieved under conventional and nonconventional methods like the ultrasound and microwave methods, respectively. With respect to the substituent present on the aromatic ring of aldehyde, under the optimized conditions, the corresponding products were obtained in high to excellent yields (Table 1).

More importantly, hetero aryl aldehydes were observed to be well tolerated under optimized conditions,





**SCHEME 3** Synthesis of 3-(trifluoromethyl)-1-(perfluorophenyl)-1H-pyrazol-5(4H)-one derivatives (**4a-d**, **5a-f**, and **6a-e**). Reaction conditions: **a** = Refluxed in acetic acid. **b** = Under ultrasound irradiation in acetic acid. **c** = Under microwave irradiation using acetic acid as a solvent

furnishing the product in good yields. All the synthesized compounds (**4a-d**, **5a-f**, and **6a-e**) were confirmed by IR, <sup>1</sup>H NMR, <sup>13</sup>C NMR, and mass spectra.

The formation of (4E)-3-(trifluoromethyl)-1-(perfluorophenyl)-4-((1-phenyl-3-(thiophen-2-yl)-1H-pyrazol-4-yl)methylene)-1H-pyrazol-5(4H)-one **4a-d** was confirmed by IR, <sup>1</sup>H NMR, <sup>13</sup>C NMR, and mass spectra. In the IR spectrum of compound **4a**, the peaks observed at 1,681 cm<sup>-1</sup> indicate the presence of C=O group. In the <sup>1</sup>H NMR spectrum of compound **4a**, two singlets were observed at δ 8.11 and 10.10 ppm for pyrazolyl and olefinic proton, respectively. The <sup>13</sup>C NMR spectrum of compound **4a** revealed that the peak appearing at δ 161.4 ppm is due to the presence of carbonyl carbon. The structure of compound **4a** was also confirmed by a molecular ion peak at *m/z* 555.01 (M + H)<sup>+</sup>. Similarly, the

synthesis of (4E)-3-(trifluoromethyl)-1-(perfluorophenyl)-4-((1,3-diphenyl-1H-pyrazol-4-yl)methylene)-1H-pyrazol-5(4H)-ones **5a-f** was also confirmed by spectral techniques. In the IR spectrum of compound **5a**, the peak observed at 1,701 cm<sup>-1</sup> corresponded to the C=O group. In the <sup>1</sup>H NMR spectrum of compound **5a**, the three singlets observed at δ 3.92, 8.11, and 10.10 ppm confirm the presence of -OCH<sub>3</sub>, pyrazolyl proton, and olefinic proton, respectively. The <sup>13</sup>C NMR spectrum of compound **5a** showed peaks at δ 162.5 and 55.5 ppm, confirming the presence of carbonyl carbon and methoxy carbon, respectively. Furthermore, the structure of compound **5a** was also confirmed by a molecular ion peak at *m/z* 573.21 (M + H)<sup>+</sup>.

Furthermore, the formation of (Z)-4-([4-oxo-4H-chromen-3-yl]methylene)-2-(perfluorophenyl)-5-(trifluoromethyl)-2,4-dihydro-3H-pyrazol-3-one **6a-e** was

confirmed by various spectral techniques. The IR spectrum of compound **6a** showed absorption peaks at 1,707 and 1,666  $\text{cm}^{-1}$  corresponding to two carbonyl groups present in the molecules. The  $^1\text{H}$  NMR spectrum of compound **6a** showed four singlets at  $\delta$  2.54 and  $\delta$  3.01 ppm for two  $-\text{CH}_3$ ,  $\delta$  8.50 ppm for chromone ring proton, and  $\delta$  10.54 ppm for olefinic proton. The  $^{13}\text{C}$  NMR spectrum of compound **6a** showed that two signals appear at  $\delta$  175.4 and 164.2 ppm for the carbonyl carbon of chromone and pyrazolone ring, respectively. In addition, two signals for methyl carbon appear at  $\delta$  22.2 and 18.6 ppm. The structure of compound **6a** was also confirmed by mass spectra and by a molecular ion peak observed at  $m/z$  537.11 ( $\text{M} + \text{H}$ ) $^+$ . Similarly, all the synthesized compounds were characterized by the spectral analysis. Structures of all the synthesized derivatives are shown in Figure S1 (Supporting Information).

## 2.2 | Biological activity

### 2.2.1 | Anti-inflammatory activity

The newly synthesized 3-(trifluoromethyl)-1-(perfluorophenyl)-1*H*-pyrazol-5(4*H*)-one derivatives (**4a-d**, **5a-f**, and **6a-e**) ( $\text{EC}_{50}$  range =  $0.6483 \pm 0.221$ – $0.8519 \pm 0.281$   $\mu\text{g}/\text{ml}$ ) exhibited moderate anti-inflammatory activity compared to the standard drug diclofenac sodium. Among all the synthesized compounds, except compounds **4c**, **5c**, **5e**, **6d**, and **6e**, all other compounds exhibited a minimum inhibitory concentration (MIC) of 200  $\mu\text{g}/\text{ml}$  compared to the standard drug diclofenac sodium (Table 2).

The percent inhibition of compounds in the in vitro anti-inflammatory model is shown in Figure 2. Furthermore, the comparative percent inhibition of compounds in the in vitro anti-inflammatory model is shown in Figure 3.

### 2.2.2 | Antioxidant activity

In the present study, antioxidant activity of the synthesized compounds has been assessed in vitro by the DPPH radical scavenging assay.<sup>[28]</sup> Ascorbic acid (AA) has been used as a standard drug for the comparison of antioxidant activity, and the observed results are summarized in Table 2.

According to the DPPH assay, compounds **5a**, **5d**, **5e**, **5f**, **6a**, **6b**, and **6e** ( $\text{IC}_{50}$  = <100  $\mu\text{g}/\text{ml}$ ) exhibited excellent antioxidant activity compared to the standard antioxidant drug AA ( $\text{IC}_{50}$  = <50  $\mu\text{g}/\text{ml}$ ). The remaining synthesized compounds display comparable antioxidant activity than

**TABLE 2** Anti-inflammatory and antioxidant activity of 3-(trifluoromethyl)-1-(perfluorophenyl)-1*H*-pyrazol-5(4*H*)-one derivatives (MIC in  $\mu\text{g}/\text{ml}$ )

Compound	Anti-inflammatory	Antioxidant
<b>4a</b>	200	>100
<b>4b</b>	200	>400
<b>4c</b>	400	>200
<b>4d</b>	200	>200
<b>5a</b>	200	<100
<b>5b</b>	200	>200
<b>5c</b>	NT	NT
<b>5d</b>	200	<100
<b>5e</b>	800	<100
<b>5f</b>	200	<100
<b>6a</b>	200	<100
<b>6b</b>	200	<100
<b>6c</b>	200	>200
<b>6d</b>	800	>100
<b>6e</b>	400	<100
Diclofenac sodium	50	-
Ascorbic acid	-	<50

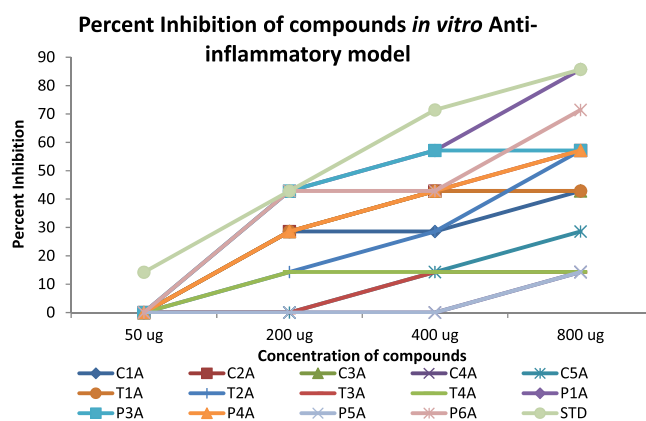


**FIGURE 2** The percent inhibition of compounds in an in vitro anti-inflammatory model

the standard drug butylated hydroxytoluene (Table 2). The percent inhibition of compounds in the in vitro antioxidant model is shown in Figure 4.

## 2.3 | Computational study

### 2.3.1 | In silico ADME

An important task for the lead compounds is early prediction of drug likeness properties as it resolves the cost

**FIGURE 3** The comparative percent inhibition of compounds in an in vitro anti-inflammatory model

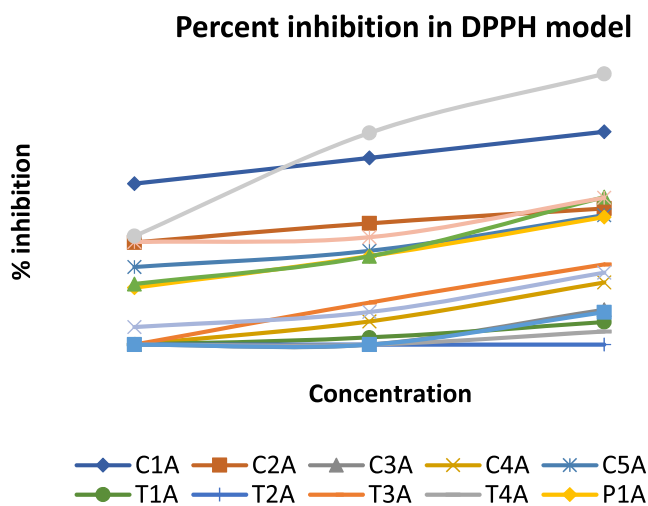
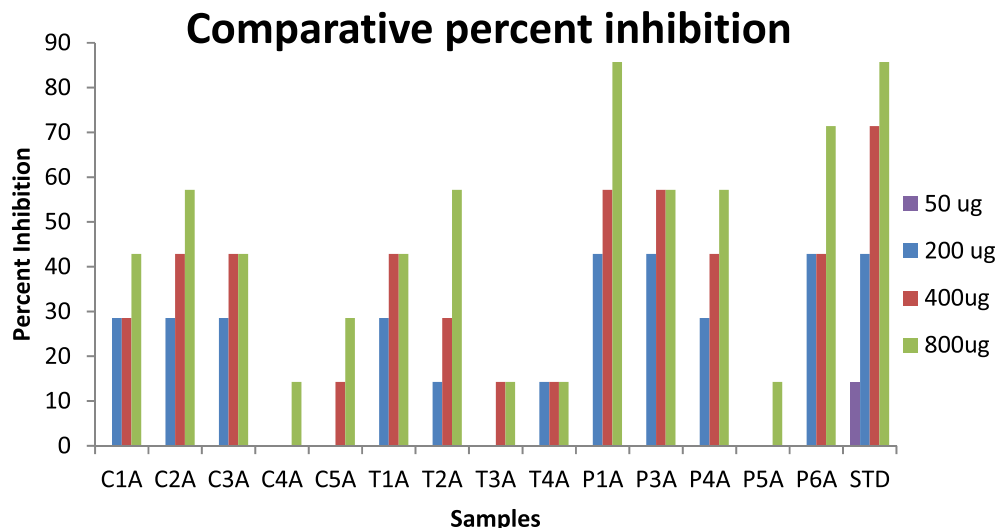


**FIGURE 4** The percent inhibition of compounds in an in vitro antioxidant model

and time issues of drug development and discovery. Due to the inadequate drug likeness properties of many active agents with a significant biological activity, these compounds have failed in clinical trials.<sup>[29]</sup> On the basis of Lipinski's rule of five, the drug likeness properties were analyzed by ADME parameters using the Molinspiration online property calculation toolkit,<sup>[30]</sup> and data are summarized in Table 3.

All the compounds exhibited noteworthy values for the various parameters analyzed and showed good drug-like characteristics based on Lipinski's rule of five and its variants, which characterized these agents to be likely orally active. For the synthesized compound **6e**, the data obtained were within the range of accepted values. Parameters such as the number of rotatable bonds and total polar surface area are linked with the intestinal absorption; results showed that all

synthesized compounds had good absorption. The in silico assessment of all the synthetic compounds has shown that they have very good pharmacokinetic properties, which are reflected in their physicochemical values, thus ultimately enhancing the pharmacological properties of these molecules.

### 3 | EXPERIMENTAL SECTION

All organic solvents were acquired from Poona Chemical Laboratory, Pune and Research-Lab Fine Chem Industries, Mumbai and were used as such without further purification. The melting points were measured on a DBK melting point apparatus and are uncorrected. Microwave irradiation was carried out in Raga's synthetic microwave oven. IR spectra were recorded on Shimadzu IR Affinity 1S (ATR) fourier transform infrared spectrophotometer. <sup>1</sup>H NMR (500 MHz) and <sup>13</sup>C NMR (125 MHz) spectra were recorded on Bruker Advance neo 500 spectrophotometers using tetramethylsilane as an internal standard, and CDCl<sub>3</sub> and dimethyl sulphoxide-*d*<sub>6</sub> as solvent and chemical shifts, respectively, were expressed as  $\delta$  ppm units. Mass spectra were obtained on Waters quadrupole time-of-flight micromass (ESI-MS) mass spectrometer.

#### 3.1 | General procedure for the synthesis of synthesize new 3-(trifluoromethyl)-1-(perfluorophenyl)-1H-pyrazol-5(4H)-one derivatives (4a-d, 5a-f and 6a-e)

**Conventional method:** An equimolar amount of 2-(perfluorophenyl)-5-(trifluoromethyl)-2,4-dihydro-3H-pyrazol-3-

TABLE 3 Pharmacokinetic parameters of (4a-d, 5a-f, and 6a-e) compounds

Entry	% ABS	TPSA (Å <sup>2</sup> )	n-ROTBT	MV	MW	miLog P	n-ON	n-OHNH	Lipinski violation	Drug likeness model score
Rule	-	-	-	-	<500	≤5	<10	<5	≤1	-
4a	90.81	52.72	5	397.75	554.42	5.83	5	0	2	-0.68
4b	90.81	52.72	5	420.56	651.31	6.92	5	0	2	-0.84
4c	90.81	52.72	5	411.28	588.87	6.63	5	0	2	-0.25
4d	90.81	52.72	5	415.63	633.32	6.76	5	0	2	-0.56
5a	87.62	61.96	6	432.58	578.42	6.10	6	0	2	-0.46
5b	90.81	52.72	5	407.04	548.39	6.04	5	0	2	-0.80
5c	87.62	61.96	6	437.51	596.41	6.19	6	0	2	-0.22
5d	90.81	52.72	5	423.60	562.42	6.49	5	0	2	-0.51
5e	87.62	61.96	7	447.32	632.39	7.01	6	0	2	-0.45
5f	90.81	52.72	5	434.11	617.28	7.33	5	0	2	-0.36
6a	86.53	65.11	3	374.21	536.76	6.25	5	0	2	-0.53
6b	86.53	65.11	3	357.65	522.74	5.87	5	0	2	-0.36
6c	86.53	65.11	3	341.09	508.71	5.49	5	0	2	-0.32
6d	86.53	65.11	3	354.62	543.15	6.10	5	0	2	-0.93
6e	86.53	65.11	3	344.11	488.29	5.26	5	0	1	-0.81

Abbreviations: % ABS, percentage absorption; TPSA, topological polar surface area; n-ROTBT, number of rotatable bonds; MV, molecular volume; MW, molecular weight; miLogP, logarithm of partition coefficient of compound between n-octanol and water; n-ON acceptors, number of hydrogen bond acceptors; n-OHNH donors, number of hydrogen bonds donors.

one (3) (0.002 mol) and substituted aldehydes (0.002 mol) was taken in a round-bottom flask using glacial acetic acid (5 ml) as a solvent and were refluxed for the period of time indicated in Table 1. The progress of the reaction was monitored by thin layer chromatography (TLC). After completion of reaction, the mixture was cooled and poured into ice-cold water. The obtained solid was filtered and washed with water and dried and purified by crystallization from ethyl acetate to obtain pure compounds (4a-d, 5a-f, and 6a-e).

**Ultrasound method:** A mixture of 2-(perfluorophenyl)-5-(trifluoromethyl)-2,4-dihydro-3H-pyrazol-3-one (3) (0.002 mol) and substituted aldehydes (0.002 mol) in acetic acid (5 ml) was taken in a 50-ml round-bottom flask. The mixture was irradiated in the water bath of an ultrasonic cleaner at 35–40°C for a period of time indicated in Table 1. After completion of the reaction (monitored by TLC), the mixture was poured into ice-cold water, and the obtained solid was collected by simple filtration and washed successively with water. The crude product was purified by crystallization from ethyl acetate to obtain pure compounds (4a-d, 5a-f, and 6a-e).

**Microwave irradiation method:** An equimolar amount of 2-(perfluorophenyl)-5-(trifluoromethyl)-

2,4-dihydro-3H-pyrazol-3-one (3) (0.002 mol) and substituted aldehydes (0.002 mol) was taken in a round-bottom flask (RBF) using glacial acetic acid (5 ml) as a solvent, and the contents of RBF were subjected to MW irradiation for the period of time indicated in Table 1 at 350 W. The progress of the reaction was monitored by TLC. After completion of reaction, the mixture was cooled and poured into ice-cold water. The obtained solid was filtered and washed with water and dried and purified by crystallization from ethyl acetate to obtain pure compounds (4a-d, 5a-f, and 6a-e).

### 3.1.1 | (4E)-3-(Trifluoromethyl)-1-(perfluorophenyl)-4-((1-phenyl-3-(thiophen-2-yl)-1H-pyrazol-4-yl)methylene)-1H-pyrazol-5(4H)-one (4a)

Orange solid; Wt. 930 mg, Yield 84%; IR( $\nu_{\max}$ /cm<sup>-1</sup>): 2,926 (=C–H), 1,681 (C=O), 1,598 (C=N), 1,519 (C=C), 1,234 (C–F); <sup>1</sup>H NMR spectrum,  $\delta$ , ppm: 7.35–7.91 (m, 8H, Ar–H), 8.11 (s, 1H, pyrazolyl-H), 10.10 (s, 1H, =C–H); <sup>13</sup>C NMR spectrum,  $\delta_C$ , ppm: 161.4 (C=O), 151.7, 140.1, 137.8, 134.9, 131.1, 130.0, 129.6, 129.1,

128.70, 128.6, 119.7, 115.7, 113.5; MS (ESI-MS):  $m/z$  555.01 (M + H)<sup>+</sup>.

### 3.1.2 | (4E)-4-((3-(5-Bromothiophen-2-yl)-1-(4-fluorophenyl)-1H-pyrazol-4-yl)methylene)-3-(trifluoromethyl)-1-(perfluorophenyl)-1H-pyrazol-5(4H)-one (4b)

Orange solid; Wt. 1.05 g; Yield 81%; IR ( $\nu_{\max}/\text{cm}^{-1}$ ): 2,927 (C–H), 1,680 (C=O), 1,598 (C=N), 1,516 (C=C), 1,231 (C–F); <sup>1</sup>H NMR spectrum,  $\delta$ , ppm: 7.16 (d, 1H,  $J$  = 3.50 Hz, Ar–H), 7.26–7.19 (m, 3H, Ar–H), 7.84 (dd, 2H,  $J$  = 5.00 Hz and 9.00 Hz, Ar–H), 8.10 (s, 1H, pyrazole-H), 10.11 (s, 1H, =C–H); MS:  $m/z$  651.03 (M + H)<sup>+</sup>.

### 3.1.3 | (4E)-4-((3-[5-Chlorothiophen-2-yl]-1-phenyl-1H-pyrazol-4-yl)methylene)-3-(trifluoromethyl)-1-(perfluorophenyl)-1H-pyrazol-5(4H)-one (4c)

Orange solid; Wt. 873 mg; Yield 80%; IR ( $\nu_{\max}/\text{cm}^{-1}$ ): 2,926 (C–H), 1,682 (C=O), 1,597 (C=N), 1,518 (C=C), 1,232 (C–F); <sup>1</sup>H NMR spectrum,  $\delta$ , ppm: 7.07 (s, 1H, Ar–H), 7.26–7.18 (s, 1H, Ar–H), 7.44 (d, 1H,  $J$  = 6.00 Hz, Ar–H), 7.52 (m, 2H, Ar–H), 7.86 (d, 2H,  $J$  = 7.00 Hz, Ar–H), 8.11 (s, 1H, pyrazole-H), 10.16 (s, 1H, =C–H); <sup>13</sup>C NMR spectrum,  $\delta_{\text{C}}$ , ppm: 162.4 (C=O), 151.3, 139.5, 138.3, 135.0, 133.5, 130.8, 130.0, 128.8, 127.6, 127.4, 120.0, 116.3, 114.6; MS:  $m/z$  547.11 (M + H)<sup>+</sup>.

### 3.1.4 | (4E)-4-((3-(5-Bromothiophen-2-yl)-1-phenyl-1H-pyrazol-4-yl)methylene)-3-(trifluoromethyl)-1-(perfluorophenyl)-1H-pyrazol-5(4H)-one (4d)

Orange solid; Wt. 960 mg; Yield 76%; IR ( $\nu_{\max}/\text{cm}^{-1}$ ): 2,926 (C–H), 1,681 (C=O), 1,597 (C=N), 1,520 (C=C), 1,235 (C–F); <sup>1</sup>H NMR spectrum,  $\delta$ , ppm: 7.16 (d, 1H,  $J$  = 4.00 Hz, Ar–H), 7.21 (d, 1H,  $J$  = 3.50 Hz, Ar–H), 7.44 (t, 1H,  $J$  = 7.50 Hz, Ar–H), 7.52 (t, 2H,  $J$  = 7.50 Hz, Ar–H), 7.75–7.86 (d, 2H,  $J$  = 7.50 Hz, Ar–H), 8.47 (s, 1H, pyrazole-H), 10.16 (s, 1H, =C–H); <sup>13</sup>C NMR spectrum,  $\delta_{\text{C}}$ , ppm: 183.2 (C=O), 162.3, 151.2, 143.2, 142.9, 139.4, 138.3, 134.9, 133.7, 133.4, 131.2, 130.6, 129.8, 129.1, 128.8, 128.5, 128.2, 120.6, 119.9, 119.6, 116.2, 115.9, 114.6; MS:  $m/z$  633.05 (M + H).

### 3.1.5 | (4Z)-3-(Trifluoromethyl)-4-((3-[4-methoxyphenyl]-1-phenyl-1H-pyrazol-4-yl)methylene)-1-(perfluorophenyl)-1H-pyrazol-5(4H)-one (5a)

Orange solid; Wt. 971 mg; Yield 84%; IR ( $\nu_{\max}/\text{cm}^{-1}$ ): 3,141 (C–H), 1,703 (C=O), 1,595 (C=N), 1,514 (C=C), 1,224 (C–F); <sup>1</sup>H NMR spectrum,  $\delta$ , ppm: 3.92 (s, 3H, –OCH<sub>3</sub>), 7.10 (d, 2H,  $J$  = 8.50 Hz, Ar–H), 7.51 (t, 2H,  $J$  = 8.50 Hz, Ar–H), 7.62 (d, 2H,  $J$  = 8.50 Hz, Ar–H), 7.90 (d, 2H,  $J$  = 9.00 Hz, Ar–H), 7.99 (s, 1H, pyrazole-H), 10.19 (s, 1H, =C–H); <sup>13</sup>C NMR spectrum,  $\delta_{\text{C}}$ , ppm: 162.5 (C=O), 161.1, 158.7, 143.3, 141.4, 138.6, 134.9, 130.7, 129.7, 128.5, 122.6, 120.1, 116.8, 114.7, 113.7, 55.5 (OCH<sub>3</sub>); MS:  $m/z$  579.21 (M + H)<sup>+</sup>.

### 3.1.6 | (4Z)-3-(Trifluoromethyl)-1-(perfluorophenyl)-4-([1,3-diphenyl-1H-pyrazol-4-yl)methylene)-1H-pyrazol-5(4H)-one (5b)

Orange solid; Wt. 876 mg; Yield 80%; IR ( $\nu_{\max}/\text{cm}^{-1}$ ): 3,142 (C–H), 1,701 (C=O), 1,595 (C=N), 1,510 (C=C), 1,223 (C–F); <sup>1</sup>H NMR spectrum,  $\delta$ , ppm: 7.42 (m, 1H, Ar–H), 7.52 (t, 2H,  $J$  = 7.50 Hz, Ar–H), 7.57–7.58 (m, 3H, Ar–H), 7.68 (dd, 2H,  $J$  = 7.50 and 2.00 Hz, Ar–H), 7.90 (d, 2H,  $J$  = 8.00 Hz, Ar–H), 8.00 (s, 1H, pyrazole-H), 10.22 (s, 1H, =C–H); <sup>13</sup>C NMR spectrum,  $\delta_{\text{C}}$ , ppm: 162.5 (C=O), 158.8, 143.0, 141.2, 138.6, 134.9, 130.3, 129.9, 129.7, 129.4, 129.2, 128.6, 120.0, 116.8, 114.0; MS:  $m/z$  549.19 (M + H)<sup>+</sup>.

### 3.1.7 | (4Z)-4-((3-[2-Fluoro-4-methoxyphenyl]-1-phenyl-1H-pyrazol-4-yl)methylene)-3-(trifluoromethyl)-1-(perfluorophenyl)-1H-pyrazol-5(4H)-one (5c)

Orange solid; Wt. 1.06 g; Yield 82%; IR ( $\nu_{\max}/\text{cm}^{-1}$ ): 3,145 (C–H), 1,702 (C=O), 1,596 (C=N), 1,512 (C=C), 1,221 (C–F); <sup>1</sup>H NMR spectrum,  $\delta$ , ppm: 3.91 (s, 3H, –OCH<sub>3</sub>), 6.82 (dd, 1H,  $J$  = 2.50 and 12.00 Hz, Ar–H), 6.91 (dd, 1H,  $J$  = 2.00 and 8.50 Hz, Ar–H), 7.42 (t, 1H,  $J$  = 7.50 Hz, Ar–H), 7.58–7.49 (m, 2H, Ar–H), 7.79 (d, 1H,  $J$  = 2.50 Hz, Ar–H), 7.88 (d, 2H,  $J$  = 7.50 Hz, Ar–H), 8.52 (s, 1H, pyrazole-H), 10.20 (s, 1H, =C–H); <sup>13</sup>C NMR spectrum,  $\delta_{\text{C}}$ , ppm: 162.7 (C=O), 162.6, 162.5, 154.1, 141.2, 138.6, 134.7, 132.5, 129.7, 128.5, 120.0, 117.6, 113.9, 111.2, 110.3, 102.2, 102.0, 55.8 (OCH<sub>3</sub>); MS:  $m/z$  653.26 (M + H)<sup>+</sup>.



### 3.1.8 | (4Z)-3-(Trifluoromethyl)-1-(perfluorophenyl)-4-([1-phenyl-3-p-tolyl-1H-pyrazol-4-yl]methylene)-1H-pyrazol-5(4H)-one (5d)

Orange solid; Wt. 887 mg; Yield 79%; IR ( $\nu_{\max}/\text{cm}^{-1}$ ): 3,143 (=C–H), 1,701 (C=O), 1,594 (C=N), 1,511 (C=C), 1,220 (C–F);  $^1\text{H}$  NMR spectrum,  $\delta$ , ppm: 2.44 (s, 3H, –CH<sub>3</sub>), 7.45 (d, 1H,  $J = 7.50$  Hz, Ar–H), 7.51 (t, 1H,  $J = 7.50$  Hz, Ar–H), 7.62 (d, 1H,  $J = 8.00$  Hz, Ar–H), 7.65 (d, 1H,  $J = 8.00$  Hz, Ar–H), 9.90 (s, 1H, pyrazole-H), 11.96 (s, 1H, =C–H); MS:  $m/z$  563.08 (M + H)<sup>+</sup>.

### 3.1.9 | (4Z)-3-(Trifluoromethyl)-1-(perfluorophenyl)-4-((1-phenyl-3-(4-[trifluoro methoxy]phenyl)-1H-pyrazol-4-yl)methylene)-1H-pyrazol-5(4H)-one (5e)

Orange solid; Wt. 960 mg; Yield 76%; IR ( $\nu_{\max}/\text{cm}^{-1}$ ): 3,145 (=C–H), 1,700 (C=O), 1,595 (C=N), 1,517 (C=C), 1,225 (C–F);  $^1\text{H}$  NMR spectrum,  $\delta$ , ppm: 7.42–7.44 (m, 3H, Ar–H), 7.51–7.54 (m, 2H, Ar–H), 7.71 (d, 1H,  $J = 2.00$  Hz, Ar–H), 7.73 (d, 1H,  $J = 2.00$  Hz, Ar–H), 7.88 (d, 1H,  $J = 2.00$  Hz, Ar–H), 7.90 (d, 1H,  $J = 3.50$  Hz, Ar–H), 7.92 (s, 1H, pyrazole-H), 10.21 (s, 1H, =C–H);  $^{13}\text{C}$  NMR spectrum,  $\delta_{\text{C}}$ , ppm: 162.4 (C=O), 157.3, 150.5, 143.2, 142.9, 140.3, 138.5, 134.9, 130.9, 129.8, 129.0, 128.7, 121.5, 120.6, 120.0, 118.4, 116.6, 114.4; MS:  $m/z$  633.23 (M + H)<sup>+</sup>.

### 3.1.10 | (4Z)-4-((3-[3,4-Dichlorophenyl]-1-phenyl-1H-pyrazol-4-yl)methylene)-3-(trifluoromethyl)-1-(perfluorophenyl)-1H-pyrazol-5(4H)-one (5f)

Orange solid; Wt. 1.03 g; Yield 84%; IR ( $\nu_{\max}/\text{cm}^{-1}$ ): 3,144 (=C–H), 1,701 (C=O), 1,596 (C=N), 1,517 (C=C), 1,227 (C–F);  $^1\text{H}$  NMR spectrum,  $\delta$ , ppm: 7.44 (m, 1H, Ar–H), 7.48 (d, 1H,  $J = 2.00$  Hz, Ar–H), 7.50 (d, 1H,  $J = 2.00$  Hz, Ar–H), 7.53 (d, 1H,  $J = 7.50$  Hz, Ar–H), 7.67 (d, 1H,  $J = 8.50$  Hz, Ar–H), 7.83 (d, 1H,  $J = 2.00$  Hz, Ar–H), 7.87–7.89 (m, 2H, Ar–H), 7.89 (s, 1H, pyrazole-H), 10.18 (s, 1H, =C–H);  $^{13}\text{C}$  NMR spectrum,  $\delta_{\text{C}}$ , ppm: 162.3 (C=O), 156.1, 143.2, 142.9, 139.7, 138.4, 135.0, 134.5, 133.7, 131.2, 131.1, 130.3, 129.8, 128.8, 128.3, 120.0, 116.4, 114.7; MS:  $m/z$  617.15 (M + H)<sup>+</sup>.

### 3.1.11 | (Z)-4-([6-Chloro-5,7-dimethyl-4-oxo-4H-chromen-3-yl]methylene)-2-(perfluorophenyl)-5-(trifluoromethyl)-2,4-dihydro-3H-pyrazol-3-one (6a)

Orange solid; Wt. 900 mg; Yield 84%; IR ( $\nu_{\max}/\text{cm}^{-1}$ ): 3,074 (=C–H), 1,707 (C=O), 1,666 (C=O), 1,624 (C=N), 1,508 (C=C), 1,192 (C–F);  $^1\text{H}$  NMR spectrum,  $\delta$ , ppm: 2.54 (s, 3H, –CH<sub>3</sub>), 3.01 (s, 3H, –CH<sub>3</sub>), 7.26 (s, 1H, Ar–H), 8.50 (s, 1H, chromone-H), 10.54 (s, 1H, =C–H);  $^{13}\text{C}$  NMR spectrum,  $\delta_{\text{C}}$ , ppm: 175.4 (C=O), 164.2 (C=O), 162.3, 155.1, 144.5, 143.4, 143.3, 139.7, 134.7, 120.9, 120.2, 119.4, 118.3, 118.2, 118.1, 22.2 (–CH<sub>3</sub>), 18.6 (–CH<sub>3</sub>); MS:  $m/z$  537.11 (M + H)<sup>+</sup>.

### 3.1.12 | (Z)-4-([6-Chloro-7-methyl-4-oxo-4H-chromen-3-yl]methylene)-2-(perfluorophenyl)-5-(trifluoromethyl)-2,4-dihydro-3H-pyrazol-3-one (6b)

Orange solid; Wt. 783 mg; Yield 75%; IR ( $\nu_{\max}/\text{cm}^{-1}$ ): 3,076 (=C–H), 1,705 (C=O), 1,664 (C=O), 1,627 (C=N), 1,508 (C=C), 1,192 (C–F);  $^1\text{H}$  NMR spectrum,  $\delta$ , ppm: 2.54 (s, 3H, –CH<sub>3</sub>), 7.47 (s, 1H, Ar–H), 8.24 (s, 1H, Ar–H), 8.48 (s, 1H, chromone-H), 10.62 (s, 1H, =C–H); MS:  $m/z$  523.08 (M + H)<sup>+</sup>.

### 3.1.13 | (Z)-4-([6-Chloro-4-oxo-4H-chromen-3-yl]methylene)-2-(perfluorophenyl)-5-(trifluoromethyl)-2,4-dihydro-3H-pyrazol-3-one (6c)

Orange solid; Wt. 812 mg; Yield 80%; IR ( $\nu_{\max}/\text{cm}^{-1}$ ): 3,074 (=C–H), 1,707 (C=O), 1,662 (C=O), 1,621 (C=N), 1,509 (C=C), 1,193 (C–F);  $^1\text{H}$  NMR spectrum,  $\delta$ , ppm: 7.55 (d, 1H,  $J = 9.00$  Hz, Ar–H), 7.73 (d, 1H,  $J = 2.50$  and  $9.00$  Hz, Ar–H), 8.26 (d, 1H,  $J = 2.50$  Hz, Ar–H), 8.47 (s, 1H, chromone-H), 10.63 (s, 1H, =C–H); MS:  $m/z$  509.08 (M + H)<sup>+</sup>.

### 3.1.14 | (Z)-4-([6,8-Dichloro-4-oxo-4H-chromen-3-yl]methylene)-2-(perfluorophenyl)-5-(trifluoromethyl)-2,4-dihydro-3H-pyrazol-3-one (6d)

Orange solid; Wt. 845 mg; Yield 78%; IR ( $\nu_{\max}/\text{cm}^{-1}$ ): 3,078 (=C–H), 1,707 (C=O), 1,665 (C=O), 1,626 (C=N), 1,506 (C=C), 1,194 (C–F);  $^1\text{H}$  NMR spectrum,  $\delta$ , ppm: 7.83 (d, 1H,  $J = 2.50$  Hz, Ar–H), 8.17 (d, 1H,  $J = 2.50$  Hz, Ar–H), 8.40 (s, 1H, chromone-H), 10.66 (s, 1H, =C–H); MS:  $m/z$  543.07 (M + H)<sup>+</sup>.

### 3.1.15 | (Z)-4-([7-Methyl-4-oxo-4H-chromen-3-yl]methylene)-2-(perfluorophenyl)-5-(trifluoromethyl)-2,4-dihydro-3H-pyrazol-3-one (6e)

Orange solid; Wt. 800 mg; Yield 82%; IR ( $\nu_{\max}/\text{cm}^{-1}$ ): 3,076 (C–H), 1,703 (C=O), 1,666 (C=O), 1,627 (C=N), 1,510 (C=C), 1,193 (C–F);  $^1\text{H}$  NMR spectrum,  $\delta$ , ppm: 2.51 (s, 3H,  $-\text{CH}_3$ ), 7.48 (d, 1H,  $J = 8.00$  Hz, Ar–H), 7.60 (dd, 1H,  $J = 8.00$  and 2.00 Hz, Ar–H), 8.08 (d, 1H,  $J = 1.50$  Hz), 8.54 (s, 1H, chromone-H), 10.64 (s, 1H, =C–H);  $^{13}\text{C}$  NMR spectrum,  $\delta_{\text{C}}$ , ppm: 174.5 (C=O), 165.5 (C=O), 162.4, 154.2, 143.4, 142.4, 137.5, 136.3, 126.2, 120.9, 123.3, 120.2, 118.6, 118.5, 118.2, 118.1, 21.1 ( $-\text{CH}_3$ ); MS:  $m/z$  489.14 (M + H) $^+$ .

## 3.2 | Anti-inflammatory activity

All the synthesized compounds were screened for their in vitro anti-inflammatory activities against the standard drug diclofenac sodium. The minimum inhibitory concentration was determined by the well diffusion method at 1 mg/ml of concentration. (Table 2). A volume of 1 ml of diclofenac sodium at different concentrations (50, 100, 200, 400, 800, and 1,000  $\mu\text{g}/\text{ml}$ ) was homogenized with 1 ml of aqueous solution of bovine serum albumin (5%) and incubated at 27°C for 15 minutes. The mixture of distilled water and bismuth sulphite agar constituted the control tube. Denaturation of the proteins was caused by placing the mixture in a water bath for 10 minutes at 70°C. The mixture was cooled within the ambient room temperature, and the activity of each mixture was measured at 255 nm. Each test was conducted thrice. The following formula was used to calculate inhibition percentage:

$$\% \text{inhibition} = \frac{\text{absorbance of control} - \text{absorbance of sample}}{\text{absorbance of control}} \times 100.$$

## 3.3 | In silico ADME

In the present study, we have calculated molecular volume (MV), molecular weight (MW), logarithm of partition coefficient ( $\text{miLog } P$ ), number of hydrogen bond acceptors (n-ON), number of hydrogen bonds donors (n-OHNH), topological polar surface area (TPSA), number of rotatable bonds (n-ROTB), and Lipinski's rule of five<sup>[31]</sup> using the Molinspiration online property calculation toolkit.<sup>[30]</sup> Absorption (% ABS) was calculated by: %

ABS =  $109 - (0.345 \times \text{TPSA})$ .<sup>[32]</sup> Drug likeness model score (a collective property of physicochemical properties, pharmacokinetics, and pharmacodynamics of a compound that is represented by a numerical value) was computed by MolSoft software.<sup>[33]</sup>

## 4 | CONCLUSIONS

In conclusion, we have constructed pyrazole and fluorine in one molecular framework as new 3-(trifluoromethyl)-1-(perfluorophenyl)-1H-pyrazol-5(4H)-one derivatives under conventional and nonconventional methods like microwave irradiation and ultrasonication, respectively, via Knoevenagel condensation and evaluated their biological activity. Ultrasonication and microwave irradiation can shorten the reaction time from a few hours to a few minutes and increases the product yield (74–84%) compared to the conventional method (59–75%). The synthesized compounds exhibited promising anti-inflammatory activity compared to the standard drug diclofenac sodium. Similarly, the synthesized compound displayed promising antioxidant activity compared to the standard drug. Furthermore, an analysis of the ADME parameters for synthesized compounds showed good drug-like properties and can be developed as an oral drug candidate, thus suggesting that compounds from the present series can be further optimized and developed as a lead molecule.

## ACKNOWLEDGMENT

The authors are thankful to the Department of Science and Technology, New Delhi for providing research facilities under FIST scheme and to CIF, Savitribai Phule Pune University, Pune and SAIF, Panjab University, Chandigarh for providing spectral facilities.

## CONFLICT OF INTEREST

The authors declare no conflict of interest, financial or otherwise.

## REFERENCES

- [1] M. Bhat, G. K. Nagaraja, R. Kayarmar, S. K. Peethamber, M. Shefeeulla, *RSC Adv.* **2016**, 6, 59375.
- [2] A. L. Luz, C. D. Kassotis, H. M. Stapleton, J. N. Meyer, *Toxicology* **2018**, 393, 150.
- [3] P. Khloya, S. Kumar, P. Kaushik, P. Surain, D. Kaushik, P. K. Sharma, *Bioorg. Med. Chem. Lett.* **2015**, 25, 1177.
- [4] (a) Y. R. Li, C. Li, J. C. Liu, M. Guo, T. Y. Zhang, L. P. Sun, C. J. Zheng, H. R. Piao, *Bioorg. Med. Chem. Lett.* **2015**, 25, 5052. (b) S. A. Ali, S. M. Awad, A. M. Said, S. Mahgouba, H. Tahaa, N. M. Ahmed, *J. Enzyme Inhib. Med. Chem.* **2020**, 35, 847.
- [5] X. L. Deng, J. Xie, Y. Q. Li, D. K. Yuan, X. P. Hu, L. Zhang, Q. M. Wang, M. Chi, X. L. Yang, *Chin. Chem. Lett.* **2016**, 27, 566.

- [6] H. Jia, F. Bai, N. Liu, X. Liang, P. Zhan, C. Ma, X. Jiang, X. Liu, *Eur. J. Med. Chem.* **2016**, *123*, 202.
- [7] C. I. Nieto, M. P. Cabildo, M. P. Cornago, D. Sanz, R. M. Claramunt, I. Alkorta, J. Elguero, J. A. Garcia, A. Lopez, D. A. Castroviejo, *J. Mol. Struct.* **2015**, *1100*, 518.
- [8] S. Shu, X. Cai, J. Li, Y. Feng, A. Dai, J. Wang, D. Yang, M. W. Wang, H. Liu, *Bioorg. Med. Chem.* **2016**, *24*, 2852.
- [9] R. Dummer, P. A. Ascierto, H. J. Gogas, A. Arance, M. Mandala, G. Liskay, C. Garbe, D. Schandendorf, L. Krajsova, R. Gutzmer, V. C. Sileni, C. Dutriaux, J. W. Groot, N. Yamazaki, C. Loquai, L. A. M. D. Parseval, M. D. Pickard, V. Sandor, C. Robert, K. T. Flaherty, *Lancet Oncol.* **2018**, *19*, 6035.
- [10] E. Therrien, G. Larouche, N. Nguyen, J. Rahil, A. M. Lemieux, Z. Li, M. Fournel, T. P. Yan, A. J. Landry, S. Lefebvre, J. J. Wang, K. Macbeth, C. Heise, A. Nguyen, J. M. Besterman, R. Deziel, A. Wahhab, *Bioorg. Med. Chem. Lett.* **2015**, *25*, 2514.
- [11] X. H. Lv, Q. S. Li, Z. L. Ren, M. J. Chu, J. Sun, X. Zhang, M. Xing, H. L. Zhu, H. Q. Cao, *Eur. J. Med. Chem.* **2016**, *108*, 586.
- [12] M. A. Tabrizi, P. G. Baraldi, E. Ruggiero, G. Saponaro, S. Baraldi, R. Romagnoli, A. Martinelli, T. Tuccinardi, *Eur. J. Med. Chem.* **2015**, *97*, 289.
- [13] E. Kick, R. Martin, Y. Xie, B. Flatt, E. Schweiger, T. L. Wang, B. Busch, M. Nyman, X. H. Gu, G. Yan, B. Wagner, M. Nanao, L. Nguyen, T. Stout, A. Plonowski, I. Schulman, J. Ostrowski, T. Kirchgessner, R. Wexler, R. Mohan, *Bioorg. Med. Chem. Lett.* **2015**, *25*, 372.
- [14] a) K. Muller, C. Faeh, F. Diederich, *Science* **2007**, *317*, 1881. b) W. K. Hagmann, *J. Med. Chem.* **2008**, *51*, 4359. c) R. E. Banks, B. E. Smart, J. C. Tatlow, *Organo Fluorine Chemistry. Principles and Commercial Applications*, Plenum, New York **1994**. d) S. Purser, P. R. Moore, S. Swallow, V. Gouverneur, *Chem. Soc. Rev.* **2008**, *37*, 320. e) P. Jeschke, *ChemBioChem* **2004**, *5*, 570.
- [15] a) D. O'Hagan, *Chem. Soc. Rev.* **2008**, *37*, 308. b) H. J. Bohm, D. Banner, S. Bendels, M. Kansy, B. Kuhn, K. Muller, U. ObstSander, M. Stahl, *ChemBioChem* **2004**, *5*, 637. (c) P. Nagender, D. Pulakesh, G. Gouverneur, N. Shibata, *Org. Lett.* **2018**, *20*, 1526. (d) D. Pulakesh, G. Satoshi, P. Nagender, U. Hiroto, T. Etsuko, N. Shibata, *Chem. Sci.* **2018**, *9*, 3276. (e) P. Nagender, S. Takuya, K. Mikhail, T. Etsuko, S. Yuji, N. Shibata, *Chem. Commun.* **2018**, *54*, 4294. (f) D. K. Swaroop, N. Ravi Kumar, P. Nagender, G. Jitender Dev, N. Jagadeesh Babu, B. Narsaiah, *Eur. J. Org. Chem.* **2019**, *2019*, 3654. <https://doi.org/10.1002/ejoc.201900482>. (g) P. Nagender, H. Kyosuke, N. Shibata, *Chem. Commun.* **2018**, *54*, 7171.
- [16] (a) I. I. Gerus, R. X. Mironetz, I. S. Kondratov, A. V. Bezdudny, Y. V. Dmytriv, O. V. Shishkin, V. S. Starova, O. A. Zaporozhets, A. A. Tolmachev, P. K. Mykhailiuk, *J. Org. Chem.* **2012**, *77*, 47. (b) B. D. Maxwell, *J. Labell. Compd. Radiopharm.* **2000**, *43*, 645.
- [17] T. G. Leighton, *The acoustic bubble*, Academic Press, London **1994**, p. 531.
- [18] C. O. Kappe, A. Stadler, D. Dallinger, *Microwaves in Organic and Medicinal Chemistry*, 2nd ed., Wiley-VCH, Weinheim **2012**.
- [19] (a) A. S. William, F. B. Aleksel, C. Ron, Organic synthesis: The science behind art. in *Royal Society of Chemistry (Great Britain)*, RSC publications, Cambridge, **1998**. (b) *Organic Synthesis Co. II vol*; **1935**. (c) *Comprehensive Organic Synthesis Book Volumes*, John Wiley & Sons, Hoboken, NJ, **1991**.
- [20] (a) T. Syed, A. Yahya, J. A. Alsheri, *Lett. Org. Chem.* **2020**, *17*, 157. (b) S. Mallouk, K. Bougrin, A. Laghzizil, R. Benhida, *Molecules* **2010**, *15*, 813. (c) J. S. Biradar, B. S. Sasidhar, *Eur. J. Med. Chem.* **2011**, *46*, 6112. (d) M. B. Ansari, H. Jin, M. N. Parvin, S. E. Park, *Catal. Today* **2012**, *185*, 211.
- [21] (a) M. A. Pasha, K. Manjula, J. Saudi, *Chem. Soc.* **2011**, *15*, 283. (b) Y. Ogiwara, K. Takahashi, T. Kitazawa, N. Sakai, *J. Org. Chem.* **2015**, *80*, 3101. (c) P. Leelavathi, S. R. Kumar, *J. Mol. Catal. A Chem.* **2005**, *240*, 99. (d) J. V. Schijndel, A. C. Luiz, D. Molendijk, J. Meuldijk, *Green Chem. Lett. Rev.* **2017**, *10*, 404.
- [22] S. Ramesh, F. Devred, D. P. Debecker, *ChemistrySelect* **2020**, *5*, 300.
- [23] R. B. Ardakani, N. Safaeian, M. Oftadeh, M. F. Mehrjardi, *Theor. Chem. Acc.* **2020**, *139*, 45.
- [24] N. Zengin, H. Burhan, A. Savk, H. Goksu, F. Sen, *Scie. Rep.* **2020**, *10*, 12758.
- [25] A. R. Bhat, M. H. Najjar, R. S. Dongre, M. S. Akhter, *Res. Green Sust. Chem.*, **2020**, *3*, 100008. <https://doi.org/10.1016/j.jrgsc.2020.06.001>.
- [26] (a) K. S. Hon, H. N. Akolkar, B. K. Karale, *J. Het. Chem.* **2020**, *57*, 1692. (b) S. P. Kunde, K. G. Kanade, B. K. Karale, H. N. Akolkar, S. S. Arbuj, P. V. Randhavane, S. T. Shinde, M. H. Shaikh, A. K. Kulkarni, *RSC Adv.* **2020**, *10*, 26997. (c) S. J. Takate, A. D. Shinde, B. K. Karale, H. Akolkar, L. Nawale, D. Sarkar, P. C. Mhaske, *Bioorg. Med. Chem. Lett.* **2019**, *29*, 1999. (d) S. P. Kunde, K. G. Kanade, B. K. Karale, H. N. Akolkar, P. V. Randhavane, S. T. Shinde, *Res. Chem. Intermed.* **2017**, *43*, 7277. (e) R. S. Endait, B. K. Karale, H. N. Akolkar, P. V. Randhavane, *Indian J. Het. Chem.* **2016**, *26*, 141.
- [27] B. S. Furniss, A. J. Hannaford, P. W. G. Smith, A. R. Tatchell, *Vogel's Text Book of Practical Organic Chemistry*, 5th ed., Addison Wesley Longman Limited, England **1998**.
- [28] S. Kandia, A. L. Charles, *Food Chem.* **2019**, *287*, 338.
- [29] S. Zhang, Y. Luo, L. Q. He, Z. J. Liu, A. Q. Jiang, Y. H. Yang, H. L. Zhu, *Bioorg. Med. Chem.* **2013**, *21*, 3723.
- [30] Molinspiration Chemoinformatics Brastislava, Slovak Republic. <http://www.molinspiration.com/cgi-bin/properties>; **2014**.
- [31] C. A. Lipinski, L. Lombardo, B. W. Dominy, P. J. Feeney, *Adv. Drug Del. Rev.* **2001**, *46*, 3.
- [32] Y. Zhao, M. H. Abraham, J. Lee, A. Hersey, N. C. Luscombe, G. Beck, B. Sherborne, I. Cooper, *Pharm. Res.* **2002**, *19*, 1446.
- [33] Drug-Likeness and Molecular Property Prediction. <http://www.molsoft.com/mprop/>.

## SUPPORTING INFORMATION

Additional supporting information may be found online in the Supporting Information section at the end of this article.

**How to cite this article:** Dengale SG, Akolkar HN, Karale BK, et al. Synthesis of 3-(trifluoromethyl)-1-(perfluorophenyl)-1H-pyrazol-5 (4H)-one derivatives via Knoevenagel condensation and their biological evaluation. *J Chin Chem Soc.* 2020;1–12. <https://doi.org/10.1002/jccs.202000357>



## COLLEGE CAMPUS AS A ROLE MODEL FOR ENVIRONMENTAL CONSCIOUSNESS

Mohamed Rizwan Khan

Dept. of Zoology, Radhabai Kale Mahila Mahavidyalaya, Ahmednagar (M.S.) India.

\*Corresponding Author: [mail: rizwan\\_khan672@yahoo.com](mailto:rizwan_khan672@yahoo.com)

Communicated: 23.02.2020

Revision :27.03.2020 & 28.04.2020

Accepted: 25.05.2020

Published: 30.05.2020

### ABSTRACT:

India is a young country. College is the place where this youth come to learn and spend lot of time. These students are the future and part of the society. As our planet earth faces many environmental issues, college is the best place for sensitization of students regarding environment. Students propagate this to their locality also. This paper deals with measures the college can adopts for ecofriendly campus and to become a role model for environmental consciousness like green audit, e governance, vermicompost plant, rainwater harvesting project, biogas plant, botanical garden, hydroponics, use of renewable energy, waste management, biodiversity posters & environmental slogans, students projects based on environment and offering compulsory course on environmental education.

**Key words:** - *Campus, College, Consciousness, Environment.*

### INTRODUCTION:

The human society is facing many environmental issues like pollution, population explosion, deforestation, resource depletion, loss of biodiversity etc. Sustainable development is a significant social, economic or environmental challenge for any country (Wynn Calder, 2003). The youth should get sensitive about environment. Education is one solution to solve environmental problem. The teaching and learning must begin to reflect environmental issues; there is an emerging consensus that institutions must also model sustainable practices (Erin Redman, 2013). Students take with them the green practices and approaches they were involved with at their institution (Will Toor, 2003). Environmental education becomes integral part in syllabus. National Assessment and Accreditation Council an autonomous institution of the University Grants Commission play important role in periodic assessment and accreditation of higher education institutions also gives importance to

environment consciousness and sustainability. In Criteria 7 Institutional Values and Best Practices of NAAC manual for the college, environmental consciousness and sustainability is incorporated which includes metrics regarding use of alternate energy sources, management of waste, water conservation facilities, green campus initiatives and quality audits on environment. Eco friendly college means “environmental sustainability within the college”. Eco friendly college campus mainly focuses on the efficient uses of energy and water, minimize waste generation or pollution and also economic efficiency. Eco friendly college focuses on the reduction of the emissions of green house gases, more use of renewable energy, rainwater harvesting, encourages staff and student for environmental issues, to have significant environmental impacts. Following measures and activities can be adopted by college to make campus ecofriendly.

**Vermicompost Plant:** Construction of vermicompost pit for the waste from gardens

and office can be converted to vermicompost which is used as compost for plants in campus.

**Rainwater harvesting:** Collection of rain water in ponds and using it for laboratory purpose.

**Biogas plant:** Construction of biogas plant for the biodegradable waste from hostel can be converted to biogas.

**Solar Panels:** Installation of solar panels at prominent places to utilize renewable solar energy for laboratory work.

**Botanical Garden:** Maintenance of botanical garden for aesthetic purpose and to attract insects specially butterflies which help in biodiversity study.

**Green campus:** Plantation programme for green campus so that more carbon dioxide can be fixed and tree attract many birds for their nesting and green initiatives like observation of no vehicle day, environment days etc.

**E-waste management:** E-waste produced by Information Technology Department is managed by recycling and by doing annual maintenance contract.

**Green audit:** Green audit of the college should be done regularly.

**Biodiversity Posters & Environmental Slogans:** Local Biodiversity posters and environmental slogans at prominent places in campus should be displayed which aware students and staff.

**Dust bin:** Separate dust bin for liquid and solid waste should be placed and properly used.

**Hydroponics:** Plants can be cultivated in mineral rich water without soil.

**E governance:** Use of mobile applications, SMS and email for admission and governance.

**LED and CFL:** To decrease the energy consumption use of CFL and LED should be promoted, five star electronic appliances can be preferred and students and staff should be promoted to switch off appliances after use.

Organization of environmental awareness activities like poster presentation, environmental related day celebration, plays, seminar, conference etc. and involvement of students and staff.

To frame various college level committees related to environment like water management committee, green audit committee, energy conservation committee, waste recycling committee.

#### CONCLUSION:

College is the place where students spend more time. These young students are the future of any nation. Awareness of these students regarding environmental issues is very important. Eco friendly college campus can be a very good model to learn and sanitizes the students regarding environment that can be passed to society also. For that, college can establish eco friendly college committee to look and implement eco-friendly measures

#### REFERENCES:

- Erin Redman, (2013): Advancing educational pedagogy for sustainability: Developing and implementing programs to transform behaviors, International Journal of Environmental and Science education, Vol. 8, No. 1, January, 1-34.
- Wynn Calder and Richard M. Clugston, 2003, Progress Toward Sustainability in Higher Education, ELR News & Analysis Environmental Law Institute®,





Washington, DC. Reprinted with permission from ELR®, <http://www.eli.org>, 1-800-433-5120.  
Will Toor, (2003): “The Road Less Traveled: Sustainable Transportation for Campus,”

Planning for Higher Education, March-May 137-140.  
[http://www.naac.gov.in/images/docs/Manuals/Affiliated\\_Constituent-UG-PG-Colleges-04\\_Feb2020.pdf](http://www.naac.gov.in/images/docs/Manuals/Affiliated_Constituent-UG-PG-Colleges-04_Feb2020.pdf)

**OCCURRENCE OF *TENODERA SUPERSTITIOSA SUPERSTITIOSA* (FABRICIUS, 1781) (INSECTA: MANTODEA: MANTIDAE: MANTINAE) FROM THE DECCAN PLATEAU OF MAHARASHTRA STATE, INDIA.**

**G. A. Raut, M. R. Khan and S. M. Gaikwad\***

Department of Zoology, Radhabai Kale Mahila Mahavidyalaya, Ahmednagar (MS).

\*Department of Zoology, Shivaji University Kolhapur (MS).

**ABSTRACT**

*Tenodera superstitionosa superstitionosa* (Fabricius, 1781) has been reported for the first time from Kolhapur and Satara Districts of Maharashtra. Present record adds to its geographical distribution apart from Andaman, Bihar, Kerala, Punjab and Uttar Pradesh.

**Key words:** *Tenodera superstitionosa superstitionosa*, first record, Deccan Plateau.

Praying Mantids are well known predators with about 56 species reported from Maharashtra state (Ghate et. al. 2012). Out of these, *Tenodera superstitionosa superstitionosa* is distributed in Andaman, Bihar, Kerala, Punjab and Uttar Pradesh (Mukherjee et. al. 1995). Later on it was reported in Maharashtra by Mukherjee et. al. (2014) without mentioning specimen examined or deposition records. This leads to a question mark on its distribution in Maharashtra state. Present communication reports collection of this species from Kolhapur district along with brief description.

**Material and Methods**

The specimen was collected from Karveer Tehsil of Kolhapur district, and Dahiwadi region of Satara district, of Maharashtra state. The nymphs and adults were collected from Panchganga river bank, Karveer, reared in laboratory at the Department of Zoology, Shivaji University, Kolhapur till adult stage. Specimens were properly spread, dried, preserved and deposited at the Department of Zoology, Shivaji University, Kolhapur and Western Regional Centre, Zoological Survey of India, Pune. The specimens were observed under microscope and photographed. The identification and nomenclature was done

following Mukherjee et al. (1995).

**Material Examined:** 7 nymphs, Karveer, Kolhapur. 18.08.2014, NZC,ZSI,WRC, Ent.-12/106, coll. G.A. Raut. 1 male, Karveer, Kolhapur. 10.09.2015, NZC,ZSI,WRC,Ent.-12/107, coll. G.A. Raut, 1 Female, Dahiwadi, Satara. 12.vii. 2018, ZSUK.MANT.F221, coll. Raut G.A.

**Diagnosis:** Male (Figure1) and female greenish straw colored. Frontal sclerite 2X wide than high; upper edge sinus on each side. Pronotum long, supra coxal dilation little, the metazona depressed, lateral edges carinated strongly in female, little in male, much longer than the fore coxa; prosternum with small band at the junction of coxa. In fore legs, coxa smooth; femora with 4 external, 4 discoidal, 15 internal spines in which 8 small and 7 large; tibia with 13 internal and 9 external spines; all spines black at the tip. Elytra acute, longer than abdomen, costal area opaque remaining hyaline; in hind wings. costal and discoidal areas crossed by line of dark smoky patches on veins.

Both male and females are in faint brown in the middle and at the lateral green; males were brownish than females. In rainy season both male and female having much green shade while in dry season it become

more brownish; nymphs mostly green in colour.

**Measurements:** Body length: M-82.78, F-92.67; Pronotum: M-28.41, F-39.1; Fore wing: M-59.3, F-68.7.(M: Male, F: Female)

**Distribution:** India: Andaman, Bihar, Kerala, Punjab, Uttar Pradesh (Mukherjee et al. 1995) and Maharashtra (present record)

**Distribution** Elsewhere: Singapore, Angola, Java, Malay, Africa (Mukherjee et al. 2014).

The species has been reported for the first time from Deccan Plateau of Maharashtra. The present record extends its known geographical range notably from Andaman, Bihar, Kerala, Punjab, Uttar Pradesh towards western India and adds information on its known distributional range.

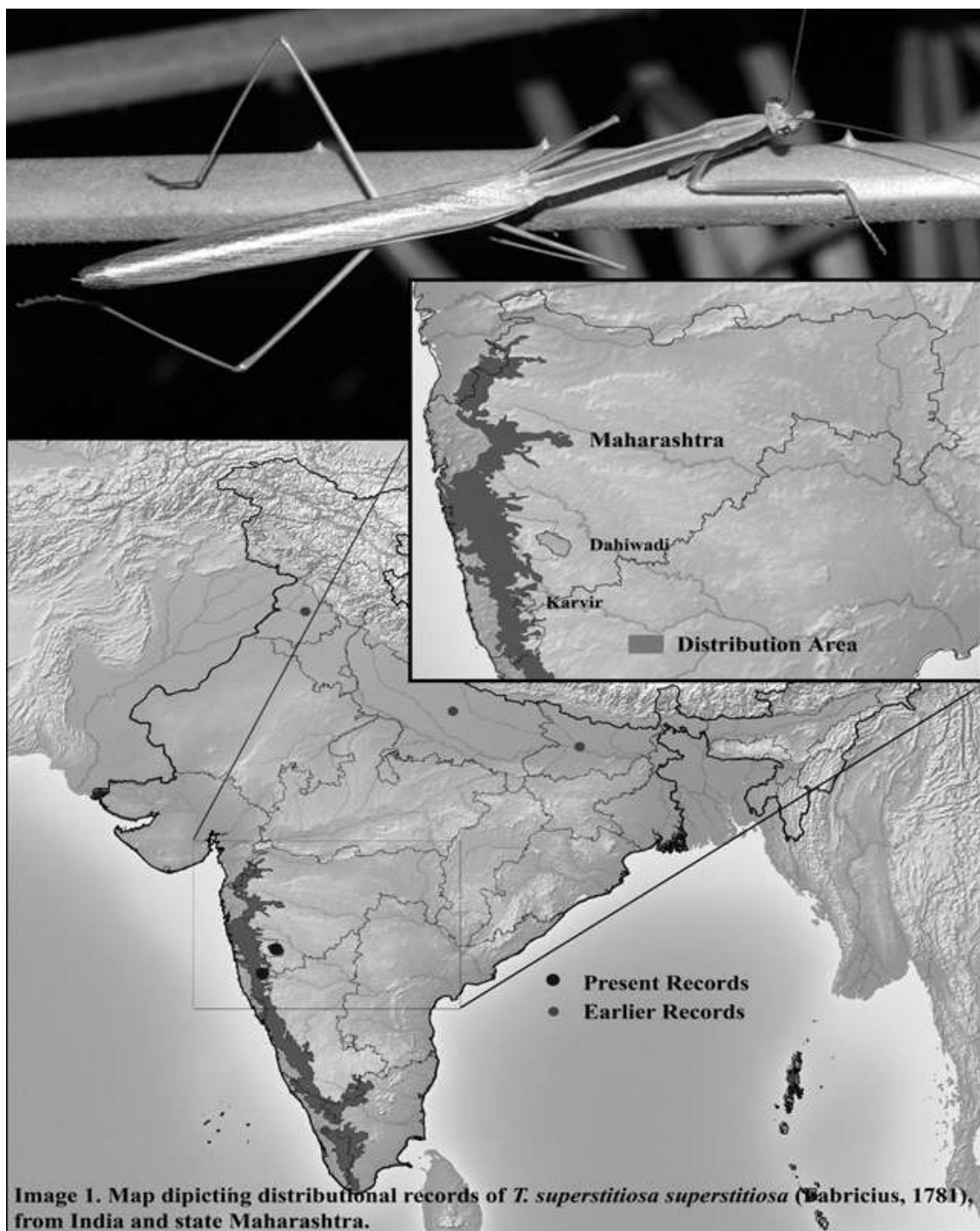
Due to limited literature on this species, misidentifications and confusion, *T. superstiosa superstiosa* is frequently reported as *T. fasciata*. However, present study will enable its correct identification and distribution pattern.

### Acknowledgements:

Authors are grateful to the Head, Department of Zoology, Shivaji University, Kolhapur, and the Principal, Radhabai Kale Mahila Mahavidyalay, Ahmednagar for providing necessary facilities and DST-FIST Phase-I for financial assistance for field and laboratory work. The authors are also thankful to Dr. Amrut Bhosale for continuous help for collection and also for technical support.

### References:

- Ghate, H. V., Jadhav, S. S. and R. M. Sharma. (2012). "*Insecta: Mantodea*". Fauna of Maharashtra State, State Fauna Series. Zoological Survey of India.
- Mukherjee, T. K., Hazra, A. K. and A. K. Ghosh. (1995). *Oriental Insects*. **29(1)**: 185.
- Mukherjee, T.K., Ehrmann, R. and P. Chatterjee. (2014). "*Checklist of Mantodea (Insecta) from India*". Priamus, Serial Publication of the Centre for Entomological Studies Ankara. (suppl.). **(30)**: 1-61.



**OCCURRENCE OF *TENODERA SUPERSTITIOSA SUPERSTITIOSA* (FABRICIUS, 1781) (INSECTA: MANTODEA: MANTIDAE: MANTINAE) FROM THE DECCAN PLATEAU OF MAHARASHTRA STATE, INDIA.**

**G. A. Raut, M. R. Khan and S. M. Gaikwad\***

Department of Zoology, Radhabai Kale Mahila Mahavidyalaya, Ahmednagar (MS).

\*Department of Zoology, Shivaji University Kolhapur (MS).

**ABSTRACT**

*Tenodera superstitionosa superstitionosa* (Fabricius, 1781) has been reported for the first time from Kolhapur and Satara Districts of Maharashtra. Present record adds to its geographical distribution apart from Andaman, Bihar, Kerala, Punjab and Uttar Pradesh.

**Key words:** *Tenodera superstitionosa superstitionosa*, first record, Deccan Plateau.

Praying Mantids are well known predators with about 56 species reported from Maharashtra state (Ghate et. al. 2012). Out of these, *Tenodera superstitionosa superstitionosa* is distributed in Andaman, Bihar, Kerala, Punjab and Uttar Pradesh (Mukherjee et. al. 1995). Later on it was reported in Maharashtra by Mukherjee et. al. (2014) without mentioning specimen examined or deposition records. This leads to a question mark on its distribution in Maharashtra state. Present communication reports collection of this species from Kolhapur district along with brief description.

**Material and Methods**

The specimen was collected from Karveer Tehsil of Kolhapur district, and Dahiwadi region of Satara district, of Maharashtra state. The nymphs and adults were collected from Panchganga river bank, Karveer, reared in laboratory at the Department of Zoology, Shivaji University, Kolhapur till adult stage. Specimens were properly spread, dried, preserved and deposited at the Department of Zoology, Shivaji University, Kolhapur and Western Regional Centre, Zoological Survey of India, Pune. The specimens were observed under microscope and photographed. The identification and nomenclature was done

following Mukherjee et al. (1995).

**Material Examined:** 7 nymphs, Karveer, Kolhapur. 18.08.2014, NZC,ZSI,WRC, Ent.-12/106, coll. G.A. Raut. 1 male, Karveer, Kolhapur. 10.09.2015, NZC,ZSI,WRC,Ent.-12/107, coll. G.A. Raut, 1 Female, Dahiwadi, Satara. 12.vii. 2018, ZSUK.MANT.F221, coll. Raut G.A.

**Diagnosis:** Male (Figure1) and female greenish straw colored. Frontal sclerite 2X wide than high; upper edge sinus on each side. Pronotum long, supra coxal dilation little, the metazona depressed, lateral edges carinated strongly in female, little in male, much longer than the fore coxa; prosternum with small band at the junction of coxa. In fore legs, coxa smooth; femora with 4 external, 4 discoidal, 15 internal spines in which 8 small and 7 large; tibia with 13 internal and 9 external spines; all spines black at the tip. Elytra acute, longer than abdomen, costal area opaque remaining hyaline; in hind wings. costal and discoidal areas crossed by line of dark smoky patches on veins.

Both male and females are in faint brown in the middle and at the lateral green; males were brownish than females. In rainy season both male and female having much green shade while in dry season it become



more brownish; nymphs mostly green in colour.

**Measurements:** Body length: M-82.78, F-92.67; Pronotum: M-28.41, F-39.1; Fore wing: M-59.3, F-68.7.(M: Male, F: Female)

**Distribution:** India: Andaman, Bihar, Kerala, Punjab, Uttar Pradesh (Mukherjee et al. 1995) and Maharashtra (present record)

**Distribution** Elsewhere: Singapore, Angola, Java, Malay, Africa (Mukherjee et al. 2014).

The species has been reported for the first time from Deccan Plateau of Maharashtra. The present record extends its known geographical range notably from Andaman, Bihar, Kerala, Punjab, Uttar Pradesh towards western India and adds information on its known distributional range.

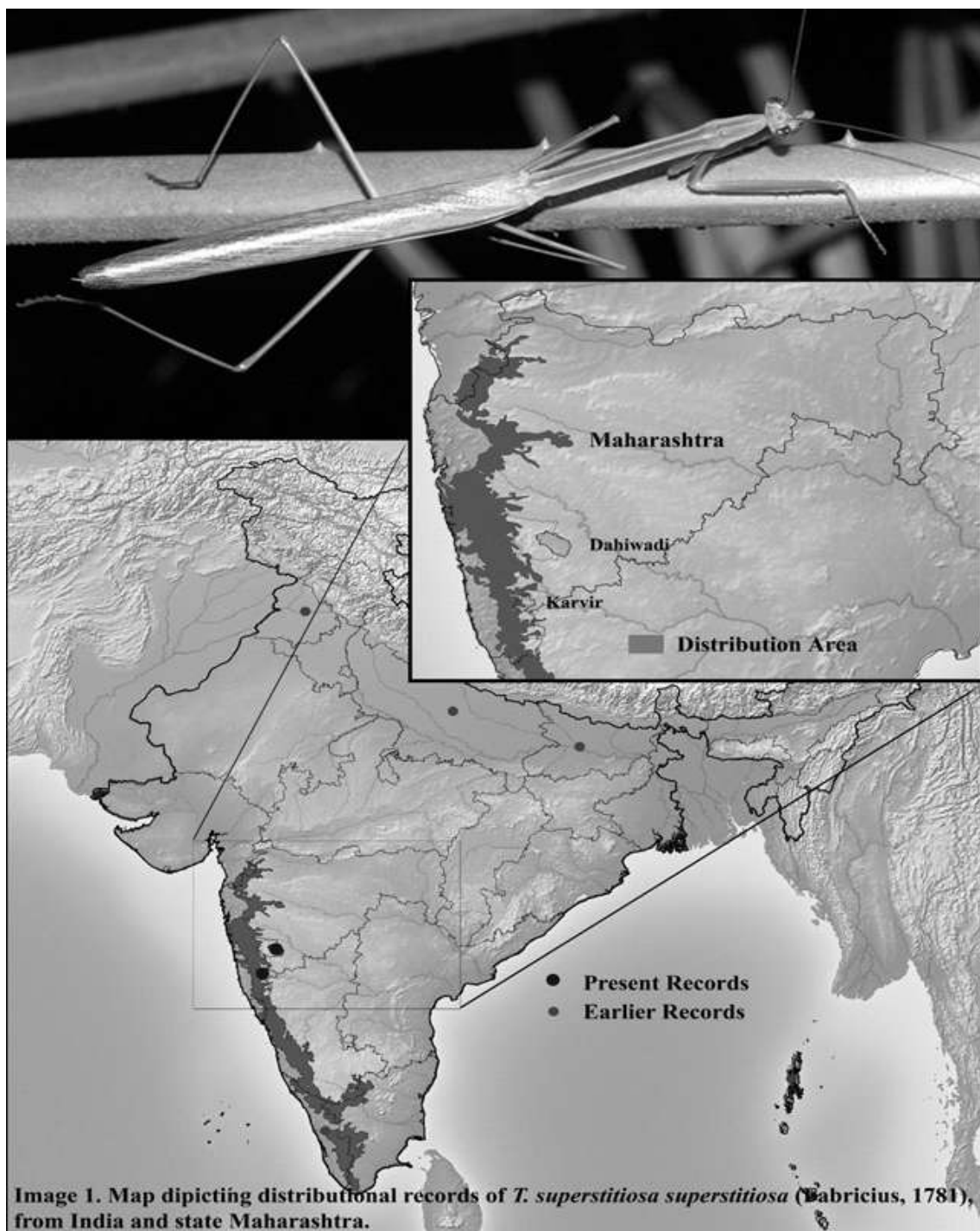
Due to limited literature on this species, misidentifications and confusion, *T. superstiosa superstiosa* is frequently reported as *T. fasciata*. However, present study will enable its correct identification and distribution pattern.

### Acknowledgements:

Authors are grateful to the Head, Department of Zoology, Shivaji University, Kolhapur, and the Principal, Radhabai Kale Mahila Mahavidyalay, Ahmednagar for providing necessary facilities and DST-FIST Phase-I for financial assistance for field and laboratory work. The authors are also thankful to Dr. Amrut Bhosale for continuous help for collection and also for technical support.

### References:

- Ghate, H. V., Jadhav, S. S. and R. M. Sharma. (2012). "*Insecta: Mantodea*". Fauna of Maharashtra State, State Fauna Series. Zoological Survey of India.
- Mukherjee, T. K., Hazra, A. K. and A. K. Ghosh. (1995). *Oriental Insects*. **29(1)**: 185.
- Mukherjee, T.K., Ehrmann, R. and P. Chatterjee. (2014). "*Checklist of Mantodea (Insecta) from India*". Priamus, Serial Publication of the Centre for Entomological Studies Ankara. (suppl.). **(30)**: 1-61.





## NUTRITIONAL STATUS OF BASIDIOMYCETOUS FUNGI ASSOCIATED WITH CASUARINA FROM TAMILNADU

<sup>1</sup>Kulkarni Sangita\* and <sup>2</sup>Kulkarni Abhijit

<sup>1</sup>Radhabai Kale Mahila Mahavidyalaya, Ahmednagar

<sup>2</sup>Department of Botany, Ahmednagar College, Ahmednagar

\*Corresponding Author: [sangitakulkarni69@gmail.com](mailto:sangitakulkarni69@gmail.com)

Communicated : 16.02.2020

Revision : 18.03.2020 & 22.4.2020

Accepted : 18.05.2020

Published: 30.05.2020

### ABSTRACT:

Present study dealt with study of nutritional status of Basidiomycetous fungi associated with Casuarina. During the investigation various carbon and nitrogen sources were used and the basidiomycetous fungi such as *Podaxis pistillaris* and *Clavaria* species were grown invitro. It was found that *Podaxis pistillaris* flourishes best with xylose and Raffinose sugars as carbon sources and sodium nitrate and sodium ammonium nitrate as nitrogen sources. *Clavaria* sp. grows best with the carbon sources like mannitol and maltose. Glutamine and sodium ammonium nitrate as nitrogen sources for the growth of *Clavaria*. The inorganic sources help in faster growth of fungus. The effect of growth is positive when the sources are used in combinations.

**Key words:** - *Podaxis pistillaris*, *Clavaria*

### INTRODUCTION:

*Casuarina*, a member of the family Casuarinaceae, is a native of Australia. They are successfully introduced in the east coast of Indian Peninsula in 1960s and then cultivated in all parts of the country. Species of *Casuarina* is planted on a large scale in different parts of our country where there is longer dry season and less water contents. Casuarinas are salt tolerant and adaptable to poor soils with least requirements for their growth. In South India they are grown on coastal areas with sandy soils as well as in interiors with loam soils. The *Casuarina* plantations are abundant along the seashores of Tamilnadu. The plant is a multipurpose tree in Agro-forestry. The tree gives diffused shade, improves physical and chemical properties of soil, suppresses the weeds, helps in maintaining the fertility of soil, used as food, fuel and fodder and acts as good wind breaker.

Fungi utilize dead plant tissues and the soluble substrates including root

exudates and develop themselves in rhizoplane and rhizosphere. Members of Ascomycetes and Basidiomycetes are reported to be present in rhizosphere. *Casuarina* plants from different localities were surveyed for Basidiomycetous fungi and their ectomycorrhizal association. During the study, *Podaxix pistilaris*, *Clavaria* sp., *Lycoperdon* sp., *Calvatia* sp. and some mushrooms were found associated with *Casuarina* plantations. These forms did not have any Ectomycorrhizal association with the plants.

Present investigation dealt with studies on Basidiomycetous fungi occurring in the rhizosphere of *Casuarina* from Tamilnadu and their nutritional requirements.

### MATERIAL AND METHODS:

In the present study the material of basidiomycetous fungi *Podaxix pistilaris*, *Clavaria* species associated with *Casuarina* was collected from sites of Chennai, Mahabalipuram and Trichur (Tamilnadu)

state). The species of *podaxis* and *Clavaria* were selected for nutritional studies. The work was undertaken in following steps:

1. Two fungi *Podaxis* and *Clavaria* were selected for study. The fungal spores were collected and grown in axenic cultures on Malt agar plates incubated at 27° C for 48 hours.
2. After the growth of hyphae, the hyphal mat was punched with the help of corn borer and used as a source of inoculum.
3. The inoculum was added to the agar plates with different nitrogen and carbon sources were inoculated at 27°C for 48 hours till 144 hours in diffused light conditions and recorded in tables ( Table – I & II).
4. The different nitrogen sources included Cysteine, Alanine, Glutamine, Sodium nitrate, Threonine, Ammonium oxalate, Sodium nitrate and Sodium ammonium nitrate which were added in the concentrations of 0.05% in the basal medium (Modified Pridham & Gottlieb medium ;1948).
5. Different carbon sources included were Sorbitol, Lactose, Xylose, Mannitol, Galactose, Maltose and Raffinose which were added in the concentrations of 3.5% in the basal medium.

#### OBSERVATIONS AND RESULTS:

Based on the nutritional requirements it is concluded that

1. *Podaxis pistillaris* flourishes best with xylose and Raffinose sugars as carbon sources and sodium nitrate and sodium ammonium nitrate as nitrogen sources.
2. *Clavaria* sp. grows best with the carbon sources like mannitol and

maltose as well as Glutamine and sodium ammonium nitrate as nitrogen sources.

3. The inorganic sources help in faster growth of fungus.
4. The effect of growth is positive when the sources are used in combinations.
5. Structurally the fungi belonged to gastromycetes group and the nutritional analysis indicated the use of inorganic nitrogen sources and disaccharides as carbon sources either single or in combination has helped in better growth of fungi.
6. The *Casuarina* plant litter and residue provides the inorganic sources of carbon and nitrogen for the growth of the fungi around them.

#### REFERENCES:

- Abhijit Kulkarni 1995. Thesis: Mycroflora associated with the roots of *Casuarina*.
- Brown G.D. 1984. Trees roots and the use of soil nutrients. In: Nutrition of plantation Forests (eds. G.D. Brown and S.K.S. Nambair) Academic press, London, pp. 147-167.
- Costas Theodorou and Paul Reddell. 1991. *In vitro* synthesis of ectomycorrhizas on Casuarinaceae with a range of mycorrhizal fungi. New Phytologist: Pp. 279-288.
- Garrett S.D. 1955. Microbial ecology of the soil. Trans. Brit. Mycol. Soc. 38 (1): 1-7.
- Nair L. N and V.P.Kaul 1984. Nutritional studies on *Pleurotus* I nitrogen and carbon J. Univ. Pune. Sci. Tech. 56: 99-104.
- Nair L.N. and Veena Ganju 1989. Nutritional studies on *Pleurotus* II – Growth regulators. Vegetos 2 (2) : 206-211.

**TABLE: I**A. Carbon nutrition studies - *Podaxis*

Diameter of colony in cms							
Hours	Sorbitol	Lactose	Xylose	Mannitol	Galactose	Maltose	Raffinose
48	1.0	1.8	2.7	1.0	2.0	2.8	2.4
72	1.9	3.0	3.5	3.0	2.1	3.2	3.4
96	1.9	3.0	4.5	4.0	2.8	3.9	4.0
120	2.0	3.9	5.8	5.5	3.0	3.9	5.0
144	2.3	4.1	6.5	5.5	3.8	4.1	5.9
Mean	1.8± 0.9	3.1±0.1	<b>4.6±0.9</b>	3.8±0.2	2.7±0.9	3.5±0.2	<b>4.1±0.1</b>
Type of growth	Scanty	Scanty	<b>Normal</b>	Moderate	Scanty	Scanty	<b>Normal</b>

B. Carbon nutrition studies - *Clavaria*

Diameter of colony in cms							
Hours	Sorbitol	Lactose	Xylose	Mannitol	Galactose	Maltose	Raffinose
48	2.0	3.4	2.5	2.5	2.0	4.4	1.9
72	2.7	4.4	4.2	4.6	3.6	5.7	3.5
96	3.0	5.6	5.3	7.5	5.2	7.5	3.5
120	3.4	6.3	5.7	8.4	7.0	8.8	3.7
144	4.0	6.8	6.0	9.3	7.2	10.0	4.0
Mean	3.0± 0.4	5.3±0.8	4.7±0.9	<b>6.4±0.1</b>	5.0±0.3	<b>7.2±0.1</b>	3.3±0.1
Type of growth	Scanty	Scanty	Scanty	<b>Normal</b>	Scanty	<b>Normal</b>	Scanty

**TABLE: II**A. Nitrogen nutrition studies - *Podaxis*

Diameter of colony in cms							
Hours	Cystiene	Alanine	Glutamine	Threonine	Amm. oxalate	Na nitrate	NaNH <sub>4</sub> nitrate
48	1.2	1.5	1.5	1.4	1.5	1.5	1.5
72	1.7	2.1	2.1	2.0	2.0	2.4	2.4
96	2.5	2.7	2.7	2.6	2.4	3.0	3.0
120	3.1	3.4	3.0	3.0	3.1	3.6	3.6
144	3.3	3.6	3.1	3.0	3.3	4.1	4.1
Mean	2.3± 0.9	2.6±0.1	2.4±0.1	2.4±0.1	2.4±0.1	<b>2.9±0.2</b>	<b>2.9±0.2</b>
Type of growth	Scanty	Scanty	Scanty	Scanty	Scanty	<b>Normal</b>	<b>Normal</b>

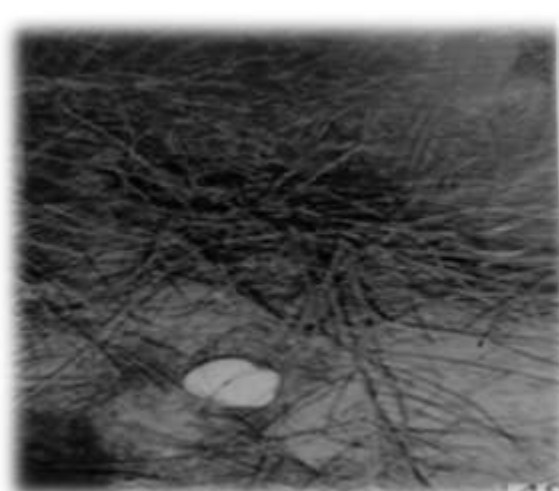


B. Nitrogen nutrition studies - *Clavaria*

Diameter of colony in cms							
Hours	Cystiene	Alanine	Glutamine	Threonine	Amm. Oxalate	Na nitrate	NaNH <sub>4</sub> nitrate
48	0.7	3.2	4.2	4.9	4.5	1.9	3.5
72	0.7	5.4	6.0	6.4	6.0	4.4	5.8
96	0.7	6.4	7.4	7.0	7.0	6.0	7.2
120	0.7	7.5	8.5	8.0	7.5	6.7	9.0
144	0.8	8.5	9.0	8.5	8.0	7.9	9.5
Mean	0.7± 0.2	6.2±0.1	<b>7.0±0.2</b>	6.9±0.8	6.8±0.2	5.3±0.2	<b>7.0±0.2</b>
Type of growth	Scanty	Moderate	<b>Normal</b>	Moderate	Moderate	Scanty	<b>Normal</b>



*Podaxis pistillaris*



*Clavaria sp.*



## Online Teaching and Learning: Threat or Opporurtity

Dr. Raviprakash. D. Thombre

Head, Department of Geography Radhabai Kale Mahila Mahavidyalaya,  
Ahmednagar,(Maharashtra)

### Abstract

We are seeing education institutions adapting these developments into their systems And relying on group resources and mechanisms to improve the student life. The use of social media in education provides students with the ability to get more useful information, to connect with learning groups and other educational systems that make education convenient.

**Key Words:Online Teaching Threat, opportunity.**

### Introduction:

Social network tools afford students and institutions with multiple opportunities to improve learning methods. Through these networks, you can incorporate social media plugins that enable sharing and interaction. Students can benefit from online tutorials and resources that are shared through social networks and LMS's. There is valuable knowledge to be gained through social media such as analytics and insights on various topics or issues for study purposes.

Connecting with experts on topics via social media

The great thing about using social media is that you soon learn who the experts are in particular fields and subjects. When you start following these experts you learn more and gain useful content from them, this empowers you to produce great results. Social media has the ability to broaden your perspective on various subjects and gives illuminating, instant content that is new. You have the opportunity of engaging experts to get answers on topics that you may need help in. Institutions communicate with students via YouTube and Facebook

Learning colleges have the ability to connect with students through social media networks such as Facebook, Google Plus groups, and YouTube. These channels can be used to communicate campus news, make announcements and provide students with useful information. This builds engagement between the College and students which help tackle many student issues through the group interactions.

### It helps in Research process

Social media offers audience and subject monitoring tools that are useful and it is one of the best platforms to extract data. You can find out how the majority people feel about a particular topic or how experts perceive and advice on specific issues.

### Positive effects of Social Media:

Encourage Online Learning: With the advance use of Social Media platforms in boarding school Dehradun, the students get encouraged and motivated to learn. Educational videos on YouTube, The use of YouTube to watch educational videos, easy access to e-books, online notes, learning via video calling are some of the major aspects which contribute to educational development.





# तिफण

वर्ष : ११ वे अंक : २ रा व ३ रा  
जुलै ते डिसेंबर - २०२०

लोककला विशेषांक

साहित्य, कला आणि लोकसंस्कृतीला वाहिलेले त्रैमासिक

# तिफण

वर्ष अकरावे, अंक- २रा व ३रा, जुलै-डिसेंबर २०२० (जोडअंक)

UGC Care Listed Journal

ISSN 2231 - 573X

- संपादक -

डॉ. शिवाजी हुसे

पत्ता : संपादक, तिफण, 'शिवार', श्रीराम कॉलनी,  
हिवरखेडा रोड, कन्नड, जि. औरंगाबाद - ४३११०३,

मोबा. ९४०४०००३९८



## अनुक्रमणिका

अ.क्र.	शीर्षक / लेखक	पृ.क्र.
*	लोककला विशेषांकाच्या निमित्ताने... - डॉ. शिवाजी हुसे	
*	संपादकीय - प्रा. डॉ. चंद्रशेखर कणसे (अतिथी संपादक)	
१.	'कीर्तन' समाजप्रबोधनाचे प्रभावी माध्यम: एक अभ्यास - डॉ. चंद्रशेखर कणसे (परळी वैजनाथ, बीड)	९
२.	महाराष्ट्रातील लोककला : कीर्तन - प्रा. डॉ. सोमनाथ महादेव दडस (दापोडी, पुणे)	१८
३.	वारकरी दिंडी लोककला : एक आनंदयात्रा - धन्यकुमार प्रल्हाद तारळकर (ता. फलटण जि. सातारा)	२४
४.	'सोंगी भारूडी भजन' - डॉ. आनंद बल्लाळ (आजरा, कोल्हापूर)	३२
५.	प्रयोगात्मक लोककलाप्रकार - 'भारूड' - डॉ. नाना झगडे (पुरंदर)	३९
६.	विदर्भातील झाडीपट्टी येथील लोककला 'दंडार' - प्रा. अमृता डोरलीकर (नागपूर)	४७
७.	महाराष्ट्रातील लोककला 'बोहडा' - डॉ. भास्कर शेळके (अकोले)	५२
८.	गोमंतकीय लोककला : विशेष संदर्भ 'धालोत्सव' - डॉ. नीता तोरणे (पेडणे, गोवा)	५५
९.	'गोंधळ : स्वरूप आणि आविष्कार' - डॉ. पांडुरंग भोसले (हडपसर, पुणे)	६७
१०.	महाराष्ट्रातील लोककला : 'गोंधळ' - डॉ. पद्माकर तामगाडगे (मुंबई) व प्रा. राजू शनवार (ठाणे)	७१
११.	महाराष्ट्राचे विधिनाट्य 'गोंधळ' आणि 'जांभूळ आख्यान' - प्रा. शिल्पा नेवे (मुंबई)	७५
१२.	'गोंधळ' कला प्रकाराचे बदलते स्वरूप - डॉ. जयदेवी पनार (बाभळगाव, ता. जि. लातूर)	८९
१३.	गोंधळ : महाराष्ट्राची लोककला - डॉ. वैशाली श्रीकृष्ण भालसिंग (अहमदनगर)	९५



१४. 'जागरण' - डॉ. राखी सलगर (औरंगाबाद) १०२
१५. गोवा येथील लोककला 'जागर' - प्रा. विनय मडगांवकर (गोवा) १०६
१६. महाराष्ट्रातील लोककला : 'दशावतार व नमन' - प्रा. प्रियंका कुंभार (तासगाव, जि. सांगली) ११४
१७. महाराष्ट्रातील लोकनाट्याचा आविष्कार - 'लळीत' - प्रा. पुरुषोत्तम महाजन (भुसावळ) १२१
१८. 'लळीत' - डॉ. प्रतिभा सोनी (शिक्रापूर, शिरूर) १२८
१९. सर्वाना एकत्र बांधून ठेवणारा सांस्कृतिक ठेवा - 'भोंडला' - प्रा. तारळेकर (सांगली) १३३
२०. 'लोककला तमाशा' - एक अभ्यास - प्रा. डॉ. रामहारी मायकर (वडवणी जि. बीड) १३८
२१. 'लोकरंगभूमीवरील डाका विधीनाट्य' - डॉ. सुनिल टाक (औरंगाबाद) १४३
२२. 'लोकसाहित्यातील लोककला प्रकार' - डॉ. भाऊसाहेब गव्हाणे (केडगाव, ता. दौंड, जि. पुणे) १४८
२३. लोककला : स्वरूप व वाटचाल - प्रा. डॉ. विजय विष्णूपंत केसकर (कळंब, जि. उस्मानाबाद) १५५
२४. 'महाराष्ट्रातील लोककला : एक चिंतन' - कु. वर्षा तांदळे (कोल्हापूर) व प्रा. बाळासाहेब चव्हाण (कोरेगाव) १६०
२५. आदिवाशी यांच्या लोककला - प्रा. चिंतामण धिंदळे (नगर) १६५
२६. महाराष्ट्रामधील आदिवाशी लोककलांचे विवेचन - डॉ. सुनिल घनकुटे (अकोले जि. नगर) १७१
२७. महाराष्ट्र लोकसंस्कृती उपासकांचे कलाविष्कार : वासुदेव आणि पोतराज - डॉ. किरण नामदेव पिंगळे (नाशिक) १७८
२८. लोकसंस्कृतीचे लोककलेतून सहज सुंदर आविष्कार घडविणारा 'वासुदेव' - डॉ. नानासाहेब पवार (हडपसर, पुणे) १८४
२९. पोतराजाची आराधना : एक लोककला - डॉ. नितीन मोटे (वडगाव, पुणे) १९४
३०. महाराष्ट्राच्या लोककलेचा सहजसुंदर आविष्कार - लावणी - डॉ. धबडगे (औरंगाबाद) २००

# महाराष्ट्रातील आदिवासींच्या लोककला

- प्रा. चिंतामण धिंदळे

(मराठी विभागप्रमुख)

राधाबाई काळे महिला महाविद्यालय, अहमदनगर

प्रस्तावना :-

भारतीय आदिवासी हा स्वातंत्र्योत्तर काळात अनेकांच्या आकर्षणाचा विषय झाला होता. उदा. भारतात येणारे हौसी पर्यटक आदिवासी क्षेत्राला आवर्जून भेट देत. आदिवासी लोककलांच्या महोत्सवी कार्यक्रमात हौशी पर्यटकांची उपस्थिती लक्षणीय प्रमाणात वाढत असल्याचे दिसून येते. महाराष्ट्रात जवळजवळ ४७ आदिवासी जमाती आहेत. प्रत्येक आदिवासी जमातीचा अभ्यास करता, त्यांची संस्कृती, वेगळी असल्याचे जाणवते. त्यांची बोलीभाषा, सण-उत्सव, लग्न समारंभ पद्धतीमध्ये साम्य आढळत असले तरी, ते वेगळे आहेत. आदिवासींच्या जीवनातील समान गुणधर्म जर काय असेल तर तो प्रत्येक आदिवासी जमाती या निसर्गपूजक आहेत. निसर्गालाच त्या देव मानतात. निसर्गाच्या सानिध्यात ते आपले जीवन जगत असतात. आयुष्यभर काबाडकष्टाचे जीवन वाट्याला आलेला आदिवासी माणूस लोककलांच्या माध्यमातून आपल्या जीवनात विरंगुळा शोधत असतो. जवळपास प्रत्येक जमातीची एक स्वतंत्र लोककला आज अस्तित्वात आहे. कलेच्या माध्यमातून ते आपल्या समाजाची संस्कृती दुसऱ्या समाजासमोर मांडण्याचा प्रयत्न करतांना दिसतात. नृत्य, गाणे, वाद्य, अशा प्रमुख कलांबरोबरच तमाशा, वगनाट्य, भारूड, दशावतार, बोहाडा, जत्रा अशा माध्यमातून ते आपल्या उपजत कलागुणांना वाव देताना दिसतात. काळाच्या ओघात बहुतांशी जमातींच्या कला कालबाह्य होण्याच्या मार्गावर आहेत. शासन दरबारी ह्या कला संवर्धन करण्याचे जोरदार प्रयत्न चालू आहेत. मात्र औपचारिकपणामुळे त्यात यश येताना दिसत नाही. साक्षरता वाढली पण आपली उपजत कला मात्र हा समाज विसरत चालला आहे. तरूण पिढीला ह्या कलांविषयी फारशी आस्था नाही. एकूणच काय तर या कला जतन करायला हव्यात. या कलांचे संवर्धन व्हायला हवे. सरकारी दरबारी असणारी उदासीनता दूर व्हायला हवी. आदिम संस्कृती नष्ट होऊ पाहात आहे. लोककलांच्या माध्यमातून आदिवासी संस्कृती टिकविणे आज काळाची गरज आहे. आदिवासींच्या लोककला म्हणजे पांढरपेशीय समाजाच्या मनोरंजनाचा उपक्रम नव्हे तर त्यांच्या कला त्यांच्या जगण्याचा मूलाधार व्हावा ही संकल्पना त्यांच्या ठायी रुजवणे काळाची गरज आहे.



## आदिवासी संकल्पना :-

आदिवासीबाबत विविध अभ्यासकानी, संशोधकांनी विविध व्याख्या मांडल्याचे दिसते. त्या व्याख्यांच्या अनुषंगाने आपल्याला आदिवासी म्हणजे काय, व त्याविषयीची संकल्पना स्पष्ट करता येईल. डॉ. धुये यांनी आदिवासींना 'मागासलेले हिंदू' असे संबोधले आहे. काही अभ्यासक आदिवासी हे मुळचे रहिवासी आहेत असे मानतात. आंतरराष्ट्रीय श्रम संघटनेने कोणत्याही देशातील मूळ रहिवाश्यांना संबोधण्यासाठी आदिवासी ही संज्ञा वापरावी असे म्हटले आहे. अजून काही अभ्यासकांनी विविध व्यापाराच्या द्वारे आदिवासी संकल्पना स्पष्ट केल्या आहेत.

१. **बोआम :-** यांच्या मते जगात म्हणजे आर्थिकदृष्ट्या असा स्वातंत्र लोकसमूह की जो एक भाषा बोलतो व बाह्य आक्रमणापासून स्वताःचे संरक्षण करण्यासाठी संघटीत झालेला असतो.
२. **गिलीन व गिलीन :-** यांचे मते एका विशिष्ट भूप्रदेशावर राहणारा, समान बोली भाषा बोलणारा व समान सांस्कृतिक जीवन जगणारा पण अक्षर ओळख नसलेल्या स्थानीय समूहाला आदिवासी समाज असे म्हणतात.
३. **डॉ. मुजुमदार :-** यांच्या मते आदिवासी समुदाय म्हणजे नातेदारीने संबंधित असणाऱ्या अनेक कुटूंबांचा असा समुच्चय होय की ज्याचे एक सामान्य नाव व समान भाषा असते. हा समुदाय एका विशिष्ट भूप्रदेशावर वसलेला असतो. तसेच या समुदायाला सभासद विवाह व व्यवसायाबद्दल समान नियमांचे पालन करतात.
४. १९६२ साली शिलाँगमध्ये आदिवासी समितीच्या परिषदेने आदिवासी समुदायाची व्याख्या पुढीलप्रमाणे केली आहे. 'आदिवासी समुदाय हा एकाच पूर्वजापासून उत्पत्ती सांगणारा असा एक सजातीय गट आहे की, ज्यातील सभासद एक भाषा किंवा बोली बोलतात. त्यांचे एका विशिष्ट भूप्रदेशात वास्तव्य असते. हे लोक विज्ञान व तंत्रज्ञानाच्या दृष्टीने मागासलेले असतात. अक्षर ओळख नसलेल्या व रक्तसंबंधावर आधारित सामाजिक व राजकीय रीतिरिवाजांचे प्रामाणिक पालन करणाऱ्या एकजिनसी गटाला आदिवासी समुदाय असे म्हणतात.'

आदिवासी जमात, आदिवासी समाज, आदिवासी समुदाय अशा संज्ञांच्याव्याख्या विचारवंतानी केल्या आहेत. या सर्व व्याख्यामधून आदिवासी जमात या शब्दाचा अर्थ स्पष्ट करण्याचा प्रयत्न केला आहे. एकूणच आदिवासी समाज ह्या भूमीवरचा प्रथम समाज आहे, असा निकष लावता येऊ शकेल. कोणत्याही देशाचा मूळ रहिवाशी आदिवासी समाज असा अर्थ लावता येऊ शकेल.

## महाराष्ट्रातील आदिवासी जमाती:-

महाराष्ट्रात आजमितीस जवळ-जवळ ४५ आदिवासी जमाती आहेत. सह्याद्री, सातपुडा, ब्रह्मगिरी, भीमाशंकर, महादेवाच्या टेकड्या या डोंगररांगाच्या पायथ्याशी आदिवासी जमातींची वस्ती आढळून येते. औद्योगिकरणाचापरिणाम त्यांच्या जीवनरहाटीवर पडलेला दिसून येतो. डोंगरदऱ्यातून वस्ती करून राहणाऱ्या या जमाती आता सपाट प्रदेशात, शहराच्या जवळ यायला लागल्या आहेत. शिक्षणाचा झालेला प्रसार आणि प्रचार यामुळे आदिवासी समाज शिकून नोकरी व्यवसायानिमित्त, रोजगाराच्या शोधात शहरात राहू लागला आहे. आदिवासी जमातींची नावे भिन्न अशी आहेत. उदा. गोंड, भिल्ल, कोलम, कोरकू, माडिया, अंध, इत्यादी. आदिवासींच्या वसतीस्थानाचा विचार करता उदा. कोळी महादेव, ठाकर ह्या जमाती पुणे, अहमदनगर, ठाणे, रायगड, नाशिक या जिल्यात आढळतात. कोरकू, वापेची, भावासी, वापी व निहाल ह्या जमाती अमरावती जिल्यातील मेळघाट भागातच आढळून येतात. थोडक्यात आदिवासी जमातींची विशिष्ट भाषा, प्रदेश, चालीरीती-रिवाज, संस्कृती असे वेगळेपण आपणास जाणवते. आदिवासी जमातींचा मुख्य व्यवसाय शेती करणे व त्याबरोबरच पशुपालन हा पूरक व्यवसाय करणाऱ्या काही आदिवासी जमाती आहेत. तर अजूनही बहुतांशी जमाती या जंगल व त्यातून मिळणारे वनउपज, मजुरी, यावर अवलंबून आहेत. पूर्वी शेती व्यवसायाकडे वळण्याअगोदर जंगलात जाऊन शिकार करणे, जंगलातील सरपण, फळे, हिरडा, बेहडा, गोळा करून आपला उदरनिर्वाह करित असत. शिक्षणाने समाज बदला व सुधारित तशीच पारंपारिक शेती करणे, गुरे पाळणे, शहरात जाऊन रोजगार मिळविणे, नोकरी, व्यवसाय करणे, हा बदल झाल्याचे दिसते.

आर्थिकदृष्ट्या मागास असलेला हा समाज मात्र सांस्कृतिकदृष्ट्या संपन्न आहे. निसर्गाला देव मानणारा, निसर्गाच्या नियमांप्रमाणे जीवन जगणारा हा समाज आपल्या कला-गुणांसाठी प्रसिद्ध आहे. जवळ-जवळ सर्वच आदिवासी जमातीमध्ये काहीना काही कला ह्या उपजतच असतात. त्यांच्या विवाहप्रसंगी, शेतीच्या कामाच्या वेळी, कामे संपल्यावर रिकाम्यावेळी मनाला विरंगुळा मिळावा, श्रम कमी व्हावेत म्हणून नाच-गाण्यांचा कार्यक्रम हमखास होत असतो. लग्नविधी, जत्रा विशेषतः सामुदायिक कार्यक्रमात स्त्रियांची नृत्ये होतात, प्रत्येक आदिवासी जमातीत अशाप्रकारची नृत्ये होत असतात. मात्र स्त्रियांच्या नृत्याला विशेष महत्त्व असते. आदिवासींचा भूप्रदेश हा शहरापासून दूर असल्याने नागर संस्कृतीचे विशेष अजूनही त्यांच्यापर्यंत पोहचले नाहीत, थोड्याफार प्रमाणात शहरातील संस्कृती आज आदिवासी समाजाची झाल्याचे दिसते. परंतु सगळ्या आदिवासी जमाती आपल्या पारंपारिक लोककला जतन करून आहेत. देशातील इतर राज्यांचा विचार करता



ज्या ठिकाणी आदिवासी समूह आहे, त्यांची आजची स्थिती पाहता महाराष्ट्र, पूर्वांचल, दक्षिण भारत या राज्यातील आदिवासी जमाती मुख्य प्रवाहामध्ये आल्या आहेत. मात्र मध्यप्रदेश, छत्तीसगड, गुजरात, हिमाचलप्रदेश, ओरिसा, प. बंगाल, तेलंगाना, बिहार, झारखंड या राज्यातील आदिवासींची स्थिती वाईट आहे. राज्यस्थान मधील मीना नावाच्या जमातीचा जितका विकास झालेला दिसतो तितका विकास इतर जमातींचा झालेला नाही.

### आदिवासींच्या लोककलाः -

आदिवासी समाज म्हटला की कला ही आलीच. कारण आदिवासींचे जगणे कलेशिवाय अधुरे आहे. लोकलेमधून आदिवासींची जीवनरहाटी, संस्कृती व एकूणच जगण्याचा आशय त्यातून व्यक्त होत असतो. उदा. नृत्य, वाद्य, गायन, चित्रकला, विणकाम इ. कला आढळून येतात. त्यातही 'नृत्य' ही लोककला सर्वच आदिवासी जमातीमध्ये आढळून येते. उदा. ठाकर जमातीचा कांबडनाच, ठाकर स्त्रियांची 'फुगडी' ह्या कला इतर जमातीत दिसून येत नाहीत. फुगडी हा नाच सर्वच जमातीत असला तरी ठाकर स्त्रिया फुगडी बसून घालतात, बाकी जमातीच्या स्त्रिया फुगडी उभ्याने खेळतात. कोळी महादेव जमातीत 'घेवडा' व 'वरमाई' हे दोन नाच प्रमुख आहेत. वाध्यांचा विचार करता पावा, बासरी, ढोल, ढोलकी, झांज, इत्यादी वाद्यंचा समावेश होतो. सर्वच आदिवासी जमातींना गायनाची कला अवगत असते. किंबहुना ती कला त्यांना निसर्गतःच मिळालेली देणगी आहे. चित्रकलेचा विचार करता वारली चित्रकला जगप्रसिद्ध म्हणून मान्यता पावली आहे. विणकाम ही कला सर्वच आदिवासी जमातींना अवगत असते. जंगलात मिळणाऱ्या बांबूपासून गृह उपयोगी वस्तू ते बनवित असतात. उदा. टोपल्या, कुरकुले, हारा, किरकिंडा, कणगा, कणगी, काठवळा, मळई, बोक्सी, सुपाट, इरले, चटया जवळजवळ सर्व उपयोगी वस्तू ते घरच्या घरी बनवितात. मासेमारीसाठी बऱ्याच वस्तू बनवितात. ससे मारण्यासाठी वाघुर बनवितात. एकूणच आदिवासी जमातीमध्ये कलेचा वारसा दिसून येतो. आदिवासींच्या कला ह्या केवळ कला नसून त्या उपयोजित कला म्हणून त्यांचा विचार व्हायला हवा.

१. आदिवासी नृत्य :- महाराष्ट्रामध्ये एकूण ४७ आदिवासी जमाती आहेत. प्रत्येक आदिवासी जमातीचा एक वेगळा नृत्य प्रकार आहे. नाच संस्कृती आदिवासींची आहे. त्यांच्या नाच संस्कृतीनेच त्यांचे जीवन समृद्ध केले आहे. आनंदाच्या प्रसंगी हा समाज एकत्र येतो आणि बेधुंद रात्रभर नाचतो. नाचताना सर्व दुःख विसरून नाचतो. निसर्गाच्या साथीने, निसर्गाच्या संगतीने तो नृत्य करित असतो. सह्याद्रीच्या पायथ्याशी व कोकणात 'ठाकर' नावाची जमात वास्तव्य करून राहते. ठाकर आदिवासींमध्ये 'कांबड' नाच विशेष प्रसिद्ध आहे. दहा ते पंधरा पुरुष मंडळी एकत्र येतात, मोठे (कोंडोळे) रिंगण केले जाते,



मध्येढोल वाजवणारा एक ढोल्या असतो. त्याच्या समोर ढोलाला पकडून राहणारा एक व गाणे म्हणणारा असा हा कांबड नाच सुरु होतो. शेतीची कामे आटोपल्यावर रात्री चांदण्यात ही मंडळी एकत्र जमते व कांबड नाच सुरु होतो. वेशभूषा अशी विशेष नसते मुळातच अंगभर कपडे नसणारा हा समाज डोक्याला मुंडास, अंगात कोपरी, किंवा बंडी पायात मात्र चाळ (धुंगरू), हाताला (मनगटाला) फुलांचा गजरा बांधून आपला नाच सुरु करतात. त्यांच्या गीतात उत्साह असतो. नाचणे हा त्यांचा छंद आहे. बेफाम होऊन नाचणे, त्यांचा हा नाच रांगडा आहे, वेगात नाचले जाते. म्होरक्या मध्येच शिळ घालून इशारे करतो, कुठे मुरडायचे, वळायचे कुठे, कुठे आवाज काढून नाचायचे हे ठरलेले असते. मर्दानी अशा नाचातून ठाकरांचा चपळपणा, काटकपना जाणवतो. ज्या पद्धतीने पुरुष मंडळी कांबडा नाच सादर करतात, त्याचप्रमाणे स्त्रिया सुद्धा फुगडी नाच सादर करतात. १० ते १५ स्त्रिया रिंगण करून गोलाकार उभ्या राहतात. कधी पायाच्या चवड्यावर बसून गाणी म्हणत फुगडी नाच करतात. या नृत्यात तरून मुली, वृद्ध स्त्रिया, मध्यम वयाच्या स्त्रिया नाचत सहभागी होतात. या नाचासाठी कोणत्याही वाद्याची गरज नसते. टाळ्यांच्या तालावर गाणी म्हणत फुगडी नाच सादर केला जातो.

**२. आदिवासी कोळी महादेव जमातीचा घेवडानृत्य :-** कोळी महादेव ही जमात महाराष्ट्रातील सहा जिल्यात वास्तव्य करून राहत आहे. पुणे, अहमदनगर, नाशिक, ठाणे, रायगड, पालघरसह्याद्रीच्या कुशीत व कोकणच्या पायथ्याशी राहणारी ही जमात शेती, पशुपालन, मजुरी करून आपला उदरनिर्वाह करतांना दिसते आहे. जागतिकीकरणात बहुतांशी शिकलेला तरुण शहरात नोकरी, रोजगारानिमित्त गेला आहे. कोळी महादेव या जमातीची एक वेगळी अशी बोली प्रचलित आहे. त्या बोलीस 'डांगणी' व 'मावळी' बोली असे संबोधले जाते. पुणे जिल्यात 'मावळी' बोली म्हणून प्रसिद्ध आहे. तर अहमदनगर, नाशिक जिल्ह्यात 'डांगानि' बोली म्हणून प्रसिद्ध आहे. या जमातीचे दोन नृत्य प्रसिद्ध आहेत. ती दोन्ही नृत्य लग्ना प्रसंगी नाचली जातात. एक आहे 'वरमाई' नृत्य व दुसरे आहे 'घेवडा' नृत्य. हळदीच्या दिवशी आदिवासी स्त्रिया वरमाई नृत्य नाचतात. वाजंत्री वाजवितात, व या स्त्रिया हातात आहेर घेऊन नाचविण्याच्या नृत्यला वरमाई नृत्य म्हणतात. वरातीच्या रात्री नवऱ्या मुलीला व नवऱ्या मुलाला कडेवर घेऊन दोन पुरुष वाजंत्र वाजवतील त्या तालावर वधु-वराला नाचविले जाते. त्या नृत्याला 'घेवडा' नृत्य म्हणतात. नवरा. नवरीच्या हातात, कपड्याचे चाबूक तयार करून दिले जातात. त्या चाबकाने एकमेकाला मारण्याचा कार्यक्रम होत असतो. अतिशय गमतीशीर हे नृत्य असते. प्रत्येक आदिवासी जमातीचे असे स्वतंत्र बोली व नृत्य असते.

आदिवासी जमाती त्यांच्या कलांनी ओळखल्या जातात. आदिवासी संस्कृती ही

अतिशय समृद्ध आहे. त्यांच्या लोककलांमधून त्यांचे जीवन, संस्कृतीचे दर्शन होत असते. या लेखामध्ये आदिवासी ठाकर व कोळी महादेव या जमातीच्या लोककलांचा परिचय करून देण्याचा प्रयत्न केला आहे.

**मूलभूत संदर्भ :-**

अकोले तालुक्यातील 'चाळीसगाव डांगण' आंबेगाव तालुक्यातील 'घोडनयार' जुन्नर तालुक्यातील 'कुकडेनयार' इगतपुरी तालुक्यातील 'महालदेश' मूळनयार, पेहरा, या प्रदेशातील आदिवासी जमातीच्या लोककलांचा अभ्यास करून वरील नोंदी केल्या आहेत.

\* \* \* \* \*



आदिवासी साहित्य, संस्कृती आणि अस्मितेचे प्रतीक

ISSN 2319-6033



१५ मार्च ते नोव्हेंबर २०२०  
वर्ष १३ वे, अंक ४ ते १२  
पृष्ठे ४०, किंमत रु.४०/-



# फडकी

(मासिक)



संपादक- डॉ. मारुती आढळ । देवराज आढळ



- मुख्य संपादक : डॉ. संजय लोहकरे
- सहसंपादक : प्रा. डॉ. तुकाराम रोंगटे  
डॉ. मारुती आढळ
- उपसंपादक : डॉ. सोनू लांडे  
मधुचंद्र भुसारे
- कार्यकारी संपादक : मा. संजय इंदे  
डॉ. सुनील घनकुटे

- प्रसिद्धी  
देवराम आढळ सुनील फलके  
पंकज इरनक प्रा. रामदास गिळंदे

- संपादक मंडळ  
कृष्णा साबळे तुकाराम धांडे  
देवदत्त चौधरी कैलास धिंदळे  
अभिजित करवंदे राहूल शेंगाळ  
डॉ. कुंडलिक पारधी सीता भोजने  
रोहिदास डगळे मेजर विठ्ठल बांगर

- अक्षर जुळवणी  
संजय रा. महल्ले  
मेधा पब्लिशिंग हाऊस  
'अक्षरवेल', नरसम्मा कॉलेजजवळ  
किरणनगर, अमरावती ४४४६०६ (महाराष्ट्र)  
मोबा. ९४२३६२२६६७  
E-mail-medhaphouse@gmail.com

- प्रकाशन स्थळ/पत्र व्यवहार  
संपादक - डॉ. संजय यशवंत लोहकरे  
निरगुडेवाडी (विठे) ४२२ ६०४  
ता. अकोले जि. अहमदनगर  
मोबा. 09657549076, 9404979683  
E-mail-phadki@rediffmail.com

- मूल्य : रु. ४०/-

(मासिकातील लेखांशी संपादक सहमत असेलच असे नाही.)

## \* अनुक्रमणिका \*

- \* कोरोना काळी भुकेचे बळी-तुकाराम चौधरी
- \* कोरोनाविषयी आदिवासींची धारणा -श्री. संजय घोरपडे ३
- \* सिंदीचा काला-प्रा. चिंतामण धिंदळे ११
- \* प्रतिकारशक्ती वाढवा, आरोग्य जपा -वाहरु सोनवणे ११
- \* कोरोना प्रादुर्भावामुळे जव्हार तालुक्यातील आदिवासींच्या  
जीवनावर झालेला परिणाम -प्रा. राजू शंकर शनवार २१
- \* वाडीतला कोरोना- कैलास धिंदळे २३
- \* समाजाचा दुष्मन- मारुती कोंडू आढळ २५
- कविता \* कोरोना म्हणत्यात मला-प्रशांत गायकवाड ८/काळजी  
घ्या-श्वेता आवारी १४/कोरोना आला विमानात बसून-वाहरु  
सोनवणे २०/संवसार मूडी पडणा-प्रमोद (पोम्या) कांदीलाल  
बागूल ३१/मजबूर मी मजदूर-संजय इंधे ३२/हिदगी ज आगोही  
(डांगी भाषेत)-भावेश बागूल ३२/भरलंय कोरोनाचं वारं-देवदत्त  
चौधरी ३३/चल ना वं आये, घरला आता -संजय दोबाडे ३३/  
गर्दी करणं टाळ-पंकजकुमार गवळी ३४/कोरोनाचे वारे-  
वैजनाथ अनमुलवाड ३४/चला हरवुया या कोरोनाला- देवदत्त  
चौधरी ३५/डॅंगन मामा-वैजनाथ अनमुलवाड ३५/आला आला  
कोरोना-किरण निरवार ३६/नाव माझे मयत नोंदल्यावर-किशोर  
डोके ३६/पायपीट-विठ्ठल निरवारे ३७/पसरू देवू नका कोरोना-  
रोशनी आवारी ३७/विषाणू- कोरोना-सोनाली डगळे ३७/  
लॉकडाऊन काळातील आदिवासी हायकू -मधुचंद्र भुसारे ३८

## वर्गणीचे दर

वार्षिक : 300 रु., दशवार्षिक : 2500 रु.

आजीव : 5000 रु.

संपादकीय पत्त्यावर मनी ऑर्डर, चेक  
किंवा डिमांड ड्राफ्टने वर्गणी पाठवावी  
'फडकी' या नावाने चेक/डिमांड ड्राफ्ट असावा.  
बँक ट्रान्सफरने वर्गणी भरण्यासाठी तपशील  
बँक ऑफ महाराष्ट्र शाखा, अकोले जि. अहमदनगर  
'फडकी' या नावाने बचत खाते  
क्र. 60307966854  
IFSC Code : MAHB 0001641  
MICR No. : 422014502

ISSN 2319-6033



## सिंदीचा काला

प्रा.चिंतामण धिंदळे (मराठी विभाग प्रमुख)

राधाबाई काळे महिला महाविद्यालय, अहमदनगर

मो. ८१०४४८४४६५

‘कोरोना’ म्हणजे ‘कोविड-१९’ या नव्या रोगाची लागण प्रथम चीनमधील ‘वुहान’ या शहरात झाल्याचे निदर्शनास आले. ‘कोरोना’ हा संसर्गजन्य आजार चीनमध्ये फोफावला. वुहान शहरात जवळजवळ ९०% लोकांना ‘कोरोनाची’ बाधा झाल्याचे जगासमोर आले. आजमीतीस कोरोनामुळे चीनमध्ये ४५०० च्या वर लोकांचा बळी गेल्याचा आकडा समोर आला आहे. डिसेंबर २०१९ ते मार्च २०२० पर्यंत हा आजार हळूहळू कमी झाल्याचे चीनने नमूद केले आहे. असे असले तरी मे २०२० ला पुन्हा काही रुग्ण आढळल्याचा दावा चीनने केला आहे. चीनमधून तो आजार थेट युरोप, अमेरिका, इराक, इराण व संपूर्ण जगभर आज कोरोनाचे ३५ लाख रुग्ण आहेत. संपूर्ण जगभर २ लाखाच्यावर मृतांचा आकडा पोहोचला आहे. इटली, स्पेन, अमेरिका सारख्या देशाने तर अक्षरशः हात टेकले आहेत. सध्यःस्थित एकट्या अमेरिकेत ९० हजार व्यक्तींचे बळी गेले आहेत. साधारणतः फेब्रुवारीच्या शेवटच्या आठवड्यात ‘कोरोना’ भारतात दाखल झाला. पहिला रुग्ण केरळमध्ये सापडल्याची नोंद आहे. आजच्या तारखेला भारतात कोरोनाग्रस्तांची संख्या ९८ हजारावर गेली आहे. मृतांचा आकडा कमी असला तरी, बाधितांची संख्या दर २४ तासाला ५००० ते ५२०० अशा पटीने वाढते आहे. बऱ्या होणाऱ्या रुग्णांचा दर ३८.१२% च्या आसपास आहे.

‘कोरोना’ या आजाराची लक्षणे उशिरा दिसत असल्याने संसर्ग झालेल्या व्यक्तीला किमान १४ दिवसानी रोगाची लक्षणे जाणवू लागतात. झपाट्याने वाढणारा हा संसर्ग भारतातील सर्वच राज्यात दाखल झाला आहे. त्यातही महाराष्ट्रात बाधितांची संख्या ३६ हजारांवर जाऊन पोहोचली आहे. देशातील सर्वात गर्दीची शहरे मुंबई, ठाणे, पुणे, नागपूर, नाशिक (मालेगाव) ही महाराष्ट्रात आहेत. एकट्या मुंबईत

कोरोना बाधितांची संख्या २६ हजारांवर पोहोचली आहे. सरकारने यावर प्रतीबंधात्मक उपाययोजना म्हणून संपूर्ण देशात ‘टाळेबंदी’ घोषित केली आहे. पहिली टाळेबंदी १७ मार्च २०२० ते २४ मार्च २०२० अशी जाहीर केली होती. ती पुढे वाढवून ३१ मार्च २०२० पर्यंत करण्यात आली. रुग्णांची संख्या वाढत असल्याने टाळेबंदी १४ एप्रिल २०२० पर्यंत वाढविली, पुढे ३ मे २०२०, त्याही पुढे १८ मे आणि आता ३१ मे २०२० पर्यंत टाळेबंदी वाढविण्यात आली आहे. रुग्णांचा वाढता दर हा शहरात ज्यास्त आहे, त्या मानाने खेडी अजून सुरक्षित आहेत. परंतु सध्यःस्थिती पाहता सरकारने शहरात अडकलेले परराज्यातील, परजिल्ह्यातील मजुरांना आप-आपल्या गावी जाण्यास परवानगी दिली आहे. केवळ मुंबई, ठाणे, पुणे या महानगरातील कोरोना संसर्ग रोखता यावा म्हणून ही उपाययोजना करण्यात येत आहे. जर हाच निर्णय दीड महिन्यापूर्वी घेतला गेला असता तर कोरोनाचा संसर्ग टाळता आला असता. परदेशातून आलेले नागरिक घरीच राहता ते इतर गर्दीच्या ठिकाणी जात होते, त्यामुळेही संसर्ग वाढला. दुसरी अत्यंत महत्त्वाची घटना म्हणजे दिल्ली येथील ‘मरकज’ या धार्मिक कार्यक्रमासाठी गेलेले ‘तबलिगी’ जमातीच्या २२०० लोकांना कोरोनाची बाधा झाली. हे सर्व लोक आपापल्या राज्यात गेल्याने त्याठिकाणी कोरोनाचा संसर्ग झपाट्याने वाढल्याचे समोर आले आहे. पहिल्या स्टेपमधील कोरोना संपून आता तो गर्दीच्या ठिकाणी जाऊन पोहोचला आहे. आतापर्यंत देशात २ हजारांच्या आसपास मृतांचा आकडा समोर आला आहे. मृत व्यक्तींमध्ये वृद्धांची संख्या अधिक आहे. त्याखालोखाल दुर्धर आजार असणारे रुग्ण आहेत, म्हणजेच ज्या व्यक्तींची रोगप्रतिकार शक्ती कमी आहे अशा लोकांचा समावेश जास्त आहे. युरोप अमेरिकेत मृतांचा व बाधितांचा आकडा वाढण्याचे प्रमुख कारण म्हणजे



तेथील लोकांची जीवनशैली हा महत्वाचा घटक आहे. युरोप अमेरिकेतील लोक 'वातानुकुलीत' जागेत काम करतात व 'वातानुकुलीत' घरात राहतात. तसेच जेवणात पिझ्झा, बर्गर, न्यूडल अशा पदार्थांचा समावेश असतो. या आहारामुळे व्यक्तीमध्ये रोगप्रतिकार शक्ती कमी होते. सदरच्या लेखात आपण आदिवासी लोकांच्या रोगप्रतिकार शक्ती व जीवनशैली याविषयावर भाष्य करणार आहोत. 'कोरोना' सारख्या जागतिक महामारीत या आजाराला आपल्यापासून आदिवासी लोक कसे दूर ठेवू शकतात? अपवाद, बाधित व्यक्ती व त्यांच्या संपर्कात आल्यास हा संसर्ग होऊ शकतो. परंतु त्यांच्याकडे असणारी नैसर्गिक रोगप्रतिकार शक्तीमुळे या संसर्गावर मात करू शकतील.

आदिवासी लोकांची रोगप्रतिकार शक्ती इतर लोकांपेक्षा २० ते ३० टक्के जास्त असण्याची करणे त्यांची जीवनशैली व आहार यावर अवलंबून आहे. भारतात फेब्रुवारी महिन्यात 'कोरोना' आला याविषयी समजताच सगळ्या आदिवासी जमातींनी जंगलात सापडणारे कंदमुळे आणून सेवन करायला सुरुवात केली. चाळीसगाव डांगानातील आदिवासी लोकांनी सिंदीचा काला शिरपुंजे येथील मुडाच्या डोंगरावर जाऊन आणून प्रत्येक माणसाला देण्यात आला. सिंदीचा काला खाऊन, साथीच्या आजारात डोंगरावर राहून माणसे जिवंत राहिल्याचे दाखले या भागात उपलब्ध आहेत. साधारणतः १८५६ सालाच्या आसपास मानमोडी, पटकी, प्लेग असे साथीचे आजार आले होते. त्यावेळी या आदिवासींनी डोंगरचा रस्ता धरला व जंगलात डोंगरावर मिळणाऱ्या रानभाज्या, रानकंद यांचे सेवन करून साथीपासून आपला बचाव केल्याचे दाखले उपलब्ध आहेत. महामारीच्या साथीत 'सिंद' नावाच्या झाडाचा कंद 'काला' खाऊन माणसे जिवंत राहिली होती. सह्याद्रीच्या पट्ट्यात डोंगरावर 'सिंद' जातीची झाडे मुबलक प्रमाणात आढळतात. खजुराच्या झाडाच्या जातकुळीची ही वनस्पती आहे. खजुराच्या चवीची फळे या झाडाला लागतात. या झाडाचा 'गर्भ' म्हणजे आतील 'गर' काला काढून बारीक तुकडे करून खातात. तसेच तुकडे पिण्याच्या पाण्यात टाकून

आठ दिवस ते पाणी संपूर्ण कुटुंब पिते. त्या काल्याचा संपूर्ण अर्क पाण्यात उतरतो. काल्यामुळे फुफुस स्वच्छ राहते. साधारणतः पुढील तीन महिने फुफुसाला संसर्ग होत नाही. कोरोनाचा विषाणू प्रथम हल्ला करतो तो श्वसन यंत्रणेवर म्हणजे घसा आणि फुफुसावर. थोडक्यात, श्वसन यंत्रणा सुरक्षित राहिली तर अशा विषाणूची बाधा व्यक्तीला होण्याची शक्यता नसते. त्याचबरोबर आदिवासी भागात महुचे फूल मिळते. त्यापासून ही माणसे दारू तयार करतात. महुच्या फुलांसोबत जंगलातील काही औषधी वनस्पतींच्या मुळ्या उकळून ही दारू तयार केली जाते. जांभूळ या फळापासून सुद्धा दारू तयार केली जाते. महुच्या दारूमुळे कफ, खोकला बरा होतो. श्वसन यंत्रणा चांगल्या प्रकारे कार्यरत राहते. जांभळा पासून तयार केलेली दारू सेवनामुळे मधुमेहासारखे आजार बरे होतात. पोट साफ करण्याचे उत्तम औषध म्हणून जांभळ्याची दारू उपयुक्त ठरते. अशा प्रकारची मद्ये आदिवासी आपल्या घरात नेहमी ठेवतात. करवंदापासून सुद्धा दारू तयार करतात. या दारूमुळे पित्ताचे आजार होत नाहीत. रोगप्रतिकार शक्ती वाढते. वरील सर्व प्रकारच्या दारू आदिवासी, औषध म्हणून वापरतात. आदिवासी आणि जंगल यांचे नाते अतूट आहे. जंगलातील प्रत्येक वनस्पती मानवी शरीरास काही ना काही प्रतिजैविके देत असते. यांचे ज्ञान आदिवासींना आहे. प्रत्येक ऋतूमध्ये जंगलात उगवणाऱ्या रानभाज्या, रानकंद हे आदिवासी सेवन करीत असतात. सृष्टीचे व आयुर्वेदाचे ज्ञान त्यांना आहे. महामारीचा आजार, साथीचे आजार हे उन्हाळ्यात व पावसाच्या पहिल्या सत्रात जास्त फैलावतात. त्यामुळे त्यापूर्वी नेमके काय प्रतिबंधात्मक उपाय आदिवासींना माहित आहेत ?

मकरसंक्रारातीच्या दुसऱ्या दिवशी 'कर' असते. करीच्या दिवशी हे लोक जंगलात जातात व 'आणीव' नावाचा कंद खणून आणतात. 'आणीव' हा संजीवनी देणारा रानकंद आहे. चविष्ट असणारा हा कंद सर्वात जास्त रोगप्रतिकार शक्ती वाढवितो. संपूर्ण वर्षभर रोगप्रतिकार शक्ती टिकवून ठेवणारा हा कंद आहे, म्हणून आदिवासी त्याला संजीवनी म्हणतात.



याबरोबरच अजून बरेच रानकंद आहेत की ज्यामुळे प्रतिकारशक्ती टिकून राहते. हायंदा, चाय, खुरपुडी हे कंद शरीरातील वेगवेगळ्या अवयवाना संजीवनी देत असतात, तसेच त्या अवयवांची प्रतिकारशक्ती वाढवतात. पावसाळ्यात 'हायंदा' खणून आणला जातो व त्याच्या फोडीपासून कालवण, सुकी भाजी करतात. त्याच्या फुलांची सुद्धा भाजी केली जाते. हायंदा खाल्यामुळे पोटाचे विकार बरे होतात. चायचा कंद किंवा चाविंद हा कंद चिकट असतो. तो भूजून अथवा शिजवून खातात. त्याच्या चिकट गुणधर्मांमुळे घसा साफ होतो, मल मार्ग स्वच्छ होतो. 'खुरपुडी' हा कंद चवीला अत्यंत कडू आहे. तो भाजून किंवा शिजवून खातात. त्याच्या कडू गुणधर्मांमुळे पित्त, कफ असे विकार बरे होतात. श्रावण महिन्यात जंगलात अनेक फळभाज्या असतात, त्या कच्च्या किंवा कमी शिजवून खातात. 'करटूली', 'गोमेटा' या भाज्या सेवन केल्याने भूक वाढते. पहिल्या पावसात चाईची भाजी, कोंबड्याची भाजी, कुरडूची भाजी, भात्याची भाजी, बडद्याची भाजी, बरकीची, कौल्याची, तांदुरड्याची भाजी, घायपताची भाजी आदिवासी लोक खातात. यामुळे पचनसंस्था चांगले कार्य करते. भाज्यांमधून मिळणारे 'क' जीवनसत्त्वे प्रतिकारशक्ती वाढवितात. पावसाळ्यात आदिवासींचे आवडते खाद्य म्हणजे किरवे, चिंबोरी, गींधोडी, मुरे मासे. हे अन्न यांच्या जेवणात वर्षभर असते. या अन्नापासून त्यांना भरपूर प्रमाणात प्रथिने मिळतात. खेकड्यांपासून कॅल्शियम मिळते. माशांच्या सेवनामुळे दृष्टी कमजोर होत नाही. निसर्गातून मिळणाऱ्या रानभाज्या, रानकंद, खेकडे, मासे यांच्या सेवनाने त्यांची प्रतिकारशक्ती चांगली राहते. कार्तिक महिन्यात 'चिचूरडा' नावाचे वांग्याच्या जातीचे बारीक फळ येते. त्याची भाजी आदिवासी लोक आवर्जून खातात. चवीला अत्यंत कडू असणारी ही भाजी खाल्यामुळे कफ, पित्त, वात यांचा त्रास होत नाही. जवळजवळ सहा महिने पित्ताचा त्रास होत नाही. अशा रानभाज्या खाल्यामुळे आदिवासी माणसे सुदृढ राहतात. चैत्र, ज्येष्ठ महिन्यात 'कुसर' नावाच्या फळांची भाजी खातात. कुसरे अतिशय कडू असतात. कुसरे आणून

उखळात कांडतात, मग शिजवून त्यातील कडू पाणी काढून टाकले जाते व मग तव्यावर 'खुरसनी' तेलात, कांद्याबरोबर परतून भाजी केली जाते. पावसाळ्यात डोंगराच्या कुशीत उगवलेले 'पंदा' नावाचा कंद शिजवून, कधी दळून भाकरी करून खातात. पूर्वी अन्नधान्य मुबलक प्रमाणात होत नव्हते, तेव्हा हा कंद अन्न म्हणून आदिवासी खात असत. या कंदाच्या सेवनाने भरपूर कर्बोदके मानवी शरीरास मिळतात. रानकेळी, त्यास आदिवासी 'कवदरा' असे म्हणतात. तो कंद सुद्धा शिजवून भातासारखा लागतो. तसेच 'हमर-कंद' यास आदिवासी संजीवनी म्हणतात. आदिवासी हे कष्टाची कामे करतात, कंबरदुखीवर अत्यंत रामबाण औषध असणारा हा कंद आदिवासी लोक पावसाळ्यात भाजी करून खातात. बाळंत स्त्रीला खारीक, खोबरे व हमरकंद यांचे कूट खायला देतात. त्यामुळे बाळंतपनात स्त्रीला कमरेचा त्रास होत नाही. असे अनेक कंद आहेत, ज्यांचे सेवन आदिवासी अन्न म्हणून उपयोग करतात. त्यामुळे त्यांची प्रतिकारशक्ती व रोगप्रतिकारशक्ती उत्तम असते. उन्हाळ्यात काही खास रानभाज्या हे लोक जाणूनबुजून खातात. त्यात भोकराची भाजी, सायरधोडे, रान निरगुडीच्या फुलांची भाजी खातात, ज्यामुळे उन्हाळ्यात येणाऱ्या साथीच्या, तापसरीच्या रोगापासून बचाव होऊ शकेल. लहान मुलांना या ऋतूत कांजण्या, गोवर हे साथीचे आजार होतात. त्याला जलसंजीवनी म्हणून उंबराच्या झाडाच्या मुळीचे पाणी पाजतात.

डोकेदुखीवर रामबाण उपाय म्हणून एक छोटीशी वनस्पती आदिवासी भागात सापडते, ती म्हणजे 'चित्रुक'. चित्रुकाचे दोन प्रकार आहेत. एक कांड्या चित्रुक व दुसरे पताड्याचित्रुक. या चित्रुकाचा लेप कपाळावर देतात. सर्दी पडसे झाल्यावर गरम-गरम नाचण्याची (नागल्याची) भाकरी, गरम उडीदाची डाळ, लसणाची लाल मिरची, विशेषतः खुरसणी तेलात तळलेली, असा आहार घेतल्यास अर्ध्या तासात सर्दी पडसे गायब होते. आदिवासी जीवन आणि निसर्ग हे एकमेकांवर अवलंबून आहेत. निसर्ग चक्राप्रमाणे आदिवासींचे



जीवन आहे. त्यांच्या आहारापासून ते दैनंदिन जीवनापर्यंत निसर्ग आणि त्यातील वनस्पती यांचे नाते अतूट आहे. आदिवासी भागात साथीचा आजार आल्यास संपूर्ण गाव, घरे, रस्ते 'निरगुडी' च्या फांद्याचा झाडू करून सात दिवस स्वच्छता केली जाते. 'निरगुडी' ही वनस्पती निर्जंतुकीकरना (सानिटाईझर) चे कार्य करते. या विषयीचे ज्ञान आदिवासींना पूर्वीपासूनच आहे. 'विलगीकरण' ही संकल्पना आदिवासींना माहित आहे. 'कोरोना' सारख्या साथीच्या आजारात बाहेरून आलेल्या व्यक्तीला 'मरीआईच्या' देवळात कोरंटाईन केले जाते असे. साथीच्या आजाराव्यतिरिक्त 'क्षय' सारख्या आजारी रुग्णास बकरीच्या गोठ्यात रात्रभर झोपवले जाते. बकरीचे गोमुत्र उपासीपोटी प्यायला देतात. त्यामुळेही ज्यांची रोगप्रतिकारशक्ती चांगली आहे, असे रुग्ण बरे झाले आहेत. प्रत्येक आदिवासीच्या वाड्यात पूर्वी 'कोरपड' असायचे, जे पित्तावर अत्यंत गुणकारी आहे. उन्हाळ्यात लहान मुलांना डांग्या खोकला होत असे. त्यावर उपाय म्हणून हिरड्याची पूड मधात कालवून चाटण दिले जायचे. त्यामुळे खोकला बरा होत असे. जंगलाचे ज्ञान, आयुर्वेदाचे ज्ञान असणारे आदिवासी इतर लोकांपेक्षा आरोग्याने सुदृढ आहेत. त्यांच्या राहायच्या घरापासून ते शेतीच्या आवजारासाठी लागणारे लाकूड सुद्धा विशिष्ट झाडाचे असायचे. उदा. घराचा 'उंबरा' भुस्कूटाच्या झाडाचा असायचा. बुस्कूट ही वनस्पती जंतुनाशक आहे. तसेच वास नष्ट करणारी आहे. जंगलात एखाद्या विषारी जातीच्या सापावर चुकून पाय पडला अथवा त्याचा स्त्राव पायाला चिकटला तर तो साप घरापर्यंत येत असे, परंतु तो उंबरा (उमतरा) कधीच ओलांडत नसे. भुस्कूटाच्या उंबऱ्यामुळे सापाचा स्त्राव गंदहिन होऊन जातो. त्यामुळे तो साप घरात प्रवेश करित नसे.

'कोरोना' या विषाणूने जगभर थैमान माजवले आहे. संपूर्ण जग या महामारीने हतबल झालेले आहे. मात्र आदिवासी लोक बिनधास्त आहेत. त्यांना माहित आहे की, अशा महामारीला रोखण्यासाठी आपले शरीर सक्षम आहे. 'कोरोना' मुळे आदिवासी लोक बाधित होतील, परंतु त्यांची

रोगप्रतिकार शक्ती चांगली असल्यामुळे त्यावर ते मात करू शकतील. सामाजिक अंतर म्हणजेच 'सोशल डीस्टन्स' कसे पाळावे याचे ज्ञान त्यांना आहे. कारनटाईण, सानिटायझर याविषयी पुरेसे ज्ञान त्यांना आहे. साथीच्या आजारात विहिरीवरून 'दुडीने' हंडे आणायचे नाहीत याचे ज्ञान त्यांना आहे. खनिजयुक्त पाणी, सेंद्रिय अन्न यामुळे आदिवासी लोक 'कोरोना' सारख्या दुर्धर साथीच्या आजाराचा सामना नक्कीच करतील. कारण रानमेवा, कंदमुळे आणि शुद्ध हवा, निसर्ग हे घटक आदिवासींच्या जीवनाचा अविभाज्य भाग आहेत.

संदर्भ:- अकोले तालुक्यातील चाळीसगाव डांगणातील (शिरपुंजे गाव) आदिवासी लोकांकडून मिळालेली माहिती.

\*\*\*

### काळजी घ्या...

पाऊस वारे गाती छान  
 सृष्टी हिरवळ आहे ना  
 हे जग किती सुंदर  
 पण आला एक व्हायरस असा  
 भारतातून जाणार कसा ?  
 त्याच्यावर एकच उपाय... घरात बसा  
 मानव पशु-पक्षी कसे राहणार  
 घरात राहून आंबे कसे खाणार ?  
 घरात बसून व्हायरसला सामोरे जाणार  
 बाहेरून आल्यावर स्वच्छ हात धुवू  
 भारतातून कोरोनाला पळवून लावू  
 हॅंडवॉश आणि सॅनिटायझर घरात ठेवू  
 भारतवासीयांना कोरोनाचा आला कंटाळा  
 त्यामुळे घराबाहेर पडायचे टाळा  
 नाहीतर पोलीस मारून करतील काळा निळा  
 - श्वेता आवारी (इ. ९ वी)

\*\*\*

**AAYUSHI INTERNATIONAL INTERDISCIPLINARY  
RESEARCH JOURNAL**

PEER REVIEW & INDEXED JOURNAL  
Email Id : [airjpramod@gmail.com](mailto:airjpramod@gmail.com)  
[www.airjournal.com](http://www.airjournal.com)

**SPECIAL ISSUE No. 90  
Volume - 01**

**Literature, Society and Culture**

**SPECIAL ISSUE PUBLISHED BY  
AAYUSHI INTERNATIONAL INTERDISCIPLINARY  
RESEARCH JOURNAL**

Peer Review & Indexed Journal | Impact factor 7.149  
Email Id : [airjpramod@gmail.com](mailto:airjpramod@gmail.com)  
[www.airjournal.com](http://www.airjournal.com)  
Mob. 999250451

**Executive Editor**  
Dr. P. B. Patil  
Principal,  
Karmaveer Hire, Arts, Science, Commerce  
and Education College, Gargoti

**Co-Editor**  
Mr. Rajratna S. D.  
Dr. Dewale Y. D.  
Dr. Desai S. B.  
Mr. Chitrakar R. A.

**Chief Editor**  
Prof. Pramod Tandale

**Aayushi International Interdisciplinary  
Research Journal (AIIRJ)**

Peer Reviewed And Indexed Journal

ISSN 2349-638x

Impact Factor 7.149

Website :- [www.airjournal.com](http://www.airjournal.com)

**Theme of Special Issue**

**Literature, Society and Culture**

(Special Issue No.90)

**Chief Editor**

**Mr. Pramod P. Tandale**

**Executive Editor**

**Dr. P.B.Patil**

Principal,

Karmaveer Hire Arts, Science, Commerce and Education College, Gargoti

**Co-Editor**

**Mr. S.D.Rajratna**

**Dr. Y.D. Dewale**

**Dr. S.B. Desai**

**Mr.R.A.Chitrakar**



No part of this Special Issue shall be copied, reproduced or transmitted in any form or any means, such as Printed material, CD – DVD / Audio / Video Cassettes or Electronic / Mechanical, including photo, copying, recording or by any information storage and retrieval system, at any portal, website etc.; Without prior permission.

## **Aayushi International Interdisciplinary Research Journal**

ISSN 2349-638x

Special Issue No.90

27<sup>th</sup> March 2021

### **Disclaimer**

Research papers published in this Special Issue are the intellectual contribution done by the authors. Authors are solely responsible for their published work in this special Issue and the

## Volume 01

Sr.No.	Name of the Author	Title of Paper	Page No.
1.	Mr. S.D. Rajratna	Socio-Political Issues in Margie Orford's Crime Novel, Like Clockwork	1
2.	Chandrakant K. Chavan	The struggle and suffering in Hemingway's 'The old man and the sea'	5
3.	Dr. Madhavi Pawar	The Fractured Identity That Long Silence	8
4.	Dr. Uttam Ramchandra Patil	Literature: A Gateway to Social Change	10
5.	Dr. Prashant Kale	A Study of Reading Habits of B.Ed. Teacher Trainees	11
6.	Dr. A. S. Arbole	Society and Symbols Depicted in the Novel <i>Train to Pakistan</i>	12
7.	Mrs. Jadhav Jyoti Mohan	Provincial Customs and Attitudes Dictate the Future of Children in Anita Desai's Novel <i>Fasting, Feasting: A Social Study</i>	20
8.	Mr. Sorate J.B.	Role Of Literature in Social Change	23

## Marathi Language

9.	प्रा.डॉ.आनंद वारके	सामाजिक चळवळी आणि राजन गवस यांच्या कादंबऱ्या	25
10.	प्रा. डॉ. सुभाष पाटील	मराठीतील आदिवासी साहित्य प्रवाह	31
11.	डॉ. कुंडलिक विंधू पारधी	सामाजिक चळवळी आणि आदिवासी साहित्य	38
12.	डॉ. लता पां. मोरे	'ज्याचा त्याचा प्रश्न'मधील स्त्रीवादी दृष्टिकोन	42
13.	प्रा.चिंतामण हुंदा धिंदळे	सामाजिक चळवळी आणि आदिवासी कविता	47
14.	डॉ. योगिता मारुती रांधवणे	नव्वदोत्तर ग्रामीण कादंबरीतील बदलेली ग्रामीण मानसिकता	52
15.	प्रा. आशालता नारायण खोत	मराठी कादंबरीतील बदलते चित्रण (बनगरवाडी)	55
16.	प्रा. सुजाता संजय घोपडे	'सूड' कयेची नायिका जानकी या ज्वालाप्रसाद पर्यंतचा प्रवास	60
17.	प्रा. मोहन बाबुराव चव्हाण	सामाजिक चळवळी आणि ग्रामीण कथा	65



## सामाजिक चळवळी आणि आदिवासी कविता

प्रा.चिंतामण दुंदा थिंदळे  
रयत शिक्षण संस्थेचे,  
राधाबाई काळे महिला महाविद्यालयात  
जि. अहमदनगर  
एरलत्र- cddhindale@gmail.com

### प्रास्ताविक

महाराष्ट्रातील ख्रिस्ती मिशनरीतर्फे संस्थेचे शैक्षणिक व आरोग्यविषयक कार्य, ठाणे जिल्हयातील 'कल्याण' चर्च ऑफ ब्रेदरेन मिशन' या अमेरिकन संस्थेतर्फे रेन्हरंड अॅडॅम एबी यांनी इ.स.१९०३ साली वारली आदिवासीकरीता दवाखाना उघडला होता. याच मिशनतर्फे शिक्षणाचे कार्य सुरू झाले. याशिवाय पुणे, नाशिक, धुळे, विदर्भातील चंद्रपूर, गडचिरोली या सर्व प्रादेशिक भूभागात ख्रिस्ती मिशनरींनी सेवाभावी वृत्तींनी आदिम जमातींची सामाजिक गरज लक्षात घेऊन त्यांच्या उत्थानाचे कार्य केले. या सर्व प्रक्रियेतून कळत-नकळत आदिवासी जागृतीची चळवळ अधिक विकसित होत गेली. एतदेशियांपैकी नामदार गोपाळ कृष्ण गोखले (भारत सेवक समाज) पू. ठक्करबाप्पा (भिल्ल सेवा मंडळ) पालघरचे वि.वा ऊर्फ बाबासाहेब दांडेकर, बोडीचे आचार्य भिसे (आदिवासी सेवा मंडळ, मुंबई) बाळासाहेब खेर, म. गांधीजींची समाजसेवेची प्रेरणा घेऊन काकासाहेब बर्वे, शंकरराव ठकार, दादासाहेब बिडकर, भाऊसाहेब हिरे, डॉ. ए. के. मोरे, कोंडू मारती बोकड (जूजर) गोपाळराव कडू, ओंकार होळक्या पाडवी, मारोती महादेव केंगले, नागपूर विदर्भाकडील पंचमबाबू मडावी.

भारतीय संविधानाने भारतीय नागरिकांना जे संरक्षण आणि हक्क दिले ते सर्वसामान्य आदिवासीलाही प्राप्त झाले. विशेष म्हणजे आदिवासींची विशिष्ट परिस्थिती लक्षात घेता त्यांना संविधानाव्दारे विशेष संरक्षण व अधिकारही मिळाले. डॉ. बाबासाहेब आंबेडकर व पू. ठक्करबाप्पा यांच्यासारख्या द्रष्ट्या नेत्यांचे हे ऋण आदिवासी कधीही उतराई होऊ शकणार नाही. आदिवासी जंगली आणि अशिक्षित, अडाणी आहेत. त्यांना सर्व हक्क व अधिकार प्रदान करावेत की नाहीत ? त्यांना त्यांचा वापर करता येईल का नाही ? असाही त्याकाळी एक विचार प्रवाह होता. परंतु थोर नेत्यांच्या प्रयत्नांमुळे हा विचार प्रवाह निर्माण झाला तिथेच संपला. परिणामतः संविधानाव्दारे आदिवासींची शैक्षणिक, आर्थिक आणि सामाजिक मागासलेपणातून सोडवणूक करण्याचे सर्व थरावर प्रयत्न सुरू झाले. जरी खरे असले तरी आदिवासींचे जे जटिल प्रश्न होते, विशेषतः जमीन, जंगल, सावकारी शोषण त्यांची तातडीने सोडवणूक होण्यापरिस्थिती निर्माण होऊ न शकल्याने देशभर आदिवासींनी चळवळी, लढे आणि संस्था संघटनांव्दारे जन आंदोलने सुरू केली. आणि जमिनीवरील हक्क प्रस्थापित करण्यासाठी व अन्याय, अत्याचार आणि शोषणा विरुद्ध आवाज उठविण्यासाठी स्वातंत्र्यपूर्व काळात अनेक चळवळी आणि लढे उभे राहिले. या चळवळीचा इतिहास आणि त्यावर आधारीत ललित साहित्याची निर्मिती हा खरं म्हणजे आदिवासी साहित्याचा ठेवाच ठरेल. त्यात प्रामुख्याने बिरसा मुंडाची चळवळ, बिहारमधील ताना भगत चळवळ, बस्तरच्या आदिवासींचा लढा, तेलंगणातील आदिवासी लढा, गोंड आणि कोलामांचा आदिलाबादमधील लढा, कोयांचा लढा, ओरिसातील कोरापूटचा लढा, नागाचा लढा, मुंडा आदिवासींची सरदारी चळवळ, मनिपूरचा लढा, मुंबई राज्यातील वारली लढा, सावकार जमीनदारांविरुद्ध लाल बावट्यांची चळवळ, जुआंग रिबेल्स, जोरिया नाईक रिहोल्ड, १९३७ सालचा जंगल सत्याग्रह, गुजरातमधील भगत मुळमेट आणि आप की जय अस्तीत्ववादी चळवळ, संताळ परगण्यातील संताळी लढे, लुशाई टेकड्यातील मिझोंच्या चळवळी, चणकापूरचे बंड इत्यादींचा प्रामुख्याने उल्लेख करता येईल. विसाव्या शतकाच्या पूर्वार्धात झालेल्या या चळवळी आणि लढ्यांनी आदिवासींचे प्रश्न सुटले असे नाही. परंतु स्वातंत्र्यानंतरच्या पूर्वार्धात ह्या चळवळीचा शोषभाग आणि नव्याने चळवळी उभ्या राहिल्या. अनेक आंदोलने झाली. त्यात आदिवासींची अस्मिता, अस्तित्व आणि प्रादेशिक स्वातंत्र्यतेचे लढे आणि चळवळी अग्रस्थानी होत्या. याशिवाय अलीकडील काळात आदिवासी जमातीत जन्म घेऊन समाजसेवेचा वसा घेणारे अनेक समाजसेवक व कार्यकर्ते यांनी आदिम जमातींना शैक्षणिक सुविधा पुरविल्या आहेत. महाराष्ट्रातील शासन संस्थेनेही आदिवासी उपाय योजनेच्या माध्यमातून त्यांचा



जीवनस्तर उंचावण्याचा प्रयत्न केला आहे. याशिवाय महाराष्ट्रातील डाव्या विचारसरणीच्या आश्रयाखाली येऊन घुळे येथील काँ. शरद पाटील यांच्या मार्गदर्शनाखाली नजूबाई गावीत व वाहरु सोनवणेसारखी प्रतिभावंत लेखक मंडळी उदयास आली आहेत. वरील सर्वांच्या अथक परिश्रमातून, समाजसेवेतून आदिवासी मुक्ती चळवळ आणि पर्यायाने आदिवासी कविता निर्माण झाली आहे.

मराठी साहित्यात १९६० नंतर दलित व ग्रामीण असे साहित्य प्रवाह निर्माण झाले. त्यांच्याकडून आदिवासींच्या खूप अपेक्षा होत्या परंतु ते साहित्य त्या पूर्ण करू शकले नाही. त्यामुळेच आदिवासींची आपला वेगळा प्रवाहा निर्माण करण्याच्या दृष्टीने पावूल उचलून १० व ११ नोव्हेंबर १९७९ साली प्रा. विनयाक तुमराम यांच्या पुढाकाराने व भराणी दुर्गावती' वाचनालयाच्या वतीने पहिले आदिवासी साहित्य संमेलन चंद्रपूर जिल्ह्यात भद्रावती' या गावी भरविण्यात आले. व या निमित्ताने आदिवासी साहित्याचे स्वतंत्र दालन मराठी साहित्यात उघडले गेले. त्यानंतर दुसरे आदिवासी साहित्य संमेलन श्री राजाभाऊ राजगडकर यांच्या पुढाकाराने २३ मे १९८२ रोजी बवतमाळ जिल्ह्यात भवणी' या गावी घेण्यात आले. या साहित्य संमेलनाच्या उदघाटन प्रसंगी चळवळी विषयी शिवाजीराव मोघे म्हणतात की, "निसर्गाशी समरस होऊन आदिवासी आनंदात राहतो. वाघाशी मुकाबला करताना भित नाही. पण शहरातील उच्चभू अधिकाऱ्यांची त्याला भिती वाटते. शेकडो वर्षांपासून जपलेला साहित्यसाठा रानावनात आहे. साहित्य संमेलनापासून प्रेरणा घेऊन त्यातील अनिष्ट ते काढून सोज्वळ व चांगले साहित्य प्रकाशात आले पाहिजे आदिवासी साहित्य चळवळ ही केवळ साहित्यापुरती मर्यादित नाही तर ती आदिवासींच्या सर्वांगीण विकासासाठी आहे. त्याद्वारे मार्गदर्शन मिळाले पाहिजे." १ स्वातंत्र्यानंतरच्या काळातच आदिवासीतीच्या शैक्षणिक विकासाचा वेग खऱ्या अर्थाने वाढलेला दिसतो. शिक्षणाचे महत्त्व पटल्यावरून म्हणा अथवा सामाजिक सर्वंकष मदतीसाठी ज्या शिक्षणसंस्था उभारल्या त्या संस्थातून म्हणा, अनेक आदिवासी कार्यकर्त्यांनी शिक्षणसंस्था उभारल्या. त्या संस्थांमधून शिक्षण घेऊन बाहेर पडलेले शेकडो आदिवासी तरुण उच्च पदांवर असलेले आज पाहावयास मिळतात. डॉ. विनायक तुमराम हयांनी १९७८ साली ग्रंथाल्याची चळवळ उभारून भद्रावती, जिल्हा चंद्रपूर येथे भराणी दुर्गावती वाचनालय' नावाचे पहिले वहिले वाचनालय सुरु केले. तर १९८१ साली भएकलव्य शिक्षण प्रसारक मंडळ' स्थापन केले. १९८५ साली तेलवार येथे भगवान पेरसापेन ग्रंथालय' स्थापन केले. महिलांसाठी १९८६ साली, आदिवासी महिला विकास ग्रंथालय' अशा अनेक संस्था स्थापन करण्यात आल्यामुळे आदिवासी तरुणवर्ग वाचन आणि लेखनाकडे वळल्याचे दिसून येतो. यानंतर पाच वर्षांनी ६ व ७ जून १९८७ साली तिसरे आदिवासी साहित्य संमेलन नांदेडजिल्ह्यात किनवट' या गावी श्री. राम भिराणे यांनी आयोजित केले होते. त्यानंतर चौथे आदिवासी साहित्य संमेलन १९८९ यावर्षी आदिवासी साहित्यिकांचे दोन मेळावे गडचिरोली येथे डॉ. सुभाष सावरकर यांचे अध्यक्षतेखाली १८ व १९ फेब्रुवारी १९८९ रोजी भरविला होता. तर दुसरा मेळावा पांढरकवडा येथे ८ मे १९८९ रोजी आदिम' चे लेखक डॉ. भाऊ मांडकर यांचे अध्यक्षतेखाली संपन्न झाला. या दोन्ही मेळाव्यांचे अध्यक्ष बिगर आदिवासी साहित्यिक व अभ्यासक होते. दुसऱ्या मेळाव्याचे उदघाटकही डॉ. जयंतराव धावडे हे बिगर आदिवासी होते. त्यामुळे ६ व्या आदिवासी साहित्य संमेलनाच्या अध्यक्षीय भाषणात कवी भुंजग मेश्राम म्हणतात की, "आपल्याला आपली वाट, आपली दिशा निश्चिंत करणे महत्त्वाचे आहे. आदिवासी साहित्य कृतीशील बनवून त्यास आत्मसन्मानाच्या चळवळीशी जोडणे आवश्यक आहे. आम्हांला आदिवासींच्या आत्मसन्माची चळवळ तीव्र करायची आहे. आदिवासी साहित्य हे तिचे अविभाज्य अंग आहे." २ भुंजग मेश्राम यांनी जे मत व्यक्त केले आहे त्याचा परिणाम आदिवासी कवितेवर नक्कीच झालेला आहे. त्यामुळेच वाहरु सोनवणे' यांच्या स्टेज' नावाच्या कवितेतून मांडलेले आहे. ते लिहितात.

"आम्ही स्टेजवर गेलो नाही.

आणि आम्हाला बोलावलही नाही

बोटाच्या इशान्याने

आमची पायरी आम्हाला दाखवून दिली

आम्ही तिथंच बसलो.....

ते आले नि स्टेजवर गेले

आमचेच दुःख आम्हाला सांगत राहिले

आम्ही चुळबुळलो.....







आपणास परिचय होतो. हे ऐतिहासिक वास्तव विसरून चालणार नाही.'६ असे मत आदिवासी अभ्यासक विनायक तुमराम नोंदवतात वरील अभ्यासकांच्या मताचा विचार करून आदिवासी काव्यातून चळवळीचे सूर येतात. आदिवासींच्या शिक्षणातील समस्या मांडतांना, कधी तरी भरणाऱ्या शाळेचे वर्णन पुरुषोत्तम आगाशे' आपल्या कवितेत करतात.

''ऐसी इधली शाळा  
नाही खडू नाही फळा  
हवेशीर इधल्या भिंती  
छपराला लागते पळती  
पोर इथं शिकायला जाती

कधीतरी मास्तर आल्यावरती..''७

आदिवासींच्या समस्या कवितेतून मांडण्यामागील प्रेरणा ह्या चळवळीच्याच असल्याचे लक्षात येते. म्हणूनच कवितेतून आदिवासी कुपोषण, दारिद्र्य, आरक्षण, स्त्रियांवरील अन्याय, अत्याचाराचे चित्रण कविनी केल्याचे पाहावयास मिळते. आदिवासी कविता हा आदिवासी हा आदिवासी जीवनाचा आरसाच आहे. कवितेतून आदिवासी कवींनी सूचकपणे यथार्थवादी दृष्टिकोनातून आदिम भावना मांडून नवआदिवासी कवींनी एक दिशाव प्रेरणा देण्याचे काम केले आहे. आदिवासी कवींची कविता असल आदिमत्व प्रकट करते व ती विविध भाषिक सौंदर्यांनी नटलेली आहे. आदिवासी साहित्याबरोबरच आदिवासी संस्कृतीचे जतन व संवर्धन आदिवासी चळवळीने आवश्यक आहे. त्यासाठी आदिवासी कविनी प्रयत्न केले आहे. आदिवासींच्या शोषण मुक्तीचा विचार आदिवासी चळवळीने मांडलेला आहे. त्याचा परिणाम, प्रभाव कवितेवर असल्याचे दिसून येते. नवसमाज निर्माण करण्यासाठीचे सामर्थ्य आदिवासी साहित्य परिषद व आदिवासी चळवळीत प्राप्त झाले आहे. त्यामुळे नवोदीत आदिवासी कविच्या काव्यातून नवा विचार पुढे येतो आहे. आदिवासी समाजातील मुक्या भावनांना व्यक्त स्वरूप देण्यासाठी चळवळीनी प्रयत्न केले आहे. अशा प्रकारे आदिवासी चळवळी आणि कवितेचा सहसंबंध असल्याचे दिसून येते.

आदिवासी साहित्याची निर्मिती ही स्वातंत्र्योत्तर काळातील आहे. त्याअगोदर आदिवासी साहित्य नव्हते, असे नाही. मात्र, मुळातच हा समाज आणि साहित्य स्वातंत्र्यापूर्वी आणि स्वातंत्र्यानंतरही मोठ्या प्रमाणात उपेक्षित राहिला आहे. अर्थातच जाणूनबुजून उपेक्षित ठेवले, हे या उपेक्षित राहण्यामागचे कारण आहे. १९७५ पासून आदिवासी साहित्य खऱ्याअर्थाने पावले टाकत आलेला पाहावयास मिळतो. आदिवासींच्या धार्मिक व सामाजिक रूढी परंपरागत निसर्गपूजेतून निर्माण झाल्या आहेत. निसर्गातील जे जे निरनिराळे गूढ, अनाकलनीय ते सर्व पूजनीय असं ते मानतात. आकाशात चमकणारी चीज, चंद्र, सूर्य, प्रचंड वृक्ष, वाघ, सिंह, साप, विंचू अशा निसर्गनिर्मित सजीव-निर्जीव वस्तुंची आणि प्राण्यांची ते पुजा करतात, त्यांच्यात हिरवा, हिमाई, वनदेव, बडादेव, गावदेव, कणसरी, घरतरी, वाघदेव, वाघिया, चित्ता, डोंगरदेव अशा निसर्गातून झालेल्या देवतांचीही पूजा केली जाते. त्यामुळेवास्तविक 'आदिवासी साहित्य' हे खऱ्या अर्थाने. साहित्याचे मूळ आहे. त्याचा कर्ता कोण हे कोणाला सांगता येत नाही. वेदाचा कर्ता कोण हे कुठे सांगता येते कुणाला ?वेद ब्रह्म्याच्या मुखातून प्रगट झाले असे सांगतात, म्हणून ते परिपूर्ण आहे असे मानले जाते. 'वेद वाक्य प्रमाण' असे मानण्याचा प्रघात जनमाणसांत त्यामुळेच रूढ झालेला आहे. आदिवासींच्या अभिजात जनसाहित्याच्या विशेषतः आदिवासींच्या लोककथा, लोकगीते, जानपदगीते, गुराखी गीते, देव-देवतांच्या, मनुष्य - प्राण्याच्या उत्पत्ती आणि मरण्याच्या कथा, जनव्यवहाराचे वाद संवाद, घात-प्रघात, बोलण्या-चालण्याचे अडाखे, म्हणी आणि वाक्प्रचार हा आदिवासी साहित्याचा आद्य प्रकार म्हणता येईल. त्यांचा उगम कुठे झाला, केव्हा झाला, त्याचा कर्ता कोण हे कुणाला सांगता येणार नाही. आदिवासी मात्र अनादी काळापासून या साहित्यावर जगाला आहे. अनादी काळापासून त्यांचे हे मौखिक साहित्य एका पिढीकडून दुसऱ्या पिढीकडे केवळ मौखिक परंपरेने चालत आलेले आहे. खरेतर त्यांचे हे साहित्य अक्षरवाङ्मय आहे. परंतु आजचे आदिवासी साहित्यिक त्याला विसरून गेले आहेत. या निमित्ताने त्याची आठवण मी करून देऊ इच्छितो. या मौखिक वाङ्मयाचा शोध घेण्याची, विकास करण्याची, त्यातील शब्द सौंदर्य, लालित्य, भावना प्रधानता, शृंगार, प्रेम आणि निसर्गाशी विलीन होण्याची व त्यात स्वतःला विसरून जाण्याची क्रिया

साहित्य प्रेमींना सुस्पष्ट झाली पाहिजे आणि हे उत्तरदायित्व आजच्या आदिवासी साहित्य संमेलनाला जमणाया साहित्यिकांवर आहे. आदिवासी कवितेच्या प्रेरणा शोधतांना, निसर्ग हीच पहिली प्रेरणा असल्याचे सांगता येईल. प्रस्थापित भौतकदृष्ट्या प्रगत अशा संस्कृतीपासून अलिप्त असलेला, निसर्ग ज्याच्या जीवनाचा अविभाज्य भाग आहे, कृत्रिम, तथाकथित सुसंस्कृत वातावरणापासून दूर राहून स्वाभाविक नैसर्गिक जीवन व्यतीत करणारा आणि किमान प्राथमिक गरजांपासून वंचित ठेवण्यात आलेला जो आदिवासी समाज आहे त्या समाजातून जिरीने प्राप्त परिस्थितीशी संघर्ष करीत आदिवासींच्या व्यथा-वेदनांची दाहकता आदिवासी कविते तून मांडली आहे.

#### समारोप-

स्वातंत्र्योत्तर सामाजिक चळवळीचा विचार केला असता. आदिवासी साहित्य प्रवाहाची सुरुवात ही आदिवासी कवितेनी झालेली आहे. नव्या जगाची नवीन अनुभवविश्वाची भर घातली गेली आहे. अन्याय, अत्याचार विरुद्ध आवाज उठवला आहे. आदिवासी कला, संस्कृती, निसर्ग यांची ओळख येथील प्रस्थापित समाजाला करून देण्याचे काम कथा, कविता, कादंबरी आणि नियतकालिकांनी केले आहे. त्यामुळे मराठी साहित्य समृद्ध होण्यास नक्कीच मदत झाली आहे.

#### संदर्भ आणि टिपा -

१. वाल्हेकर ज्ञानेश्वर, आदिवासी साहित्य: एक अभ्यास, स्वस्व प्रकाशन औरंगाबाद. प्र.आ. २००९. पृ. २५.
२. वाल्हेकर ज्ञानेश्वर तत्रैव. पृ. २५.
३. सोनवणे वाहरु, गोधड, सुगावा प्रकाशन पुणे. प्र.आ. १९८७.
४. घोदडेकाळूराम, 'आदिवासी साहित्याचा आदिवासी चळवळीशी समन्वय', हाकारा, जानेवारी- जून १९९१ पृ. ३९.
५. तुमराम विनायक, 'साहित्याचा युगप्रवास' हाकारा, जुलै-सप्टेंबर १९८२. पृ. १७.
६. तुमराम विनायक, आदिवासी साहित्य : स्वस्व आणि संकल्पना स्वस्व प्रकाशन, औरंगाबाद प्र.आ. १५ नोव्हेंबर २०१२. पृ. ५
७. आगाशे पुरुषोत्तम, 'हाकारा', जुलै-सप्टें. १९९५. पृ. १७.

ISSN 2349-638X

www.aairjournal.com

ISSN 2349-638x  
Impact Factor 7.149

AAYUSHI INTERNATIONAL INTERDISCIPLINARY

RESEARCH JOURNAL

PEER REVIEW & INDEXED JOURNAL

Email id : [airjpramod@gmail.com](mailto:airjpramod@gmail.com)

[www.airjournal.com](http://www.airjournal.com)

SPECIAL ISSUE No. 90

Volume - 01

**Literature, Society and Culture**

SPECIAL ISSUE PUBLISHED BY  
AAYUSHI INTERNATIONAL INTERDISCIPLINARY  
RESEARCH JOURNAL

Peer Review & Indexed Journal | Impact factor 7.149  
Email id : [airjpramod@gmail.com](mailto:airjpramod@gmail.com)  
[www.airjournal.com](http://www.airjournal.com)  
Mob. 8999250451

Executive Editor

Dr. P. B. Patil  
Principal  
Karmaveer Hire, Arts, Science, Commerce  
and Education College, Gargoti

Co-Editor

Mr. Rajratna S. D.  
Dr. Dewale Y. D.  
Dr. Desai S. B.  
Mr. Chitrakar R. A.

Chief Editor

Prof. Pramod Tandale

## **Aayushi International Interdisciplinary Research Journal (AIRJ)**

Peer Reviewed And Indexed Journal

ISSN 2349-638x

Impact Factor 7.149

Website :- [www.airjournal.com](http://www.airjournal.com)

**Theme of Special Issue**

**Literature, Society and Culture**

(Special Issue No.90)

**Chief Editor**

**Mr. Pramod P. Tandale**

**Executive Editor**

**Dr. P.B.Patil**

Principal,

Karmaveer Hire Arts, Science, Commerce and Education College, Gargoti

**Co-Editor**

**Mr. S.D.Rajratna**

**Dr. Y.D. Dewale**

**Dr. S.B. Desai**

**Mr.R.A.Chitrakar**



---

No part of this Special Issue shall be copied, reproduced or transmitted in any form or any means, such as Printed material, CD – DVD / Audio / Video Cassettes or Electronic / Mechanical, including photo, copying, recording or by any information storage and retrieval system, at any portal, website etc.; Without prior permission.

**Aayushi International Interdisciplinary Research Journal**

ISSN 2349-638x

Special Issue No.90

27<sup>th</sup> March 2021

**Disclaimer**

Research papers published in this Special Issue are the intellectual contribution done by the authors. Authors are solely responsible for their published work in this special Issue and the

---

Special Issue Theme :- Literature, Society and Culture (Special Issue No.90) ISSN 2349-638x Impact Factor 7.149	27 <sup>th</sup> March. 2021
--	---------------------------------

## Volume 01

Sr.No.	Name of the Author	Title of Paper	Page No.
1.	Mr. S.D. Rajratna	Socio-Political Issues in Margie Orford's Crime Novel, Like Clockwork	1
2.	Chandrakant K. Chavan	The struggle and suffering in Hemingway's 'The old man and the sea'	5
3.	Dr. Madhavi Pawar	The Fractured Identity That Long Silence	8
4.	Dr. Uttam Ramchandra Patil	Literature: A Gateway to Social Change	10
5.	Dr. Prashant Kale	A Study of Reading Habits of B.Ed. Teacher Trainees	13
6.	Dr. A. S. Arbole	Society and Symbols Depicted in the Novel <i>Train to Pakistan</i>	17
7.	Mrs. Jadhav Jyoti Mohan	Provincial Customs and Attitudes Dictate the Future of Children in Anita Desai's Novel <i>Fasting, Feasting: A Social Study</i>	20
8.	Mr. Sorate J.B.	Role Of Literature in Social Change	23
<b>Marathi Language</b>			
9.	प्रा.डॉ.आनंद वारके	सामाजिक चळवळी आणि राजन गवस यांच्या कादंबऱ्या	25
10.	प्रा. डॉ. सुभाष पाटील	मराठीतील आदिवासी साहित्य प्रवाह	31
11.	डॉ. कुडतिक चिंधू पारधी	सामाजिक चळवळी आणि आदिवासी साहित्य	38
12.	डॉ. लता पां. मोरे	'ज्याचा त्याचा प्रश्न'मधील स्त्रीवादी दृष्टिकोन	42
13.	प्रा.चिंतामण दुंदा धिंदळे	सामाजिक चळवळी आणि आदिवासी कविता	47
14.	डॉ. योगिता मारुती रांधवणे	नव्योत्तर ग्रामीण कादंबरीतील बदलते ग्रामीण मानसिकता	52
15.	प्रा. आशालता नारायण खोत	मराठी कादंबरीतील बदलते चित्रण (बनगरवाडी)	55
16.	प्रा. सुजाता संजय चोपडे	'सूड' कथेची नायिका जानकी चा ज्वालाप्रसाद पर्यंतचा प्रवास	60
17.	प्रा. मोहन बाबुराव चव्हाण	सामाजिक चळवळी आणि ग्रामीण कथा	65

### नवदोत्तर ग्रामीण कादंबरीतील बदलेली ग्रामीण मानसिकता

डॉ. योगिता मारुती रांधवणे

रयत शिक्षण संस्थेचे

राधाबाई काळे महिला महाविद्यालय, अहमदनगर

ईमेल- [yogitarandhavane9@gmail.com](mailto:yogitarandhavane9@gmail.com)

#### प्रास्ताविक

ग्रामीण अर्थव्यवस्थेचा कणा असलेली शेती ही सुरुवातीपासूनच संकटात आहे. शेतकऱ्याचे वर्षाचे उत्पन्न आणि शेतीचा व जगण्याचा खर्च याचा ताळेबंद आजपर्यंत जुळलेला दिसत नाही. याशिवाय खाऊजा अर्थनीतीमुळे ग्रामीण शेतकऱ्यांच्या जीवनावर अनिष्ट परिणाम झाले आहेत. याचाच परिणाम मराठी ग्रामीण कादंबरीतून येणाऱ्या समकालीन शेतकरी जीवन चित्रणावर झालेले आहे. आत्महत्येच्या वाटेवर चालणारा शेतकरी, वांझोटया ठरलेल्या शेतकरी चळवळी, शहर खेडे यांच्यात रुंदावलेली दरी गावातील नवतरुणांत वाढत चाललेले शहराचे आकर्षण, यामुळे मोडत चाललेली ग्रामसंस्कृती, नात्यात येत असलेला फोलपणा स्वतःपुरते पाहण्याची वाढत चाललेली वृत्ती, प्रामाणिक माणसाची होणारी दमछाक, पैशाला आलेले देवपण हे सारे जागतिकीकरणाचे देणे असून त्याचा परिणाम ग्रामजीवनावर खूपच पडलेला आहे. या सर्व घडामोडीचा प्रभाव मराठी ग्रामीण कादंबरीवरही पडलेला असून त्याचे प्रतिबिंब या दशकातील कादंबरीत रेखाटले आहे.

#### नवदोत्तरग्रामीण कादंबरी वाटचाल व वेगळेपण :-

भारतासारख्या कृषीप्रधान देशाने १९९१ मध्ये नवे आर्थिक धोरण स्वीकारले. त्याचा ग्रामीण साहित्यातील कथा, कविता, नाटक साहित्याप्रमाणे मराठी, ग्रामीण कादंबरीवरही जागतिकीकरणाचा प्रभाव पडलेला आहे. त्याचे कारण म्हणजे ग्रामीण लेखक ग्रामीण समाजजीवनात वावरत असताना त्यांना अलेले अनुभव, ग्रामीण संस्कृती, रूढी, परंपरा, ग्रामनिष्ठा कृषिसंस्कृती, ग्रामीण माणसांचे राहणीकमान, त्याची केशभूषा, वेशभूषा, त्याचे सण-उत्सव खेड्याची रचना, व्यापार, उद्योग, रोजगार अशा विविधांगी घटकांचे ग्रामीण कादंबरीच्या माध्यमातून चित्रण केले आहे. मुक्त अर्थव्यवस्थेची स्वीकार व त्यामुळे जगाला आलेले एक मोठया खेड्याचे स्वरूप या शहरी आणि ग्रामीण माणसाच्या जगण्यात अमुलाग्र बदल झाले. शहरे बदलली तशी खेडीही बदलली याचे प्रतिबिंब तत्कालीन साहित्यात बरोबरच कादंबरीत पहावयास मिळते. १९९० नंतर रा.रं बोराडे, बाबाराव मुसळे, संदानंद देशमुख, अशोक कोळी, राजन गवस, रंगनाथ पठारे, विश्वास पाटील, किशोर सानप, पुरुषोत्तम बोरकर, प्रवीण दशरथ बांदेकर, जी. के. ऐनापुरे यांच्या ग्रामीण कादंबऱ्यातून खाजगीकरण, उदारीकरण आणि जागतिकीकरणाचे होणारे चांगले, वाईट परिणाम मांडण्यात आलेले आहेत. याशिवाय मराठी ग्रामीण कादंबरीकारांच्या कादंबऱ्यातून 'खाऊजा' अर्थनीतीचे आजतागायत चित्रण केले जात आहे. त्यामुळे जागतिकीकरण आणि मराठी ग्रामीण कादंबरीची वाटचाल आज २१ व्या शतकातही सुरुच आहे. संदानंद देशमुख यांच्या 'बारोमास' या कादंबरीतील जागतिकीकरण संदर्भात प्रा. शेटकार रामशेट्टी असे म्हणतात की, "बारोमास या कादंबरीत जागतिकीकरणामुळे शेतकऱ्याच्या मुलाला म्हणजे एकनाथाला दुःखाचे जीवन जगावे लागत आहे. तो एम.ए. बी. एड प्रथम श्रेणीत उत्तीर्ण होऊनही त्याला नौकरी मिळत नाही. तो शेतीत काम करीत असल्यामुळे त्याची पत्नी त्याच्यासोबत राहत नाही. त्याच्या स्वप्रांच्या चुराडा होतो. 'बारोमास' या कादंबरीत मांडलेल्या एकनाथ या एका शेतकऱ्याच्या मुलाची कहाणी नसून संबंध देशातील शेतकरी मुलांची कहाणी आहे. प्रत्येक शेतकऱ्यांच्या नशिबी बेकारीचा प्रश्न 'आ' वासून उभा राहिलेला आहे. म्हणजेच, सर्वसामान्य शेतकरी हा आर्थिक विवंचनेत दिवस काढत आहे."१



शेतकऱ्यांच्या मुलांची होणारी फरफट ग्रामीण कादंबरीतून चित्रित होताना दिसून येते. राजन गवस यांनी 'कळप' व 'तणकट' या कादंबरीतून शहर व गाव यातील नेमके अंतर प्रभाविपणे व्यक्त केले आहे. किशोर सानप यांच्या 'पांगुळवाडा' या कादंबरीतून खेडयातून शहराकडे जाणाऱ्या लोकांची मानसिकता, ग्रामीण जीवनाचे होणारे 'स्थित्यंतर' या कादंबरीत टिपले आहे. तर रमेश इंगळे यांनी 'निशाणी डावा अंगठा' २००५ या कादंबरीतून आजची बदलत चालेली ग्रामव्यवस्था, शाळा, दवाखाने याचे यथार्थ चित्रण केलेले आहे. तर प्रतिमा इंगोल यांची बुढाई, अप्पासाहेब खोत यांची गाव पांढरीच्या वाटेवरी, प्रशांत पोखरकर यांची गाव ढासळत आहे, भारत काळे यांची ऐसे कुणबी भूपाळ, प्रकाश देशपांडे यांची बारदान, कृष्णात खोत यांची रौंदाळा, अशोक कोळी - कुंधा, महेंद्र कदम-धुळपावल, कैलास दौंड - कापूस काळ, पांडुरंग कुंभार- गावकूस, पाणधुई, मोहन पाटील- साखरपेरा, हया कादंबऱ्या नव्वदोत्तरी ग्रामीण कादंबरीची वाटचाल सांगणाऱ्या आहेत.

### बदलेली ग्रामीण मानसिकता :-

पारंपरिक ग्रामीण अर्थव्यवस्थेत ग्रामीण माणूस, ग्रामीण शेतकरी हा सुखी-समाधानी होता. परंतु जागतिकीकरणाने ग्रामीण पारंपरिक अर्थव्यवस्था बदलून नवी अर्थव्यवस्था वसत आहे. आज शेती करणे परवडण्याजोगी राहिली नाही. जागतिकीकरणामुळे सामान्य माणसाच्या हातात नवे तंत्रज्ञान आले. मोबाईलव्दारे घरात बसून शेतीतील मोटरपंप चालू किंवा बंद करता येईल, असे तंत्रज्ञान विकसित झाले. शिक्षणाच्या माध्यमातून नोकरी उद्योगात शिरकाव झाल्यामुळे खेडेगावातील नव्या पिढीचे राहणीमान बदलले. गावातील प्रत्येक घरावर टि. व्ही. डिश. लावलेल्या दिसू लागल्या, मॉल संस्कृती वाढीस लागली, प्रसारमाध्यमांच्या प्रसारामुळे जगात घडणारी प्रत्येक गोष्ट क्षणात सर्वत्र पसरू लागली. दुसरीकडे बहुराष्ट्रीय कंपन्यांच्या मुक्त संचारामुळे शेतकऱ्यांच्या शेतात पिकलेली फळे, भाजीपाला, धान्य हे कवडीमोल भावाने विकले जाऊ लागले. तोच माल आकर्षक पॅकिंगमध्ये या कंपन्या बाजारात आणून जास्त किमतीत विकून मोठ्या होऊ लागल्या. नव्या तंत्रज्ञानाच्या आगमनासोबत अवर्षणासारख्या आपत्तीमुळे अपेक्षाभंगाचे दुःख वाढून कर्जाचे ओझे शेतकऱ्यांच्या मानगुटीवर वाढायला लागले. असह्य होणाऱ्या ताणाची परिणीती शेतकऱ्यांच्या आत्महत्येस होऊ लागली. "शेती नीट पिकत नसेल तर ती विकून टाकावी आणि त्या पैशात पोटापाण्यासाठी दुसरा उद्योगधंदा बघावा दुकान टाकावे किंवा पाण्याची व्यवस्था करून बागाईत करावी अर्थात बागायती शेती करून शेतीमालाला भाव मिळत नसेल तर मग सरळच विकून टाकावी. अशीही भयंकर मानसिकता ग्रामीण भागातील शेतकरी कुटुंबातून निर्माण झाली"२ आधुनिकीकरण व जागतिकीकरणाची ही दुसरी बाजूही विचारात घ्यावी लागेल. या सर्वांचे दर्शन या कालखंडातील ग्रामीण कादंबरीतून घडत गेले. अशोक कोळी यांच्या 'पाडा' (२००६) सुरेंद्र पाटील यांच्या चिखलवाटा (२००७) अशा काही कादंबऱ्यातून हे नव्या यंत्राचे आधुनिकतेचे वारे आणि त्याच्या झंझावात वाहून जाणारा ग्रामीण समाज याचे चित्रण आलेले आहे.

### भ्रष्टाचाराचा भयंकर विळखा :-

ग्रामीण भागात या कालखंडात भ्रष्ट व्यवस्थेचा शिरकाव होत गेला. शिक्षण संस्थामधून नवशिक्षितांची पिळवणूक होऊ लागली. साखर कारखाने, दुध संस्था, सहकारी सोसायट्यां मध्ये मक्तेदारी वाढीस लागली. या संस्था आपल्याकडे टिकवून ठेवण्यासाठी राजकारण गलिच्छ धरावर पोहोचले पैशातून सत्ता व सत्तेतून पैसा असे नवे समीकरण उद्घास आले. गुंडाचा शिरकाव झाल्यामुळे राजकारणातील स्वच्छ चारित्र्याची माणसे बाजूला गेली. सामान्य माणूस या भ्रष्ट व्यवस्थेत भरडला गेला. शेती करणारे, व्यवसाय करणारे नोकरी करणारे असे सारेच या व्यवस्थेतील सत्तास्थानाचे गुलाम झाले. या सगळ्या परिस्थितीचा परिणाम म्हणजे शेतकऱ्यांची आर्थिक स्थिती कमालीची खालावली. त्यामुळे यांचे पडसात ग्रामीण कादंबरीवरती पडणे साहाजिक होते. शेतकऱ्यांच्या आर्थिक परिस्थिती विषयी लिहिताना देशपांडे म्हणतात की, " ग्रामीण जनतेवरील म्हणजे मुख्यत्वे शेतकऱ्यांवरील कर्जाचे



ओझे वाढले. भारतातील बहुसंख्य शेतकऱ्यांना दारिद्र्यामुळे विविध गरजा भागविण्यासाठी वेळोवेळी कर्ज काढावे लागले. मग त्या गरजा कृषीसंबंधी असोत की अनुत्पादक स्वरूपाच्या (लग्न ,धार्मिक सणसभारंभ अथवा कार्य ) असोत कर्जाचा उपयोग उत्पादक कार्यासाठी करूनही त्यांची आर्थिक स्थिती विशेष न सुधारल्यामुळे कर्जाचा व त्यावरील व्याजाचा भार सतत वाढतच जाऊन ग्रामीण जनता ऋणग्रस्त होते.”<sup>३</sup> तसेच राजकीय लोक स्वार्थासाठी समाजाची विभागणी गटागटात करतात. त्यामुळे सामान्य माणूस आपआपसात भांडत बसतो. देश स्वतंत्र होऊनही त्याच्या नशिबी पारतंत्र्यच आहे. “स्वातंत्र्यानंतरचा समतेचा लढा इथेच उभारला गेला. शेतकऱ्यांच्या हक्कासाठी संघर्ष घडले ते इथेच अमेरिकन मिशनर इथ शैक्षणिक व सामाजिक सेवेचा आदर्श उभा केला. इथल्या सेवाभावी कार्यकर्त्यांनी शिक्षण संस्थांचे जाळ गुफलं आणि खेडयापाडयापर्यंत ज्ञानाचे पाझर पोहोचले”<sup>४</sup> आर्थिक दारिद्र्य त्यातून व्यसनाधिनता आजार अशा समस्यांच्या गर्तेत ग्रामीण समाज ओढला गेला. सारी ग्रामव्यवस्था रसातळाला जाऊ लागल. एकविसाव्या शतकातील ग्रामीण कादंबरीत हेच चित्रित व्हायला लागले. व. बा. बोधे यांची ‘पाननिवळी’ (२००७) आणि सुरेशकुमार लोंढे यांची ‘शाळा आणि माती’ (२००७) अशा काही कादंबऱ्या यादृष्टीने महत्त्वाच्या ठरतात.

#### वाढती बेकारी :-

ग्रामीण भागात शिक्षणाचा प्रसार वाढल्यामुळे नवीन पिढी शिक्षित झाली. शिक्षणाच्या काळात त्यांची शेतीकामाची सवय मोडते. पदवीधर झालेले हे तरुण शेतीकाम करीत नाही. दुसरीकडे एवढे शिक्षण घेतलेल्या या तरुणांना नोकऱ्या मिळत नाहीत. त्यांनी घेतलेले शिक्षण निकामी ठरते. शिकवण्यासाठी आई बापांनी केलेल्या खर्च वाया जातो. अनेकांनी शेती विकून कर्ज काढून मुलांना शिकवलेले असते. काहीनी कष्ट करून मुलांना शिकवलेले असते. त्यांच्याही आशा फोल ठरतात. नवशिक्षितांची ही नवी पिढी सैरभैर झालेली आहे. मुले शिकली तरी नोकरी मिळत नसल्यामुळे बेकारी वाढते. काही शेतात काम करतात. उपवर मुलींचे बाप आपल्या मुलींचे लग्न अशा नोकरी नसलेल्या मुलांबरोबर करण्यास तयार होत नाहीत. लग्नासाठी नोकरी मिळणे महत्त्वाचे होऊ लागले आहे. सदानंद देशमुख यांच्या (बारोमास ) २००२ या कादंबरीत याचे चित्रण येते.

#### समारोप :-

शेतकऱ्याला बारा महिने शेतात राबावे लागते. श्रम हेच त्यांचे भांडवल असते व त्याचीच गुंतवणूक करावी लागते. नवी पिढी शिकल्यामुळे तिला हे श्रम नको वाटतात त्यातून आर्थिक समस्या निर्माण होतात व त्यांना आत्महत्येसारख्या वाईट मार्गाला जावे लागते. वाढता खर्च कमी उत्पन्न यामुळे ग्रामीण भागातील माणसाला संसाराचा भार सहन होत नाही. तो आत्महत्येकडे वळतो. आज नवनविन तंत्रज्ञान येत आहे परंतु त्यासाठी पैसा शिल्लक राहत नाही. निसर्गाची अवकृपा, अतिवृष्टी, दुष्काळ शेतमालाला भाव न मिळणे, वाढती महागाई यामुळे शेतकरी हवादिल झालेला दिसतो व या सर्व परिस्थितीचे वर्णन या कालखंडातील कादंबऱ्यातून आलेले आहे.

#### संदर्भ ग्रंथ :-

१. नाईकवाडे शेषराव, (संपा) ‘जागतिकीकरण समकालीन बदलते संदर्भ’, अलंकार प्रकाशन, उमरी, प्र. आ. २०१२ पृ. १६९.
२. पाटील मोहन, ‘ग्रामीण साहित्य आणि संस्कृती’ स्वरूप प्रकाशन, औरंगाबाद प्र. आ. २००२ पृ.८४.
३. देशपांडे स.ह, ‘मराठी विश्वकोश’, खंड ०५ वा (संपा) जोशी लक्ष्मणशास्त्री (प्रकाशन) म.रा.सा.सं.मंडळ मुंबई १९७७ पृ. ३६१.
४. शेवते अरुण (संपा) ७० वे अखिल भारतीय मराठी साहित्य संमेलन, गडाख यशवंतराव व्दितीय आवृत्ती ०३ जानेवारी पृ. ७, ८.



# ENTIRE RESEARCH

MULTI-DISCIPLINARY

**INTERNATIONAL JOURNAL**

INDEXING WITH ISRA  
Peer Reviewed and Refereed Journal



MM's  
Chandrashekhar Agashe  
College of Physical  
Education, Pune, Maharashtra





# INDEX

Sr. No.	Title	Author Name	Page No.
1	Study of Muscular Endurance of School Students from Nashik District	Dr. Sopan Kangane Dr. Sunil More	1
2	Comparison of Psychological Barriers Among Competitive and Amateur Players	Dr. Yogesh Bodke Dr. Santosh Pawar	4
3	A Comparative Study Of Motion Examination Of Forehand Overhead Clear Stroke And Relationship Of Anthropometric Estimations At The time of Contact Stage in Badminton	Mr. Vijay B. Singh Dr. Balwant Singh	8
4	A Study On Speed And Strength Variables Of Indian Male Long Jumpers In Relation To Performance	Dr. Nilima Deshpande Dr.R. Subramanian Dr. Neha Ms Chaitaly Nandy	16
5	Comparative Study of Selected Physiological and Physical Variables of Inter Collegiate Level Baseball and Softball Players	Mr. Ravindra A. Kadane Dr. Bhaskar Reddy S. N.	21
6	Effect Of Meditation And Yogic Pranayama On Selected Physical And Physiological Variables	Mrs.S.Anbu Nisha Jeba Soundar Dr.S.Saroja	25
7	A Comparative Study Of Agility Ability Among The Kho-Khoand Football Players	Mr. Rupesh Vasant Rupwate	29
8	A Comparative Study On Body Composition And Physical Fitness Of Amature, State And National Level Adolescent Archers Residing In Mumbai.	Urmi Hariya Subhadra Mandalika	32
9	A Comparative Study on Selected Physical Fitness Components of Karate and Taekwondo Male School Players	Shiva Raj Bhatt	39
10	A Study on Injuries during Badminton Sports	Dr. Rajendra S. Raykar	43
11	Effect of Integrated Training Program on Selected Social Variables of Degree College Male Students	Dr. Aditya Anil Kulkarni Vishal Prakash Gaikwad	47
12	Effect of Pranayama on Recovery of Students undergoing Police Recruitment Training at Maharashtra Mandal Vyayamshala, Pune	Dr. Ameet Dattaram Prabhu	52
13	A Study of Anthropometrical, Physical fitness and Skills of Indian Roll Ball players participating at the International Level	Mr. Anand Mohan Yadav Dr. Sharad Shankarrao Aher	55
14	Study of Attitude towards and Physical Fitness Knowledge of Physical education Teachers of Elementary School Ahmednagar District	Mr. Satish D. Chormale Dr. Bhaskar Reddy S. N.	62
15	Effect of Yoga Training Program on Selected Skill Related Physical Fitness Factor & Shooting Performance of Inter School Male Basketball Players	Mr. Navanath M. Sarode Dr. D. K. Kamble	68
16	Assessment Tools for Physical Literacy Self Perception among Children and Adolescents: A Review	Beulah Sebastian Savio Viegas	72

95	Effect of Acupressure Program on Selected Fitness Variable of Kho-Kho Players Aged Between 14 to 18 Years	Dr. Shirish More Dr. Yogesh Bodke	436
96	Effect of Suryanamaskar on Selected Physical Fitness Variables of Stay at Home Peoples of Nashik City	Ravindra R. Chavan Dr. Vishwasrao. K. Kadam	439
97	Health Related Fitness And Its Impact On Sports Performance	Dr. Vijay L. Mhaske Prof. Vilas Uttam Elke	444
98	The Study of Exercise Adherence Ttechniques Used by Male Exercise participants at Maharashtra Mandal	Mr. Kumar Krishnanand Upadhyay Dr. Balaji Satwaji Pote	449
99	Caparison of Health-Related Physical Fitness Factors of Pune City and Pune District First Year Under-Graduate Girl Students of Savitribai Phule Pune University	Dr. Shrikant Mahadik	452
100	Psychological Effect of Injury on the Athlete	Ulhas V. Bramhe	456
101	Relationship Of Yoga, Immunity, Diet And Corona Virus-19 (Covid-19)	Dr. Rahul Rajan Bhosale	460
102	A Brief Study on new innovative factors to analyze coaching patterns for Indian Sports	Dr. Pradeep S Patil	464
103	Study of Health-Related Physical Fitness and Teaching Ability of Male Teacher Trainer	Dr. Balaji S. Pote	475
104	The Super Food Daliya Upma, the Nutritionally Dense Recipe for Fueling & Nourishing Athlete	Samarth Mahesh Deshpande Dr. Mahesh Deshpande	478
105	To Study the Health Effects of Slum Area in Pune City	Dr. Sheetal Laxman Shendkar	485
106	Analysis of Motor Fitness Components Between Different Sports	Dr. Yogesh Bodke Mr. Sachin Kamble	488



# HEALTH RELATED FITNESS AND ITS IMPACT ON SPORTS PERFORMANCE

**Dr. Vijay L. Mhaske**

Director of Physical Education & Sports  
Sharadchandra Pawar Mahavidyalaya, Lonand, Satara (Maharashtra)  
Email - mhaskevijay9@gmail.com

**Prof. Vilas Uttam Elke**

Director of Physical Education & Sports  
Radhabai Kale Mahila Mahavidyalaya, Ahmednagar (Maharashtra)

---

## ABSTRACT

*Regular exercise and physical activity promotes strong muscles and bones. It improves respiratory, cardiovascular health, and overall health. Staying active can also help you maintain a healthy weight, reduce your risk for type 2 diabetes, heart disease, and reduce your risk for some cancers. Aerobic exercise, like running and swimming, appears to be best for brain health. That's because it increases a person's heart rate, "which means the body pumps more blood to the brain," says Okonkwo. But strength training, like weight lifting, may also bring benefits to the brain by increasing heart rate. Health related physical fitness is primarily oriented towards systematic development of motor abilities and their manifestation through sports skills. Health related physical fitness help to improve sports performance. In Sports performance stamina, muscle strength, and body movement is important. It is develop by physical fitness training. Health-related components focus on factors that promote optimum health and prevent the onset of disease and problems associated within activity.*

## INTRODUCTION

To improve health and fitness effectively through physical activity or exercise, we need to understand how this comes about. For many of these changes, the stimulus has been grossly defined in terms of type, intensity, duration, and frequency of exercise, but for others a dose-response relationship has not been determined. Physical activity that appears to provide the most diverse health benefits consists of dynamic, rhythmical contractions of large muscles that transport the body over distance or against gravity at a moderate intensity relative to capacity for extended periods of time during which 200 to 400 kilocalories (or 4 kilocalories per kilogram of body weight) are expended. For optimal health benefits, such activity should be performed daily or at least every other day and should be supplemented with some heavy resistance and flexibility exercises. The greatest benefits are achieved when the least active individuals become moderately active; much less benefit is apparent when the already active individual becomes extremely active. Overexertion or inappropriate exercise can produce significant health risks. Research is needed to characterize better the health-promoting features of physical activity and exercise.

Sports performance is to enhance one's performance in competition and increase one's potential for success in a chosen sport or everyday activity. Sports performance is the execution of specific physical routines or acts by an athlete while participating in a sport or activity.



**Components of health related fitness :****Health related fitness divided into five parts****Cardiovascular Endurance**

Cardiovascular fitness is the ability of the heart (cardio) and circulatory system (vascular) to supply oxygen to muscles for an extended period of time. Cardiovascular is also called cardiorespiratory (lungs) fitness. Usually the mile run or some other type of continuous fitness activity (12 minute run, cycling, step-test, etc.) is used to assess

Cardiovascular fitness. Cardiovascular, which is synonymous with cardiopulmonary exercise or "Cardio", is aerobic physical activities that last longer than 90 seconds. Cardiovascular or cardiopulmonary endurance is your physical ability to maintain aerobic exercise for prolonged periods of time. Physiologically, cardiovascular endurance deals with the efficiency of your body's (heart, lungs and vascular system) ability to transfer oxygen rich blood to your working muscles during activities that last longer than 90 seconds.

**Important of Cardiovascular Endurance**

Life without exercise or physical Fitness contributes to the early onset and progression of life style disease such as cardiovascular disease, hypertension, diabetes and obesity.

The importance of cardiovascular fitness to health for all individuals has been well documented. Physical fitness is a required element for all the activities in our life. Cardiovascular fitness of an individual is mainly dependent on lifestyle related factors such as daily physical activity levels. It was believed that the low cardiovascular fitness level of an individual is associated with higher mortality rate. (jourklesh et.al.2012). Cardiovascular endurance is very important because the more cardiovascular fit you are, the healthier your lungs, heart and vascular system is. While exercising this may be obvious to you but there is more. If you demonstrate high levels of cardiovascular endurance during exercise you also have more efficient heart, lungs and vascular system while at rest which takes up the bulk of your time. This means less stress is put on your heart and lungs around the clock which enables you to avoid illness and live a long healthy life. Many argue that cardiovascular endurance is the most important of the 5 components to physical fitness.

In sports cardiovascular endurance is important for improves your posture and health, Enhances stamina which improves your performance ability, Boosts your immune system and reduces the risk of injury, Increases oxygen supply to muscles – efficient functioning Improves your anaerobic ability, Reduces the risk of fatigue, enhances concentration and reduces stress levels.

**MUSCULAR STRENGTH**

Muscular strength refers to the maximum amount of force a muscle can exert against an opposing force. Fitness testing usually consists of a one-time maximum lift using weights (bench press, leg press, etc.). Muscular strength is the amount of force your muscle can exert against resistance for short duration, anaerobic (without oxygen) activities. Resistance includes external objects such as free weights or household objects as well as your own body weight. Physiologically, muscular strength it is the ability to your body to supply ATP (Adenosine Tri-Phosphate or muscle energy) to your muscle fibers for concentric, eccentric and isometric contractions in short times, which range from 0 to around 15 seconds.



## **IMPORTANT OF MUSCULAR STRENGTH**

While muscular strength may be subjective, the primary reason why muscular strength is important is your efficiency at Activities of Daily Living (ADLs). ADLs one of the most important reasons why being proficient at all 5 components of physical fitness is important. At the very least, to be physically fit for in the muscular strength department, you should demonstrate the basic muscular strength needed to efficiently your ADLs. While ADLs vary from person to person, you can also consider activities such as push-ups, pull-ups and carrying heavy objects as ADLs. Even though each of the 5 components of fitness depends on one another, poor muscular strength can also affect aerobic fitness and muscular endurance negatively.

Muscular strength can enhance the ability to perform general sport skills such as jumping, sprinting, and change of direction tasks. Muscular strength allows an individual to potentiate earlier and to a greater extent, but also decreases the risk of injury. Greater muscular strength when it comes to improving an individual's performance across a wide range of both general and sport specific skills while simultaneously reducing their risk of injury when performing these skills.

In sports muscular strength is important for increase your ability to do performance in sports without getting tired, Reduce the risk of injury, Help you keep a healthy body weight, Lead to healthier, stronger muscles and bones and Improve confidence and how you feel about yourself.

## **MUSCULAR ENDURANCE**

Muscular endurance refers to the ability of the muscle to work over an extended period of time without fatigue. Performing pushups and sit-ups or crunches for one minute is commonly used in fitness testing of muscular endurance. While muscular strength deals with short duration muscle contractions muscle endurance deals with sustained muscle contractions and other anaerobic activities lasting less than about 90 seconds. Muscular endurance is the bridge between muscular strength and cardiovascular endurance. In order to be cardiovascular fit, you must demonstrate muscular endurance. Physiologically while muscle strength deals primarily with type II, fast twitch muscle fibers, muscular endurance deals with primarily type I, slow twitch muscle fibers. Your body contains both but only anaerobic exercises which last longer than around 15 seconds and less than 90 seconds strengthen your type I muscle fibers.

In sports muscular endurance is important for helping maintain good posture and stability for longer periods, improving the aerobic capacity of muscles, improving the ability to carry out sports performance activities, increasing athletic performance in endurance-based sports.

## **FLEXIBILITY**

Flexibility is the range of motion possible for each of your joints or groups of joints. To some degree, your flexibility determines how efficiently your muscles are. Increased flexibility has also been associated with decreased risk of acute and chronic (overuse) injuries. Poor flexibility can directly affect cardiovascular endurance, muscle strength and muscular endurance. Physiologically flexibility can include extra-muscular (range of motion at a joint) and intramuscular factors such as hyper tonicity (knots) within the muscles themselves.

Flexibility is important for completing sports activities with ease, increased joint mobility, better posture, decreased back pain and a lower risk of injury. Improved performance of daily sport performance activities, Improved performance in sport, Enhanced joint health, Relief of pains. Relief of muscle cramps, Relaxation and stress relief (mental and physical), Improved posture and balance.



## **BODY COMPOSITION**

Body composition is the percentage of your body's tissues which you exhibit. The easiest way to look at body composition is with a 2 compartment analysis which estimates the amount of body fat you have with lean body mass which includes muscle, bone, water, and organs. It takes expensive equipment for a 3 compartment analysis which isolates bone mass which can also be considered an important part of body composition. You could say body composition depends on the other components of physical fitness. Having a poor body composition has many negative physical and psychological effects such as increased chance of a host of chronic diseases and depression. As mentioned previously, improper exercise habits and choices can not only lead to being overweight and obesity, but decreased bone mass associated with osteopenia and osteoporosis.

## **NEED OF PHYSICAL FITNESS**

Regular physical activity can improve your muscle strength and boost your endurance. Exercise delivers oxygen and nutrients to your tissues and helps your cardiovascular system work more efficiently. And when your heart and lung health improve, you have more energy to tackle daily chores. Regular physical activity can help children and adolescents improve cardio respiratory fitness, build strong bones and muscles, control weight, reduce symptoms of anxiety and depression, and reduce the risk of developing health conditions. Exercise can help provide: Sharper memory and thinking. The same endorphins that make you feel better also help you concentrate and feel mentally sharp for tasks at hand. Exercise also stimulates the growth of new brain cells and helps prevent age-related decline

## **IMPACT ON SPORTS PERFORMANCE**

Health related physical fitness training can improve stamina, strength, body movement and body posture. Physical fitness leads to better athletic performance, and persistent training will usually develop physical fitness. Ability of the endurance athlete to use oxygen is related to circulatory and respiratory capacity, but in sprints, weight lifting, and swimming there are many other important specifics. In sports, good physical fitness can increase the efficiency of learning sports skills, but also can reduce the incidence of injuries and accidents caused by the movement. Maintain and improve sports performance by health related physical fitness training.

## **REFERENCES**

- Caspersen C. J., Powell K. E., Christenson G.M. (1985) "Physical activity, exercise, and physical fitness: definitions and distinctions for health-related research", *Public Health Rep* 100:126-131
- Hulens M, Vansant G, et.al. (2002), "Health-related quality of life in physically active and sedentary obese women", *Am J Hum Biol.* 2002 Nov-Dec; 14(6):777-85.
- Ismailov R. M. , Leatherdale S. T. (2010), "Rural-urban differences in overweight and obesity among a large sample of adolescents in Ontario." *Int. Journal of / .PPediatrObes.* Aug; 2010, 5(4):351-60.
- Jourkeshet. al. (2011) *Annals of Biological Research*, , 2 (2):460-467
- Juhee Kim, Aviva Must et. al. (2005), "Relationship of Physical Fitness to Prevalence and Incidence of Overweight among Schoolchildren", *Obesity Research* (2005) 13, 1246-1254; doi: 10.1038/oby.2005.148
- Lamb KL, Brodie DA, Roberts K (1988) "Physical fitness and health-related fitness as indicators of a positive health state", *Health Promoting* 3:171-182.
- L. O. Amusa, D. T. Goon (2011), "Health-related physical fitness among rural primary school children in Tshannda, South Africa" *Scientific Research and Essays Vol. 6(22)*, pp. 4665-4680, 7 October, 2011, Available online at <http://www.academicjournals.org/SRE> ISSN 1992-2248 ©2011 Academic Journals



- Maria Eugenia Peña Reyes, SweeKheng Tan, et. al., (2003), "Urban-rural contrasts in the physical fitness of school children in Oaxaca, Mexico", Article first published online: 27 OCT 2003 DOI: 10.1002/ajhb.10218
- MehtapÖzdirenc, AyseÖzcan, et.al (2005), "Physical fitness in rural children compared with urban children in Turkey", Article first published online: 2 FEB 2005 DOI: 10.1111/j.1442-200x.2004.02008.x
- Pongprapai S, Mo-suwan L, et. al. (1994) "Physical fitness of obese school children in Hat Yai, southern Thailand", Jun;25(2):354-60.
- Sallis, J.F., McKenzie, et. al. (1999) "Effects of health – related physical education on academic achievement", Project SPARK, Research Quarterly for Exercise and Sport, 70:127-134.
- Retrieved from <https://www.danceacademyusa.com/2014/09/19/the-importance-of-cardiovascular-endurance-for-the-dancer/>
- Retrieved from <https://thesportsedu.com/muscular-endurance-definition/>
- Retrieved from <https://www.acefitness.org/education-and-resources/professional/expert-articles/5598/the-impact-of-flexibility-training-on-performance/>
- Retrieved from <https://pubmed.ncbi.nlm.nih.gov/26838985/>
- Retrieved from <https://thesportsedu.com/cardiovascular-endurance-definition/>
- Retrieved from <https://www.healthlinkbc.ca/physical-activity/muscular-strength-and-endurance>
- Retrieved from <https://www.medicalnewstoday.com/articles/muscular-endurance#how-to-improve>

ISSN 2277 - 5730  
AN INTERNATIONAL MULTIDISCIPLINARY  
QUARTERLY RESEARCH JOURNAL

# AJANTA

Volume - IX

Issue - III

JULY - SEPTEMBER - 2020

ENGLISH / MARATHI PART - II  
Peer Reviewed Referred  
and UGC Listed Journal

Journal No. 40776



ज्ञान-विज्ञान विमुक्तये

IMPACT FACTOR / INDEXING  
2019 - 6.399  
[www.sjifactor.com](http://www.sjifactor.com)

❖ EDITOR ❖

**Asst. Prof. Vinay Shankarrao Hatole**

M.Sc (Maths), M.B.A. (Mktg.), M.B.A. (H.R.),  
M.Drama (Acting), M.Drama (Prod. & Dir.), M.Ed.

❖ PUBLISHED BY ❖



**Ajanta Prakashan**

Aurangabad. (M.S.)



## CONTENTS OF ENGLISH



S. No.	Title & Author	Page No.
1	Strategic Location of Bhaje Caves with Respect to Ancient Trade Routes in Western India <b>Samir Vasant Mankar</b>	1-9
2	Hostel Movement in Solapur <b>Dr. Dhanaji B. Masal</b>	10-16
3	Review of Literature on Lokmanya Bal Gangadhar Tilak <b>Dr. Nalini Avinash Waghmare</b>	17-24
4	Tilak Views on Nationalism <b>Dr. Suma. S. Nirni</b>	25-29
5	Political Ideas of Bal Gangadhar Tilak's <b>Dr. Nivedita Swami</b>	30-36
6	Mesolithic Culture of Karha Basin, Pune District, Maharashtra <b>Dr. Kshirsagar Shivaji Dadaso</b>	37-42

## ❧ CONTENTS OF MARATHI PART - II ❧

अ.क्र.	शोधनिबंध आणि लेखकाचे नाव	पृष्ठ क्र.
१	अण्णाभाऊ साठे यांचे संयुक्त महाराष्ट्राच्या चळवळीतील योगदान <b>डॉ. गंगणे जीवन सुदामराव</b>	१-५
२	सत्यशोधकीय विचारवंत आण्णाभाऊ साठे <b>प्रा. डॉ. सावंत जे. सी.</b>	६-९
३	साहित्यिक अण्णाभाऊ साठे यांचे योगदान <b>डॉ. उर्मिला क्षीरसागर</b>	१०-१४
४	अण्णाभाऊ साठे यांच्या निवडक कथात्मक साहित्यातील स्त्री चित्रण <b>प्रा. डॉ. सौ. कल्पना राजीव मोहिते</b>	१५-२१
५	आण्णाभाऊ साठे यांच्या साहित्यातील मानवतावाद संघर्ष आणि स्थानिक इतिहासाचे वास्तववादी चित्रण <b>प्रा. डॉ. वंदना रा. लोंढ</b>	२२-२५
६	खिरविरे येथील सावकारांच्या वद्दांची होळी (७ नोव्हेंबर १९४९) <b>डॉ. गणेश शंकर विधाटे</b>	२६-२८
७	दुसऱ्या महायुद्धातील यशवंत घाडगे यांची कामगिरी <b>किरण गणपत कुंभार</b>	२९-३१
८	प्रजाहितदक्ष जयसिंगराव घाटगे <b>राजेंद्र मा. घाडगे</b>	३२-३६
९	घारापुरी लेणीचा एक ऐतिहासिक अभ्यास <b>डॉ. भानुदास धोंडिबा शिंदे</b>	३७-४१
१०	डॉ. संजीवनी सतीष केळकर यांचे कार्य <b>डॉ. एस. एन. गायकवाड</b>	४२-४५
११	उत्तर पेशवेकालीन तुरुंग व्यवस्था <b>प्रिया ब्रिजेश कुलकर्णी</b>	४६-४८
१२	शेतकऱ्यांच्या व्यथा व महात्मा फुले यांचे उपाय <b>प्रा. कोकाटे अनिल दत्तात्रय</b>	४९-५२



## ६. खिरविरे येथील सावकारांच्या वहांची होळी (७ नोव्हेंबर १९४९)

डॉ. गणेश शंकर विघाटे

इतिहास विभाग, राधाबाई काळे महिला महाविद्यालय, अहमदनगर, ता. जि. अहमदनगर.

**महत्वाचे शब्द :-** रोखेफाडी, गहाणखते, खरेदीखते, सालखते, लाल वावटा

### प्रस्तावना

अहमदनगर जिल्हा हा जहाल शेतकऱ्यांचा जिल्हा म्हणून ओळखला जातो. 'शेतकरी आम्ही झालो समदं लाल वावटेवाल' असे अहमदनगर जिल्हयातील कम्युनिस्ट विचारांचे शेतकरी अभिमानाने म्हणत असत. जिल्हयातील कम्युनिस्ट पक्ष मजबूत करण्याचे काम या शेतकरी चळवळीच्या माध्यमातून झालेले दिसून येते. अशा या शेतकऱ्यांची नगर जिल्हयातील संघटित चळवळ खऱ्या अर्थाने सुरू झाली ती कम्युनिस्ट पक्षाच्या नेतृत्वाखाली किसान सभेची स्थापना झाल्यापासून. किसान सभेच्या अजेड्यावर असलेला महत्वाचा कार्यक्रम म्हणजे सावकारशाही विरोधी दस्तऐवजे ताब्यात घेऊन ती फाडणे अगर नष्ट करणे होय. या सावकारशाही विरोधी चळवळीचा महत्वाचा भाग म्हणजे नगर जिल्हयातील खिरविरे येथील सावकारांच्या वहांची होळी होय.

१. **खिरविरे गावातील सावकारांची पूर्वपीठिका :-** सावकारशाहीला विरोध हा कम्युनिस्टांचा एक प्रभावी कार्यक्रम होता. अहमदनगर जिल्हयातील अकोले तालुक्याच्या वायव्य भागात खिरविरे हे एक दुर्गम गाव आहे. गावातील बहुसंख्य लोक आदिवासी शेतकरी होते.<sup>१</sup> या गावात शहा, मेहता या आडनावांची व्यापारी सावकारांची ७-८ कुटुंबे मोठमोठ्या वाड्यात वास्तव्य करून होती. डांग, टोकद, घोटी, इगतपूरी, समशेरपूर इत्यादी गावांमध्ये त्यांची मोठी सावकारी होती. ते लोकांच्या निश्चरता, अडचणीचा गैरफायदा घेऊन कर्जाच्या बदल्यात खोटी दस्तऐवज लिहून घेत असत. फसवला गेलेला शेतकरी न्यायालयात गेला असता तेथे त्याचा टिकाव लागत नसे. अनेक शेतकऱ्यांच्या जमिनी या सावकारांनी गिळंकृत केलेल्या होत्या. त्यामुळे या शेतकऱ्यांमध्ये मोठा असंतोष होता.<sup>२</sup>
२. **सावकारी दस्तऐवज बाहेर काढून त्याची होळी करण्याचा कार्यक्रम :-** महाराष्ट्र राज्य किसान सभेची पहिली परिषद टाणे जिल्हयातील टिटवाळ्याला १२ जानेवारी १९४५ रोजी भरली. महाराष्ट्रातील किसान सभेची अध्येक्ष्य होते कॉ.शामराव परुळेकर आणि गोदूताई परुळेकर. ऐतिहासिक कम्युनिस्ट पक्षाच्या नेतृत्वाखालील वारली आदिवासींचे बंड सुरू झाले ते किसान सभेच्या या परिषदेतून स्फूर्ती घेवूनच. मे १९४५ मध्ये टिणगी पडलेल्या या बंडाचा वणवा सर्व आदिवासी भागात दोन वर्षांत पसरला. या वणव्यात सर्व प्रकारची वेंटविगारी आणि गुलामगिरी

जळून राख झाली.<sup>३</sup> या परिषदेतील कार्यक्रमानुसार सन १९४६ साली गुहा, गहुरी येथील शिवीगमध्ये कॉ.शामराव परुळेकर व गोदूताई परुळेकर यांनी सावकारांचे दस्तऐवज बाहेर काढून त्यांची सार्वजनिक ठिकाणी होळी करवयाची, आदिवासी कर्जमुक्त झाला असे घोषित करवयाचे असा विचार मांडला होता.<sup>४</sup>

३. **सावकारशाही विरोधी चळवळीची कार्यवाही :-** कॉ. मुरलीधर नवले, कुशाबा नवले, भाऊसाहेब थोगत, कॉ. धर्मा कमा भांगरे, कॉ. सकुभाई मंगळ यांनी अकोले व संगमनेर तालुक्यातील कार्यकर्त्यांची एक बैठक बोलावली. बैठकीत सावकारांच्या घरावर मोर्चा काढून त्यांच्या ताब्यातील शेतकऱ्यांची गहाणखते, खरेदीखते, सालखते ताब्यात घेऊन त्यांची भर चौकात होळी करवे असा कार्यक्रम ठरला.<sup>५</sup>

या मोहिमेचे नेतृत्व कॉ. मुरलीधर नवले यांनी करवले असे ठरले. ७ नोव्हेंबर हा रशियन राज्यक्रांतीचा स्मृतीदिन. सावकारांजवळची कागदपत्रे जाळण्यासाठी कार्यकर्त्यांनी हा दिवस जाणीवपूर्वक निवडला. गजूर, अकोले, गजापूर, संगमनेर, खिरविरे इत्यादी गावातील १०० कार्यकर्त्यांनी लाल बावट्याचा जयजयकार करित खिरविरे गावात प्रवेश केला व सावकारांच्या घराला वेढा घातला. आपल्याकडील सर्व कागदपत्रे जमा करण्याचे सावकारांना आवाहन केले. सावकारांनी त्यांच्याकडे दुर्लक्ष करून दरवाजे बंद केले. अखेर बळजबरीने एकएका सावकारांच्या घरात प्रवेश करून तिजोरीतील कर्जाचे दस्तऐवज गोळा केले आणि गावातील मंदिरसमोर उपस्थित लोकांसमोर त्यांची जाहीर होळी केली. यावेळी सावकारांच्या घरातील बायकांमुलांना कोणत्याही प्रकारचा त्रास कार्यकर्त्यांनी दिला नाही. तसेच त्यांच्या गेकड व दागिन्यांना हातही लावला नाही. जमलेल्या जमावाला उद्देशून कॉ. मुरलीधर नवले म्हणाले, "भावा-बहिणींनो सावकारांच्या जाचातून तुम्ही आता मुक्त झाला आहात. तुमच्या जमिनीचे खोटे दस्तऐवज तुमच्या सर्वांच्या साक्षीने आगीच्या भक्षस्थानी पडले आहेत. आता तुम्ही घाबरायचे कारण नाही. तुम्ही कर्जमुक्त झालात. तुमच्या जमिनी जर सावकारांनी ताब्यात घेतल्या असतील, तर लगेच आजपासून तुम्ही कसायला सुरुवात करा. किसान सभा सदैव तुमच्या पाठीशी आहे. सावकारांनी अरेगवी व अत्याचार केले तर आम्हाला बोलवा. बोला लाल बावटे की जय."<sup>६</sup>

४. **सरकारी दडपशाही :-** खिरविरे प्रकरणाची बातमी जिल्ह्यात वाऱ्यासारखी पसरली. कॉ.बुवासाहेब नवले, कॉ. कुशाभाऊ नवले, कॉ. मुरलीधर नवले यांच्याकडे बंदुका असूनही त्यांनी त्याचा प्रत्यक्ष वापर केला नाही.<sup>७</sup> मात्र एका सावकाराने पोलीस स्टेशनला या नेत्यांच्या विरोधात खून आणि दरोड्याची तक्रार केली. परंतु पोलीसांची धाड पडण्याआधीच प्रमुख नेते भूमिगत झाले. मात्र काहींना अटक करण्यात आली. अटक झालेल्यांमध्ये निवृत्ती गोडसे, विठ्ठल हासे यांचा समावेश होता. सरकारने या घटनेनंतर कॉ. मुरलीधर नवले, रावसाहेब शिंदे, भाऊसाहेब थोगत, कॉ. धर्मा कमा भांगरे यांच्यावर हजारे रूपांची बक्षिसे लावली. अहोरात्र त्यांच्या मागे पोलीसांचा ससेमारा लागला. त्यांना आश्रय देणाऱ्यांचा पोलीसांनी छळ आरंभला. पोलीसांच्या दडपशाहीचा सर्वत्र वखटा फिरू लागला.<sup>८</sup>

खिरविरे प्रकरण हे दक्षिणेतील गेखेफाडीच्या (दख्खनचे दगे) चळवळीशी साधर्म्य दाखविणाऱ्या चळवळ होती. सावकारांच्या व्ह्याची होळी करणाऱ्याची घटना ही आदिवासी भागातील एक क्रांतिकारी घटना ठरली. या घटनेचा निर्णय स्थानिक नेत्यांनी घेतलेला होता. आपल्यावर अन्याय करणाऱ्यांना कम्युनिस्टांनी धडा शिकवल्याचे उदगार जनतेच्या मुखातून निघत होते. त्यामुळे त्यांनी या कृतीचे भरभरून समर्थन केले अशी नोंद गवसाहेब शिंदे आपल्या 'ध्यासपर्व' या आत्मचरित्रात करतात.<sup>१</sup>

### संदर्भसूची

१. <https://www.swapp.co.in/site/newvillage.php?stateid=8y68qEDJ0ugeDsGafWxiUw%3D%3D&districtid=Gzqu0R2%3BQznAgPCZAHkdA%3D%3D&subdistrictid=cJBMqm8xqVILPwNDLFeFuW%3D%3D&areaid=P%2F8CBV%2FYHKhxJYqUIDZ9OQ%3D%3D>, last seen at 01/09/2020
२. शिंदे गवसाहेब, 'ध्यासपर्व. A Rebel for a Cause', अमेय प्रकाशन, पुणे, चौथी आवृत्ती २००९, पृ.क्र. २२६.
३. <https://www.mahacpim.in/our-history-marathi/>, last seen at 02/09/2020
४. कडू पी.बी., क्रांतिपंढरीचा वारकरी (शब्दांकन: सविता भावे), प्रकाशक, अरूण पुंजाजी कडू, सात्रळ, गहुरी, सप्टेंबर २०१४, पृ.क्र.६२.
५. [https://mr.wikipedia.org/wiki/%E0%A4%AD%E0%A4%BE%E0%A4%B8%E0%A4%8D%E0%A4%95%E0%A4%B0%E0%A4%B0%E0%A4%BE%E0%A4%B5\\_%E0%A6%E0%A5%81%E0%A4%B0%E0%A5%8D%E0%A4%B5%E0%A5%87](https://mr.wikipedia.org/wiki/%E0%A4%AD%E0%A4%BE%E0%A4%B8%E0%A4%8D%E0%A4%95%E0%A4%B0%E0%A4%B0%E0%A4%BE%E0%A4%B5_%E0%A6%E0%A5%81%E0%A4%B0%E0%A5%8D%E0%A4%B5%E0%A5%87), last seen at 02/09/2020
६. शेवाळ विद्दल, पेटलेले दिवस — संगमनेर अकोल्याच्या कम्युनिस्ट पक्षाचा प्रेरक इतिहास, प्रकाशक कॉ. गोविंद पानसरे अमृत महोत्सव समिती, रेड फ्लॅग बिल्डिंग, विंदू चौक, कोल्हापूर, पहिली आवृत्ती, २००९, पृ.क्र.५३, ५४.
७. ढोल अशोक एकनाथ, कॉ.पी.बी.कडू पार्टील जीवन व कार्य : एक चिकित्सक अभ्यास (१९२१-१९९६), टिळक महाराष्ट्र विद्यापीठ, पुणे, २०१४
८. <http://nawalewadi.com/history.html>, last seen at 03/09/2020
९. शिंदे गवसाहेब, ध्यासपर्व. A Rebel for a cause, उपरोक्त, पृ.क्र.२२७.



## अहमदनगर जिल्ह्यातील कम्प्युनिस्ट पक्षाचा जमीन बळकाव लढा

प्रा. डॉ. विश्वाटे गणेश शंकर

इतिहास विभाग, राधाबाई काळे महिला महाविद्यालय, अहमदनगर, ता.जि. अहमदनगर.

### प्रास्ताविक

आशिया खंडात सहकार चळवळीची पायाभरणी करणाऱ्या अहमदनगर जिल्ह्यास महाराष्ट्रातील कम्प्युनिस्ट चळवळीच्या इतिहासात महत्त्वाचे स्थान आहे. कारण कष्टकरी शेतकरी समुदायात व ग्रामीण भागात कम्प्युनिस्ट पक्षाने याच जिल्ह्यात भक्कमपणे पाय रोवले. स्वातंत्र्योत्तर काळात अहमदनगर जिल्ह्यातील शेतकऱ्यांच्या जमीन विषयक प्रश्नावर कम्प्युनिस्ट पक्षाने केलेल्या चळवळीमध्ये जमीन बळकाव लढ्याच्या चळवळीस अनन्यसाधारण महत्त्व असल्याचे दिसून येते. या चळवळीच्या माध्यमातून स्वकीय सरकारच्या शोषक व जुलमी धोरणांचे जिल्ह्यातील कम्प्युनिस्ट पक्षाने हिंडीम स्वरूप दर्शवून वंचित घटकांच्या प्रति आपली बांधिलकी स्पष्ट केल्याचे दिसते.

महत्त्वाचे शब्द : सिलिंग, लाल बावटा, कॉंग्रेस, ज्या जमीन धारणा कमाल कायदा, जबरन जोत,

### शोधनिबंधाचा उद्देश :

१. जमीन बळकाव लढ्याची पार्श्वभूमी समजून घेणे.
२. भारतीय कम्प्युनिस्ट पक्षाचा जमीन बळकाव लढ्याच्या हेतूचा मागोवा घेणे.
३. कॉंग्रेस सरकारची जमीन बळकाव लढ्यासंबंधीची प्रतिक्रिया जाणून घेणे.
४. १९६२ च्या महाराष्ट्र सरकार जमीन धारणा कमाल मर्यादा ठरविणाऱ्या कायद्याची वस्तुस्थिती जाणून घेणे.
५. भारतीय कम्प्युनिस्ट पक्षाच्या सिलिंग कायद्यामागच्या भूमिकेचा आढावा घेणे
६. अहमदनगर जिल्ह्यातील कम्प्युनिस्ट पक्षाच्या जमीन बळकाव लढ्यातील कामगिरीचा आढावा घेणे.

### 1. जमीन बळकाव लढ्याच्या पार्श्वभूमी :

१९५२ च्या दुष्काळाच्या पार्श्वभूमीवर अहमदनगर जिल्ह्यात कम्प्युनिस्ट पक्ष, रिपब्लिकन पक्ष व लाल निशाण पक्षाने सरकारकडे असलेली हजारो एकर जमीन आदिवासी, हरिजन भूमिहीनांना मिळावी या करिता भूमिहीनांच्या चळवळीची यशस्वी मुहूर्तमेढ रोवली होती. या चळवळीतील जमीन बळकाव लढा हा पुढचा महत्त्वाचा टप्पा होता. भारतीय कम्प्युनिस्ट पक्षाने संपूर्ण देशामध्ये सिलिंगचा कायदा झाला पाहिजे याकरिता १९७० साली अखिल भारतीय पातळीवर एक मोठा जमीन बळकाव लढ्याचा कार्यक्रम हाती घेण्याचा निर्णय घेतला. कारण कम्प्युनिस्ट पक्षाच्या मते स्वातंत्र्य मिळून २३ वर्षे होऊनही कॉंग्रेस सरकार शेतकऱ्यांना त्यांच्या उदरनिर्वाहाचे साधन (शेतकीचे मालकी हक्क) उपलब्ध करून देण्यात अपयशी ठरले होते. राज्यातील कॉंग्रेस सरकारने शेतीबाबत अनेक कायदे केले. शेती विकासावर प्रचंड पैसा खर्च केला. तरीही ग्रामीण भागातील ८० टक्के शेतमजूर, गरीब शेतकरी दरिद्री जीवन जगत होते. खेड्यातील ४० टक्के जनता भूमिहीन होती. जे शेतकरी भूमालक होते त्यांच्याकडे तुटपुंजी जमीन होती. याउलट ८ टक्के लोक असे होते, की त्यांच्याकडे लागवडीखाली असलेल्या जमिनीचा ३६ टक्के मालकी भाग होता. त्यात जुने राजेरजवाडे, वडे जमीनदार, पूर्वीचे जहागीरदार, बडे उद्योगपती आदींचा समावेश होता. त्यामुळे जमिनीवरची ही प्रस्थापितांची मक्तेदारी नष्ट करून त्यांच्याकडील जमिनी भूमिहीनांना दिल्या जात नाही, तोपर्यंत शेतमजूर आणि गरीब शेतकऱ्यांचे जीवनमान सुधारणे शक्य नाही असे कम्प्युनिस्टांचे मत होते. १ कॉंग्रेस सरकार मात्र देशात पुरेशी जमीनच नाही, आहे त्या जमिनीचे आम्ही वाटप करून टाकले आहे अशा थापा मारीत होते. एम. एस. दांतवालांसारखे सरकारधार्जिणे अर्थशास्त्रज्ञ जमीन मालकी संबंधाबाबत पंजाब, तामिळनाडू व आंध्रप्रदेश या राज्यात पुरोगामी कायदे झालेले नसतानाही तेथे हरितक्रांतीने अपेक्षेपेक्षा जास्त यश प्राप्त केल्याचे दिसून येते. याउलट महाराष्ट्र व गुजरातसारख्या राज्यात जमीनविषयक विशेषतः कुळांच्या बाबत प्रगत कायदे झालेले आहेत त्या राज्यात शेती उत्पादनक्षमतेची वाढ वेताचीच आहे असा निष्कर्ष काढण्यात मशगुल होते. शेती उत्पादनाला आणि उत्पादनक्षमतेला हानीकारक अशा जमीनविषयक सुधारणा सरकारने टाळाव्यात असे त्यांचे मत होते. सरकारनेही हरितक्रांतीला, वाढत्या शेतीउत्पादनाला महत्त्व देऊन त्यामागे जमीनवाटप व जमीनसुधारणा घडवून आणून शेती उत्पादनात वाढ करण्याचा मार्ग अवरूद्ध करून टाकला. काँ. डांगे सरकारच्या या धोरणावर टिका करताना म्हणतात, "जमीनमालकी संबंधात सामाजिक जीवनात, शासनसंस्थेत एकूण समाज व अर्थव्यवस्थेत रचनात्मक बदल न करता शेती व्यवस्थेतील तांत्रिक प्रगतीवर दिलेला एकांगी भर हा प्रगतीविरोधाचा धोका वाढवीत आहे." अमेरिकन अर्थतज्ञ सोलोन वारक्लोभ भारत सरकारच्या जमीन सुधारणेवर भाष्य करताना म्हणतो, "शेती मालकी संबंधात फेरबदल करण्याच्या प्रश्नाला वगळ दिली तरी त्या प्रश्नाशी चार डोळे करण्याचा क्षण टळत नाही आणि राज्यकर्त्यांनी टाळाटाळ केली तरी अविकसीत देशातील कष्टकरी जनता तो अशा पद्धतीने सोडविल की ती सुखावलेल्या जमीनदारांना सुखावह



होणार नाही."२ त्यातच जमीनधारणेच्या कमाल मर्यादेच्या कायद्यात सरकारने अनेक पळवाटा करून ठेवल्या होत्या. उदा: १९६२ साली महाराष्ट्र सरकारने जमीन धारणेची कमाल मर्यादा ठरविणारा कायदा केला. हा कायदा म्हणजे जमीन मालकी संबंध सुधारणेचा अखेरचा टप्पा व जमीन मालकी संबंधात विषमता नष्ट करणारा कायदा होय असे काँग्रेसजन आत्मप्रौढीने सांगू लागले. मात्र वस्तुस्थिती वेगळीच होती. महाराष्ट्रात ३० एकर जमिनीवर ११ टक्के खातेदार आहेत व शेतकऱ्यांच्या ६ टक्के खातेदार आहेत. परंतु त्यांच्याजवळ ४२ टक्के जमीन आहे. ह्याउलट ५ एकरपर्यंत ३७ टक्के खातेदार व १५ टक्के शेतकरी असून फक्त ७ टक्के जमीन त्यांच्याजवळ आहे. त्यामुळे ही जमीन मालकी संबंधात विषमता नव्हे तर आणखी काय असा सवाल कम्युनिस्ट सरकारला विचारू लागले. या कायद्यात जमीनदारांना पळवाटा असल्यामुळे आणि मर्यादेचे क्षेत्र अधिक ठेवल्यामुळे जमिनीचे केंद्रीकरण अव्यधित राहिले. उदा: १९५६ सालच्या भाऊसाहेब हिरे यांच्या कुळ कायद्यातील तरतुदीनुसार बारमाही पाणी, दोन व एका हंगामातील पाणीपुरवठा जमिनीसाठीचे प्रमाण व कोरडवाहू जमीनसाठीचे कमाल जमीन धारण प्रमाण अनुक्रमे १२, २४, २७ व ४८ एकर असे ठेवण्यात आले. याउलट १९६२ च्या जमीन धारणा कमाल कायद्यानुसार बारमाही पाणी, दोन व एका हंगामातील पाणीपुरवठा जमिनीसाठीचे प्रमाण व कोरडवाहू जमीनसाठीचे कमाल जमीन धारण प्रमाण अनुक्रमे १८, २७, ३० व ६६ ते १२६ एकर (व्यक्तिगत मालकीच्या जमिनीवर व कुटुंबाला सवलत) असे ठेवण्यात आले. त्याचा फायदा घेऊन मत्तेदार, जमीनदार, उच्च अधिकारी, मंत्री यांनी लाखो शेतकऱ्यांना त्यांच्या हक्काच्या जमिनीपासून वंचित ठेवले. ३

**1. भारतीय कम्युनिस्ट पक्षाची जमीन बळकाव लढ्याची भूमिका व उद्देश :** भारतीय कम्युनिस्ट पक्षाने काँग्रेस सरकारचा हा धूर्त डाव ओळखून जनतेचे या प्रश्नावर प्रबोधन करावयास सुरुवात केली. एकीकडे जनतेला समाजवादाचे डोस पाजावयाचे तर दुसरीकडे जमीनदारशाही नष्ट करून भूमिहीनांना हक्काची जमीन मिळवू द्यावयाची नाही असा धूर्त खेळ सरकार वाटप करायला पडजमिनच शिल्लक नाही असा प्रचार . आपल्याशी खेळत आहे हे जनतेने ओळखलेर प्रस्थापित सरकार, जनसंघ व हितसंबंधी करीत असतांना देशात ९ कोटी एकर सरकारी पडजमिन, ३ कोटी एकर जंगलाची जमीन व ९ कोटी एकर वरकड जमीन अशी एकूण २१ कोटी एकर जमीन वाटपासाठी उपलब्ध आहे हे कम्युनिस्ट पक्षाने दाखवून दिले व सरकारचा हा प्रचार धादांत खोटा असल्याचे जनतेच्या निदर्शनास आणून दिलेच्या निवडणुकीच्या काळात १९६७ . कम्युनिस्ट पक्षाने मत्तेदार, जमीनदार, सरकारी मंत्री, बडे अधिकारी आणि त्यांचे पाठीराखे सरकार यांच्या विरुद्ध प्रचार करून १९६९ च्या सुरुवातीला जमीन बळकाव लढा उभारण्याचा निश्चय केला. ५

**2. भारतीय कम्युनिस्ट पक्षाचा सरकारी पडजमिनी ताब्यात घेण्याचा अहमदनगर जिल्ह्यातील कार्यक्रम :** १९६९ मध्ये भाकप, भारतीय खेत मजदूर युनियन आणि अखिल भारतीय किसान सभा या संघटनांनी एकत्र येऊन लागवडीस लायक अशा सरकारी पडजमिनी ताब्यात घेण्याची मोहीम हाती घेतली. सप्टेंबर . १९६९ मध्ये भारतीय कम्युनिस्ट पक्षाच्या राष्ट्रीय कौन्सिलने एक ठराव पास केला " .सरकारी जमिनी ताब्यात घेण्याची मोहीम हिरहिरिने हाती घ्या; आपल्या पक्षाशी सहकार्य करून ज्या ज्या जनसंघटना आपल्याबरोबर यायला तयार असतील त्यांना बरोबर घेऊन या मोहिमेला हात घाला ही .सत्याग्रहाची लक्षणात्मक मोहीम आहे, या दृष्टीने तिच्याकडे न पाहता सरकारी जमिनीचा प्रत्यक्ष ताबा घेऊन तेथे पिके काढवयाची आहेत या दृष्टीने या मोहिमेकडे आपण पहिले पाहिजे", असा सर्व पक्षघटकांना आदेश दिला. ५

भारतीय कम्युनिस्ट पक्षाच्या आदेशानुसार दिफेब्रुवा ८ .री १९७० रोजी अहमदनगर जिल्ह्यातील श्रीरामपूर येथे भारतीय कम्युनिस्ट पक्ष, मार्क्सवादी कम्युनिस्ट पक्ष, लाल निशाण पक्ष व, संयुक्त समाजवादी पक्ष यांच्या वतीने भूमिहीन शेतकरी, शेतमजूर व आदिवासींची एक परिषद काँडांगे .दत्ता देशमुख यांच्या अध्यक्षतेखाली व काँ ., काँगोदूताई परळकर ., साथी एसपरिषदेत महाराष्ट्रातील लागवडी लायक जंगल व पडीक जमीन .जोशी यांच्या उपस्थितीत संपन्न झाली .एम . ना कसण्यास द्यावी.भूमिहीन शेतकऱ्यां, जमीनदार व बागायतदार शेतकऱ्यांचे जमिनीवरील केंद्रीकरण नष्ट करून जमिनीचे फेरवाटप व्हावे, आदिवासींनी बहितास आणलेल्या 'जंगल जमिनी' काढून घेऊ नये इत्यादी मागण्यांचे ठराव पास करण्यात आले.मार्च रोजी विधानसभेवर भव्य मोर्चा नेण्याचा निर्णय घेण्यात आला ४च्या प्रश्नावर तसेच भूमिहीन शेतकऱ्यां .५ श्रीरामपूर परिषदेतील निर्णयानुसार ४ मार्च रोजी काँडांगे यांच्य .ा अध्यक्षतेखाली २५ हजार शेतकऱ्यांचा भव्य मोर्चा विधानसभेवर नेण्यात आला" .एप्रिल पर्यंत जमिनीचे फेरवाटप केले नाही तर २० हजार भूमिहीन शेतकरी जमिनीत नांगर घालून तिचा कब्जा करतील .असा निर्णायक इशारा काँ "सारा महाराष्ट्र पेटविल्याशिवाय आम्ही गप्प राहणार नाही .डांगे यांनी सरकारला दिला. ७ सरकारने मात्र बहिरेपणाचे सोंग घेऊन भूमिहीनांच्या मागण्यांना वाटाण्याच्या अक्षता लावल्या . रोजी १९७० एप्रिल १४ .त्यामुळे भाकप व महाराष्ट्र राज्य शेतमजूर संघ यांच्या आवाहनाला प्रतिसाद देऊन दि जिल्ह्यातील हजारो भूमि १५ महाराष्ट्रातील हीन व आदिवासींनी लालबावट्याच्या जयघोषात पडित जमिनीत नांगर



घातले व २३ हजार एकर जमिनीवर कब्जा केला या 'जबरन जोत' आंदोलनात सुमारे ५ हजार भूमिहीन व आदिवासींना अटक करून त्यांना दिर्घ मुदतीच्या शिक्षा टोठावण्यात आल्या.८ अहमदनगर जिल्ह्यात संगमनेर तालुक्यातील ८, अकोले तालुक्यातील ०५, श्रीरामपूर तालुक्यातील ०५ व राहुरी तालुक्यातील ०६ केंद्रांवर भूमिहीनांनी जमिनीत नांगर फिरवून सत्याग्रह केलाकडू .बी .पी .या सत्याग्रहात काँ ., आमदार गोंदेशमुख .के .बी ., कौसहाणे मास्तर ., कौरामभाऊ नागरे ., कौबाबुराव थोरात यांनी स .हभाग घेतलाया .भूमिहीनांच्या प्रश्नावर झालेला हा पहिलाच राज्यव्यापी भव्य लढा होता . लढ्याने गरीब जनतेच्या जमिनीच्या मागणीबाबत सरकारचे धोरण बदल्याखेरीज आपणास जमीन मिळू शकणार नाही ही जाणीव भूमिहीनांना झाल्यामुळे या लढ्याला प्रचंड पाठिंबा मिळाला असे आपल्या मुलाखती दरम्यान कौपंडरीनाथ . सहाणे मास्तर यांनी सांगितले९

३. भूमिहीनांच्या लढयासंबंधी इंदिरा गांधींची भूमिका :

भूमिहीनांची लढाऊ चळवळ आणि जमिनीची भूक लक्षात घेऊन प्रधानमंत्री इंदिरा गांधी यांनी सर्व मुख्यमंत्र्यांना एक पत्र लिहिले. 'सरकारी पडजमिनी गरीब भूमिहीन शेतकऱ्यांना लवकर वाटून द्या, कुळ कायद्यात योग्य त्या दुरुस्त्या करण्यासाठी आणि त्या अंमलात आणण्यासाठी उपाय योजा', असे आदेश या पत्रान्वये देण्यात आले. पंतप्रधानांच्या नेतृत्वाखाली 'आम्ही मूलगामी जमीनसुधारणा कायदे करणार आहोत, जमिनीचे वाटप करणार आहोत अशा घोषणा काँग्रेसकडून केल्या गेल्या.१० भाकपचे अहमदनगर जिल्ह्यातील अकोल्याचे आमदार काँ. बी. के. देशमुख यांनी विधानसभेत सरकारच्या शेतजमीन (जमीनधारणेची कमाल मर्यादा) (तृतीय सुधारणा) विधेयकाची चिरफाड करताना ४ मे १९७० च्या भाषणात शेतकऱ्यांची वस्तुनिष्ठ व्याख्या करून सरकारच्या दुटप्पी धोरणाचे सातत्याने वाभाडे काढले. ते म्हणाले, "ज्याने कधी शेतात नांगर धरला नाही, नांगर कसा धरायचा याची ज्याला माहिती नाही, तो शेतकरी झाला आहे. अध्यक्षमहाराज, जो स्वतः शेती करतो, थोडीफार मजुरी लावून कष्ट करतो, राबतो त्याला शेतकरी समजले पाहिजे. असा जो शेतकरी आहे तो जी जमीन कसतो तेवढी जमीन त्याला देण्यात यावी. तशी दुरुस्ती कायद्यामध्ये केली तरच आपल्याला जी हरितक्रांती करावयाची आहे, ती यशस्वी होऊ शकेल. तरच गोरगरिवांचे प्रश्न सुटतील. अन्नधान्याची गरज भागेल. पण अध्यक्षमहाराज ह्या गोष्टी करण्याच्या दृष्टीने शासन कधीही पाऊल टाकणार नाही. कारण मध्यमवर्ग व वरच्या वर्गाचे विशिष्ट लोक यांचे-संरक्षण हे सरकार करते. कारण ते लोक निवडणुकीत शासनाला मदत करतात. त्यामुळे त्यांच्या हिताचे संरक्षण करणे ही शासनाची जबाबदारी समजली जाते. तेव्हा आपण सिलिंगचा कायदा करून योग्य ते पाऊल उचलावे. तसा कायदा केला तरच देशाचे उत्पादन वाढू शकेल व भूमिहीनांना आणि शेतकऱ्यांना जमिनी कसण्यास मिळू शकतील. परंतु अशा प्रकारचे पाऊल सरकार उचलणार नाही याची मला खात्री आहे."११

४. भारतीय कम्युनिस्ट पक्षाचा जमीन बळकाव लढ्याचा कार्यक्रम :

दि. ८ ते १३ मे १९७० या काळात भारतीय कम्युनिस्ट पक्षाच्या राष्ट्रीय कौन्सिलची बैठक दिल्ली येथे पार पडली. या बैठकीत आजचे बिनबुडाचे सिलिंगचे कायदे सुधारण्याच्या प्रश्नावर काँग्रेस, अकाली-जनसंघ, डी.एम.के, स्वतंत्र पक्षाचे मुख्यमंत्री मृग गिळून बसले आहेत. सिलिंगच्या कायद्यात सुधारणा करण्याचा प्रश्नच उद्भवत नाही असे ही काही मुख्यमंत्री उघडपणे बोलत आहेत. त्यामुळे प्रधानमंत्री व काही राज्यांच्या मुख्यमंत्र्यांनी कितीही चांगल्या घोषणा केल्या तरी गरीब शेतकरी, शेतमजूर आणि आदिवासींनी लढाऊ आंदोलने उभारल्याशिवाय या घोषणांमधून फारसे काही निष्पन्न होणार नाही असा बैठकीत निष्कर्ष काढण्यात आला. म्हणून सिलिंगच्या कायद्यात मूलभूत सुधारणा करून सरकारी जमिनीचे वाटप व्यवस्थित घडवून आणणे यासाठी भूमिहीनांच्या खालील मागण्यांवर अखिल भारतीय पातळीवर जमीन बळकाव लढ्याची भारतीय कम्युनिस्ट पक्षाने हाक दिली.

१. सर्व सरकारी जमिनी, लागवडी लायक पडजमिनी, जंगल जमिनी सोडून ग्रामपंचायतीच्या ताब्यातील उपजाऊ जमिनी, जमीनदार, मत्सेदार आदींच्या ताब्यात असलेल्या सरकारी जमिनी भूमिहीन गरीबांना देण्यात याव्यात. ज्या भूमिहीनांच्या ताब्यात सरकारी जमिनी आहेत त्यांचा होणारा छळ बंद करून त्यांचे पट्टे त्यांना करून देण्यात यावेत.

२. कुळांच्या ताब्यातील जमिनीवरून त्यांना बेदखल करण्याचे सर्व मार्ग ब्रेकायदेशीर घोषित करून त्यांचे उल्लंघन करणाऱ्या जमिनदारांना दंड ठोठावले पाहिजेत. कुळ कायद्यात योग्य त्या दुरुस्त्या करणारे कायदे केले पाहिजेत. भरमसाठ दर कमी करून त्याचे प्रमाण निश्चित केले पाहिजे. सरजामी जमीनदारी नष्ट करून कुळांना जमिनीचे ठरविले पाहिजे. ३. आजचे सिलिंगचे कायदे पूर्णतः बदलावेत. त्यात खालील मुद्यांचा समावेश करावा. सा.स. कारखान्यांच्या मालकीचे फार्म, गवताळ जमिनी, फळवागा आणि देवस्थानांच्या जमिनी यांना मिळणाऱ्या सवलती बंद कराव्यात. काही कायद्यांमध्ये सिलिंगचा कायदा व्यक्तींना लागू आहे. त्यामुळे हा कायदा कुटुंबाला लागू केला पाहिजे. जमिनदारांच्या मालकीच्या जमिनीवर आज जी कमालमर्यादा आहे ती कमी केली पाहिजे. जमिनीची परिस्थिती आणि



चळवळीची तीव्रता या बाबी लक्षात घेऊन भिन्नभिन्न राज्यात सिलिंगच्या मर्यादा खाली आणल्या पाहिजेत. ४. आदिवासींच्या बळकावलेल्या जमिनी त्यांना परत करून त्यासंदर्भात कडक कायदा करावा. त्यांना जंगलाच्या जमिनी दिल्या जाव्यात आणि विवड (भटक्या पद्धतीने) शेती कसण्याचे त्यांनी सोडून देऊन कायम शेती करावी म्हणून त्यांना आर्थिक व तांत्रिक मदत दिली जावी. ५. जमीनदारांच्या मालकीच्या गावठाणाच्या जमिनीवर वस्ती करून राहणाऱ्या लोकांना या जमिनीचे मोफत मालकी हक्क दिले पाहिजेत. ६. सिलिंग कायद्याची अंमलबजावणी केल्यानंतर वरकड, सरकारी पडजमीन व जंगलाची जमीन भूमिहीन शेतकऱ्यांना वाटून द्यावी किंवा त्यांची सहकारी शेते स्थापन करावीत. ७. जमिनीचे योग्य वाटप व्हावे या करिता ज्या वेगवेगळ्या भूमीसमित्या केल्या जातील त्यात भूमिहीनांच्या संघटनांना योग्य प्रतिनिधित्व मिळाले पाहिजे. १२ १४ एप्रिलच्या लढ्यानंतर सरकारने '१९७० च्या आत आम्ही हा प्रश्न सोडवू' अशी घोषणा केली असली व त्याप्रमाणे हालचाली सुरू केल्या असल्या तरी १४ एप्रिल सरकारची व ७ जून आपली! या जिद्दीने आपण पुढील लढ्याची तयारी केली पाहिजे. १४ एप्रिलच्या लढ्यात जी जंगल, वरकड व पडजमीन आपण सरकारकडे मागितली आहे ती "७ जून नंतर मृग नक्षत्राचा पाऊस पडल्यावर आम्ही पेरणार, त्याचे पीक घेणार व त्याचे प्रत्यक्ष फायदे भूमिहीन शेतकऱ्यांना मिळवून देणार". म्हणून या लढ्याच्या तयारीला त्वरित सुरुवात करून '७ जून नंतर पेरते व्हा' असा संदेश देऊन जमिन बळकाव लढ्याचा कार्यक्रम सर्व राज्यांत पावसाळा सुरू होताच हाती घेण्याचा आदेश कम्युनिस्ट पक्षाने दिला. १३

#### 5. अहमदनगर जिल्ह्यातील कम्युनिस्ट पक्षाचे जमीन बळकाव लढ्यातील योगदान व कामगिरी:

दि. १ जुलै १९७० रोजी भाकप, अ. भा. किसान सभा व आदिवासी भूमिहीन शेतमजूर संघ यांच्या नेतृत्वाखाली राहुरी तालुक्यात सहा केंद्रांवर जमीन पेरणी सत्याग्रह करण्यात आला. त्याचे नेतृत्व जिल्हा किसान सभेचे अध्यक्ष कॅ. बाबुराव थोरात, कॅ. गंगाधर जाधव यांनी केले. १४ १४ जुलै रोजी महाराष्ट्र राज्य कम्युनिस्ट पक्षाच्या सभेत जमीन बळकाव लढा तीव्र करण्याचा निर्णय घेण्यात आला. कम्युनिस्ट पक्षाच्या आदेशानुसार १५ ऑगस्ट १९७० रोजी भाकप, किसान सभा, लाल निशाण पक्ष, प्रजा समाजवादी पक्ष, संयुक्त समाजवादी पक्ष व भूमिहीन शेतमजूर संघटना यांच्या नेतृत्वाखाली संपूर्ण भारतात व महाराष्ट्रभर बऱ्या बागायतदारांकडील जमिनी ताब्यात घेण्याचा सत्याग्रह करण्याचा निर्णय घेण्यात आला. १५

अहमदनगर जिल्ह्यात श्रीरामपूर तालुक्यात खाजगी साखर कारखानदारी व बऱ्या बागायतदारांचे मोठे प्रस्थ होते. त्यामुळे सर्वपक्षीय नेतृत्वाने या तालुक्यात ४ केंद्रांवर जमीन बळकाव लढा कार्यक्रम घेण्याचा निर्णय घेतला. तालुका मॅजिस्ट्रेटने या भागाच्या आसपास १४४ कलम जारी केले. त्याचा भंग करून सत्याग्रह करण्याचा सर्वांनी निश्चय केला. अहमदनगर जिल्ह्यात सोमय्या (९०० एकर जमीन) यांच्या श्रीरामपूर तालुक्यातील फार्मवरील सत्याग्रहात अहमदनगर वीड व औरंगाबाद जिल्ह्यातील ८०० सत्याग्रहींनी भाग घेतला. त्याचे नेतृत्व कॅ. चंद्रगुप्त चौधरी व कॅ. निवृत्ती उगले यांनी केले. कॅ. बाळासाहेब नागवडे, कॅ. वकीलराव लंघे, कॅ. नामदेवराव आव्हाड, कॅ. जगनाथ सोनवणे, कॅ. बाबुराव थोरात, कॅ. अचपळराव लांडे पाटील, कॅ. सातपुते पाटील, कॅ. लक्ष्मणराव लांडे, कॅ. शांतीलिंग आप्पा लोहकरे, कॅ. विनायकराव औटी आदी कम्युनिस्ट पुढाऱ्यांनी या सत्याग्रहात भाग घेतला. फार्म भोवती पोलिस व एस. आर. पी. चा कडक पहारा ठेवण्यात आला होता. फार्ममधील शेतमजुरांनी १५ ऑगस्ट रोजी एक दिवसांचा लाक्षणिक संप करून सत्याग्रहाला आपला पाठिंबा व्यक्त केला. सत्याग्रहींनी सिलींग मर्यादेंपेक्षा जादा जमीन काढून घ्या, भूमिहीन व आदिवासींना जमीन मिळालीच पाहिजे, जान देंगे जमीन लेंगे अशा घोषणा देत फार्ममध्ये घुसण्याचा प्रयत्न केला. पोलिसांनी १४४ कलमाचा भंग केल्याबद्दल सर्व सत्याग्रहींना अटक केली. स्त्रियांना २०० रु. दंड अगर दोन दिवसांची शिक्षा ठोठावण्यात आली. श्रीरामपूर तालुक्यातील जमीनदार खटोड (१३०० एकर जमीन) यांच्या मालुंजा येथील फार्ममध्ये कॅ. एकनाथ भागवत व आमदार दराडे यांच्या नेतृत्वाखाली ६०० भूमिहीन सत्याग्रहींनी जबरदस्तीने जमीन बळकावण्याचा प्रयत्न केला. पोलिसांनी त्यांनाही ताब्यात घेतले. स्टेट फार्म हरेगाव येथे सुमारे ७६ सत्याग्रहींनी जमीन ताब्यात घेण्याचा प्रयत्न केला. या तुकडीचे नेतृत्व कॅ. माधवराव गायकवाड, आमदार कॅ. बी. के. देशमुख व कॅ. पी. बी. कडू पाटील यांनी केले. १६ कोल्हार येथे केंद्रीय मंत्री अण्णासाहेब शिंदे यांच्या ६० एकर शेतीत २२३ सत्याग्रहींनी घुसल्याबद्दल त्यांना १८८ कलमाखाली अटक करण्यात आली. या सत्याग्रहाचे नेतृत्व कॅ. गंगाधर ओगले यांनी केले. १७

#### 6. जमीन बळकाव लढ्याचे मूल्यमापन :

१५ ऑगस्टचा जमीन बळकाव लढा संपूर्ण भारतभर झाला. या लढ्यात ३१,१८३ सत्याग्रहींना अटक झाली व १, ६१, ९९० एकर जमीन ताब्यात घेण्यात आली. महाराष्ट्रातील २६ पैकी २२ जिल्ह्यातील २० हजारापेक्षा जास्त सत्याग्रहींनी लढ्यात भाग घेतला. त्यात १२०० स्त्रिया होत्या. ७५०० जणांना अटक झाली व ४ हजारापेक्षा जास्त सत्याग्रहींना ७

दिवस ते ४॥ महिन्यांची शिक्षा झाली. या लढ्यात १२ हजार एकर पडजमिनीचा कब्जा घेण्यात आला. १८ महाराष्ट्रात अहमदनगर जिल्हा हा या लढ्यामध्ये सर्वात आघाडीवर होता. जिऱ्यात १७०० सत्याग्रहींना अटक करण्यात आली. ११६७ जणांना १ महिन्यांची शिक्षा झाली. या लढ्यामुळे जिऱ्यातील बऱ्या वागायतदारांनी आज ना उद्या आपल्या ताब्यातील जमीन जाणारे याची धास्ती घेतली. ेच स्वतःकडे हजारो एकर जमीन ठेवून त्या जमिनीवर रावणाऱ्या कुळांना उपाशी मारणारे व शेतमजुरांची पिळवणूक करणारे शासकीय व खासगी भांडवलदारांचे लुटारू शोषक स्वरूप समोर आले. भूमिहीनांना वाटण्यासाठी थोडीच जमीन शिल्लक आहे ह्या प्रचारातील फसवेपणा दिसून आला. बऱ्या जमीनदार व भांडवलदारांनी हजारो एकर जमीन वेकायदेशीर मार्गाने बळकावली आहे हे या लढ्यामुळे स्पष्ट झाले. १९ या लढ्याच्या परिणामस्वरूप केंद्र सरकारच्या सूचनेनुसार महाराष्ट्र सरकारने १९६१ च्या भूमीधारणेची मर्यादा कमी करण्यासंबंधीचा बट्टुकूम १९७१ साली काढला. त्यानुसार वागायतीची कमालमर्यादा १० ते १८ एकर, विहीरीच्या पाण्याखालील जमिनीची २७ एकर व कोरडवाहू जमिनीची कमालमर्यादा ५४ एकर एवढी निश्चित केली. गरीब शेतकरी, शेतमजूर व आदिवासी शेतकऱ्यांच्या परिपदेत कम्युनिस्ट पक्षाचे मेक्रेटरी काँ. एकनाथ भागवत यांनी या बट्टुकूमला विरोध करून जमीनधारणेची कमाल मर्यादा निम्यावर आणून ही मर्यादा साधारण जमिनीसाठी ३० एकर, हलक्या जमिनीसाठी ५० एकर व ओलीताखालील जमिनीसाठी ८ एकरपेक्षा अधिक न ठेवण्याची मागणी केली. तसेच जमिनीची कालमर्यादा ठरवितांना जमिनीच्या मालकीऐवजी त्या जमिनीत किती उत्तपन्न निघते हा निकष लावण्याची मागणी केली. सिलींगची अंमलबजावणी सप्टेंबर १९७० ऐवजी जानेवारी १९७१ पासून करण्याच्या सूचनेला कम्युनिस्टांनी विरोध केला. कारण अनेक वागायतदारांनी आपल्या लाखो एकर जमिनी नातेवाईकांच्या नावे केल्या होत्या. शेतकरी कोणाला म्हणावे याची स्पष्ट व्याख्या न केल्याने सधन व्यापारी, दलाल, सरकारी अधिकारी, काळा पैसेवाले यांना एक प्रकारे अभय मिळून त्यांना जमीन ठेवण्याची मुभा मिळाली. त्यामुळे कम्युनिस्ट पक्षाने जमीन धारणेची कमाल मर्यादा ठरविणाऱ्या बट्टुकूमाला विरोध करण्याची भूमिका चालूच ठेवली. २० पुढे १९७५ साली देशात आणीबाणी जाहीर झाल्यानंतर पंतप्रधान इंदिरा गांधी यांनी २० कलमी कार्यक्रम घोषित केला आणि त्यामध्ये कम्युनिस्ट पक्षाच्या धोरणानुसार सिलींग कायदा करून त्यात मोठ्या जमीनदारांकडील अतिरिक्त जमिनी भूमिहीन शेतमजुरांना देण्याची तरतूद केली. २१ अशा प्रकारे कम्युनिस्ट पक्षाने देशपातळीवर जमीन बळकाव लढ्याच्या माध्यमातून उभी केलेली चळवळ यशस्वी करण्यात अहमदनगर जिल्ह्यातील कम्युनिस्ट पक्षाने मोठी भागीदारी केलेली दिसते.

#### संदर्भ ग्रंथ सूची

१. दैनिक नगर टाइम्स, वर्ष ११ वे, अंक ४५ वा., दि. १८/१२/१९७६, पृ. क्र. २.
२. दैनिक नगर टाइम्स, वर्ष १३ वे, अंक २३९ वा., दि. १२/०७/१९७८, पृ. क्र. १.
३. साप्ताहिक युगांतर, महाराष्ट्र राज्य कम्युनिस्ट पक्षाचे मुखपत्र, दि. ०५/१०/१९८०, पृ. क्र. १.
४. काँ. भगवान गायकवाड, 'मुलाखत दि. २३/०८/२०१४', तालुका सचिव भाकप, शेवगाव, मु. पो. खरडगाव, ता. शेवगाव, जि. अहमदनगर.
५. साप्ताहिक युगांतर, महाराष्ट्र राज्य कम्युनिस्ट पक्षाचे मुखपत्र, दि. ३०/०३/१९६९, पृ. क्र. ९.
६. ढोले अशोक एकनाथ, 'काँ. पी. बी. कडू पाटील जीवन व कार्य: एक चिकित्सक अभ्यास (१९२१-१९९६)', (अप्रकाशित शोध प्रबंध), टिळक महाराष्ट्र विद्यापीठ, पुणे, २०१४, पृ. क्र. २८२.
७. कडू पी. बी., 'क्रांतिपंढरीचा वारकरी (शब्दांकन: सविता भावे), प्रकाशक, अरुण पुंजाजी कडू, सात्रळ, राहुरी, सप्टेंबर २०१४, पृ. क्र. १८४.
८. भागवत एकनाथ, 'जमिनीचा लढा लढवा', भारतीय कम्युनिस्ट पक्षाच्या महाराष्ट्र राज्य कौन्सिलचे प्रकाशन, राजभुवन, सरदार पटेल रोड, मुंबई, प्रथम आवृत्ती, १० जुलै १९७०, पृ. क्र. ३.
९. उद्धृत, देशमुख सुदाम, 'महाराष्ट्रातील ग्रामीण गरिबी आणि जमिनीचे फेरवाटप', भारतीय कम्युनिस्ट पक्षाच्या महाराष्ट्र राज्य कौन्सिलचे प्रकाशन, राजभुवन, सरदार पटेल रोड, मुंबई, प्रथमावृत्ती, जून १९६९, पृ. क्र. १-२.
१०. साप्ताहिक युगांतर, महाराष्ट्र राज्य कम्युनिस्ट पक्षाचे मुखपत्र, दि. १३/०२/१९७२, पृ. क्र. ३-४.
११. भागवत एकनाथ, 'जमिनीचा लढा लढवा', उपरोक्त, पृ. क्र. ३.



## जायकवाडी बांध आंदोलन में जिला अहमदनगर के साम्यवादी दल का योगदान

★ प्रा.डॉ. विघाटे गणेश शंकर ★★ डॉ.राजाराम कानडे

### सारांश:

जायकवाडी जलसिंचन परियोजना में सरकार की भूमिका और विस्थापित लोगों पर हुए सितम के कारण, विस्थापितों का पुनर्वास संबंधी प्रश्नों की ओर सरकार का नजरअंदाज की वजह से उभरा जन आंदोलन को सही अंजाम देने की भूमिका में अहमदनगर जिले के साम्यवादी दल के योगदान को उजागर करने के प्रयोजन में प्रस्तुत शोध आलेख पाठक, संशोधक को आंदोलन के प्रति सजग करेगा। इसमें जन आंदोलन के बढ़ते प्रभाव के कारण सरकार द्वारा पारित विभिन्न अधिनियम की जानकारी है। साथ ही आंदोलन कर्मियों का विश्वास कायम रखने के प्रयास में साम्यवादी अनुयायियों का अथक प्रयास ही मानवतावादी विचारधारा की तरफ पाठक को ले जाता है।

### महत्त्वपूर्ण शब्द:

महाराष्ट्र राज्य सरकार तथा साम्यवादी भूमिका की फल निष्पत्ति.

### उद्देश्य:

1. जायकवाडी जलसिंचन परियोजना निर्माण में सरकार की भूमिका पर प्रकाश डालना।
2. बांध निर्माण कार्य में पीड़ितों की मानसिकता को उजागर करना एवं जन आंदोलन के विषय पर प्रकाश डालना।
3. साम्यवादी विचारकों की भूमिका और उनका मानवतावादी प्रयास की दिशा पर प्रकाश डालना।
4. जायकवाडी बांध निर्माण एवं जन आंदोलन की शुरुआत और पुनर्वास संबंधी अधिनियम के प्रति वाचक कोसजग करना।
5. बांध पीड़ितों के आंदोलन की दिशा और फलनिष्पत्ति का अध्ययन करना।

### प्रस्तावना:

महाराष्ट्र की मशहूर नदी गोदावरीके तट पे स्थित 'पैठण' के समीप स्थापितजायकवाडी बांध के कारण विस्थापित हुए किसान, खेती मजदूरों के आवास के प्रश्नों पर अहमदनगर के साम्यवादी विचार दलने बांध पीड़ितों के आंदोलन हेतु बिगुल बजाया जो अहमदनगर जिले के किसान आंदोलन एक यशस्वी आंदोलन के रूप में समझा जाता है। बेघरं भूमिहीन किसान

तथा मजदूरों की विपन्न अवस्था में वे बांध के वास्ते मृत्यु को गले लगान सके, पुनर्वासके साथ बांध योजना इस तत्व के अनुसरण में अहमदनगर के साम्यवादी दल के अनुयायियों ने 'गोदावरी बांध परिषद' की सहयोग में राज्यव्यापी आंदोलन जारी रखने का ऐलान किया और उसे जिम्मेदारी के साथ निभाया।

### 1. जायकवाडी बांध योजना का ऐलान

तत्कालीन जलसंधारण मंत्री शंकरराव चौहान ने जनवरी 1965 में ख्यातनाम नदी गोदावरी एवं पैठण के पश्चिम दिशा में स्थित 'कावसन' गांव में जायकवाडी बांध निर्माण करने का ऐलान किया। जायकवाडी बांध की ऊंचाई 120 फीट और लंबाई 7मीलथी। इसकी बृहददीवारलगभग 120 फीट की थी। इस बांध से उपलब्ध पानी लगभग 25 मील दूर और 12 से लेकर 15 मील चौड़ाई के अहाते में रहनेवाला था।बांध का कुल खर्चा 70 करोड़ था। बांध की एक ओर 115 मील तथा दूसरी ओर 178 मील की दो नहरे निकालने का ऐलान किया गया।<sup>1</sup> सामान्यतः यह बांध मराठवाड़ा के अकाल को दूर करके वहां

\* इतिहास विभागाध्यक्ष,राधाबाई काळे महिला महाविद्यालय, अहमदनगर

\* \* हिंदी विभागाध्यक्ष एस.एस.जी.एम.कॉलेज,कोपरगांव, जि. अहमदनगर

शैक्षिक, व्यवसायिक, औद्योगिक विकास की दृष्टि के तहत बांध निर्माण किया जा रहा था। "इस बांध परियोजना से मराठवाड़ा की 7.5 लाख एकड़ जमीन जलसिंचनमें आने वाली थी।" इसलिए जायकवाडी बांध परियोजना मराठवाड़ा के चहुँमुखी विकास की एक मौलिक चाबी प्रतीत हो रही थी।

## 2. जायकवाडी बांध पीड़ितों के सत्याग्रह आंदोलन की नींव

महाराष्ट्र के तत्कालीन मुख्यमंत्री यशवंतराव चौहान ने 7 दिसंबर 1960 में स.गो.बर्वे की अध्यक्षता में समिति गठित की थी।<sup>3</sup> प्रस्तुत समिति ने पुनर्वास के बारे में निम्न सूचनाएं दी—बांध परियोजना में जिन किसानों की जमीन शासन ने अपने कब्जे में की हैं, उनके लिये पुनर्वास योजना तैयार करना और परियोजना के साथ ही मंजूर होना अनिवार्य है।<sup>4</sup> गुल्हाटी समिति के सम्मुख महाराष्ट्र की ओर से महाराष्ट्र शासन ने अकाल से पीड़ितों को इस योजना में सबसे पहले हक देने का मुद्दा प्रस्तुत किया था। लेकिन जायकवाडी बांध के ऐलान में शासन ने इसके बारे में कोई भी प्रारूपण प्रस्तुत नहीं किया। अतः 1962 की बर्वे सिंचन समिति की सिफारिशों को रोकने की संभावनाएं किसानों में तीव्र होने लगी। इस बांध के कारण शेवगांव, नेवासा, पैठण तथा गंगापुर जैसे चार तहसीलों के 66 गांव, 7 लाख किंटल से ज्यादा जवार फसल देने वाली 92 हजार एकड़ उपजाऊ जमीन और लगभग एक लाख से ज्यादा लोग बेघर होने वाले थे। इनमें से शेवगांव तहसील के 20 और नेवासा तहसील के 24 गांव बांध में डूबने वाले थे।<sup>5</sup> स्वातंत्र्योत्तर महाराष्ट्र में वीर, पानशेत तथा कोयना इन बांध पीड़ितों के ढेर सारे प्रश्नों को सरकार ने अनदेखा किया था। इसलिए कई लोग दिशाहीन हो गए थे अतः 'वीर' बांध परियोजना परिषद के सामने भारतीय कम्युनिस्ट दल के कॉमरेड वसंतराव तुळपुळे ने 'पहले पुनर्वास फिर बांध' यह नारा देकर बांधों के आंदोलन का बिगुल बजाया था।<sup>6</sup>

बांध परियोजना निर्माण और उससे संबंधित प्रश्नों के कारणविपन्न किसानों ने नापसंदगी दिखाई। पैठण में आयोजित कांग्रेस की सभा में अहमदनगर के कांग्रेस अध्यक्ष घुले पाटील ने शंकरराव चव्हाण की निंदा की। उनकी राय द्रष्टव्य है, "जायकवाडी बांध परियोजना की जगह जब निश्चित की गई तब शंकर चव्हाण और बाळासाहेब भारदे ने बांध की जगह यदि बदलने का प्रस्ताव भी सामने आया तो वे उसका जमकर विरोध करते क्योंकि शेवगांव, नेवासा तथा पैठण इन तहसीलों में साम्यवादी दल का काफी प्रभाव था और उनका प्रभाव या असर कम करने हेतु उनकी धनयुक्त जमीन को जल परियोजना में डूबने पर उन्हें बेघर करने का एक सुअवसर प्राप्त हो रहा था। इसलिए सत्ताधारियों ने अपनी पूरी शक्ति इस कार्य में लगाई।"

साम्यवादियों ने 1 मार्च 1965 में शेवगांव तहसीलके 'आगरनांदुर' में बांध पीड़ितों की एक सभा कॉमरेड नाना पाटीलकीअगुवाई में आयोजित की। इस परिषद में 'गोदावरी बांध परिषद' की स्थापना की गई। इस संगठन के सचिव कॉमरेड वसंतराव तुळपुळे, अध्यक्ष कॉमरेड विश्वनाथ कर्डिले थे। पुनर्वास प्रश्नके बारे में 'गोदावरी बांध परिषद' में कई मांगे स्वीकृत की गईं।

1. पुनर्वास का आलेखन तैयार करके उसे बांध परियोजना में स्थान मिलना चाहिए।
2. बांध में जिनकी जमीन जाने वाली है, उन्हें उतनी ही जमीन नहर पानी की मिलनी चाहिए।
3. जमीन का कब्जा लेते समय नई जमीन हक का ठहराव शीघ्र तैयार होना चाहिए।
4. पुनर्वास बांध योजना में गैर किसान को समाकर उन्हें उचित आर्थिक मदद करनी चाहिए।
5. बांध विकास में तबाह हो गई जमीन पर जितना भी कर्ज का बोझ हो उसे मिटाया जाए।
6. सरकार बांध पीड़ितों की संतानों को मुफ्त में शिक्षा देने का ऐलान करें।

सरकार ने उपर्युक्त बातों की ओर गौर करके उनपर यथाशीघ्र अमल करके उन्हें पूर्ण किया जाए।<sup>7</sup> साथ इन माँगों की पूर्ति हेतु किसानों ने आंदोलन के लिए तैयार होने का नारा दिया।

## 3. जायकवाडी बांध और सत्याग्रह आंदोलन का प्रारंभ:



संगमनेरककोंमरेड दत्ता देशमुख ने जायकवाडी बांध पीड़ितों के असंतोष का अध्ययन करके 'गोदावरी परियोजना व महाराष्ट्र शासन' इस प्रकाशित निबंध में जायकवाडी बांध योजनाअशासकीय होने तथा गलत जगह पर निर्माण करने के प्रति मुहर लगाई।<sup>9</sup> सरकार ने इस खयाल की ओर अनदेखा किया। इसलिए कॉमरेड विश्वनाथ पाटील कर्डिले एवं कॉमरेड एकनाथ भागवत केमोरचा में तत्कालीन मुख्यमंत्री वसंतराय नाईक बांध स्थल को देखने हेतु पधारे उस वक्त साम्यवादियों ने 2000 किसानों के मोर्चा में उन्हें आवेदन दिया।

महाराष्ट्र राज्य के सब बांध पीड़ितों की सभा का आयोजन दिनांक 26 तथा 27 जून 1965 को हुआ। जिसकी अध्यक्षता कॉमरेड डांगे ने की और यह सभा 'महाराष्ट्र राज्य बांध और पुनर्वास परिषद' तथा साम्यवादी दल के निर्देशन में हुई। इसमें काकासाहेब गाडगीळ ने जायकवाडी बांध योजनाका सबसे ज्यादा फायदा महाराष्ट्र के अलावा आंध्र प्रदेश को होने वाली बात कहकर इस योजना पर प्रश्नचिह्न लगाने का प्रयास किया। इसलिए गोदावरी घाटमें बन रहे महाराष्ट्र केबांधों का अधिक खर्चा उठाने संबंधी प्रस्ताव यदि आ भी जाता है तो उसे मंजूर करने का सवाल निर्माण न हो इस लियें तत्कालीन केंद्रीय जलसंधारन मंत्री के.एल.राव नेजायकवाडी बांध को अतिशीघ्र मंजूरी दी। परिणामतः गोदावरी का ज्यादातर पानी आंध्र प्रदेश को ही मिलने वाला है यह निश्चितहो गया।<sup>10</sup>

बाँध और पुनर्वास परिषदकेआदेश मुताबिक 29 जुलाई 1965 में मुंबई कोअहमदनगर जिले के हजारों बांध पीड़ित किसानों का विधानसभा पर मोरचानिकाला। उन्होंने सरकार को यह इशारा दिया कि पुनर्वास के प्रश्नों को कानून के तौर पर हक प्रदान नहीं किया तो प्रस्तुत बांध योजना को रोका जाएगा। महाराष्ट्र शासन ने इस बात की ओर अनदेखा करके जायकवाडी बांध परियोजना निर्माण हेतु भूमिपूजन समारोह को 18 अक्टूबर 1965 में प्रधानमंत्री लाल बहादुर शास्त्री के कर कमलों से निश्चित किया। साम्यवादी दल ने इस समारोह के खिलाफ विगुल बजाया। पुलिसों की सजगता में भूमि पूजन के पहले कॉमरेड एकनाथ भागवत, कॉमरेड अचपळराव लांडेपाटील, कॉमरेड शशिकांत कुलकर्णी आदि साम्यवादी अनुयायियों को गिरफ्तार कर नासिक के हरसुल नामक कारागृह में बंद किया और भूमि पूजा समारोह संपन्न होने पर उन्हें रिहा किया।<sup>11</sup> इससे यह स्पष्ट होता है कि सरकार की ऐसी मनचाही भूमिका में कहीं ना कहीं उनकी तानाशाही भूमिका प्रतीत होती है। गोदावरी बांध परिषद द्वारा नियुक्त सभासद मंडल नेभुतपूर्व प्रधानमंत्री लाल बहादुर शास्त्री के सामने बांध पीड़ितों के प्रश्न प्रकट किए जिसे प्रधानमंत्री लाल बहादुर शास्त्री ने अपनी स्वीकृति दी।<sup>12</sup> "जिन बांध पीड़ितों को जिस गांव में पुनर्वासके लिए जमीन मिलेगी वहाँ जलसिंचन तथा पीने के लिए यथा योग्य पानी की सुविधा मिले।" उन्होंने इसकी सूचना महाराष्ट्र शासन को दी।<sup>12</sup> इसके बावजूद महाराष्ट्र सरकार ने परियोजना पीड़ितों के लिए यथा योग्य सुविधाएं न देने के कारण 18 मार्च 1966 में हो गई महाराष्ट्र राज्य बांध परिषद की कार्यकारी मंडल की सभा में पुनर्वास के अधिनियम के लिए गोदावरी बांध परिषद ने सत्याग्रह की राह पर तूट करके गोदावरी बांध कार्य रोकने का निर्णय लिया।<sup>13</sup>

ऊपरी फैसले के मुताबिक 14 मई 1966 को कॉमरेड रामराव पाटील थोरात के अगुवाई में, 19 मई को एरंडगांव के सरपंच कॉमरेड चंद्रभान पाटील के अगुआपन में; 26 मई को नेवासा तहसील के वकीलराव लंधे, 2 जून 1966 को कॉमरेड विश्वनाथ पाटील कर्डिले के आगुआपन में सत्याग्रह किए जिसमें क्रमशः 29, 77, 130, 114 अनुयायी प्रतिभागी हुए थे और इन्हें कई दिनों का कारावास भी हुआ था।<sup>14</sup> 9 जून को श्रमिक महिजा परिषद की अध्यक्ष वत्सलाबाई भागवत, अंजनाबाई दादा पाटील, सीताबाई काशीनाथ कर्डिले और सत्यभामा विश्वनाथ पाटील के आगुआपन में 101 किसान महिला सत्याग्रही की टुकड़ी ने सत्याग्रह करके बांध का कारोबार पूर्ण रूप से बंद किया। हालाँकि त्रेन वाहक खोजर तथा रोडरोलर को अपने कब्जे में करने वाली 24 महिलाओं को पुलिस ने हिरासत में लिया था। शेष महिलाओं



ने पूरा दिन क्रेन वाहक के सम्मुख बैठकर अपना आंदोलन किया। शाम पाँच बजे आयोजित की गई सभा में अगले आंदोलन के स्वरूप की दिशा तय करने में अपने पारिवारिक सदस्यों को भी इस आंदोलन में प्रतिभागी करने का नारा दिया गया।<sup>15</sup> महिलाओं के इसी प्रयास में आंदोलन को एक मौलिक दिशा मिल गई।

#### 4. जायकवाड़ी बांध और पुनर्वास में सरकार की भूमिका:

महाराष्ट्र शासन ने 'जायकवाड़ी बांध परियोजना' के ऐलान के पश्चात बांध पीड़ितों के पुनर्वास संबंधी एकयोजनाबनाई। जिसके अनुसार सरकार ने 1884 के भूसंपादन अधिनियम के तहत 1000 रुपये की क्षतिपूर्ति की रकम देनी चाही। मगर यह मदद विलंब से मिलने के कारण बांध पीड़ितों का असंतोष बढ़ गया। इसलिए सन 1965 में सरकार ने 'पुनर्वास मंडल' की स्थापना की। इसका कार्यक्षेत्र केवल बांध पीड़ितों को क्षतिपूर्ति के लिए आर्थिक बँटवारा ही थाना की पुनर्वास की कानूनी योजना बनाना। उसमें उन्होंने 1 एकड़ के लिए 1000 रुपये के बदले 2000 रुपये कर दिए थे फिर भी महंगाई के परिप्रेक्ष्य में यह रकम काफी न थी इसलिए आंदोलन जारी रहा।<sup>16</sup>

'महाराष्ट्र राज्य बांध एवं पुनर्वास परिषद' का दूसरा अधिवेशन अहमदनगर में 18 मार्च 1969 में कॉमरेड डांगे की अध्यक्षता में संपन्न हुआ। इस अधिवेशन के परिणाम स्वरूप सरकार ने किसानों की क्षतिपूर्ति की केवल नाममात्र रकम बढ़ाकर विद्रोही लोगों को खुश करने की कोशिश की। इसमें किसानों के जमीन का उचित साक्ष्यपत्र न देना, भ्रष्टाचार तथा किसानों के अज्ञान का नाजायद फायदा लेकर किसानों के कानूनी हक को नकारने कार्य प्रशासकीय अधिकारी कर रहे थे यह इल्जाम कॉमरेड डांगे ने किया। डांगे की राय से किसानों के लिए 'पुनर्वास कानून' ही एकमात्र राहत देने में सक्षम है। उसके लिए आवश्यक अधिनियम की आवश्यकता है और बांधपीड़ितों पर हो रहे सितम को रोकने हेतु उन्होंने एक कार्यक्रम सप्ताह का नारा दिया। इसके अनुसार 2 से लेकर 9 अप्रैल तक महाराष्ट्र में जहाँ कहीं पुनर्वास के प्रश्न हैं उन तहसिलों में सप्ताह में हर रोज सैकड़ों किसानों का जमघट तहसीलदार कार्यालय या कचहरी के सामने करने का ऐलान किया।<sup>17</sup> यदि सरकार इसकी ओर अनदेखा करेगी तब महाराष्ट्र के प्रशासकीय अधिकारी तथा मंत्रीगण को रोकने की बात तय हो गई।

परिषद के आदेश के अनुसार शेवगांव में 9 अप्रैल को कॉमरेड विश्वनाथ कर्डिले के आगुआपन में पहले 98 और बाद में 68 किसानों ने 144 दफा खारिज करके कचहरी के सम्मुख सत्याग्रह किया। पी.बी. कडुपाटील की आगुआपन में राहुरी में 45 किसानों के सहयोग में सत्याग्रह किया। उन्हें 7 दिनों का कारावास मिला। जिन्हें कारावास मिला उनमें पुणे की कॉमरेड कमलाबाई भागवत, कॉमरेड विश्वनाथ कर्डिले, कॉमरेड बाबासाहेब नागवडे, कॉमरेड वकील राव लंधे, कॉमरेड पी.बी. कडु, कॉमरेड चंद्रभान थोरात आदि का समावेश था।<sup>18</sup> इन्हें येरवड़ा कारागृह में भेज दिया गया। इस तरह क्षतिपूर्ति के प्रयास में सरकार की ओर से केवल नाममात्र प्रयास हुआ जिसका खंडन साम्यवाद के अनुयायियों ने बलपूर्वक करके आंदोलन को योग्य दिशा दी।

#### 5. बांध पीड़ितों को जमीन और आर्थिक क्षतिपूर्ति करने का अधिनियम:

जायकवाड़ी बांध पीड़ितों के निरंतर आंदोलन के कारण महाराष्ट्र सरकार को इसकी ओर ध्यान आकृष्ट करना पड़ा। जायकवाड़ी बांध में भूमिहीन हुए किसानों, मजदूरों अथवा वंचितों को जमीन देने का फैसला लिया गया। नये पुनर्वास में पाटशाला, बिजली, पीने का पानी, अस्पताल आदि अत्यावश्यक सुविधाएँ नए गांव में स्थापित करने में सरकारके कटिबद्ध होने का ऐलान है। अगले छह माह में शेवगांव, नेवासा तहसील के बांध को 30 हजार एकड़ जमीन का बँटवारा किया जाएगा। इसकी घोषणा तत्कालीन राज्य पुनर्वासमंत्री माननीय शरद पवार ने 20 जुलाई 1974 को शेवगांव में आयोजित सभा में की।<sup>19</sup>



नेवासा तहसील के भूतपूर्व विधायक कॉमरेड वकीलराव लंघे की आगुआपनमें स्थापित समिति ने माननीय शरद पवार के सम्मुख बांध पीड़ितों को सीलिंग की सीमा तक जमीन उपलब्ध कराने की माँग की। शरद पवारजी ने अतिशीघ्र बांध पीड़ितों का पुनर्वास के संबंधी अधिनियम करने का विश्वास व्यक्त किया।<sup>20</sup>

सन 1976 में महाराष्ट्र सरकार ने बांध पीड़ितों के 'पुनर्वास अधिनियम' को मंजूरी दी। इसके अनुसार

1. बांध पीड़ितों को सीलिंग सीमा के तहत सरकार की ओर जमीन प्रदान की जाएगी।
2. यदि किसानों को जमीन के बदले आर्थिक क्षतिपूर्ति की चाहत है तो उसे आर्थिक भुगतान दिया जाए।
3. ग्रामस्थल के गृह निर्माण के तहत किसान को उसके पारिवारिक सदस्य संख्या के मुताबिक भूखंड प्रदान किए जाएं। भूमिहीन किसान मजदूर व्यापारी अथवा उद्योजक को 186 से 280 चौरस मीटर के भूखंड देने का प्रावधान हो।

सन 1976 के अधिनियम को कानूनी दर्जा प्राप्त हुआ और पुनर्वास परियोजना के निर्वाह हेतु नेक प्रणाली तैयार करने की बात तय हो गई।<sup>21</sup> मगर प्रावधान में कुछ समस्याएँ निर्माण हो गईं। बाढ़ पीड़ितों को जमीन देने का प्रावधान अधिनियम में करने पर भी सरकार पर इसका बंधन न था। पुनर्वास गाँव में वहाँ के बड़े जमींदार जमीन देने में आनाकानी कर रहे थे। इसलिए अनेक किसानों को आर्थिक रूप में सहायता देने का प्रयास रहा जिसे बांध पीड़ितों ने ठुकराया। अतः गोदावरी बांध परिषद के नेताओं ने बांध पीड़ितों के सुशिक्षित युवकों को नौकरी में 10 प्रतिशत आरक्षण देने, बेघरों को 1500 रुपयों में मकान देने, खेतीकार्य के लिए मुफ्त में बिजली, आंतरिक सड़क, सुजल एवं पाठशालाओं का इंतजाम करने की माँग पुनर्वास मंत्री प्रतापराव भोसले के सम्मुख रखी थी जिसपर यथायोग्य अमल करने का विश्वास परिषद के नेताओं को प्रतापराव भोसले ने दिया।<sup>22</sup>

### 6. जायकवाड़ी बांध प्रथम के आंदोलन की फल निष्पत्ति:

सन 1976 के पुनर्वास अधिनियम के तहत कई बांध पीड़ितों का मूल गाँव के नजीक पुनर्वास किया गया। जायकवाड़ी बांध निर्माण में शेवगांव तथा नेवासा के जो गाँव डूब गए थे वहाँ के रास्ते, पाठशाला एवं अस्पतालकी 70 प्रतिशत तक की कार्यपूर्ति सन 1978 ई. तक पूरी की गई।<sup>23</sup> बांध पीड़ितों को सन 1979 तक मकान के लिए 94 लाख तथा जमीन खरीदी के लिए 4.8 करोड़ रुपये दिए गए। बांध पीड़ितों की संतानों के लिए सरकारी नौकरी में 10 प्रतिशत जगह आरक्षित की।<sup>24</sup> शेवगांव तहसील के बांध पीड़ितों को जिस गाँव में जमीन मिली, उन जमीनों के सिंचन की सुविधा हेतु जायकवाड़ी बांध योजना से पानी उठाकर ताजनापुर गाँव सेलिफ्ट के माध्यम से कर देने की माँग की गई थी। सरकार ने 'ताजनापुर' लिफ्ट योजना को मंजूरी दी लेकिन यह योजना शुरू होने में विलंब हुआ।<sup>25</sup>

1976 के पुनर्वास अधिनियम से बांध पीड़ित असंतुष्ट थे। जिन किसानों की जमीन बांध में गई उन किसानों की बहुत कम क्षतिपूर्ति होने का इल्जाम साम्यवादियों ने किया। कुछ किसानों ने कोर्ट कचहरी के जरिए यथा योग्य क्षतिपूर्ति कर ली थी। साथ ही कुछ किसानों को पुनर्वास के आहाते में जमीन प्राप्त नहीं हो सकी। उपरी दिक्कतों के अलावा 1976 में महाराष्ट्र सरकार ने पुनर्वास कानून के जरिए जायकवाड़ी बांध पीड़ितों के पुनर्वास करने का जो प्रयास किया, उससे बांध सरकार के प्रति का क्रोधभाव कम होने में मदद हो गई। बांध के प्रारूपण के साथ ही पुनर्वास प्रारूप तैयार हो जाना चाहिए। जमीन के बदले जमीन और मकान के बदले मकान देने के कानूनी अधिकार मिलने चाहिए। इस तरह की साम्यवादी नेताओं की दृढ़ता एवं तद्संबंधी के आंदोलन को अनुपम सफलता मिल गई। यह साम्यवादी दल को प्राप्त हुई सबसे बड़ी कामयाबी समझी जाती है।

## निष्कर्ष:

1. जायकवाडी बांध परियोजना की कार्य गतिविधियों के स्पष्ट प्रारूपण को विशद न करके उसका ऐलानबांध पीड़ितों को धोखा देने के समान प्रतीत होता है।
2. साम्यवादियोंका अकालग्रस्त मराठवाड़ा के विकास के खातिर सरकारी योजनाओं के प्रति विरोध न था। बांध के जरिए एक प्रदेश के विकास के साथ-साथ वहां के अनगिनत लोगों का विस्थापनसाम्यवादियोंको नामंजूर था।
3. कोयना और वीर बांध योजना में पुनर्वासके दर्द को पूरी तरह मिटाया नहीं था। इसलिए 'पहले पुनर्वास फिर बांध योजना' इस खयाल को सम्मुख रखकर 'गोदावरी बांध परिषद' के माध्यम से बांध पीड़ितों का भव्य मोर्चा मार्क्सवादियों ने खड़ा करके लगभग दो शतक तक सरकार के साथ अथक संघर्ष करने का ऐलान ही उनके योगदान पर प्रकाश डालता है।
4. सन 1894 ई. के भूमिअधिग्रहण अधिनियम की तहत सरकार का बांध परियोजना ग्रस्त या पीड़ितों को मराठवाड़ा के विकास के नाम पर सितम करने का प्रयास शुरूसे देखा जाता है। साम्यवाद के दबाव तथा जन आंदोलन के परिणाम स्वरूप 1976 के पुनर्वास अधिनियम के प्रावधानों के अनुसार पीड़ितों को अपने गाँव के नजीक पुनर्वास की सुविधा देकर महाराष्ट्र सरकार ने लोगों के असंतोष को कम जरूर किया है, इसमें कोई संदेह नहीं है।

## संदर्भ सूची:

1. तुळपुळे, मालिनी, कॉमरेड वसंतराव तुळपुळे: कार्य व परिचय, शलाका प्रकाशन मुंबई 1979, पृ. 85
2. पाक्षिक 'युगांतर', महाराष्ट्र राज्य कम्युनिस्ट पक्ष का मुखपत्र, दिनांक 25 जुलाई 1965, पृ. 3.
3. राजदेव, त्रिंबक, महाराष्ट्र के विकास में कॉमरेड दत्ता देशमुख का कार्य (अप्रकाशित शोधप्रबंध), डॉ. बाबासाहेब आंबेडकर मराठवाडा विद्यापीठ, औरंगाबाद, 2002, पृ. 213 और 214.
4. डीतीतं 'जंजम पतपहंजपवद ब्वउउपेपवद त्मचवतजए 1962ए च्त्तपदजमक ज जीम ळवअमतदउमदज च्त्तमेए छंहचनतए 1962ए चण116ए
5. तुळपुळे, वसंतराव, महाराष्ट्र राज्य धोरण व पुनर्वसन परिषद 26, 27 जून 1965 अहवाल, कल्पना मुद्रणालय, पुणे, 1965, पृ. 14.
6. तैत्रव, पृ. 2
7. गवंडी, पुंडलिक, लाल सूर्य, अमोल प्रकाशन, नारायण पेठ पुणे, 20 नवंबर 199, पृ. 139.
8. पाक्षिक, 'युगांतर', महाराष्ट्र राज्य कम्युनिस्ट दल का एजेंडा (मुखपत्र). दि. 14/03/1965, पृ. 13.
9. कॉमरेड देशमुख, दत्ता, गोदावरी परियोजना और महाराष्ट्र शासन सिंचन आयोग, दैनिक केसरी, दिनांक 3 व 4 जून 1965 (पुनर्मुद्रित).
10. पाक्षिक, 'युगांतर', महाराष्ट्र राज्य कम्युनिस्ट दल का एजेंडा (मुखपत्र), दिनांक 25 जुलाई 1965, पृ. 13
11. कॉमरेड पवार, कृष्णा, साक्षात्कार, दिनांक 15 नोव्हेंबर 2015, भूतपूर्व तहसिल सचिव भाकप, शेवगाव जि. अहमदनगर.
12. लाड श्रीकांत (संपादक), भारतीय कम्युनिस्ट दल के 50 वर्ष, भारतीय कम्युनिस्ट दल प्रकाशन, मुंबई, जनवरी 1976, पृ. 56.
13. दैनिक नगर टाइम्स, वर्ष प्रथम, अंक 170, दिनांक 2 मे 1966, पृ. 2.
14. पाक्षिक, 'युगांतर', महाराष्ट्र राज्य कम्युनिस्ट दल का मुखपत्र, दिनांक 12 जून पृ. 1.
15. पाक्षिक, 'युगांतर', महाराष्ट्र राज्य कम्युनिस्ट दल का मुखपत्र, दिनांक 19 जून 1966 पृ. 3 व 8.





ISSN 2319-4766

PEER REVIEWED & REFEREED JOURNAL

# RESEARCH JOURNAL INTERDISCIPLINARY

APRIL-JUNE, 2021, VOL. 10, 1331-31

Special Issue of Department of History,  
Lokmanya Mahavidyalaya Warora, Dist. Chandrapur (MS)

5<sup>th</sup> June 2021

## RECENT TRENDS IN MODERN HISTORY



**Chief Editor**

Dr. Subodh Kumar Singh  
Principal

**Editor**

Dr. Dipak P. Lonkar  
Head, Dept. of History

Book  
1



## RELIGIOUS FUNDAMENTALISM: CONCEPT, CAUSES, AND REALITY

Dr. Ganesh Shankar Vidhate

Department of History, Rayat Shikshan Sanstha's, Radhabai Kale Mahila Mahavidyalaya,

Ahmednagar, Tal. Dist. Ahmednagar. 414001

Email : rkmm.history1989@gmail.com Mob : 9225222241, 8999148844

**Keywords:** Sacred texts, Fanaticism, Christianity, Apocalyptic orientation, Chauvinism, Protestantism, Doctrine of monotheism.

Preface: Fundamentalism is defined as 'forming a foundation or Basis'. Yet the word today resonates with destruction and annihilation. It evokes strong emotions and impulses. Originally characteristic of American conservative Protestantism, Fundamentalism is now associated with violence and terror. Fundamentalism was a world problem. In this complex world there are so many peoples lived which belongs to different race, religion, cast and community. Each community rewards its religious superiority with furioso. Love of religion is the main element of nationalism. But extreme religiosity is the cause of hatred of other religions. This creates an atmosphere of unrest and instability in society. The present research paper discusses various factors related to fundamentalism.

1. Concept and meaning of Fundamentalism: Fundamentalism is a words which seem to have a curious charge to them an emotional, spiritual, religious charge. Fundamentalism usually has a religious connotation that indicates unwavering attachment to a set of irreducible beliefs.<sup>1</sup> However, fundamentalism has come to be applied to a tendency among certain groups – mainly, although not exclusively, in religion – that is characterized by a markedly strict literalism as it is applied to certain specific scriptures, dogmas, or ideologies, and a strong sense of the importance of maintaining ingroup and outgroup distinctions.<sup>2</sup> The term is used to refer to extremism, fanaticism, and literal thinking in connection with a religious faith. When used by the West with reference to Muslim groups, religious fundamentalism also implies terrorism and oftentimes evokes a powerful image of persons who are irrational, immoderate, and violent.<sup>3</sup> Fundamentalism, type of conservative religious movement characterized by the advocacy of strict conformity to sacred texts. Indeed, in the broad sense of the term, many of the major religions of the world may be said to have fundamentalist movements. It has a close commitment to religion.<sup>4</sup> Karen Armstrong underscores the meaning of Fundamental and the power it evokes:

One of the most startling developments of the Twentieth century has been the emergence within every major religious tradition of a militant piety popularly known as "fundamentalism." Its manifestations are sometimes shocking. Fundamentalists have gunned down worshipers in a mosque, have killed doctors and nurses who work in abortion clinics, have shot their presidents, and have even toppled a powerful government. It is only a small minority of fundamentalists who commit such acts of terror, but even the most peaceful and law-abiding are perplexing, because they seem so adamantly opposed to many of the most positive values of modern society. Fundamentalists have not time for democracy, pluralism, religious toleration, peace-keeping, free speech, or the separation of church and state.<sup>5</sup>

2. Causes of Fundamentalism: The main causes of Fundamentalism are modernism and Secularism. But religions fundamentalism also stimulate the wave of the fundamentalist movements. Modernization has undermined religion in at least three ways:

- Social life has become separated from religious life.
- In a Rationalist view people are more likely to seek scientific explanations for behavior rather than religious explanations.
- In certain societies 'religious traditionalist' feel as if their way of life is under threat, and so they take steps to defend their traditions against the erosive influence of modernization.
- Where there is 'ideological cohesion' around a single God and sacred text Fundamentalism seems to be stronger in Christianity and Islam, not so strong in Hinduism and Buddhism.
- When there is a common enemy to unite against Islamic Fundamentalism is often united against the USA.
- The existence of marginalized individuals facing oppression Fundamentalism needs recruits, and if a Fundamentalist group emerges with claims that it can provide a better life for people if they just adhere to the faith, it is more likely to grow
- The nature of Fundamentalism is shaped by how the political institutions deal with Fundamentalist movements where they are blocked access to political representation, movements are more likely to turn to violence.
- The specific histories of Christianity and Islam have affected the way the see politics. Christianity spent much of its early life as an obscure sect, on the political fringes, so is more concerned with 'day to day' (non-political) life, whereas Islam quickly came to dominate states in its early history – thus Islam is more concerned with politics than Christianity.
- Christianity tends to emphasize the importance of belief, while Islam emphasizes the importance of actions, thus Islam is more likely to develop violent forms of fundamentalism compared to Christianity.<sup>6</sup>
- Religious fundamentalism serves to reduce anxiety by promising justice. Indeed, structural conditions, over which the individual has little or no control, bring about many frustrations hard to bear with. The powerful use the underprivileged, some exercise power over others. In most parts of the world, economic and social conditions are such that some enjoy prosperity and well-being, while some others hardly survive. Thus, in the face of earthy injustices, religion functions as a palliative pill by promising that justice will be done and all sins will be punished eventually.<sup>7</sup>
- Origin of Fundamentalism: The growth of fundamentalism represents a culture war – a clash between the sacred and the secular. Religious fundamentalism first appeared in the 1880s in the USA. At that time, liberal Protestants attempted to adapt their views to the modern world, while conservative Protestants opposed. The conservative Protestants believed that the bible must be understood literally and wrote a set of pamphlets named 'The Fundamentals'.<sup>8</sup>



*Source: Internet, done by Interdisciplinary Studies*

4. **Founder of Fundamentalism:** The term fundamentalist was coined in 1920 to describe conservative Evangelical Protestants who supported the principles expounded in *The Fundamentals: A Testimony to the Truth* (1910-15), a series of 12 pamphlets that attacked modernist theories of biblical criticism and transferred the authority of the Bible. There is no single founder of Fundamentalism. American Evangelist **Daigle L. Moody** (1837-99) and British preacher and father of dispensationalism **John Nelson Darby** (1800-1882). Also associated with the early beginnings of Fundamentalism were **Cyrus**

5. **Teaching of Fundamentalism:**

- Supremacy of own religion
- Creates motivation to sacrifice for Dharma
- The doctrine of monotheism
- Only one particular religion will exist in the world in the future. Fundamentalism therefore denies religious freedom to other religions and opposes their existence
- The Fundamentalists teach a violent way to destroy the existence of opposing religions through traditional thinking and religious fanatic.
- The deities of other religions and their mention are also not tolerated. According to the essence of Islam, Allah is the only supreme power. Christian fundamentalists say that Jesus is the deity of all mankind, not Allah. At the same time, they worship the gods of other religions as Devil. Occasionally there is an emphasis on forcible conversion by the force of the sword or by financial temptation.<sup>10</sup>

5. **Characteristics of Fundamentalism:**

- Religious texts are seen as perfect. As such, they might be read literally be it the Bible, the Quran, Bhagavadgita or the Torah. One consequence of this is that fundamentalism rejects religious pluralism.
- There is a profound rejection of modern society. Modern society is seen as morally corrupt. Living in the modern world is seen as problematic because of the variety of choice. Fundamentalists reject the idea of choice and assert the value of tradition.
- Chauvinism is another defining characteristic of fundamentalism. While a fundamentalist of a religious type talks in the power of God, he is one who denies himself the power of God; while he makes a full cry of equality, he is, by nature, a patriarchalistic; while he claims all life based around faith, he declares all science to be wrong. While he pays a great deal of lip service to the ideals, he ignores them in practice and occasionally is contemptuous of them in private. He plays foul with ideology for which he claims to live and die, if necessary.
- Activism is strongly encouraged. Fundamentalists are vocal in their struggle of good against evil e.g. media images often focus on fundamentalists protesting against modernity.
- Fundamentalism reinforces nationalism. Fundamentalists often appeal to deep-seated fears of 'strangers'

- Fundamentalism is always without a base. It starts with a conclusion and, thereafter, searches for evidence of support for the conclusion and if the fundamentalist does not find any, he creates one.
- Fundamentalists have a political agenda. Absolute opposition to homosexuals, abortion and birth control.<sup>11</sup>

The specific histories of Christianity and Islam have affected the way the see politics. Christianity spent much of its early life as an obscure sect, on the political fringes, so is more concerned with 'day to day' (non-political) life, whereas Islam quickly came to dominate states in its early history – thus Islam is more concerned with politics than Christianity.

6. **Features of Fundamentalism:**

- **Dualism:** The fundamentalist divide the world into binary categories: good/evil, right/wrong lines.
- **Paranoia:** A deep feeling of suspicion towards those on the wrong side of the dualistic dividing lines.
- **An Apocalyptic orientation:** An obsession with the ultimate endpoint for society or humanity. Usually positively disposed to bring about that ultimate end.
- **Charismatic leadership:** A commitment or devotion to Charismatic leader. Often accompanied with a cult of leadership.
- **Totalized conversion experience:** Once the fundamentalist converts or embrace the ideology, they do so completely.<sup>12</sup>

7. **Comparing Fundamentalism:** Religions like ideologies vary. They differ in their potential for becoming fundamentalistic. The more monolithic a religion or ideology is, the more are the chances of it turning to fundamentalism. Islam and the evangelical Protestant strand of Christianity are monolithic religions; they believe that there is just one God; they are also dogmatic; they believe it is possible to express his nature and will in specific propositions both these things are the necessary pre-conditions for fundamentalism.<sup>13</sup>

Hinduism as a religion, in the context of Islam and Protestant Christianity as they are, is less monolithic and dogmatic and hence, less fundamentalistic. There are a number of reasons for that: there is diffuseness in Hinduism, different deities, a variety of gods. So diffused is the society as well: a variety of traditions, groups, sects. It might be, Bruce says, "better described not as a religion, but as a loose collection of religions: that of the Shaivites, the Vaishnavas, the Shalcras, the Smartas, and others that share some common themes but they tolerate a huge variety of expressions of these themes. As those expressions can vary from village to village and caste to caste, there is a little scope for enforcing conformity, criticizing laxity, or vigorously rejecting moderate reconstructions of the tradition. Instead of the single Bible or Quran, there are a large numbers of holy books and holy traditions." Hindu fundamentalism is rare and arises only when anti-Hindu fundamentalism challenges it. Within itself, revivalistic attempts have been at work in Hinduism: sometimes in the forms of Buddhism, Jainism or Sikhism at an early period of history or in the forms of Brahma Samaj, Arya Samaj, Ramakrishna Mission or Ved-Samaj during the greater part of the nineteenth century. Orthodoxy has always been



met with revivalism in Hinduism. To that extent and arguably, monolithic religions such as Judaism, Christianity and Islam offer relatively more fertile soil for fundamentalism than Hinduism.<sup>14</sup>

Protestantism and Islam have much in common. Their potentials are the same. Both can generate fundamentalism; their aims are similar. Each wishes to assert the primacy of its religious belief systems and the patterns of behavior each belief system requires. But both differ in their methods. The Islamic fundamentalists believe that coercion is proper; most of them believe that it is necessary as well, while others feel that it is required, declaring 'Jihad' literally. The Protestant fundamentalists do not believe so. Christ preached against the old law of 'eye for an eye' and instead recommended to offer another cheek to the person who has already hit the first cheek. Though radical Protestants have created militant sects, the Protestants are relatively pacifists. Protestants and Islamists differ in their attitudes to toleration. By and large, the Protestants are tolerant while the Islamists are less so; the USA, for example, permits freedom of religious expression and attempts to prevent the state promoting one religion as superior to any other. As against this, most of the Muslim countries are far less tolerant. Referring to this, Bruce writes: 'Note that this is a matter of description and not value judgement. Nothing about what I have said requires us to believe that permissiveness is better than authoritarianism.' Differences in the two monolithic religions can be cited in abundance. But that apart, what is more significant here is that Islamic fundamentalism is more potent, and more severe than Christian fundamentalism. We can turn to them briefly. Christianity and politics, for most of the time stayed apart. It became official religion of the Roman Empire in only AD 373, though it was officially tolerated from sixty years before, i.e., 313 AD. During the Middle Ages, the theory of the two swords kept the two domains, temporal and ecclesiastical, distinct from each other. The Reformation not only brought to the fore the two sects, Catholics and Protestants, it made religion a private affair of the individual. Liberalism, in the West, is not due to Christianity but due to its absence. Lewis says: "The distinction between the church and the state is rooted in Christendom". This is not to say that Christians are not religious. They are as religious minded as the followers of any other religions: many of them live a life-style which is particularly godly. Bruce says, "The core of Protestantism is correct belief, not correct action; orthodoxy rather than ortho-praxis." With the emergence of the modern state, century after century, Christianity remained aloof from the state, though most of the citizens in the western nations were Christians. Christian fundamentalists, in relation to the state and the law, operate in a more legitimate manner and largely, in secular countries.<sup>15</sup>

Islamic fundamentalism is more pronounced, more vocal and more action-oriented. From the beginning, Islam, unlike Christianity, remained political. The Prophet and the subsequent Caliphs were both spiritual and political leaders. The founder of the Muslim Brotherhood, an Islamic fundamentalist organization, puts it as: "Politics is part of religion. Caesar and what belongs to Caesar is for God Almighty alone." The Islamic fundamentalist promotes a life-style which is not only conformity to the creed, it demands actions also in conformity with what the fundamentalist wants. A hostage, held by Hezbollah, puts the case of Islamic fundamentalism, saying: "All our activities, from the way we slept to the way we entered a lavatory, were watched so that we could not violate the laws of Islam. Khomeini had written that on entering a lavatory, a believer must put his left foot forward first. We were taken to task for violating that rule." And Bruce adds: "For Islam, religion is a matter of obeying the Holy Law. As what God requires is obedience to the Law, then its imposition is not just acceptable but necessary."

Most of the Muslim countries, especially in the Middle East, have not been able to shed their religion which is Islam, despite all their efforts to westernize themselves. Islam, for them, is more than a religion: it is their eye, it is their way. The Islamic fundamentalists in relation to the state, operate largely in theocratic countries and seek Muslim brotherhood and Islamic unity.<sup>16</sup>

Thus the religious and cultural conflict among various nations creates threat among various community in the world. Religion in such situations offers support and a sense of cultural identity in an uncertain or hostile environment. Defending a community against a threat often gives religion a prominent role in politics. Fundamentalism happens in monotheistic religions with one God. There is a comparison of fundamentalism in the West and in the Third World; West; fundamentalism is a reaction to change in modern society, either because of increasing diversity or postmodernity. Third world; fundamentalism is a reaction to outside values being thrust upon them.

**Conclusion:** Although the terms *fundamentalism* and *fundamentalist* have entered common parlance and are now broadly applied, it should not be forgotten that the myriad movements so designated vary greatly in their origins, character, and outlook. Thus, Islamic fundamentalist movements differ from their Christian and Jewish counterparts in having begun as essentially defensive responses to European colonial domination. Early Islamic fundamentalists were reformers who wished to affirm the value of their religion by returning to what they sought to portray as its pristine original form; their movements only gradually acquired the militancy characteristic of much religious fundamentalism today. On the other hand, these movements share with Christian and Jewish fundamentalism

an antipathy to secularism, an emphasis on the importance of traditional religiosity as their members understand it, and a strict adherence to sacred texts and the moral codes built upon them. Although these and other common features are important as sources of insight, each fundamentalist movement is in fact unique and is best understood when viewed in its own historical and cultural context.

#### References:

- Nagata, Judith, "Beyond Theology: Toward an Anthropology of "Fundamentalism" *American Anthropologist*, June 2001, p. 103.  
[www.https://en.wikipedia.org/wiki/Fundamentalism](http://en.wikipedia.org/wiki/Fundamentalism), last seen at 01-04-2021 at 2.30 pm.  
 Mizaffer Ercan Yilmaz, A Research article published in *International Journal of Human Sciences*, Volume: 2 Issue: 2, June 23, 2006, p.2  
[www.https://www.britannica.com/topic/fundamentalism](http://www.britannica.com/topic/fundamentalism), last seen at 01-04-2021 at 2.30 pm.  
 Karen Armstrong, *The Battle for God*, New York: Alfred A. Knopf, March 2000, p. 9.  
<https://revisesociology.com/2018/11/23/the-cause-of-fundamentalism>, last seen at 02-04-2021 at 6.35 pm.  
 Mizaffer Ercan Yilmaz, *Op.cit*, p.6.  
[www.https://sociologysaviour.wordpress.com/2015/08/04/fundamentalism-uit-3/](http://sociologysaviour.wordpress.com/2015/08/04/fundamentalism-uit-3/), last seen at 01-04-2021 at 3.30 am.  
[www.https://link.springer.com/chapter/10.1057%2F9780230616585\\_7](http://link.springer.com/chapter/10.1057%2F9780230616585_7), last seen at 01-04-2021 at 5.00 pm.  
 Kudu Anil, *Fundamentalism: Concept and Reality*, research article published in *Navjyot/Vol.X/Issue-I, 2015*, p.51.  
<http://egyankosh.ac.in/bitstream/123456789/23766/1/Unit-22.pdf>, last seen at 02-04-2021 at 9.30 am.